Genetic and culture diversity of Planctomycetes from different habitats of India

Thesis submitted for the degree of

Doctor of Philosophy

Kumar Gaurav

(Reg. No. 15LPPH16)

Department of Plant Sciences
School of Life Sciences
University of Hyderabad
Hyderabad – 500 046, INDIA

March, 2021

University of Hyderabad
(A Central University established in 1974 by an act of parliament)
HYDERABAD – 500 046, INDIA

CERTIFICATE

This is to certify that **Mr. Kumar Gaurav** has carried out the research work embodied in the present thesis under the supervision and guidance of Prof. Ch. Venkata Ramana for a full period prescribed under the Ph.D. ordinances of this University. We recommend his thesis entitled **"Genetic and culture diversity of Planctomycetes from different habitats of India"** for submission for the degree of Doctor of Philosophy of the University.

18/08/2021
Head,
Department of Plant Sciences

HEAD
Dept. of Plant Sciences
School of Life Sciences
University of Hyderabad
Hyderabad-500 046. INDIA

18/8/2021
Prof. Ch. Venkata Ramana
(Research Supervisor)

Prof. Ch. Venkata Ramana Ph.D
Department of Plant Sciences School of Life Sciences
University of Hyderabad, P.O. Central University,
Hyderabad - 500 046, India

Dean,
School of Life Sciences

DEAN
School of Life Sciences
University of Hyderabad
Hyderabad - 500 046.

Scanned with CamScanner

University of Hyderabad
(A Central University established in 1974 by an act of parliament)
HYDERABAD – 500 046, INDIA

DECLARATION

This is to declare that the work embodied in this thesis entitled **"Genetic and culture diversity of Planctomycetes from different habitats of India"** has been carried out by me under the supervision of Prof. Ch. Venkata Ramana, Department of Plant Sciences, School of Life Sciences. The work presented in this thesis is a bonafide research work and has not been submitted for any degree or diploma in any other University or Institute. A report on plagiarism statistics from the University Librarian is enclosed.

18/8/2021

Prof. Ch. Venkata Ramana
(Research Supervisor)

Prof. Ch. Venkata Ramana M.Tech., Ph.D
Department of Plant Sciences School of Life Sciences
University of Hyderabad, P.O. Central University,
Hyderabad - 500 046, India

Kumar Gaurav

Scanned with CamScanner

Department of Plant Sciences
School of Life Sciences
University of Hyderabad
Hyderabad – 500046, Telangana, India

CERTIFICATE

This is to certify that this thesis entitled **"Genetic and culture diversity of Planctomycetes from different habitats of India"** is a record of bonafide work done by **Mr. Kumar Gaurav**, research scholar for Ph. D. program under the Department of Plant Sciences, School of Life Sciences, University of Hyderabad under my guidance and supervision. This thesis is free from plagiarism and has not been submitted in part or in full to this or any other University or institution for the award of any degree or diploma.

Parts of the thesis have been:

Published in the following publications:

Gaurav Kumar., Dhanesh K., Jagadeeshwari U., Sreya PK., Shabbir A., Sasikala Ch. and Ramana Ch.V (2021) *Crateriforma spongiae* sp. nov., isolated from a marine sponge. *Antonie van Leeuwenhoek*. (doi.org/10.1007/s10482-020-01515-1)

[$]Dhanesh Kumar., [$]**Gaurav Kumar.,** [$]Jagadeeshwari U., Sasikala, Ch. and Ramana Ch.V (2021) *Candidatus* Laterigemmans baculatus" gen. nov. sp. nov., the first representative of rod shaped planctomycetes with lateral budding in the family *Pirellulaceae. Syst Appl Microbiol. (*doi.org/10.1016/j.syapm.2021.126188)

[$]**Gaurav Kumar.,** [$]Radha Vaddavalli., [$]Jagadeeshwari, U., Sasikala, Ch. and Ramana, Ch.V (2020) Bacterial communities of sponges from the wetland ecosystem of Little Rann of Kutch, India with particular reference to Planctomycetes. *3 Biotech* 10:1-10

[$]Dhanesh Kumar., [$]**Kumar Gaurav.,** Jagadeeshwari U., Deepshikha G., Sasikala Ch. and Ramana Ch.V (2020) *Roseimaritima sediminicola* sp. nov., a new member in Planctomycetaceae isolated from Chilika lagoon. *Int J Syst Evol Microbiol* 2020.70:2613-2623.

[$]Dhanesh Kumar., [$]**Gaurav Kumar.,** Shabbir A., Jagadeeshwari U., Sasikala Ch. and Ramana Ch.V (2020) Descriptions of *Roseiconus nitratireducens* gen. nov. sp. nov. and *Roseiconus lacunae* sp. nov. *Arch. Microbiol* 12:1-14

[$]Dhanesh Kumar., [$]**Kumar Gaurav.,** Sreya PK., Shabbir A., Jagadeeshwari, U., Sasikala Ch., and Ramana Ch.V (2020) *Gimesia chilikensis* sp. nov., a haloalkali tolerant planctomycete isolated from Chilika lagoon and emended description of the genus *Gimesia. Int J Syst Evol Microbiol* 70:3647-3655.

Note:- $, First and equal Authorship

Presented in the following conference

Kumar Gaurav., Radha Vaddavalli., Jagadeeshwari Uppadda., Ramana ChV. and Sasikala Ch. (2018). "Anaerobic ammonium oxidation bacteria (anammox) bacteria associated with sponges collected from little Rann of Kutch, Gujarat, India". Poster presentation in 59th Annual conference of AMI during 9th-12th December, 2018 in Hyderabad, India.

Further, the student has passed the following courses towards the fulfillment of the coursework requirement for Ph.D.

S. NO	Course	Name	Credits	Pass/Fail
1	PL801	Analytical Techniques	4	Pass
2	PL802	Research ethics, Data analysis and Biostatistics	3	Pass
3	PL803	Lab Work and Seminar	5	Pass

18/3/2021

Supervisor

Prof. Ch. Venkata Ramana Ph.D
Department of Plant Sciences School of Life Sciences
University of Hyderabad, India

Head 18/03/2021

HEAD
Dept. of Plant Sciences
School of Life Sciences
University of Hyderabad
Hyderabad-500 046. INDIA

Dean

DEAN
School of Life Sciences
University of Hyderabad
Hyderabad - 500 046.

Scanned with CamScanner

ACKNOWLEDGEMENTS

I would like to take this opportunity to extend my gratitude to my supervisor Prof. Ch. Venkata Ramana for his unrelenting encouragement and constant support, without whom, this endeavor would not have been possible. Working under him gave me a true sense of freedom, broadened my scientific outlook, and inculcated a spirit of positive attitude in me. I am deeply indebted of his unfailing support in every scientific aspect like writing, communication, presentation skills, which enabled me towards the successful completion of this Ph.D. program. Above all, I can't forget his care and help showed towards me at difficult times during the entire tenure of my doctoral research, cheerful time which I had with him during samples collection.

I thank my doctoral committee members, Prof. S. Rajagopal and Dr. K. Gopinath for their suggestions during my work. I also thank them for allowing me to use their lab facilities.

I thank the former Deans, Prof. P. Reddanna, Prof. Ramaiah and the present Dean, Prof. S. Dayananda School of Life Sciences and former Head, Prof Ch. Venkata Ramana, and present Head Prof. Padmaja Dept. of Plant Sciences, for their support in all possible ways.

I am grateful to Prof. Ch. Sasikala, CEN, IST, JNTU for allowing me to work in her lab. I extend my sincere gratitude for her immense support and guidance in every scientific aspect and her help in nurturing my writing skills which helped in successful completion of this Ph.D. program. Thank you madam for making this thesis possible.

I thank Jagadeeshwari uppadda, JNTU for helping me in the genome analysis of the various isolates.

I thank Prof. Bernhard Schink for suggesting the etymology of the newly isolated species. I would also like to thanks curators of KCTC, South Korea and NBRC, Japan

for depositing strains and providing reference strains for my work. I Thank prof. Michelle Kelly for identifying sponges and algal specimens.

I am extremely grateful to my teachers, who taught me just not science, also ethics and morals in life.

I thank Department of Biotechnology (DBT) for the research fellowship. Infrastructural support provided by UGC-SAP, DBT-CREBB and DST-FIST to the Dept. of Plant Sciences are highly acknowledged.

I am extremely happy to gratefully acknowledge my present (Dr.Suresh, Shabbir, Kim, Smita, Indu, Anusha, Sreya, Ipsita, Deepshikha, Ashif and Krishnaiah) and former lab mates, friends at SLS, UoH, *friends at JNTU Hyderabad for their friendly association, encouragement, suggestions, care and help offered to me.*

I thank all my friends including Satyam, Priyanka and Ranay for their unconditional supports and other research scholars of the school of life sciences for their cooperation and for making my stay in HCU memorable.

Words fail to express my heartfelt gratitude for my parents, and all my family members including my elder brother, Bhabhi, elder sister, brother in law and all my niece and nephew to whom I'm forever indebted for their love, unconditional support, endless patience, without their cooperation I would not have come so far.

Thank you everyone

Kumar Gaurav

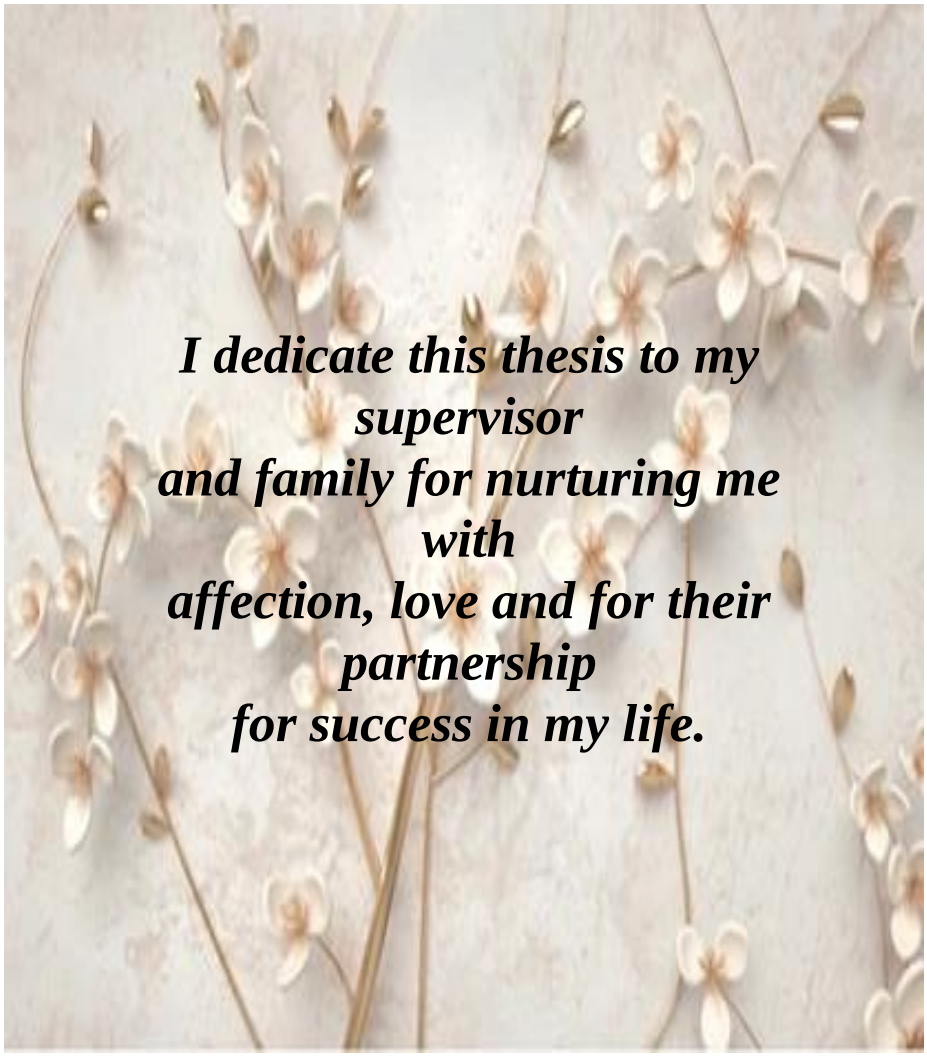
I dedicate this thesis to my supervisor
and family for nurturing me with
affection, love and for their partnership
for success in my life.

CONTENTS P. No

Abbreviations, list of tables and figures I-XV

1. Introduction 1-23

1.1 Planctomycetes 1
1.2 Cell plans of the Planctomycetes 2
1.3 Planctomycetes wheel of life 5
1.4 Planctomycetal shape determination and cell division 7
1.5 Planctomycetal Genome 9
1.6 Chemotaxonomy of Planctomycetes 10
1.7 Taxonomy of Planctomycetes 11
1.8 Anaerobic ammonia-oxidizing (anammox) bacteria 12
1.9 Ecology and Physiology of Planctomycetes 13
1.10 Planctomycetal diversity associated with sponges 17
1.11 Planctomycetal diversity associated with Algae 19
1.12 Biotechnological aspects of Planctomycetes 21
1.13 Objectives 23

2. Material and methods 24-45

2.1 Glasswares 24
2.2 Cleaning 24
2.3 Distilled water, double distilled water and Milli-Q water 24
2.4 Chemicals and solvents 24
2.5 Gases used 24
2.6 Determination of pH 24
2.7 Sterilization 24
2.8 Sample collection 25
2.9 Enrichment and isolation of Planctomycetes member 26
2.9.1 The three steps enrichment strategy for anammox bacteria 26
2.9.2 The enrichment strategy for Planctomycetes 27
2.10 Fluorescence in-situ hybridization (FISH) 32
2.11 Purification of Planctomycetes 32
2.12 Maintenance of the cultures 32
2.13 Morphological characterization 33
2.13.1 Morphological observation 33
2.13.2 Microscopic observation 33
2.13.3 Field emission scanning electron microscopy (FFSEM) 33
2.13.4 Negative staining for Transmission Electron Microscopy (TEM) 33
2.13.5 Transmission electron micrographsection for ICM structures 34
2.14 Biochemical characterisation 34
2.14.1 Oxidase and catalase test 34

2.14.2 Organic carbon substrate utilization test 34
2.14.3 Utilization of various nitrogen sources 35
2.14.4 Vitamin B_{12} requirement 35
2.14.5 NaCl requirement for optimal growth 36
2.14.6 Temperatures for optimum growth 36
2.14.7 pH for optimum growth 36
2.15 Chemotaxonomic characterisation 36
2.15.1 Cellular fatty acid composition 36
2.15.2 Polar lipid extraction and identification 37
2.15.3 Quinone extraction and identification 38
2.15.4 Polyamine extraction and identification 38
2.16 DNA isolation, PCR, 16SrRNA gene sequencing and BLAST analysis 39
2.16.1 Phylogenetic analysis 40
2.16.2 Digital/ *In-silico* DNA-DNA hybridization (dDDH) 40
2.16.3 Orthologous Average Nucleotide Identity (OrthoANIu) 41
2.16.4 Average Amino acid Identity (AAI) and Percentage of Conserved Proteins (POCP) 41
2.16.5 Construction of phylogenomic tree using UBCG (Up-todate Bacterial Core Gene) pipeline 41
2.16.6 Genomic information and in-silico metabolic characterisation 41
2.17 Amplicon based metagenome analysis 42
2.17.1 Extraction of metagenomic DNA from sponge/Algal samples 42
2.17.2 16SrRNA amplicon-based Illumina Library preparation 42
2.17.3 DNA processing and assessment for taxonomic diversity 43
2.17.4 Functional Profile Prediction 45
2.17.5 “Sporotan” staining of fruiting bodies 45
3 Results 46-211
3.1 Bacterial communities of selected habitats with particular reference of Planctomycetes 47
3.1.1 Bacterial communities of sponges from the wetland ecosystem of little Rann of Kutch, India 47
3.1.1.1 Sampling strategy 47
3.1.1.2 Metagenomic DNA extraction, sequencing and quality control 48
3.1.1.3 Bacterial abundance and diversity analysis 49
3.1.1.4 Planctomycetes diversity among sponges 54
3.1.1.5 Functional profile Prediction 55

	3.1.2	Bacterial communities of sponges, collected from Tamil Nadu coast, India		57
		3.1.2.1	Sampling strategy	57
		3.1.2.2	Metagenomic DNA extraction, sequencing and quality control	57
		3.1.2.3	Bacterial abundance and diversity analysis of sponges	57
		3.1.2.4	Planctomycetal abundance and diversity analysis of sponges	61
	3.1.3	Bacterial communities of the algal samples, collected from Tamil Nadu coast, India		63
		3.1.3.1	Sampling strategy	63
		3.1.3.2	Metagenomic DNA extraction, sequencing and quality control	64
		3.1.3.3	Bacterial abundance and diversity analysis of algal samples	64
		3.1.3.4	Planctomycetal abundance and diversity analysis of algal samples	67
	3.1.4	Temporal based bacterial communities analysis of Satpada region of Chilika Lagoon, India		69
		3.1.4.1	Sampling strategy	69
		3.1.4.2	Metagenomic DNA extraction, sequencing and quality control	69
		3.1.4.3	Bacterial abundance and diversity analysis of sediment samples of Satpada region of Chilika Lagoon	69
		3.1.4.4	Planctomycetal abundance and diversity analysis of sediment samples of Satpada region of Chilika Lagoon	70
3.2	Enrichment			72
	3.2.1	The three enrichment strategy for Planctomycetes		72
	3.2.2	FISH for detection of Planctomycetes from the enrichment		72
	3.2.3	Phylogenetic analysis of anammox-Planctomycetes from the culture-dependent study		76
3.3	Isolation of Planctomycetes			79
3.4	Phylo-taxogenomic studies of newly isolated axenic cultures of Planctomycetes from Chilika lagoon			85
	3.4.1	Phylo-taxonomic study of strain JC635^{T} and JC654^{T}		85
		3.4.1.1	Habitat and Nucleotide sequence accession number	85
		3.4.1.2	Genomic characteristics	86

3.4.1.3 BLAST analysis and phylogenetic inference 86
3.4.1.4 *In-silico* metabolic characterization 92
3.4.1.5 Morphological and physiological analyses 93
3.4.1.6 Chemotaxonomic characterization 96
3.4.1.6.1 FAME profile 96
3.4.1.6.2 Polar lipid profile 96
3.4.1.6.3 Polyamine profile 98
3.4.2 Phylo-taxogenomic study of strain JC646^T 102
3.4.2.1 Habitat and Nucleotide sequence accession number 102
3.4.2.2 Genomic characteristics 102
3.4.2.3 BLAST analysis and phylogenetic inference 103
3.4.2.4 *In-silico* metabolic characterization 108
3.4.2.5 Morphological and physiological analyses 109
3.4.2.6 Chemotaxonomic characterization 111
3.4.2.6.1 FAME profile 111
3.4.2.6.2 Polar lipid profile 111
3.4.2.6.3 Polyamine profile 113
3.4.3 Phylo-taxogenomic study of strain JC651^T 115
3.4.3.1 Habitat and Nucleotide sequence accession number 115
3.4.3.2 Genomic characteristics 115
3.4.3.3 BLAST analysis and phylogenetic inference 116
3.4.3.4 Morphological and physiological analyses 119
3.4.3.5 Chemotaxonomic characterization 121
3.4.3.5.1 FAME profile 121
3.4.3.5.2 Polar lipid profile 121
3.4.4 Phylo-taxogenomic study of strain JC650^T, JC657^T, JC636, JC649 124
3.4.4.1 Habitat and Nucleotide sequence accession number 124
3.4.4.2 Genomic characteristics 124
3.4.4.3 BLAST analysis and phylogenetic inference 126
3.4.4.4 *In-silico* metabolic characterization 128
3.4.4.5 Morphological and physiological analyses 133
3.4.4.6 Chemotaxonomic characterization 135
3.4.4.6.1 FAME profile 135
3.4.4.6.2 Polar lipid profile 136
3.4.4.6.3 Polyamine profile 136
3.4.5 Characterization of the strains JC640 and CH01 138
3.4.5.1 Habitat and Nucleotide sequence accession number 138
3.4.5.2 Genomic characteristics 138

3.4.5.3 BLAST analysis and phylogenetic inference 138
3.4.5.4 *In-silico* metabolic characterization 139
3.4.5.5 Morphological analyses 151
3.5 Phylo-taxogenomic studies of the newly isolated axenic cultures of Planctomycetes from Tamil Nadu 155
3.5.1 Phylo-taxogenomic study of strain JC647^T 155
3.5.1.1 Habitat and Nucleotide sequence accession number 155
3.5.1.2 Genomic characteristics 156
3.5.1.3 BLAST analysis and phylogenetic inference 157
3.5.1.4 *In-silico* metabolic characterization 161
3.5.1.5 Morphological and physiological analyses 168
3.5.1.6 Chemotaxonomic characterization 169
3.5.1.6.1 FAME profile 169
3.5.1.6.2 Polar lipid profile 169
3.5.1.6.3 Polyamine profile 171
3.5.2 Phyto-taxogenomic study of strain JC658^T 173
3.5.2.1 Habitat and Nucleotide sequence accession number 173
3.5.2.2 Genomic characteristics 173
3.5.2.3 BLAST analysis and phylogenetic inference 173
3.5.2.4 *In-silico* metabolic characterization 175
3.5.2.5 Morphological and physiological analyses 180
3.5.2.6 Chemotaxonomic characterization 181
3.5.2.6.1 FAME profile 181
3.5.2.6.2 Polar lipid profile 181
3.5.2.6.3 Polyamine profile 181
3.5.3 Phyto-taxogenomic study of strain JC639^T and JC637 185
3.5.3.1 Habitat and Nucleotide sequence accession number 185
3.5.3.2 Genomic characteristics 185
3.5.3.3 BLAST analysis and phylogenetic inference 185
3.5.3.4 *In-silico* metabolic characterization 189
3.5.3.5 Morphological and physiological analyses 191
3.5.3.6 Chemotaxonomic characterization 191
3.5.3.6.1 FAME profile 191
3.5.3.6.2 Polar lipid profile 191
3.5.3.6.3 Polyamine profile 193
3.6 Phyto-taxogenomic studies of the newly isolated axenic culture of Planctomycetes from Loktak lake 197
3.6.1 Phyto-taxogenomic study of strain JC669^T 195
3.6.1.1 Habitat and Nucleotide sequence accession number 195

3.6.1.2 Genomic characteristics 196
3.6.1.3 BLAST analysis and phylogenetic inference 198
3.6.1.4 *In-silico* metabolic characterization 200
3.6.1.5 Morphological and physiological analyses 202
3.6.1.6 Chemotaxonomic characterization 205
3.6.1.6.1 FAME profile 205
3.6.1.6.2 Polar lipid profile 206
3.6.1.6.3 Polyamine profile 207

4 Discussion 209- 239

4.1 Culture independent studies of bacterial communities with special emphasis on taxa belonging to Planctomycetes 209
4.1.1 Bacterial communities of sponges collected from the Little Rann of Kutch, India 209
4.1.2 Bacterial communities of seventeen sponges samples collected from Tamil Nadu 210
4.1.3 Bacterial communities of fourteen algal samples collected form Tamil Nadu 211
4.1.4 Bacterial communities of sediment samples collected form Satapada region of Chilika Lagoon 212
4.1.5 Comparative analysis of bacterial communities of sample collected from different habitats of India 213
4.2 The three step enrichment protocol helps in successful cultivation of Planctomycetes 214
4.3 Proposal and description of new taxa of Planctomycetes 215
4.3.1.1 Proposal of a new genus to accommodate strains JC635^T and JC645^T 216
4.3.1.2 Description of *Roseiconus* gen. nov. 216
4.3.1.3 Description of *Roseiconus nitratireducens* sp. nov. 217
4.3.1.4 Description of *Roseiconus lacunae* sp. nov. 218
4.3.2.1 Proposal of a new species to accommodate strain JC646 ^{T} 219
4.3.2.2 Description of *Gimesia chilikensis* sp. nov. 219
4.3.2.3 Proposal of amending the genus description of *Gimesia* 220
4.3.2.4 Emended description of the genus *Gimesia* 221
4.3.3.1 Proposal of new species to accommodate strain JC651^T 222
4.3.3.2 Description of *Roseimaritima sediminicola* sp. nov. 222
4.3.4.1 Proposal of a new species to accommodate strains JC650 ^{T} and JC657 ^{T} 224
4.3.4.2 Description of *Tautonia marina* sp. nov. 225

4.3.4.3	Description of *Tautonia rosea* sp. nov.	226
4.3.4.4	Proposal to amend the genus description of Tautonia	227
4.3.4.5	Emended description of the genus Tautonia	227
4.3.5.1	Proposal of the new genus to accommodate strain JC640 and CH01	228
4.3.5.2	Description of "*Candidatus* Laterigemmans" gen. nov.	228
4.3.5.3	Description of "*Candidatus* Laterigemmans baculatus" sp. nov.	228
4.3.6.1	Proposal of a new species to accommodate strain JC647 ^{T}	230
4.3.6.2	Description of *Crateriforma spongiae* sp. nov.	230
4.3.6.3	Proposal to emend the genus description of "*Crateriforma*"	231
4.3.6.4	Emended description of the genus "*Crateriforma*"	231
4.3.7.1	Proposal of the new genus to accommodate strain JC658 ^{T}	233
4.3.7.2	Description of *Thalassoroseus* gen. nov.	233
4.3.7.3	Description of *Thalassoroseus pseudocratinae* sp. nov.	234
4.3.8.1	Proposal of a new species to accommodate strain JC639^{T}	235
4.3.8.2	Description of *Roseiconus marina* sp. nov.	235
4.3.9.1	Proposal of a new species to accommodate strain JC669^{T}	237
4.3.9.2	Description of *Aquisphaera insulae* sp.nov.	238
5.0	Major findings	240
	References	241-64
	Annexure	265-96
	Publication list	297-99
	Publication copies	
	Plagiarism report	

LIST OF ABBREVIATIONS

Abbreviations	Expansion
AAI	Average amino acid identity
AL	Aminolipid
ANI	Average nucleotide identity
BLAST	Basic Local Alignment Search Tool
BLASTn	Nucleotide Basic Local Alignment Search Tool
BLASTP	Protein Basic Local Alignment Search Tool
bp	Base pair
BPGA	Bacterial pan-genome analysis
CDS	Coding sequence
CTP	Cytidine triphosphate
*d*DDH	Digital DNA-DNA hybridization
DNA	Deoxyribonucleic acid
DPG	Diphosphatidylglycerol
DSMZ	Deutsche Sammlung von Mikroorganismen und Zellkulturen GmbH
ECR	Extra chromosomal replicons
EDTA	Ethylenediaminetetraaceticacid
EMBL	European molecular biology laboratory
FAME	Fatty acid methyl esters
g	Gram
$g.l^{-1}$	Gram per liter
G+C	Guanine+cytosine
GC	gas chromatography
GC-MS	Gas chromatography mass spectrophotometry
GL	Glycolipid
GPS	Global positioning system
h	Hour
HMM	Hidden Markov Model
HPLC	High-performance liquid chromatography
HSPs	high-scoring segment pairs
ICM	Intracytoplasmic membrane
ICNB	International Code of Nomenclature of Bacteria

JCM	Japan collection of microorganisms
KCTC	Korean collection for type cultures
L	Litre
LDL	low-density lipoprotein
LH	Light harvesting
Mb	Mega base pairs
MCL	Markov Cluster
ME	Minimum Evolutionary
MEGA	Molecular Evolutionary Genetics Analysis
Mg	Milligram
Min	Minute
MK	Menaquinone
ml	Milliliter
ML	Maximum Likelihood
mM	Millimolar
NaCl	Sodium chloride
NBRC	NITE Biological Resource Center
NCBI	National Center for Biotechnology Information
NJ	Neighbor-Joining
nm	Nanometer
nt	Nucleotide
OD	Optical density
OrthoANI	Orthologous average nucleotide identity
PCR	Polymerase chain reaction
PDA	Photodiode array
PGA	Pan-genome analyses
PGAP	Pan-genome analysis pipeline
PGC	Photosynthetic gene cluster
POCP	Percentage of conserved proteins
Q	Ubiquinone
RAST	Rapid Annotation using Subsystem Technology
Rba.	*Rhodobacter*

RC	Reaction center
RNA	Ribonucleic acid
RQ	Rhodoquinone
rRNA	Ribosomal ribonucleic acid
s	Seconds
SDS	Sodium dodecyl sulfate
SEM	Scanning electron microscopy
TEAP	Triethylamine phosphate
TEM	Transmission electron microscopy
TLC	Thin layer chromatography
UBCG	Up-to-date bacterial core gene
UV	Ultraviolet
v/v	Volume per volume
w/v	Weight per volume
WGS	Whole Genome Sequencing
ΔTm	melting temperature
µg	Microgram
$\mu g l^{-1}$	Microgram per liter
(w/v)	Weight/volume
≤	Less than or equal to
°C	Degree Celsius
µl	Microliter
µM	Micromolar
$^{0}C.min^{-1}$	Degree Celsius per minute
10K	10000
2D	Two dimensional
1D	One dimensional

Sl.No	List of Figures and Tables	P. No
Fig. 1.1	Cell plans of Planctomycetes (A) and Eukaryotes (B) is adopted from Wiegand et al. (2018)	03
Fig. 1.2	Cell plans of Planctomycetes (a) and canonical bacteria (b) is adopted from Wiegand et al. (2018)	03
Fig. 1.3	Hypothesis of Planctomycetal life cycle is adopted from Wiegand et al. 2018	06
Fig. 1.4	Planctomycetal cell division and cell shape is adopted from Wiegand et al. (2020)	06
Fig. 1.5	Taxonomy of the phylum Planctomycetes (Based on the information from different literatures.	11
Fig. 1.6	Unique feature of anammox cell. (a) Cell shows anammoxosome (A), (b) an …….	14
Fig. 1.7	Distribution of Planctomycetes across globe, is adopted from Wiegand et al. 2018	14
Fig. 1.8	Planctomycetal secondary metabolite BGCs, is adopted from Wiegand et al. (2020)	22
Fig. 2.1	Three steps enrichments of Planctomycetes including anammox bacteria.	28
Fig. 2.2	The flowchart of phylogenetic tree reconstruction using the UBCG pipeline is adopted from Na et al. 2018.	42
Fig. 2.3	Bioinformatics workflow for amplicon based metagenome analysis of various samples.	44
Fig. 3.1.1.a	culture dependent and independent studies to assess the bacterial diversity of……	48
Fig. 3.1.1.b	Rarefaction analysis of the three sponge samples. Rarefaction curves of OTUs…….	50
Fig. 3.1.1.c	Heat map showing Phylum level comparison of bacterial community structure……	51
Fig. 3.1.1.d	Heat map showing Class-level comparison of bacterial community structure……	52

Fig. 3.1.1.e	Venn diagram representing diversity of core and shared OTUs with in the three sponge……	53
Fig. 3.1.1.f	Non-metric multidimensional scaling (nMDS) plot representing the diversity based……	54
Fig. 3.1.1.g	Heat map depicting the abundance and distribution of Planctomycetes at family……	55
Fig. 3.1.1.h	KEGG Annotation of reads obtained from metagenome of three sponge samples……	56
Fig. 3.1.2.a	Detail about the samples collected for the metagenome and culture -based studies……	58
Fig. 3.1.2.b	Rarefaction analysis of seventeen sponge samples. Rarefaction curves of OTUs……	59
Fig. 3.1.2.c	Heat map showing Phylum level comparison of bacterial community ……	59
Fig. 3.1.2.d	Heat map depicting the abundance and distribution of Planctomycetes at family level……	62
Fig. 3.1.2.e	Heat map depicting the abundance and distribution of Planctomycetes at genus level……	62
Fig. 3.1.3.a	Detail about the samples collected for the metagenome and culture -based studies……	64
Fig. 3.1.3.b	Rarefaction analysis of fourteen algal samples. Rarefaction curves of OTUs	65
Fig. 3.1.3.c	Heat map showing Phylum level comparison of bacterial community structure obtained…….	65
Fig. 3.1.3.d	Heat map depicting the abundance and distribution of Planctomycetes at family……	67
Fig. 3.1.3.e	Heat map depicting the abundance and distribution of Planctomycetes at genus level from……	68

Fig. 3.1.4.a	Heat map showing Phylum level comparison of bacterial community structure obtained……	71
Fig. 3.1.4.b	Heat map showing family level comparison of Planctomycetes community……	71
Fig. 3.2.1	Fluorescence micrograph of few sponge samples showing enrichment of ……	73
Fig. 3.2.2	Fluorescence micrograph of few algal samples showing enrichment of Planctomycetes from……	73
Fig. 3.2.3	Fluorescence micrograph of few algal samples showing enrichment of Planctomycetes……	74
Fig. 3.2.4	Sample based relative enrichments of Planctomycetes based on the FISH analysis	75
Fig. 3.2.5	Geographical based relative enrichments of Planctomycetes based on the FISH analysis.	75
Fig. 3.2.6	Fluorescence micrograph of Planctomycetes bacteria from five sponges enriched CY3……	77
Fig. 3.2.7	Phylogenetic tree constructed using the partial sequences of 16S r RNA gene of isolates…….	78
Fig. 3.3.1	Fluorescence micrograph of few cultures of isolated Planctomycetes using CY3 Pla46 ……	79
Fig. 3.3.2	Phylogeny of the newly isolated axenic Planctomycetal strains.	80
Fig. 3.4.1	Detail about the total Planctomycetal strains isolated, remain viable and strains……	85
Fig. 3.4.1.1	Analysis of phylogenetic markers for delineation of the novel isolates JC635^{T}and JC645^{T}……	88

Fig. 3.4.1.2	The 16S rRNA gene sequences based phylogenetic tree showing the phylogenetic relationship……..	89
Fig. 3.4.1.3	The phylogenomic tree based on RAxML of strain JC645^{T}and JC635^T along with Publically……..	91
Fig. 3.4.1.4	Common and unique biochemical pathways between strain JC635^T and strain JC645^T……	92
Fig. 3.4.1.5	Electron microscopic image of strain JC635^T: (a, b) SEM image; (c) TEM image……	95
Fig. 3.4.1.6	Electron microscopic image of strain JC645T: (a) SEM image; (b) TEM image of……	95
Fig. 3.4.1.7	Two dimensional chromatograms showing polar lipids of (a) strain JC635T and (b) strain ……	97
Fig. 3.4.1.8	HPLC data showing the presence of different polyamine present in strain JC645T and JC635T	98
Fig. 3.4.2.1	Genome organization of strain JC646^T and G. maris DSM 8797^T.	105
Fig. 3.4.2.2	Genome map based on protein sequence identity among strains JC646^T and some other……	105
Fig. 3.4.2.3	The 16S rRNA gene sequences based phylogenetic tree showing the phylogenetic relationship…….	105
Fig. 3.4.2.4	Phylogenomics tree based on RAxML of strain JC646^T along with publicly……	107
Fig. 3.4.2.5	Common and unique biochemical pathways between strain JC646^T and *G. maris* DSM ……	109
Fig. 3.4.2.6	Confocal microscope image of (a) strain JC646^T and (b) *G. maris* DSM 8797^T……..	110

Fig. 3.4.2.7	Electron microscopic images of strain JC646^T. (a) SEM image showing intact cells……..	111
Fig. 3.4.2.8	Two dimensional chromatograms showing polar lipids of (a) strain JC646^T and…….	113
Fig. 3.4.2.9	HPLC chromatogram of polyamines of *Gimesia* spp.	113
Fig. 3.4.3.1	Genome organization of strain JC651^T and *R. ulvae* DSM 25454^T.	116
Fig. 3.4.3.2	Genome map based on protein sequence identity between *Roseimaritima* sp……	116
Fig. 3.4.3.3	Phylogenetic tree based on 16S rRNA gene sequences showing the phylogenetic relationship……..	117
Fig. 3.4.3.4	RAxML-based phylogenomic tree of strain JC651T along with publicly available……	118
Fig. 3.4.3.5	Common and unique biochemical pathways between strain JC651^T and *R. ulvae* DSM 25454^T	120
Fig. 3.4.3.6	Electron microscopic images of strain JC651T: (A) SEM image showing the aggregate	120
Fig. 3.4.3.7	Two-dimensional chromatogram showing polar lipids of A). strain JC651^T and B). *R. ulvae*……..	122
Fig. 3.4.4.1	Genome organization of strains *T. sociabilis* GM2012^T, *T. plasticadhaerens* ElP^T. JC650……..	125
Fig. 3.4.4.2	Genome map based on protein sequence identity. Genome of *Tautonia sociabilis*……	125
Fig. 3.4.4.3	Analysis of phylogenetic markers for delineation of the novel isolates JC650^T and JC657^T……	127
Fig. 3.4.4.4	16S rRNA gene sequences based Phylogenetic tree showing the phylogenetic relationship……	129

Fig. 3.4.4.5	Phylogenomic tree of strains JC636, JC649, JC650^{T}and JC657^{T} along with publicly available……..	129
Fig. 3.4.4.6	Functional classification COGs clusters of orthologs of two isolates and related strains……	130
Fig. 3.4.4.7	Comparative analysis of CAZymes of strains JC650^{T}, JC657^{T} and related species of genus *Tautonia*…….	130
Fig. 3.4.4.8	Common and unique biochemical pathways between strains JC650^{T} and *T. sociabilis* GM2012^{T}.	131
Fig. 3.4.4.9	Common and unique biochemical pathways between strains JC650T and……	132
Fig. 3.4.4.10	Common and unique biochemical pathways between strains JC650^{T} and JC657^{T}……	132
Fig. 3.4.4.11	Number of genetic clusters putatively involved in the production of secondary.	133
Fig. 3.4.4.12	Electron micrographs of strain JC650^{T}: SEM image showing spherical to oval cells……..	134
Fig. 3.4.4.13	Electron micrographs of JC657^{T}: SEM image showing spherical to oval cells in aggregates……	135
Fig. 3.4.4.14	Two dimensional chromatograms showing polar lipids of strain JC650^{T} …….	136
Fig. 3.4.4.15	HPLC data showing the presence of major polyamines in strains JC650T and JC657^{T}	136
Fig. 3.4.5.1	The phylogenetic tree based on 16S rRNA gene sequences showing the phylogenetic…….	143
Fig. 3.4.5.2	phylogenomic tree based on RAxML of strains JC640 and CH01 along with publicly…….	148

Fig. 3.4.5.3	Comparative analysis of CAZymes of strain JC640 CH01 and *Roseimaritima ulvae*……	150
Fig. 3.4.5.4	Functional classification COGs clusters of orthologs of strain JC640 , CH01……	150
Fig. 3.4.5.5	Transmission electron microscopic images of negatively stained cells of strains JC640 and……	152
Fig. 3.5.1	Detail about the total Planctomycetal strains isolated, remain viable and strains……	155
Fig. 3.5.1.1	Genome organization of strains JC647^{T} and "*Crateriforma conspicua*" Mal65^{T}……	157
Fig. 3.5.1.2	Genome map based on protein sequence identity.. List of tracks, from outside……..	157
Fig. 3.5.1.3	Analysis of phylogenetic markers for delineation of the novel isolate JC647^{T}……..	158
Fig. 3.5.1.4	Phylogenetic tree based on 16S rRNA gene sequences showing the phylogenetic…….	159
Fig. 3.5.1.5	RAxML based phylogenomics tree of strain JC647^{T} along with publicly…….	160
Fig. 3.5.1.6	Functional classification COGs clusters of orthologs of strain JC647^{T}……..	164
Fig. 3.5.1.7	Comparative analysis of CAZymes of strain JC647T and "*Crateriforma conspicua*"……..	164
Fig. 3.5.1.8	Common and unique biochemical pathways between strain JC647T and "*Crateriforma*……	165
Fig. 3.5.1.9	Electron microscopic images of strain JC647^{T}. (A) SEM image showing……	169

Fig. 3.5.1.10	Two dimensional chromatograms showing polar lipids of the strain (a) JC647^T and……	170
Fig. 3.5.1.11	HPLC chromatogram of polyamines of Strain JC647^T	170
Fig. 3.5.2.1	Phylogenetic tree based on 16S rRNA gene sequences showing the phylogenetic…….	174
Fig. 3.5.2.2	RAxML based phylogenomics tree of strain JC658^T along with publicly available…….	175
Fig. 3.5.2.3	Comparative analysis of CAZymes of strain JC658^T and closely related strains of……	180
Fig. 3.5.2.4	Electron micrographs of JC658^T, SEM image showing oval to pear shaped……	181
Fig. 3.5.2.5	Two-dimensional thin-layer chromatograms of whole cell polar lipids of strain 1. JC658……..	182
Fig. 3.5.2.6	Polyamine profile of the strain JC658^T	182
Fig. 3.5.3.1	Analysis of phylogenetic markers for delineation of the novel isolates JC637 and……..	188
Fig. 3.5.3.2	Phylogenetic tree based on 16S rRNA gene sequences showing the phylogenetic…….	188
Fig. 3.5.3.3	RAxML based phylogenomic tree of strain JC637 and JC639^T along with publically…….	188
Fig. 3.5.3.4	Number of genetic clusters putatively involved in the production of secondary metabolites…….	190
Fig. 3.5.3.5	Electron microscopic image of strain JC639^T and JC637: (A,B) SEM……	191
Fig. 3.5.3.6	Two dimensional chromatograms showing polar lipids of (A) strain JC637 and (B)……	192

Fig. 3.5.3.7	Polyamine profile of the strains JC639^T, JC637**,** *R. lacunae* JC635^T, *R. nitratereducens* JC645^T	193
Fig. 3.6.1	Detail about the total Planctomycetal strains isolated, remain viable and strains……..	195
Fig. 3.6.1.1	Genome organization of strain JC669^T and *Aquisphaera giovannonii* OJF2^T.	197
Fig. 3.6.1.2	Genome map based on protein sequence identity between genome of strain JC669^T……	197
Fig. 3.6.1.3	Analysis of phylogenetic markers for delineation of the novel isolates JC669^T….....	199
Fig. 3.6.1.4	Phylogenetic tree based on 16S rRNA gene sequences showing the phylogenetic……	199
Fig. 3.6.1.5	RAxML based phylogenomics tree of strain JC669^T along with publicly available……	200
Fig. 3.6.1.6	Comparative analysis of CAZymes of strains JC669^T *and Aquisphaera giovannonii*……	200
Fig. 3.6.1.7	Common and unique biochemical pathways between strain JC669^T and *A. giovannonii*……	201
Fig. 3.6.1.8	Transmission (a) and scanning (b,c,d,e) electron micrographs of cell of Strains JC669^T……	203
Fig. 3.6.1.9	LSCM images: Sporotan stained fruiting bodies and unstained mother cells of……	204
Fig. 3.6.1.10	Heat map representing the Percentage identity of some sporulating proteins in the strains JC669…….	204
Fig. 3.6.1.11	Two dimensional chromatograms showing polar lipids of (a) strain JC669^T …….	207
Fig. 3.6.1.12	HPLC chromatograms showing polyamines strain JC669^T and *A. giovannonii* DSM 22561^T……..	207

Fig. 4.1	Venn diagram representing diversity of core and shared bacterial (a) and Planctomycetal (b)…….	214
Table. 2.1	Anammox bacteria media composition (Modified)	26
Table. 2.1.1	Trace element solution 1 composition	27
Table. 2.1.2	Trace element solution 2 composition	27
Table. 2.2	M30 Modified media Composition	28
Table. 2.2.1	Composition of the artificial sea water	29
Table. 2.2.2	Metal 44 components	29
Table. 2.2.3	Hutner's Basal salts compositions	30
Table. 2.2.4	Vitamin solution compositions	30
Table. 2.3	MN Media Composition	31
Table. 2.4	MYM media compositions	31
Table. 3.1.1.a	Comparison of Microbial community richness and diversity indices of three sponge samples	49
Table. 3.3.1	Details about the isolated axenic strains of Planctomycetes from different geographical locations	81
Table. 3.4.1.1	Comparative genomic features among members of genus *Rhodopirellua*. and genus *Roseimaritima* with	87
Table. 3.4.1.2	POCP values (%) Matrix among some members of planctomycetaceae and Pirellulaceae	90
Table. 3.4.1.3	AAI values (%) Matrix among some members of planctomycetaceae and Pirellulaceae including	91
Table. 3.4.1.4	Cellular fatty acid composition (%) of 1. Strain JC635^T and 2. Strain	97
Table. 3.4.1.5	Differentiating characters of the novel genus *Roseiconus* from	99
Table. 3.4.1.6	Differentiating characteristics between strains 1. JC635^T and 2. JC645^T	99
Table. 3.4.2.1	Genome features of members of the genus Gimesia.	104
Table. 3.4.2.2	POCP Values among the selected genomes of the family *Planctomycetaceae*.	106
Table. 3.4.2.3	AA1Values among the selected genomes of the family Planctomycetaceae.	106

Table. 3.4.2.4	Cellular fatty acid composition (%) of strain JC646T and G. maris DSM8797^T	112
Table. 3.4.2.5	Differential characteristics of (1) *Gimesia chilikenesis* JC646^T and 2. *G. maris* DSM 8797^T.	114
Table. 3.4.3.1	Cellular fatty acid composition (%) of 1. strain JC651^T and 2. *R. ulvae* DSM 25454^T.	122
Table. 3.4.3.2	Differential characteristics of 1. Strain JC651^T and 2. *R. ulvae* DSM 25454^T.	123
Table. 3.4.4.1	Cellular fatty acid composition (%) of the newly isolated strains	136
Table. 3.4.4.2	Comparison of phenotypic, chemotaxonomic and genomic features of 1. strain JC650^T	137
Table. 3.4.5.1	AAI values of strains JC640 and CH01 with other members of Family Pirellulaceae	144
Table. 3.4.5.2	POCP values of strains JC640 and CH01 with other members of Family Pirellulaceae.	146
Table. 3.4.5.3	Genome-based analysis of the central carbon metabolism of "*Candidatus* Laterigemmans baculatus…….	148
Table. 3.4.5.4	Phenotypic and genotypic information of strains JC640 and CH01 compared ……..	153
Table. 3.5.1.1	Genome-based analysis of the central carbon metabolism of genus "*Crateriforma*	166
Table. 3.5.1.2	Cellular fatty acid composition (%) of Strains JC647^T and "*Crateriforma conspicua*" Mal65^T	169
Table. 3.5.1.3	Differentiating characters between strain JC647^T and "*Crateriforma conspicua"* Mal65^T	171
Table. 3.5.2.1	Genome-based analysis of the central carbon metabolism of genus strain JC658^T	179
Table. 3.5.2.2	Distribution of fatty acids in the strain JC658^T	182
Table. 3.5.2.3	Differentiating characters between strains JC658^T and other members of Planctomycetaceae	183
Table. 3.5.3.1	Comparative genomic features among members of genus *Roseiconus*, JC637, and JC639^T	187

Table. 3.5.3.2	Fatty acids distributions among the strains JC639^T, JC637, *R. lacunae* JC635^T, *R. nitrateducens* JC645^T.	194
Table. 3.5.3.3	Differentiating characters between strain JC639^T, JC637 and other members of……	195
Table 3.6.1.1	**:** Major **(>1%)** Cellular fatty acids composition (%) of 1. strain JC669^T and 2. *A. giovannonii* OJF2^T.	206
Table 3.6.1.2	Differential characteristics of (1) strain JC669^T and 2. *A. giovannonii* DSM 22561^T.	208

Introduction

1. Introduction

1.1 Planctomycetes

On studying the model organisms, mostly belonging to the phyla Actinobacteria, Firmicutes, Bacteroidetes and Proteobacteria provide knowledge on vital bacterial features of their genetics, cell biology, metabolism, virulence and biotechnological exploitability. However, the most critical question comes to our mind: Do these bacterial phyla represent general bacterial traits and concepts? To date, approximately 105 bacterial phyla are recognized (Wiegand et al. 2020) of which many of them belong to "Candidatus phyla" with no cultivated representatives. Investigating more genomes of uncultivated bacteria is now possible due to the advent and low cost of metagenomics and next-generation sequencing. Uncultivated members' metagenome-assembled genomes were comparatively analysed to explore their hidden and potential characters. Nevertheless, discovering and analysing yet unplumbed or unexplored potential (Wiegand et al. 2020). bacterial traits, axenic cultures are crucial for detail studies of their physiological and morphological characterisation and genetic manipulation. Hence, detailed exploration of less understood bacterial phyla like Planctomycetes may help to explore some of the yet unexplored bacterial traits.

The phylogeny of Planctomycetes was a subject of controversy since its discovery in the year 1924. These members were first recognised as eukaryotes due to their morphology resembling fungi (Gimesi 1924). However, it was corrected and subsequently acknowledged as bacteria (Hirsch 1972). The Planctomycetes along with other bacterial phyla like Verrucomicrobia, Kiritimatiellaeota, Lentisphaerae, "*Candidatus* Omnitrophica" and Chlamydiae form the PVC superphylum (Wagner and Horn 2006).

Members of the phylum Planctomycetes are ubiquitous in distribution and are most commonly isolated from aquatic habitats (Wiegand et al. 2018). Species of this phylum have unique physiology and cell morphology compared to other bacteria (Lagae et al. 2014; Wiegand et al. 2020).

1.2 Cell plans of the Planctomycetes

At first, cells of Planctomycetes were thought to significantly differ from those typical Gram-negative bacteria or Gram-positive bacteria bacteria (Fuerst and Webb 1991; Lindsay et al. 1997). Planctomycetal cells were thought to have proteinaceous cell walls instead of peptidoglycan (PG). Intracytoplasmic membrane (ICM) divided the cytoplasm into pirellulosome and paryphoplasm (Ko¨nig et al. 1984; Liesack et al. 1986; Stackebrandt et al. 1984; Stackebrandt et al. 1986; Lindsay et al. 2001). Species like *Gemmata obscuriglobus*, the nucleoid is enclosed by double membranes having the distribution of nuclear pores which resemble the nuclear enveloped of eukaryotic and separate transcription and translation was suggested in this species (Fuerst and Sagulenko 2011; Fuerst and Webb 1991; Gottshall et al. 2014). Further, it was also reported in the same species to possess the clathrin-coated endocytic vesicles within paryphoplasm. If this is validated, Planctomycetes would be the first group of bacteria to possess eukaryotic feature of endocytosis-like vesicle-based uptake system (Devos et al. 2004; Santarella-Mellwig et al. 2010; Lonhienne et al. 2010; Jermy 2010). (Fig. 1.1a, b). The above scenario has now changed with the advent of genetic tools and high-resolution microscopic techniques used for the studies of planctomycetes. Multiple studies focusing on planctomycete cell's biology eventually induced a paradigm shift from what it was thought earlier. One of the bacterial cell wall's hallmark traits is the presence of peptidoglycan, which maintain the

integrity of the bacterial cells against osmotic pressure (Boedeker et al 2017). Peptidoglycan (PG) is a linear glycan

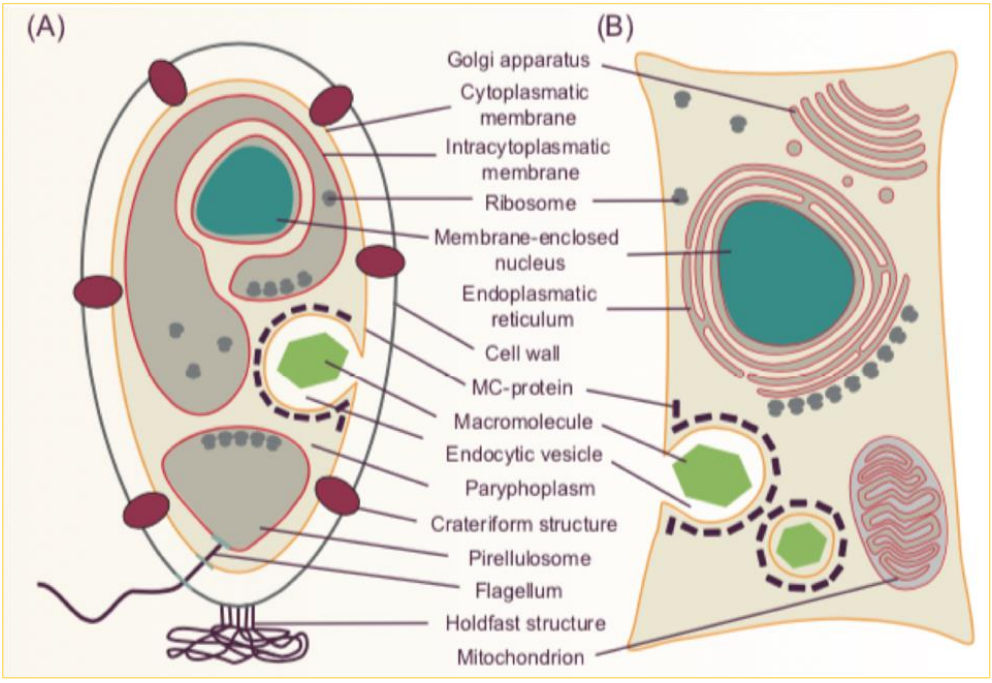

Fig. 1.1. Cell plans of Planctomycetes (A) and Eukaryotes (B) is adopted from Wiegand et al. (2018)

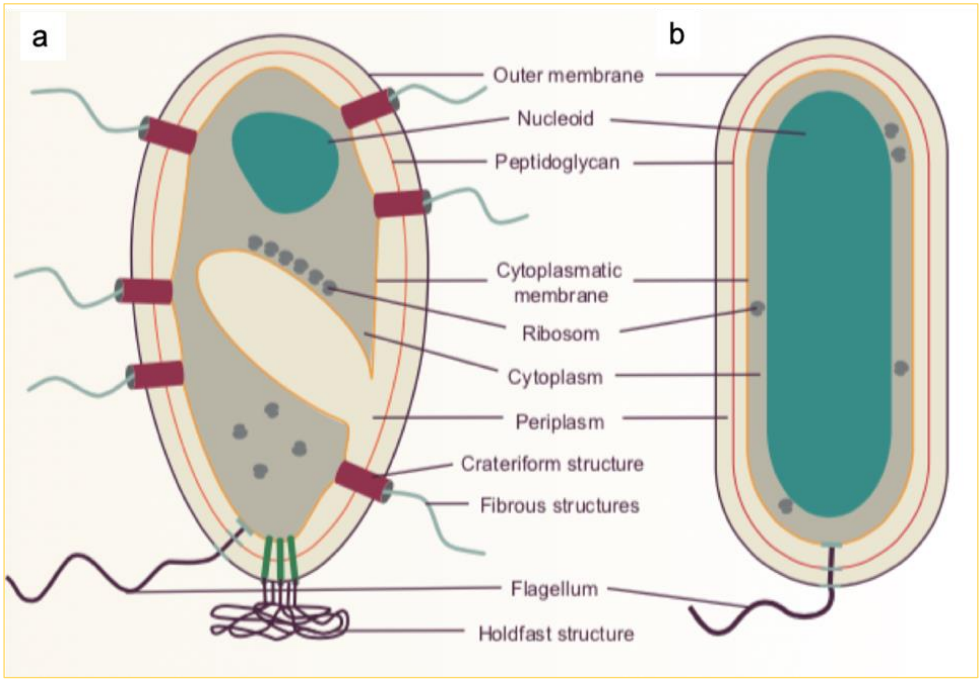

Fig. 1.2. Cell plans of Planctomycetes (a) and canonical bacteria (b) is adopted from Wiegand et al. (2018)

cross-linked *via* short peptides and subsequently forms a rigid polymeric mesh cross (Lovering et al. 2012; Vollmer and Holtje 2004). The action of FtsZ and other related proteins are vital during cell division for septal formation and for the synthesis of Peptidoglycan (Egan and Vollmer 2013). Further, the absence or presence of PG was the needed to be addressed experimentally among Planctomycetes. Several multiple independent analysis, experiments and methods like Planctomycetal genome analysis, GC-MS based studies on cellular component like diaminopimelic acid, several biochemical assays to find sugar components of peptidoglycan, isolation of peptidoglycan sacculi and its lysozyme treatments to analyse the cell wall composition of Planctomycetes by cryo-electron tomography clearly established peptidoglycan presence in the cell wall of Planctomycetes and are closely related to Verrucomicrobia (Van Teeseling et al. 2015; Jeske et al. 2015). Further, the absence of true nucleus is confirmed through the membrane staining and Cryo-electron tomography experiments in *Gemmata obscuriglobus* (Santarella-Mellwig et al. 2013) (Fig. 1.2a, b).

Recent characterization of some planctomycetes outer membrane proteins, reconceptualised the Planctomycetal 'cytoplasmic membrane' from the previous studies as the ‘outer membrane’ (Fig.1.2a), while 'intracytoplasmic membrane' (Fig.1.1a) from then is now reinterpreted as the ‘cytoplasmic membrane’ (Lindsay et al. 2001; Van Teeseling et al. 2017) (Fig.1.2a). Thus according to observations in their cell plan, Planctomycetes are now considered as exceptional Gram-negative bacteria. Due to the presence of enlarged periplasmic space or invaginations of the CM, the planctomycete cell plan is exceptional to Gram-stain-negative bacteria (Boedeker et al. 2017). On employing recent technologies like SIM super-resolution microscopy, dSTORM and cryo-electron tomography revealed

the subcellular membrane organization inside the cells of Planctomycetes (Boedeker et al. 2017). Compartmentalization inside the cell was nothing but the invagination of cytoplasmic membranes (Acehan et al. 2013; Boedeker et al. 2017; Santarella-Mellwig et al. 2013), with few exceptions present in "*Candidatus* Brocadiales" clade as anammoxosome (Kartal et al. 2013; Kartal et al. 2010). Endocytosis which is the hallmark trait of early eukaryotic cells and in the prokaryote endocytosis became difficult for the vesicle to pass mesh-like structure of peptidoglycan (Jeske et al. 2015). Hence, possibility for the endocytosis like uptake in Planctomycetes is ruled out by the presence of peptidoglycan in the cell wall of Planctomycetes. Furthermore, super-resolution microscopy and cryo-electron tomography experiments revealed that macromolecules which are stored in the continuous enlarged periplasmic space are indeed cytoplasmic invaginations rather than endocytic vesicles (Jeske et al. 2015; Lonhienne et al. 2010; Boedeker et al. 2017) (Fig. 1.2a, b).

1.3 Planctomycetal wheel of life

Members of Planctomycetes mostly divides through polar budding, but binary fission was also reported in few members of Planctomycetes (*Phycisphaeraceae*) (Fuerst and Sagulenko 2011; Fukunaga et al. 2009). Recently, it was reported that some members also divides through lateral budding (Wiegand et al. 2020). Most members of Planctomycetes have a dual lifestyle. Young cells of Planctomycetes are swimmer bearing flagella and subsequently attach to the surface through its hold fast and become sessile stalk mother cells. The stalk cells starts reproducing to produce swimmer daughter cells (Jogler et al. 2011) (Fig 1.3). The differences in the planctomycete cell architecture regarding different shapes and lifestyles are also reflected in their diversity (Jogler et al. 2011). Some members are non-motile through their lifestyle and some members like *Isosphaera pallida*

lack holdfast as it forms filament. This indicates that the lifestyle switch is not a universal mechanism for the Planctomycetes (Giovannoni et al. 1987) (Fig 1.3).

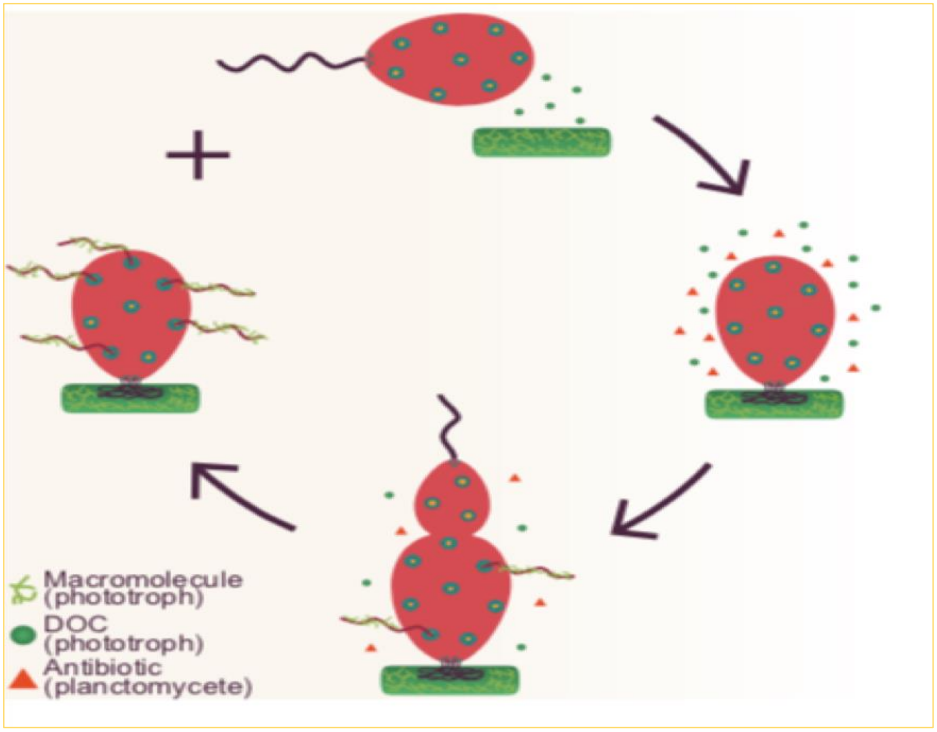

Fig. 1.3 Hypothesis of Planctomycetal life cycle is adopted from Wiegand et al. 2018

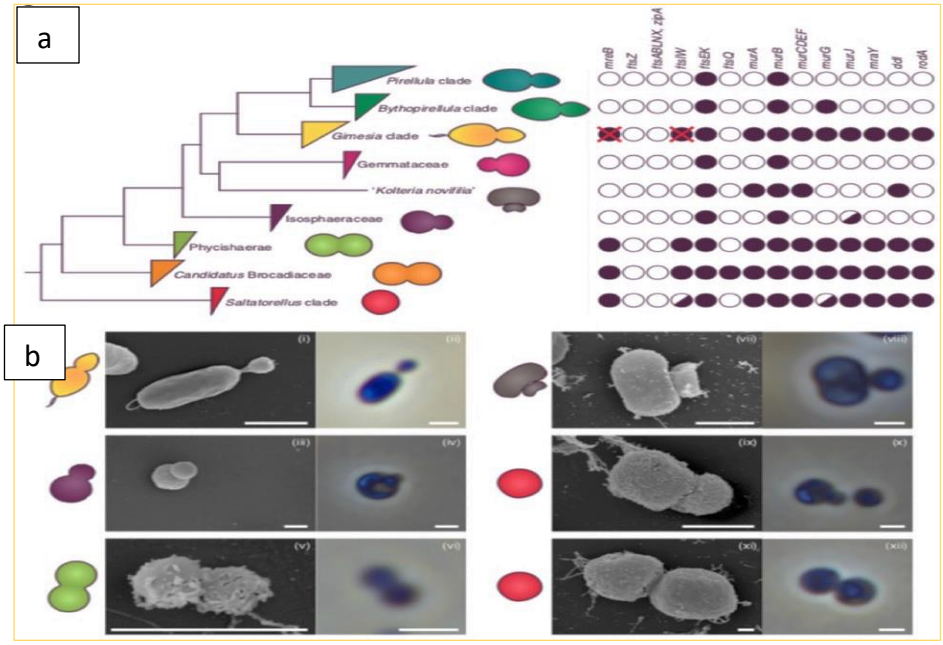

Fig. 1.4. Planctomycetal cell division and cell shape is adopted from Wiegand et al. (2020)

1.4 Planctomycetal shape determination and cell division

The advent of microscopy technology provides the swotting of the cell divisions and morphologies of the bacterial axenic cultures. As expected, Planctomycetal members which belongs to the class Planctomycetia frequently divides by polar budding. In the pear-shaped or axial symmetric cells, like *P. limnophila*, divide by polar budding in which daughter cells originate in opposite to the pole from the bulge region, forms stalk (as in *Gimesia maris*) (Jogler et al. 2011) or holdfast structure. Cells multiplication through budding in Planctomycetes is observed in an elongated shaped cell as well as in radial symmetric/coccoid cells such as '*Aeolisphaera plasticia*'. Strikingly, '*Kolteria novifilia*', deviated from that pattern of polar budding which forms a distinct phylogenetic clade within the order Planctomycetale. '*Kolteria novifilia'* cells divide by idiosyncratic 'lateral budding' originated from mid-position of the cell, perpendicular to the mother cell's longitudinal axis (Wiegand et al. 2020). Members of the family *Isosphaeraceae* divides by habitual polar budding (Kaushik et al. 2020) (Fig 1.4). In disparity to the budding class Planctomycetia, the classes 'Brocadiaceae' and Phycisphaerae usually divide by binary fission (Kartal et al. 2013; Wiegand et al. 2018, 2020). Surprisingly, coccoid cells of '*Saltatorellus'* clade can switch between binary fission and budding even in the same culture (Fig 1.4) (Wiegand et al. 2020).

In contrast to binary fission, the budding process is incomprehensible at the molecular level. Twelve essential conserved proteins forms the divisome in the free-living bacteria (Wagstaff et al. 2018; Jogler et al. 2012). FtsZ, bacterial tubulin-homolog, is the crucial component. Several genomes analysis verified the absence of *ftsZ* in all analysed planctomycete genomes, including the *Kolteria* and *Saltatorellus* deep branching clades (Wiegand et al. 2020; Jogler et al. 2012) (Fig 1.4). Some strains of Planctomycetes encode an FtsZ-like protein (FtsZl-1) but are superfluous to form filaments (Jogler et al. 2012).

The divisome proteins like FtsE and FtsK are encoded in all Planctomycetes genome, while FtsI and FtsW selectively encoded in some species of Planctomycetes genome. This conspicuously shows that the proteins FtsW and FtsI are superfluous for planctomycete cell division and same was further validated by constructing and investigating of *P. limnophila; ftsI* and *ftsW* deletion mutants. All planctomycetes encode the DNA translocase FtsK and cells deficient of FtsK (*ftsK* deletion mutant) do not survive. Hence, FtsK seems essential and could serve as one of the starting candidate to reveal the planctomycete cell division's molecular background in the future (Wiegand et al. 2020). The correlation between the canonical cell-division genes and the mode of planctomycetal cell divisions are still elusive. This indicates that except FtsK, other the canonical bacterial cell-division proteins might redundant to planctomycetal reproduction (Jogler et al. 2012; Wiegand et al. 2020) (Fig 1.4). The cell division and cell-shape determination of planctomycete is an enigmatic process. Peptidoglycan sacculus define bacterial shape in the absence of a static and rigid cytoskeleton (Wagstaff et al. 2018). The experimental demonstration, along with detailed and stringent computational analysis revealed that Planctomycetal clades utilises the certain set of genes to build cell wall compose of peptidoglycan (Van Teeseling et al. 2015; Jeske et al. 2015). Some members belonging to the family *Pirellulaceae and Gemmataceae* lack most of the peptidoglycan synthesis related genes, despite possessing a clear peptidoglycan cell wall (Fig 1.4). The cytoskeletal filaments proteins, such as MreB, the actin homolog regulate the making and breaking of the cell wall's peptidoglycan component (Wagstaffet al. 2018; Van Teeseling et al. 2017; Shi et al. 2018; Hussain et al. 2018). MreB protein during the peptidoglycan synthesis process organises the elongasome, which is the multi-enzyme complex present in the majority of the bacterial species (Hussain et al. 2018). However, members of the class Planctomycetia along with strain '*Kolteria novifilia*', devoid of MreB (Wiegand et al. 2020; Shi et al. 2018). However, the coccoid

'Brocadiaceae' and Phycisphaerae as well as members of the *Saltatorellus* clade, encode MreB. Further, a mutant study in the *P. limnophila* revealed that the role of MreB is still elusive for the main Planctomycetes clade. There were no significant differences in their cell shape observed between the mutant and wild type. Mutant *P. limnophila (ΔmreB)* divided like the wild type showed no phenotypic difference than the wild type (Fig 1.4) (Jacquier et al. 2015; Wiegand et al. 2020).

1.5 Planctomycetal genomes

From a genomic view point, bacteria of the phylum Planctomycetes are very unusual. From all validly described and sequenced isolates, the average genome size is 7.9Mb. Out of which, *Phycisphaera mikurensis* has the smallest (3.9 Mb) genome and the *Fimbriiglobus ruber* belonging to the family *Gemmataceae* has the largest genome size of 12.4 Mb. While, genome size of usual heterotrophic free-living environmental bacterium is around 5 Mb, making planctomycetal genomes exceptionally large. Most sequenced Planctomycetes harbour only one replicon while some members also display additional plasmids (Wiegand et al. 2018). On an average, function of 57% of genes within the Planctomyetes genome are still unknown. Members of the family *Gemmataceae*, particularily, *Zavarzinella formosa* and *Fimbriiglobus ruber* have large genomes with 67.2% and 68.9% genes of unknown function (Jeske et al. 2013). Previous studies on Planctomycetes have established a linear relation between genome size and number of predicted secondary metabolite-related genes and gene clusters. Actinobacteria and Myxobacteria are well known to produce small bioactive molecules, have many secondary metabolite-related genes which are rather large in size >5kb. These large genes are called as giant genes (Reva and Tummler 2008). Now, Planctomycetes were also identified as one of seven bacterial phyla to have such giant genes with potential to produce small bioactive secondary metabolites. All planctomycetal genomes contain such giant genes of size 20-30

kb (Kohn et al. 2016). But, it is not correct to relate all giant genes to small molecules production. For example, in the genus *Paludisphaera*, they are plasmid borne and rather encode enzymes of carbohydrate metabolism (Ivanova et al. 2017a).

1.6 Chemotaxonomy of Planctomycetes

Members of Planctomycetes have various specialized pieces of machinery to utilize a wide ranges of organic carbon sources, including high molecular weight polysaccharides like N-acetylglucosamine (Jeske et al. 2016). For the utilisation of these high molecular weight polysaccharides like N-acetylglucosamine, three possibilities other than endocytosis was inferred: (i) the extracellular degradation of complex substrates into monosaccharides by secreting the enzymes and subsequently these monosaccharides are then transported inside the cell through the outer and cytoplasmic membrane (Jeske et al. 2015, 2016). (ii) Planctomycetes anchor complex high molecular weight polysaccharides to their cell surface and complex polysaccharides are further degraded into simple oligosaccharides. These molecules are then relocated to the periplasm with the help of Sus proteins for further degradation. This selfish mechanism was already reported in Bacteriodetes. These oligosaccharides cannot be consumed or benefited by non-enzyme producing heterotrophic bacteria (Cuskin et al. 2015; Reintjes et al. 2017). (iii) Crateriform structures associated with fibres help internalize most of the high molecular weight polysaccharides like N-acetylglucosamine into their enlarged periplasm for further degradation into the oligosaccharides and subsequently to monosaccharides (Boedeker et al. 2017). Nevertheless, these specialized mechanisms are now irrespective of habitats because all members of planctomycetes grow well in the presence of N-acetylglucosamine. These intracellular digestion mechanisms of complex polysaccharides could proffer an

advantage during the competition for nutrients in their natural habitats polysaccharides (Boedeker et al. 2017).

1.7 Taxonomy of the phylum Planctomycetes

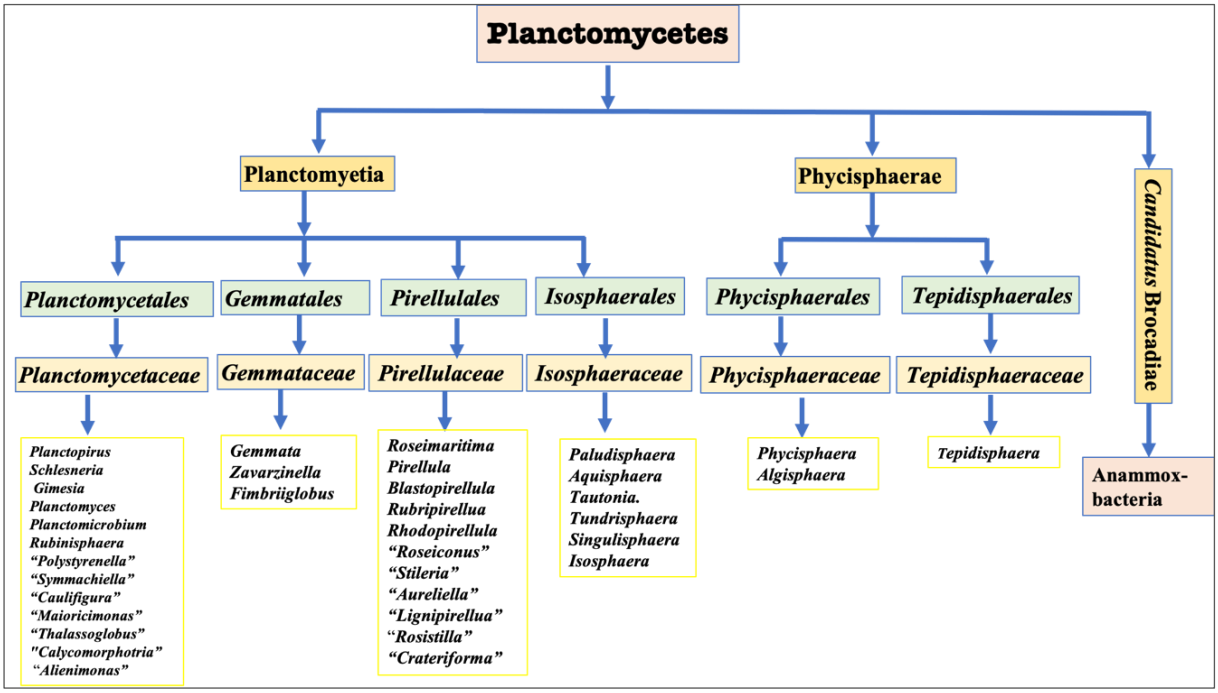

Fig. 1.5 Taxonomy of the phylum Planctomycetes (Based on the information from different literatures.

Taxonomically, the phylum Planctomycetes is subdivided into three classes: Phycisphaerae, Planctomycetia, and *Candidatus* Brocadiae (Wiegand et al. 2018) (Fig. 1.5). At present, the class Planctomycetia consists most of the valid described members in the phylum Planctomycetes. The class Planctomycetia consists of the four orders with validly published names viz., Planctomycetales, Gemmatales, Pirellulales and Isosphaerales (Dedysh et al. 2020) and each order contain single family *Planctomycetaceae, Gemmataceae, Isosphaeraceae* and *Pirellulaceae,* respectively. The families *Pirellulaceae* and *Planctomycetaceae* contain majority of the genera in which maximum are monospecies till now. The class Phycisphaerae have two orders Phycisphaerales and Tepidiphaerales and the latter consists of one family Tepidisphaeraceae with only one genus *Tepidisphaera*. Phycisphaerales contain single

family *Phycisphaeraceae* having two genera *Phycisphaera* and *Algisphaera;* Wiegand et al. 2018, 2020) (Fig. 1.5). It is conspicuous that Phylum Planctomycetes is still under sampled and more hidden members need to be isolated in the laboratory from different sources as an axenic culture.

1.8 Anaerobic ammonium-oxidizing (anammox) bacteria

Anammox is an abbreviation for ANaerobic AMMonium OXidation. It is a recently discovered bacterial process and is a significant component of the biogeochemical nitrogen cycle (Kartal et al. 2010). Anammox bacteria primarily grow by the process of oxidation of ammonium coupled to nitrite/nitrate reduction, utilizing carbon dioxide as the sole carbon source. Despite being neglected for a long time, anammox bacteria are encountered in enormous anoxic environments containing fixed nitrogen and NH_3 (Kartal et al. 2013). Anammox bacteria are believe to produce about 50% of all nitrogen gas released into the atmosphere from the oceans (Arrigo 2005; Lam and Kuypers 2011). Anammox processes most likely takes place in a particular cell organelle like structure, the anammoxosome (Van Niftrik et al. 2008a, b) (Fig. 1.6). It is hypothesized that a variety of heme c proteins, such as the hydrazine synthase (HZS) complex and hydroxylamine oxidoreductase (HAO)-like proteins, that participate in anammox catabolism are reside inside the anammoxosome (Lindsay et al. 2001; Jetten et al. 2009; Karlsson et al. 2009). During the anammox process, proton-motive force for ATP synthesis is generated by nitrite reduction and ammonium oxidation proceed in cyclic electron flow via two intermediates, hydrazine and nitric oxide. Localisation of all heme c complement near the anammoxosome membrane was confirmed through the Diaminobenzidine staining (Van Niftrik et al., 2008a, b). The membrane of anammox bacteria consists of unique (ladder-like) lipid known as ladderane lipids (Kuypers et al. 2003) (Fig. 1.6). Anammox bacteria's ladderane lipids compose of saturated C_{17}-C_{20} fatty acid having three linearly concatenated cyclobutane rings and one

cyclohexane or five cyclo-butane rings. Fatty acids are esterified with either methanol or the glycerol backbone (Boumann et al. 2006; Rattray et al. 2008; Rattray et al. 2010). The ladderane alcohols are ether-linked with glycerol, all in different combinations. Nevertheless, the current concepts regarding the anammox process and presence of ladderane lipid around anammoxosome membranes are hypothetical to a greater extent and further put forward the most intriguing questions that need specific protocols for the isolation of anammoxosomes with a high yield.

Taxonomically, ten anammox species have been recognised, including seven that are available in laboratory as the enrichment cultures from various sources ranging from sludge, waste water treatment plants and marine environments (Kartal et al. 2013). Till now, none of these strains were obtained as axenic cultures, so all have the taxonomical status of 'Candidatus'. All the Candidatus species are placed under five genera: (1) *Kuenenia*, represented by *Kuenenia stuttgartiensis*, (2) *Anammoxoglobus* (one species: *A. propionicus*, (3) *Brocadia* (three species: *B. anammoxidans*, *B. fulgida*, and *B. sinica* (4) *Jettenia* (one species: *J. asiatica*, and (5) *Scalindua* (four species: *S. S. brodae*, *S. sorokinii*, *S. wagneri*, and *S. profundal*) (Kartal et al. 2013). Although 2500, 16S rRNA gene sequences belonging to anammox bacteria have been deposited to the Genbank (http://www.ncbi.nlm.nih.gov/genbank/), only ten anammox species have been described so far, which represent a minute fraction of anammox biodiversity. Hence, it is still challenging for the bacterial taxonomist to culture anammox bacteria in their laboratories.

1.9 Ecology and Physiology of Planctomycetes

In marine habitats, Planctomycetes are sometimes considered as leading players within bacterial community. For example, bacteria associated to the macroalgae *Ecklonia radiata* present on the Australian shore composed of 70% of the Planctomycetes community (Wiegand et al. 2018).

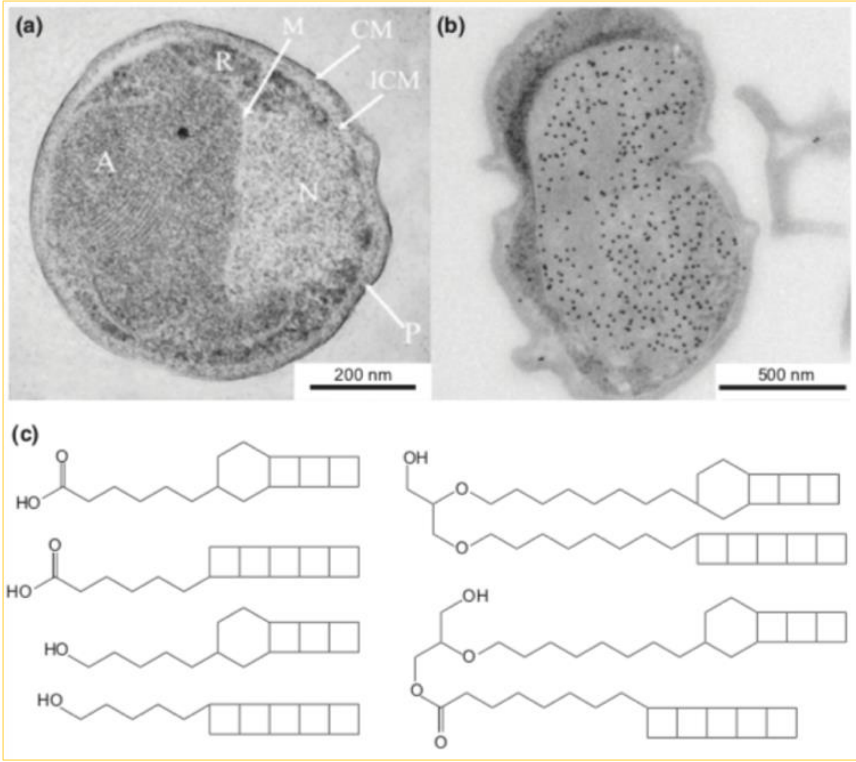

Fig. 1.6 Unique feature of anammox cell. (a) Cell shows anammoxosome (A), (b) anammoxosome having hydroxylamine Oxidoreductase, (c) cell membrane have ladderane lipid (C17-C20), is adopted from Kartal et al. (2013)

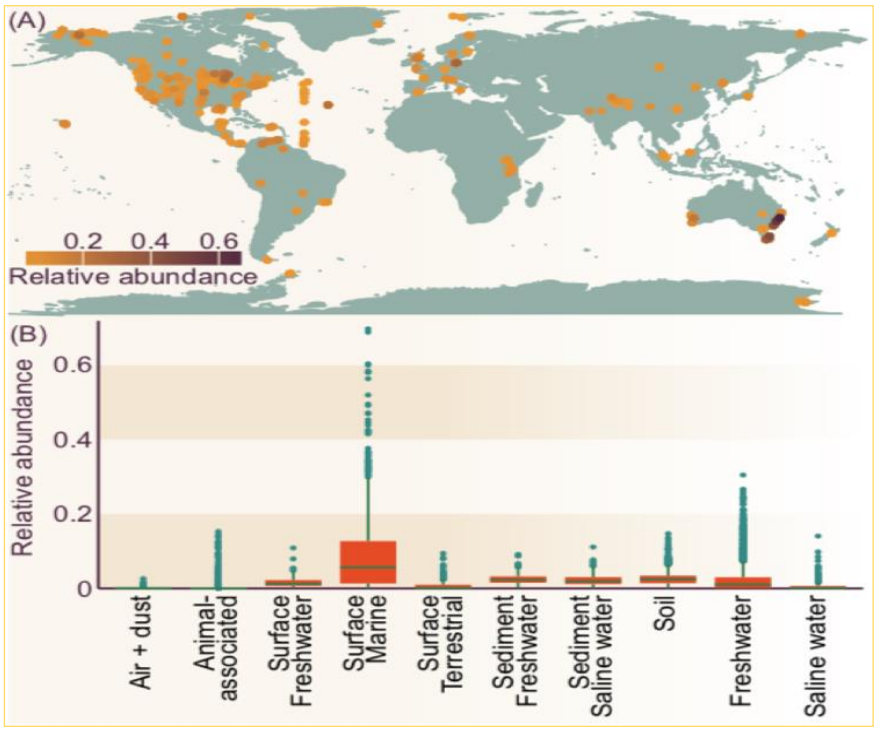

Fig. 1.7 Distribution of Planctomycetes across globe, is adopted from Wiegand et al. 2018

Due to a consonant mismatch in a universally used, 16S rRNA gene specific primer (Zielin´ska et al. 2017), the phylum Planctomycetes has been overlooked in natural communities (Vergin et al. 1998). However, that scenario changed with the recent advent of next-generation sequencing technologies and the usage of new and specific primer sets.

Data analysed from various project like the Earth Microbiome Project database (Gilbert et al. 2014) gave an outline of the current knowledge on the planctomycetal ecology. They mapped the Planctomycetal relative abundance in their respective sampling sites. Metagenomics approach studies revealed that Planctomycetes live primarily in diverse aquatic habitats (Santos-Junior et al. 2017). Planctomycetes consists of 8.2%, 5%, and 2.7% of the total bacterial community in the upper Amazon basin, subseafloor aquifer, and rain-collected groundwater, respectively (Tully et al. 2017a,b; Jongman et al. 2017) (Fig. 1.7).

A significant amount of Planctomycetes are associated with various microbial mats. For examples, Planctomycetes composition in the microbial mats of the hypersaline Laguna Tebenquiche (Chile), an iron-rich thermal spring (South Africa), Little Hot Creek (USA), and black mats collected from the hypersaline lake (Chile) are 21%, 3%, 5%, and 42% of the bacterial community respectively (Fernandez et al. 2016; Selvarajan et al. 2017; Bradley et al. 2017; Farias et al. 2017). It is also reported that 15% of the stromatolite-associated bacteria belong to the phylum Planctomycetes (Proemse et al. 2017). Microbial mats from harsh environments like Antarctic marine and saltpans (pH of 8.0 and salinity of 12.8%) are rich in Planctomycetes; 21% and 12.5%, respectively. Planctomycetes are believed to degrade polymers of the marine snow e.g. sulfated polysaccharides as twenty-one percent of the bacterial communities on marine macroscopic detrital aggregates studied as marine snow can be Planctomycetes (DeLong et al. 1993; Woebken et al. 2007).

In the Great Barrier Reef in Australia, Planctomycetes also account for about 10% of the microbiome associated to calcifying benthic foraminifera *Amphistegina lobifera* (Prazeres et al. 2017). In the coral *Montastraea cavernosa*, Planctomycetes form up to 5% of their microbiome (Jarett et al. 2017). In the shrimp cultural ecosystems, Planctomycetes account for 10.71% of the bacterial community. A significant amount (2.9%) of Planctomycetes were also reported from intestine microbiota of white shrimp (*Litopenaeus vannamei*) (Zeng et al. 2017; Hou et al. 2017) which are also commercially important, and in carp intestine (7.3%) (Li et al. 2014; In the fecal samples of pigs (Leser et al. 2002), wild gorilla (Frey et al. 2006) and soil-feeding termites (*Cubitermes* spp.), In the guts, which are alkaline parts, Planctomycetes constitute about one-fourth of the microbiota (Kohler et al. 2008). Increased in significant amount of Planctomycetes are detected in mice's gut when fed with fungal derived polysaccharides and are absent when fed with a regular die (Xu and Zhang 2015). On the chitin-tube forming worms (*Escarpia* sp.) residing in the deep sea, cold seeps have maximum OTUs (21.1%) belonging to the Planctomycetes (Kellogg et al. 2016). Planctomycetes dominate in the deep-sea sediments of Mexico's gulf (28%) and have an indispensable role in the nitrogen cycle through the disintegration of detrital organic matter delivered to the sediment as marine snow (Vigneron et al. 2017).

Notwithstanding living primarily in the aquatic habitats, Planctomycetes are widespread and significantly abundant in soils worldwide (Buckley et al. 2006). In the mangrove wetlands (5.70%) (Yun et al. 2017), agriculture fields (4.69% or 10.74%) (Niu et al. 2016; She et al. 2016), and in Siberia, lichen-dominated subarctic ecosystems (7.2%–14%) (Danilova et al. 2016; Ivanova et al. 2016), Planctomycetes are well widespread. The abundance of Planctomycetes also varies according to the temporal and spatial variation of the particular ecosystem. For example, if grazed pasture soil was influenced by elevated pCO_2 to simulate climate change in salty and sandy coastal soils in China, Planctomycetes

abundance increased by 50% (Xia et al. 2017). In the arid regions of China, Planctomycetes are abundant (23.7%) and their abundancy decreases along the salinity gradient (9.8%) (Chen et al. 2017a). Hence, these findings clearly correlates with an abundance of Planctomycetes with environmental changes (Bacci et al. 2015). In the rhizosphere of Chinese leek, Planctomycetes account for 7.2% of the bacterial community (Hou 2017). Planctomycetes are well distributed in the moist acidic soil of the tundra region (up to 2.5%; Kim et al. 2016), Fennoscandian boreal forest and in the active layer above permafrost soils (4%; Chen et al. 2017b). From the acidic tundra region and boreal forest, few Planctomycetes were isolated and characterized as well. In the natural temperate forests, Planctomycetes are well associated with decomposing dead wood (Tla´skal et al. 2017). Planctomycetes are more significantly enriched in the rhizosphere collected from an Amazon rainforest as compared to the surrounding soil (Fonseca et al. 2018). As previously discussed, the Planctomycetal abundance might still be overlooked or underestimated as few DNA extraction methods or kits from soil reduce the amount of Planctomycetal sequences and also due to the consistent mismatch in a universally used 16S rRNA gene specific primers. However, in soil Planctomycetes represents the fifth most abundant bacterial phylum (Zielin´ska et al. 2017).

1.10 Planctomycetal diversity associated with sponges

Sponges belong to the phylum Porifera and have more than 8700 formally described and 16,000 estimated species. Sponges are pivotal benthic aquatic animals having significant ecological, biopharmaceutical and commercial importance (Bergquist 1978). Sponges have highly diverse and specific symbiont communities (Mohamed et al. 2010). Due to the filter-feeding activities of sponges, they maintain a constant influx of seawater microorganisms. Approximately 40% of sponge volume comprises sponge-associated microorganisms having densities over 109 CFU. sponge tissue^{-1}, several higher orders than

those typical for seawater (Abdelmohsen et al. 2014). The sponge microbiome consists of all three life domains, i.e., Bacteria, Archaea and Eukarya (single cell). The sponge microbiome plays an essential role in shaping sponge evolution (Hentschel et al. 2012, 2003; Imhoff and Stohr 2003; Taylor et al. 2007).

Sponge symbionts are capable of producing secondary metabolites and provide a chemical defence to the sponge. Sponge symbionts probably contribute to the host's nutrition by involving themselves in various metabolic processes such as photosynthesis, nitrification, nitrogen fixation, and sulfate reduction (Wilkinson 1979; Hoffmann et al. 2006; Hoffmann et al. 2009; Bayer et al. 2008; Mohamed et al. 2010; Weisz et al. 2007). Culture-independent, as well as culture-dependent studies in the past revealed that sponges have diverse microbial populations (Mohamed et al. 2010). Phylogenetic studies have shown that sponges contain more than 30 different bacteria phyla, including the candidate phylum 'Poribacteria' that is almost exclusively found within sponges (Schleifer 2004; Webster et al. 2008; Sipkema et al. 2009). On the basis of microbial abundance sponges are categorised into two types: (1) the high microbial abundance (HMA) sponges and (2) The low microbial abundance (LMA) sponges (Hentschel et al. 2003; Webster et al. 2008; Lafi et al. 2009; Fieseler et al. 2004). The microbial communities in HMA sponges are more diverse than LMA sponges and generally single bacterial clades dominate in LMA sponges (Taylor et al. 2013; Giles et al. 2013). For example, in the sponge *Crambe crambe*, a single Beta-proteobacterium symbiont dominates that particular sponge associated microbial community (Croue et al. 2013). In sponge *Niphates* sp., the phylum Planctomycetes usually dominates (Izumi et al. 2013). In the past decade, various culture-independent studies showed richness of the Planctomycetes diversity associated with marine sponges. Through culture-dependent studies, planctomycetes are also isolated from both marine as well as freshwater sponges. Association of anammox bacteria with sponges

reveals the crucial role of Planctomycetes in the process of denitrification within the sponges (Mohamed et al. 2010). In the past several amplicon based metagenome studies were carried out in several marine sponges. For example, *Carteriospongia foliascens* (collected from the Red Sea coast), *I. strobilina* and *M. laxissima* (Conch Reef, Key Largo, Florida), *Xestospongia muta* (Florida Keys, Atlantic Ocean), *Xestospongia testudinaria*, (Indonesia, Pacific Ocean) where they have shown the domination of Proteobacteria, Firmicutes and Bacteroidetes and Planctomycetes as well (Mohamed et al. 2010). Domination of Planctomycetes among sponges are also supported by the culture based studies of *sponges Niphates* sp. (Moreton Bay) and *Aplysina* sp. (offshore of Banyuls-sur-Mer, France) where several Planctomycetal strains where successfully isolated as axenic strains (Kaboré et al. 2020).

1.11 Planctomycetal diversity associated with Algae

In the marine environment, bacteria frequent colonize on the biotic surfaces through the process of epibiosis (Wahl 2008). Wide range of interactions of prokaryotes with many eukaryotic hosts like bryozoans, sponges, corals, ascidians and microalgae are very recurrent. These host associated bacteria are the potential candidates for the production of new bioactive products (Burke et al. 2011). Since last one decade, microbial biofilms associated with macroalgae or microalgae was extensively studied (Wahl 2008; Goecke et al. 2013), but the understanding of their interactions and ecology is still scanty. Nutritional and protective role of epiphytic bacteria can have positive relations with host macroalgae. Epiphytic bacteria prevent host against biofouling, protection against toxic substances and invasion by pathogens (Kaboré et al. 2020). Bacteria isolated from the macroalgae are capable of mineralization and nitrogen fixation which aids bacteria to provide nutrients and growth factors to the host macroalgae. Nevertheless, bacteria can also induce diseases and decomposition of macroalgae and hence, show noxious effects on

macroalgae (Dimitrieva et al. 2006; Goecke et al. 2013). Various culture dependent and metagenome studies revealed that the dominant bacterial phyla associated to macroalgae are Proteobacteria, Bacteroidetes, Planctomycetes, Firmicutes and Actinobacteria Goecke et al. 2010; Friedrich 2012; Hollants et al. 2013). Variations or specificity in the distributions of bacteria also exists among the various macroalgae species (Lage and Graca 2016). For example, red and brown algae are rich in *Firmicutes*, *Actinobacteria* and *Planctomycetes* while, Alphaproteobacteria and Bacteroidetes are more abundant on green macroalgae (Hollants et al. 2013). Recently lots of planctomycetes were isolated from macroalgae and successfully characterised as new taxa. For example, some genera like *Roseimaritima, Crateriforma* (belong to family *Pirellulaceae)* and *Algisphaera* (Phycisphaeraceae) were reported for taxa isolated from marine macroalgae. Also, fluorescence *in situ* hybridization (FISH) analysis of biofilms present on the kelp *Laminaria hyperborea* divulged that Planctomycetes accounted for 50–53% of all bacteria population. Distribution of Planctomycetes are not only limited to marine macroalgae, but it was well distributed or associated to fresh water macrophytes like *Nuphar lutea* (yellow lily). Hence, this show that Planctomycetes are good candidate of biofilm present on the surface of various macroalgae. In addition to this, genome mining of several *Planctomycetes* genome have unveiled the putatively existence of a high number of sulfatase genes, which assist in the degradation of complex sulphated hetero-polysaccharides (carrageenans and agars) commonly produced by macroalgae (Wegner et al. 2013). This provide conspicuous advantage of *Planctomycetes* living on macroalgal surface.

1.12 Biotechnological aspects of Planctomycetes

The removal of toxic ammonium from wastewater and oceans by anammox bacteria (Strous et al. 1999), is one of the primary applications of Planctomycetes. At the industrial scale, anammox process is well established (Kartal et al. 2010). Consequently, aerobic Planctomycetes are also presupposed to be an untapped 'adroited producers' of bioactive small molecules that might comprise putative novel antimicrobial compounds with a potential therapeutic character such as novel antibiotics (Graca et al. 2016; Jeske et al. 2016). Planctomycetal genome analysis revealed that Planctomycetal genomes encode up to 15 biosynthetic gene clusters (BGCs). The recognised BGCs are significant in producing various polyketides, non-ribosomal peptides, terpenes, bacteriocins, ectoine, ladderanes, and others. The polyketide synthases (PKS) or non-ribosomal peptide synthases (NRPSs) are known to produce various bioactive secondary metabolites like antibiotics. Gene clusters encoding putative PKSs vary among the members of Planctomycetes. Among the members of Planctomycetes, the *Pirellulaceae* and Isosphaeraceae clades encode maximum PKS (three to seven). The NRPSs abundance is lower than the PKSs, and is limited to the *Bythopirellula* and *Pirellula* clades and reaches up to five in '*Rosistilla oblonga*' CA51^{T} (Fig. 1.8).The BGCs encoding bacteriocin and ectoine dominate in the *Gimesia* clade and narrowly present in the *Bythopirellula* and *Pirellula* clades. Thus, BGCs are not evenly distributed among the Planctomycetes members (Fig. 1.8). All planctomycetal clades show a difference in the production of small bioactive molecules. Fewer BGCs are present in the members of 'Saltatorellus', 'Brocadiaceae', Phycisphaerae clades than other Planctomycetal strains. In-depth, genome analysis showed that most of the putative Planctomycetal BGCs are unique and are different from the known BGCs of other bacteria.

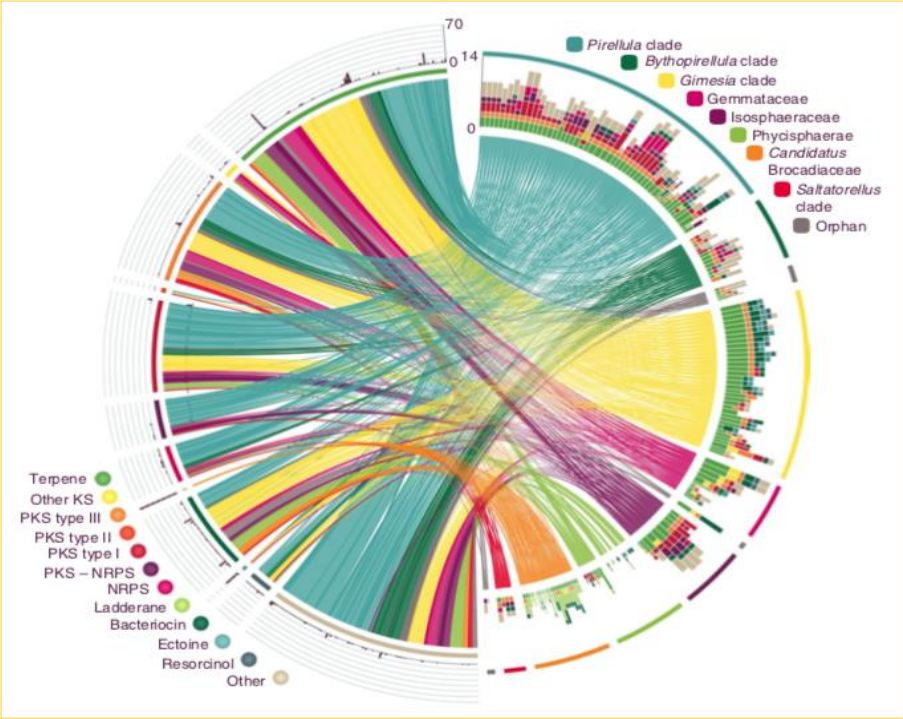

Fig. 1.8 Planctomycetal secondary metabolite BGCs, is adopted from Wiegand et al. (2020)

Hence, Planctomycetal BGCs are indicated as an untapped metabolic potential (Fig. 1.8). However, the presence of BGCs among Planctomycetes members depends extensively on their lifestyle either in term of environmental conditions or in term of competing with other bacteria. Actinobacteria and Myxobacteria are the most talented producers. They contain more BGCs (up to 40 BGCs) compared to Planctomycetes (up to 15 BGCs). However, these findings could be misleading as genome-mining algorithms that were employed are mainly optimised on well-described BGCs, Actinobacteria, and Myxobacteria. Hence, there are high probability of missing Planctomycetal BGCs. The presence of 'giant genes' in the large genomes of Planctomycetes makes them suitable candidates for the production of novel and yet unknown antibiotics biosynthetic pathways.

Planctomycetes' role were also observed for the polyhydroxyalkanoate production in dark fermented paperboard mills in the presence of acetate. As in the enrichment, 7.46% of the bacterial community is the Planctomycetes only (Farghaly et al. 2016). Planctomycetes might also have an essential role in facilitating halotolerant organisms for

the bauxite and uranium remediation where their abundance is about 14% of total bacterial community (Bray et al. 2017; Akob et al. 2007). In arsenic-contaminated sediments and herbicide degradation bacterial enrichment, Planctomycetes accounted for almost up to 10% of the bacterial community (Caracciolo et al. 2005; Halter et al. 2011). However, further investigations on large as well as diverse sample sizes are necessary to confirm possible roles of Planctomycetes members in the process of bio-remediation. Planctomycetes are also reported as useful candidate for the production biotechnologically potential enzymes like sulfatases for industrial chemistry and demonstrated as well (Wallner et al. 2005).

1.13 Objectives

(1) To catalogue planctomycetes of different habitats using amplicon-based metagenome study.

(2) Phylo-taxogenomic including polyphasic taxonomic studies of newly isolated strains of Planctomycetes.

Materials and methods

2. Materials and methods

2.1 Glasswares

Borosil and Anumbra make glassware's were used include Petri plates, Erlenmeyer flasks, measuring cylinders, round bottom flasks, screw cap test tubes, 15 x 150 mm rimless test tubes, serum vials, Durham tubes, etc.

2.2 Cleaning

'Teepol' was used to clean all plasticware's and glassware's. Prior to cleaning, these plasticware's and glassware's were soaked in the chromic acid solution for four hours. It were then cleaned, washed and rinsed with tap water.

2.3 Distilled water, double distilled water, and Milli-Q water

Media and buffer solutions were prepared routinely by distilled water. For TLC, Milli-Q water was obtained from the MilliQ plant facility at the School of chemistry and School of Life sciences, University of Hyderabad.

2.4 Chemicals and solvents

All the analytical grade chemicals, solvents were procured from Merck, Genetix, Sigma-Aldrich, and HiMedia, and were used in this study.

2.5 Gases used

Ultra-pure carbon dioxide and argon gases were used in the study and supplied by Goyal gasses Pvt. Ltd., Hyderabad

2.6 Determination of pH

pH strips (HiMedia make) and digital pH meter (Digisun Electronics DI-707) was used for checking the pH of the buffer and growth medium.

2.7 Sterilization

Sterilization of glassware's, plasticware's , buffers and growth media were done by autoclaving (heat-tolerant materials) manufactured by LTE scientific. Filter sterilization for heat-labile compounds like antibiotics, glucose, and NAG solution using a 0.2 µm acrodisc syringe filter manufactured by Pall's Life Sciences and Millex.

2.8 Samples collection

Samples for the study of diversity and isolation of Planctomycetes were collected from India's diverse geographical locations for three years. Sampling was done across the coastal regions of India for the search of Planctomycetes. The salinity, pH, and temperature of sampling sites were measured through conductivity meter, pH meter, and thermometer. Along the coastal region, we mainly collected sediments, specimens of macroalgae, seaweeds, and sponges specimens present on-shore at the time of sampling. A total of 380 samples were collected from India's western coastal region, including Gujarat and Kerala. Approximately, 520 samples were collected from the eastern coast of India, Tamil Nadu. Some 50 samples were also collected from a different region of Chilika lagoon, Odisha. Four hundred samples, including freshwater lake sediments and Lichens, algae, sponges, were also collected from different regions of Telangana, Andhra Pradesh, Karnataka, Maharashtra, Chhattisgarh, Jharkhand, West Bengal, Bihar, Odisha, Sikkim, and Manipur. All the samples were inoculated on-site in 2 ml microcentrifuge tubes having planctomycetes and Anammox bacteria-specific media. The same time specimens and sediments were also preserved in formalin for the metagenome based study (Annexure 1a,b,c,d,e). These samples were further incubated in the enrichments medium at 25 °C for 1-6 months in the laboratory for the culture based studies.

2.9 Enrichment and isolation of Planctomycetes members

2.9.1 The three steps enrichment strategy for anammox bacteria

All collected samples were inoculated on-site in 2 ml microcentrifuge (Eppendorf) tubes along with a Durham tube containing oligotrophic anammox bacterial mineral salts medium (Egli et al. 1997) (Table. 2.1, 2.1.1, 2.1.2). On-site inoculation of the samples minimises the loss of Planctomycetes including anammox bacteria.The inoculated microcentrifuge tubes were sealed with para-film. After 30 days of anaerobic/anoxic incubation, enrichment cultures were transferred into 15 x 150 mm rimless test tubes containing 5 ml of anammox medium and Durham tubes. Rimless tubes were tightly closed by suba-seals. Anaerobic conditions were maintained by flushing with ultra-pure argon gas and incubated at room temperature for 45 days. One ml of culture from these test tubes were drawn and inoculated into serum vials (20 ml) containing 15 ml of anammox medium pre-flushed with ultra-pure argon gas to maintain anaerobic condition (Fig.2.1).

Table. 2.1 Anammox bacteria media composition (Modified):-

Media composition	**Amount (mM)**
$NaNO_2$	06
$KHCO_3$	25
$(NH_4)_2SO_4$	03
K_2HPO_4	01
$CaCl_2.5H_20$	0.5
$MgCl_2.7H_20$	0.5
Trace element solution 1	2 ml per litre
Trace element solution 2	1 ml per litre
Distilled water	1 litre

Table. 2.1.1 Trace element solution 1 composition:-

Composition	**Amount (g.l-1)**
$Na_2EDTA \cdot 2H_2O$	10
$FeSO_4.7H_2O$	05
MilliQ water	1 litre

Table. 2.1.2 Trace element solution 2 composition:-

Composition	**Amount (g.l-1)**
$Na_2EDTA \cdot 2H_2O$	15
$ZnSO_4 \cdot 7H_2O$	0.43
$CoCl_2 \cdot 6H_2O$	0.24
$MnCl_2 \cdot 4H_2O$	1.0
$CuSO_4 \cdot 5H_2O$	0.25
$NaMoO_4 \cdot 2H_2O$	0.22
$NiCl_2 \cdot 6H2O$	0.20
Na_2SeO_3	0.08
H_3BO_4	0.02
Distilled water	1 litre

Note:- $KHCO_3$ is flushed or saturated with ultra-pure CO_2 gas for 5 minutes prior to autoclave,. It was autoclaved in a bottle with tightly closed lid and is added separately after the autoclave. Trace element solution 1 and 2 are filter sterilised in serum vial and are added to the media after autoclave. Trace element solution 1 and 2 can be store for one year at 4 °C.

2.9.2 The enrichment strategies for Planctomycetes.

For the enrichments and purifications of planctomycetes, several growth media were used. The media optimized according to the environmental condition (pH, salinity, and temperature) of that particular samples. Generally, two growth media was used for the marine samples of the various coastal regions of India (M30 modified media and MN media). For fresh water samples of the Loktak lake and wetland samples of Kerala, MYM

media were used. Based on the sources, 200 mg of samples were inoculated into serum vials (20 ml) containing 10 ml of medium (M30 media and MN media for marine samples; MYM media for freshwater and wetland samples). To maintain aerobic conditions, serum vials were not flushed with argon gas. For the enrichments of Planctomycetes, samples were incubated at 25 °C for the periods of 1-4 months.

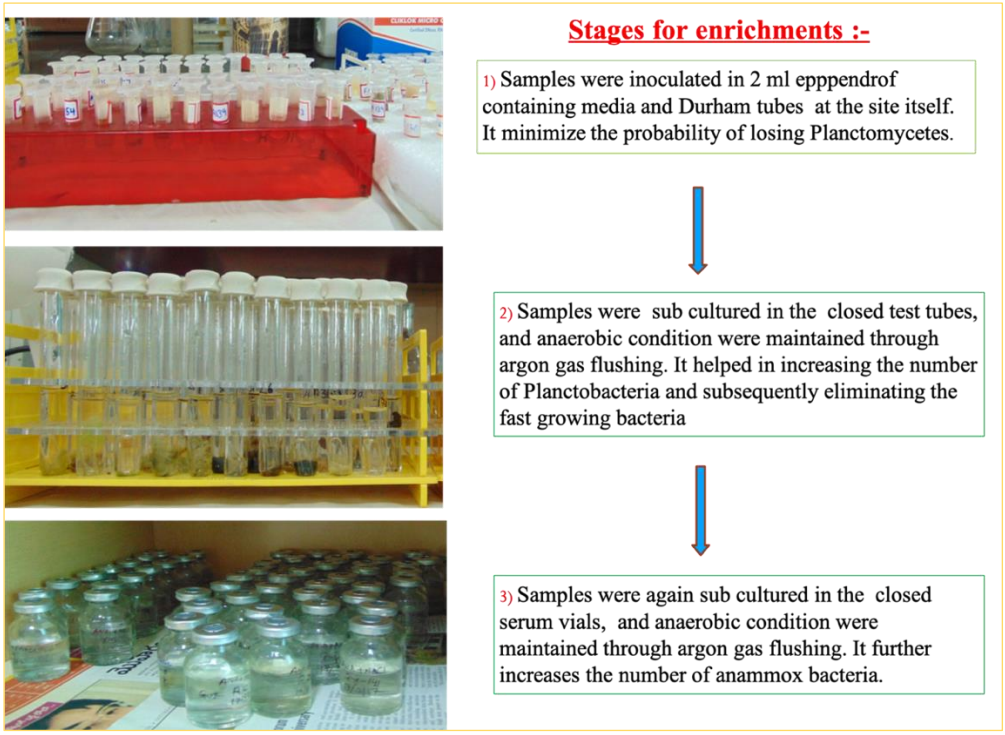

Fig. 2.1 Three steps enrichments of Planctomycetes including anammox bacteria.

Table 2.2 M30 Modified media Composition (Staley et al. 1992):-

Media Composition	**Amount/Litre**
Hutner's basal salts	20 ml
10M Tris-HCl (pH 8)	5.0 ml
$MgCl_2.7H_2O$	1.0 gm
Agar (Sigma make)	20.0 gm
N-Acetyl glucosamine (NAG)	1.0 gm
$Na_2HPO_4.2H_2O$	100 mg
Vitamin's Solution	10.0 ml
Artificial sea water	970.0 ml

Note:- Filter-sterilized vitamin's Solution, $Na_2HPO_4.2H_2O$, and NAG are added to the media after autoclaved and use pH strips to adjust the pH of media to 8.0, with pre-autoclaved 1M HCl or 5M NaOH.

Table 2.2.1 Composition of the artificial sea water (ASW):-

Composition	gm/litre
NaCl	24
Na_2SO_4	4.0
$MgCl_2.6H_2O$	5.0
$CaCl_2.2H_2O$	1.1
$NaHCO_3$	0.2
KCl	0.7
KBr	0.1
H_3BO_3	0.03
$SrCl_2$	0.03
NaF	0.03
Distilled Water	1 litre

Table 2.2.2 Metal 44 components: -

Components	Amount/Litre
Na-EDTA	250.0 mg
$ZnSO_4 \times 7H_2O$	1095.0 mg
$FeSO_4 \times 7H_2O$	500.0 mg
$MnSO_4 \times H_2O$	154.0 mg
$CuSO_4 \times 5H_2O$	39.2 mg
$Co(NO_3)_{2-} \times 6H_2O$	24.8 mg
$Na2B4O_7 \times 10H_2O$	17.7 mg
Autoclaved distilled water	1000 ml

Note:- Dissolve Na-EDTA and add a few drops of concentrated H_2SO_4 to retard precipitation of the heavy metal ions. Filter sterilize METAL 44 and can be store for three months at 4 °C.

Table 2.2.3 Hutner's Basal salts compositions: -

Components	**Amount/Litre**
Nitrilotriacetic acid (NTA)	10.0 gm
$MgSO_4$ x 7 H_2O	29.7 gm
$CaCl_2$ x 2 H_2O	3.335 gm
$(NH_4)_6MoO_7O_{24}$ x $4H_2O$	9.250 mg
$FeSO_4$ x $7H_2O$	99.0 mg
"Metals 44" (see above)	50 ml
Autoclaved distilled water	950 ml

Note:- Nitrilotriacetic acid (NTA) was dissolved in distilled water and pH was adjusted to 7.0 with KOH (about 7.3 gm/litre). Other salts were then dissolved separately. It can be store at 4 °C until it precipitated.

Table 2.2.4 Vitamin solution compositions: -

Vitamin solution	**Amount/Litre**
Vitamin solution	0.2 mg
Thiamine-HCl x$2H_2O$	10.0 mg
Folic acid	1 mg
Ca-pantothenate	10 mg
Biotin	4.0 mg
Riboflavin	10 mg
Nicotinamide	10 mg
p-Aminobenzoic acid	10 mg
Pyridoxine hydrochloride	10 mg
Autoclaved distilled water	1000 ml

Note: Filter sterilize vitamin solution and can be store for one year at 4 °C

Table 2.3 MN Media Composition (Wiegand et al. 2020):-

Media Composition	**Amount/Litre**
Hutner's basal salts	20 ml
10M Tris-HCl (pH 8)	5.0 ml
Glucose	0.25 gm
Peptone	0.25 gm
Yeast extract	0.25 gm
Agar (Sigma make)	20.0 gm
N-Acetyl glucosamine (NAG)	1.0 gm
Vitamin's Solution	10.0 ml
Artificial sea water	970.0 ml

Table 2.4 MYM media compositions (Kaushik et al. 2020):-

Media Composition	**Amount/Litre**
Hutner's basal salts	20 ml
Yeast extract	0.1gm
$(NH4)_2SO4$	0.5gm
Glucose	2.0 gm
NAG	1.0 gm
Vitamin's Solution	10.0 ml
Distilled water	970.0 ml
Agar	20.0 gm (2%)

2.10 Fluorescence in situ hybridization (FISH)

To corroborate the presence of Planctomycetes including anammox bacteria in the anaerobically and aerobically enriched samples, fluorescence in situ hybridization was performed for different enriched samples, according to Parsley et al. 2010, with slight modifications. Samples were pre-treated with TritonX100 (0.04%) for 30 minutes at 37°C. FISH was performed using CY3 labelled Planctomycetes bacteria-specific probes, Pla46 (5'-GACTTGCATGCCTAATCC-3') (Parsley et al. 2010) supplied by BIOMERS, Germany. Probe concentration was 6ng.µl-1used for the hybridization at 58°C for overnight (Schmid et al. 2005). Samples were washed with SSC buffer (0.2X) and observed under a confocal microscope (Carl Zeiss LSM880).

2.11 Purification of Planctomycetes

After enrichments for 1-4 months, aerobic enriched samples given complimentary for FISH were taken and spread individually on the Petri plate containing their respective solid media having agar (2%). Petri-plates were incubated at 23 °C to 25 °C, and after every three days, all plates were screened for the growth of pinkish colonies. After 15-30 days of incubation, pink colonies were started emerging, and it continued until three months. All the pink colonies were purified further on the Petri plate containing their respective solid media having agar (2%). Simultaneously, some shiny and white colonies were also purified for the search non pigmented Planctomycetal colonies.

2.12 Maintenance of the cultures:-

All Planctomycetes are known for their fastidious nature. Thus, all the isolated strains of Planctomycetes were maintained on their respective media agar plate by repeated sub-culturing at the regular intervals of two months.

2.13.2 Microscopic observation

Morphological characters like cell shape, cell size, and cell division were observed using phase contrast microscope at JNTUH, Hyderabad (Olympus- B201).

2.13.3 Field emission scanning electron microscopy (FESEM)

One ml of log-phase culture was centrifuged at 7000g for 10 min at 04 °C. The resulted cell pellet was washed by suspending in autoclaved MilliQ and centrifuged at 7000g for 10 min at 04 °C. The pellet or cells were fixed in 2.5% glutaraldehyde solution and kept for six hours incubation at 4 °C. cells were dehydrated sequentially with an increased ethanol concentration from 10- 100% (20% interval). At last, the cells were resuspended in 100% ethanol. Ten µl of samples were kept on the small size glass slide, which is placed on the stab with adhesive tape. Finally, stabs kept for gold sputtering for six minutes and then cells morphology and division were viewed under the FESEM (Philips XL3O) facility of school of Physics, UOH.

2.13.4 Negative staining for Transmission Electron Microscopy (TEM)

Planctomycetal cells were negatively stained by 2% uranyl acetate and staining procedure is according to Kumar et al. 2020. The grids were visualized under TEM microscopy (H-7500 Hitachi) facility of CCMB, Hyderabad.

2.13.5 Transmission electron micrograph sections for ICM structures

Ultrathin sectioning of the log phase Planctomycetal cells were outsourced at RUSKA Diagnostic, Hyderabad and is processed according to Kumar et al. 2020. The sections of the Planctomycetal cells were mounted on copper grids and observed under TEM (H-7500 Hitachi) facility of CCMB, Hyderabad.

2.14 Biochemical characterisation

2.14.1 Oxidase and catalase test

one loopful of Planctomycetal culture (log-phase) was put onto a glass slide (HiMedia), and culture/pellet was treated with three to four drops of 3% H_2O_2. Bubble formation show positive result for the catalase otherwise negative. Oxidase disc (HiMedia) was used for the oxidase test according to the instructions of the manufacturer.

2.14.2 Organic carbon substrate utilization tests

Various organic carbon substrates were used to test its utilisation by the various isolated Planctomycetal strains like, ethanol, fumarate, glycerol, lactate, malate, succinate, sucrose, D-glucose, D-rhamnose, fructose, acetate, ascorbate, cysteine, , tartrate, lactose, glutamate, D-sorbitol, D-galactose, D-cellobiose, D-mannose, D-mannitol) utilization were tested by on liquid basal medium. For the marine isolates, organic carbon substrates utilization by the strain was determined on M30 modified liquid basal medium by replacing N-acetylglucosamine (NAG) with $(NH_4)_2SO_4$ (0.1% w/v) as the nitrogen source in modified M30 media and different organic carbon substrates were used at a concentration of 0.1% (w/v). Similarly, for the fresh water isolates of the Loktak lake liquid basal medium was used for various organic carbon substrates utilisation by the strain as described by Bondoso et al. (2011) with slight modifications. Organic substrates Medium was supplemented with 0.05% w/v yeast extract. For organic carbon substrate utilisation, $(NH_4)_2SO_4$ (0.1% w/v) was used as a sole nitrogen source and cell growth was tested on different organic carbon substrates at a concentration of 0.1% (w/v).

2.14.3 Utilisation of various nitrogen sources

Diiferent nitrogen substrates were used to test its utilisation by the various isolated Planctomycetal strains like L-methionine, DL-ornithine, D-valine, L-proline, L-phenylalanine, DL-threonine, Peptone, D-alanine, L-arginine, L-glycine, L-histidine, L-

leucine, L-glutamine, L-isoleucine, NAG, yeast extract, casamino acid, L-serine, L-lysine, L-glutamic acid, L-tryptophan, L-glycine, L-aspartic acid, L-tyrosine, cysteine) utilization were tested on the liquid basal medium. For the marine isolates, nitrogen substrates utilization by the strain was determined on M30 modified liquid basal medium by replacing N-acetylglucosamine (NAG) with D-glucose (0.1% w/v) as the organic source and different nitrogen substrates were used at a concentration of 0.1% (w/v). Similarly, for various nitrogen substrates utilisation for the fresh water Planctomycetal isolate of the Loktak lake, liquid basal medium was used as described by Bondoso et al. (2011) with slight modifications. Liquid basal medium was supplemented with 0.05% w/v yeast extract. For different nitrogen substrates utilisation, D-glucose (0.1% w/v) was used as a sole organic carbon source and cell growth was tested on different nitrogen substrates at a concentration of 0.1% (w/v).

2.14.4 Vitamin B_{12} requirement

Planctomycetal colonies were inoculated in their respective liquid basal media supplemented with sole filter-sterilized vitamin B_{12} solutions (0.22 µm Acrodisc syringe filter, Pall make). For determining the absolute requirement of vitamin B_{12}, the Planctomycetal cells were repeatedly grown in a basal liquid medium without vitamin B_{12} (0.02 mM), and contained glucose (0.1% w/v) and ammonium sulphate (0.1% w/v) as carbon and nitrogen sources, respectively.

2.14.5 NaCl requirement for optimum growth

NaCl tolerance (0-7% w/v; final salt concentration in the media) for the isolated planctomycetal strains were tested at 25 °C and pH 7.

2.14.6 Temperatures for optimum growth

The Planctomycetal cultures in their respective growth media were incubated at various temperatures (05, 10, 15, 20, 25, 30, 35, and 40 °C) and growth was observed.

2.14.7 pH for optimum growth

pH range (4.0, 5.0, 6.0, 7.0, 8.0, 9.0, 10.0) for growth of all Planctomycetal strains were tested at 25 °C in buffered (Bondoso et al. 2015) liquid growth medium and confirmed by repeated sub-culturing.

2.15 Chemotaxonomic characterisation

2.15.1 Cellular fatty acid composition

For fatty acid analysis, healthy growing cells were harvested by centrifugation (10,000 g for 15 min at 4 ºC) at a cell density of 70% of the maximum optical density (100% = 0.9 OD_{660}). Cellular fatty acids were methylated, separated and identified according to the instructions of the Microbial Identification System (Microbial ID; MIDI 6.0 version; method, RTSBA6) (Sasser 1990), which was carried out by Royal Research Labs, Secunderabad, India.

2.15.2 Polar lipid extraction and identification

Five ml of 0.3% NaCl was used to dissolve the 0.5-1.0 grams of lyophilized Planctomycetal cultures, and pellets were dissolved in 8-10 ml of methanol and vortexed for 5 min. Once the pellets are dissolved then the cell membranes were disrupted by boiling it till whole methanol gets evaporated. 10 ml of chloroform was added and then vortexed for 10 minutes. Then 5 ml of 0.3% NaCl was added and centrifuged for 10 minutes at 08 °C, which resulted in the formation of two layers of chloroform at the bottom and water layer at top. Whole bottom layer of chloroform was transferred into a round bottom flask. This step is repeated again by adding 5-10 ml of chloroform in the centrifuge tube and was then centrifuged for 10 minutes at 08 °C. Bottom layer of chloroform was again transferred into the same round bottom flask and chloroform is evaporated using the flash evaporator (ROTAVAC). The extract is now dissolved in 0.5-1.0 ml of the solution of chloroform and

methanol in a 2:1 ratio, from which 10-20 µl was spotted on to the left corner of the silica gel TLC plate (7x7 cm in size):

Solvent system for the first dimension:

Chloroform: methanol: water (30:12:1.5).

Solvent system for the second dimension:

Chloroform: methanol: glacial acetic acid: water (35:7:6:1).

TLC is then dipped for 20 seconds into 4% ethanolic molybdophosphoric acid and whole extracted polar lipids were visualised by drying TLC using a hot air blower.

Ninhydrin reagent

0.1% (w/v) of ninhydrin dissolved in ethanol was sprayed onto the TLC plate it was dried using a hot air gun to visualize amino lipid. Spots on the TLC plates corresponding to amino lipid give pink colour.

Dragendorff's reagent

Dragendorff's reagent was procured from Sigma, Merck. This reagent was used to visualise choline containing lipid which give yellow colour spot on treatment.

Molybdenum blue reagent

Molybdenum blue reagent was procured from Sigma, Merck. This reagent was used to visualise all phosphate containing lipid which give blue colour spot.

Glycolipids identification

The visualization of glycolipids on TLC plate was done by spraying solvents containing 3.2% (w/v) alpha-naphthol dissolved in methanol, H_2SO_4, and H_2O (25:3:1.5, vol/vol/vol). Pink/purple colour spot develop after heating the plate using a hot air gun.

2.15.3 Quinone extraction and identification

Quinones were extracted with a chloroform/methanol (2:1, v/v) mixture, purified by TLC and analysed by HPLC (Imhoff 1984).

2.15.4 Polyamine extraction and Identification

Polyamines were extracted according to Dion and Herbst (1970). Logarithmic cultures of both strains were harvested by centrifuging the culture for 10 minutes at 4°C. The pellet was washed thrice with 50 mM phosphate buffer (pH 7.5). It was further resuspended in 0.2M perchloric acid and disrupted by sonication. The cell lysate was neutralized with $NaHCO_3$ (1 M) and centrifuged (10 minutes at 4°C). Polyamines of the supernatant were derivatized with dansyl chloride (3 mg ml-1) (Dion and Herbst 1970), and the unbound dansyl chloride was removed by adding proline (50 mM). Polyamines were extracted by toluene for thrice, separated and evaporated in a flash rotatory evaporator, and finally dissolved in HPLC grade methanol. Polyamine (Sigma Aldrich) standards were also derivatized with dansyl chloride and finally suspended in HPLC grade methanol. Polyamines were analysed using HPLC (Shimadzu) with Photo Diode Array (PDA) detector, C-18 Luna (5µm, 250 X 4.6 mm) column. A linear gradient method was used to separate polyamines. 1% (v/v) acetic acid in water (solvents A) and acetonitrile: methanol:: 4: 1 (solvent B) was used as a mobile phase with a 0.8 ml min-1 flow rate. Polyamines were confirmed by their retention time, peak absorption spectra of standards, and spiking using internal standards.

2.16 DNA isolation, PCR, 16S rRNA gene sequencing and BLAST analysis

DNA was isolated from the pure cultures using a commercial DNA isolation kit (Nucleo-pore gDNA Fungal Bacterial Mini Kit, from M/s. Genetix Biotech Asia Pvt. Ltd, India) which was used for PCR amplification and genome sequencing. PCR was performed for 16S rRNA gene amplification using planctomycetes specific primers F40 and R1388. Purified PCR products were sent to AgriGenome Pvt. Ltd. (Kochi, India) for 16S rRNA gene sequencing. Sequence was used for identification using BLAST search analysis on EzBioCloud database (Yoon et al. 2017).

Primers sequences are as follows:

S No	Primer	Name	Sequence 5'to 3'
1	Forward	F8	5´- AGAGTTTGATCCTGGCTCAG -3´
2	Forward	F27	5´- GTTTGATCCTGGCTCAG- 3´
3	Reverse	R1492	5´-GGTTACCTTGTTACGACT-3´
4	Reverse	R1525	5´-AGAAAGGAGGTGATCCAGCC-3´

For PCR amplification TAKARA master mix (EmeraldAmp® GT PCR Master Mix) was used instead of individual components. PCR Reaction mixture prepared as follows;

Component	**Volume (µl)**
Milli-Q water	16
MasterMix	25
Forward Primer	2
Reverse Primer	2
Template DNA (from denatured colony, 50 µl)	5

PCR conditions for 16S rRNA gene amplification were as follows;

S No	Step	Temp (°C)	Time
1.	Initial denaturation	94	10 minutes
2.	Denaturation	94	1 minute
3.	Annealing	54	54 second
4.	Elongation	72	1.5 minutes
	Number of cycles: 32		
5.	Final elongation	72	15 minutes in last cycle

1.0% agarose gel was prepared in the TAE buffer to run the amplified product along with the DNA marker at 80 voltage for 40 min. Ethidium bromide staining was used for visualization, and the amplified products were observed using the BIO-RAD gel documentation system. Desired amplified products were outsourced to Agrigenome Labs Pvt. Ltd. for sequencing where the 16S rRNA gene sequencing was carried out in an ABI 3730 XL DNA Analyzer automatic sequencer using the BigDye1 Terminator v.3.1 Cycle Sequencing Kit. The sequences obtained from different primers were assembled using

DNA Lasergene SeqMan Pro software. The assembled sequence similarity with existing bacteria was found by BLAST search using the EzBioCloud database (Yoon et al. 2017). For multiple sequence alignment, MUSCLE (https://www.ebi.ac.uk/Tools/msa/muscle/), for pairwise sequence alignment LALIGN algorithms (https://www.ebi.ac.uk/Tools/psa/lalign/) was used.

2.16.1 Phylogenetic analysis

The 16S rRNA gene sequences of the Planctomycetal strains obtained by amplicon based sequencing and sequences extracted from their respective genomes using ContEst16S (https://www.ezbiocloud.net/tools/contest16s) were analysed for the closest identity using BLAST search of NCBI and EzBioCloud database as well (Johnson et al. 2008). The 16S rRNA gene sequences of strains and other closest members belonging to the Phylum Planctomycetes (obtained from NCBI) were aligned using the MUSCLE implemented in MEGA7.0 (Kumar et al. 2016) and the distances were calculated using Kimura 2-parameter (Kimura 1980) in a pairwise deletion procedure. Neighbor-joining (NJ) (Saitou and Nei 1987), minimum evolution (ME) (Rzhetsky and Nei 1992) and maximum likelihood (ML) (Yang 1997) methods in the MEGA7 software were used to construct phylogenetic trees having bootstraps of 1000 replication (Felsenstein 1985).

2.16.2 Digital/ In-silico DNA-DNA hybridization (dDDH)

dDDH replaces the error-prone conventional DNA-DNA hybridization. dDDH estimate among strains were calculated based on the genome sequences using the Genome-to-Genome Distance Calculator (GGDC 2.1; http://ggdc.dsmz.de/distcalc2.php; Meier-Kolthoff et al. 2014).

2.16.3 Orthologous Average Nucleotide Identity (OrthoANIu)

OrthoANI score was calculated from the Planctomycetal genome sequences using online service in the EzBioCloud (https://www.ezbiocloud.net/tools/ani) (Yoon et al. 2017).

2.16.4 Average Amino acid Identity (AAI) and Percentage Of Conserved Proteins (POCP)

Average Amino Acid Identity (AAI) was calculated using AAI calculator developed by Kostas lab (Rodriguez and Konstantinidis 2014). Percentage of Conserved Protein (POCP) was calculated as described by Qin et al. (2014).

2.16.5 Construction of phylogenomic tree using UBCG (Up-to-date bacterial core gene) pipeline

The phylogenomic tree was also constructed using 92 core genes from all the publicly available genomes of both Planctomycetaceae and Pirellulaceae families. These 92 core genes were retrieved using the Up-to-date Bacterial Core Gene (UBCG) tool (Na et al. 2018). A concatenated sequence of 92 genes was used to construct the RAxML based phylogenomic tree. The tree was generated with random samples of 50% of homology groups used for the main tree, in a process known as gene-wise jackknifing. Hundreds of these 50% gene-wise jackknife trees were made using RAxML and the support values at the nodes indicate the number of times a particular branch was observed in the support tree (Fig. 2.2).

2.16.6 Genomic information and in-silico metabolic characterisation

Whole-genome sequencing (WGS) was carried out using Illumina HiseqX10 platform and paired-end library were generated with sequence coverage of 100x.WGS job was outsourced to AgriGenome Pvt. Ltd, Kochi, India. De novo assembly was performed using Unicycler (Wick et al. 2017) assembly software. Unicycler assembly was used for all further downstream analysis. The genome sequence was checked for any possible contamination using ContEst service of EZBiocloud (Yoon et al. 2017) which yielded the 16S rRNA sequence of only one organism indicating the WGS was free from sequences of other organisms. The genome was further annotated using online freely available RAST server (http://rast.theseed.org/FIG/rast.cgi) (Aziz et al. 2008).

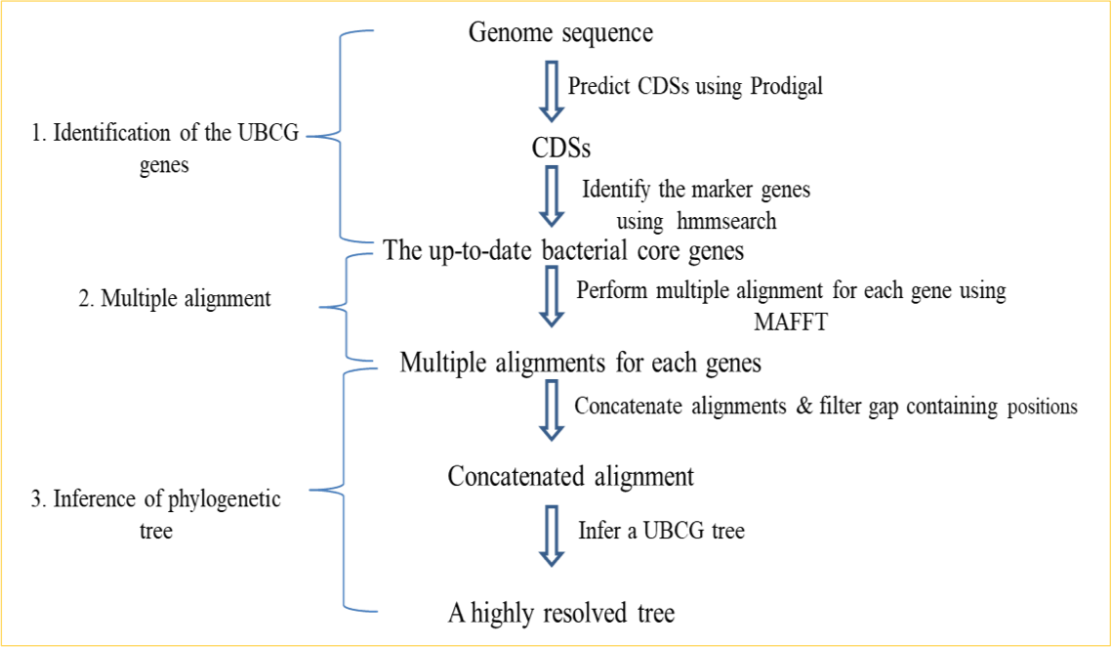

Fig. 2.2 The flowchart of phylogenetic tree reconstruction using the UBCG pipeline is adopted from Na et al. 2018.

In-silico metabolic characterization was carried out based on its genome information through online tool PATRIC 3.6.2 (https://www.patricbrc.org/) (Wattam et al. 2017). In- silico identification for the presence of putative genetic clusters responsible for the biosynthesis of secondary metabolites was carried out using online freely available tool antiSMASH5.1 (http://antismash.secondarymetabolites.org) (Blin et al. 2019).

2.17 Amplicon based metagenome analysis

2.17.1 Extraction of metagenomic DNA from sponge/Algal samples

300 mg of sponge/Algal specimens preserved in formalin were macerated in liquid nitrogen with the help of mortar and pestle. Metagenomic DNA was extracted from the macerated sponge specimens using MO BIOs' Power Soil DNA Isolation kit (QIAGEN make) and processed according to the kit's protocols with few modifications. For the lysis of sponge/Algal tissues, vortex was subjected for longer period of 40 minutes. Extracted DNA was analyzed using 1% (w/v) agarose gel electrophoresis and was visualized with a UV transilluminator after staining with 0.5 g ml-1 of ethidium bromide. Extracted DNA

was quantified using Qubit fluorometer and Nanodrop according to the manufacturer's instructions. The extracted DNA was stored at -20°C until further analysis.

2.17.2 16s rRNA amplicon-based Illumina Library preparation

The microbial community structure was investigated using 16S rRNA amplicon sequencing analysis to unveil bacterial species' dwellings. DNA samples were sent for Illumina Mi-Seq (2x300 bp) sequencing to Research and Testing Laboratory (RTL) LLC (Lubbock, TX, USA) and M/S Eurofin, Bangalore, India. The samples underwent 16S rRNA gene amplification for V3-V4 regions using universal primers Pro341F (5′-TACGGGNBGCASCAG-3′), and Pro805R (5′-GACTACNVGGGTATCTAATCC-3′).

2.17.3 DNA processing and assessment of taxonomic diversity

The raw sequence reads obtained after Illumina paired-end sequencing was processed using mothur software (Schloss 2009). The two sets of data from each sample were joined to form contigs and further processed to reduce the sequencing and PCR errors. Sequences shorter than 350 nucleotides with homopolymers longer than eight nucleotides and all reads containing ambiguous base calls or incorrect primer sequences were removed (Kozich et al. 2013). The improved sequences were further processed to remove redundant sequences. Next, the processed sequences were aligned against the SILVA v 132 database (Pruesse et al. 2007) (http://www.mothur.org/wiki/Alignment_database). Putative chimeric sequences were detected and removed via Chimera Uchime, an integrated algorithm in mothur (Edgar et al. 2011). All taxonomic classification was performed using the Bayesian classifier (Qiong et al. 2007), using a Greengenes dataset (gg_13_8_99) https://www.mothur.org/wiki/Greengenes-formatted_databases. Data has been normalized to obtain seven taxonomic levels for each sequence at 80% Naïve Bayesian bootstrap cut-off with 1000 iterations (Fig. 2.3).

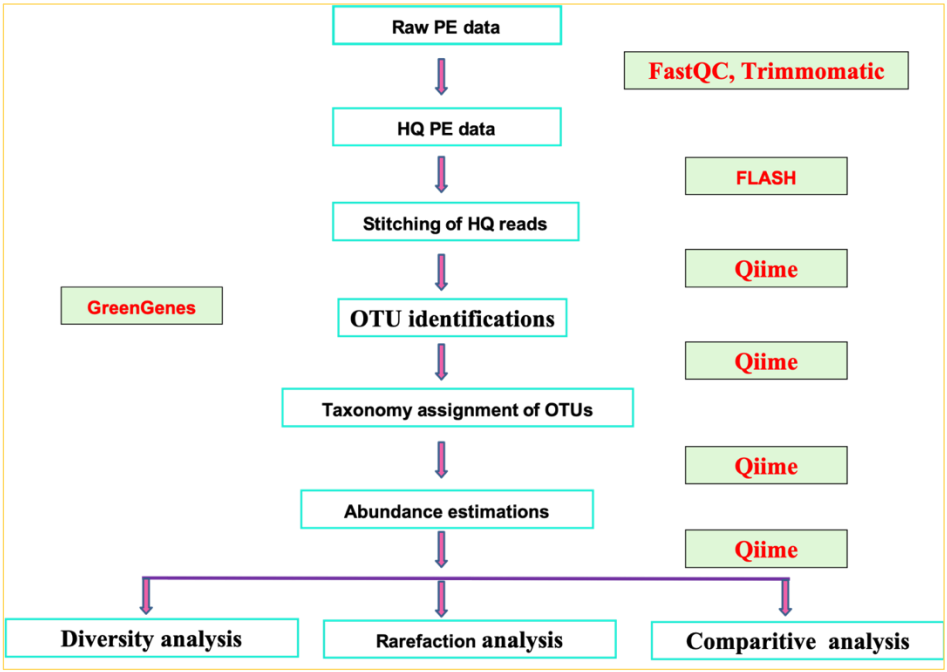

Fig. 2.3 Bioinformatics workflow for amplicon based metagenome analysis of various samples.

Operational taxonomic units (OTUs; at 97% and 98% sequence similarity) were calculated using the mothur platform. The undesirable sequences belonging to Mitochondria, Chloroplast, Archaea, and Eukaryota were removed. The constructed OTU table was corrected to comply with the current official nomenclature (List of Prokaryotic names with Standing in Nomenclature: LPSN-www.bacterio.net). The rarefaction analysis was carried out using a single rarefaction function of mothur, and alpha diversity was estimated by calculating the diversity indices like Inverse Simpson, Shannon diversity (H), and observed richness sub sampling. The statistical analysis was carried out using PAST v3.18 (Hammer et al. 2001). Statistical tests like ANOVA and Tukey's posthoc tests were used to detect remarkable differences in diversity indices between sponge samples. To further examine the community relationship among all three sponge samples, non-metric multidimensional scaling (NMDS) uses Bay-Curtis distance. The number of shared OTUs among all the sponge samples was calculated and represented using a Venn diagram (subsampled OTU table) by mothur. The samples' microbial composition was characterized, and results are displayed by bacterial phyla abundances. The bacterial

families and genera with abundances greater 0.5% in at least one of the samples were also identified. Remarkable differences between samples were assessed using the Kruskal-Wallis test and Dunn's posthoc test (non-normal data). The heatmap showing relative abundance were constructed using Morpheus web-based tool (https://software.broadinstitute.org/morpheus).

2.17.4 Functional Profile Prediction

KEGG (Kyoto Encyclopedia of Genes and Genomes) annotation of the OTU table obtained from mothur was performed using PICRUSt (Phylogenetic Investigation of Communities by Reconstruction of Unobserved States) to predict the functional composition of microbial community obtained from amplicon metagenome data (Langille et al. 2013).

2.17.5 "Sporotan" staining of fruiting bodies

The protocol used by Senthilnathan et al. (2020) and Ali et al. (2020) was adapted in this study also. Late stationary phase liquid cultures (approximately 4 months old) of both the strain JC669^T and A. giovannonii DSM 22561^T were pellet down by centrifugation (10,000 rpm at 4 °C for 5 min) and the deposited pellet was re-suspended and washed with PBS buffer (pH 7.8) for 2 times. 100 µl of the pellet suspension was incubated with 6 µl of 4 mM solution of "Sporotan" in DMSO ("sporotan" is water insoluble) for 20 min at room temperature (~26 °C). Stained cultures were centrifuged (10,000 rpm at 4 °C for 5 min) and the pellet was resuspended in 20 µl Milli- Q water. A drop of suspension was smeared on the cleaned microscopic glass slide, protected with a coverslip and observed under confocal laser microscope (Carl Zeiss LSM900). Fluorescence signals of "Sporotan" were detected at excitation: 405 nm; emission: 410–480 nm long pass. (Senthilnathan et al. 2020; Ali et al. 2020).

Results

3.1 Bacterial communities of selected habitats with particular reference to Planctomycetes

3.1.1 Bacterial communities of sponges from the wetland ecosystem of Little Rann of Kutch, India

3.1.1.1 Sampling strategy

During our survey for Planctomycetes from the wetland ecosystem, we collected five sponges from puddles at the Joghad Eco Park (part of Little Rann of Kutch). The GPS of the sampling site is N 22°43'26", E 70°28'40". The salinity, pH, and temperature of sampling sites were measured through conductivity meter, pH meter and thermometer, respectively. Sponges were identified to the genus through the world Porifera Database (http://www.marinespecies.org/porifera/). Three sponges belonged to the genus *Spongilla* (*Spongilla sp.* S8, *Spongilla* sp. S9, and *Spongilla* sp. S10), while two belonged to the genus *Ciocalypta* (*Ciocalypta* sp. S11, and *Ciocalypta* sp. S12). *Spongilla* spp. were collected from three puddles having at a depth of about 20 cm with continuous flow of surface water from different resources and the samples were collected at a distance of about 20 meters between puddle. While *Ciocalypta* sp. S11 and *Ciocalypta* sp. S12 were collected from the salt marsh puddles on the road side at a distance of about 100 meters between the puddles. Salinity, pH and temperature of the puddle water ranged between 1-5%, 7-9 and 26-30 °C respectively. The collected sponges were processed separately for metagenome and cultured diversity analyses (Fig. 3.1.1.a).

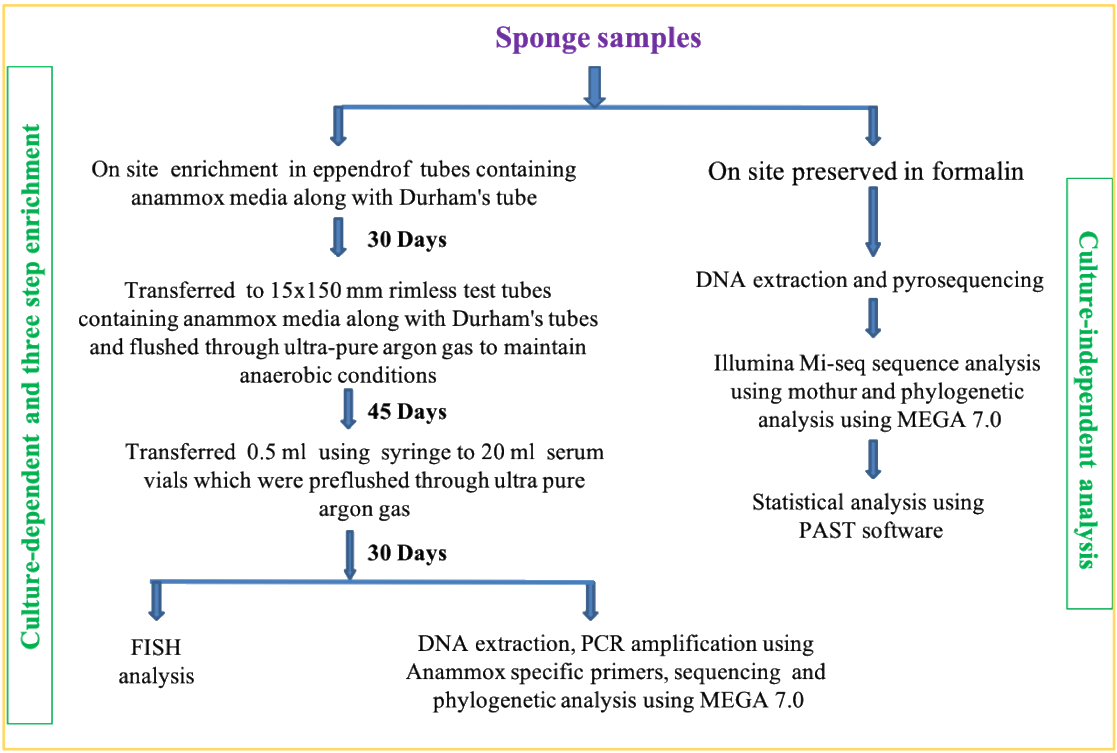

Fig. 3.1.1.a Protocol used for culture dependent and independent studies to assess the bacterial diversity of sponge samples collected from Little Rann of Kutch.

3.1.1.2 Metagenomic DNA extraction, sequencing and quality control

DNA was extracted successfully from all the five formalin preserved sponges for further study. However, metagenomic DNA extracted from *Spongilla sp.* S8 and *Spongilla* sp. S10 failed when subjected to amplicon sequencing on the Illumina Mi-Seq platform, though the genomic DNA quality was good. The metagenomic sequences of the sponge samples, *Spongilla* sp. S9, *Ciocalypta* sp. S11 and *Ciocalypta* sp. S12 were submitted to the NCBI-SRA (Sequence Read Archive) under accession numbers SRR6347343, SRR6347342, and SRR6347344 respectively.

3.1.1.3 Bacterial abundance and diversity analysis

A total of 10161operational taxonomic units (OTUs) belonging to 41 different phyla (376 different species) were obtained from the three sponge samples, *Spongilla* sp.S9 (growing at pH 8 and salinity 1%), *Ciocalypta* sp. S11 (pH 8; salinity 5%) and *Ciocalypta* sp. S12 (pH 9; salinity 1.5%) with 98% cut-off and 9148 OTUs with 97%

cut-off. There were no significant differences in the abundance of bacterial diversity obtained using both the cut-off's (Table. 3.1.1.a); hence 98% cut-off was used for further analysis.

Cut-off	Sponge Sample ID	Number of Sequences	Shannon (H)	Inverse Simpson	Observed Richness
98%	*Ciocalypta* sp. S11	4828	4.8 ± 0.0	44.5 ± 0.0	585 ± 0.0
	Ciocalypta sp. S12	4828	5.7 ± 0.0	121.1 ± 4.4	778.7 ± 16.9
	Spongilla sp. S9	4828	8.2 ± 0.0	425.2 ± 26.3	3146.6 ± 26.4
97%	*Ciocalypta* sp. S11	4826	4.8 ± 0.0	44.4 ± 0.0	613 ± 0.0
	Ciocalypta sp. S12	4826	5.6 ± 0.0	111.7 ± 4.0	685.6 ± 15.5
	Spongilla sp. S9	4826	7.9 ± 0.0	376.2 ± 20.4	2908.2 ± 27.1

Table. 3.1.1.a Comparison of Microbial community richness and diversity indices of three sponge samples *Spongilla* sp S9, *Ciocalypta* sp. S11 and *Ciocalypta* sp. S12. All statistical diversity indices and estimators were performed under 1000 iterations and by rarefying the OUT table to 4828 sequences. The results of statistical analyses for bacterial communities show that *Spongilla* sp. S9 has higher OTUs, species richness, and diversity compared to other two sponge samples. a. Shannon: Shannon diversity index (>0, higher, more diverse). b Inverse Simpson is the reciprocal of Simpson diversity index where higher the value, the greater the diversity c. Observed Richness (sobs) is a richness estimator that returns number of observed OTUs from observed definition

The abundance here refers to the percentage of sequence reads in the final OTU table. The unclassified OTUs observed were 5.8% in 97% cut-off and 5.9% in 98% cut-off. In this analysis, OTU represents a cluster of a particular group of sequences. Thus, some sequences representing OTUs constructed at 97% were not classifiable by the RDP classifier and were labelled as unclassified. At 98% cut-off, these longer unclassifiable sequences were placed in separate OTUs with fewer sequences and shorter abundant classifiable sequences placed in other OTUs, consequently increasing identifiable sequences. Rarefaction curves were generated (Fig. 3.1.1.b) for each sample at a sequence similarity cut-off of 98%, which indicated that the majority of taxonomic diversity was covered in all the three samples. The curves showed saturation indicating proper sampling to continue with further analysis.

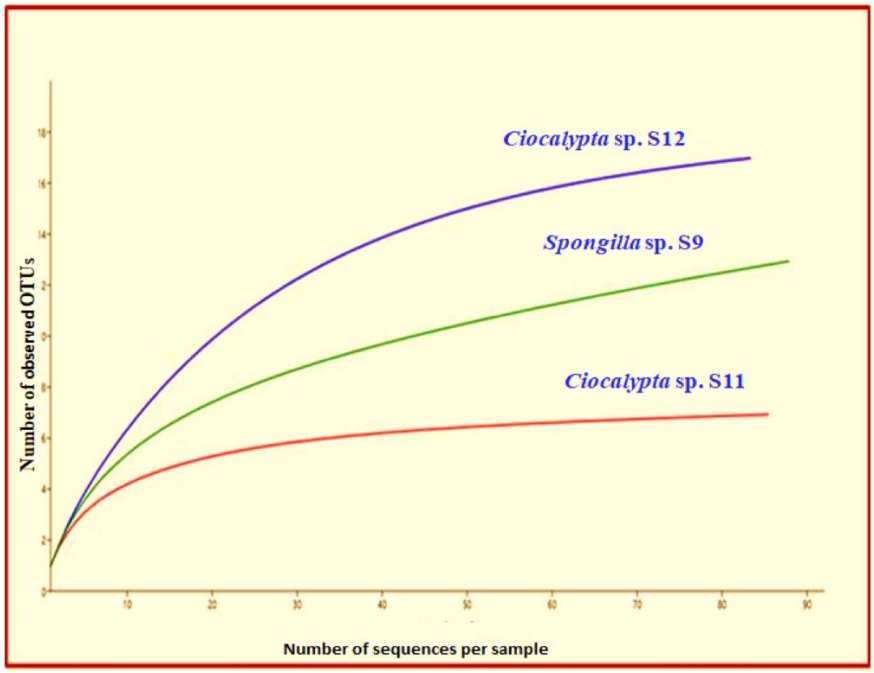

Fig. 3.1.1.b Rarefaction analysis of the three sponge samples. Rarefaction curves of OTUs clustered at 98% sequence identity across different samples.

Bacterial abundance or distributions at the level of phylum (Fig. 3.1.1.c) and classes (Fig. 3.1.1.d) are shown in the form of heat map. Overall, 8792 OTUs (at 98% sequence similarity cut-off) belonging to 41 different bacterial phyla (23 known bacterial phyla, 17 "*Candidatus*" phyla, and one unclassified phylum) were obtained from the three sponge samples. Detected OTUs belong to the phyla Actinobacteria, Firmicutes, Bacteroidetes, Chloroflexi, Planctomycetes, Acidobacteria, and Gemmatimonodetes accounting to 40% of the observed OTUs. Seventeen OTUs belong to the Candidatus phyla which include BRC1, GN02, GN04, H-178, KSB3, NKB19, OD1, OP8, SR1, TM6, TM7, WPS2, WS1, WS3, WS4, WWE1 and ZB31. Members of the phylum "*Candidatus* Poribacteria" which are widely associated with many marine sponges (Schmitt et al. 2012) were not detected in our study. Majority of the OTUs belong to unclassified taxa and taxa belonging to the phylum Aquificae, Caldiserica, Dictyoglomi, Nitrospira, and Thermodesulfobacteria were absent in all the sponges studied (Fig. 3.1.1.c).

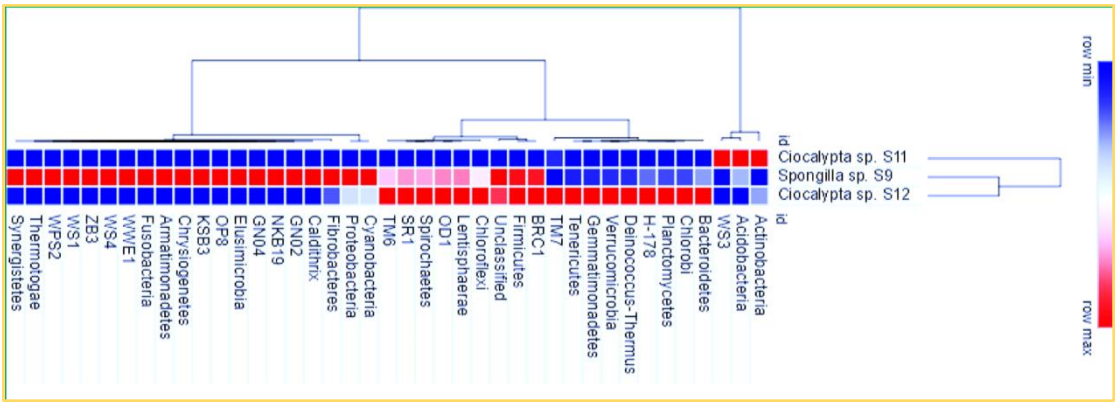

Fig. 3.1.1.c Heat map showing Phylum level comparison of bacterial community structure obtained from amplicon metagenome of three sponge samples, Spongilla sp. S9, Ciocalypta sp. S11 and Ciocalypta sp. S12. The relative abundance is represented as the percentage of each phylum to the total effective bacterial sequences of each sample. The relative abundance is represented as the percentage of each phylum to the total effective bacterial sequences of each sample. The heat map was hierarchically clustered in two dimensions. The horizontal axis refers to relative abundance of each phylum and vertical axis represents the sponge sample.

The most abundant OTUs belong to the phylum Proteobacteria with 11810 sequences distributed across all the five classes (Alphaproteobacteria, Betaproteobacteria,Gammaproteobacteria,Deltaproteobacteria, and Epsilonproteobacteria). OTUs belonging to the class Alphaproteobacteria is the most dominant in all the three sponge (Fig. 3.1.1.d). Among the phylum Planctomycetes, OTUs belonging to the Class Phycisphaerae and Planctomycetia are dominant in Ciocalypta sp. S12 (Fig. 3.1.1.d). At the family level, OTUs belonging to Rhodobacteraceae (27-48%) is dominant in all the sponge samples. The dominant families were similar in *Spongilla* sp. S9 and *Ciocalypta* sp. S12. However, *Spongilla* sp. S9 showed a higher ratio of unique families compared to *Ciocalypta* sp. S12 and *Ciocalypta* sp. S11 (Data not shown).

Among the 4828 OTUs used for constructing Venn diagram by mothur, no OTU represented core microbiome of the three sponges' samples analyzed (Fig. 3.1.1.e). *Spongilla* sp. S9 and *Ciocalypta* sp. S12 shared about 80 OTUs, mostly belonging to Proteobacteria. *Spongilla* sp.

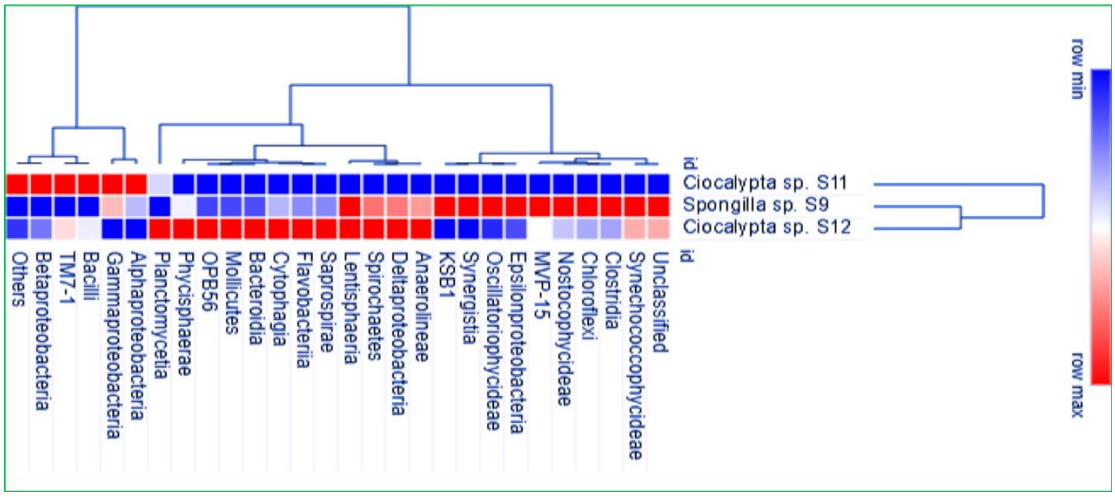

Fig. 3.1.1.d Heat map showing Class-level comparison of bacterial community structure obtained from amplicon metagenome of three sponge. samples *Spongilla* sp. S9, *Ciocalypta* sp. S11 and *Ciocalypta* sp. S12. The relative abundance is represented as the percentage of each class to the total effective bacterial sequences of each sample. Classes with greater than 0.5% of abundance in atleast two samples ((28 out of 89 classes of bacteria) were shown here. The class Alphaproteobacteria is most abundant and present in all samples. *Anaerolineae* as the next dominant and absent in *Ciocalypta sp.* S11.

S9 contains more unique OTUs (3072), accounting for 70% of total OTUs, followed by *Ciocalypta* sp. S12 (700 OTUs, 15.6%) and finally, *Ciocalypta* sp. S11 contained 583 unique OTUs (11.8%). *Ciocalypta* sp. S12 and *Ciocalypta* sp. S11 shared only 2 OTUs (Fig. 3.1.1.e). To further examine the community relationship among all three sponge samples, non-metric multi-dimensional scaling (nMDS) was performed using PAST software. The Bay-Curtis distance was taken into consideration. The nMDS analysis positioned them at altogether different places (Fig. 3.1.1.f). Various alpha diversity indices (Mean and Standard deviation) like Shannon (H), Inverse Simpson, and Observed Richness were calculated using mothur by rarefying the OTU table to 4828 OTUs.

Alpha diversity indices were similar between the cut-off percentages (97% & 98% sequence similarity) for the three samples analysed. Shannon diversity index varied between the sponge samples, with the highest diversity found in *Spongilla* sp. S9 (H=8.2 $\pm$ 0.0) and the lowest in *Spongilla* sp. S11 (4.8 $\pm$ 0.0).

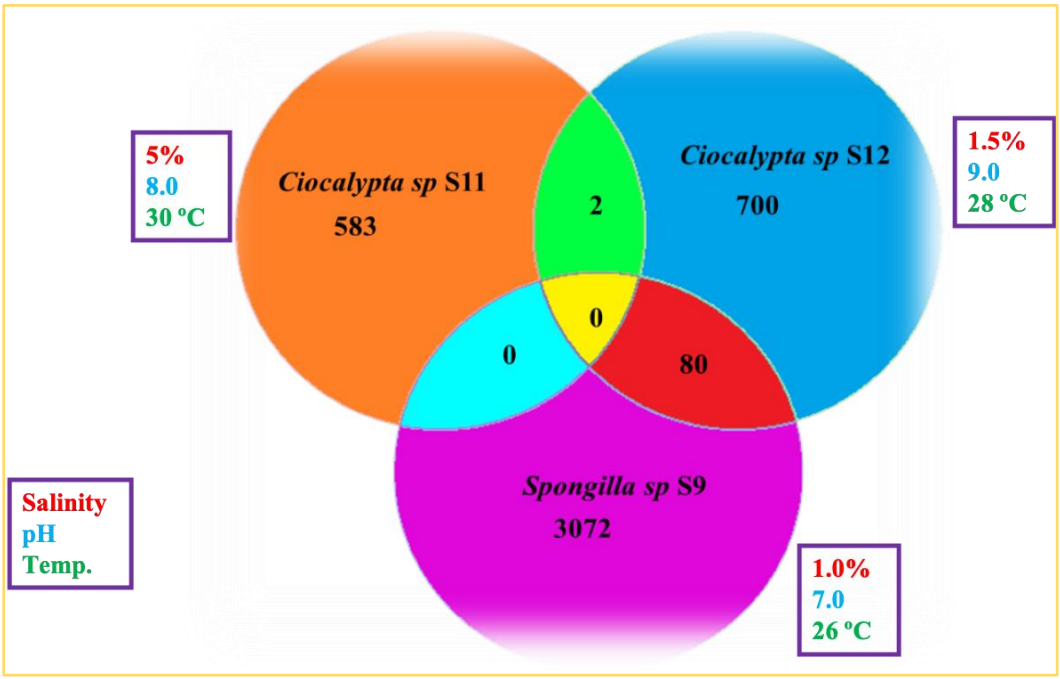

Fig. 3.1.1.e Venn diagram representing diversity of core and shared OTUs with in the three sponge samples Spongilla sp. S9, Ciocalypta sp. S11 and Ciocalypta sp. S12. The number in the overlapping zone indicates how many OTUs were shared between sponge samples, and the numbers in the non-overlapping zone indicate how many OTUs were exclusively found in each sponge. The overlapping zone of three circles represent the shared OTUs between three sponges.

Observed Richness and Inverse Simpson indices were also higher for *Spongilla* sp. S9, followed by *Ciiocalypta* sp. S12 and lowest for *Ciiocalypta* S11 (Table. 3.1.1.a). The *Spongilla* sp. S9 showed the most diverse bacterial community (Shannon's diversity, which considers how evenly the OTUs are distributed), followed by *Ciocalypta* sp. S12 and *Ciocalypta* sp. S11.

3.1.1.4 Planctomycetes diversity among sponges

Planctomycetes in all three sponge samples were analysed using the abundance values obtained by amplicon sequencing. Planctomycetes, although not a dominant phylum, was observed in all the three samples ranging from 1.0-4.3% (Fig. 3.1.7). The sponge sample *Ciocalypta* sp. S12 contains more OYUs (4.3%) belonging to Planctomycetes, followed by *Ciocalypta* sp. S11 (1.1%) and *Spongilla* sp. S9 (1.2%).

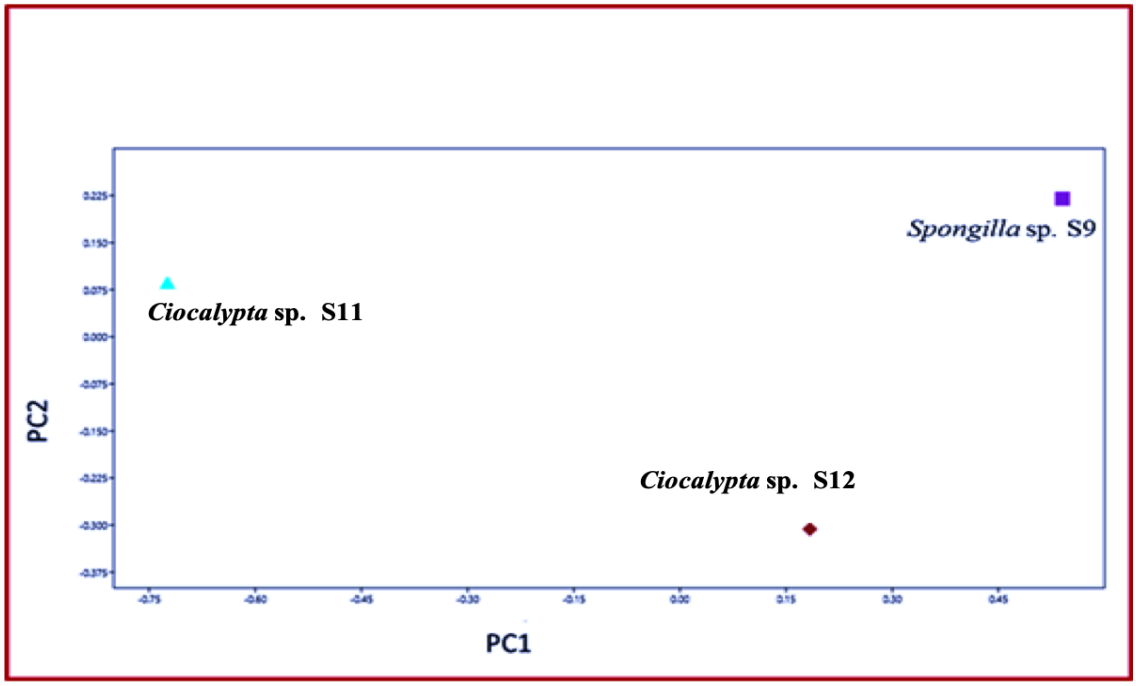

Fig. 3.1.1.f Non-metric multidimensional scaling (nMDS) plot representing the diversity based on Bay-curtis distance among three sponge samples Spongilla sp. S9, Ciocalypta sp. S11 and Ciocalypta sp. S12.The plot is constructed based on the abundance of OTUs found in sponge sample at phylum level. The distance between the sample demonstrates the difference in diversity. The three sponge samples are distantly related and shared less OTUs.

Family level distribution showed a different diversity among the three sponges. *Ciocalypta* sp. S11 contained OTUs belonging to Isosphaeraceae (unclassified at genus level), whereas *Ciocalypta* sp. S12 and *Spongilla* sp. S9 showed similar distribution with different dominant families (Fig. 3I). *Spongilla* sp. S9 is dominated by OTUs belonging to the family Phycisphaeraceae (unclassified) followed by OTUs of the family Pirellulaceae (unclassified), Planctomycetaceae (Planctomyces sp.), and Isosphaeraceae whereas in Ciocalypta sp. S12, Pirellulaceae family is dominant, followed by Planctomycetaceae, Phycisphaeraceaeand Isosphaeraceae (Fig. 3.1.1.g).

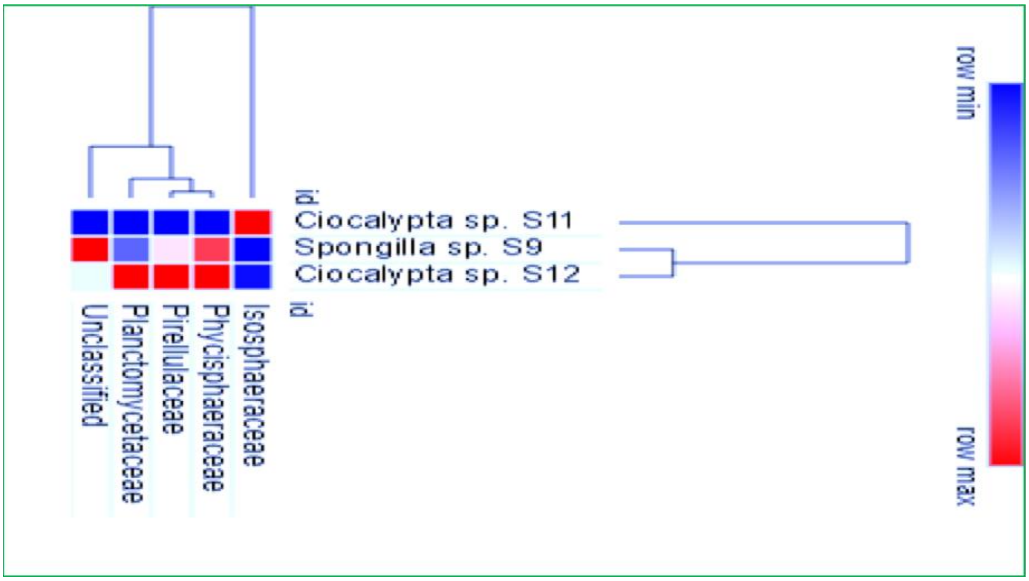

Fig. 3.1.1.g Heat map depicting the abundance and distribution of Planctomycetes at family level from amplicon sequence data of three sponge samples. The heat map was hierarchically clustered in two dimensions. The horizontal axis refers to relative abundance and vertical axis represents the sponge sample**.**

3.1.1.5 Functional Profile Prediction

The metabolic capacity of the microbiomes inferred from amplicon genomic libraries will provide a better understanding of the role of the microbiome in host metabolism and disease **(**Steinert et al. 2019). Functional metabolic profiling by using PICRUSt, a predictive approach, provide insights into potential functional aspects of sponge-associated bacterial communities. The KEGG annotation predicted a total of 6909 KEGG Orthologs (KOs; i.e., sets of homologous sequences) mapping to 328 different KEGG pathways (Fig. 3.1.1.h). Out of the total predicted KOs, 4448 were shared in microbiomes of all the three sponges . Most of the KOs are associated with membrane transport, followed by amino acid metabolism, carbohydrate metabolism, and energy metabolism. Besides, the occurrence of different classes of energy metabolism (e.g., carbon or nitrogen metabolism) or symbiosis factors (e.g., eukaryotic-like proteins, ankyrin repeats, or tetratricopeptide repeats), KOs related to synthesis of secondary metabolites and bioactive natural products were predicted. Sponges, are acknowledged widely often to synthesize secondary metabolites and bioactive natural products and the same may be

contributed by the associated microbiome. All the three sponge microbiomes showed functional genes related to xenobiotic degradation (1,1,1-Trichloro-2,2-bis(4-chlorophenyl)ethane (DDT), aminobenzoate, atrazine, benzoate, caprolactam, Polycyclic aromatic hydrocarbons). The functionally related genes for biosynthesis of secondary metabolites like carotenoids, neomycin, streptomycin, vancomycin, penicillin, and cephalosporin were predicted in the samples. Such a vast secondary metabolite repertoire may play pivotal roles in microbiome community assembly, host-symbiont signalling, and host defence. They also showed genes related to beta-Lactam resistance. They also showed KOs mapped to terpenoid backbone biosynthesis; terpenoids represent the most extensive natural products group and are a highly diverse class of organic chemicals. Terpene synthases have also been shown to be widely distributed in bacteria and represent a potentially important source for discovering novel natural products (Fig. 3.1.1.h).

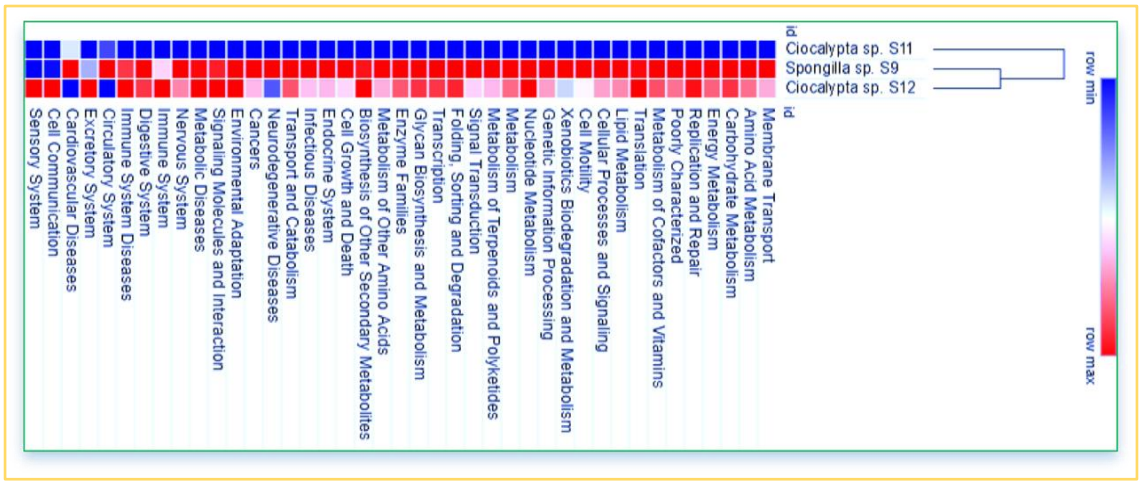

Fig. 3.1.1.h KEGG Annotation of reads obtained form metagenome of three sponge samples *Spongilla sp.* S9, *Ciocalypta* sp. S11 and *Ciocalypta* sp. S12.

3.1.2 Bacterial communities of sponges, collected from Tamil Nadu coast, India

3.1.2.1 Sampling strategy

During our survey for Planctomycetes from the Tamil Nadu coast, we collected seventeen sponge's specimen lying on-shore in various geographical regions. The salinity, pH, and temperature of sampling sites were measured through conductivity meter, pH meter and thermometer, respectively. Sponges were identified to the level of species/genus/order/family through the world Porifera Database (http://www.marinespecies.org/porifera/) or with the assistance to the sponge taxonomist. The collected sponges were processed separately for metagenome and cultured diversity analyses (Fig. 3.1.2.a) (Annexure 1c,e).

3.1.2.2 Metagenomic DNA extraction, sequencing and quality control

DNA was extracted successfully from all thirty one formalin preserved sponges for further study. The metagenomic DNAs were outsourced to M/s Eurofins Pvt. Ltd, India for amplicon based sequencing on the Illumina Mi-Seq platform. The metagenomic sequences of all seventeen sponge samples were submitted to the NCBI-SRA (Sequence Read Archive) under accession numbers SRP280073 and BioProject ID: PRJNA639208.

3.1.2.3 Bacterial abundance and diversity analysis of sponges.

A total of 9,463 operational taxonomic units (OTUs) belonging to 43 different phyla were obtained from the seventeen sponge samples, with 98% and 97% cut-off. There were no significant differences in the abundance of bacterial diversity obtained using both the cut-off's, hence 98% cut-off was used for further analysis. The abundance here refers to the percentage of sequence reads in the final OTU table. The unclassified OTUs observed were 7.0% in 97% cut-off and 6.9% in 98% cut-off. In this analysis, OTU represents a cluster of a particular group of sequences.

Fig. 3.1.2.a Detail about the samples collected for the metagenome and culture -based studies along with their GPS location. Level of identification is given in the brackets.

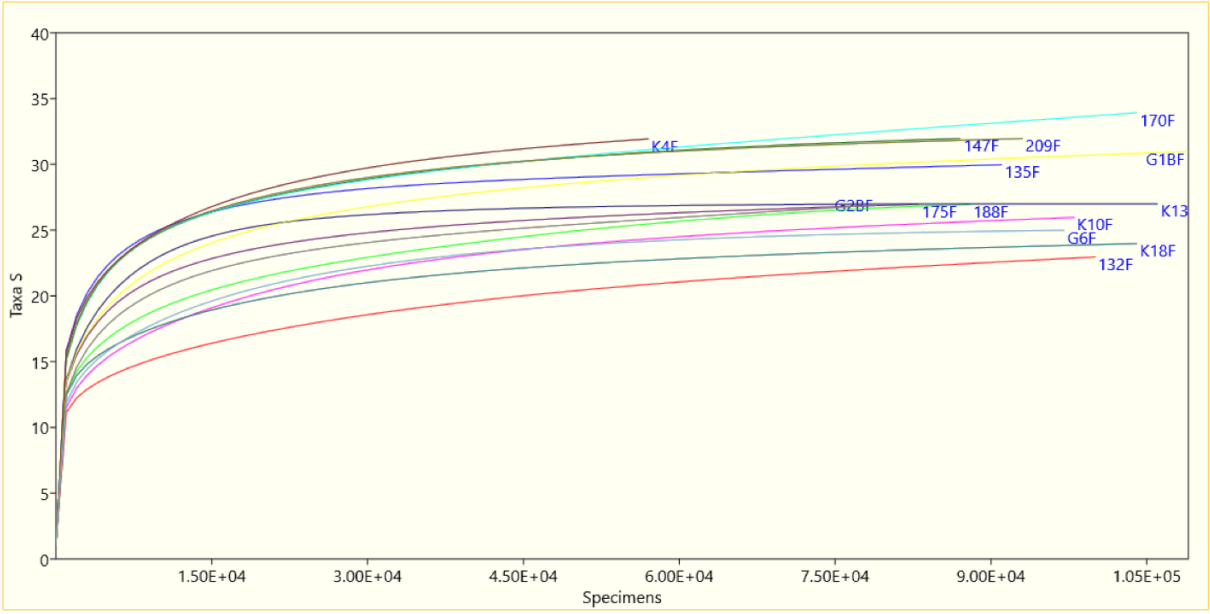

Fig. 3.1.2.b. Rarefaction analysis of seventeen sponge samples. Rarefaction curves of OTUs clustered at 98% sequence identity across different samples.

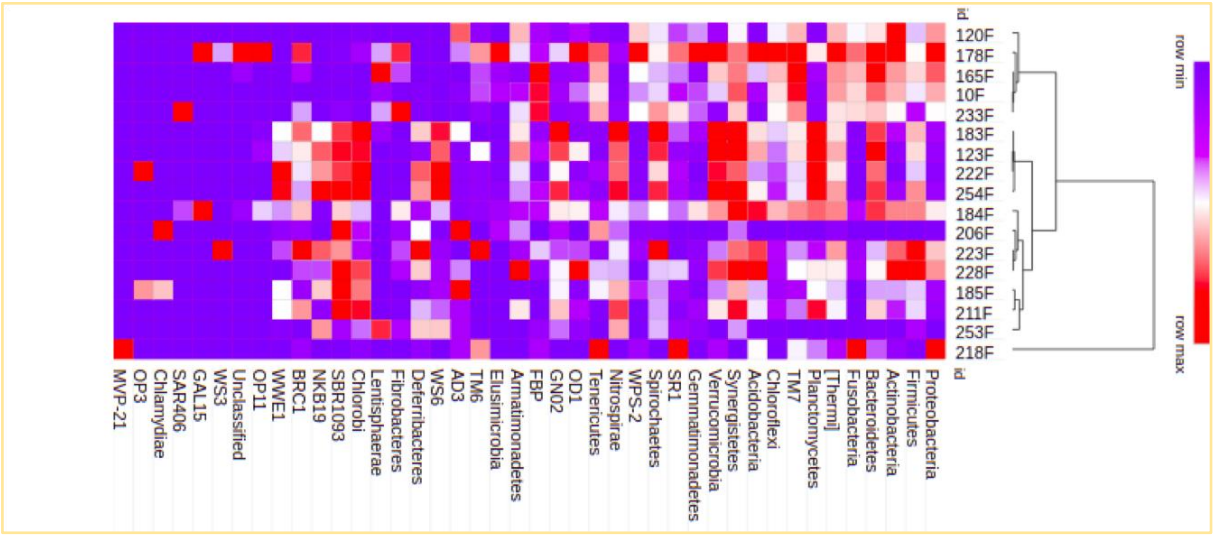

Fig. 3.1.2.c Heat map showing Phylum level comparison of bacterial community structure obtained from amplicon metagenome of seventeen sponge samples. The relative abundance is represented as the percentage of each phylum to the total effective bacterial sequences of each sample. The relative abundance is represented as the percentage of each phylum to the total effective bacterial sequences of each sample. The heat map was hierarchically clustered in two dimensions. The horizontal axis refers to relative abundance of each phylum and vertical axis represents the sponge sample.

Thus, some sequences representing OTUs constructed at 97% were not classifiable by the RDP classifier and were labelled as unclassified.At 98% cut-off, these longer unclassifiable sequences were placed in separate OTUs with fewer sequences and shorter abundant classifiable sequences placed in other OTUs, consequently increasing identifiable sequences. Rarefaction curves were generated for each sample at a sequence similarity cut-off of 98%, which indicated that the majority of taxonomic diversity was covered in all the seventeen samples (Fig 3.1.2.b). The curves showed saturation indicating proper sampling to continue with further analysis.

Bacterial abundance or distributions at the level of phylum are shown in the form of heat map. Overall, 9,463 OTUs (at 98% sequence similarity cut-off) belonging to 42 different bacterial phyla (22 known bacterial phyla, 19 "*Candidatus*" phyla, and one unclassified phylum) were obtained from all the sponge samples. Detected OTUs belong to the phyla *Actinobacteria, Firmicutes, Bacteroidetes, Chloroflexi, Planctomycetes, Acidobacteria, and Gemmatimonodetes* accounting to 40-50% of the observed OTUs and their relative abundance varies according to the samples. In the samples, 10, 165, 178, and 218 maximum OTUs (45%) corresponds to the *Proteobacteria.* In the samples, 218 and 223 maximum OTUs (40%) corresponds to the *Firmicutes.* In the samples, 120, 178, 228 the maximum OTUs (30-40%) corresponds to the Actinobacteria. In the samples, 183, 123, 222, 254, 184, 10, 165 and 178 the maximum OTUs (30-50%) corresponds to the *Bacteriodetes.* In the samples, 183, 123, 222, 254 and 211 contain maximum of 15-20% of Planctomycetal OTUs and other samples contain only 5-8% of Planctomycetal OTUs (Fig. 3.1.2.c)

Nineteen OTUs belong to the Candidatus phyla which include MVP-21, OP3, SAR406, GAL15, OP11, WWE1, BRC1, SBR1093, WS6, AD3, FBP, GN02, SR1,

NKB19, OD1, TM6, TM7, WPS2, WS3. Members of the phylum "*Candidatus* Poribacteria" which are widely associated with many marine sponges (Schmitt et al. 2012) were not detected in our study. Majority of the OTUs belong to unclassified taxa and taxa belonging to the phylum *Caldiserica, Dictyoglomi, and Thermodesulfobacteria* were absent in all the sponges studied (Fig. 3.1.2.c).

3.1.2.4 Planctomycetal abundance and diversity analysis of sponges.

Among the phylum Planctomycetes, OTUs belonging to the families Planctomycetaceae, Pirellulaceae, Gemmataceae and Isosphaereaceae are predominant in all the sponge samples (Fig. 3.1.2.d). Also, 20-40% of the OTUs belong to unclassified Planctomycetes are present among the sponges. At the genera level, OTUs belonging to *Gemmata, Pirellula and Isosphaera* (27-48%) is dominant in all the sponge samples. OTUs belonging to unclassified and Candidatus order (A1) are also present among all the sponges. The dominant families and genera were similar in all the sponge samples (Fig. 3.1.2.e).

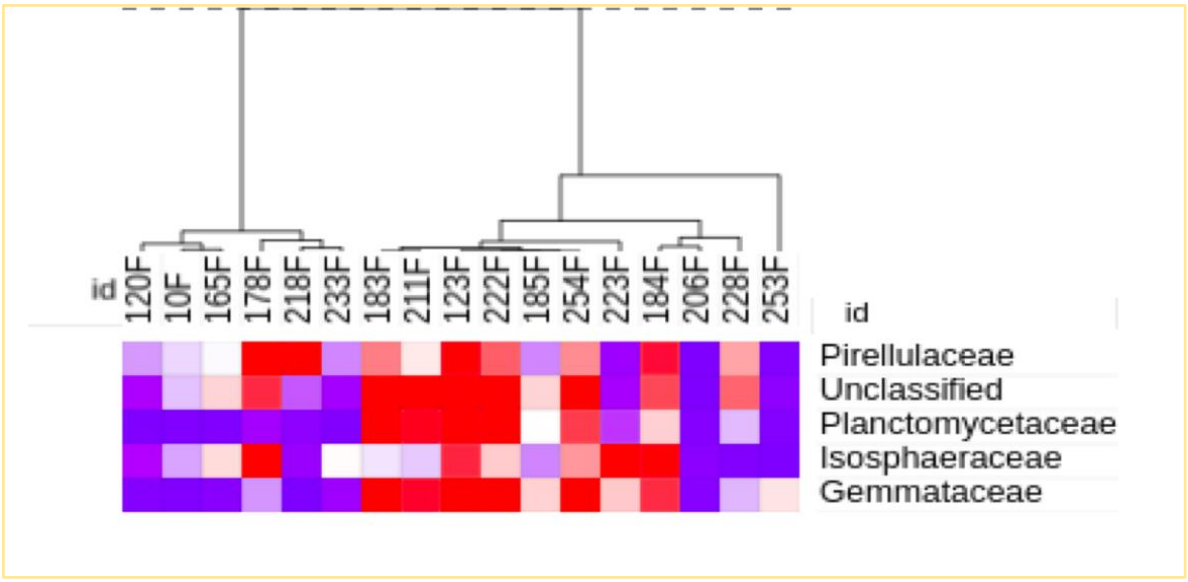

Fig. 3.1.2.d Heat map depicting the abundance and distribution of Planctomycetes at family level from amplicon sequence data of sponge samples. The heat map was hierarchically clustered in two dimensions. The horizontal axis refers to relative abundance and vertical axis represents the sponge sample.

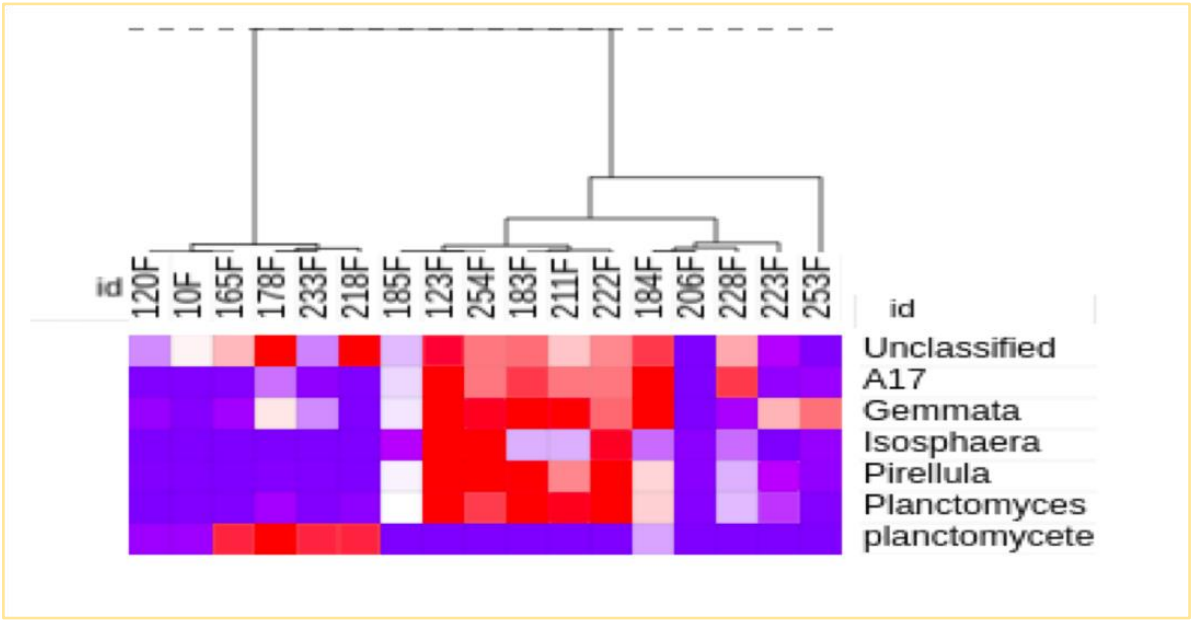

Fig. 3.1.2.e Heat map depicting the abundance and distribution of Planctomycetes at genus level from amplicon sequence data of sponge samples. The heat map was hierarchically clustered in two dimensions. The horizontal axis refers to relative abundance and vertical axis represents the sponge sample**.**

3.1.3 Bacterial communities of the algal samples, collected from Tamil Nadu coast, India

3.1.3.1 Sampling strategy

During our survey for Planctomycetes from the Tamil Nadu coast, we collected fourteen algal specimen lying on-shore from various geographical locations. The salinity, pH, and temperature of sampling sites were measured through conductivity meter, pH meter and thermometer, respectively. The collected algal were processed separately for metagenome and cultured diversity analyses (Fig. 3.1.3.a) (Annexure 1c,e).

3.1.3.2 Metagenomic DNA extraction, sequencing and quality control

DNA was extracted successfully from all the fourteen formalin preserved algae for further study. The metagenomic DNAs were outsourced to M/s Eurofins Pvt. Ltd, India for amplicon based sequencing on the Illumina Mi-Seq platform. The metagenomic sequences of all thirty one samples were submitted to the NCBI-SRA (Sequence Read Archive) under accession numbers SRP280073 and BioProject ID: PRJNA639208.

3.1.3.3 Bacterial abundance and diversity analysis of Algal samples.

A total of 8,622operational taxonomic units (OTUs) belonging to 42 different phyla were obtained from the fourteen algal samples, with 98% and 97% cut-off. There were no significant differences in the abundance of bacterial diversity obtained using both the cut-off's, hence 98% cut-off was used for further analysis. The abundance here refers to the percentage of sequence reads in the final OTU table. The unclassified OTUs observed were 8.0% in 97% cut-off and 7.0% in 98% cut-off. In this analysis, OTU represents a cluster of a particular group of sequences. Thus, some sequences representing OTUs constructed at 97% were not classifiable by the RDP classifier and were labelled as unclassified. At 98% cut-off, these longer unclassifiable sequences were placed in separate OTUs with fewer

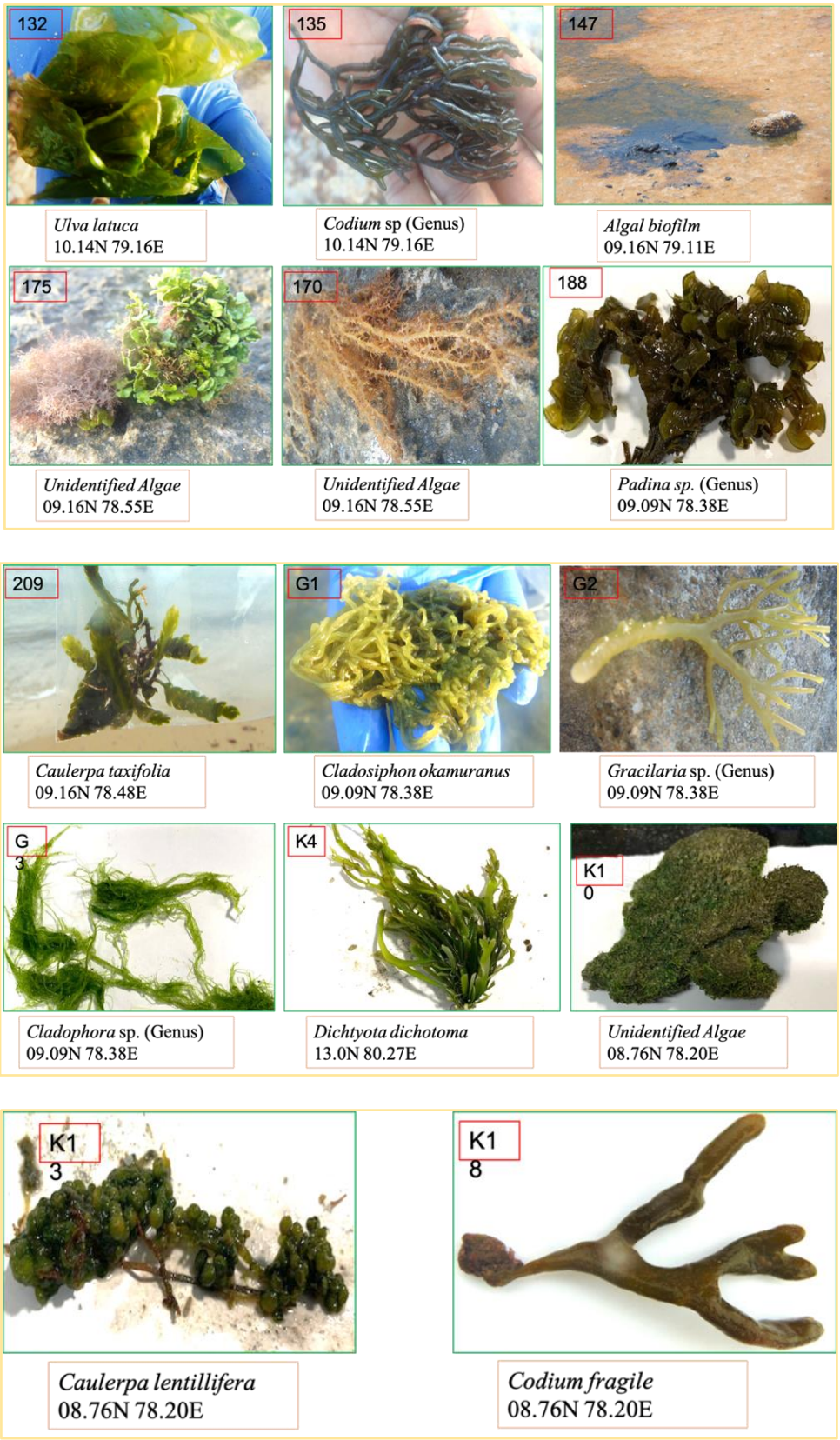

Fig. 3.1.3.a Detail about the algal samples collected for the metagenome and culture -based studies along with their GPS location. Level of identification is given in the bracket.

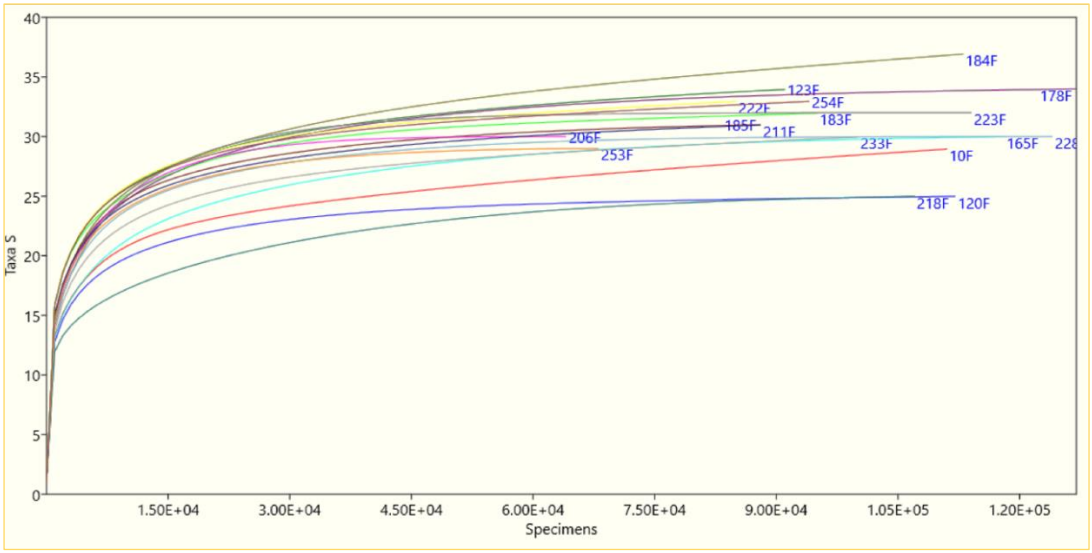

Fig. 3.1.3.b Rarefaction analysis of fourteen algal samples. Rarefaction curves of OTUs clustered at 98% sequence identity across different samples.

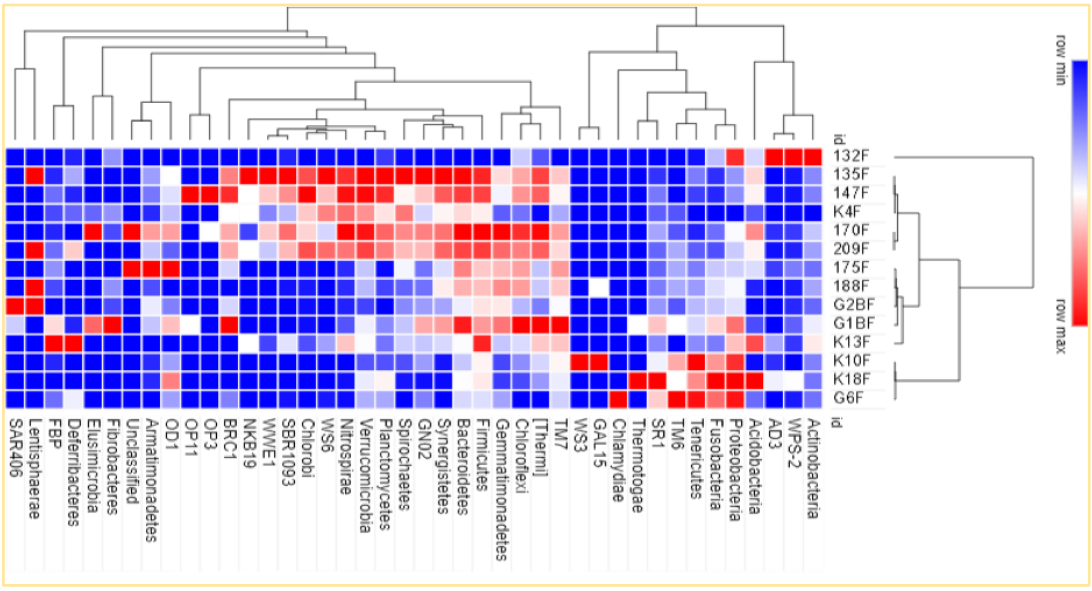

Fig. 3.1.3.c Heat map showing Phylum level comparison of bacterial community structure obtained from amplicon metagenome of fourteen algal samples. The relative abundance is represented as the percentage of each phylum to the total effective bacterial sequences of each sample. The relative abundance is represented as the percentage of each phylum to the total effective bacterial sequences of each sample. The heat map was hierarchically clustered in two dimensions. The horizontal axis refers to relative abundance of each phylum and vertical axis represents the algal sample.

sequences and shorter abundant classifiable sequences placed in other OTUs, consequently increasing identifiable sequences. Rarefaction curves were generated for each sample at a sequence similarity cut-off of 98%, which indicated that the majority of taxonomic diversity was covered in all the three samples (Fig 3.1.3.b). The curves showed saturation indicating proper sampling to continue with further analysis. Bacterial abundance or distributions at the level of phylum are shown in the form of heat map. Overall, 8,622 OTUs (at 98% sequence similarity cut-off) belonging to 42 different bacterial phyla (23 known bacterial phyla, 18 "*Candidatus*" phyla, and one unclassified phylum) were obtained from all the algal samples. Detected OTUs belong to the phyla *Actinobacteria, Firmicutes, Bacteroidetes, Chloroflexi, Planctomycetes* ,and *Acidobacteria* accounting to 40-50% of the observed OTUs and their relative abundance varies according to the samples. In the samples, G6, K10, K18, and 132 maximum OTUs (30-35%) corresponds to the *Proteobacteria.* In the samples, 135, 147, 170, K13 and 209 maximum OTUs (30%) corresponds to the *Firmicutes.* In the sample, 132 the maximum OTUs (30%) corresponds to the *Actinobacteria*. In the samples, G1B, 135, 147, 170, and 209 the maximum OTUs (30-35%) corresponds to the *Bacteriodetes.* In the samples, 135, 147, 170, and 209 contain maximum of 15-20% of Planctomycetal OTUs and other samples contain only 5-8% of Planctomycetal OTUs. Eighteen OTUs belong to the Candidatus phyla which include OP3, SAR406, GAL15, OP11, WWE1, BRC1, SBR1093, WS6, AD3, FBP, GN02, SR1, NKB19, OD1, TM6, TM7, WPS2, WS3. Like sponge samples, members of the phylum "*Candidatus* Poribacteria" which are widely associated with many marine sponges (Schmitt et al. 2012) were not detected in the algal samples. Majority of the OTUs belong to unclassified taxa and taxa belonging to the phylum *Caldiserica, Dictyoglomi, and Thermodesulfobacteria* were absent in all the algal studied (Fig. 3.1.3.c).

3.1.3.4 Planctomycetal abundance and diversity analysis of algal samples.

Among the phylum Planctomycetes, OTUs belonging to the families Planctomycetaceae, Pirellulaceae, Gemmataceae and Isosphaereaceae are predominant in all the algal samples. Also, 20-40% of the OTUs belong to unclassified Planctomycetes are present among all the sponges (Fig. 3.1.3.d). At the genera level, OTUs belonging to *Gemmata*, *Pirellula and Isosphaera* (27-48%) is dominant in all the algal samples. OTUs belonging to unclassified and Candidatus genera (A1) are also present among all the algal samples. The dominant families and genera were similar in all the algal samples (Fig. 3.1.3.e).

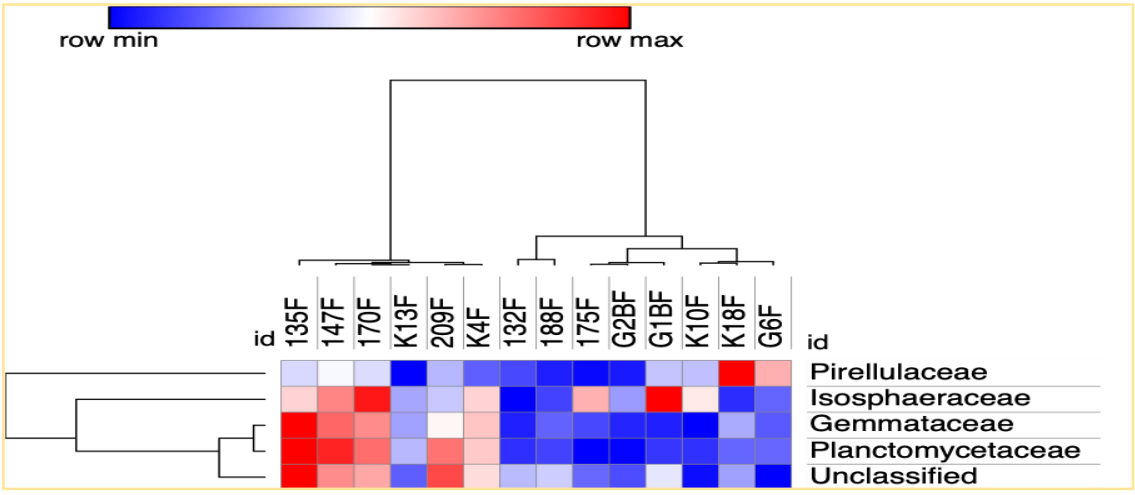

Fig. 3.1.3.d Heat map depicting the abundance and distribution of Planctomycetes at family level from amplicon sequence data of algal samples. The heat map was hierarchically clustered in two dimensions.The horizontal axis refers to relative abundance and vertical axis represents the algal sample**.**

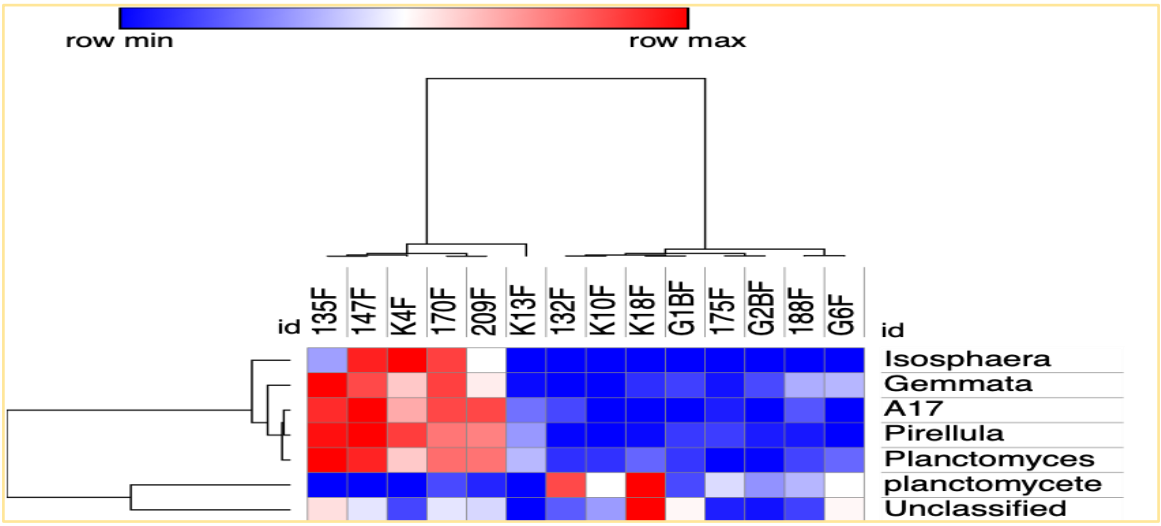

Fig. 3.1.3.e Heat map depicting the abundance and distribution of Planctomycetes at genus level from amplicon sequence data of algal samples. The heat map was hierarchically clustered in two dimensions. The horizontal axis refers to relative abundance and vertical axis represents the algal sample**.**

3.1.4 Temporal based bacterial communities' analysis of Satpada region of Chilika Lagoon, India

3.1.4.1 Sampling strategy

To analyse the temporal based bacterial communities of Satpada region of Chilika Lagoon, sediment samples were collected in three different seasons. Samples were collected in the months of August, December and May to analyze the bacterial communities for the autumn, winter and summer seasons respectively. The salinity, pH, and temperature of sampling sites were measured through conductivity meter, pH meter and thermometer, respectively. The collected sediments were processed separately for metagenome and cultured diversity analyses.

3.1.4.2 Metagenomic DNA extraction, sequencing and quality control

DNA was extracted successfully from all the formalin preserved sediment samples for further study. The metagenomic DNAs from all three seasons were outsourced to M/s Eurofins Pvt. Ltd, India for amplicon based sequencing on the Illumina Mi-Seq platform. The metagenomic sequences of all thirty one samples were submitted to the NCBI-SRA (Sequence Read Archive) under accession numbers SRP280073 and BioProject ID: PRJNA639208.

3.1.4.3 Bacterial abundance and diversity analysis of sediment samples of Satpada region of Chilika Lagoon

A total of 6,547 operational taxonomic units (OTUs) belonging to approximately 17 different phyla were obtained from the sediment samples of all the seasons, 98% cut-off. The abundance here refers to the percentage of sequence reads in the final OTU table. The unclassified OTUs observed were 8.0% in 97% cut-off and 7.0% in 98% cut-off. In this analysis, OTU represents a cluster of a particular group of sequences. Thus, some sequences representing OTUs constructed at 97% were not classifiable by the RDP classifier and were labelled as unclassified sequences placed in other OTUs, consequently

increasing identifiable sequences. Rarefaction curves were generated for each sample at a sequence similarity cut-off of 98%, which indicated that the majority of taxonomic diversity was covered in all the three samples**.** The curves showed saturation indicating proper sampling to continue with further analysis (Data not shown). Bacterial abundance or distributions at the level of phylum are shown in the form of heat map. Overall, 6,547 OTUs (at 98% sequence similarity cut-off) belonging to 17 different bacterial phyla (13 known bacterial phyla, 3 "*Candidatus*" phyla, and one unclassified phylum) were obtained from all the sediment samples irrespective of seasons. Detected OTUs belong to the phyla Actinobacteria, Firmicutes, Bacteroidetes, Chloroflexi, Planctomycetes, and Spirochaetes accounting to 50-60% of the observed OTUs and their relative abundance varies according to the samples. Interestingly, 15% of the OTUs also belongs to the Cyanobacteria. In winter season bacterial abundance of all the phyla is highest followed by autumn and the summer seasons. In summer season (May). Some bacterial phyla like Cyanobacteria, Actinobacteria and Planctomycetes are more abundant as compare to autumn season (August) (Fig. 3.1.4.a).

3.1.4.4 Planctomycetal abundance and diversity analysis of sediment samples of Satpada region of Chilika Lagoon

Among the phylum Planctomycetes, OTUs belonging to the families Planctomycetaceae, Pirellulaceae, Gemmataceae and Isosphaereaceae are predominant in all the sediment samples. Like overall bacterial abundance, the members of the phylum Planctomycetes are most abundant during winter season. In the Satpada region, about 40% of the OTUs belong to unclassified Planctomycetes or ‘candidatus’ members are present among all the samples (Fig. 3.1.4.b). This showed the vast existence of Planctomycetes diversity in the Chilika lagoon and as a result it helped in the cultivation of novel taxas within the Phylum Planctomycetes (Table. 3.3.1)

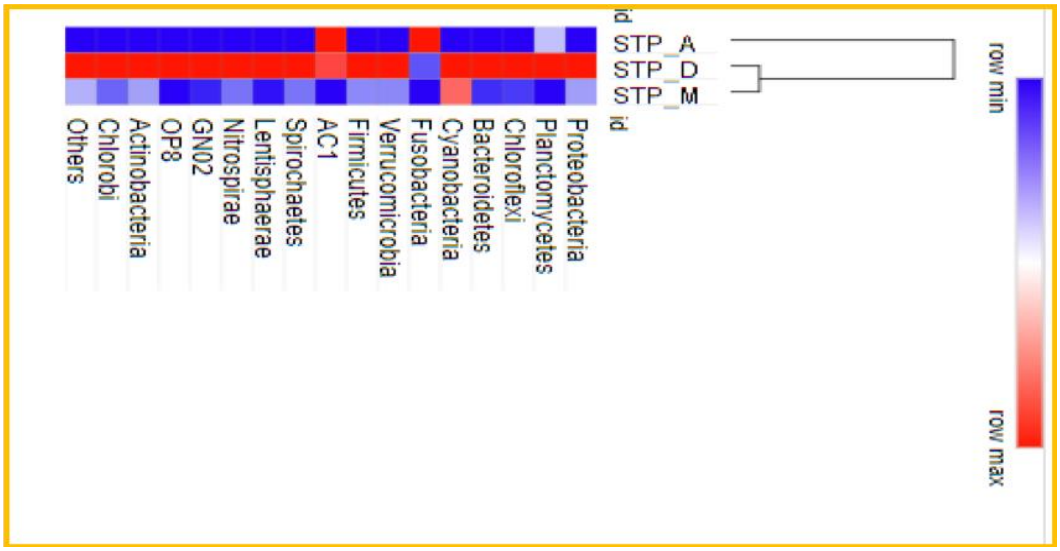

Fig. 3.1.4.a Heat map showing Phylum level comparison of bacterial community structure obtained from amplicon metagenome of sediment from Satpada region of Chilika lake. A, August; D, December; M, May.

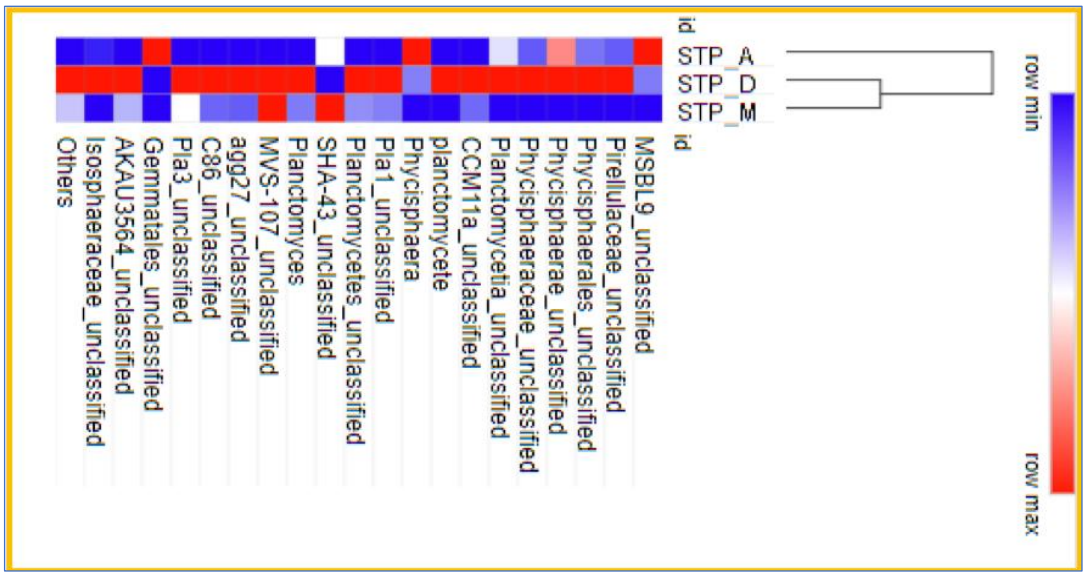

Fig. 3.1.4.b Heat map showing family level comparison of Planctomycetes community structure obtained from amplicon metagenome of sediment from Satpada region of Chilika lake. A, August; D, December; M, May.

3.2 Enrichments

3.2.1 The three steps enrichment strategy for planctomycetes

Metagenome based studies provide clear clues about the existence of Planctomycetes in the association to sponges and algal samples. Due to the fastidious nature of Planctomycetes, it is difficult to cultivate under the laboratory conditions. So, it require altogether different strategies of enrichments prior to cultivations of the Planctomycetes in laboratory.

On-site inoculation of the sample in Planctomycetes medium (in microcentrifuge tube having Durham's tube inside) ensured positive enrichment of anammox-planctomycetes and aerobic Planctomycetes (in co-cultured communities) and thus enhanced chances of recovering them in culture and minimizing the probability of losing. A three-step enrichment strategy proved quite useful in cultivating different Planctomycetes along with anammox-planctomycetes. This finding was confirmed through the FISH using Planctomycetes specific probe.

3.2.2 FISH for the detection of Planctomycetes from the enrichments

In different enrichment samples, the relative abundance of planctomycetes bacteria in samples was 1.0-4.3% (from metagenome data), which was enhanced to 60-70% (deduced from microscopic observation during FISH) in the enrichment cultures. Positive fluorescence for the enrichment of Planctomycetes (which are growing either as clusters or in isolation) were observed mostly in all type of the samples using CY3 labelled Pla46 probes (Fig. 3.2.1,2,3).

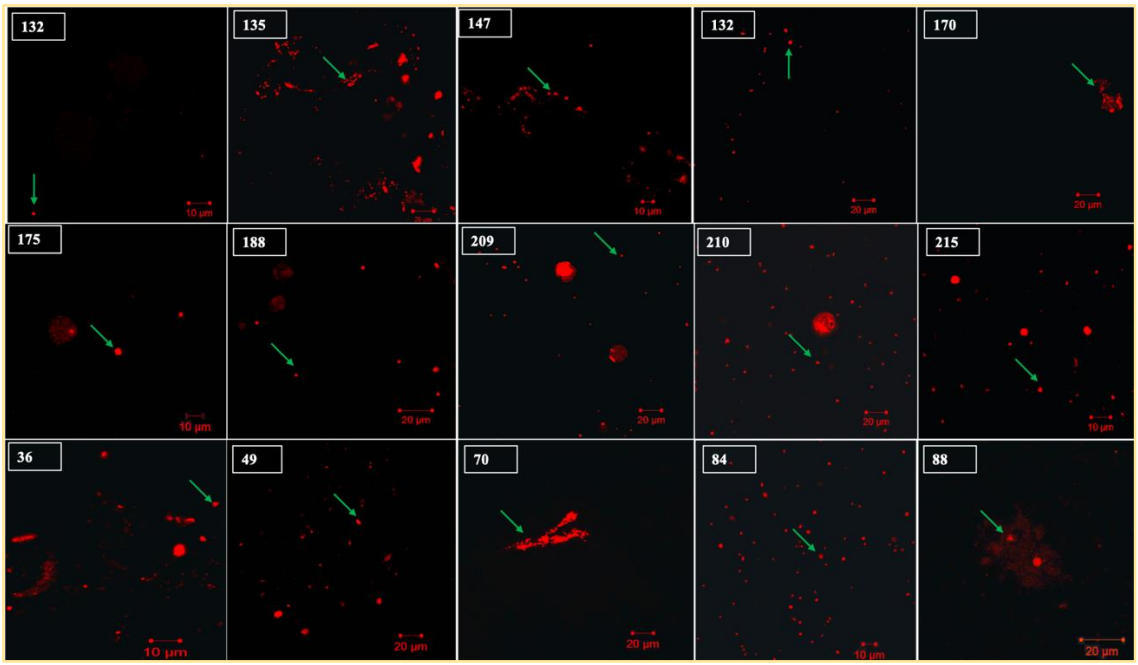

Fig. 3.2.1 Fluorescence micrograph of few sponge samples showing enrichment of Planctomycetes from various geographical locations. Number in the box indicates sample detail of sponge specimen (Annexure 1a,b,c,d,e). Arrow indicates Planctomycetal cells hybridised by CY3 labelled Pla46 probe using red filter.

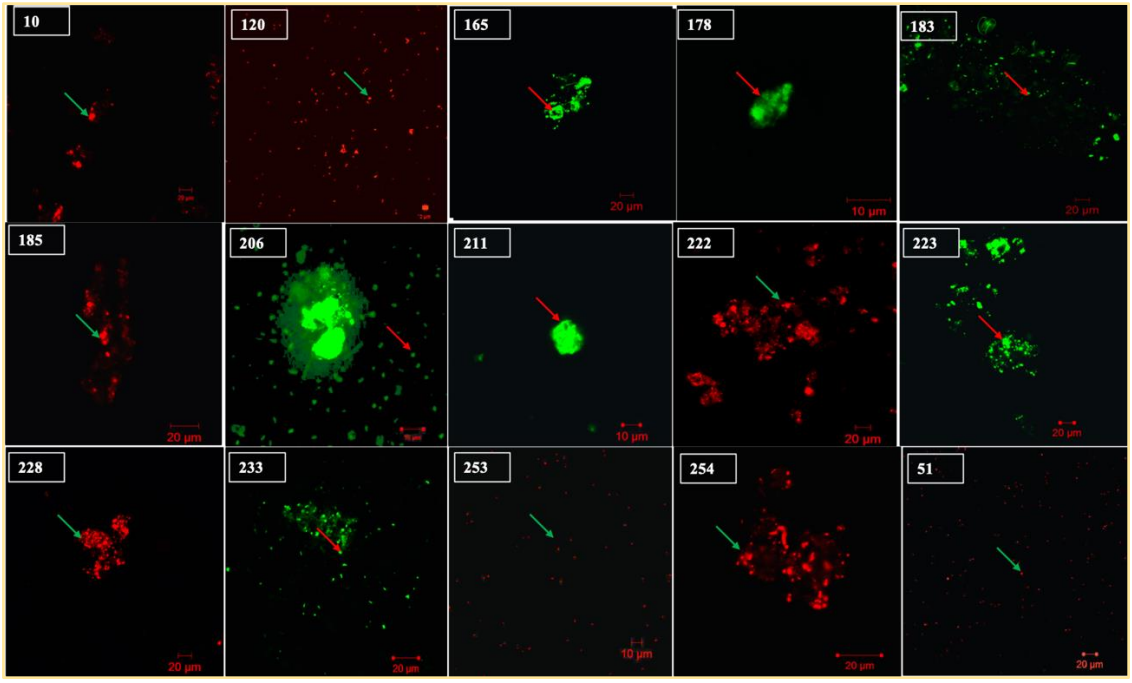

Fig. 3.2.2 Fluorescence micrograph of few algal samples showing enrichment of Planctomycetes from various geographical locations of Tamil Nadu. Numbers in the box indicates sample detail of algal sample (Annexure 1a,b,c,d,e). Arrow indicates Planctomycetal cells hybridised by CY3 labelled Pla46 probe using red filter and green filter.

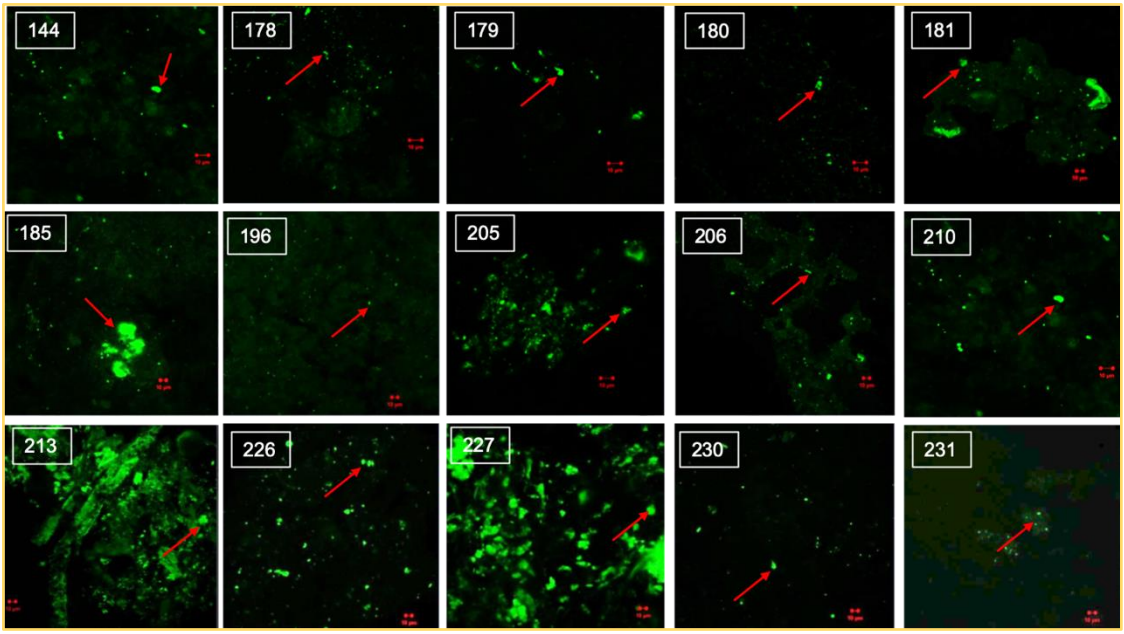

Fig. 3.2.3 Fluorescence micrograph of few algal samples showing enrichment of Planctomycetes from various geographical locations of Gujarat. Number in the box indicates sample detail of algal sample (Annexure 1a,b,c,d,e). Arrows indicate Planctomycetal cells hybridised by CY3 labelled Pla46 probe using green filter.

Eighty three out of 221 algal samples have shown positive enrichment for Planctomycetes which were confirmed through FISH studies. Similarly, 37 out of 102 sponge samples yielded positive enrichments for planctomycetes. Of the 221 sediment samples, 46 samples yielded positive enrichments. Thirty five lichen samples and a sixteen fungi belonging to the genus *Polyporous* have also shown the enrichment for Planctomycetes. Maximum (about 40%) enrichment of Planctomycetes was observed from algal and sponge samples (Fig. 3.2.4).

The geographical based enrichments show maximum of about 40% of samples enriched from both Tamil Nadu and Gujarat, while about 30% of enrichments form Kerala, Odisha and Sikkim (Fig. 3.2.5). This show that Marine samples (mostly collected from Tamil Nadu and Gujarat) harbours more Planctomycetal diversity as compared to other samples like freshwater, lichen, *Polyporous* and soil.

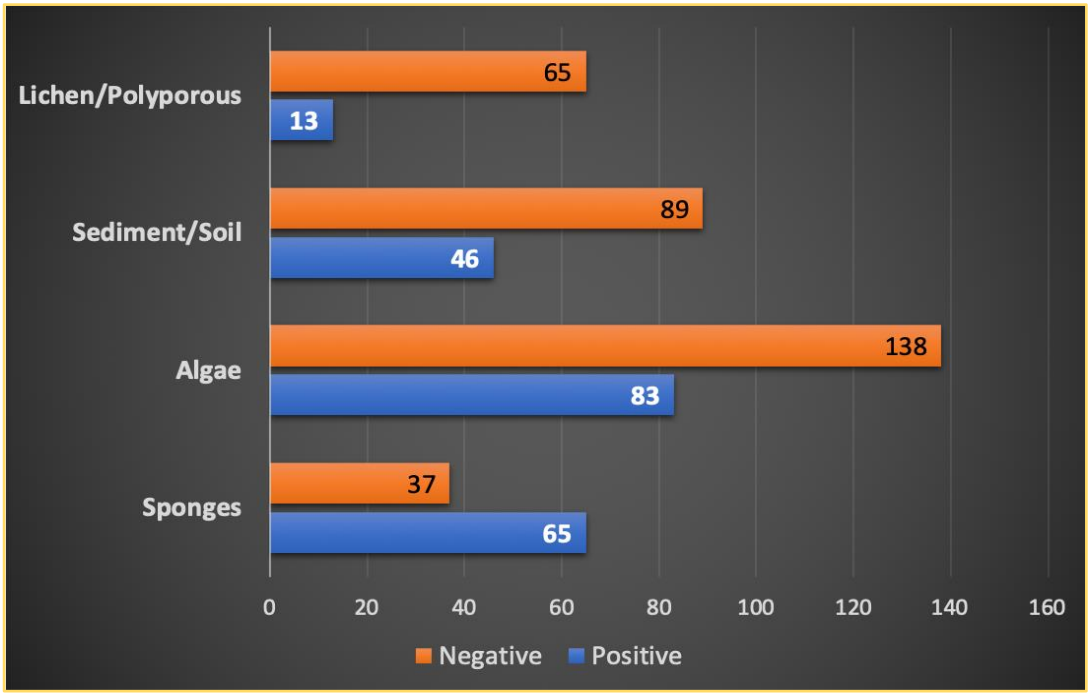

Fig. 3.2.4 Sample based relative enrichments of Planctomycetes based on the FISH analysis.

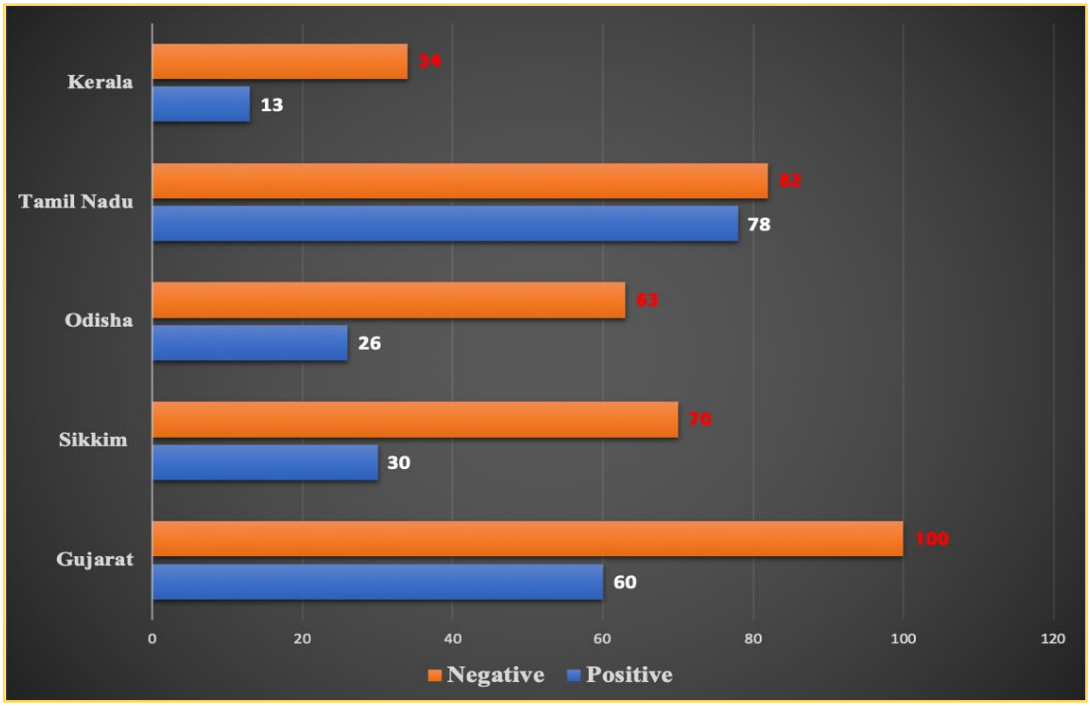

Fig. 3.2.5 Geographical based relative enrichments of Planctomycetes based on the FISH analysis.

3.2.3 Phylogenetic analysis of anammox-planctomycetes from the culture-dependent study

On-site inoculation of five sponge samples collected from wetland ecosystem of Jogadh, Gujarat in anammox-planctomycetes medium (in microcentrifuge tube having Durham's tube inside) ensured positive enrichment of anammox-planctomycetes (in co-cultured communities) and thus enhanced chances of recovering them in culture and minimizing the probability of losing. A three-step enrichment strategy (Fig. 3.2.6) proved quite useful in cultivating different Planctomycetes bacteria. The relative abundance of planctomycetes bacteria in samples was 1-4.3% (from metagenome data), which could be enhanced to 60-70% (deduced from microscopic observation during FISH) in the enrichment cultures. Positive fluorescence (Fig. 3II) observed with all the five co-cultured communities using CY3 labeled Pla46 probes for hybridization confirms the presence of anammox-planctomycetes cells (which are growing either as clusters or in isolation) in all the enrichments.

Further, sequential sub-culturing in the test tubes and serum vials in anaerobic conditions helped increase the number of Planctomycetes and reduce relative abundance of other bacteria. The16S rRNA gene sequences having a sequence length greater than 500 bp representing different orders of Planctomycetes were obtained from NCBI. The five 16S rRNA gene sequences from the enrichment cultures of the present study were used for phylogenetic analysis using the Maximum Likelihood (ML) method of MEGA-7. 16S rRNA gene sequences obtained from the isolates JC541, JC542, and JC544 cladded with CTUs of "*Candidatus* Brocadia anammoxidans*",* but distinctly out-grouped (Fig. 3.2.7), suggesting that they represent new taxa. In contrast, the sequences of isolates, JC543, and JC545 have formed a separate clade with the uncultured *Phycisphaerae* class.

Since the enrichment cultivation conditions mostly favour the growth of anammox bacteria, we suspect the two isolates (JC543 and JC545) representing putative novel taxa

of *Phycisphaerae* might also have anammox property, which is under investigation since, so far, no members of *Phycisphaerae* are reported as anammox bacteria.

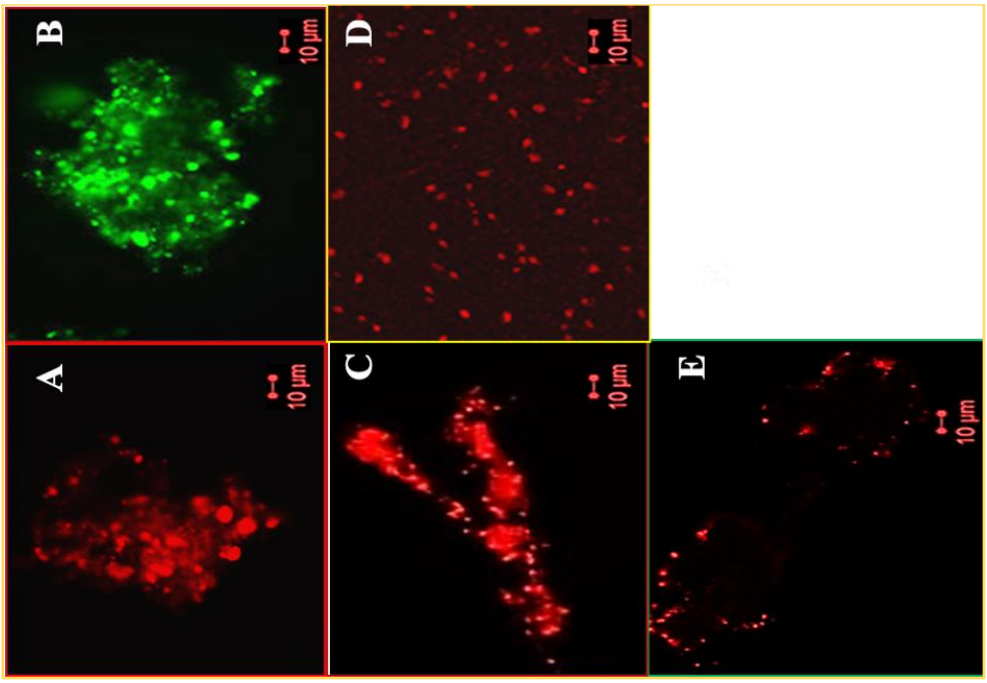

Fig. 3.2.6 Fluorescence micrograph of Planctomycetes bacteria from five sponges enriched samples using CY3 labeled Pla46 probe. (A) JC541, (B) JC542, (C) JC543, (D) JC544, (E) JC544. Scale is of 10 µm.

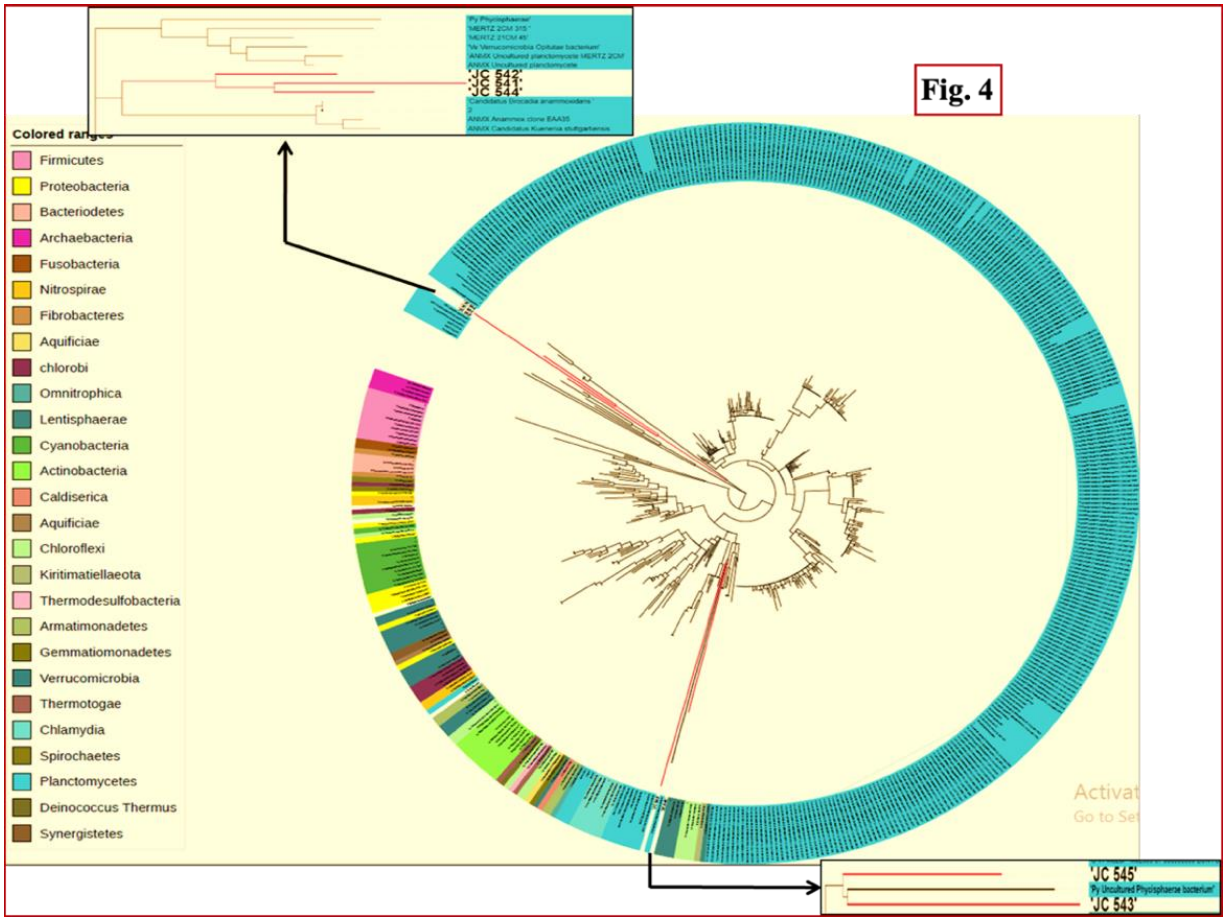

Fig.3.2.7 Phylogenetic tree constructed using the partial sequences of 16S r RNA gene of isolates JC 541, JC542, JC543, JC544 and JC545 along with the sequences belonging to phylum Planctomycetes obtained from amplicon metagenome of three sponge samples. Type strains of different members belonging to different phyla were also taken for phylogenetic analysis. Tree was constructed by the neighbour joining method using MEGA-7 software. The constructed tree was visualized and coloured using online available software Interactive Tree Of Life (iTOL).

3.3 Isolation of Planctomycetes

Various enriched samples from different geographical regions were spread plated onto different growth media after 30-90 days of incubation. Marine samples enrichments, including algae, sponges, and sediments, were spread plated onto the MY and MN media. Soil samples, freshwater sediments, lichen, and *Polyporus* were spread plate onto the MYM media. After 45 to 60 days of incubation, we observed pink colonies along with shiny white colonies. These cultures were further streaked onto their respective media for purification. Planctomycetes of the purified cultures were confirmed through the FISH studies, using Pla46 CY3 labelled probe (Fig. 3.3.1).

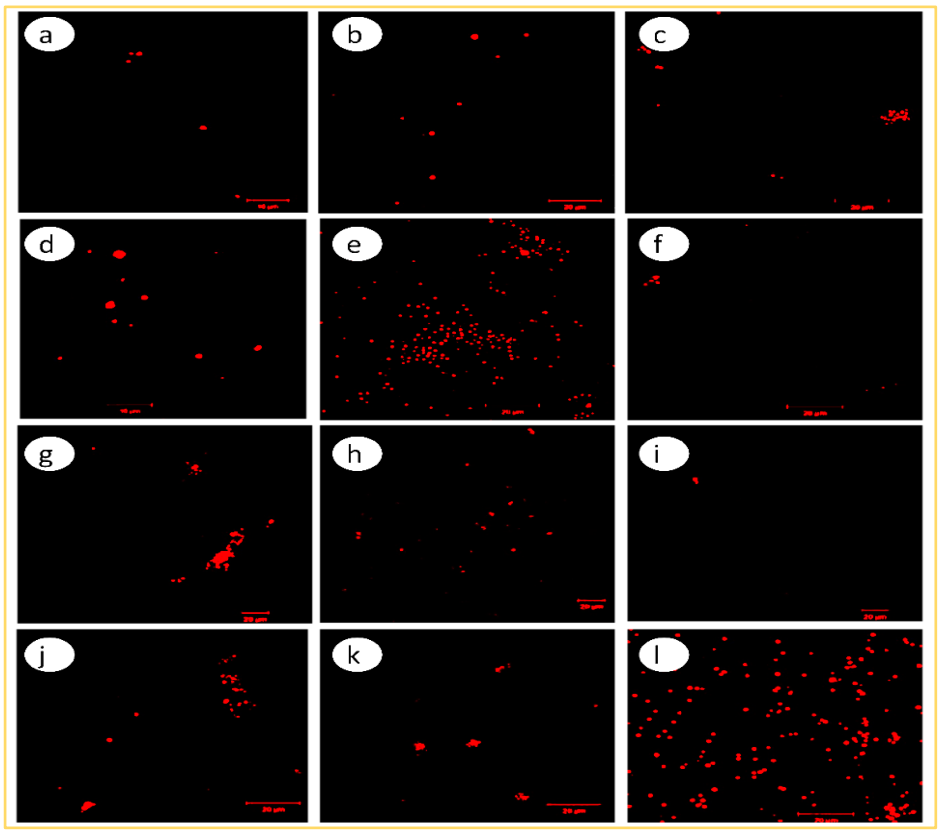

Fig. 3.3.1 Fluorescence micrograph of few cultures of isolated Planctomycetes using CY3 Pla46 labelled probe. a, JC635; b, JC636; c, JC637; d, JC638; e, JC639; f, JC640; g, JC647; h, JC648; i, JC650; j, JC658; k, JC665; l, JC673.

Total, 53 cultures of planctomycetes were purified, of with only 36 strains survived and remained viable. Twenty seven strains became silent or non-viable after seventh to ninth streaking. These axenic but non-viable strains could be the Candidatus members within the Planctomycetes. The axenic strains were further sequenced to assign their strain numbers and putatively their taxonomic rank (Table 3.3.1). These axenic viable strains are further characterized to assign their valid taxonomic rank (Fig. 3.3.2).

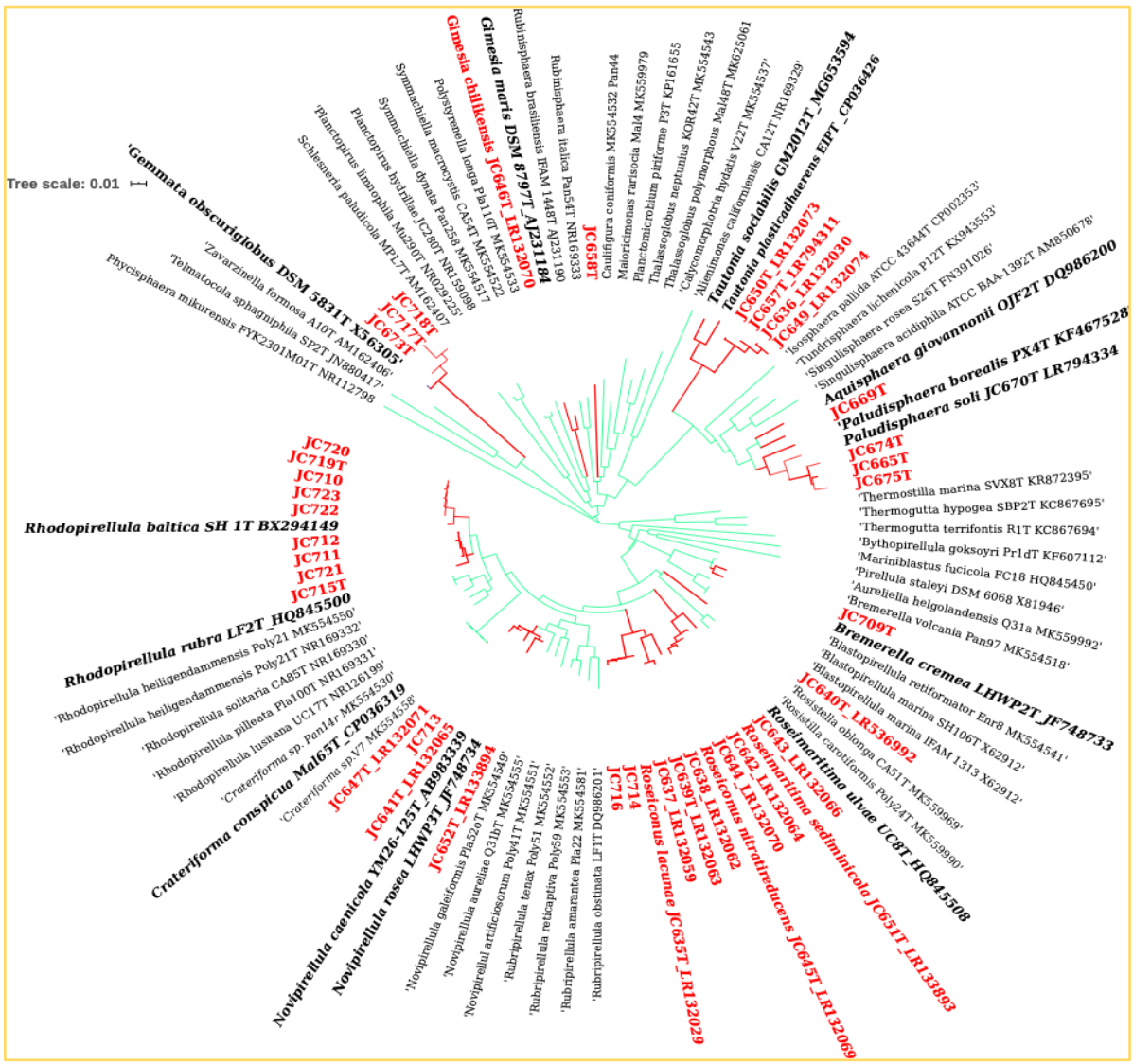

Fig 3.3.2 Phylogeny of the newly isolated axenic Planctomycetal strains. Strains marked in red colour indicates newly isolated strains from our laboratory. Strains marked in black colour are reference strains either validated in IJSEM or effectively published but not validated (present within the inverted comma).

Table. 3.3.1 Details about the isolated axenic strains of Planctomycetes from different geographical locations

Strains Isolated	Place	Source of Isolation	GPS	EzBioCloud based 16S rRNA sequence identity	EMBL accession no.	Culture Deposition
JC635 *Rhodopirellula* sp.	Chilika Lagoon, Odisha	Sediment	19°40'12" N 85°25'48" E	95.8% *Rhodopirellula* baltica SH1^T	LR132029	KCTC 72164 NBRC113875
JC636 *Singulisphaera* sp.	Chilika Lagoon, Odisha	Sediment	19°42'51" N 85°11'54" E	89.1% *Singulisphaera* rosea S26^T	LR132030	NBRC113882
JC638 *Rhodopirellula* sp.	Chilika Lagoon, Odisha	Sediment	19°40'12" N 85°25'48" E	95.8% *Rhodopirellula* baltica SH1^T	LR132062	KCTC72167 NBRC113877
JC640 *Roseimaritima* sp.	Chilika Lagoon, Odisha	Sediment	19°42'51" N 85°11'54" E	91% *Roseimaritima* ulvae DSM 25454^T	LR536992	-
JC645 *Rhodopirellula* sp.	Chilika Lagoon, Odisha	Sediment	19°40'12" N 85°25'48" E	94.2% *Rhodopirellula rubra* LF2^T	LR132069	KCTC72174 NBRC113879
JC646 *Gimesia* sp.	Chilika Lagoon, Odisha	Sediment	19°40'12" N 85°25'48" E	97.4% *Gimesia chilikensis* JC646^T	LR132072	KCTC72175 NBRC113881
JC648 *Singulisphaera* sp.	Chilika Lagoon, Odisha	Sediment	19°42'51" N 85°11'54" E	88.9% *Singulisphaera* rosea S26^T	LR536993	NBRC113884
JC649 *Singulisphaera* sp.	Chilika Lagoon, Odisha	Sediment	19°30'54" N 85°05'53" E	88.9% *Singulisphaera* rosea S26^T	LR132074	NBRC113874
JC650 *Tautonia* sp.	Chilika Lagoon, Odisha	Sediment	19°42'51" N 85°11'54" E	94.5% *Tautonia* sociabilis GM2012^T	LR132073	KCTC72177 NBRC113885
JC651^T *Roseimaritima* sp.	Chilika Lagoon, Odisha	Sediment	19°40'12" N 85°25'48" E	100% *Roseimaritima* sediminicola JC651^T	LR133893	KCTC72178 NBRC113926
JC652 *Rhodopirellula* sp.	Chilika Lagoon, Odisha	Sediment	19°40'12" N 85°25'48" E	98.9% *Rhodopirellula* baltica SH1^T	LR133894	KCTC72179 NBRC114069

JC657 *Tautonia* sp.	Chilika Lagoon, Odisha	Sediment	19°30'54" N 85°05'53" E	94.8% *Tautonia* sociabilis GM2012^T	LR794311	KCTC72597 NBRC113883
JC637 *Rhodopirellula* sp.	Tamil Nadu, Coastal region	Sponge specimen	11°44'17" N 79°43'45" E	94.1% *Rhodopirellula* caenicola YM26-125^T	LR132059	KCTC72166 NBRC 113876
JC639 *Rhodopirellula* sp.	Tamil Nadu, Coastal region	Sponge specimen	10°14'59" N 79°16'43" E	95.8% *Rhodopirellula* baltica SH1^T	LR132063	KCTC72168 NBRC113878
JC641 *Rhodopirellula* sp.	Tamil Nadu, Coastal region	Sponge specimen	09°59'02" N 79°12'09" E	99.1% *Rhodopirellula* caenicola YM26-125^T	LR132065	KCTC72170 NBRC113880
JC642 *Roseimaritima* sp.	Tamil Nadu, Coastal region	Sponge specimen	09°16'52" N 79°10'20" E	99.2% *Roseimaritima* sediminicola JC651^T	LR132064	KCTC72171 NBRC113923
JC643 *Roseimaritima* sp.	Tamil Nadu, Coastal region	Sponge specimen	09°16'52" N 79°10'20" E	99.4% *Roseimaritima* sediminicola JC651^T	LR132066	KCTC72172 NBRC113924
JC644 *Roseimaritima* sp.	Tamil Nadu, Coastal region	Sponge specimen	09°16'52" N 79°10'20" E	99.1% *Roseimaritima* sediminicola JC651^T	LR132070	KCTC72173 NBRC113925
JC647 *Rhodopirellula* sp.	Tamil Nadu, Coastal region	Sponge specimen	09°16'52" N 79°10'20" E	94.4% *Rhodopirellula* rubra LF2^T	LR132071	KCTC72176 NBRC114068
JC658 *Planctomicrobium* sp.	Tamil Nadu, Coastal region	Sponge specimen	09°09'55" N 78°38'33" E	87.4% *Planctomicrobium* piriforme	LR898466	KCTC72881
JC669 *Aquisphaera* sp.	Loktak, Lagoon	Rhizosphere	24°30'21"N 93°47'43"E	96% *Aquisphaera* giovannoni	LR782133	KCTC72672 NBRC 114306
JC673/P56 *Gemmata* sp.	Kerala Wetland	Algal mat	11° 30' 11" N 75° 38' 09" E	99.1% *Gemmata* obscuriglobus	LR898467	-
JC717T *Gemmata* sp.	Kerala, Wetland	Algal mat	11° 30' 11" N 75° 38' 09" E	99.2% *Gemmata* obscuriglobus	ERZ1756645	-

JC718 *Gemmata* sp.	Kerala, Wetland	Algal mat	11° 30' 11" N 75° 38' 09" E	99.3% *Gemmata* obscuriglobus	ERZ1756646	-
JC675/P58 *Paludisphaera* sp.	Kerala, Wetland	Algal mat	11° 30' 11" N 75° 38' 09" E	94% *Paludisphaera* borealis	-	-
JC709 Blastopirellula sp.	Tamil Nadu, Coastal region	Sponge	09°09'55" N 78°38'33" E	98.6% *Blastopirellula* cremea	ERZ1756633	-
JC710 Rhodopirellula sp.	Tamil Nadu, Coastal region	Sponge	09°09'55" N 78°38'33" E	98.5% *Rhodopirellula* baltica	ERZ1756634	-
JC711 Rhodopirellula sp.	Tamil Nadu, Coastal region	Algae	09°59'02" N 79°12'09" E	98.9% *Rhodopirellula* rubra LF2^{T}	ERZ1756635	-
JC712 Rhodopirellula sp.	Tamil Nadu, Coastal region	Algae	09°16'52" N 79°10'20" E	98.9% *Rhodopirellula* rubra LF2^{T}	ERZ1756636	-
JC713 Rhodopirellula sp.	Tamil Nadu, Coastal region	Algae	09°16'52" N 79°10'20" E	98.9% *Rhodopirellula* caenicola YM26-125^{T}	ERZ1756637	-
JC714 Rhodopirellula sp.	Tamil Nadu, Coastal region	Algae	09°09'55" N 78°38'33" E	94.1% *Rhodopirellula* caenicola YM26-125^{T}	ERZ1756638	-
JC715 Rhodopirellula sp.	Tamil Nadu, Coastal region	Sponge specimen	09°09'55" N 78°38'33" E	98.9% *Rhodopirellula sallentina*	ERZ1756639	-
JC716 Rhodopirellula sp.	Tamil Nadu, Coastal region	Sponge specimen	09°09'55" N 78°38'33" E	93.32% *Rhodopirellula* caenicola YM26-125^{T}	ERZ1756641	-
JC719 Rhodopirellula sp.	Tamil Nadu, Coastal region	Algae	09°09'55" N 78°38'33" E	98.5% *Rhodopirellula* baltica	ERZ1756642	-
JC720 Rhodopirellula sp	Tamil Nadu, Coastal region	Algae	09°09'55" N 78°38'33" E	98.5% *Rhodopirellula* baltica	ERZ1756643	-

JC721 Rhodopirellula sp	Tamil Nadu, Coastal region	Algae	09°09'55" N 78°38'33" E	98.9% *Rhodopirellula* rubra LF2^{T}	ERZ1756644	-
JC722 Rhodopirellula sp	Tamil Nadu, Coastal region	Algae	09°09'55" N 78°38'33" E	99.0% *Rhodopirellula* baltica	ERZ1756647	-
JC723 Rhodopirellula sp	Tamil Nadu, Coastal region	Algae	09°09'55" N 78°38'33" E	98.6% *Rhodopirellula* baltica	ERZ1756648	-

3.4 Phylo-taxogenomic studies of the newly isolated axenic cultures of Planctomycetes from Chilika lagoon

Twenty axenic strains of Planctomycetes were isolated from the Chilika lagoon. Total eleven isolated strains of Planctomycetes remained viable and nine strains became silent after 9^{th}-11^{th} sub culturing. Further, phylo-taxogenomic studies of nine strains were carried out (Fig. 3.4.1).

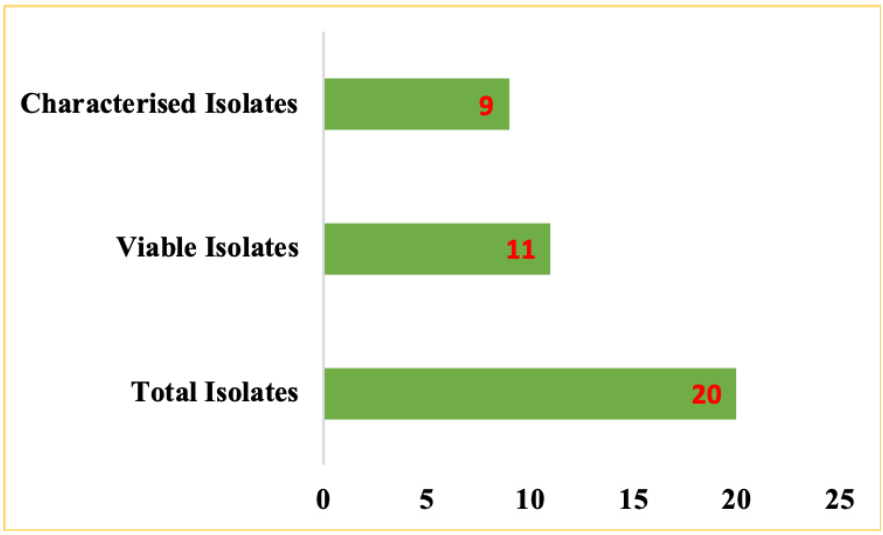

Fig. 3.4.1 Detail about the total Planctomycetal strains isolated, remain viable and strains Phylo-taxogenonomic studied (Characterised) from the Chilika lagoon.

3.4.1 Phylo-taxogenomic study of the strains JC635^T and JC645^T

3.4.1.1 Habitat and Nucleotide sequences accession numbers

The strains JC635^T and JC645^T isolated from the sediment samples collected from Satpada region (19°40'12"N; 85°25'48"E) of Chilika lagoon, Odisha, India. The 16S rRNA gene sequences of both the taxa was deposited with European Molecular Biology Laboratory (EMBL) with accession numbers LR132029 and LR132069. The whole genome sequences of strains JC635^T and JC645^T (7951142 nt and 8196902 nt) was deposited to NCBI with accession numbers VSZO00000000and VWOX00000000, respectively.

3.4.1.2 Genomic characteristics

Genome size of the strain JC635^T is 7.9Mb with N_{50} value of 466,683 while the genome size of strain JC645^{T}is 8.2Mb with N_{50} value of403,299. Genome of strain JC635^T has 5,570genes of which 5,410 are protein coding genes, 79 genes code for RNAs and 81genes are pseudogenes. While strain JC645^T has 5,806 genes of which 5,637 are protein coding genes, 83 genes code for RNAs and 86 genes are pseudogenes (Table 3.4.1.1). Genomic DNA G+C content of strains JC635^T and JC645^T are 55.1mol% and 60.0 mol%, respectively. The G+C content between the two taxa varied by 8.2% which is more than 3% for species delineation (Meier-Kolthoff et al. 2014).

3.4.1.3 BLAST Analysis and Phylogenetic inference

BLAST analysis of amplicon based 16S rRNA gene sequence of strains JC635^T (1414 nt) and JC645^T (1268 nt) in EzBiocloud server showed that these strains share highest identity with members of the genus *Rhodopirellula* (<94%) and *Roseimaritima* (<94). The 16S rRNA sequence similarity between strains JC635^T and JC645^T is 96.1% (Fig. 3.4.1.1). The OrthoANI value between strains JC635^T and JC645^T is 71.0%. The *d*DDH value between strains JC635^T and JC645^T is 21.2%. OrthoANI and *d*DDH values (Fig. 3.4.1.1) between strains JC635^{T}and JC645^T is far less (95-96% cut off for ANI and 70% cut off for *d*DDH) than the recommended cut-off values for species delineation (Goris et al. 2007; Richter and Rossello-Mora 2009) thus, both strains represent two different species. Comparison of POCP values (Table 3.4.1.2; Fig. 3.4.1.1) of strains JC635^T and JC645^T with *Rhodopirellula* spp. and *Roseimaritima* spp. yielded a minimal similarity of 49.1% and 50.4%, respectively.

Table 3.4.1.1 Comparative genomic features among members of genus *Rhodopirellua*. and genus *Roseimaritima* with strain JC635^T and JC645^T.

	Organism	Accession No	Sequencing Technology	Genome coverage	Genome size (Mb)	No of contigs	GC %	N50 (bp)	Genes (total)	CDS (Total)	CDS (Protien)	rRNA	tRNA	Other RNA	Pseudogene	CRISPR s
1	**JC635^T**	NZ_VSZO01000000	Illumina HiSeqX10	100.0x	7.9	97	55.1	466,683	5,570	5,491	5,410	3	72	4	81	0
2	**JC645^T**	NZ_VWOX00000000	Illumina HiSeqX10	100.0x	8.2	108	60.0	403,299	5,806	5,723	5,637	4	74	5	86	
3	***Rhodopirellula baltica* SH1^T**	NC_005027	Combination of a clone-based and a whole-genome shotgun	NA	7.15	1	55.4	7,145,576	5,447	5,358	5,239	3	83	3	119	0
4	***Roseimaritima ulvae* DSM 25454^T**	NZ_LWSJ01000001	Illumina MiSeq	50.0x	8.11	103	59.1	127,469	5,796	5,723	5,625	3	67	3	98	0
5	***Roseimaritima sedimincola* JC651^T**	NZ_WIAD01000001	Illumina HiSeqX10	100.0x	6.25	185	62.4	92,046	4,546	4,494	4,405	3	46	3	89	0

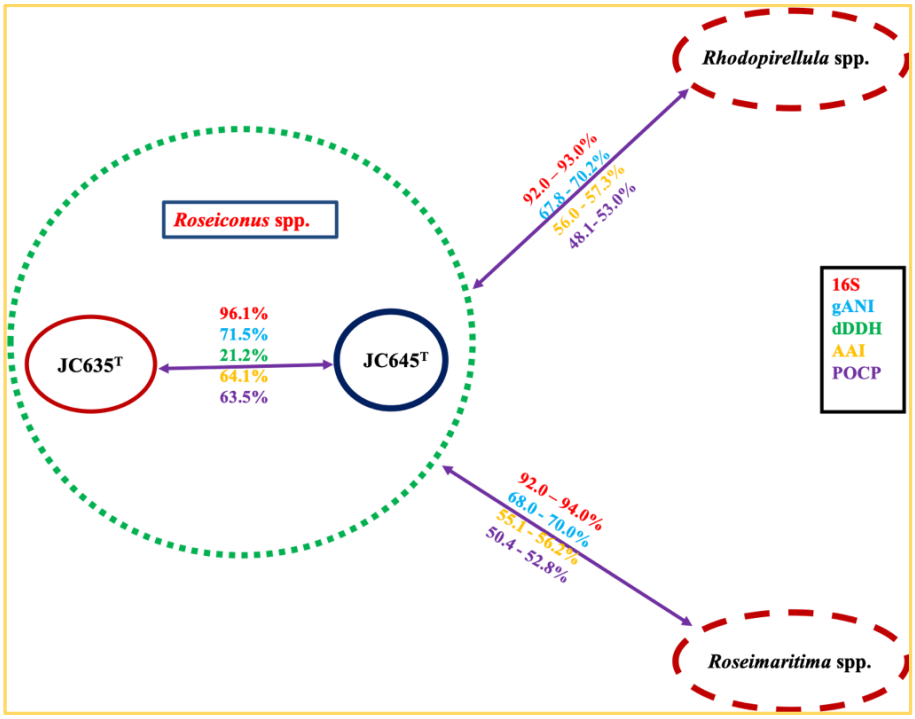

Fig. 3.4.1.1 Analysis of phylogenetic markers for delineation of the novel isolates JC635^{T}and JC645^T. Methods used: 16S rRNA gene identity (16S), average amino acid identity (AAI), average nucleotide identity (ANI) and percentage of conserved proteins (POCP).

These values are below or very close to the POCP value of 50% for delineating taxa of Planctomycetes at the level of genus (Peeters et al. 2020a), affirming that both strains represent a novel genus within the family Pirellulaceae. The AAI values (Table 3.4.1.3; Fig. 3.4.1.1) of both strains with *Rhodopirellula* spp. and *Roseimaritima* spp. yielded a minimal similarity of 56.4% and 55.1%, respectively. These values are also below the genus delineating threshold AAI value of 60% (Rodriguez and Konstantinidis 2014) supporting the proposal of a novel genus. High POCP value (63.8%) and high AAI value (64.1%) between the strains JC635^T and JC645^T (Table 3.4.1.2,3) allow these strains to be classified under the same genus as per the recommended standards (Qin et al. 2014, Luo et al. 2014). The 16S rRNA gene sequences of strains JC635^T and JC645^T extracted from the genome has sequence length of 1532 nt and 1530 nt respectively and the BLAST search

results are also similar. The 16S rRNA gene sequence based phylogenetic tree with combined bootstrap values obtained from NJ, ME, ML trees (Fig. 3.4.1.2) and 92 core genes based phylogenomic tree (Fig. 3.4.1.3) confirmed the distinct monophyletic clustering of strains JC635^T and JC645^T within the family Pirellulaceae. Strains JC635^T and JC645^T are distinctly separated from each other suggesting two novel species of a novel genus in the family Pirellulaceae.

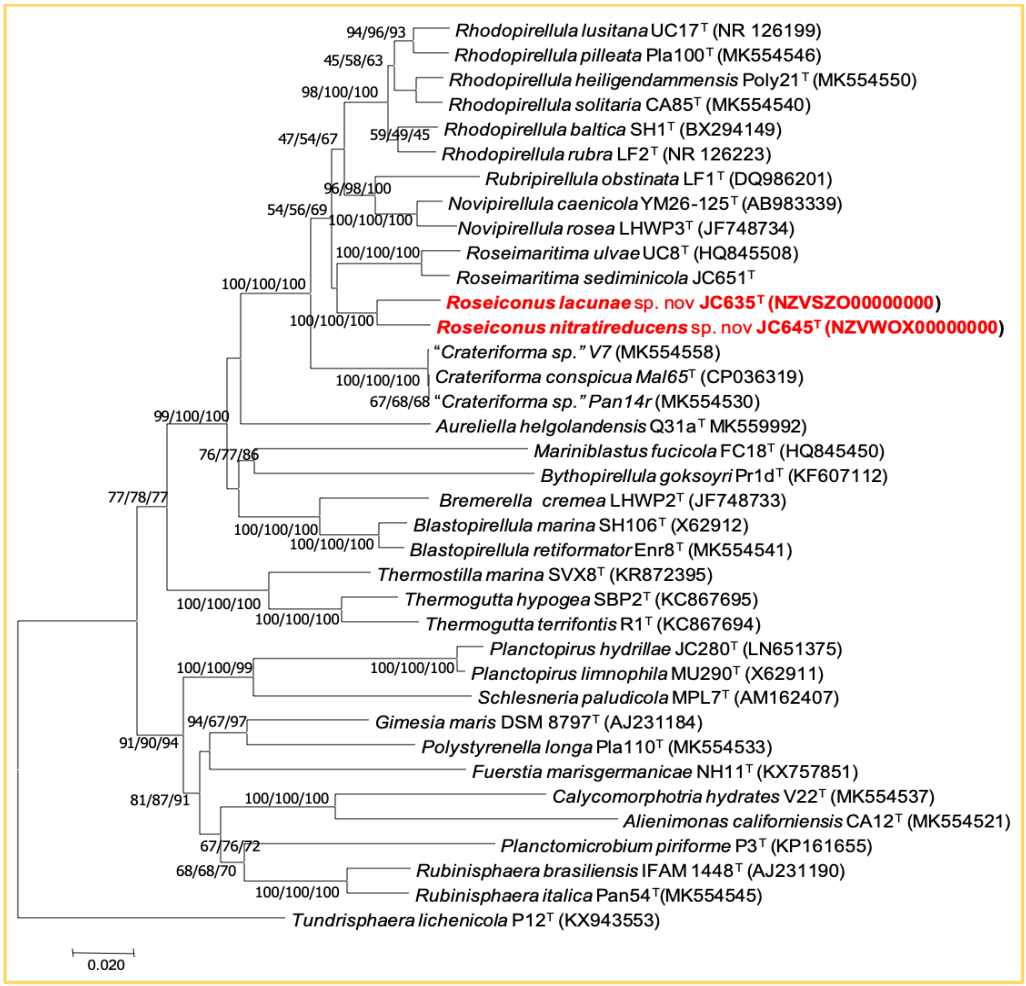

Fig. 3.4.1.2 The 16S rRNA gene sequences based phylogenetic tree showing the phylogenetic relationship of strains JC645^T, JC635^{T}within the family Planctomycetaceae and Pirellulaceae along with some of the clone sequences obtained from NCBI having >96% sequence similarities with both the strains.

Table 3.4.1.2 POCP values (%) Matrix among some members of planctomycetaceae and Pirellulaceae including strains JC635^T and JC645^T.

	1	2	3	4	5	6	7	8	9	10	11	12	13	14	15	16	17	18	19	20	21	22	23	24	25	26	27	28	29	30	31	32
1	100.0																															
2	28.7	100.0																														
3	29.2	37.0	100.0																													
4	29.8	36.6	57.5	100.0																												
5	30.0	37.1	72.6	59.7	100.0																											
6	26.2	31.4	32.8	34.0	34.3	100.0																										
7	22.5	29.0	29.5	32.3	31.0	27.6	100.0																									
8	28.8	40.9	33.6	33.4	35.4	31.0	27.6	100.0																								
9	32.2	34.7	30.8	32.0	30.9	27.8	25.9	30.3	100.0																							
10	34.5	30.6	33.5	35.6	34.3	27.8	26.5	26.9	40.9	100.0																						
11	35.2	30.9	34.4	35.2	34.7	27.8	26.8	27.6	41.3	81.1	100.0																					
12	**28.2**	**41.8**	**34.4**	**33.5**	**35.1**	**29.6**	**25.7**	**55.1**	**32.3**	**29.2**	**29.4**	**100.0**																				
13	**29.3**	**42.8**	**35.6**	**34.3**	**36.4**	**31.0**	**27.6**	**55.2**	**33.6**	**30.1**	**31.8**	**63.5**	**100.0**																			
14	25.4	29.7	33.1	34.6	33.7	47.3	26.9	27.9	25.7	26.6	26.7	**27.1**	**28.9**	100.0																		
15	24.4	32.1	30.1	30.1	30.5	27.5	23.6	32.4	28.3	25.1	25.4	**32.3**	**31.2**	26.2	100.0																	
16	28.9	41.9	33.5	34.0	34.6	28.8	26.3	51.0	32.1	29.3	29.7	**51.5**	**53.8**	26.7	31.5	100.0																
17	29.1	35.7	41.8	44.8	44.4	33.9	33.2	32.8	29.2	31.5	32.2	**33.0**	**34.1**	35.9	29.7	32.3	100.0															
18	34.0	28.1	29.5	32.3	31.2	27.1	24.3	25.8	35.3	39.8	40.2	**26.8**	**28.5**	30.2	24.1	27.2	32.8	100.0														
19	15.5	13.7	13.1	13.2	13.6	12.2	11.2	12.1	20.1	16.5	17.3	**12.9**	**13.5**	12.2	11.7	12.1	15.4	17.2	100.0													
20	35.4	27.3	29.5	30.9	30.8	25.7	23.3	25.6	32.2	38.6	38.9	**25.7**	**26.3**	26.8	23.0	25.0	34.6	41.7	17.7	100.0												
21	36.0	30.7	31.0	32.3	32.1	28.5	24.5	28.0	38.3	45.9	46.7	**27.7**	**29.4**	27.0	24.8	27.6	31.6	38.1	16.8	38.2	100.0											
22	28.5	43.4	33.9	34.1	34.7	30.7	25.6	56.5	33.1	28.8	29.1	**54.6**	**55.2**	28.0	32.4	54.6	33.4	27.0	12.1	25.8	28.7	100.0										
23	30.4	42.0	33.6	34.3	34.7	29.9	26.8	51.6	31.4	28.6	28.6	**51.2**	**52.2**	27.9	30.6	52.7	32.6	26.8	12.3	26.2	27.9	59.5	100.0									
24	28.9	43.3	33.9	33.6	34.8	30.6	25.7	56.9	33.0	28.5	29.1	**53.9**	**54.9**	27.6	32.4	54.2	33.3	26.8	12.3	26.0	28.4	82.8	58.8	100.0								
25	28.9	45.1	34.4	34.7	35.3	30.7	26.4	55.8	33.8	29.4	29.9	**53.7**	**54.4**	28.3	32.9	54.6	33.7	27.3	12.8	26.4	29.5	80.0	60.7	78.1	100.0							
26	26.6	38.9	31.0	31.5	32.5	29.7	25.1	55.0	29.2	26.1	26.5	**49.1**	**50.0**	26.4	31.6	54.3	30.8	25.2	11.2	24.4	26.2	60.9	59.2	59.9	60.8	100.0						
27	32.7	44.8	37.4	38.6	38.4	32.5	30.7	50.8	33.3	31.1	32.1	**50.4**	**51.9**	30.8	33.1	53.7	37.5	29.5	14.3	28.4	31.4	52.4	53.8	52.4	53.5	48.0	100.0					
28	31.3	46.7	37.9	38.2	38.8	31.6	29.2	50.7	35.0	32.3	32.5	**51.7**	**52.8**	29.6	33.6	56.6	36.8	29.3	14.1	27.5	30.2	53.5	51.8	53.2	54.5	49.3	71.8	100.0				
29	38.5	31.2	34.2	35.6	36.1	27.9	24.6	31.3	37.4	43.5	44.7	**31.6**	**32.5**	26.4	26.3	31.3	32.5	41.4	16.4	42.0	41.2	31.3	31.4	31.7	31.5	30.1	33.6	33.7	100.0			
30	24.2	35.0	28.2	28.8	30.0	28.2	23.7	52.2	25.6	22.9	23.1	**48.1**	**48.7**	25.8	30.4	49.3	29.3	23.2	10.5	22.8	23.6	50.9	47.7	50.7	50.2	50.4	47.0	45.3	25.3	100.0		
31	30.1	27.7	28.8	30.5	28.7	25.0	24.6	23.6	35.3	39.5	40.3	**26.0**	**27.2**	28.4	22.5	25.8	32.1	40.8	17.7	42.2	37.7	24.5	25.6	24.0	24.8	22.9	27.3	28.0	36.0	21.2	100.0	
32	26.0	27.2	30.7	33.4	32.8	30.2	36.0	28.2	22.9	25.1	25.5	**25.3**	**26.4**	29.1	23.5	24.8	34.6	25.4	12.0	26.8	26.0	25.3	26.9	24.9	26.1	25.8	30.9	27.8	27.0	24.4	23.8	100.0

1. *Alienimonas californiensis* CA12^T 2. *Aureliella helgolandensis* Q31a^T 3. *Blastopirellula cremea* HEX-1 MGV^T 4. *Blastopirellula marina* DSM 3645^T 5. *Bremerella volcania* Pan97^T 6. *Bythopirellula goksoyri* Pr1d^T 7. *Candidatus* Anammoximicrobium sp. AS06rmzACSIP 8. *Crateriforma conspicua* Mal65^T 9. *Fuerstia marisgermanicae* NH11^T 10. *Gimesia maris* DSM 8797^T 11. *Gimesia chilikensis* JC646^T **12. Strain JC635^T 13. Strain JC645^T** 14. *Lacipirellula parvula* PX69^T 15. *Mariniblastus fucicola* FC18^T 16. *Novipirellula maiorica* SM1^T 17. *Pirellula staleyi* DSM 6068^T 18. *Planctomicrobium piriforme* DSM 26348^T 19. *Planctomyces bekefii* phe10_nw2017^T 20. *Planctopirus limnophila* DSM 3776^T 21. *Polystyrenella longa* Pla110^T 22. *Rhodopirellula baltica* SH 1^T 23. *Rhodopirellula solitaria* CA85^T 24. *Rhodopirellula europaea* 6C^T 25. *Rhodopirellula islandica* K833^T 26. *Rhodopirellula sallentina* SM41^T 27. *Roseimaritima sediminicola* JC651^T 28. *Roseimaritima ulvae* DSM 25454^T 29. *Rubinisphaera brasiliensis* DSM 5305^T 30. *Rubripirellula obstinata* CECT 8602^T 31. *Schlesneria paludicola* DSM 18645^T 32. *Thermogutta terrifontis* R1^T

Table 3.4.1.3 AAI values (%) Matrix among some members of *planctomycetaceae and Pirellulaceae* including strains JC635^{T} and JC645^{T}.

	1	**2**	**3**	**4**	**5**	**6**	**7**	**8**	**9**	**10**	**11**	**12**	**13**	**14**	**15**	**16**	**17**	**18**	**19**	**20**	**21**	**22**	**23**	**24**	**25**	**26**	**27**	**28**	**29**	**30**	**31**	**32**
1	100.0																															
2	44.1	100.0																														
3	44.0	47.8	100.0																													
4	44.3	48.1	57.5	100.0																												
5	43.8	48.0	74.1	57.8	100.0																											
6	43.5	47.1	48.4	49.1	48.5	100.0																										
7	43.5	47.4	48.3	49.4	48.6	47.6	100.0																									
8	43.8	49.6	47.0	47.1	47.2	46.2	46.6	100.0																								
9	46.9	47.0	45.4	45.7	45.4	44.7	44.4	44.8	100.0																							
10	47.3	45.1	46.2	46.7	45.9	44.8	44.6	43.8	50.2	100.0																						
11	47.3	45.0	46.6	46.5	46.2	45.1	44.9	43.8	50.3	77.1	100.0																					
12	**43.5**	**49.7**	**47.1**	**46.9**	**47.2**	**45.9**	**45.8**	**57.4**	**45.8**	**44.2**	**44.3**	**100.0**																				
13	**44.3**	**50.4**	**47.8**	**47.4**	**47.9**	**46.5**	**46.4**	**58.0**	**46.3**	**44.9**	**45.2**	**64.1**	**100.0**																			
14	43.6	46.1	48.1	49.0	48.2	56.8	47.8	45.6	43.9	44.2	44.5	**45.0**	**46.0**	100.0																		
15	42.0	46.1	45.6	45.7	45.9	45.3	44.8	46.0	44.2	43.0	43.0	**46.0**	**45.8**	44.5	100.0																	
16	44.4	50.8	47.4	47.4	47.5	45.9	46.4	57.7	46.5	45.1	44.8	**57.3**	**58.5**	45.4	46.5	100.0																
17	43.8	48.1	49.9	50.9	50.2	48.8	50.9	47.0	44.6	45.2	45.2	**46.6**	**47.1**	49.5	45.8	47.0	100.0															
18	46.9	44.3	44.8	45.8	44.8	44.4	44.2	43.0	48.6	49.8	49.7	**43.4**	**43.9**	46.0	42.2	43.8	45.7	100.0														
19	43.0	40.9	41.1	41.1	41.0	40.4	40.8	40.2	48.8	44.2	44.5	**40.1**	**40.9**	40.6	39.4	40.3	41.7	44.2	100.0													
20	46.6	43.3	44.1	44.5	44.3	43.6	43.5	42.8	47.0	48.8	49.2	**42.6**	**43.5**	44.2	42.4	42.8	45.4	49.3	44.1	100.0												
21	46.8	44.8	45.1	45.4	45.2	44.7	43.7	43.4	49.6	52.2	52.3	**43.4**	**44.1**	43.8	41.6	43.9	44.8	48.9	43.5	48.0	100.0											
22	44.0	50.4	46.8	46.8	46.9	46.2	45.5	58.2	45.8	44.2	44.2	**56.2**	**56.9**	45.1	42.4	58.3	46.4	43.3	39.9	42.8	43.7	100.0										
23	43.9	50.4	46.9	47.0	46.8	46.2	45.7	58.3	46.0	44.3	44.4	**56.4**	**57.2**	45.4	46.4	58.3	46.6	43.2	39.7	42.8	43.9	87.8	100.0									
24	44.1	50.6	46.9	46.9	46.9	46.2	45.7	58.2	45.9	44.2	44.5	**56.3**	**57.3**	45.4	46.4	58.3	46.8	43.2	39.9	42.7	43.8	88.7	92.3	100.0								
25	43.6	49.5	46.3	46.5	46.5	46.0	45.5	58.0	45.1	43.6	43.6	**55.2**	**56.2**	45.0	46.3	58.4	46.3	43.0	39.2	42.4	43.4	63.3	63.5	63.2	100.0							
26	44.3	50.6	46.9	47.4	47.0	46.2	46.0	56.9	46.0	44.3	44.3	**55.9**	**56.8**	45.7	45.7	58.2	46.6	43.5	40.1	42.7	43.6	62.3	62.7	62.5	68.1	100.0						
27	45.0	51.5	48.1	48.2	48.2	47.2	48.2	55.5	46.3	45.2	45.5	**55.0**	**56.1**	46.7	46.3	57.4	48.4	44.5	40.9	43.4	44.5	55.6	55.7	55.8	55.0	56.0	100.0					
28	45.0	52.1	48.4	48.5	48.5	47.1	47.6	55.5	47.2	45.7	43.9	**54.9**	**55.7**	46.3	46.7	58.9	48.1	44.5	41.4	43.6	44.6	56.2	55.8	56.1	55.4	55.9	72.5	100.0				
29	47.7	45.3	46.2	46.0	46.5	44.6	44.0	45.1	49.1	50.4	51.1	**45.3**	**46.0**	44.3	43.5	45.9	45.0	50.0	14.4	48.5	49.7	45.2	45.2	45.2	44.7	45.1	45.8	46.0	100.0			
30	42.6	48.1	45.8	45.9	46.1	45.5	45.2	58.0	43.5	42.6	44.6	**56.7**	**57.5**	45.1	45.9	59.1	46.1	42.1	39.1	41.9	42.2	56.9	57.1	57.4	57.3	56.8	54.9	55.0	43.1	100.0		
31	46.0	44.0	44.3	45.2	44.3	44.1	44.4	42.7	47.9	49.9	49.9	**43.1**	**43.7**	45.3	41.9	43.4	45.9	50.4	15.0	52.2	49.3	42.7	42.9	42.6	42.4	43.1	43.8	44.0	48.5	41.7	100.0	
32	43.0	44.8	46.5	47.3	46.7	47.1	49.9	44.9	42.8	43.4	43.7	**43.9**	**44.8**	47.2	42.6	44.2	47.7	43.4	40.0	43.6	43.2	44.0	44.2	44.1	43.9	44.2	45.7	45.0	43.6	43.8	43.3	100.0

1. *Alienimonas californiensis* CA12^{T} 2. *Aureliella helgolandensis* Q31a^{T} 3. *Blastopirellula cremea* HEX-1 MGV^{T} 4. *Blastopirellula marina* DSM 3645^{T} 5. *Bremerella volcania* Pan97^{T} 6. *Bythopirellula goksoyri* Pr1d^{T} 7. *Candidatus* Anammoximicrobium sp. AS06rmzACSIP 8. *Crateriforma conspicua* Mal65^{T} 9. *Fuerstia marisgermanicae* NH11^{T} 10. *Gimesia maris* DSM 8797^{T} 11. *Gimesia chilikensis* JC646^{T} **12. JC635^{T} 13. JC645^{T}** 14. *Lacipirellula parvula* PX69^{T} 15. *Mariniblastus fucicola* FC18^{T} 16. *Novipirellula maiorica* SM1^{T} 17. *Pirellula staleyi* DSM 6068^{T} 18. *Planctomicrobium piriforme* DSM 26348^{T} 19. *Planctomyces bekefii* phe10_nw2017^{T} 20. *Planctopirus limnophila* DSM 3776^{T} 21. *Polystyrenella longa* Pla110^{T} 22. *Rhodopirellula bahuensis* SWK21^{T} 23. *Rhodopirellula baltica* SH 1^{T} 24. *Rhodopirellula europaea* 6C^{T} 25. *Rhodopirellula sallentina* SM41^{T} 26. *Rhodopirellula solitaria CA85^{T}* 27. *Roseimaritima sediminicola* JC651^{T} 28. *Roseimaritima ulvae* DSM 25454^{T} 29. *Rubinisphaera brasiliensis* DSM 5305^{T} 30. *Rubripirellula obstinata* CECT 8602^{T} 31. *Schlesneria paludicola* DSM 18645^{T} 32. *Thermogutta terrifontis* R1

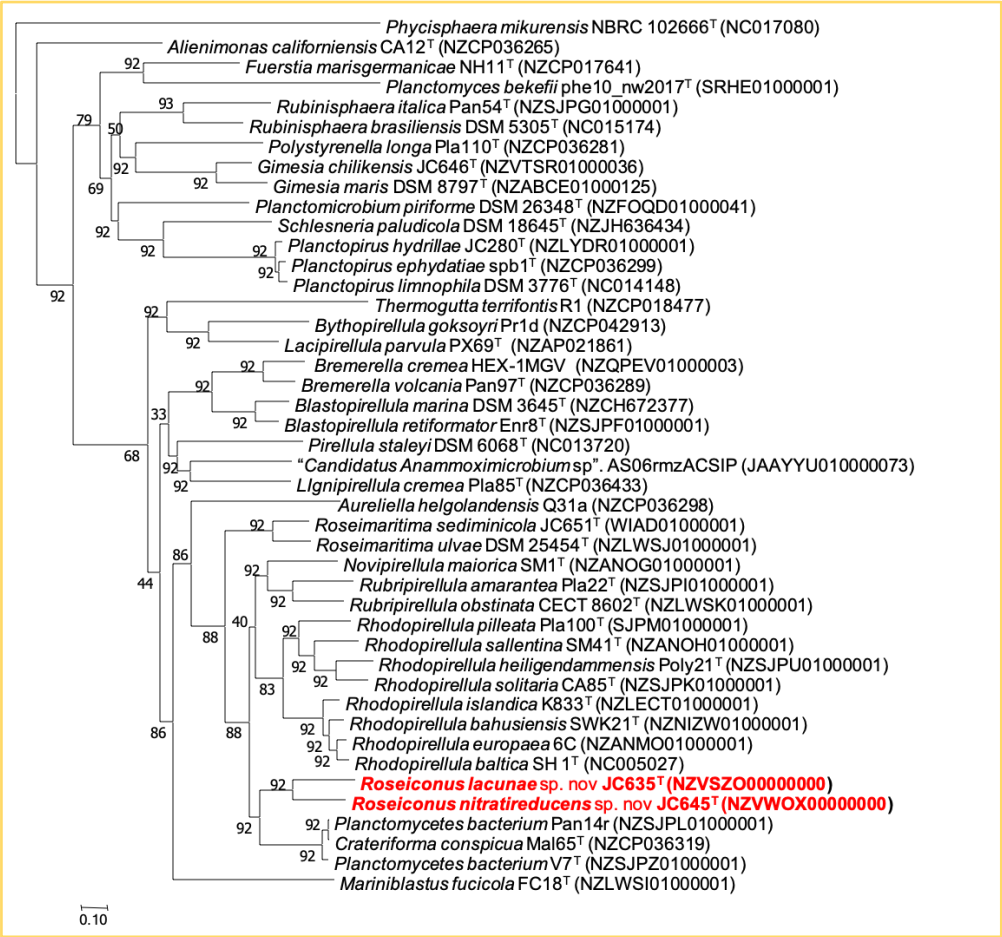

Fig. 3.4.1.3 The phylogenomic tree based on RAxML of strain JC645^{T}and JC635^T along with Publically available genome sequences of Pirellulaceae, Planctomycetaceae and Isosphaeraceae families.

3.4.1.4 *In-silico* metabolic characterization

The strains JC635^T and JC645^T have 2-C-methyl-D-erythritol 4-phosphate/1-deoxy-D-xylulose 5-phosphate (MEP) pathway for the biosynthesis of five-carbon isoprene unit (isopentenyl pyrophosphate; IPP) which is eventually the precursor for the synthesis of carotenoids and quinones (Eisenreich et al. 2004; Zhao et al.2013; Zhang 2018). Genes encoding for diapocarotenoid biosynthetic enzymes like diapolycopene oxygenase (1.14.99.44), 4,4'-diapophytoene desaturase (1.3.8.2), 15-cis-phytoene synthase (2.5.1.32) were present in both strains and are capable of forming diaponeurosporenic acid and phytoene. Strain JC635^T differs from strain JC645^T in fatty acid metabolism,

sphingolipid metabolism, glycan biosynthesis and degradations of toxic xenobiotic compounds like xylene, caprolactam, 1,4-dichlorobenzene, benzoate, fluorobenzoate and toluene. Genes coding for phosphoglycerate kinase (EC 2.7.2.3) in glycolysis pathway and choloylglycine hydrolase (EC 3.5.1.24) in primary bile salts biosynthesis pathway are exclusive for the strain JC645^T (Fig 3.4.1.4).

Genes coding for aromatic-L-amino-acid decarboxylase (EC 4.1.1.28) which helps in Isoquinoline alkaloid biosynthesis, Inositol-phosphate phosphatise (EC 3.1.3.25) for streptomycin biosynthesis, Acetyl-CoA carboxylase (EC 6.4.1.2) for Tetracycline biosynthesis are present in JC635^T only. Gene coding for creatinine amidohydrolase (EC 3.5.2.10), which helps in the degradation of creatine and creatinine degradation is present in strain JC635^T, while the same may be catalysed by cytosine deaminase (EC 3.5.4.1) in strain JC645^T. The number of putative gene clusters for the biosynthesis of secondary metabolites in the strains JC645^T and JC635^T are 8 and 10 respectively. Both strains have gene clusters coding for Type III Polyketide Synthase (TIIIPKS), TIPKS, terpenes and acyl amino acid. Non-ribosomal peptide synthetase (NRPS) genes are exclusively present in the genome of strain JC635^T. Genes coding for pyruvate dehydrogenase (EC 1.2.4.1), lactate dehydrogenase (EC 1.1.1.27), aldehyde dehydrogenase (EC 1.2.1.3) and alcohol dehydrogenase (EC 1.1.1.1) involved in fermentative metabolism are present in both strains.

3.4.1.5 Morphological and physiological analyses

Cells of strain JC635^T were cone to pear shaped (Fig. 3.4.1.5a,b), while cells of strain JC645^T were spherical to oval shaped (Fig. 34.1.6a,b). Cell size of strains JC635^T and JC645^T was 1.2-1.5x0.5-0.9 and 1.6-2.3x1.2-1.5 (LxW) respectively (Fig. 3.4.1.5a, 3.4.1.6b,c).

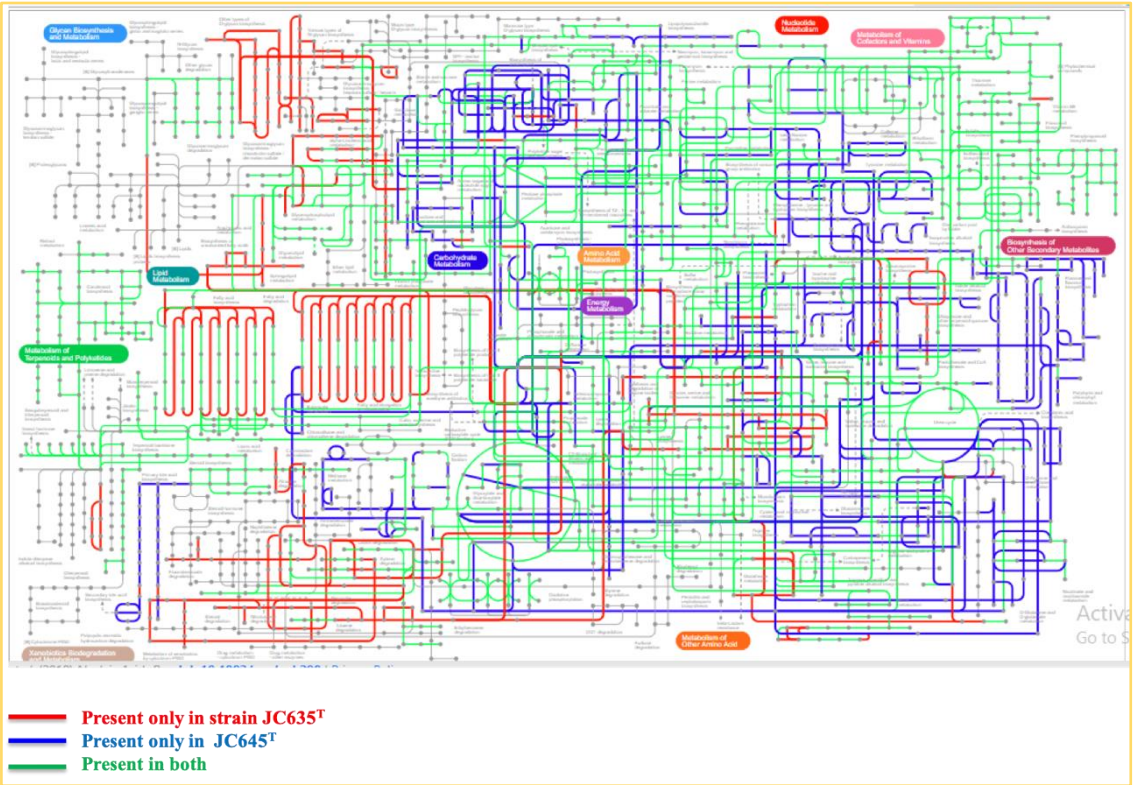

Fig 3.4.1.4. Common and unique biochemical pathways between strain JC635^T and strain JC645^T.

Cells of both the strains are either present in clusters and also singly. Cells of both strains multiply by budding (Fig. 3.4.1.6b; shown for strain JC645^T). Cells of strain JC635^T are motile by lophotrichous flagella (Fig. 3.4.1.5c), while motility could not be demonstrated in strain JC645^T. Crateriform structures are present throughout the cell surface of both the strains (Fig. 3.4.1.5c, 3.4.1.6b,c). Cell multiplication is initiated by the outgrowth of a new filament from a pole of a mature cell (Fig. 3.4.1.6b,d), which after a period of growth enlarges to form a daughter cell. Both strains show compartment like structure, concentrated nuclear region (Fig. 3.4.1.5d, 3.4.1.6e) with fimbriae like structures coming out from crateriform structures (Fig. 3.4.1.5c, 3.4.1.6b). Cellular membrane, invagination of cytoplasmic membrane, enlarged periplasm and cytoplasm are distinctly present in the TEM image of strain JC645^T (Fig. 3.4.1.5e).

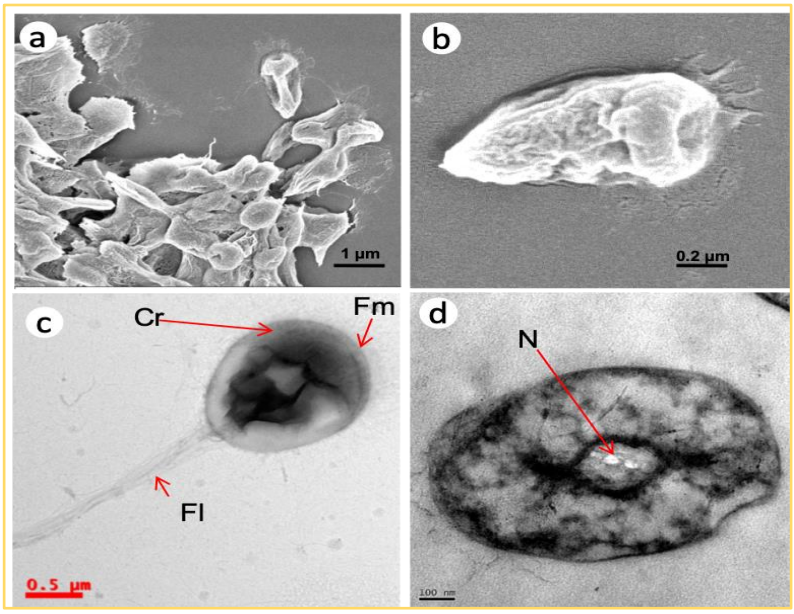

Fig. 3.4.1.5 Electron microscopic image of strain JC635^T: (a, b) SEM image; (c) TEM image of negatively stained cell showing flagella; (d) TEM image showing intracellular compartmentalization. Cr, Crateriform structures; N, Nucleoid; Fm, Fimbriae; Fl, Flagella

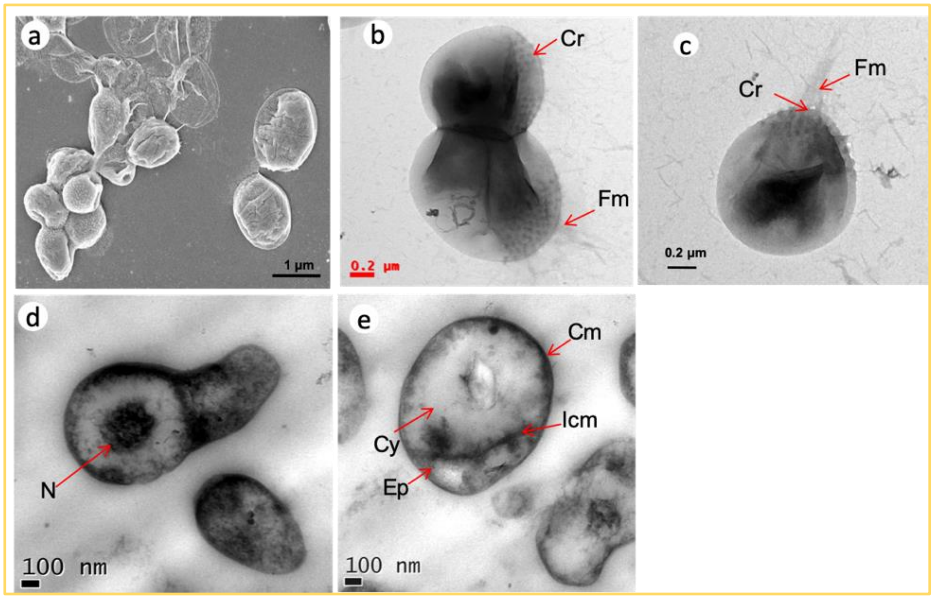

Fig. 3.4.1.6 Electron microscopic image of strain JC645^T: (a) SEM image; (b) TEM image of negatively stained cell showing reproduction by budding (c) showing crateriform structures (d) presence of nucleoid (e) TEM image showing intracellular compartmentalization. Cr, Crateriform structures; Cm, Cellular membrane; Icm, Invagination of cytoplasmic membrane; N, Nucleoid; Ep, Enlarged periplasm; Cy, Cytoplasm;Fm, Fimbriae.

Nitrate reduction is positive for the strain JC645^T only, which is also well supported by the presence of gene coding periplasmic nitrate reductase (EC 1.7.99.4) in its genome. Vitamin B_{12} is not required for the growth of strain JC635^T but it is obligate for strain JC645^T. Growth with different carbon substrates/nitrogen sources/pH range/NaCl tolerance for both strains is given in either species description or in Table 1. Strains JC635^T and JC645^T grow chemoorganoheterotrophically (aerobic dark, NAG [0.1% w/v] as electron donor and carbon source) and have fermentative growth [dark anaerobic with glucose (0.1% w/v) as carbon source]. Fermentative growth of both the strains is also supported from the genomic insights. Oxidation of carbohydrates and enzymatic activity of both the strains was determined according to the manufacturer's instructions, using API 20NE kit (BioMérieux) and API ZYM kit (BioMérieux) respectively for which the results are given in Table 3.4.1.5,6 or in species description.

3.4.1.6 Chemotaxonomic characterization

3.4.1.6.1 FAME profile

Major (>10%) fatty acids of strains JC635^T and JC645^T are $C_{18:1}\omega9c$ and $C_{16:0}$. Details about the fatty acid composition of both the strains are shown in Table 3.4.1.4. Strain JC635^T differed from strain JC645^T in having anteiso-$C_{13:0}$, anteiso-$C_{12:0}$,$C_{16:0}$ 3-OH, anteiso-$C_{16:0}$ and anteiso-$C_{17:1}$ A. Strain JC645^T alone has $C_{15:0}$2-OH, $C_{19:0}$ and $C_{20:1}\omega9c$ (Table 3.4.1.4).

3.4.1.6.2 Polar lipid profile

The polar lipid profiles of the strains JC635^T and JC645^T are similar and contain phosphatidylethanolamine (PE), phosphatidylcholine (PC), unidentified aminolipids (AL 1), and one unidentified lipid (L1) (Fig. 3.4.1.7). MK6 is the only quinone present in both the strains.

Table 3.4.1.4 Cellular fatty acid composition (%) of 1. Strain JC635^T and 2. Strain JC645^T.

Fatty acid (%)	**1**	**2**
$C_{10:0}$3-OH	2.1	1.7
$C_{12:0}$	1.0	1.5
anteiso-$C_{12:0}$	3.0	-
$C_{11:0}$3-OH	1.0	1.0
anteiso-$C_{13:0}$	10.0	-
$C_{14:0}$	1.7	1.5
$C_{15:0}$ 2-OH	-	1.5
anteiso-$C_{15:0}$	8.0	6.9
$C_{16:0}$	16.8	17.4
$C_{16:0}$ 3-OH	1.0	-
anteiso-$C_{16:0}$	1.0	-
$C_{16:1}\omega7c/C_{16:1}\omega6c$	5.4	7.0
$C_{17:0}$	1.6	2.2
$C_{17:1}\omega8c$	2.2	5.0
anteiso-$C_{17:0}$	5.5	4.6
anteiso-$C_{17:1}$ A	1.6	-
$C_{18:0}$	3.6	1.8
$C_{18:1}\omega9c$	21.4	29.5
$C_{18:1}\omega7c/ C_{18:1}\omega6c$	2.3	2.4
$C_{18:3}\omega6c$ (6,9,12)	1.5	1.2
$C_{19:0}$	-	1.4
$C_{20:1}\omega9c$	-	2.5

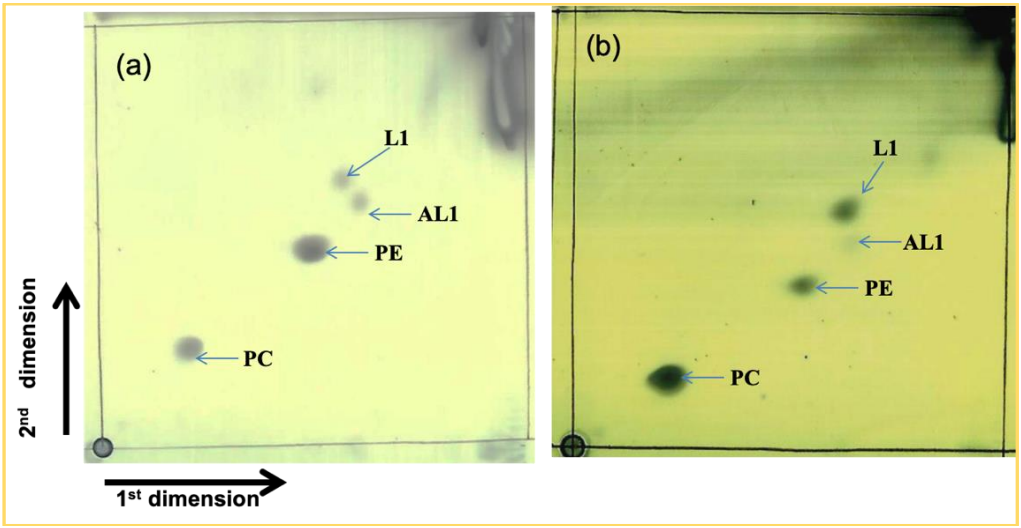

Fig 3.4.1.7 Two dimensional chromatograms showing polar lipids of (a) strain JC635^T and (b) strain JC645^T. PE, phosphatidylethanolamine; PC, Phosphatidylcholine; AL1, unidentified amino lipid; L1, unidentified lipid

3.4.1.6.3 Polyamine Profile

1,3-diaminopropane, cadaverine, spermidine, putrescine and two unidentified polyamines (UN1, UN2) are the major polyamines of strain JC635^T (Fig. 3.4.1.8). Strain JC645^T has cadaverine, putrescine and an unidentified polyamine (UN1) as major polyamines (Fig 3.4.1.8).

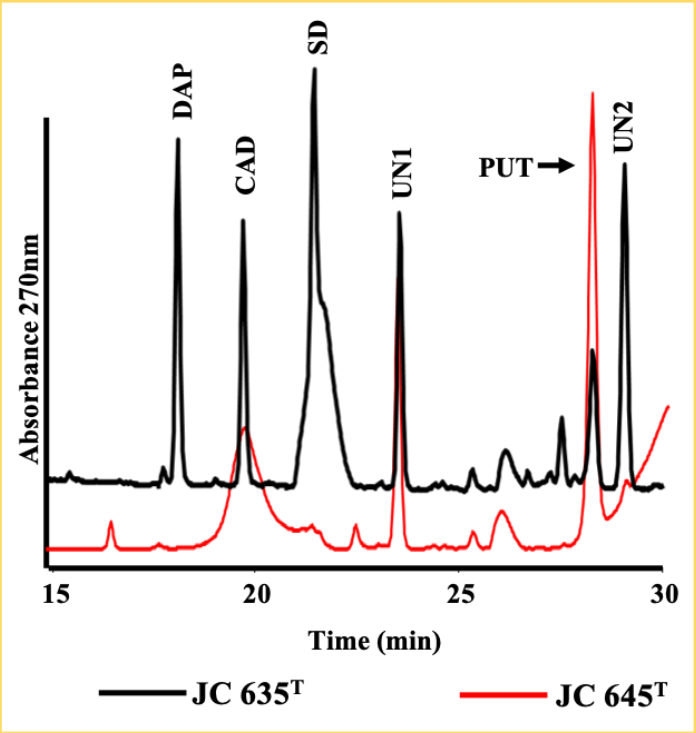

Fig 3.4.1.8. HPLC data showing the presence of different polyamine present in strain JC645^T and JC635^T. Standard polyamine: DAP- 1,2-Diaminopropane, CAD- cadaverine, SD-Spermidine, PUT – Putrescine, UN 1& 2- Unidentified polyamines.

Table 3.4.1.5 Differentiating characters of the novel genus *Roseiconus* from phylogenetically closely related genera of the family *Pirellulaceae.*

Character	**1**	**2***	**3***	**4***	**5***	**6***	**7***
Cell size (L x W, µm)	1.2-2.3× 0.5-1.5	1.0-2.5 × 1.2-2.3	1.5-2 × 1.3-1.7	1.1-1.8 × 0.9-1.5	1.8-2.1 × 0.9-1.3	1.8-2.2 × 1.3-1.5	1.8-2.1 × 0.9-1.1
Cell shape	Spherical or cone to pear	Pear to ovoid	Pear to ovoid	Spherical/round to ovoid/pear	Pear	Pear to round	Acorn
Cell arrangement	Rosettes of variable number of cells	Rosettes of variable number of cells	Rosettes 2–10 cells	Rosettes 3–40 cells	Rosette/Aggregates of variable number of cells	Aggregate of variable number of cells	Aggregate of variable number of cells
Pigmentation	pale pink	Pink to Red	Red	Light Pink	Pink	white	Lucid white
Fimbriae	+	+			+	+	+
NaCl requirement (tolerance; %)	(1-8)	(1-5)	(1-4)	(1-5)	NR	NR	NR
Temperature optima (tolerance; °C)	30 (15-35)	28 (15-35)	25 (10-30)	30 (15-40)	35 (10-36)	26 (10-30)	27 (10-33)
pH optima (tolerance)	8 (6-9)	8 (5.5–10.5)	7.5 (7.0–10.5)	7.5 (6.0–10)	7.5 (5.0-9.5)	7.5 (6.5-8.5)	7.5 (6.0-8.0)
Anaerobic (fermentative) growth	+	-	-	-	-	NR	NR
Organic substrate utilization							
NAG	+	+	-	+	+	+	+
Sucrose	+	+	-	-	NR	NR	NR
Maltose	+	+	-	+	NR	NR	NR
Lactose	+	+	-	+	NR	NR	NR
Mannitol	-	-	-	+	NR	NR	NR
Nitrogen substrate utilization							
Alanine	+	+	-	-	NR	NR	NR
Asparagine	-	-			NR	NR	NR
Phenylalanine	+	-	-	-	NR	NR	NR
Threonine	+	-	-	+	NR	NR	NR
Proline	-	+	-	+	NR	NR	NR
Catalase	+	+	-	+	NR	NR	NR
Nitrate reduction	+	-	-	-	NR	NR	NR
Starch hydrolysis	+	-	-	-	NR	NR	NR
Fatty acids							
$C_{17:1\omega}8c$	++	+++	++++	++	NR	NR	NR
$C_{16:1}\omega7c$/ $C_{16:1}\omega6c$	++	++++	+++	++	NR	NR	NR
$C_{18:1}\omega9c$	++++	-	-	-	NR	NR	NR
anteiso-$C_{15:0}$	++	-	-	-	NR	NR	NR
anteiso-$C_{13:0}$	++	-	-	-	NR	NR	NR
Polar lipids					NR	NR	NR
Phosphatidylglycerol	-	$	$$	$$	NR	NR	NR
Diphosphatidylglycerol	-	-	-	$$	NR	NR	NR
Phosphatidylethanolamine	$$	-	-	-	NR	NR	NR
Phosphatidylcholine	$$	$$	$$	$$	NR	NR	NR

[@]Carotenoid biosynthesis Genome information	DAC	DAC	DAC, NE/LY	DAC	NR	NR	NR
Size (Mbp)	7.9-8.2	7.2-8.0	6.7	6.2-8.3	7.1-7.2	9.6	8.4
G+C mol%	55.5- 60.1	53-57	56	59.1-62.4	55.4-57.8	61.4	55.3

1, *Roseiconus* (strain JC635^{T},strain JC645^{T}); 2, *Rhodopirellula* (*R. baltica*, *R. lusitana*, *R. rubra*); 3, *Rubripirellula* (*R. obstinata* CECT 8602^{T})*;* 4, *Roseimaritima* (*R. ulvae* DSM 25454^{T}, *R. sediminicola* JC651^{T}); 5, "*Crateriforma"*; 6, "*Lignipirellula"*; 7, "*Aureliella*". All strains were isolated from marine sources, have $C_{16:0}$ as major (>10%) fatty acid, phosphatidylcholine as polar lipid, N-acetyl glucose amine (NAG) is not obligate for growth. +, positive; ++, <5%; +++, <10%; ++++, >10%; $, positive with low quantities; $$, positive with high quantities; [@], Based on genomic information obtained through PATRIC resource centre; C, Cadaverine; D, 1,3-Diaminopropane; P, Putrescine, S, Sym-homospermidine; nr, not reported; B_{12}, Vitamin B_{12}; DAC, DiApoCarotene biosynthesis; NE/LY, Neurosporene/Lycopene biosynthesis; NR, Not reported *data taken from references Schlesner et al. 2004; Roh et al. 2013; Bondoso et al. 2014, 2015; Yoon et al. 2014; Peeters et al. 2020a; Kumar et al. 2020a; Peeters et al. 2020b; Kallscheuer et al. 2020.

Table 3.4.1.6. Differentiating characteristics between strains 1. JC635^T and 2. JC645^T

Characteristics	1	2
Cell shape	Cone to pear	Spherical to ovoid
Cell size (L x W)	1.2-1.5× 0.5-0.9	1.6-2.3×1.2-1.5
pH range (optimum)	6.0-9.0 (8.0)	7.0-9.0 (8.0)
NaCl tolerance range (optimum; %)	1-5 (3)	1-7 (4)
Organic substrates used for growth		
Pyruvate	-	+
Inulin	-	+
Lactose	+	-
D-galactose	+	-
Nitrogen sources used for growth		
Cysteine	-	+
L-Glutamine	-	+
L-Proline	-	+
Urea	-	+
L-isoleucine	+	-
L-phenylalanine	+	-
L-glutamate	+	-
L-aspartate	+	-
Vit B_{12} requirement	-	+
Results of API 20 NE		
$^{\&}$Nitrate reduction	-	+
$^{\&}$Starch hydrolysis	+	-
API ZYM (Biomeriux)		
Valinearylamidase	-	+
α-Glucosidase	-	+
Polyamines		
1,2-Diaminopropane	+	-
Spermidine	+	-
Unidentified polyamine (UN2)	+	-
Genome Size(Mb)	7.9	8.2
Genomic DNA G+C content (mol %)	55.5	60.1

Both strains show fermentative growth, grow from 10-35 °C (optimum at 30 °C), have MK6 as the only quinone; phosphatidylcholine, phosphatidylethanolamine, an unidentified aminolipid and an unidentified lipid as polar lipids. Both strainsJC635^{T}and JC645^{T}utilizeα-D-glucose, fructose, mannose, maltose, sucrose, starch, D-xylose and rhamnose for their growth but ascorbate, acetate, fumarate, mannitol, Na-propionate, inositol, malate, succinate, sorbitol and benzoate are not utilized by both the strains, JC635^T and JC645^T. Both strains utilize ammonium sulphate, peptone, L-serine, DL-threonine, L-leucine and DL-alanineas nitrogen sources but neither of strains utilize L-tyrosine, D-valine, DL-ornithine, L-lysine, L-methionine, L-tryptophan, L-arginine, L-histidine and L-glycine as nitrogen source; Both strains shows positive for alkaline phosphatase, esterase, esterase lipase, leucine arylamidase, acid phosphatase, napthol-AS-BI-phosphohydrolase but negative for lipase, cysteine arylamidase, trypsin, α-chymotrypsin, α-galactosidase, β-galactosidase, β-glucuronidase, β-glucosidase, N-acetyl-β-glucosamidase, α-mannosidase and α-fucosidase; ferment glucose; gelatin is not hydrolysed and indole is not produced by either strains. Cadaverine, putrescine and an unidentified polyamine (UN1) are present in both strains. +, substrate utilized/present; - substrate not utilized/absent' $^{\&}$, confirmed through biochemical test also;

3.4.2 Phylo-taxogenomic study of the strain JC646^T

3.4.2.1 Habitat and Nucleotide sequences accession numbers

The strain JC646^T isolated from the sediment samples collected from Satpada region (19°40'12"N; 85°25'48"E) of Chilika lagoon, Odisha, India. The 16S rRNA gene sequence of the taxa was deposited with European Molecular Biology Laboratory (EMBL) with accession numbers LR132072. The whole genome sequence of strain JC646^T (7,647,772 nt) was deposited to NCBI with accession number VTSR00000000.

3.4.2.2 Genomic characteristics

The genome size of the strain JC646^T was 7,647,772 nt in 45 contigs with an N50 value of 4,84,104. The genome has 5,826 genes, of which 5,703 are protein-coding genes, 67 genes for RNAs, and 50 genes are pseudogenes. No. of rRNA operons present in strain JC646^T and *G. maris* DSM 8797^T are 3 and 4, respectively. The G+C content of the genome of strain JC646T was 53.2 mol%, which is about 5% higher than G+C of *G. maris* DSM 8797^T. The difference in G+C between the strains indicate that these two are distinct species since a 3% difference in the G+C content was recommended for species delineation. Seventeen other publicly available genome sequences of genus *Gimesia* were taken from EZBiocloud, and NCBI Taxonomy and their Genomic features were compared (Table. 3.4.2.1). Genome sequences of the strains JC646^T and *G. maris* DSM 8797^T were aligned using PATRIC online software to identify the multiple maximal matches and local collinear blocks (LCBs) (https://www.patricbrc.org/). The genome sequence of the strain JC646^T is used as a reference sequence against *G. maris.* The alignment of LCB of both strains differs from each other variably (Fig. 3.4.2.1). The protein sequences identity based on a genome map was prepared using the PATRIC server's proteome comparison service. Analysis of this map indicated that most of the proteins of strain JC646^T share 20-80% similarity with

those of *G. maris* DSM 8797^T (Fig. 3.4.2.2). This suggests the well defined dissimilarity of strain JC646T with *G. maris* DSM 8797^T.

3.4.2.3 BLAST Analysis and Phylogenetic inference

OrthoANI values between strain JC646^T and *G. maris* DSM 8797^T was 74.5%. The *d*DDH values between strain JC646^T and *G. maris* DSM 8797^T was 19.0 %. The gANI and *d*DDH values of strain JC646^T with the type strain *G. maris* DSM 8797^T are far below [(95-96% cut off for ANI and 70% cut off for *d*DDH)] than the recommended (Goris et al. 2007; Richter and Rossello-Mora 2009) cut off values for species delineation and thus strain JC646^T represents a new species in the genus *Gimesia*. The AAI and POCP were calculated among the selected genomes of the family *Planctomycetaceae*. Both POCP (Table 3.4.2.2) and AAI (Table 3.4.2.3) values between the strains JC646^T and *G. maris* DSM 8797^T were approximately 77%. A POCP threshold below 50% was proposed to determine if a species belongs to two different genera. A POCP value of 77% between both strains JC646^T and *G. maris* DSM indicates that they fall within the same genus *Gimesia*. Further, the AAI value of 77% between strains falls close to the proposed cut-off of 80% used for the genus delineation. Thus, strains JC646^T represents a novel species of the genus *Gimesia*.

The 16S rRNA gene sequences of the strain JC646^T pulled out from the genome have a sequence length of 1530 nt, and the BLAST search result show similarity of 97.3% with *G. maris* DSM 8797^T. The 16S rRNA gene sequence-based phylogenetic tree with combined bootstrap values obtained from NJ, ME, ML trees **(Fig. 3.4.2.3)** and phylogenomic tree based on 92 core genes **(Fig. 3.4.2.4)** confirmed the distinct monophyletic clustering of strains JC646^T within the genus *Gimesia* clade. *The* Strain JC646^T is distinctly separated from *G. maris* DSM 8797^T, suggesting strain JC646^T is a novel species of a genus *Gimesia*.

Table 3.4.2.1: Genome features of members of the genus *Gimesia*.

Sl. no	Species /strain	Accession No	Sequencing Technology	Genome coverage	Genome size (Mb)	No of contigs	GC %	N50 (bp)	Genes (total)	CDS (Total)	CDS (Protien)	rRNA	tRNA	Other RNA	Pseudo-gene	CRISPRs
1	***Gimesia chilikensis* JC646^T**	VTSR00000000	Illumina HiSeqX10	100.0x	7.64	45	53.2	4,84,104	5,826	5,757	5,707	3	62	2	50	0
2	***Gimesia maris* DSM 8797^T**	NZ_CP043931	PacBio RSII	42.66x	7.82	1	50.4	7,816,689	5,958	5,888	5,763	4	64	2	125	0
3	*Gimesia* sp. E7	NZ_CP043930	PacBio RSII	63.33x	8.03	1	52.7	8,027,492	6,231	6,164	6,016	4	61	2	148	2
4	*Gimesia* sp. SAT87	PAJV00000000	Illumina HiSeq	NA	7.9	78	50.8	1,60,688	6,236	6,177	6,089	3	54	2	88	0
5	*Gimesia* sp.NP99	PBQK00000000	Illumina HiSeq	NA	8.4	245	52.8	54,252	6,569	6,507	6,423	4	56	2	84	0
6	*Gimesia* sp. CPC31	NYVH00000000	Illumina HiSeq	NA	7.03	433		20,642	5,892	5,849	5,772	2	39	2	77	0
7	*Gimesia maris* CA11	NZ_CP036353	PacBio RSII; Illumina MiSeq	154x	7.62	1	50.3	7,626,893	5,764	5,701	5,648	4	57	2	53	1
8	*Gimesia* sp. Pan110	NZ_CP036277	PacBio RSII; Illumina MiSeq	201x	7.98	1	53.6	7,983,903	6,014	5,952	5,895	4	56	2	57	2
9	*Gimesia maris* Mal35	NZ_CP036341	Illumina MiSeq	125x	7.53	24	50.3	7,530,055	5,683	5,621	5,552	3	57	2	69	1
10	*Gimesia* sp. V6	NZ_CP036347	Illumina Miseq	197x	8.09	15	52.8	8,097,090	6,249	6,188	6,132	3	56	2	56	1
11	*Gimesia* sp. Enr10	NZ_CP037421	Illumina MiSeq	340x	7.82	41	53.6	7,828,706	5,952	5,890	5,812	4	56	2	78	0
12	*Gimesia* sp. V144	NZ_CP037920	Illumina MiSeq	273x	7.4	4	45.1	7,397,129	5,643	5,569	5,529	4	67	3	40	1
13	*Gimesia* sp. Pan153	NZ_CP036317	PacBio RSII; Illumina MiSeq	118x	8.2	1	53.3	8,260,309	6,222	6,160	6,103	4	56	2	57	2
14	*Gimesia* sp. HG66A1	NZ_CP036266	Illumina MiSeq	461x	8.2	4	52.8	8,289,354	6,355	6,293	6,229	4	56	2	64	1
15	*Gimesia* sp. Pan241w	NZ_CP036269	Illumina MiSeq	308x	7.76	4	49.5	7,769,723	5,841	5,778	5,732	4	57	2	46	0
16	*Gimesia* sp. MalM14	NZ_CP036342	Illumina MiSeq	149x	7.8	9	53.1	7,801,558	5,915	5,854	5,807	3	56	2	47	0
17	*Gimesia* sp. Pan161	NZ_CP036343	Illumina MiSeq	378x	7.92	12	50	7,929,454	6,069	6,007	5,916	4	56	2	91	1
18	*Gimesia* sp. V202	NZ_CP037422	Illumina MiSeq	205x	7.21	7	45	7,218,541	5,457	5,386	5,350	3	65	3	36	1
19	*Gimesia* sp. Enr17	NZ_CP037452	PacBio RSII; Illumina MiSeq	131x	7.7	2	49.5	7,704,373	5,877	5,815	5,767	4	56	2	48	1

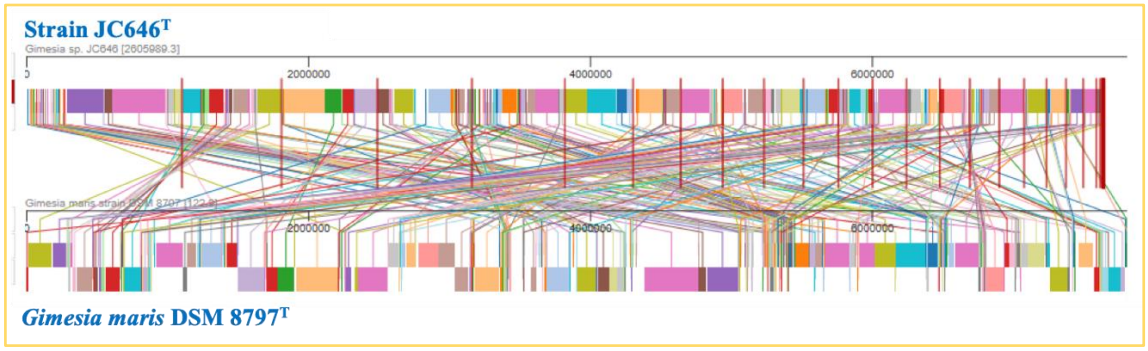

Fig. 3.4.2.1. Genome organization of strain JC646^{T} and *G. maris* DSM 8797^{T}

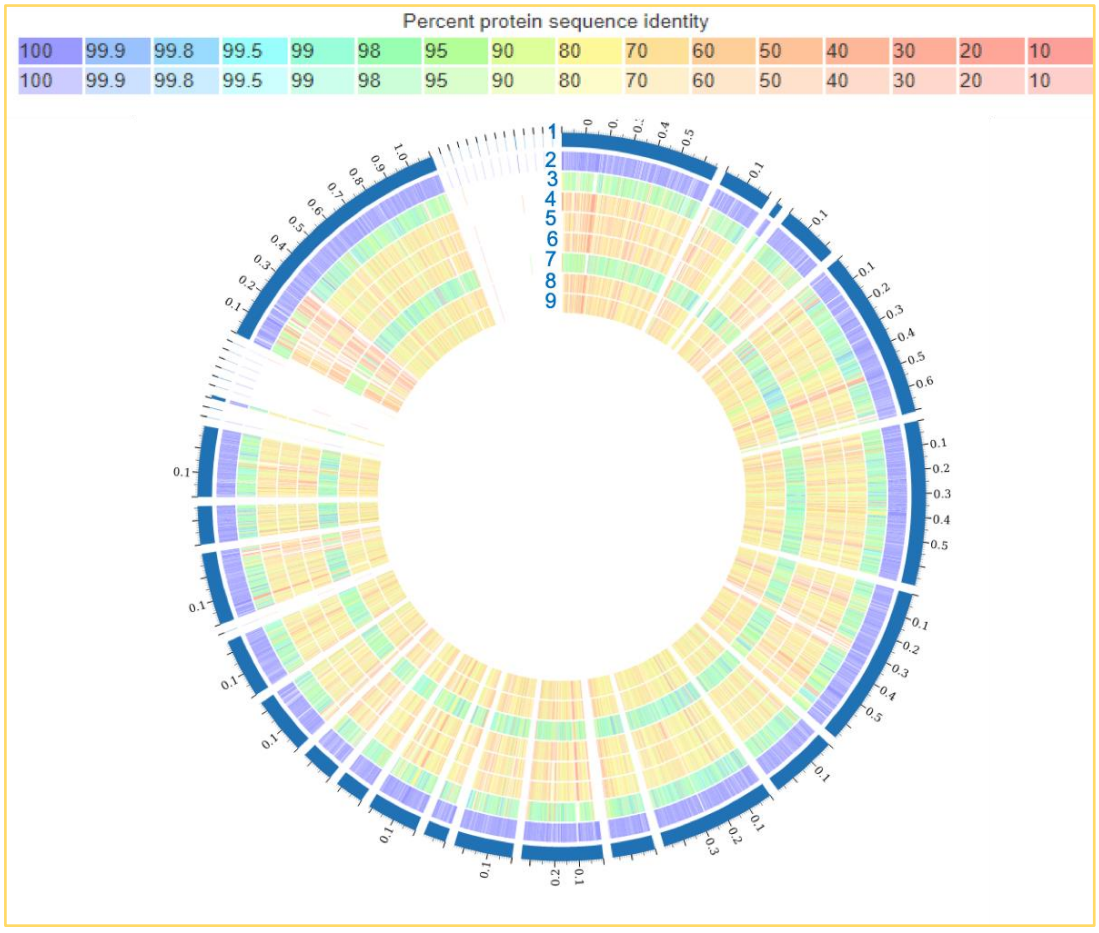

Fig. 3.4.2.2 Genome map based on protein sequence identity among strains JC646^{T} and some other members of genus *Gimesia* . Genome of strain JC646^{T} was used as reference List of tracks, from outside to inside: 1. Scale of contig length 2. *Gimesia chilikensis* JC646^{T} 3. "*Gimesia* sp." E7 4. *Gimesia maris* DSM 8797^{T} 5. "*Gimesia* sp." SAT87 6. "*Gimesia* sp." CPC31 7. "*Gimesia* sp." NP99 8. "*Gimesia maris*" UBA9375 9. "*Gimesia maris* "UBA2506.

Table 3.4.2.2. POCP Values among the selected genomes of the family *Planctomycetaceae*.

	1	2	3	4	5	6	7	8	9	10
1	100.00									
2	41.08	100.00								
3	39.35	**76.98**	100.00							
4	34.78	39.14	37.18	100.00						
5	20.17	16.48	16.04	16.78	100.00					
6	33.50	39.27	37.56	40.61	18.60	100.00				
7	31.26	36.62	35.03	38.71	16.50	80.83	100.00			
8	32.40	38.60	36.49	40.83	17.71	86.97	83.49	100.00		
9	37.60	43.61	42.07	40.82	16.46	43.30	39.65	42.15	100.00	
10	35.52	39.54	38.28	40.23	17.64	42.68	40.13	42.30	36.23	100.00

1.*Fuerstiamaris germanicae* NH11^T (NZCP017641); 2. *Gimesia maris* DSM 8797^T (NZABCE01000125); 3. Strain JC646^T (VTSR00000000); 4. *Planctomicrobium piriforme* DSM 26348^T (NZFOQD01000041); 5. *Planctomyces bekefii* phe10nw2017^T (SRHE01000001); 6. *Planctopirus ephydatiae* spb1^T (NZCP036299); 7. *Planctopirus hydrillae* JC280^T (LYDR01000001); 8. *Planctopirus limnophila* DSM 3776^T (NC014148); 9. *Rubinisphaera brasiliensis* DSM 5305^T (NC015174); 10. *Schlesneria paludicola* DSM 18645^T (NZJH636434).

Table 3.4.2.3. AA1Values among the selected genomes of the family Planctomycetaceae.

	1	2	3	4	5	6	7	8	9	10
1	100.0									
2	48.8	100								
3	50.3	**76.9**	100							
4	48.5	49.8	49.6	100						
5	50.2	43.9	44.3	44.1	100					
6	46.6	49.0	49.3	49.3	44.5	100				
7	46.9	48.5	48.8	49.0	43.9	94.2	100			
8	49.1	48.8	49.0	49.3	43.9	94.9	94.4	100		
9	47.3	50.4	51.0	50.0	43.4	48.7	48.3	48.5	100	
10	47.9	49.8	49.9	50.3	44.9	52.7	52.0	52.2	48.5	100

1.*Fuerstiamaris germanicae* NH11^T (NZCP017641); 2. *Gimesia maris* DSM 8797^T (NZABCE01000125); 3. Strain JC646^T (VTSR00000000); 4. *Planctomicrobium piriforme* DSM 26348^T (NZFOQD01000041); 5. *Planctomyces bekefii* phe10nw2017^T (SRHE01000001); 6. *Planctopirus ephydatiae* spb1^T (NZCP036299); 7. *Planctopirus hydrillae* JC280^T (LYDR01000001); 8. *Planctopirus limnophila* DSM 3776^T (NC014148); 9. *Rubinisphaera brasiliensis* DSM 5305^T (NC015174); 10. *Schlesneria paludicola* DSM 18645^T (NZJH636434).

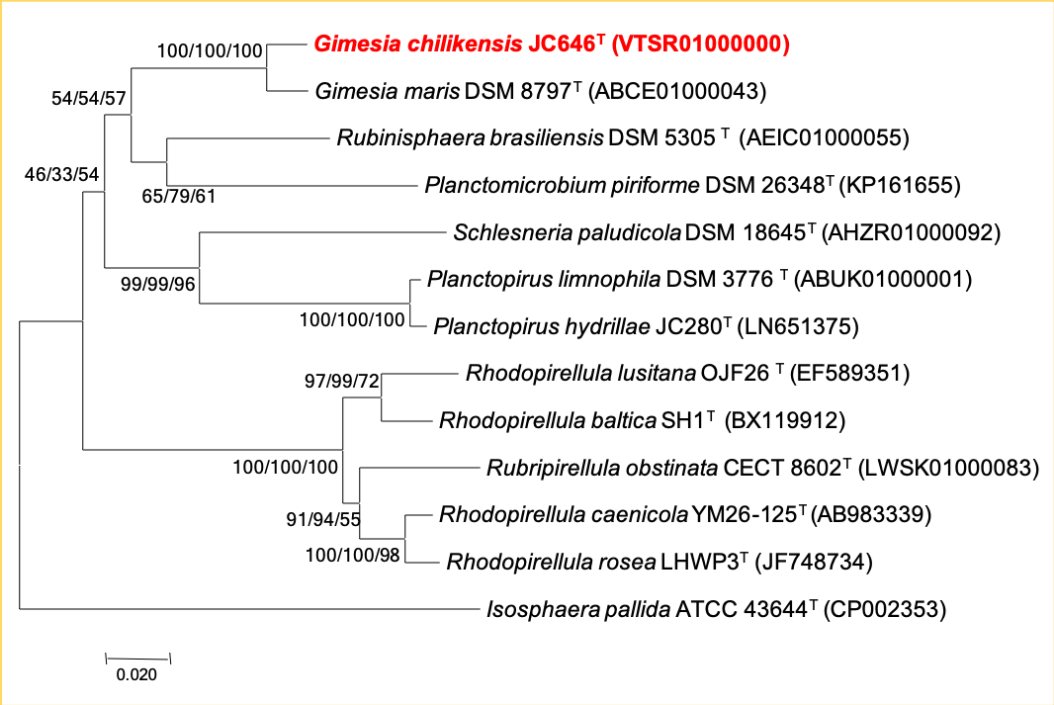

Fig. 3.4.2.3 The 16S rRNA gene sequences based phylogenetic tree showing the phylogenetic relationship of strain JC646^T with the *Gimesia maris* and other closely related species. The tree was made with MEGA 7 software and *Isosphaera pallida* ATCC 43644^T was used as out-group. The GenBank accession numbers for 16S rRNA gene sequences are shown in parentheses. Numbers at nodes indicate bootstrap value of 1000 repetition correspond to NJ/ML/ME analysis. Bar,0.02 nucleotide substitution per position.

3.4.2.4 *In-silico* metabolic characterization

In silico metabolic characterization of strain, JC646^T and *G. maris* DSM 8797^T was carried out based on its genome information through online available tool PATRIC 3.6.2 (https://www.patricbrc.org/) (Wattam et al. 2017). Both strains have the 2-C-methyl-D-erythritol 4-phosphate/1-deoxy-D-xylulose 5-phosphate (MEP) pathway for the biosynthesis of the five-carbon isoprene unit (isopentenyl pyrophosphate; IPP), which is eventually the precursor for the synthesis of carotenoids and quinones (Eisenreich et al. 2004; Zhao et al.2013; Zhang 2018). The carotenoid biosynthetic pathway is incomplete in both strains. It possibly ends with phytoene since genes coding for carotene isomerase, desaturase, hydroxylase, and lycopene cyclase are absent in both strains.

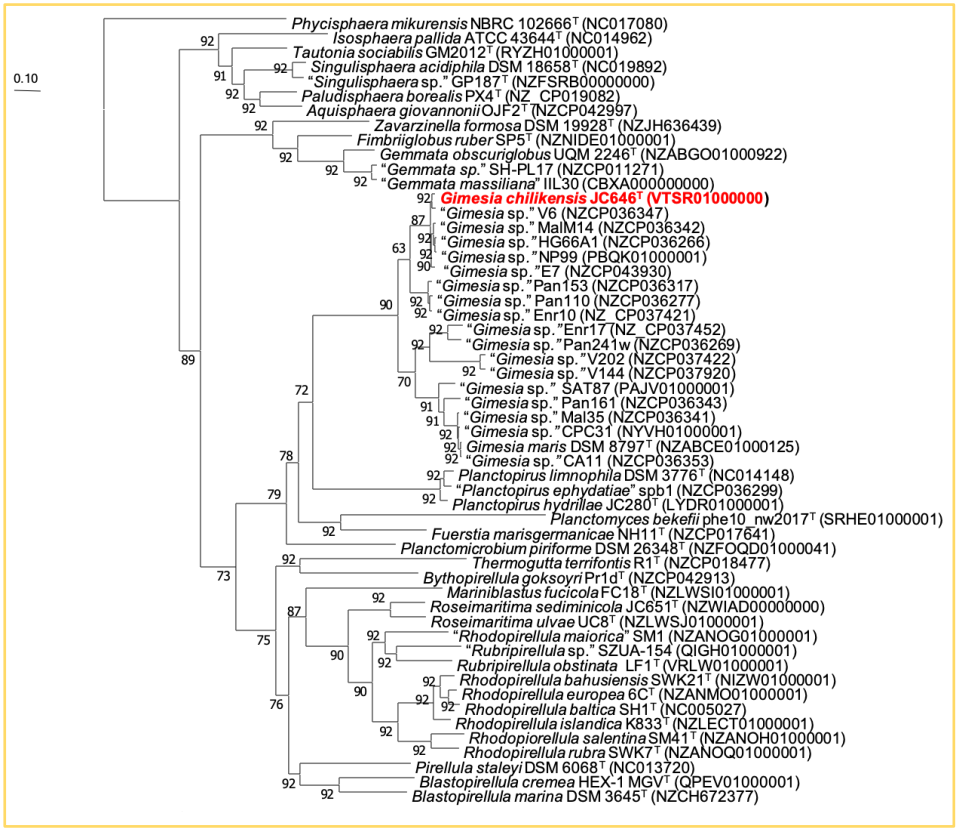

Fig 3.4.2.4 Phylogenomics tree based on RAxML of strain JC646^T along with publicly available genome sequence of *Planctomycetaceae* and *Isosphaeraceae* families. Genome sequence of *Phycisphaera mikurensis* is taken as outgroup.The GenBank accession numbers for genome sequences are shown in parentheses.Bar,0.10 nucleotide substitution per position.

This probably makes both the cultures look white compared to other planctomycetes, which are mostly pink. Cardiolipin biosynthetic pathway genes are observed only in strains JC646^T. *In silico* identification for secondary metabolites for strain JC646T and *G. maris* DSM 8797^T was carried out using online freely available tool antiSMASH5.1 (http://antismash.secondarymetabolites.org) (Blin et al. 2019). The results indicate that both strains have putative genes encoding secondary metabolites belonging to bacteriocin and Type III Polyketide Synthase (T3PKS), terpenes, and ectoine. Putative genes encoding for lanthipeptides are present only in strain JC646^T. In contrast, the putative gene encoding for resorcinol is present only in *G. maris* DSM 8797^T. Metabolic pathways of both the strains, JC646^T and *G. maris* DSM 8797^T, were compared by downloading their

EC numbers of enzymes from PATRIC and submitting it to online Interactive Pathways (iPath) explorer (https://pathways.embl.de/). Fig. 3.4.2.5 shows no significant differences in both strains' metabolic pathways, except for some differences in pentose-phosphate metabolism.

3.4.2.5 Morphological and physiological analyses

Rosette's arrangement of cells was observed among both strains JC646^T and *G. maris* DSM 8797^T (Fig. 3.4.2.6); however, the number of cells in the rosettes varied. There were about 30-50 cells in a single rosette of strain JC646^T (Fig. 3.4.2.6), while 3-8 cells in the singe rosette of *G. maris* DSM 8797^T (Fig. 3.4.2.6). Cells of strain JC646^T were oval to pear-shaped (1.2-1.6x0.7-1.0 µm; Fig. 3a) and multiplied by budding (Fig. Fig. 3.4.2.7a,b). TEM image of JC646^T cells shows the presence of the invagination of the cytoplasmic membrane, enlarge periplasm, cytoplasm, nucleoid region (Fig. 3.4.2.7c), and are surrounded by fimbriae (Fig. 3.4.2.7d). Stalks were not observed in strain JC646^T.

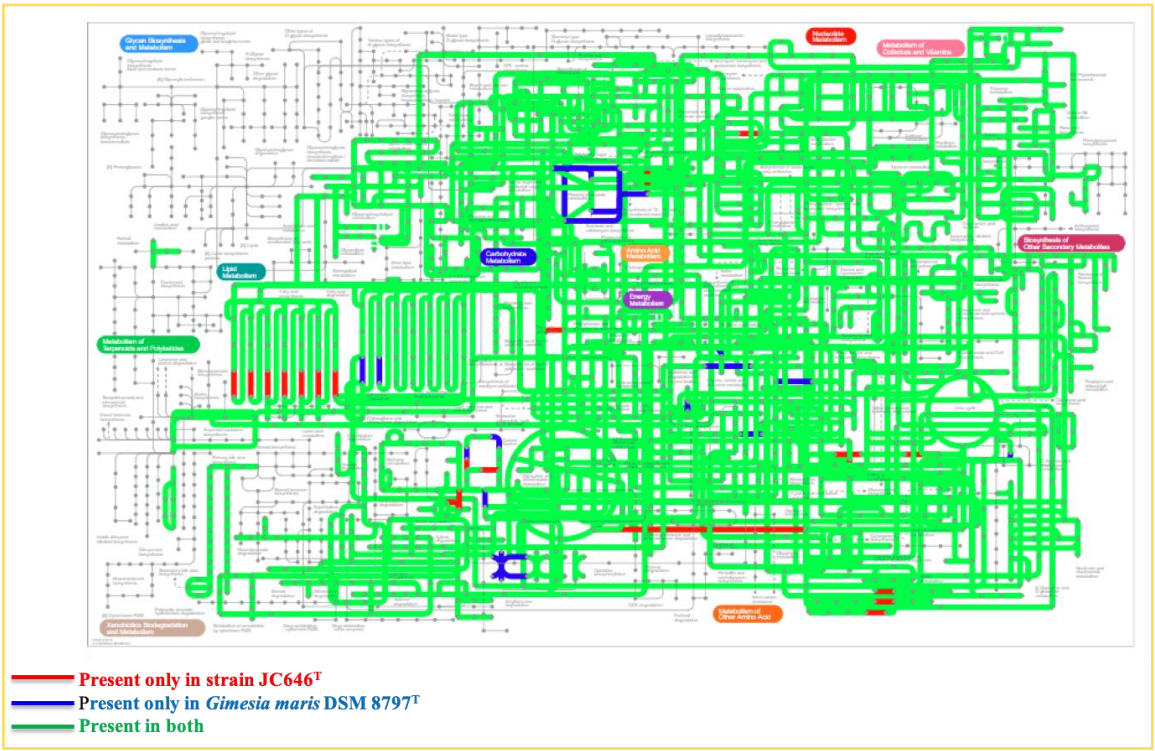

Fig. 3.4.2.5 Common and unique biochemical pathways between strain JC646^T and *G. maris* DSM 8797^T.

Vitamin B_{12} is not required for growth in both strains. Growth is monitored for both the strains with different carbon substrates/nitrogen sources/pH range/NaCl requirements of strain JC646^T are given in either species description or Table. 3.4.2.5**.** Fermentation "anaerobic growth in darkness with glucose [0.1% w/v] as electron donor and carbon source" and chemolithoautotrophy "aerobic growth in darkness with $Na_2S.9H_2O$ [1 mM]/H_2S/H_2 [5% v/v] as electron donor and $NaHCO_3$ [0.1% w/v] as carbon source" could not be observed in the strain JC646^T. The Strain JC646^T was unable to reduce nitrate. Enzyme activities of strain JC646^T were detected by API ZYM kit (BioMérieux). API ZYM kit shows positive for alkaline phosphatase, esterase, esterase lipase and acid phosphatase and negative for lipase, leucine arylamidase, valine arylamidase, cysteine arylamidase, α-chymotrypsin, α-galactosidase, β-galactosidase, β-glucuronidase, α-glucosidase, β-glucosidase, α-mannosidase, trypsin, naphthol-AS-BI-phosphohydrolase and α-fucosidase.

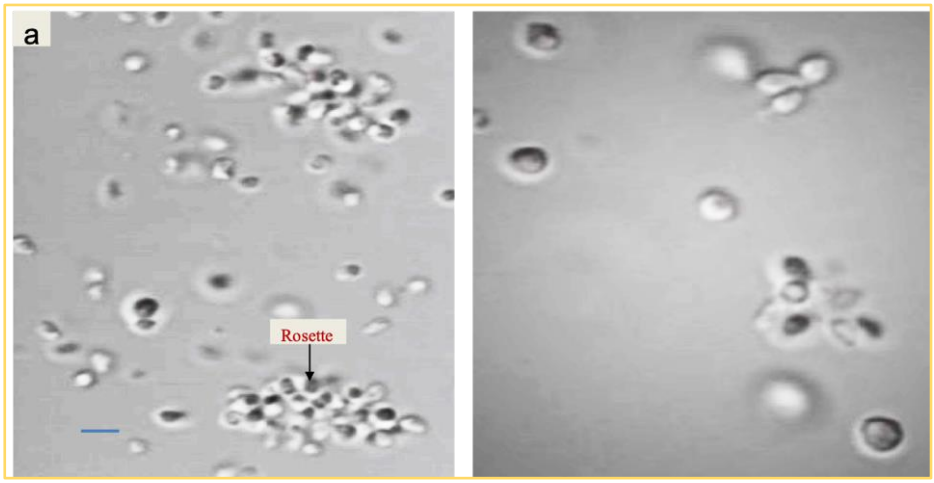

Fig. 3.4.2.6. Confocal microscope image of (a) strain JC646^T and (b) *G. maris* DSM 8797^T showing rosette formation.

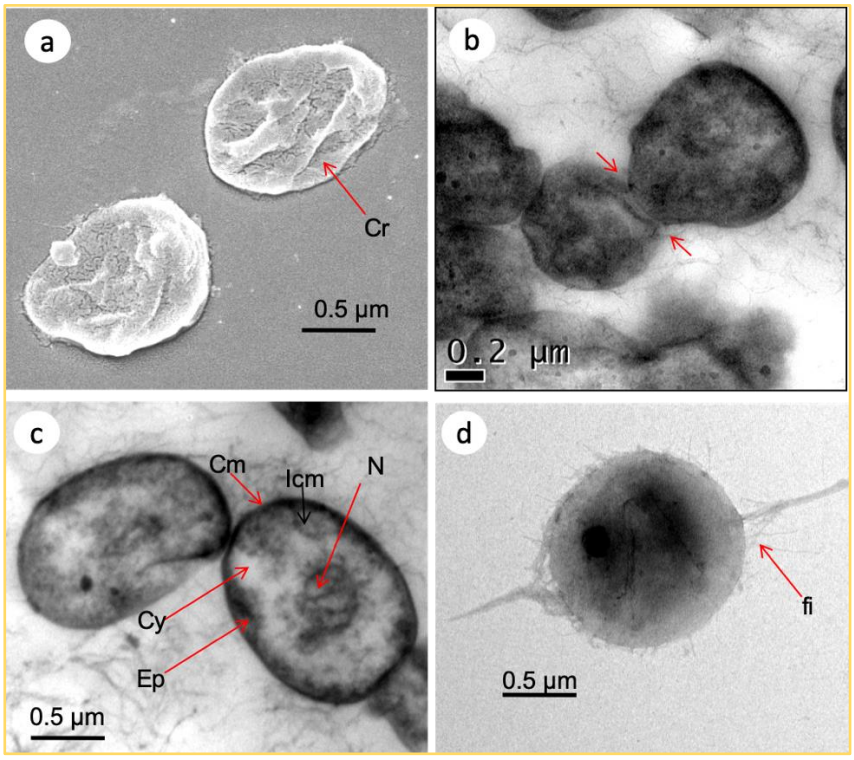

Fig. 3.4.2.7 Electron microscopic images of strain JC646^T. (a) SEM image showing intact cells having Crateriform structure (b) negative stain image showing budding process; (c) TEM image showing different parts of the cell; (d) cell showing fimbriae. Cm, Cellular Membrane; Icm, Invagination of cytoplasmic membrane; N, Nucleoid; Cy, Cytoplasm; Ep, Enlarged periplasm; fi, Fimbriae.

3.4.2.6 Chemotaxonomic characterization

3.4.2.6.1 FAME profile

The fatty acid profile of the strain JC646^T is the in congruence with the type species of the genus *Gimesia*, with major proportions of $C_{16:1}\omega7c/C_{16:1}\omega6c$ and $C_{16:0}$. $C_{10:0}3OH$, anteiso-$C_{11:0}$, $C_{12:0}3OH$, anteiso-$C_{12:0}$, anteiso-$C_{13:0}$, $C_{15:0}2OH$, $C_{15:1}\omega6c$, anteiso-$C_{15:0}$, $C_{17:0}$, iso-$C_{17:1}\omega9c$, anteiso-$C_{17:0}$, $C_{18:0}$, $C_{18:1}\omega7c$ and $C_{18:1}\omega9c$ fatty acids are also present However, the strain JC646^T differed from *G.maris* DSM 8797^T in the absence of $C_{17:1}\omega9c$ (Table. 3.4.2.4).

Table 3.4.2.4. Cellular fatty acid composition (%) of strain JC646^T and *G. maris* DSM 8797^T

Fatty acid (%)	**Strain JC646^T**	***G. maris* DSM 8797^T**
$C_{10:0}$3-OH	1.1	1.0
anteiso-$C_{11:0}$	8.5	7.0
anteiso-$C_{12:0}$	2.0	2.0
$C_{12:0}$3-OH	1.0	1.0
anteiso-$C_{13:0}$	8.8	7.4
$C_{15:0}$2-OH	2.2	2.2
anteiso-$C_{15:0}$	5.0	6.1
$C_{15:1}\omega$6C	1.1	1.3
$C_{16:0}$	**24.8**	**26.4**
$C_{16:1}\omega$7c/$C_{16:1}\omega$6c	**27.5**	**27.5**
$C_{17:0}$	1.3	1.3
anteiso-$C_{17:0}$	3.6	3.5
iso-$C_{17:1}\omega$9c	2.3	3.3
$C_{18:1}\omega$7c/$C_{18:1}\omega$9c	4.6	4.6
$C_{17:1}\omega$9c.	-	2.1

3.4.2.6.2 Polar lipid profile

The polar lipid profile of strain JC646^T (Fig. 3.4.2.8a) was not following the type species of *Gimesia*, *G. maris* (Scheuner et al. 2014). However, the polar lipids of *G. maris* DSM 8797^T in this study (Fig. 3.4.2.8b) are similar to what was reported earlier except for the absence of glycolipid (Scheuner et al. 2014; Sittig and Schlesner 1993). Polar lipids of strain JC646^T are phosphatidyl-diethanolamine, diphosphatidyl-glycerol, phosphatidylcholine, an unidentified phospholipid (PL), two unidentified lipids (L1,2) and an unidentified amino lipid (AL) (Fig. 3.4.2.8a). At the same time, *G. maris* DSM 8797^T has phosphatidylcholine, phosphatidylglycerol, unidentified phospholipid (PL), phosphatidyl-monomethylethanolamine, phosphatidyl-dimethylethanolamine and diphosphatidylglycerol (Fig. 3.4.2.8b). Strain JC646^T differs from *G. maris* DSM 8797^T in not having phosphatidyl-monoethylethanolamine and phosphatidylglycerol but additionally having an unidentified amino lipid and two unidentified lipids. MK6 is the predominant quinine of both strains.

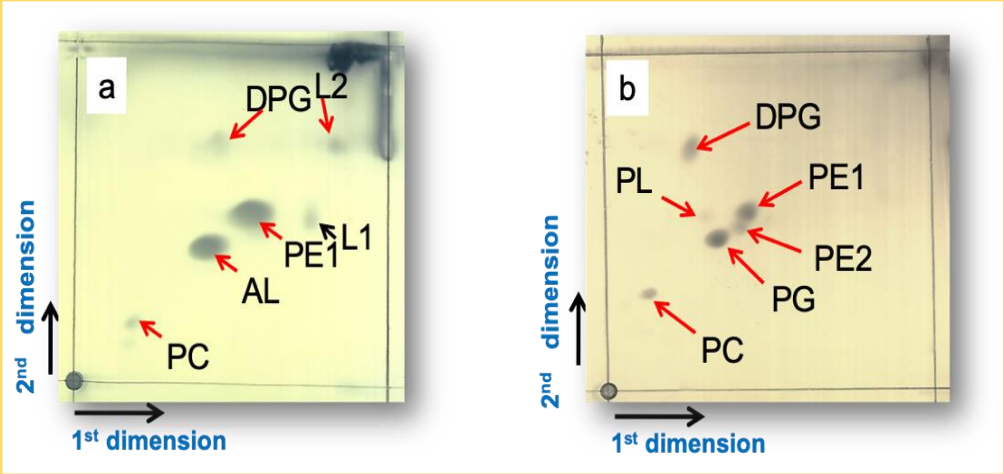

Fig. 3.4.2.8. Two dimensional chromatograms showing polar lipids of (a) strain JC646^T and (b) *G. maris* DSM 8797^T. PE1, phosphatidyl-dimethylethanolamine; PE2, phosphatidyl-monomethylethanolamine; PC, Phosphatidylcholine; PG, phosphatidylglycerol; AL, unidentified amino lipid; L1,2, unidentified lipids; DPG, Diphosphatidylglycerol; PL, unidentified phospholipid

3.4.2.6.3 Polyamine Profile

Both the strains *G. maris* DSM 8797^T and JC646^T have two polyamines; sym-homospermidine and putrescine (Fig. 3.4.2.9). While only sym-homospermidine was previously reported (Scheuner et al. 2014), in this study we also report the presence of putrescine in both strains.

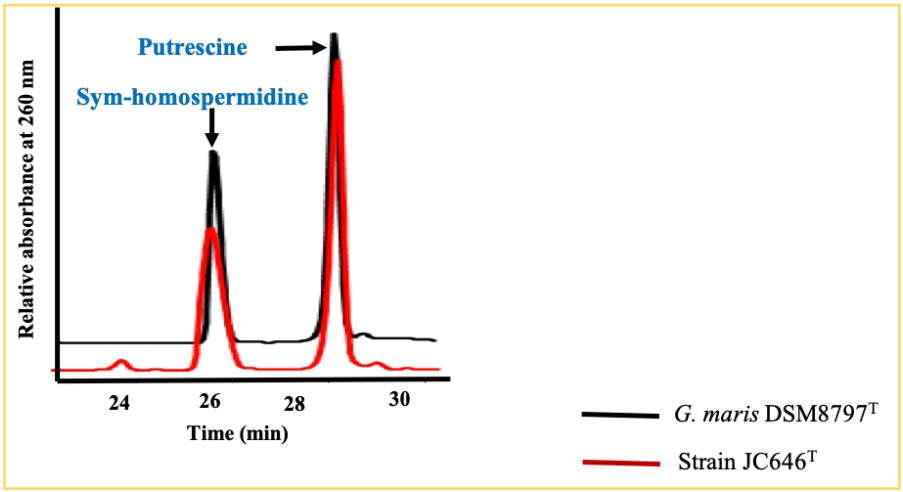

Fig. 3.4.2.9. HPLC chromatogram of polyamines of *Gimesia* spp.

Table. 3.4.2.5 Differential characteristics of (1) *Gimesia chilikensis* JC646^T and 2. *G. maris* DSM 8797^T.

Characteristics	1	2
Cell shape	Oval to pear shaped	Spherical to ovoid
Cell size (diameter µm)	0.7-1.0	0.4-1.5
Stalk	-	+
Temp range °C (optimum)	20-30 (30)	5-40 (30-35)
NaCl tolerance range (optimum) [%]	1.0-7.0 (3)	1.0-4.0 (3)
Organic substrates used for growth		
Rhamnose	-	+
Sucrose	+	-
Fumarate	+	-
Lactose	+	-
Nitrogen sources used for growth		
Nitrate	-	+
L-Glutamic acid	+	-
L-Isolucine	+	-
Nitrate reduction	-	+
Polar lipids		
PE2	-	+
PG	-	+
AL	+	-
L1,2	+	-
PL	-	+
Genomic DNA G+C content (mol %)	53.2	50.5

Data from this study

Species: 1, *Gimesia chilikensis* JC646^T; 2, *Gimesia maris* DSM 8797^T.

Both species have MK6 as the only quinone; both grow from pH 7-9 with optima at 8.0. Diphospatidylglyycerol, phosphatidyl-dimethylethanolamine and Phosphatidylcholine are common for both species; major fatty acids are $C_{16:1}\omega7c/C_{16:1}\omega6c$ and $C_{16:0}$; grow well in the presence of glucose; does not require vitamin B_{12} for growth and can grow without N-acetylglucoseamine; PE2, phosphatidyl-monomethylethanolamine; PG, phosphatidylglycerol; AL, unidentified amino lipid; L1,2, unidentified lipids; PL, unidentified phospholipid.+, substrate utilized; - substrate not utilized;

3.4.3 Phylo-taxogenomic study of the strain JC651^T

3.4.3.1 Habitat and nucleotide sequences accession numbers

The strain JC651^T was isolated from a sediment sample collected from Satapada region (19°40'12.0"N 85°25'48.0"E) of the Chilika lagoon. The 16S rRNA gene sequence of the taxa was deposited with European Molecular Biology Laboratory (EMBL) with accession numbers LR133893. The whole genome sequence of strain JC651^T (6,245,843 nt) was deposited to NCBI with accession number WIAD01000000.

3.4.3.2 Genomic characteristics

The genome size of strain JC651^T and *R. ulvae* DSM 25454^T are 6,245,843 nt and 8,119,320 nt, respectively. RAST (Aziz et al. 2008) data analysis of the genomes indicate complete coding sequences as 4904 for strain JC651^T and 6210 for *R. ulvae* DSM 25454^T. The number of RNAs present in strain JC651^T is 49, while *R. ulvae* DSM 25454^T has 67. N50 value for the genome of strain JC651^T is 92046, whereas it is 127469 for *R. ulvae* DSM 25454^T genome. The Genomic DNA G+C contents of strain JC651^T and *R. ulvae* DSM 25454^T are 62.4 and 59.1 mol%, respectively. The difference between the genome G+C content of the strains is 3.3 mol%, which is good enough to delineate species (Ritcher and Rossello-Mora 2009).

Genome sequences of the strains JC651^T and *R. ulvae* DSM 25454^T were aligned using PATRIC online software to identify the multiple maximal matches and local collinear blocks (LCBs) (https://www.patricbrc.org/) (Wattam et al. 2019). The genome sequence of the strain C651^T is used as a reference sequence against *R. ulvae.* The alignment of LCB of both strains differs from each other variably (Fig. 3.4.3.1). The protein sequences identity based on a genome map was prepared using the PATRIC server's proteome comparison service. Analysis of this map indicated that most of the proteins of strain JC651^T share 20-

80% similarity with those of *R. ulvae* DSM 25454^T (Fig. 3.4.2.2). This suggested the clear-cut dissimilarity of strain JC651^T with *R. ulvae* DSM 25454^T.

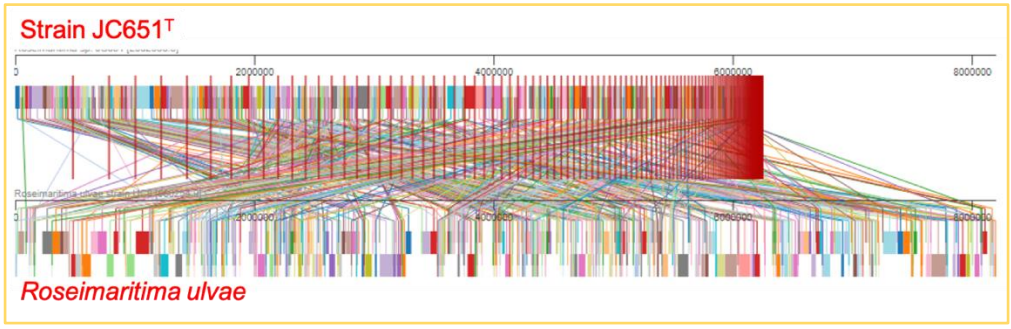

Fig. 3.4.3.1. Genome organization of strain JC651^T and *R. ulvae* DSM 25454^T.

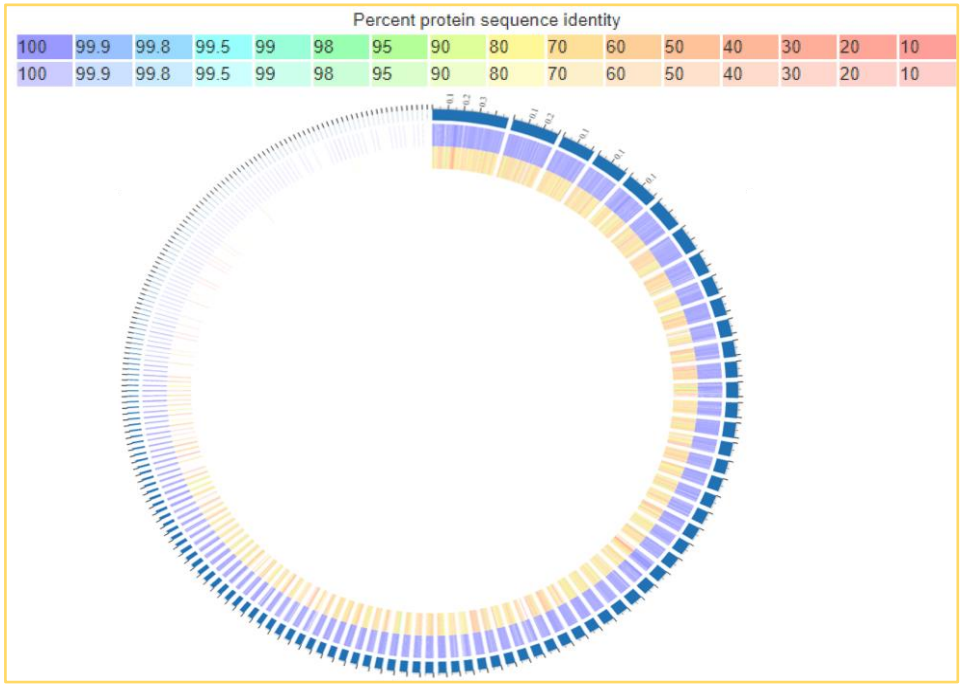

Fig. 3.4.3.2. Genome map based on protein sequence identity between *Roseimaritima* sp. strain JC651^T and *Roseimaritima ulvae*. Genome of *R.* sp. strain JC651^T was used as reference. List of track from outside to inside- *Roseimaritima* sp. strain JC651^T, *R. ulvae* DSM 25454^T

3.4.3.3 BLAST Analysis and Phylogenetic inference

The genome average nucleotide identity (gANI) score and *in silico* DNA–DNA hybridization (*d*DDH) values between strain JC651^T and *R. ulvae* DSM 25454^T were 74.9% and 19.5%, respectively. The gANI and *d*DDH values of both strains are far less [(95-96% cut off for ANI and 70% cut off for *d*DDH)] than the recommended (Goris et al.

2007; Richter and Rossello-Mora 2009) cut-off values for species delineation which is additionally supported by average amino acid identity (AAI) score of 72.2% (cut off for AAI = 95–96 %) between the taxa. The genomic information clearly distinguishes strain JC651^T from *R. ulvae* DSM 25454^T. The phylogenetic tree with combined bootstrap values obtained from NJ, ME, ML trees (Fig. 3.4.3.3) established the clustering of strain JC651^T within the genus *Roseimaritima* with 100% bootstrap value and distinctly separated from the only species of the genus, *R. ulvae* DSM 25454^T. Further, the phylogenomic tree (Fig. 3.4.3.4) and 16S rRNA gene-based tree (Fig. 3.4.3.3) showed that the strain JC651^T clade with *R. ulvae* and is a member of the genus *Roseimaritima.*

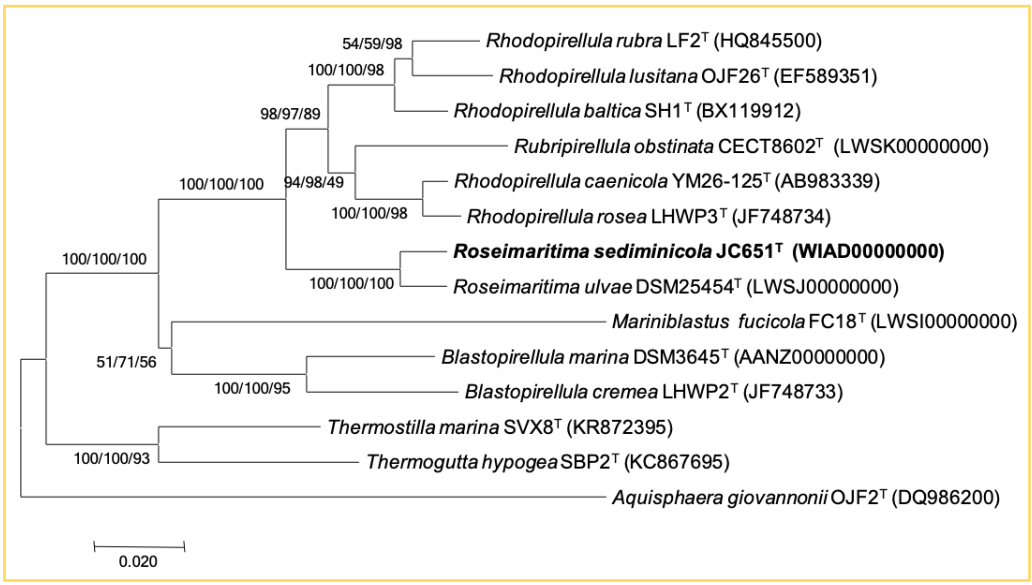

Fig. 3.4.3.3 Phylogenetic tree based on 16S rRNA gene sequences showing the phylogenetic relationship of strain JC651^T with other nearest members of *Planctomycetaceae* family. The tree was constructed using MEGA 7 software and *Aquisphaera giovannonii* OJF2^T was used as outgroup. The GenBank accession numbers for 16S rRNA gene sequences or whole genome are shown in parentheses. Bootstrap values refer to NJ/ME/ML analysis. Bar, 0.02 nucleotide substitution per position.

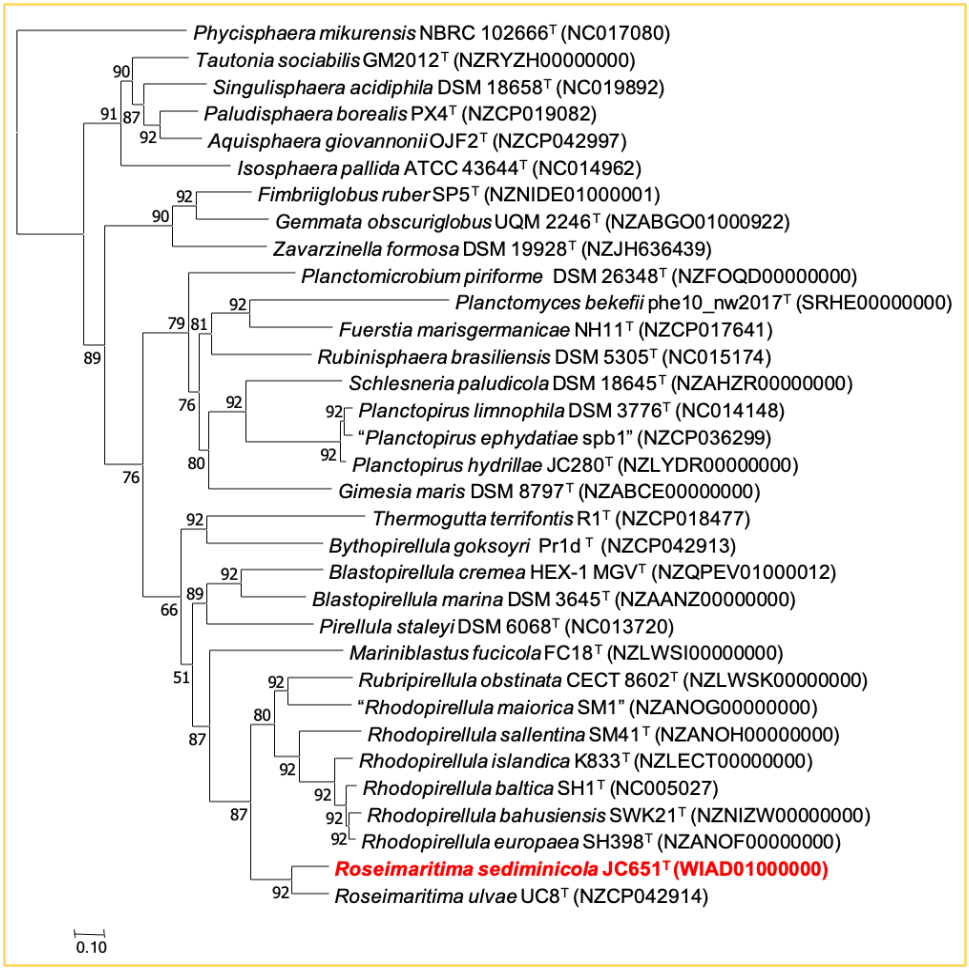

Fig. 3.4.3.4. RAxML-based phylogenomic tree of strain JC651T along with publicly available genome sequences of the families Planctomycetaceae and Isosphaeraceae. The GenBank accession numbers for genome sequences are shown in parentheses. Values at the nodes show the number of times a particular branch was observed in the support trees. The genome of *Phycisphaera mikurensis* was used as an outgroup. Bar, 0.10 nucleotide substitutions per position.

(T3PKS). NRPS (non-ribosomal peptide synthetase) and N-acyl amino acid production were exclusive to *R. ulvae* DSM 25454^T. For distinguishing the biochemical pathways between the strains, the EC numbers of the protein-coding genes were downloaded from PATRIC and then submitted to the online Interactive Pathways (iPath) explorer (https://pathways.embl.de/). Both strains have the 2-C-methyl-D-erythritol 4-phosphate/1-deoxy-D-xylulose 5-phosphate (MEP) pathway for the synthesis of isopentenyl pyrophosphate (IPP), an essential precursor for the synthesis of carotenoids

and quinones (Eisenreich et al. 2004; Zhao et al.2013; Zhang 2018). The carotenoids of the members of planctomycetes are not well studied.The genes for carotenoid biosynthesis were observed in both JC651^T and *R. ulvae* DSM 25454^T. However, genes encoding for lycopene-beta cyclase resulting in the formation of α and β-carotene were present only in JC651^T. Retinol metabolism genes were observed in both strains. Further, both strains have the capability to produces diapocarotenes. It also appears from the pathway map (Fig. 3.4.3.5) that strain JA651^T and *R. ulvae* probably choose an alternate biosynthetic route from the known pathways for diapocarotenes biosynthesis.

3.4.3.4 Morphological and physiological analyses

Colonies of strain JC651^T were round, 0.1-0.5 mm in diameter, and light pink, similar to *R. ulvae* DSM 25454^T. Cells were spherical to pear-shaped, with an average cell size of 1.0-2.0 x 0.8-1.5 (length x width, Fig. 3.4.3.6A), arranged in rosettes of 3-30 cells (Fig. 3.4.3.6B), multiplied by budding, with crateriform structures only at one side of the cells (Fig. 3.4.3.6 C) and having numerous fimbriae (Fig. 3.4.3.6D). We could not observe motile cells. The ultra-structure of strain JC651^T showed (Fig. 3.4.3.6E) the presence of nucleoid and internal cytoplasmic membrane architecture.

Growth that was observed with different carbon substrates/nitrogen sources/pH range/NaCl requirements of the strain JC651^T are given in either species description or Table 3.4.3.2. The strain JC651^T does not require vitamin B12 for its growth than *R. ulvae* DSM 25454^T. Nitrate is not reduced by strain JC651^T, which contrasts with *R. ulvae* DSM 25454^T where nitrate is reduced to nitrite. Fermentative growth is absent in either strain. Both strains are obligate aerobes with chemoorganoheterotrophic growth mode. Enzymatic activity was performed using the API ZYM kit (Biomerieux, France) following the manufacturer's protocol. Strain JC651^T was positive for alkaline phosphatase,

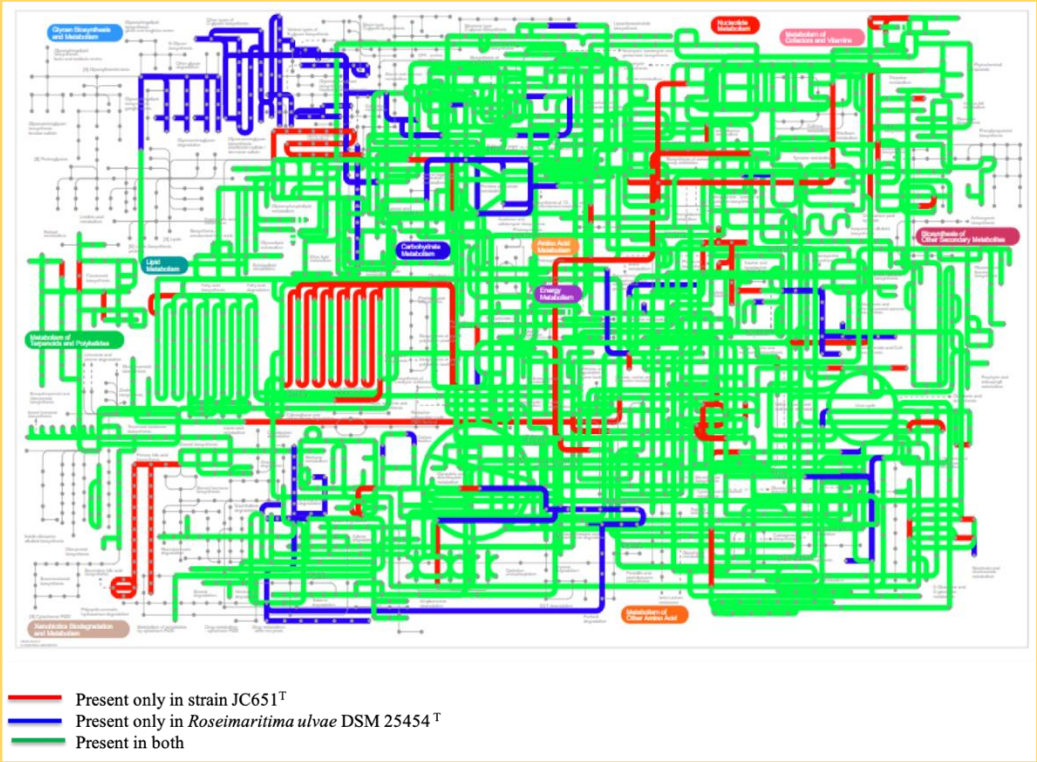

Fig. 3.4.3.5. Common and unique biochemical pathways between strain JC651^T and *R. ulvae* DSM 25454^T

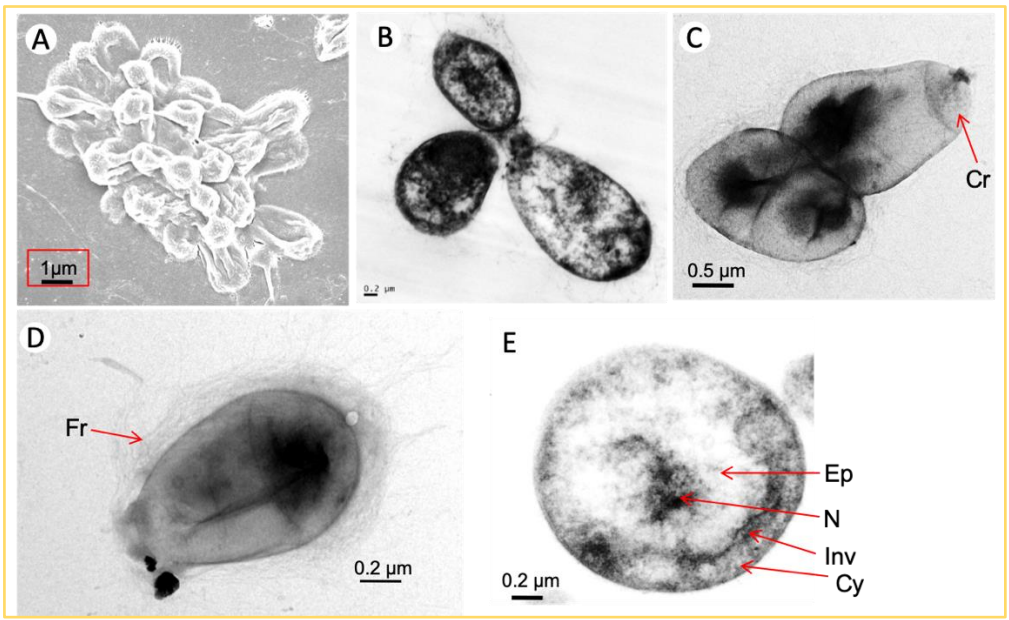

Fig. 3.4.3.6. Electron microscopic images of strain JC651^T: (A) SEM image showing the aggregate of cells, (B) showing rosette of cells in 3, (C) TEM image showing crateriform structures, (D) TEM image showing fimbriae and (E) ultrastructure of cell. Fr, fimbriae; Cr, Crateriform structures; Ep, Enlarged periplasm; Cy, Cytoplasm; N, Nucleoid; Inv, Invagination of cytoplasmic membrane.

esterase (C4), esterase lipase (C8), leucine arylamidase, valine arylamidase, acid phosphatase, naphthol-AS-BI-phosphohydrolase and negative for lipase (C14),cysteine arylamidase, trypsin, α-chymotrypsin, α-galactosidase, β-galactosidase, β-glucuronidase, α-glucosidase, β- glucosidase, N-acetyl- β-glucosaminidase, α-mannosidase, α-fucosidase in API ZYM test. *R. ulvae* DSM 25454^T differs from strain JC651^T by showing cysteine arylamidase activity, α-glucosidase, and α-galactosidase and no activity of Naphthol-AS-BI-phosphohydrolase.

3.4.3.5 Chemotaxonomic characterization

3.4.3.5.1 FAME analysis

Primary fatty acids of both strains *R. ulvae* DSM 25454^T and JC651^T are $C_{18:1}\omega9c$ (36.0%) and $C_{16:0}$ (19.3%) and the fatty acids composition is shown in Table 3.4.3.1. Strain JC651^T differs from *R. ulvae* DSM 25454^T in additionally having two hydroxy fatty acids ($C_{10:0}$3OH, $C_{15:0}$2OH), anteiso-$C_{15:0}$, anteiso-$C_{13:0}$ and anteiso-$C_{17:0}$.

3.4.3.5.2 Polar lipid profile

The polar lipids of strain JC651^T are diphosphatidylglycerol, an unidentified phospholipid, phosphatidylglycerol, and phosphatidylcholine (Fig. 3.4.3.7). The polar lipids of strain JC651^T are accordance with the type species of the genus *Roseimaritima* with diphosphatidylglycerol, phospholipid, phosphatidylglycerol, phosphatidylcholine and differ in the absence of unidentified lipid and amino lipid. MK6 is the predominant quinone of both the strains.

Table 3.4.3.1. Cellular fatty acid composition (%) of 1. strain JC651^T and 2. *R. ulvae* DSM 25454^T.

Fatty acid (%)	**1**	**2**
$C_{10:0}$3-OH	1.8	-
anteiso-$C_{13:0}$	6.4	-
$C_{14:0}$	1.0	1.2
$C_{15:0}$2-OH	3.0	-
anteiso-$C_{15:0}$	5.2	-
$C_{16:0}$	**19.3**	**32.6**
$C_{17:0}$	1.6	2.5
anteiso-$C_{17:0}$	3.8	-
$C_{17:1}\omega8c$	1.5	2.4
$C_{18:1}\omega9c$	**36.0**	**45.0**
$C_{18:0}$	4.7	3.6
$C_{18:0}$ 3-OH	1.8	1.3
$C_{20:1}\omega9c$	4.5	2.6
Summed feature 3 ($C_{16:1}\omega7c/C_{16:1}\omega6c$;)	1.5	2.4

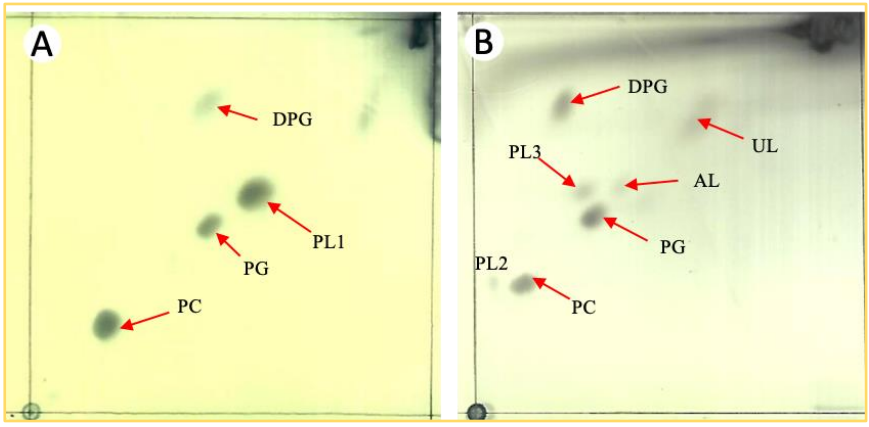

Fig. 3.4.3.7: Two dimensional chromatogram showing polar lipids of A). strain JC651^T and B). *R. ulvae* DSM25454^T.DPG, diphosphatidylglycerol; PL1,2,3, unidentified phospholipids; PG, phosphatidylglycerol; PC, phosphatidylcholine; AL, unidentified aminolipid; UL, unidentified lipid .

Table 3.4.3.2 Differential characteristics of 1. Strain JC651^T and 2. *R. ulvae* DSM 25454^T.

Characteristics	1	2
Cell shape	Round to pear	Spherical to ovoid
Cell size (lxw, in µm)	1.0-2.0x0.8-1.5	1.1–1.8 × 0.9–1.5
pH range (optima)	6.0-9.0 (7.5)	6.5-10(7.5)
NaCl range (%)(optima)	1-5 (4)	1-5 (3)
Temp range °C (optimum)	15-40 (25)	15-35 (30)
Reduction of nitrate	-	+
Nitrogen sources used for growth		
Nitrate	-	+
Peptone	-	+
L-Phenylalanine	+	-
L-Lysine	+	-
Glutamate	+	-
DL-Threonine	-	+
L-Arginine	-	+
Activity of enzymes		
Cysteine arylamidase	-	+
Naphthol-AS-BI-Phosphohydrolase	+	-
α-Galactosidase	-	+
α-Glucosidase	-	+
Vit B_{12} requirement	-	+
G+C content (mol %)	62.4	59.1
Genome size (Mb)	6.2	8.1
RNAs	49	67
Coding sequences	4904	6210

MK6 is the only quinone; polar lipids include: diphosphatidylglycerol; phospholipid; phosphatidylglycerol and phosphatidylcholine. Both strains utilized NAG, sucrose, maltose, lactose, mannitol, D-galactose, rhamnose, starch, D-galactose and D-xylose as a carbon source whereas none of the strains use Na-acetate, fumarate, pyruvate, propionate, inositol, fructose, malic acid, inulin, Na-succinate, sorbitol, benzoic acid and citrate. Both strains used ammonium sulphate, glutamine, L-proline as nitrogen source whereas both strains did not use tyrosin, cysteine, D-valine, DL-ornithine, L-methionine, L-tryptophan, L-histidine, alanine and urea as nitrogen source. Both the strains were positive for alkaline phosphatase, esterase (C4), esterase lipase (C8), leucinearylamidase, valinearylamidase andacid phosphatase. Both the strains were negative for lipase (C 14), trypsin, α-chymotrypsin, β-galactosidase, β-glucuronidase, β- glucosidase, N-acetyl- β-glucosaminidase, α-mannosidase and α-fucosidase.$C_{18:1}\omega 9c$ and $C_{16:0}$ are the major fatty acids of both strains. +, substrate utilized; - substrate not utilized.

3.4.4 Phylo-taxogenomic of strain JC650^T, JC657^T, JC636 and JC649

3.4.4.1 Habitat and nucleotide sequences accession numbers

The strains JC650^T, JC657^T, JC636 and JC649 isolated from the sediment samples collected from 3 different regions of Chilika lagoon; Satpada (GPS position: 19°40'12"N 85°25'48"E), Balugaon (GPS position: 19°42'51"N 85°11'54" E) and Rambha (GPS position: 19°30'54"N 85°05'53" E) Odisha, India. Amplicon based 16S rRNA gene sequences of all four strains (JC636, JC649, JC650^T, JC657^T) were deposited with European Molecular Biology Laboratory (EMBL) with accession numbers LR132030, LR132074, LR794306 and LR794311, respectively. The whole genomes sequences of strains JC636, JC649, JC650^T and JC657^T having 6962901, 6961268, 7069583 bp and 6965996 bp, were deposited to NCBI with accession numbers JACEHG000000000, JACEHI000000000, WEZF00000000 and JABBYO000000000, respectively.

3.4.4.2 Genomic characteristics

The genome size of strains JC650^T is 7.07 Mb with an N50 value of 2,58,013, and the genome size of strains JC657^T, JC636, and JC649 is ~6.97 Mb with an N50 value of 4,15,372. The genome of strain JC650T has 5,491genes, of which 5,338 are protein-coding genes, 65 genes are for RNAs, and 88 genes are pseudogenes. While the genome of strains JC657^T, JC636, and JC649 has ~5,372 genes, of which ~5,220 are protein-coding genes, 57-62 genes are for RNAs, and 90-92 genes are pseudogenes. Genomic DNA G+C content of strains JC650T and strain JC657^T (including strains JC636 and JC649) is 63.9 and 62.7 mol%, respectively.

Genome sequences of strains JC650^T, JC657^T, *T. sociabilis* GM2012T, and *"T. plasticadhaerens"* EIP^T were aligned using PATRIC to identify the multiple maximal

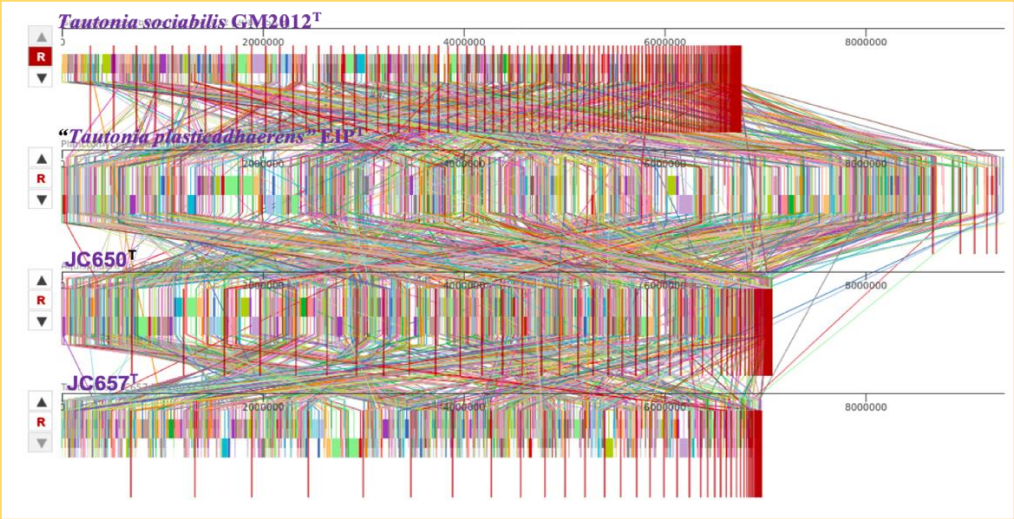

Fig 3.4.4.1. Genome organization of strains *T. sociabilis* GM2012^T , *T. plasticadhaerens* ElP^T. JC650^T, and JC657^T

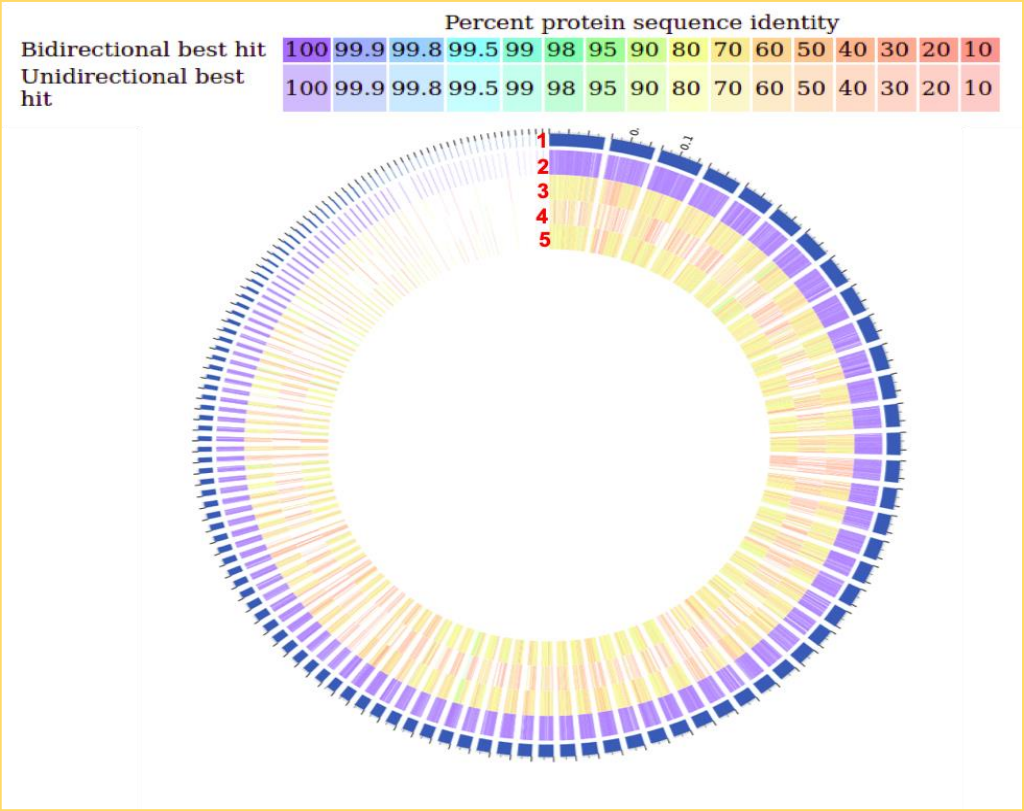

Fig 3.4.4.2. Genome map based on protein sequence identity. Genome of *Tautonia sociabilis* GM2012^T was used as reference List of tracks from outside to inside. 1. Scale of contig length 2. *T. sociabilis* GM2012^T 3. strain JC650^T 4. Strain JC657^T 5. "*T. plasticadhaerens"* ElP^T.

matches and local collinear blocks (LCBs) (https://www.patricbrc.org/). The genome sequence of *T. sociabilis* GM2012^T was used as a reference sequence against strains JC650^T, JC657^T, and *"T. plasticadhaerens"* EIP^T. The alignment of LCB of all the four Type strains differs from each other variably (Fig. 3.4.4.1). A protein sequence identity based on genome map was prepared using the PATRIC server's proteome comparison service. Analysis of this map indicated that most of the proteins of all the strains JC650^T/JC657^T, *T. sociabilis* GM2012^T and *"T. plasticadhaerens"* EIP^T share 20-80% similarity among themselves (Fig. 3.4.4.2). This suggests clear-cut dissimilarity of strains JC650^T and JC657^T (including strains JC636, JC649) with the existing species of *Tautonia* and between strains JC650^T and JC657^T as well.

3.4.4.3 BLAST Analysis and Phylogenetic inference

BLAST analysis of amplicon based 16S rRNA gene sequences of strains JC636, JC649, JC650^T and JC657^T showed highest (94.8-94.9%) identity with *Tautonia* spp. (*T. sociabilis* GM2012^T and *"T. plasticadhaerens"* EIP^T, respectively). The 16S rRNA gene sequence identity between the four strains is 99.4-100% (Fig. 3.4.4.3). The 16S rRNA gene sequence of the four strains pulled out from the genome has a sequence length of 1524 nt each and shares the highest 16S rRNA gene sequence identity with members of the genus Tautonia (<94.9%) (Fig. 3.4.4.3). These results are similar to the amplicon 16S rRNA gene sequence analysis.

The minimum AAI values of strains JC650^T and JC657^T with *Tautonia* spp. (*T. sociabilis* GM2012^T and *"T. plasticadhaerens"* EIP^T) is 76.3% and 71.0% respectively (Fig. 3.4.4.3), which fall near to the recommended cut-off of 80% used for the genus delineation (Qin et al. 2014).The maximum OrthoANI and *d*DDH value of strains JC650^T and JC657^T with *T. sociabilis* GM2012^T and *"T. plasticadhaerens"* EIP^T is 76.1-76.6% and 20.6-21.0 %, respectively, which are far less (95-96% cut off for ANI and 70% cut off

for *d*DDH) than the recommended (Goris et al. 2007; Richter and Rossello-Mora 2009) cut off values for species delineation. Further, OrthoANI and *d*DDH values between strains JC650^T and JC657^T are 84.4 % and 27.5 %, indicating that these two strains belong to two different species of the same genus *Tautonia* (Fig. 3.4.4.3). OrthoANI and *d*DDH values among strains JC636, JC649, and JC657T is >99.9 % and >99.9 %, which showed that these three strains belong to the same novel species (Fig. 3.4.4.3)**.** The characters of strain JC657^T also apply to strains JC636 and JC649, unless otherwise mentioned.

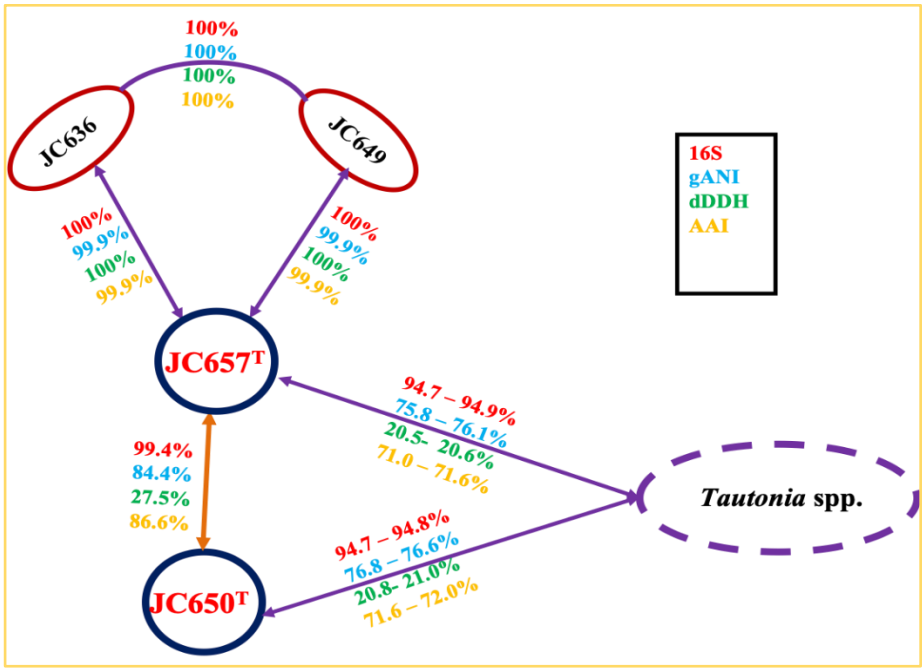

Fig. 3.4.4.3 Analysis of phylogenetic markers for delineation of the novel isolates JC650^T and JC657^T. Methods used: 16S rRNA gene identity (16S), average amino acid identity (AAI), average nucleotide identity (ANI) and digital DNA-DNA Hybridization (*d*DDH).

The 16S rRNA gene sequence-based phylogenetic tree with combined bootstrap values obtained from NJ, ME, ML trees (Fig. 3.4.4.4) confirmed the clustering of strains JC650^T, JC657^T, JC636 and JC649 within the genus *Tautonia. It separated* distinctly from the existing members of (*T. sociabilis* GM2012^T and *"T. plasticadhaerens"* EIP^T). Moreover, strains JC650^T and JC657^T are also distinctly separated from each other and

forms two distinct clades. In contrast, strains JC636, JC649, and JC657^T together form one clade. Phylogenomic tree based on 92 core genes also confirmed the clustering of strains JC650^T, JC657^T, JC636 and JC649 within the genus *Tautonia* and separated distinctly with the existing members of *Tautonia* (*T. sociabilis* GM2012^T and *"T. plasticadhaerens"* EIP^T) and strains JC650^T and JC657^T are also distinctly separated from each other, while strains JC636, JC649 and JC657^T together form one clade (Fig. 3.4.4.5). Hence, we further characterized the strains JC650^T and JC657^T (together with JC636 and JC649), which we propose to classify as two different species within the genus *Tautonia* under the family *Isosphaeraceae*.

3.4.4.4 *In-silico* metabolic characterization

COG annotation results showed that both the strains JC650^T and JC657^T are similar to other species of genus *Tautonia* in all the metabolic functions (Fig. 3.4.4.6). CAZy annotation of genomes of the strains JC650^T and JC657^T shows that they contain more genes for glycosyl transferases, followed by glycoside hydrolases similar to distribution in all the species belonging to genus *Tautonia*. The analysis also shows that 80–90% of the enzyme families account to glycoside hydrolases and glycosyl transferases (Fig. 3.4.4.7). However, the relationship between the presence of higher number of carbohydrate active enzymes and polysaccharide degradation needs further studies. Genes for linoleic acid metabolism are present in strain JC650^T and *"T. plasticadhaerens"* ElP^T. Strain JC650^T also differed from *"T. plasticadhaerens"* ElP^T in carotenoid bioynthesis, glycerolipid metabolism, Phosphonate and phosphonate metabolism, purine, pyrimidine and thiamine metabolism (Fig. 3.4.4.9). Strains JC650^{T}and JC657^T contain genes for lycopene β-cyclase, which were absent in *"T. plasticadhaerens"* ElP^T and *T. sociabilis* GM2012^T (Fig. 3.4.4.8,9,10).

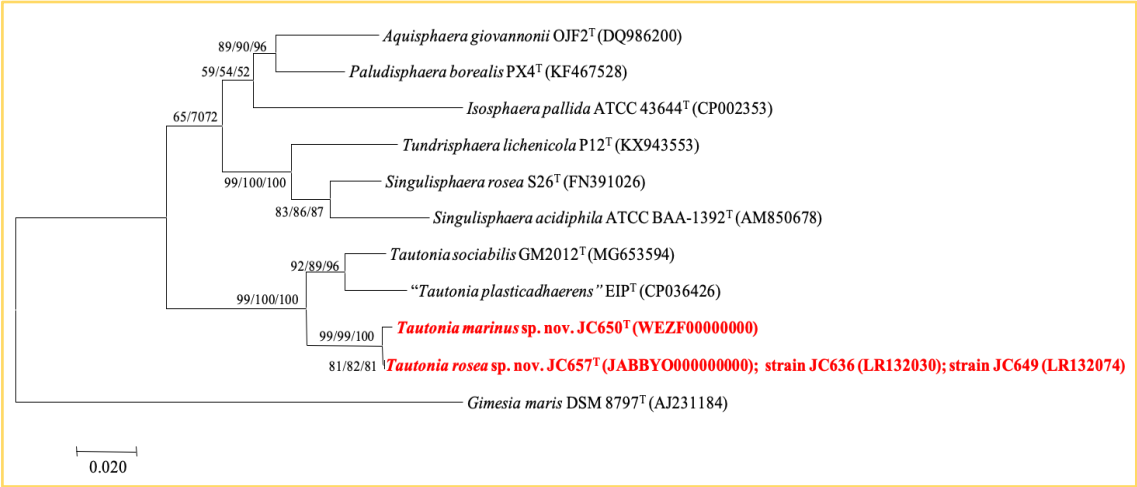

Fig.3.4.4.4 16S rRNA gene sequences based Phylogenetic tree showing the phylogenetic relationship of strains JC636, JC649, JC650^{T} and JC657^{T} within the family *Isosphaeraceae*. The tree was computed with MEGA 7 software and rooted using *Gimasia maris* DSM 8797^{T}as the out-group. The GenBank accession numbers for 16S rRNA gene sequences are shown in parentheses. Bootstrap percentages refer to NJ/ML/ME analysis. Bar, 0.02 nucleotide substitution per position.

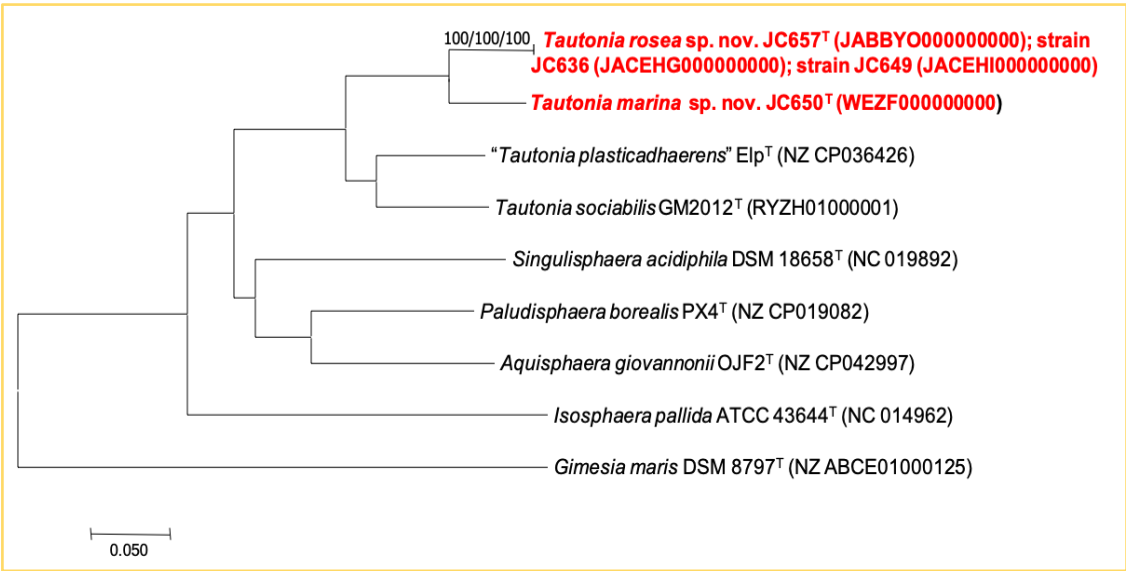

Fig. 3.4.4.5 Phylogenomic tree of strains JC636, JC649, JC650^{T}and JC657^{T} along with publicly available genome sequences of *Isosphaeraceae* family. The GenBank accession numbers for genome sequences are shown in parentheses. The tree was computed with MEGA 7 software and rooted using *Gimasia maris* DSM 8797^{T}as the out-group. Bootstrap percentages refer to ME/ML/NJ analysis. Bar, 0.02 nucleotide substitution per position.

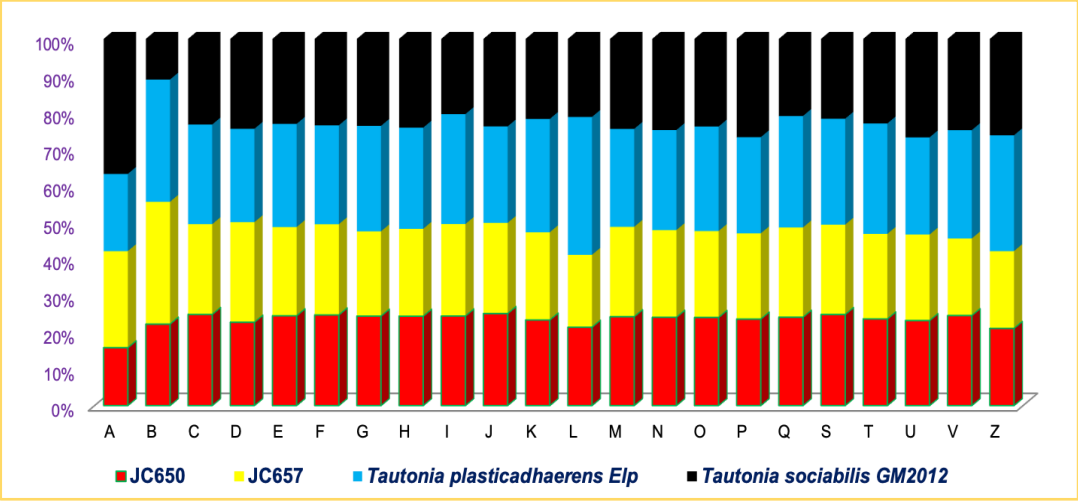

Fig 3.4.4.6 Functional classification COGs clusters of orthologs of two isolates and related strains in the genus of Tautonia. A: RNA processing and modification; B: Chromatin Structure and dynamics; C: Energy production and conversion; D: Cell cycle control and mitosis; E: Amino Acid metabolis and transport; F: Nucleotide metabolism and transport; G: Carbohydrate metabolism and transport; H: Coenzyme metabolism; I: Lipid metabolism; J: Tranlsation; K: Transcription; L: Replication and repair; M: Cell wall/ membrane/ envelop biogenesis; N: Cell motility; O: Post-translational modification, protein turnover, chaperone functions; P: Inorganic ion transport and metabolism; Q: Secondary Structure; S: Function Unknown; T: Signal Transduction; U: Intracellular trafficing and secretion; V: Defense mechanisms; Z: Cytoskeleton;

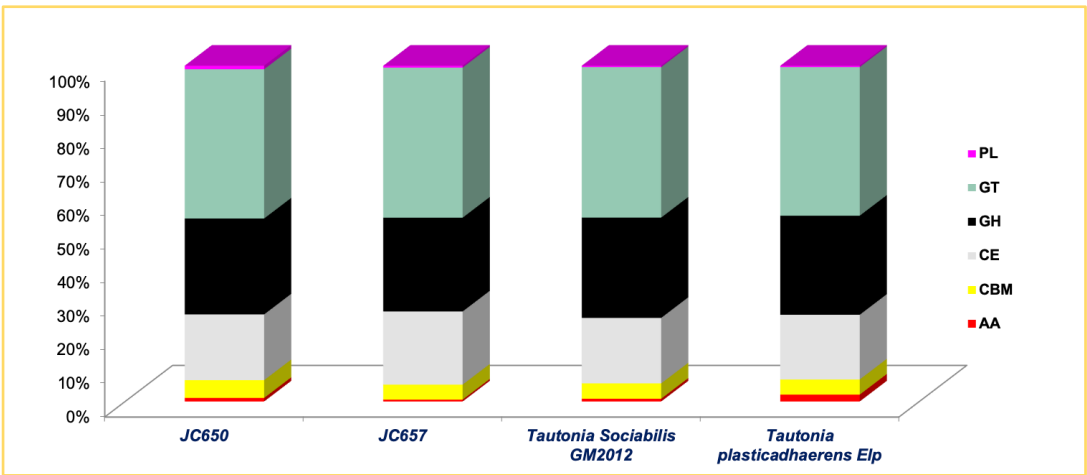

Fig 3.4.4.7 Comparative analysis of CAZymes of strains JC650^T, JC657^T and related species of genus *Tautonia*. Abbreviations: AA, Auxiliary Activities (AAs); CBM, Carbohydrate-Binding Modules (CBMs); CE, Carbohydrate Esterases (CEs); GH, Glycoside Hydrolases (GHs); GT, GlycosylTransferases (GTs); PL, Polysaccharide Lyases (PLs)

Strain JC650^T and *T. sociabilis* GM2012^T differed in carotenoid biosynthesis, fatty acid metabolism, bile acid metabolism and alanine metabolism (Fig. 3.4.4.8). Incomplete carotenoid biosynthesis pathway in *T. sociabilis* GM2012^T probably makes culture look white compared to other members of *Tautonia* which are pink in colour. Strains JC650^T and JC657^T have 2-C-methyl-D-erythritol 4-phosphate/1-deoxy-D-xylulose 5-phosphate (MEP) pathway for the biosynthesis of five-carbon isoprene unit (isopentenyl pyrophosphate; IPP) which is eventually the precursor for the synthesis of carotenoids and quinones (Eisenreich et al. 2004; Zhao et al.2013; Zhang 2018).

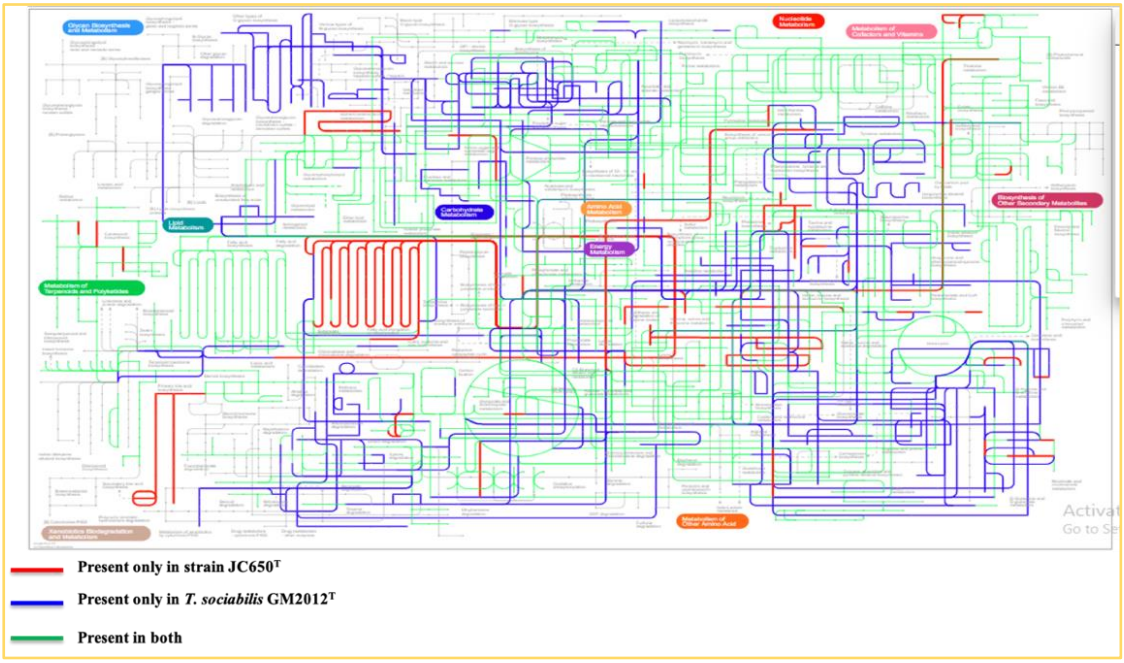

Fig. 3.4.4.8. Common and unique biochemical pathways between strains JC650^T and *T. sociabilis* GM2012^T.

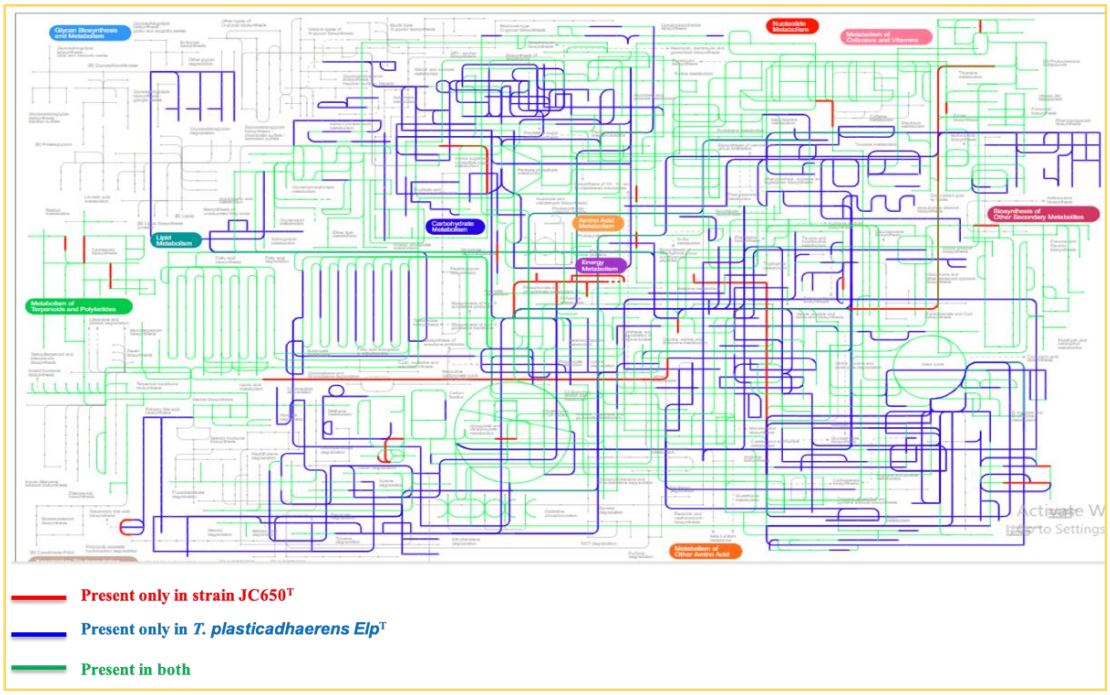

Fig. 3.4.4.9. Common and unique biochemical pathways between strains JC650^T and *T. plasticadhaerens* ElP^T.

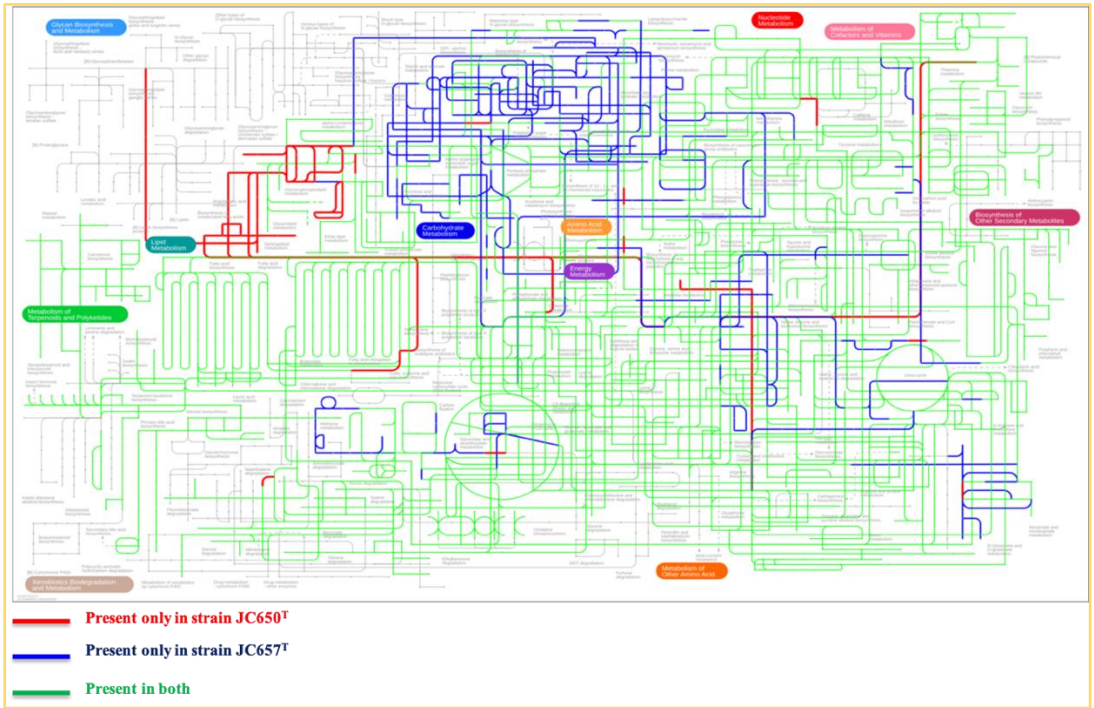

Fig. 3.4.4.10. Common and unique biochemical pathways between strains JC650^T and JC657^T

Strain JC650^T is capable of biosynthesis of unsaturated fatty acids and arachidonic acid metabolism which is absent in strain JC657^T. Both strains JC650^T and

JC657^T are putatively capable of synthesis of the anti-cancerous compound, staurosporine. The number of putative gene clusters for the biosynthesis of secondary metabolites in strains JC650^T and JC657^T are 9 and 8 respectively. Both strains have gene clusters coded for Type I Polyketide Synthase (TIPKS), terpenes and non-ribosomal peptide synthetase (NRPS-Like). Heterocyst glycolipid synthase-like PKS (hgIE-ks) is exclusive for strain JC650T only. Bacteriocin is exclusive for *T. sociabilis* GM2012^T while cyanobactin and acyl amino acids are exclusive for *"T. plasticadhaerens"* ElP^T (Fig. 3.4.4.11).

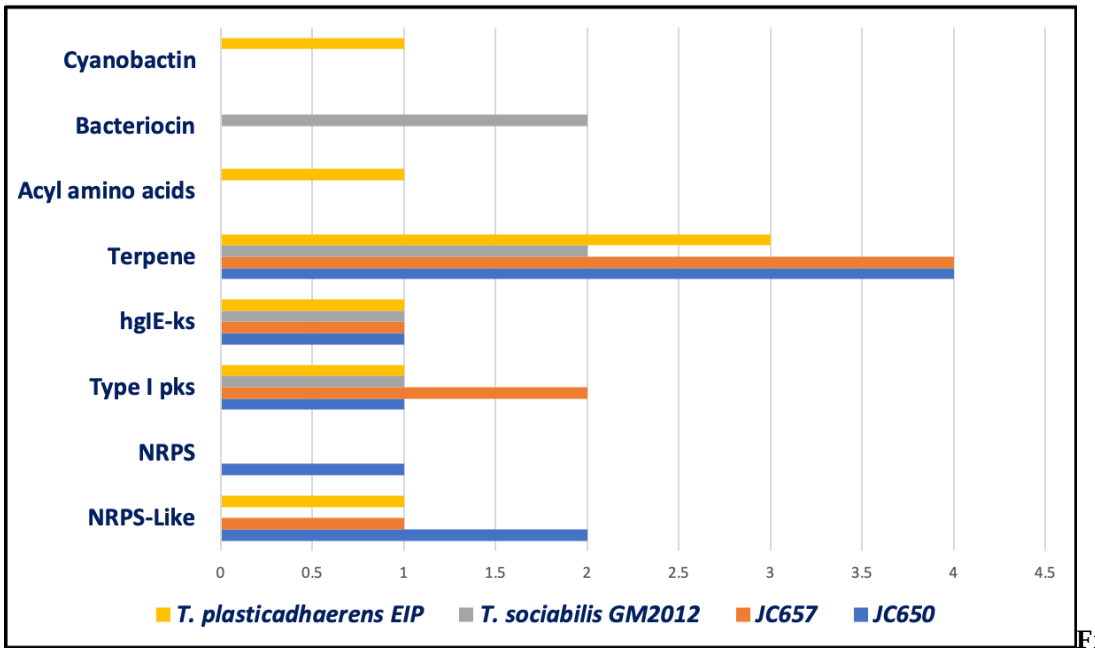

Fig. 3.4.4.11. Number of genetic clusters putatively involved in the production of secondary metabolites. The analysis is based on genome sequences of *T. sociabilis* GM2012^T, "*T. plasticadhaerens"* EIP^T, Strain JC650^T and Strain JC657^T.

3.4.4.5 Morphological and physiological analyses

SEM images of both strains JC650^T and JC657^T show that cells are spherical to oval in shape and crateriform structures are well distributed throughout their cell surface. The cells of both the strains, JC650^T and JC657^T are present as clusters (Fig. 3.4.4.12a, 3.4.4.13a). Negative staining of both strains show that their cells multiply by budding and mature cells are capable of attachment to the substrate through holdfast (Fig. 3.4.4.12b-

e, 3.4.4.13b-c). Mobility could not be observed in both the strains. TEM image of strain JC650^T shows pellucid intracellular membrane and intracellular compartments. In contrast, intracellular membrane (ICM) and intracellular compartments (ICC) are not distinct in strain JC657^T (Fig. 3.4.4.12f, 3.4.4.13d).

N-acetyl glucosamine was obligate for the growth of both the strains (JC650^T, JC657^T). Different organic carbon and nitrogen sources support growth of both the strains in the presence of NAG (Table 3.4.4.2). Enzymatic activity of both the strains JC650^T and JC657^T was determined using API ZYM kit (BioMérieux), according to the manufacturer's instructions for which results are given in Table 3.4.4.2 or in species description.

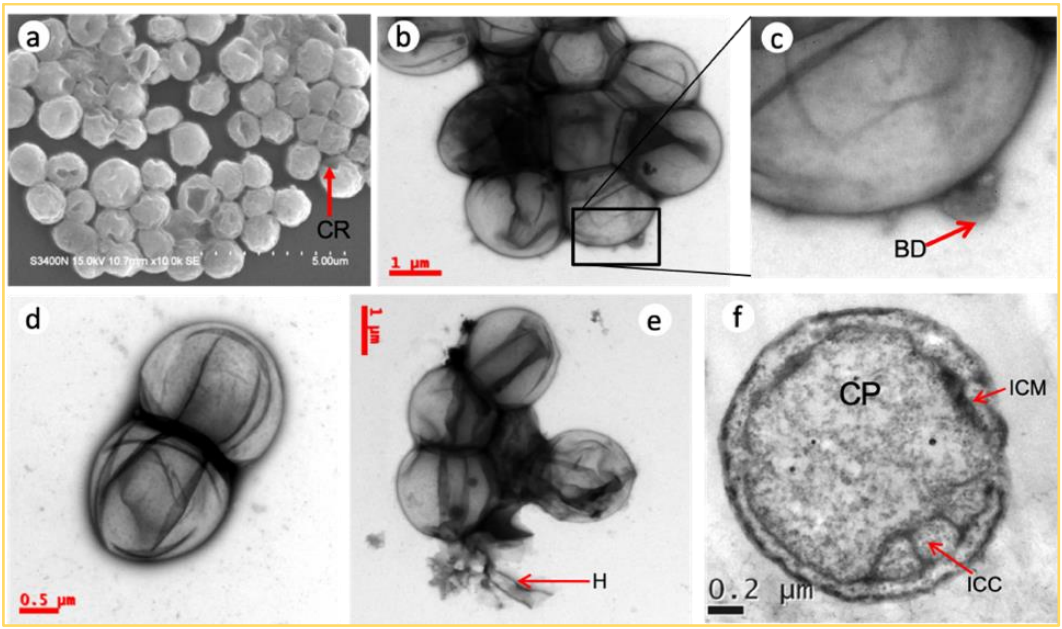

Fig. 3.4.4.12 Electron micrographs of strain JC650^T: SEM image showing spherical to oval cells in aggregates and having crateriform structures (CR) on the surface (a); TEM image of negatively stained cells (b-e), cells in aggregate (b); enlarged view of newly formed bud, shown by arrow head (c); two mature cells (d); cell aggregates showing holdfast, H (e); Ultrathin section of a cell showing intracellular membrane, ICM, intracellular compartments, ICC and cytoplasm, CP (f).

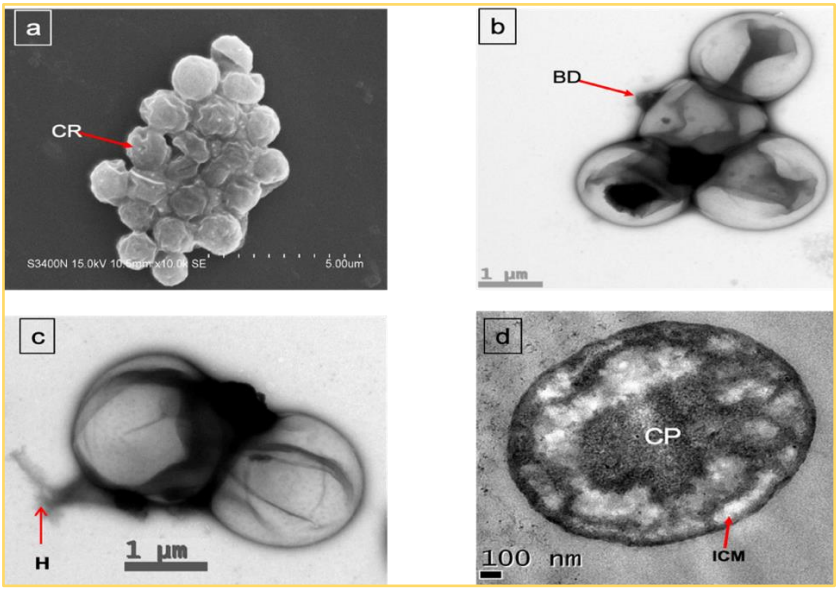

Fig.3.4.4.13 Electron micrographs of JC657^T: SEM image showing spherical to oval cells in aggregates and having crateriform structures (CR) on the surface (a); TEM image of negatively stained cells (b-c), cells in aggregate having newly formed bud, BD (b); cell aggregates showing holdfast, H (c); Ultrathin section of a cell showing intracellular membrane, ICM, intracellular compartments, ICC and cytoplasm, CP (d)

3.4.4.6 Chemotaxonomic characterization

3.4.4.6.1 FAME profile

Major (>10%) fatty acids of strains JC650^T and JC657^T are $C_{18:1}\omega9c$ and $C_{18:0}$ (Table 3.4.4.1).

Table 3.4.4.1. Cellular fatty acid composition (%) of the newly isolated strains

Fatty acid (%)	**Strains JC650^T, JC657^T, JC636, JC649**
anteiso-$C_{11:0}$	6.4-7.4
anteiso-$C_{12:0}$	1.7-2.0
anteiso-$C_{13:0}$	4.8-5.0
$C_{I4:0}$	7.4-7.7
anteiso-$C_{13:0}$	5.0
$C_{18:0}$3-OH	1.9-2.1
anteiso-$C_{15:0}$	4.3-4.7
$C_{15:0}$2-OH	1.0-1.2
$C_{19:0}$	1.5
$C_{16:0}$	7.1-7.3
$C_{18:0}$	**12.3-13.8**
anteiso-$C_{17:0}$	2.1-2.9
$C_{18:1}\omega9c$	**37.3-38.6**

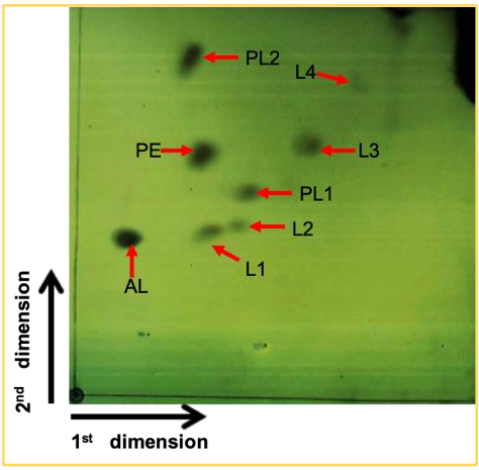

Fig. 3.4.4.14. Two dimensional chromatograms showing polar lipids of strain JC650^T (strain JC657^T also share similar polar lipids) PE, phosphatidylethanolamine; AL1, unidentified amino lipid; L1,2,3,4, unidentified lipid; PL1,2, unidentified phospholipid

3.4.4.6.2 Polar lipid profile

Polar lipid profile of strains JC650^T and JC657^T contain phosphatidylethanolamine (PE), unidentified amino lipid (AL1), and four unidentified lipids (L1) and two unidentified phospholipids (Fig. 3.4.4.14). MK6 is the only quinone.

3.4.4.6.3 Polyamine Profile

Putrescine and sym-homospermidine are the major polyamines (Fig. 3.4.15) of both the strains. No significant differences in fatty acids, polar lipids, quinone and polyamine composition was observed between the strains.

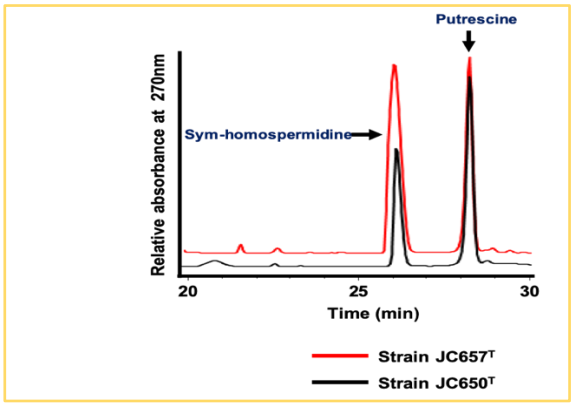

Fig. 3.4.4.15 HPLC data showing the presence of major polyamines in strains JC650^T and JC657^T.

Table 3.4.4.2. Comparison of phenotypic, chemotaxonomic and genomic features of 1. strain JC650^T 2. Strain JC657^T (including data of JC636 and JC649) 3. *T. sociabilis* GM2012^T and 4. *"T. plasticadhaerens"* EIP^T

Characteristics	**1**	**&2**	***3**	***4**
Phenotypic features				
Cell shape	Spherical to oval	Spherical to oval	Spherical	Spherical
Cell Diameter (□m)	1.8-2.0	1.8-2.0	1.7 ± 0.3	1.7-2.9
Colony colour	Pale Pink	Dark Pink	Pink	White
pH range (optimum)	7-10 (8)	7-10 (8)	6.0-8.5 (7.5)	5.5-9.0 (7.5)
Temp range °C (optimum)	15-37 (25)	10-37 (25)	10-33 (30)	37-46 (42)
NaCl tolerance range (%w/v)	1-6 (3)	1-5 (2)	nd	0-3 (0)
Holdfast Structure	+	+	nd	nd
Obligate requirement for NAG	+	+	-	-
Chemotaxonomic features				
Polar Lipids	PE, AL1, L1-4, PL1-2	PE, AL1, L1-4, PL1-2	nd	nd
Major Polyamines	Putrescine, Sym-homospermidine	Putrescine, Sym-homospermidine	nd	nd
API ZYM (Biomeriux)				
Esterase Lipase (C18)	+	-	nd	nd
Lipase (C14)	+	-	nd	nd
α-fucosidase	+	-	nd	nd
Trypsin	-	+	nd	nd
Genomic Features				
Genome Size (bp)	7,069,583	&6,965,996	9,395,224	6,760,005
G + C (mol%)	63.9	&62.7	71.1	70.1
Total genes	5482	&5369	7707	5183

&Characters based on three strains.

nd, not determined; +, Present; -, absent; PE, phosphatidylethanolamine; AL, unidentified aminolipids; L, unidentified lipids; PL, unidentified phospholipid; *data taken from literature (Jogler et al. 2020; Kovaleva et al. 2019); &genomic data of only strain JC657^T; NAG, N-acetyl glucosamine. All taxa are obligately aerobic, divide by budding, have crateriform structures, major fatty acids as $C_{18:1}\omega9c$, $C_{18:0}$ and $C_{16:0}$.

3.4.5 Characterization of the strains JC640 and CH01.

3.4.5.1 Habitat and nucleotide sequences accession numbers

Strain JC640 was isolated from a sediment sample collected from the Balugaon region (19°40'12.0"N 85°25'48.0"E) of Chilika lagoon (Odisha, India) from a depth of 2 meters with the help of a grab sampler. At the time of sampling, the salinity, pH and temperature of the sample were 2.0%, 7.5 and 24 °C respectively. Strain CH01 was isolated from a sediment soil near Karaikal beach (10°54'58.0"N 79°51'13.0"E), Puducherry, Tamil Nadu, India. The temperature, pH and salinity of the samples were 25 °C, 7.8 and 2.5 % respectively.

3.4.5.2 Genomic characteristics

The genome of strain JC640 has 5,761,926 nt arranged in 154 contigs, whereas strain CH01 has 5758428 nt arranged in 150 contigs. RAST data analysis indicates that both genomes have a GC content of 63.6 mol% and N_{50} value of 74,341. Both genomes contained 4,648 coding sequences and the total number of RNAs was 61.

3.4.5.3 BLAST Analysis and Phylogenetic inference

The strains JC640 and CH01 are closely related species based on 16S rRNA gene sequences identity (99.9 %). BLAST analysis of 16S rRNA gene sequences through EZBioCloud revealed that both strains have the highest sequence similarity (<93.3 %) with members of the genus *Roseimaritima* (*R. ulvae* and *R. sediminicola*) and <91.1 % identity with other members of the family Pirellulaceae. These values are less than the recommended cut off value (94.5 %) set for genus delineation based on 16S rRNA gene sequence (Yarza et al. 2014). To substantiate the claim of new genus, further comparative genome analyses were performed with members of different genera under the family Pirellulaceae. AAI values investigated between both strains and 33 other members of the family Pirellulaceae were in the range of 41.9-57.3 % (Table 3.4.5.1) which falls below

the cut off range (60-80 %) of AAI for genera delineation. POCP comparison of both strains with members of the family Pirellulaceae also yielded a maximum similarity range of 14.7-51.5 % except for *Roseimaritima sediminicola* for which the POCP value was 55.0 % (Table 3.4.5.2). The cut off value of POCP for genus delineation is recommended to be near to 50 % (Qin et al. 2014). The POCP value of 50-55% range with *Roseimaritima* spp. (Table 3.4.5.2) is in the overlapping range that can be considered for genus delineation as other genomic parameters strongly support it. Phylogenetic tree based on 16S rRNA gene sequences showed that both strains are within the family Pirellulaceae and are making a separate clade away from other members of family (Fig. 3.4.5.1). The 92 core genome based RAxML tree also showed that both strains make a distinct clade within the family Pirellulaceae (Fig. 3.4.5.2).

3.4.5.4 *In-silico* metabolic characterization

Both strains(JC640 and CH01)have the genes to encode for cell division related proteins;FtsK, FtsW and FtsH. Like all other Planctomycete (Wiegand et al. 2020), both strains do not have the gene to encode FtsZ, but have the gene to encode FtsK protein. Interestingly, FtsW protein coding genes were recorded from the Class *Phycisphaera* and "*Candidatus*Brocadiaceae" (Wiegand et al. 2020). Genome analysis of both the strains indicate the existences of gene encoding for FtsW protein in the class Planctomycetia as well. Further, the genome analysis of both strains also indicated the gene coding for FtsH protein which was not previously observed among the members of the phylum Planctomycetes (Wiegand et al. 2020). MreB protein, which is the homolog to the actin, plays a crucial role in the making or breaking most of the bacterial peptidoglycan cell wall (Wiegand et al. 2020). Both the strains JC640 and CH01 lack gene to encode MreB protein, following previous findings that members of the *Pirellula* clade seem to lack most

peptidoglycan-synthesis genes, despite possessing a generic peptidoglycan cell wall (Jeske et al. 2015)

The genome annotation for analysis of metabolic pathways revealed that strains JC640 and CH01 have genetic potential for fermentation and aerobic respiration. Genes coding for pyruvate dehydrogenase (EC 1.2.4.1), lactate dehydrogenase (EC 1.1.1.27), aldehyde dehydrogenase (EC 1.2.1.3), and alcohol dehydrogenase (EC 1.1.1.1) involved in fermentative metabolism are present in both strains. Both strains are putatively capable of producing acetic acid, lactic acid, ethanol and acetone as fermentation products. Genomes of both the strains revealed genes encoding for complete components of an aerobic respiratory chain, like F1F0-type ATP synthase, NADH ubiquinone oxidoreductase, succinate dehydrogenase, cytochrome bc1complex and cytochrome c oxidases. The terminal oxygen reductases in both the strains are represented by cytochrome c oxidases which are of caa_3 type having low affinity to oxygen. The genome showed no evidence that supports the growth of both the strains by anaerobic respiration. However genome showed incomplete pathways for dissimilatory nitrate reduction, methanogenesis and complete pathway of assimilatory sulfate reduction in both the strains.

The genes encoding for enzymes involved in pathways like glycolysis, gluconeogenesis, TCA cycle, phosphoenolpyruvate carboxylation and the glyoxylate shunt were predicted to obtain a better understanding on central carbon metabolism. Our prediction shows that both the strains have genes encoding for complete Embden-Meyerhof-Parnas pathway, TCA cycle and both oxidative and non-oxidative pentose phosphate pathway (Table 3.4.5.3). The essential enzymes for gluconeogenesis and glyoxylate shunt were absent and hence sugars are suitable substrates for energy and biomass formation. Both the strains showed 2-C-methyl-D-erythritol 4-phosphate/1-deoxy-D-xylulose 5-phosphate (MEP) pathway for the biosynthesis of five carbon isoprene

units (isopentenyl pyrophosphate; IPP), which is eventually the precursor for the synthesis of carotenoids and quinones. However pathway for quinone biosynthesis is absent in both the strains whereas *R. ulvae* showed complete pathway for menaquinone biosynthesis which shows that probably the strains JC640 and CH01 are depending on other organisms for uptake of quinones and hence unable to survive after several passages. The genome of both the strains showed incomplete futalosine pathway of menaquinone biosynthesis. The genes encoding for enzyme futalosine hydrolase (EC:3.2.2.26) which helps in conversion of futalosine to dehypoxanthinefutalosine an intermediary step in incomplete futalosine pathway of menaquinone biosynthesis is absent in both strains JC640 and CH01. In both the strains genes encoding for carotenoid biosynthetic enzymes like diapolycopene oxygenase (EC: 1.14.99.44), phytoene desaturase (EC: 1.3.99.26), 15-cis-phytoene synthase (EC: 2.5.1.32), 15-cis-phytoene desaturase (EC:1.3.5.5) were predicted.

. The Raetz pathway for KDO2-lipid A biosynthesis is predicted in the genus *Roseimaritima* is absent in the strains JC640 and CH01. Both the strains showed differences in Vitamin B6 metabolism i.e., genes encoding for pyridoxal phosphatase (EC 3.1.3.74), a hydrolase that converts pyridoxal 5'-phosphate (an active form of Vitamin B6) to pyridoxal in the presence of H_2O_2. Both the strains also showed differences in riboflavin metabolism, tryptophan metabolism and folate metabolism with respect to *R. ulvae*. These annotation results have provided an insight into their potential role in biogeochemical cycles such as for carbon, nitrogen and sulphur.

The genome analysis also showed the ability of both the strains to grow on glycerol. The genes encoding for glycerol uptake facilitator, glycerol kinase and other downstream enzymes were predicted in the genome. Majority of sulfatases which are helpful in degradation of sulfated glycopolymers predicted were classified as N-acetylglucosamine-6-sulfatase and N-sulfoglucosamine sulfohydrolase which aids in the degradation of

sulfated glycosaminoglycans like N-acetylglucosamine to support the growth of both the strains. The genome also showed genes encoding for iduronate-2-sulfatases which helps in hydrolysis of sulfate ester bonds from a wide variety of substrates, like steroids, carbohydrates and proteins were also predicted. The genome also showed pathways for utilization of various carbohydrates like mannose, maltose, xylose, maltodextrin and glycogen.

CAZy (Carbohydrate active enzymes) annotation by dbCAN metaserver strain JC640 and CH01 genome revealed greater than 60 genes encoding carbohydrate-active enzymes predicted to have N-terminal signal peptides and are probably involved in extracellular hydrolysis of substrates. Both the strains showed similar number of genes encoding for carbohydrate-active enzymes (CAZymes) and contains more number of carbohydrate binding molecules (CBMs) followed by glycoside hydrolases (GHs) and glycosyl transferases (GTs). Both of them contained CBM47, GT4 and CBM35 and CBM38 as major families and very few are organized in clusters (Fig 3.4.5.3).

Clusters of Orthologys (COGs) annotation classified proteins into 21 functional categories. Proteins belonging to categories general functional prediction only (R) nuclear structure (Y) and cytoskeleton (Z) were not observed in both the strains. The majority of proteins belongs to category S (unknown function) followed by energy production and conversion (C) and transport and metabolism. The strains JC640 and CH01 showed similar pattern and number of COG categories whereas *R. ulvae* UC8^{T} (Fig. 3.4.5.4). Planctomycetes are believed to produce bioactive secondary metabolites because of their complex life cycle and hence regions for secondary metabolite gene clusters were analysed using antiSMASH webserver. The number of putative secondary metabolite clusters in strain JC640 and CH01 are 7 whereas the genome of *R. ulvae* UC8^{T} showed 9 clusters respectively. All the three strains have clusters for terpenes, Type I

Polyketide Synthase (TIPKS), T III PKS, Non-ribosomal peptide synthetase(NRPS), NRPS-Like, Mixed NRPS-TIPKS and clusters coding for acyl aminoacids. Cluster for phosphonate is absent in *R. ulvae* UC8^{T}. Both the strains showed genes encoding for resistance-nodulation-cell division (RND) antibiotic efflux pump which is mainly helps in resistance of antibiotics like fluoroquinolone and tetracycline.

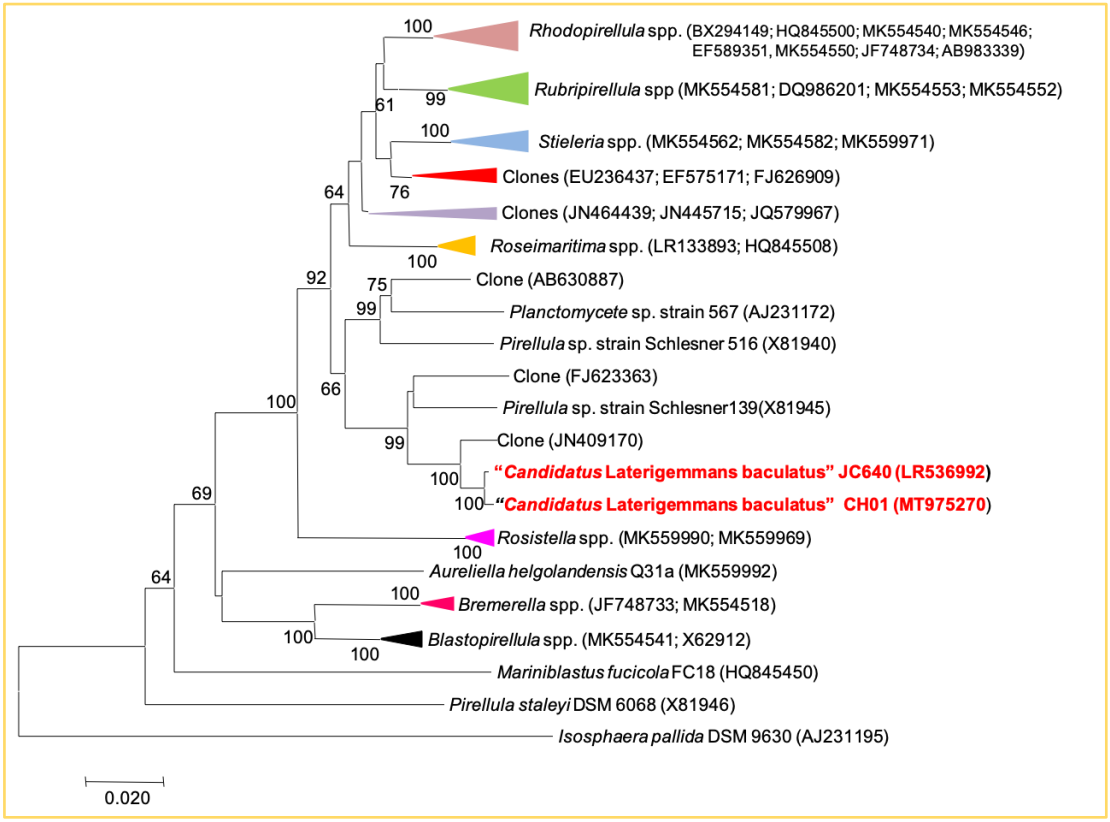

Fig. 3.4.5.1 The phylogenetic tree based on 16S rRNA gene sequences showing the phylogenetic relatedness of strains JC640 and CH01 with other members of family *Pirellulaceae.* Neighbor Joining method implemented in MEGA 7 software was used for construction of the tree and *Isosphaera pallida* DSM 9630^{T} was used as out group. (Bar, 0.02 nucleotide substitution per position with a bootstrap value of 1000).

Table 3.4.5.1 AAI values of strains JC640 and CH01 with other members of Family Pirellulaceae.

	1	2	3	4	5	6	7	8	9	10	11	12	13	14	15	16	17	18	19	20	21	22	23	24	25	26	27	28	29	30	31	32	33	34
1	100																																	
2	44.1	100																																
3	44	47.8	100																															
4	44.3	48.1	57.5	100																														
5	43.8	48	74.1	57.8	100																													
6	43.5	47.1	48.4	49.1	48.5	100																												
7	43.5	47.4	48.3	49.4	48.6	47.6	100																											
8	43.8	49.6	47	47.1	47.2	46.2	46.6	100																										
9	46.9	47	45.4	45.7	45.4	44.7	44.4	44.8	100																									
10	47.3	45.1	46.2	46.7	45.9	44.8	44.6	43.8	50.2	100																								
11	47.3	45	46.6	46.5	46.2	45.1	44.9	43.8	50.3	77.1	100																							
12	**45.2**	**50.9**	**48.6**	**49.43**	**48.7**	**47.6**	**49**	**54.1**	**46.3**	**45.9**	**46**	**100**																						
13	43.6	46.1	48.1	49	48.2	56.8	47.8	45.6	43.9	44.2	44.5	**47.7**	100																					
14	44.5	49.2	50.8	51.74	51.2	49.4	51.3	47.3	46.5	47	46.9	**50.3**	49.2	100																				
15	42	46.1	45.6	45.7	45.9	45.3	44.8	46	44.2	43	43	**46**	44.5	46.18	100																			
16	44.4	50.8	47.4	47.4	47.5	45.9	46.4	57.7	46.5	45.1	44.8	**55**	45.4	48.24	46.5	100																		
17	43.8	48.1	49.9	50.9	50.2	48.8	50.9	47	44.6	45.2	45.2	**49.4**	49.5	52.49	45.8	47	100																	
18	46.9	44.3	44.8	45.8	44.8	44.4	44.2	43	48.6	49.8	49.7	**45.1**	46	45.79	42.2	43.8	45.7	100																
19	43	40.9	41.1	41.1	41	40.4	40.8	40.2	48.8	44.2	44.5	**41.9**	40.6	41.81	39.4	40.3	41.7	44.2	100															
20	46.6	43.3	44.1	44.5	44.3	43.6	43.5	42.8	47	48.8	49.2	**43.8**	44.2	44.8	42.4	42.8	45.4	49.3	44.1	100														
21	46.8	44.8	45.1	45.4	45.2	44.7	43.7	43.4	49.6	52.2	52.3	**45.1**	43.8	46.07	41.6	43.9	44.8	48.9	43.5	48	100													
22	44	50.4	46.8	46.8	46.9	46.2	45.5	58.2	45.8	44.2	44.2	**53.6**	45.1	47.45	42.4	58.3	46.4	43.3	39.9	42.8	43.7	100												
23	43.9	50.4	46.9	47	46.8	46.2	45.7	58.3	46	44.3	44.4	**53.7**	45.4	47.73	46.4	58.3	46.6	43.2	39.7	42.8	43.9	87.8	100											
24	44.1	50.6	46.9	46.9	46.9	46.2	45.7	58.2	45.9	44.2	44.5	**53.9**	45.4	47.42	46.4	58.3	46.8	43.2	39.9	42.7	43.8	88.7	92.3	100										

25	43.6	49.5	46.3	46.5	46.5	46	45.5	58	45.1	43.6	43.6	**52.7**	45	47.1	46.3	58.4	46.3	43	39.2	42.4	43.4	63.3	63.5	63.2	100									
26	44.3	50.6	46.9	47.4	47	46.2	46	56.9	46	44.3	44.3	**53.7**	45.7	46.65	45.7	58.2	46.6	43.5	40.1	42.7	43.6	62.3	62.7	62.5	68.1	100								
27	45	51.5	48.1	48.2	48.2	47.2	48.2	55.5	46.3	45.2	45.5	**57.3**	46.7	47.74	46.3	57.4	48.4	44.5	40.9	43.4	44.5	55.6	55.7	55.8	55	56	100							
28	45	52.1	48.4	48.5	48.5	47.1	47.6	55.5	47.2	45.7	43.9	**57**	46.3	49.52	46.7	58.9	48.1	44.5	41.4	43.6	44.6	56.2	55.8	56.1	55.4	55.9	72.5	100						
29	44.1	52	49	48.4	48.3	47.5	48	53.3	47.7	46.1	46.2	**55.6**	47	49.9	46.7	55.62	48.5	44.6	41.4	43.7	45	53.6	53.7	53.6	52.9	53.8	56.9	53.8	100					
30	47.7	45.3	46.2	46	46.5	44.6	44	45.1	49.1	50.4	51.1	**45.7**	44.3	46.65	43.5	45.9	45	50	14.4	48.5	49.7	45.2	45.2	45.2	44.7	45.1	45.8	46.3	54.7	100				
31	42.6	48.1	45.8	45.9	46.1	45.5	45.2	58	43.5	42.6	44.6	**53.3**	45.1	46.43	45.9	59.1	46.1	42.1	39.1	41.9	42.2	56.9	57.1	57.4	57.3	56.8	54.9	53.1	54.1	43.1	100			
32	46	44	44.3	45.2	44.3	44.1	44.4	42.7	47.9	49.9	49.9	**44.8**	45.3	45.82	41.9	43.4	45.9	50.4	15	52.2	49.3	42.7	42.9	42.6	42.4	43.1	43.8	44.2	44.2	48.5	41.7	100		
33	43.8	50.6	47	47.1	47.6	46.2	46.6	57.8	46.8	46.1	45	**53.9**	45.3	47.87	46.3	58.71	46.9	43.8	40.6	42.9	43.8	56.9	57	57	56.1	56.1	56.2	56.3	54	45.9	57.4	43	100	
34	43	44.8	46.5	47.3	46.7	47.1	49.9	44.9	42.8	43.4	43.7	**46.3**	47.2	47.49	42.6	44.2	47.7	43.4	40	43.6	43.2	44	44.2	44.1	43.9	44.2	45.7	45.3	45.3	43.6	43.8	43	44	100

1. "*Alienimonas californiensis*" CA12^{T,} 2. "*Aureliella helgolandensis"* Q31a^{T,} 3. *Blastopirellula cremea* HEX-1 MGV^{T,} 4. *Blastopirellula marina* DSM 3645T, 5. "Bremerella volcania" Pan97T, 6. *Bythopirellula goksoyri* Pr1d^{T}, 7. "*Candidatus* Anammoximicrobium" AS06rmzACSIP, 8. "*Crateriforma conspicua*" Mal65^{T}, 9. *Fuerstia marisgermanicae* NH11^{T}, 10. *Gimesia maris* DSM 8797^{T}, 11. *Gimesia chilikensis* JC646^{T}, 12. Strain JC640/CH01, 13. *Lacipirellula parvula* PX69^{T}, 14. "*Lignipirellula cremea*" Pla85_3_4^{T}, 15. *Mariniblastus fucicola* FC18^{T}, 16. "*Novipirellula maiorica*" SM1^{T}, 17. *Pirellula staleyi* DSM 6068^{T}, 18. *Planctomicrobium piriforme* DSM 26348^{T}, 19. *Planctomyces bekefii* phe10_nw2017^{T}, 20. *Planctopirus limnophila* DSM 3776^{T}, 21. "*Polystyrenella longa*" Pla110^{T}, 22. *"Rhodopirellula bahuensis*" SWK21^{T}, 23. *Rhodopirellula baltica* SH 1^{T}, 24. "Rhodopirellula europaea" 6C^{T}, 25." Rhodopirellula sallentina" SM41^{T}, 26. "*Rhodopirellula solitaria*" CA85^{T} , 27. *Roseimaritima sediminicola* JC651^{T}, 28. *Roseimaritima ulvae* DSM 25454^{T}, 29. "Rosistilla oblonga" Poly24^{T,} 30. *Rubinisphaera brasiliensis* DSM 5305^{T}, 31. *Rubripirellula obstinata* CECT 8602^{T}, 32. *Schlesneria paludicola* DSM 18645^{T,} 33. "*Stieleria maiorica*" Mal15^{T}, 34. *Thermogutta terrifontis* R1^{T}

Table 3.4.5.2 POCP values of strains JC640 and CH01 with other members of Family Pirellulaceae.

	1	2	3	4	5	6	7	8	9	10	11	12	13	14	15	16	17	18	19	20	21	22	23	24	25	26	27	28	29	30	31	32	33	34
1	100																																	
2	28.7	100																																
3	29.2	37.0	100																															
4	29.8	36.6	57.5	100																														
5	30.0	37.1	72.6	59.7	100																													
6	26.2	31.4	32.8	34.0	34.3	100																												
7	22.5	29.0	29.5	32.3	31.0	27.6	100																											
8	28.8	40.9	33.6	33.4	35.4	31.0	27.6	100																										
9	32.2	34.7	30.8	32.0	30.9	27.8	25.9	30.3	100.0																									
10	34.5	30.6	33.5	35.6	34.3	27.8	26.5	26.9	40.9	100																								
11	35.2	30.9	34.4	35.2	34.7	27.8	26.8	27.6	41.3	81.1	100																							
12	**31.5**	**40.8**	**35.2**	**37.5**	**36.0**	**31.7**	**29.7**	**44.5**	**31.7**	**31.2**	**31.7**	**100**																						
13	25.4	29.7	33.1	34.6	33.7	47.3	26.9	27.9	25.7	26.6	26.7	**30.9**	100																					
14	28.1	36.6	39.8	42.4	41.9	32.2	33.3	31.4	32.4	34.0	35.2	**36.4**	32.1	100																				
15	24.4	32.1	30.1	30.1	30.5	27.5	23.6	32.4	28.3	25.1	25.4	**30.6**	26.2	29.2	100																			
16	28.9	41.9	33.5	34.0	34.6	28.8	26.3	51.0	32.1	29.3	29.7	**45.1**	26.7	33.1	31.5	100																		
17	29.1	35.7	41.8	44.8	44.4	33.9	33.2	32.8	29.2	31.5	32.2	**36.7**	35.9	45.4	29.7	32.3	100																	
18	34.0	28.1	29.5	32.3	31.2	27.1	24.3	25.8	35.3	39.8	40.2	**29.1**	30.2	30.4	24.1	27.2	32.8	100																
19	15.5	13.7	13.1	13.2	13.6	12.2	11.2	12.1	20.1	16.5	17.3	**14.7**	12.2	14.1	11.7	12.1	15.4	17.2	100															
20	35.4	27.3	29.5	30.9	30.8	25.7	23.3	25.6	32.2	38.6	38.9	**26.9**	26.8	28.2	23.0	25.0	34.6	41.7	17.7	100														
21	36.0	30.7	31.0	32.3	32.1	28.5	24.5	28.0	38.3	45.9	46.7	**31.2**	27.0	32.6	24.8	27.6	31.6	38.1	16.8	38.2	100													
22	28.5	42.7	33.2	33.2	33.8	30.0	25.5	55.1	32.9	28.0	28.5	**44.0**	27.3	32.2	32.0	53.3	32.1	26.3	12.1	25.1	27.7	100												
23	28.5	43.4	33.9	34.1	34.7	30.7	25.6	56.5	33.1	28.8	29.1	**45.0**	28.0	33.2	32.4	54.6	33.4	27.0	12.1	25.8	28.7	79.6	100											
24	28.9	43.3	33.9	33.6	34.8	30.6	25.7	56.9	33.0	28.5	29.1	**45.2**	27.6	32.3	32.4	54.2	33.3	26.8	12.3	26.0	28.4	80.4	82.8	100										
25	26.6	38.9	31.0	31.5	32.5	29.7	25.1	55.0	29.2	26.1	26.5	**40.9**	26.4	30.7	31.6	54.3	30.8	25.2	11.2	24.4	26.2	59.4	60.9	59.9	100									
26	30.4	42.0	33.6	34.3	34.7	29.9	26.8	51.6	31.4	28.6	28.6	**45.3**	27.9	32.3	30.6	52.7	32.6	26.8	12.3	26.2	27.9	58.1	59.5	58.8	59.2	100								
27	32.7	44.8	37.4	38.6	38.4	32.5	30.7	50.8	33.3	31.1	32.1	**55.0**	30.8	36.4	33.1	53.7	37.5	29.5	14.3	28.4	31.4	50.9	52.4	52.4	48.0	53.8	100							
28	31.3	46.7	37.9	38.2	38.8	31.6	29.2	50.7	35.0	32.3	32.5	**51.5**	29.6	37.8	33.6	56.6	36.8	29.3	14.1	27.5	30.2	52.6	53.5	53.2	49.3	51.8	71.8	100						
29	30.7	47.3	39.0	40.9	40.0	33.0	31.5	47.7	36.6	34.9	35.1	**50.6**	31.5	39.0	34.4	50.1	38.7	31.1	14.7	29.0	32.6	48.6	50.7	49.7	46.7	49.5	55.4	56.6	100					

30	38.5	31.2	34.2	35.6	36.1	27.9	24.6	31.3	37.4	43.5	44.7	**30.9**	26.4	32.1	26.3	31.3	32.5	41.4	16.4	42.0	41.2	31.1	31.3	31.7	30.1	31.4	33.6	33.7	35.3	100				
31	28.5	44.9	34.8	33.9	35.6	30.8	26.0	57.5	33.6	29.0	29.7	**45.0**	28.7	34.5	33.7	58.1	33.3	27.3	12.4	26.2	28.6	57.6	59.3	59.1	54.0	53.2	52.1	54.1	50.2	31.2	100			
32	30.1	27.7	28.8	30.5	28.7	25.0	24.6	23.6	35.3	39.5	40.3	**27.4**	28.4	30.9	22.5	25.8	32.1	40.8	17.7	42.2	37.7	24.1	24.5	24.0	22.9	25.6	27.3	28.0	28.9	36.0	25.5	100		
33	27.9	42.2	34.1	32.9	35.1	29.9	27.5	53.1	34.0	30.0	30.0	**43.6**	27.3	34.0	32.0	53.6	32.3	26.8	12.9	24.9	28.0	51.3	52.6	52.9	49.0	49.6	50.0	52.7	47.5	31.1	55.9	26.4	100	
34	26.0	27.2	30.7	33.4	32.8	30.2	36.0	28.2	22.9	25.1	25.5	**29.4**	29.1	29.5	23.5	24.8	34.6	25.4	12.0	26.8	26.0	24.4	25.3	24.9	25.8	26.9	30.9	27.8	29.2	27.0	25.1	23.8	24.5	100

1.“*Alienimonas californiensis*” CA12^{T,} 2. “*Aureliella helgolandensis”* Q31a^{T,} 3. *Blastopirellula cremea* HEX-1 MGV^{T,} 4. *Blastopirellula marina* DSM 3645T, 5. “Bremerella volcania” Pan97T, 6. *Bythopirellula goksoyri* Pr1d^{T}, 7. “*Candidatus* Anammoximicrobium” AS06rmzACSIP, 8. “*Crateriforma conspicua*” Mal65^{T}, 9. *Fuerstia marisgermanicae* NH11^{T}, 10. *Gimesia maris* DSM 8797^{T}, 11. *Gimesia chilikensis* JC646^{T}, 12. Strain JC640/CH01, 13. *Lacipirellula parvula* PX69^{T}, 14. “*Lignipirellula cremea*” Pla85_3_4^{T}, 15. *Mariniblastus fucicola* FC18^{T}, 16. “*Novipirellula maiorica*” SM1^{T}, 17. *Pirellula staleyi* DSM 6068^{T}, 18. *Planctomicrobium piriforme* DSM 26348^{T}, 19. *Planctomyces bekefii* phe10_nw2017^{T}, 20. *Planctopirus limnophila* DSM 3776^{T}, 21. “*Polystyrenella longa*” Pla110^{T}, 22. *“Rhodopirellula bahuensis*” SWK21^{T}, 23. *Rhodopirellula baltica* SH 1^{T}, 24. “Rhodopirellula europaea” 6C^{T}, 25.” Rhodopirellula sallentina” SM41^{T}, 26. “*Rhodopirellula solitaria*” CA85^{T} , 27. *Roseimaritima sediminicola* JC651^{T}, 28. *Roseimaritima ulvae* DSM 25454^{T}, 29. “Rosistilla oblonga” Poly24^{T,} 30. *Rubinisphaera brasiliensis* DSM 5305^{T}, 31. *Rubripirellula obstinata* CECT 8602^{T}, 32. *Schlesneria paludicola* DSM 18645^{T,} 33. "*Stieleria maiorica*" Mal15^{T}, 34. *Thermogutta terrifontis* R1^{T}

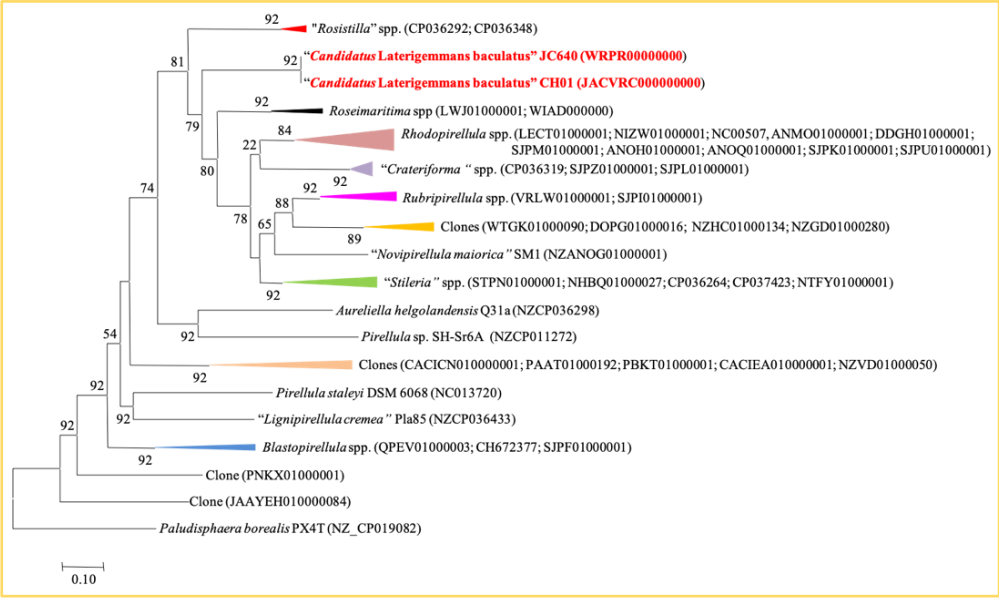

Fig. 3.4.5.2. phylogenomic tree based on RAxML of strains JC640 and CH01 along with publicly available genome sequences of *Pirellulaceae* family. Support value at the nodes shows the number of times a particular branch was observed in the support trees. Genome of *Paludisphaera borealis* PX4^T was used as an out group. Bar 0.10 nucleotide substitution per position.

Table 3.4.5.3 Genome-based analysis of the central carbon metabolism of "*Candidatus* Laterigemmans baculatus" JC640 and CH01 and *Roseimaritima ulvae* UC8^T

Enzyme/reaction	EC number	Gene	JC640	CH01	UC8
Glycolysis					
Glucose-6-phosphate isomerase	5.3.1.9	*pgi*	Yes	Yes	Yes
ATP-dependent 6-phosphofructokinase isozyme 1	2.7.1.11	*pfkA*	Yes	Yes	Yes
Fructose-bisphosphate aldolase class 2	4.1.2.13	*fbaA*	Yes	Yes	Yes
Triosephosphate isomerase	5.3.1.1	*tpiA*	Yes	Yes	Yes
Glyceraldehyde-3-phosphate dehydrogenase	1.2.1.12	*gapA*	Yes	Yes	Yes
Phosphoglycerate kinase	2.7.2.3	*pgk*	Yes	Yes	Yes
2,3-Bisphosphoglycerate-independent phosphoglycerate mutase	5.4.2.12	*gpmI*	Yes	Yes	Yes
Enolase	4.2.1.11	*eno*	Yes	Yes	Yes
Pyruvate kinase I	2.7.1.40	*pykF*	Yes	Yes	Yes
Pyruvate dehydrogenase E1 component	1.2.4.1	*aceE*	Yes	Yes	Yes
Dihydrolipoyllysine-residue acetyltransferase component of pyruvate dehydrogenase complex	2.3.1.12	*aceF*	Yes	Yes	Yes
Gluconeogenesis					
Phosphoenolpyruvate carboxylase	4.1.1.31	*ppc*	No	No	No

Pyruvate, phosphate dikinase	2.7.9.1	*ppdK*	Yes	Yes	Yes
Phosphoenolpyruvate carboxykinase (ATP)	4.1.1.49	*pckA*	Yes	Yes	Yes
Phosphoenolpyruvate carboxykinase (GTP)	4.1.1.32	*pckG*	No	No	No
Fructose-1,6-bisphosphatase class 2	3.1.3.11	*glpX*	No	No	Yes
Fructose-1,6-bisphosphatase class 1	3.1.3.11	*fbp*	No	No	No
Pyrophosphate–fructose 6-phosphate 1-phosphotransferase	2.7.1.90	*pfp*	Yes	Yes	Yes
			No	No	Yes
Pentose phosphate pathway					
Glucose-6-phosphate 1-dehydrogenase	1.1.1.49	*zwf*	Yes	Yes	Yes
6-Phosphogluconolactonase	3.1.1.31	*pgl*	Yes	Yes	Yes
6-Phosphogluconate dehydrogenase, decarboxylating	1.1.1.44	*gndA*	Yes	Yes	Yes
Transketolase 2	2.2.1.1	*tktB*	Yes	Yes	Yes
Transaldolase B	2.2.1.2	*talB*	Yes	Yes	Yes
Entner–Doudoroff pathway			Yes	Yes	Yes
KHG/KDPG aldolase	4.1.2.14	*eda*	Yes	Yes	Yes
Phosphogluconate dehydratase	4.2.1.12	*edd*	Yes	Yes	Yes
TCA cycle					
Citrate synthase	2.3.3.16	*gltA*	Yes	Yes	Yes
Aconitate hydratase A	4.2.1.3	*acnA*	Yes	Yes	Yes
Isocitrate dehydrogenase (NADP)	1.1.1.42	*icd*	Yes	Yes	Yes
2-Oxoglutarate dehydrogenase E1 component	1.2.4.2	*sucA*	Yes	Yes	Yes
Dihydrolipoyllysine-residue succinyltransferase component of 2-oxoglutarate dehydrogenase complex	2.3.1.61	*sucB*	Yes	Yes	Yes
Succinate–CoA ligase [ADP-forming] subunit alpha	6.2.1.5	*sucD*	Yes	Yes	Yes
Succinate–CoA ligase [ADP-forming] subunit beta	6.2.1.5	*sucC*	Yes	Yes	Yes
Succinate dehydrogenase flavoprotein subunit	1.3.5.1	*sdhA*	Yes	Yes	Yes
Succinate dehydrogenase iron-sulfur subunit	1.3.5.1	*sdhB*	Yes	Yes	Yes
Succinate dehydrogenase cytochrome b556 subunit	1.3.5.1	*sdhC*	No	No	No
Succinate dehydrogenase hydrophobic membrane anchor subunit	1.3.5.1	*sdhD*	No	No	No
Fumarate hydratase class I, an/aerobic	4.2.1.2	*fumA/B*	No	No	No
Fumarate hydratase class II	4.2.1.2	*fumC*	Yes	Yes	Yes
Malate dehydrogenase	1.1.1.37	*mdh*	Yes	Yes	Yes
Glyoxylate shunt					
Isocitrate lyase	4.1.3.1	*aceA*	No	No	No
Malate synthase G	2.3.3.9	*glcB*	No	No	No

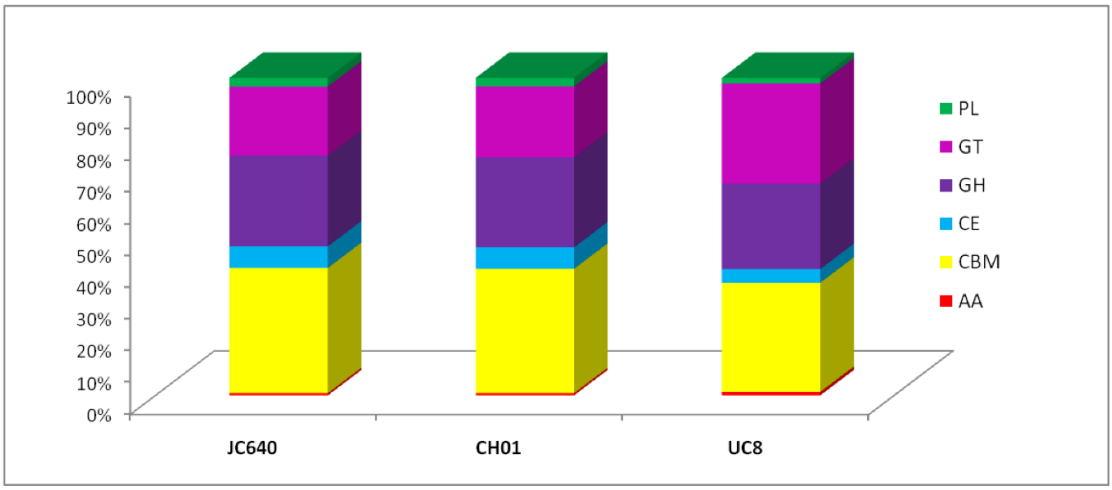

Fig. 3.4.5.3 Comparative analysis of CAZymes of strain JC640^T ,CH01^T and *Roseimaritima ulvae* UC8^T. AA, Auxiliary Activities (AAs); CBM, Carbohydrate-Binding Modules (CBMs); CE, Carbohydrate Esterases (CEs); GH, Glycoside Hydrolases (GHs); GT, GlycosylTransferases (GTs); PL, Polysaccharide Lyases (PLs)

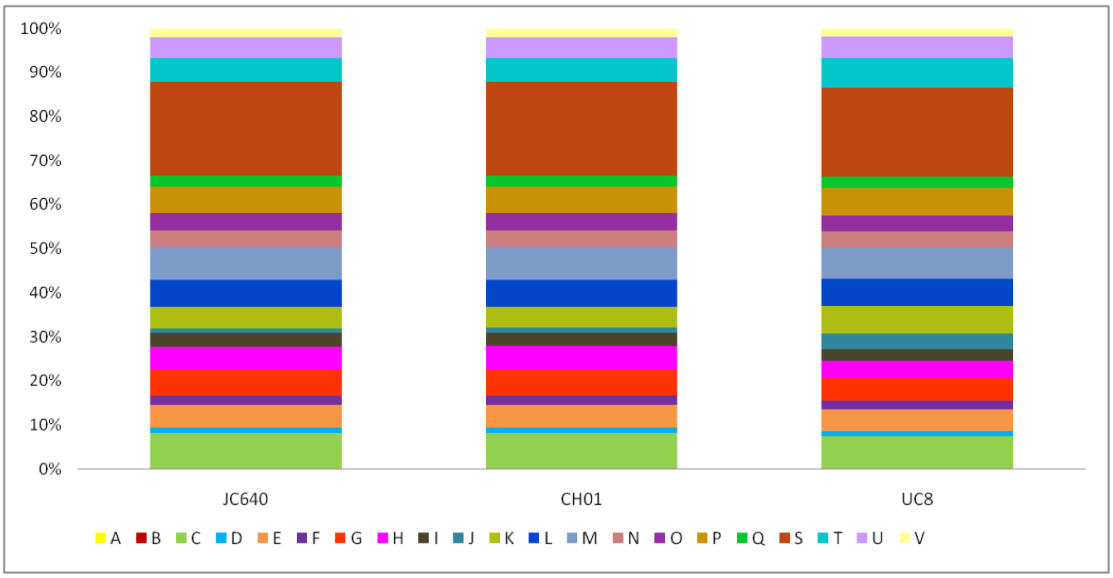

Fig 3.4.5.4. Functional classification COGs clusters of orthologs of strain JC640 , CH01 and *R. ulvae* UC8^T A: RNA processing and modification; B: Chromatin Structure and dynamics; C: Energy production and conversion; D: Cell cycle control and mitosis; E: Amino Acid metabolis and transport; F: Nucleotide metabolism and transport; G: Carbohydrate metabolism and transport; H: Coenzyme metabolism; I: Lipid metabolism; J: Tranlsation; K: Transcription; L: Replication and repair; M: Cell wall/ membrane/ envelop biogenesis; N: Cell motility; O: Post-translational modification, protein turnover, chaperone functions; P: Inorganic ion transport and metabolism; Q: Secondary Structure; S: Function Unknown; T: Signal Transduction; U: Intracellular trafficing and secretion; V: Defense mechanisms;

3.4.5.5 Morphological analyses

Both strains stain Gram-negative. Cells of both strains are rods (3.0-4.0 µm long and 0.5-0.8 µm wide) and have holdfast (Fig. 3.4.5.3a,b). Cell division is through lateral budding (Fig. 3.4.5.3a,c). Except for the members of the class Phycisphaerae and "*Candidatus* Brocadiae" which divide by binary fission, reproduction by members of the class Planctomycetia occur by budding only. Budding type is always polar until Wiegand et al (Wiegand et al. 2020) reported lateral budding in "*Kolteria novifilia"*; the only member known to date of lateral budding among *Planctomycetes*. Our study extends the existence of reproduction through lateral budding among other members of the phylum Planctomycetes. Both cultures became non-cultivable after 8-10 passages and our attempts failed to resuscitate the cultures by transferring into different media or adding supplements to the media. Electron microscopic studies of non-cultivable cells of both strains showed pleomorphic cell morphology (Fig. 3.4.5.3d,e). While cells of strain JC640 showed branching of cells with unusual cell morphology (Fig. 3.4.5.3d), strain CH01 did not show such branching but has structures similar to spheroplasts, however with cell wall (Fig. 3.4.5.3e). These structures differ from the bacterial spheroplasts (Shivani et al. 2017), where the cells lose the cell wall and appear spherical having only plasma membrane. Fluorescence observed (Fig. 3f) through staining with SYTOX green clearly indicate non-viable cells because of leaky membranes (Lebaron et al. 1998).

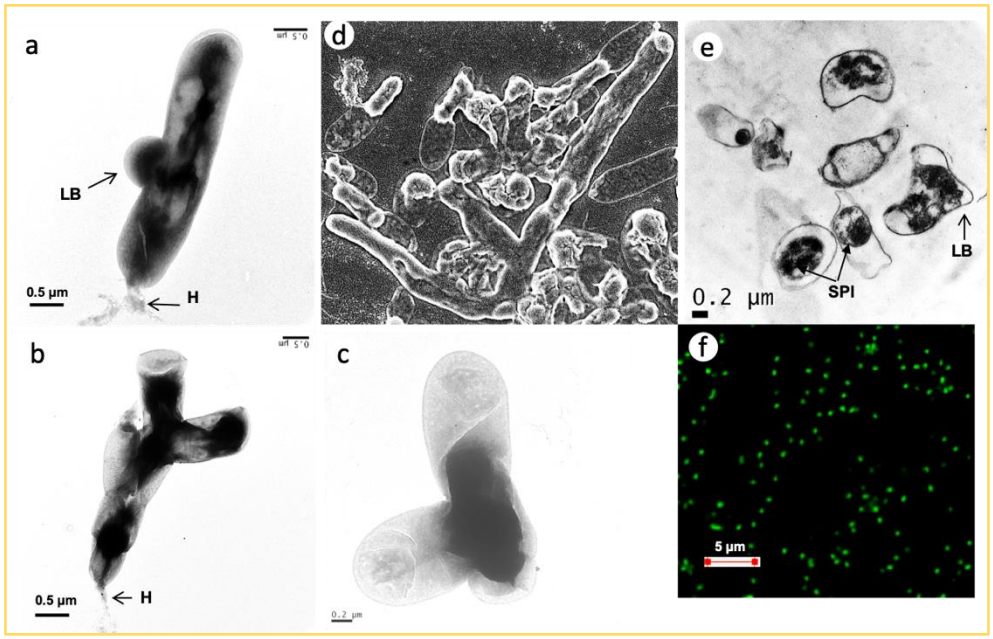

Fig. 3.4.5.5 Transmission electron microscopic images of negatively stained cells of strains JC640 and CH01 showing holdfast structures (a,b) and the reproduction by lateral budding (a,c), respectively. Electron microscopic images showing the non-cultivable cells of strains JC640 (d) and CH01 (e) having pleomorphic cell morphology. Fluorescently stained cells (f) with SYTOX green stain indicate that the cells are non-viable. LB, lateral budding; H, holdfast; SPl, spheroplasts like structures.

Table 3.4.5.4 Phenotypic and genotypic information of strains JC640 and CH01 compared with closely related taxa of different genera in the family *Pirellulaceae*.

Characteristics	1	2	3	4	5	6	7	8	9	10	11	12
Cell shape	Rods	Spherical/ Ovoid/ pear	Ovoid to pear	Pear	Round to ovoid	Acorn	Pear to ovoid	Pear to ovoid	Pear to round	Spherical to ovoid	Ovoid to spherical	round to pear
Colony colour	Pink	Light pink	Pink to red	White	Amaranth pink	Lucid white	Off-white to light brown	White- to cream	white- to cream	White to light pink	Yellowish white	Pink to light orange
Cell size (LxW, in µm)	3.0-4.0x 0.5-0.8	1.1–2.0x 0.8–1.5	1.0–2.5 x 1.2–2.3	2.5 ±0.3 x 1.5 ± 0.2	1.4-2.0 x 0.9-1.7	1.9 ± 0.2x1.0 ± 0.2	1.0–2.0x 0.7–1.5	0.6–1.5 x 0.6–1.4	2.2 ± 0.4x 1.2 ± 0.3	1.0–2.0 (diameter)	1.0–1.5x 0.9-1.0	1.6-1.9 x 0.9- 1.4
Budding	Lateral	Polar	Polar	Polar	Polar	Polar	Polar	Polar	Polar	Polar	Polar	Polar
Flagella	-	+/-	+	-	+/-	+	+	+	n.o.	-	+	+
Crateriform structures	+	+	+	+	+	+	+	+	n.o.	+	+	+
Fimbriae	-	+	+	+	+	+	+	+	+	+	+	+
Holdfast	+	+	+	n.o.	+/-	+	+	n.o.	n.o.	+	+	n.o.
16 S rRNA gene sequence similarity with strain JC640 (%)	100	93.1-93.3	90.3	90.2	88.7-90.2	87.1	85.0-86.0	84.3-85.0	89.4	83.4	83.1	89.1-90.2
***Genome characters**												
Genome size (Mb)	5.7	6.2-8.1	6.8-8.5	7.2	6.9-8.0	8.4	6.2-6.6	6.5	9.6	6.6	6.2	9.6- 11
No. of contigs	150-154	103-185	1-73	1	12-42	1	10-64	1-16	1	57	1	4-13
G+C content (mol %)	63.6	59.1/62.4	55.4-58.0	57.7	53.7-56.2	55.3	57.0-59.2	53.8-56.2	61.4	53.4	57.5	56.0-59.3
RNAs	61	49-67	48-97	44	74-120	74	59-69	71-74	122	56	45	77-79
Coding sequences	4648	4904-6210	6153-7080	6151	518-6274	6419	5003-5406	5528-6246	7178	5123	4705	6920-7797
N_{50} value	74,341	92,046-127,469	215734-7145,576	4627,310	520,663-1270004	843,9957	202613-843719	876209	9565229	268453	6196199	2318794-4804764
16S rRNA gene copies	2	1	1	1	1-2	2	1-2	2	1	1	1	1-3
Completeness (%)	97.6	98.5-99.9	99.9	98.3	96.9-98.3	98.1	96.5-98.2	98.3	98.3	98.3	98.3	98.3

1, "*Candidatus* Laterigemmans baculatus" (strains JC640 and CH01); 2, *Roseimaritima* (*R. ulvae*, *R. sediminicola*); 3, *Rhodopirellula baltica* SH1^{T}; 4, "*Rosistilla oblonga*"; 5, *"Rubripirellula tenax*" 6, "*Aureliella helgolandensis*"; 7, *Blastopirellula* (*B. marina; B. "retiformator*"); 8, "*Bremerella*" (*B. cremea*; *B. volcanica*); 9, "*Lignipirellula cremea*"; 10, *Ma iniblastus fusicola*; 11, *Pirellula staleyi*; 12, "*Stieleria"* (*S. maiorica*; *S. neptunia*; *S. varia*); n.o., not observed; n.d., not determined;

+, Present; -, Absent; +/-, Present or absent; *, genome sequences accessions numbers taken for comparisons are as given in Fig. 2. Information for this table is based on our study and information from the literature [Bondoso et al. 2015; Kallscheuer et al. 2020a,b,c; Kallscheuer et al. 2019a,b; Lage et al. 2017; Lee et al. 2013; Peeters et al. 2020; Sandargo et al. 2020; Schlesner et al. 1984, 2004]

3.5 Phylo-taxogenomic studies of the newly isolated axenic cultures of Planctomycetes from Tamil Nadu

Twenty seven strains of Planctomycetes were isolated from the Tamil Nadu coastal regions. Total twenty one isolated strains of Planctomycetes remained viable and six strains became silent after 9^{th}-11^{th} sub culturing. Further, phylo-taxogenomic studies of four strains were carried out (Fig. 3.5.1).

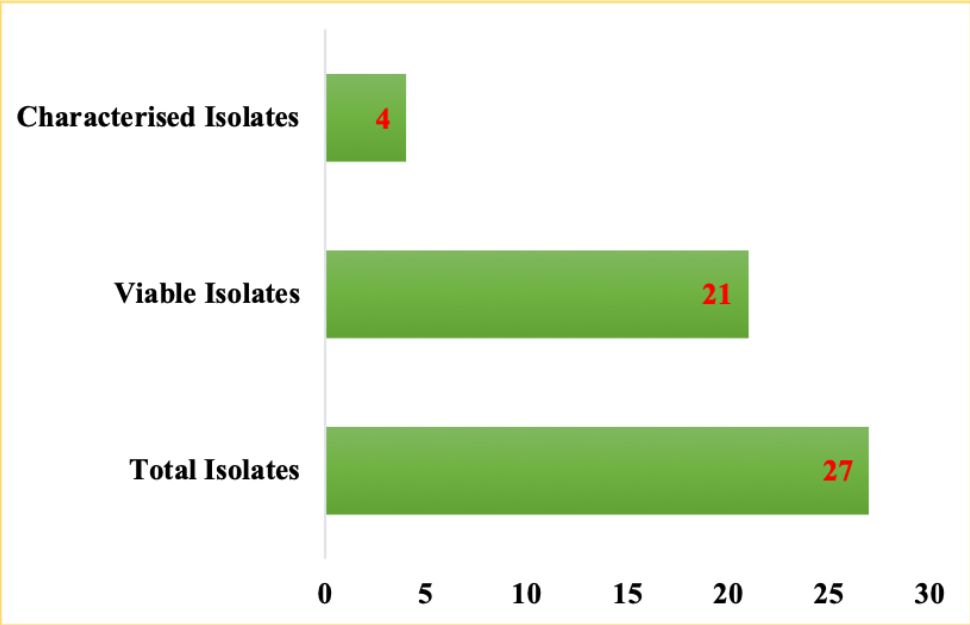

Fig. 3.5.1 Detail about the total Planctomycetal strains isolated, remain viable and strains phylo-taxogenonomic studied (Characterised) from the Tamil Nadu.

3.5.1 Phylo-taxogenomic study of the strain JC647^T

3.5.1.1 *Habitat and nucleotide sequences accession numbers*

The strain JC647^T from a specimen of sponge belonging to the genus *Spongia*, collected from the sea shore of Rameswaram, India (GPS position: 09°16'52"N 79°10'20"E). The 16S rRNA gene sequence of strain JC647^T was deposited with European Molecular Biology Laboratory (EMBL) with the accession number LR132071. The whole genome sequence of strain JC647^T (6.9 Mb) was deposited with the NCBI with accession number JAAXMS000000000.

3.5.1.2 Genomic characteristics

Genome size of strain JC647^T is 68,65,567 nt present in 48 contigs with a N50 value of 7,56,015. The genome has 6,215 genes of which 6,023 are protein coding genes, 72 genes for RNAs and 120 genes are pseudogenes. G+C content of the genome of strain JC647^T is 57.8 mol%. Whereas, the genome of type species "*Crateriforma conspicua*" Mal65^T is 71,82,433nt present in 2 contigs with N50 value of 6,685,054. The genome has 5,298 genes of which 5,165 are protein coding genes, 54 genes for RNAs and 79 genes are pseudogenes. G+C content of the genome of strain JC647^T is 57.8 mol%. Genome sequences of strains JC647^T and *"Crateriforma conspicua*" Mal65^T were aligned using PATRIC software to identify the multiple maximal matches and local collinear block (LCBs; www. patricbrc.org). The genome sequence of strain *"Crateriforma conspicua*" Mal65^T was used as a reference against JC647^T. The alignments of the LCBs in both strains differ from each other significantly (Fig. 3.5.1.1). The alignment facilitates detection of homologous regions that are shuffled or inverted due to DNA rearrangement or recombination.The comparison of the genome map based on the protein sequence identity shows that majority of the proteins of strain JC647^T share 90-95% similarity with those of *"Crateriforma conspicua*" Mal65^T (Fig. 3.5.1.2). These

results suggest a clear-cut dissimilarity between the strains JC647^T and *"Crateriforma conspicua"* Mal65^T.

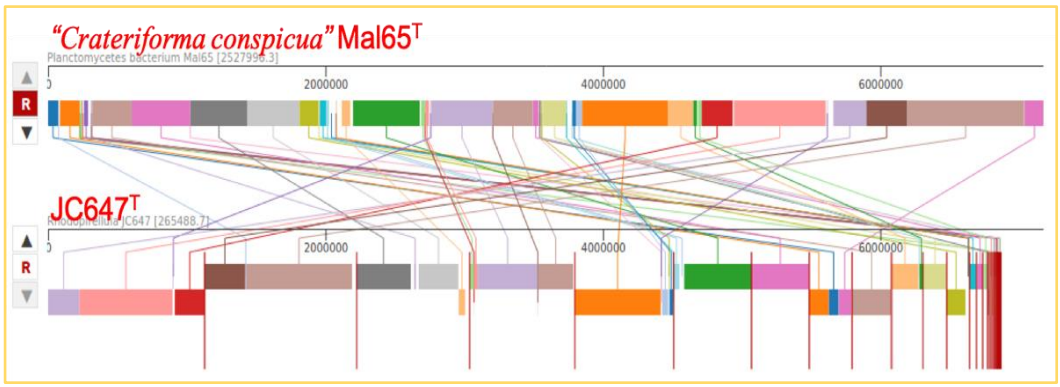

Fig. 3.5.1.1 Genome organization of strains JC647^T and "*Crateriforma conspicua*" Mal65^T

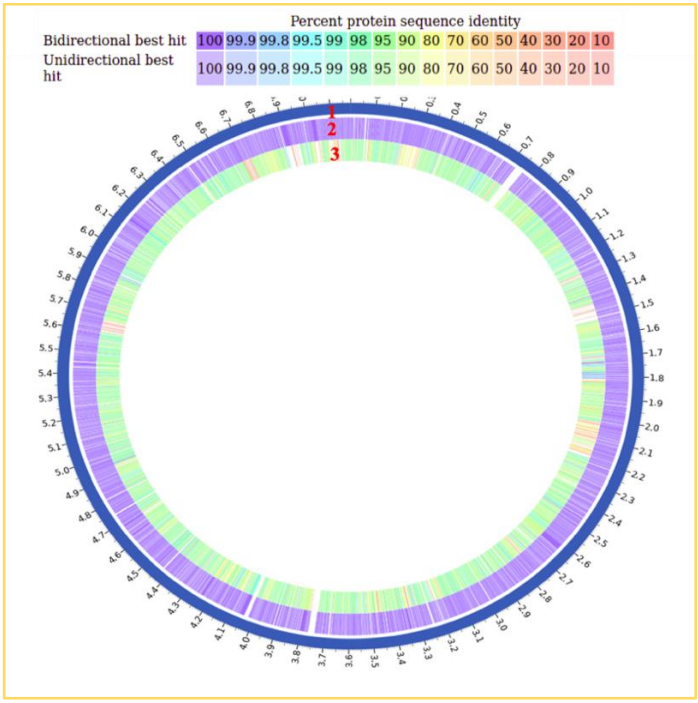

Fig. 3.5.1.2. Genome map based on protein sequence identity. List of tracks, from outside to inside: 1. Scale showing contig length 2. "*Crateriforma conspicua"* Mal65^T 3. Strain JC647^T. Genome of strain Mal65^T was used as reference.

3.5.1.3 BLAST Analysis and Phylogenetic inference

The BLAST analysis of amplicon based 16S rRNA gene sequence of strain JC647^T indicated that it shares highest identity of 99.9% with the sole species of genus "C*rateriforma*"; "*Crateriforma conspicua*" (Fig. 3.5.1.3). The 16S rRNA gene sequence of

strain JC647^T extracted from the genome has sequence length of 1533nt and the BLAST search results are similar to amplicon 16S rRNA gene sequence having identity with sole member of the genus *"Crateriforma"*; *"Crateriforma conspicua*" (Fig. 3.5.1.3).

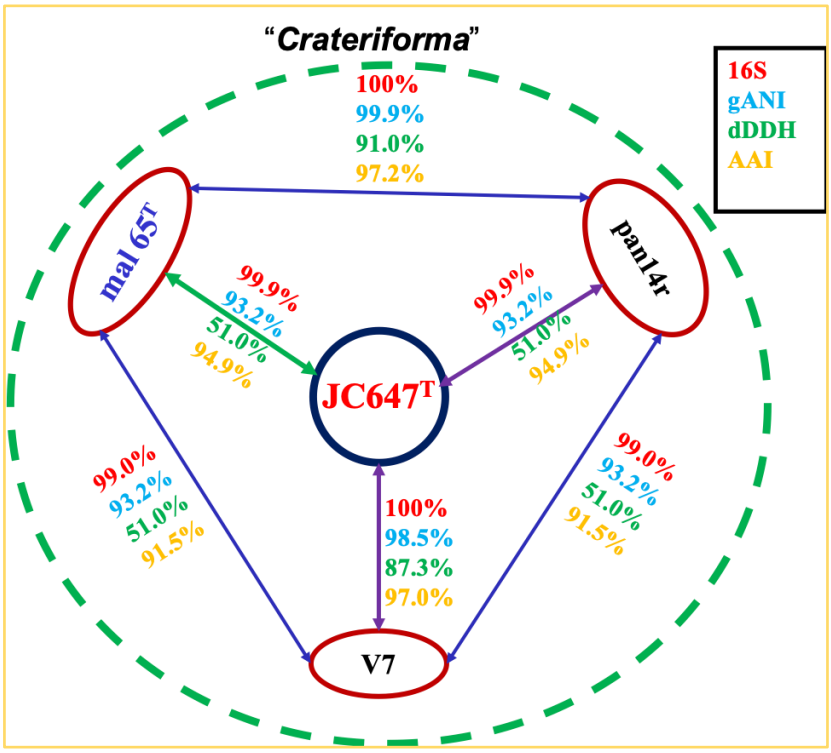

Fig. 3.5.1.3. Analysis of phylogenetic markers for delineation of the novel isolate JC647^T along with "*Crateriforma conspicua*" (strains Mal65^T, V7, Pan14r). Methods used: 16S rRNA gene identity (16S), average amino acid identity (AAI), average nucleotide identity (ANI) and digital DNA-DNA Hybridization (*d*DDH).

The 16S rRNA gene sequence based phylogenetic tree with combined bootstrap values obtained from ML, NJ, ME trees (Fig. 3.5.1.4) and 92 core genes based phylogenomic tree (Fig. 3.5.1.5) confirmed the distinct monophyletic clustering of strains JC647^T and *"Crateriforma conspicua*" Mal65^T within the family *Pirellulaceae.* Further, the cladding between strains JC647^T and *"Crateriforma conspicua*" Mal65^T are distinctly separated (Fig. 3.5.1.4,5) from each other suggesting that strain JC647^T is a novel species of the genus *"Crateriforma".*

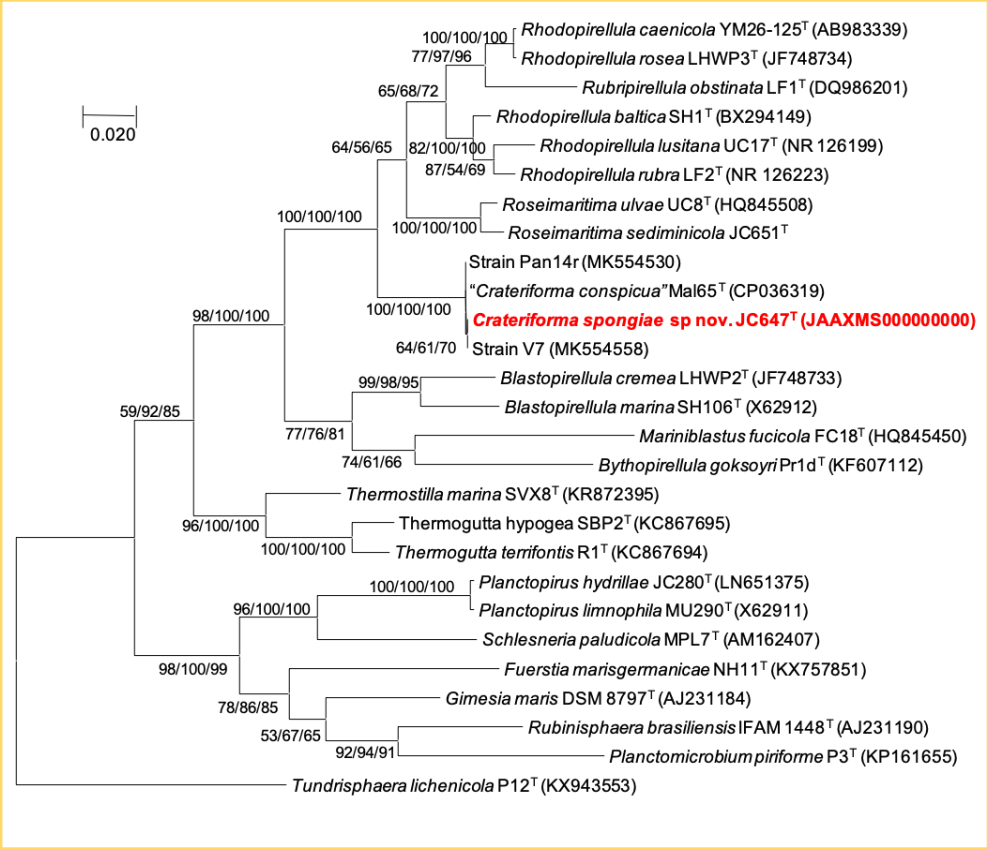

Fig. 3.5.1.4 Phylogenetic tree based on 16S rRNA gene sequences showing the phylogenetic relationship of strains JC647^T with the strains Mal65, Pan14r and V7 and other members of family *Pirellulaceae* and *Planctomycetaceae*. The tree was made with MEGA 7 software and *Tundrisphaera lichenicola* P12^{T}was used as an out-group. The GenBank accession numbers for 16S rRNA gene sequences are shown in parentheses. Numbers at nodes indicate bootstrap value of 1000 repetition correspond to ML/NJ/ME analysis. Bar,0.02 nucleotide substitution per position.

OrthoANI value between strain JC647^T and *"Crateriforma conspicua"* Mal65^T is 93.2%. The *d*DDH value between strain JC647^T and *"Crateriforma conspicua"* Mal65^T is 51.0%. OrthoANI and *d*DDH values (Fig. 3.5.1.1) between strains JC647^T and *"Crateriforma conspicua"* Mal65^T is less than the recommended cut-off values (95-96% cut off for ANI and 70% cut off for *d*DDH) for species delineation (Chun et al. 2018). The AAI value (Fig.3.5.1.1) between strain JC647^T and *"Crateriforma conspicua"* Mal65^T yielded a similarity of 94.9% and this value is close to the recommended cut-off values (95.0-95.5% cut off for AAI) for species delineation (Luo et al., 2014; Bondoso et al., 2013) supporting the proposal of a novel species.

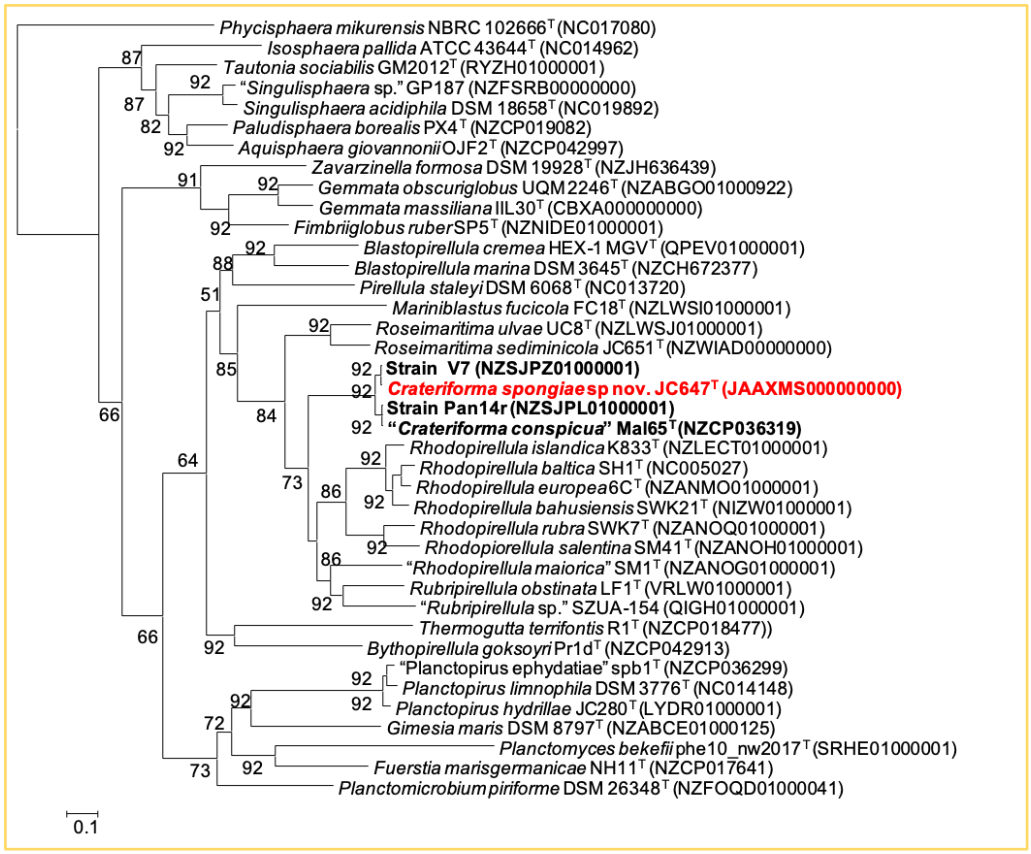

Fig. 3.5.1.5 RAxML based phylogenomics tree of strain JC647^T along with publicly available genome sequence of *Pirellulaceae*, *Planctomycetaceae*, *Gemmataceae* and *Isosphaeraceae* families. Genome sequence of *Phycisphaera mikurensis* is taken as outgroup. The GenBank accession numbers for genome sequences are shown in parentheses. Bar,0.10 nucleotide substitution per position.

Low AAI, low OrthoANI and low *d*DDH values between strains JC647^T and *"Crateriforma conspicua"* Mal65^T allow strain JC647^T to be classified as a novel species under the genus "*Crateriforma"* as per the recommended standards (Qin et al. 2014; Luo et al. 2014; Bondoso et al. 2015). Strain JC647^T, however is very close to strain V7 having high phylogenetic (Fig. 3.5.1.4,5) and genomic (Fig. 3.5.1.3) relatedness. Since V7 is not the type species of the genus *"Crateriforma conspicua"* and the authors them self-concluded that strain V7 can form as separate species (Peeters et al., 2019), we conclude strain JC647^T as a novel species of the genus "*Crateriforma*" and strain V7 as an additional strain represented from a distinct geographical habitat.

3.5.1.4 *In-silico* metabolic characterization

The genes annotated using COG database was mapped to 21 functional categories. General functional prediction only (R) and Nuclear structure (Y) were not observed in both the strains and most of the genes were associated with transport and metabolic functions which are helpful in obtaining the nutrients from host organisms. Strain JC647^T and *"C. conspicua"* Mal65^T showed a similar pattern of COGs. Strain JC647^T showed lesser number or orthologous gene clusters compared to strain Mal65^T (Fig. 3.5.1.6). CAZy annotation of genomes of the strains JC647^T and *"C. conspicua"* Mal65^T have similar number of genes encoding for carbohydrate-active enzymes (CAZymes) and contains more number of glycoside hydrolases (GHs) and followed by carbohydrate binding molecules (CBMs). Both of them contained GHs, CBM47 and CBM67 as major families and very few are organized in clusters. The genome prediction pattern agrees with the experimentally determined carbohydrate utilization. The majority of carbohydrate-active enzymes predicted in both strains are having N-terminal signal peptides which may probably help in hydrolysis of extracellular substrates (Fig. 3.5.1.7).

In-silico analysis of metabolic pathways revealed that strain JC647^T has the genetic potential for obtaining energy through fermentation and aerobic respiration. Further, strain JC647^T has genes to encode all components of an aerobic respiratory; NADH ubiquinone oxidoreductase, succinate dehydrogenase, cytochrome bc1complex, cytochrome *c* oxidases and an F1F0-type ATP synthase. Strains JC647^T and *"C. conspicua"* Mal65^T have genes encoding for cytochrome *c* oxidases of caa_3-type which have low affinity to oxygen and are usually used by aerobic microorganisms for respiration. Both strain JC647^T and *"C. conspicua"* Mal65^T are strictly aerobic and failed to grow in anaerobic conditions although the genome showed genes encoding for cytochrome bd ubiquinol oxidase which have high affinity to oxygen and are usually found in anaerobes and microaerophiles (Dedysh et al.

2020). In order to attain a better understanding on central carbon metabolism the genes encoding for the enzymes involved in pathways like glycolysis, gluconeogenesis, TCA cycle, phosphoenolpyruvate carboxylation and the glyoxylate shunt were predicted from the genomes. Strain JC647^T and *"C. conspicua*" Mal65^T have genes encoding for complete Embden-Meyerhof-Parnas pathway, TCA cycle and both oxidative and non-oxidative pentose phosphate pathway (Table. 3.5.1.1). Genes encoding for gluconeogenesis and glyoxylate shunt were absent in strain JC647^T and *"C. conspicua*" Mal65^T hence sugars are suitable substrates for energy and biomass formation.

The genome of all the four strains also showed more than 150 genes encoding for sulfatases individually. Majority of these are classified as N-acetylglucosamine-6-sulfatase and N-sulfoglucosaminesulfohydrolase which aids in the degradation of sulfated glycosaminoglycans like N-acetylglucosamine which support the growth of these strains. The genome also showed genes encoding for iduronate-2-sulfatases which aid in the hydrolysis of sulfate ester bonds from a wide variety of substrates, like steroids, carbohydrates and proteins. The presence of sulfatases in all strains indicate their probable role in the degradation of sulfated glycopolymers, which are commonly produced by potential host organisms like macroalgae and sponges (Kaboré et al. 2020). Strain JC647^T and *"C. conspicua*" Mal65^T can obtain carbon and energy through the degradation of complex host derived polysaccharides like N-acetylglucosamine which is the major postulated strategy of members of the 'Pirellula clade' (Peeters et al. 2020a). Both strains also have genes encoding for assimilatory sulfate reduction and dinitrogen fixation; whereas genes encoding for dissimilatory nitrate reduction, nitrate to ammonia were observed only with *"C. conspicua*" Mal65^T. The annotation results have provided an insight into the pivotal role by the members of the genus "*Crateriforma*" in biogeochemical cycles of carbon, nitrogen and sulphur.

Further, *in-silico* metabolic characterization show that both strains JC647^T and *"C. conspicua"* Mal65^T have 2-C-methyl-D-erythritol 4-phosphate/1-deoxy-D-xylulose 5-phosphate (MEP) pathway for the biosynthesis of five carbon isoprene units (isopentenyl pyrophosphate; IPP), which is eventually the precursor for the synthesis of carotenoids and quinones (Eisenreich et al. 2004; Zhao et al. 2013). The genes encoding for complete pathway of menaquinone biosynthesis is present in both strain JC647^T and *"C. conspicua"* Mal65^T. In both the strains genes encoding for carotenoid biosynthetic enzymes like lycopene β-cyclase (5.5.1.19), β-carotene hydroxylase (1.14.13.129), zeaxanthin epoxidase (1.14.15.21) and neoxanthin synthase (5.3.99.9) are found. Hence, both strains are putatively capable of forming neoxanthin from lycopene involving important intermediates like γ- carotene, β-carotene, zeaxanthin and violaxanthin (Fig. 3.5.1.8). Strain JC647^T and *"C. conspicua"* Mal65^T have genes encoding for the degradation and metabolism of benzoate, atrazine, caprolactam, xylene and dioxin. Genes encoding for the biogenesis of steroid hormones are absent in both taxa. Genes encoding for flavone and flavanol biosynthesis are exclusively present in the genome of *"C. conspicua"* Mal65^T (Fig. 3.5.1.8). Planctomycetes are believed to produce bioactive secondary metabolites because of their complex life cycle. The number of putative secondary metabolite clusters in strain JC647^T and *"C. conspicua"* Mal65^T are 9 and 11 respectively. Both taxa have gene clusters encoding for terpenes, Type I Polyketide Synthase (TIPKS), TIIIPKS, Non-ribosomal peptide synthetase (NRPS), NRPS-Like and Mixed NRPS-TIPKS. Cluster for nucleoside is exclusive in *"C. conspicua"* Mal65^T. *In-silico* metabolic characterization show that both strain JC647^T and *"C. conspicua"* Mal65^T have 2-C-methyl-D-erythritol 4-phosphate/1-deoxy-D-xylulose 5-phosphate (MEP) pathway for the biosynthesis of five carbon isoprene units (isopentenyl pyrophosphate; IPP), which is eventually the precursor for the synthesis of carotenoids and quinones (Eisenreich et al., 2004; Zhao et al., 2013).

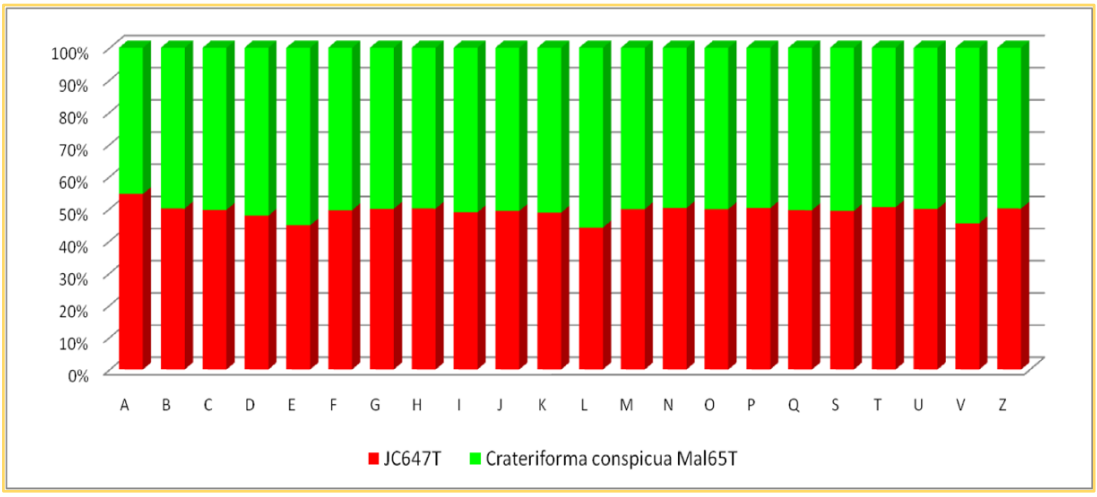

Fig 3.5.1.6. Functional classification COGs clusters of orthologs of strain JC647^T and closely related strain "*Crateriforma conspicua"* Mal65^T , A: RNA processing and modification; B: Chromatin Structure and dynamics; C: Energy production and conversion; D: Cell cycle control and mitosis; E: Amino Acid metabolis and transport; F: Nucleotide metabolism and transport; G: Carbohydrate metabolism and transport; H: Coenzyme metabolism; I: Lipid metabolism; J: Tranlsation; K: Transcription; L: Replication and repair; M: Cell wall/ membrane/ envelop biogenesis; N: Cell motility; O: Post-translational modification, protein turnover, chaperone functions; P: Inorganic ion transport and metabolism; Q: Secondary Structure; S: Function Unknown; T: Signal Transduction; Intracellular trafficing and secretion; V: Defense mechanisms; Z: Cytoskeleton.

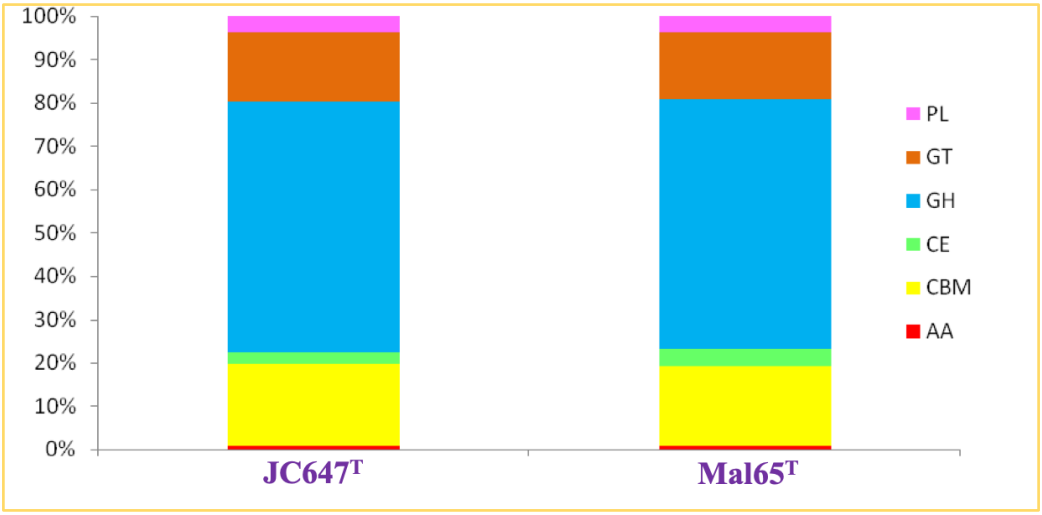

Fig. 3.5.1.7 Comparative analysis of CAZymes of strain JC647^T and "*Crateriforma conspicua"* Mal65^T.AA, Auxiliary Activities (AAs); CBM, Carbohydrate-Binding Modules (CBMs); CE, Carbohydrate Esterases (CEs); GH, Glycoside Hydrolases (GHs); GT, Glycosyl Transferases (GTs); PL, Polysaccharide Lyases (PLs)

In both the strains genes encoding for carotenoid biosynthetic enzymes like lycopene β-cyclase (5.5.1.19), β-carotene hydroxylase (1.14.13.129), zeaxanthin epoxidase (1.14.15.21) and neoxanthin synthase (5.3.99.9) are found. Hence, both the strains are putatively capable of forming neoxanthin from lycopene involving important intermediates like γ- carotene, β-carotene, zeaxanthin and violaxanthin (Fig. 3.5.1.8). Strains JC647^T and *"C. conspicua"* Mal65^T are capable of degradation and metabolism of benzoate, atrazine, caprolactam, xylene and dioxin. Whereas, naphthalene and fluorobenzoate degradation capacity is absent in both strains. Pathways of steroid hormones biosynthesis is absent in both taxa. Flavone and flavanol biosynthesis is exclusive for *"C. conspicua"* Mal65^T (Fig. 3.5.1.8).

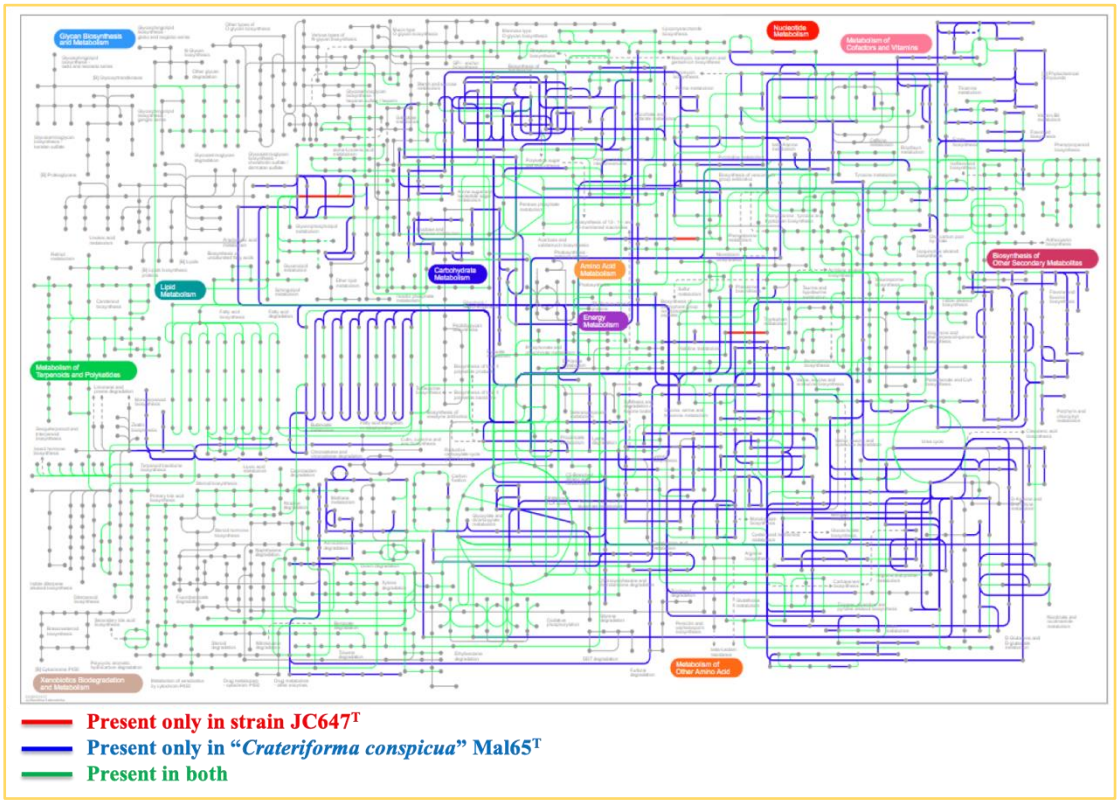

Fig. 3.5.1.8 Common and unique biochemical pathways between strain JC647^T and "*Crateriforma conspicua*" Mal65^T.

Planctomycetes are believed to produce bioactive secondary metabolites because of their complex life cycle. The number of putative secondary metabolite clusters in strain JC647^T and *"C. conspicua"* Mal65^T are 9 and 11 respectively. Both taxa have clusters for

terpenes, Type I Polyketide Synthase (TIPKS), TIIIPKS, Non-ribosomal peptide synthetase (NRPS), NRPS-Like and Mixed NRPS-TIPKS. Cluster for nucleoside is exclusive in *"C. conspicua"* Mal65^T.

Table 3.5.1.1 Genome-based analysis of the central carbon metabolism of genus "*Crateriforma*."including strain JC647^T

Enzyme/reaction	EC number	Gene	JC647^T	Mal65^T	V7	Pan14r
Glycolysis						
Glucose-6-phosphate isomerase	5.3.1.9	*pgi*	Yes	Yes	Yes	Yes
ATP-dependent 6-phosphofructokinase isozyme 1	2.7.1.11	*pfkA*	Yes	Yes	Yes	Yes
Fructose-bisphosphate aldolase class 2	4.1.2.13	*fbaA*	Yes	Yes	Yes	Yes
Triosephosphate isomerase	5.3.1.1	*tpiA*	Yes	Yes	Yes	Yes
Glyceraldehyde-3-phosphate dehydrogenase	1.2.1.12	*gapA*	Yes	Yes	Yes	Yes
Phosphoglycerate kinase	2.7.2.3	*pgk*	Yes	Yes	Yes	Yes
2,3-Bisphosphoglycerate-independent phosphoglycerate mutase	5.4.2.12	*gpmI*	Yes	Yes	Yes	Yes
Enolase	4.2.1.11	*eno*	Yes	Yes	Yes	Yes
Pyruvate kinase I	2.7.1.40	*pykF*	Yes	Yes	Yes	Yes
			Yes	Yes	Yes	Yes
Pyruvate dehydrogenase E1 component	1.2.4.1	*aceE*	Yes	Yes	Yes	Yes
Dihydrolipoyllysine-residue acetyltransferase component of pyruvate dehydrogenase complex	2.3.1.12	*aceF*	Yes	Yes	Yes	Yes
Gluconeogenesis						
Phosphoenolpyruvate carboxylase	4.1.1.31	*ppc*	No	No	No	No
Pyruvate, phosphate dikinase	2.7.9.1	*ppdK*	Yes	Yes	Yes	Yes
Phosphoenolpyruvate carboxykinase (ATP)	4.1.1.49	*pckA*	No	No	No	No
Phosphoenolpyruvate carboxykinase (GTP)	4.1.1.32	*pckG*	No	No	No	No
Fructose-1,6-bisphosphatase class 2	3.1.3.11	*glpX*	No	No	No	No
Fructose-1,6-bisphosphatase class 1	3.1.3.11	*fbp*	No	No	No	No
Pyrophosphate–fructose 6-phosphate 1-phosphotransferase	2.7.1.90	*pfp*	Yes	No	No	No
Pentose phosphate pathway						
Glucose-6-phosphate 1-dehydrogenase	1.1.1.49	*zwf*	Yes	Yes	Yes	Yes

6-Phosphogluconolactonase	3.1.1.31	*pgl*	Yes	Yes	Yes	Yes
6-Phosphogluconate dehydrogenase, decarboxylating	1.1.1.44	*gndA*	Yes	Yes	Yes	Yes
Transketolase 2	2.2.1.1	*tktB*	Yes	Yes	Yes	Yes
Transaldolase B	2.2.1.2	*talB*	Yes	Yes	Yes	Yes
Entner–Doudoroff pathway			Yes	Yes	Yes	Yes
KHG/KDPG aldolase	4.1.2.14	*eda*	Yes	Yes	Yes	Yes
			Yes	No	No	No
Phosphogluconate dehydratase	4.2.1.12	*edd*	Yes	Yes	Yes	Yes
			Yes	Yes	Yes	Yes
			Yes	Yes	Yes	Yes
TCA cycle						
Citrate synthase	2.3.3.16	*gltA*	Yes	Yes	Yes	Yes
Aconitate hydratase A	4.2.1.3	*acnA*	Yes	Yes	Yes	Yes
Isocitrate dehydrogenase (NADP)	1.1.1.42	*icd*	Yes	Yes	Yes	Yes
2-Oxoglutarate dehydrogenase E1 component	1.2.4.2	*sucA*	Yes	Yes	Yes	Yes
Dihydrolipoyllysine-residue succinyltransferase component of 2-oxoglutarate dehydrogenase complex	2.3.1.61	*sucB*	Yes	Yes	Yes	Yes
Succinate–CoA ligase [ADP-forming] subunit alpha	6.2.1.5	*sucD*	Yes	Yes	Yes	Yes
Succinate–CoA ligase [ADP-forming] subunit beta	6.2.1.5	*sucC*	Yes	Yes	Yes	Yes
Succinate dehydrogenase flavoprotein subunit	1.3.5.1	*sdhA*	Yes	Yes	Yes	Yes
Succinate dehydrogenase iron-sulfur subunit	1.3.5.1	*sdhB*	Yes	Yes	Yes	Yes
Succinate dehydrogenase cytochrome b556 subunit	1.3.5.1	*sdhC*	Yes	Yes	Yes	Yes
Succinate dehydrogenase hydrophobic membrane anchor subunit	1.3.5.1	*sdhD*	No	No	No	No
Fumarate hydratase class I, an/aerobic	4.2.1.2	*fumA/B*	No	No	No	No
Fumarate hydratase class II	4.2.1.2	*fumC*	Yes	Yes	Yes	Yes
Malate dehydrogenase	1.1.1.37	*mdh*	Yes	Yes	Yes	Yes
Glyoxylate shunt						
Isocitrate lyase	4.1.3.1	*aceA*	No	No	No	No
Malate synthase G	2.3.3.9	*glcB*	No	No	No	No

3.5.1.5 Morphological and physiological analyses

SEM image shows rosette arrangement of cells in strain JC647^T (Fig. 3.5.1.9A). Cells of strain JC647^T are oval to pear shaped (1.2-1.6 x 0.7-1.0 µm; Fig. 3.5.1.9B) having crateriform structures distributed all over the surface. TEM image of JC647^T cells shows the presence of invagination of cytoplasmic membrane, enlarged periplasm, cytoplasm, nucleoid region and cell reproduction by budding (Fig. 3.5.1.9B). Growth observations with different carbon substrates/nitrogen sources/pH range/NaCl tolerance for strain JC647^T are given in either species description or in Table 1. Enzymatic activity of strain JC647^T was determined using API ZYM kit (BioMérieux), according to the manufacturer's instructions for which results are given in species description or in Table 3.5.1.3.

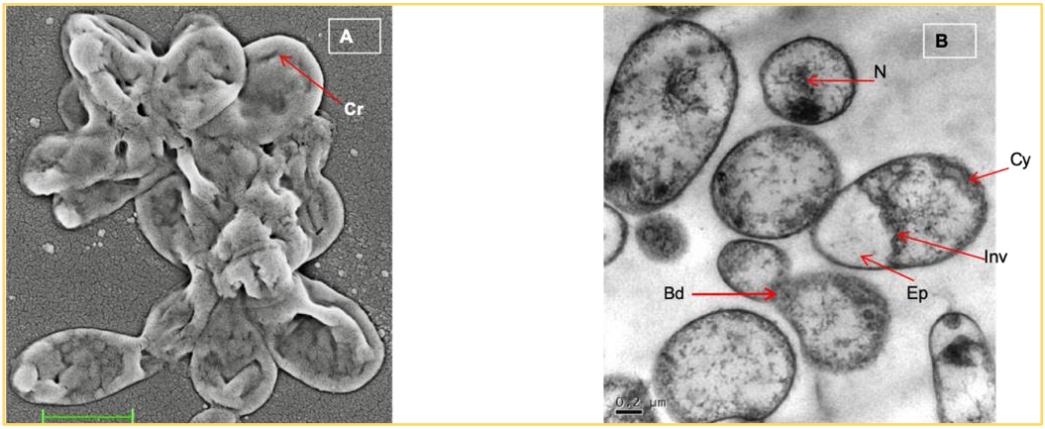

Fig. 3.5.1.9. Electron microscopic images of strain JC647^T. (A) SEM image showing intact cells and rosette formation, Scale bar 1µm; (B) TEM image showing different parts of the cells; Cm, Cellular Membrane; Inv, Invagination of cytoplasmic membrane; N, Nucleoid; Cy, Cytoplasm; Ep, Enlarged periplasm; Cr, Crateriform structure; Bd, budding.

3.5.1.6 Chemotaxonomic characterization

3.5.1.6.1 FAME profile

For the strain JC647^T, major proportions of the fatty acids are $C_{16:0}$, $C_{18:1}\omega9c$ and $C_{18:0\text{-ante}}$ /$C_{18:2}\omega6,9c$ (Table. 3.5.1.2)

Table 3.5.1.2 Cellular fatty acid composition (%) of Strains JC647^T and "*Crateriforma conspicua*" Mal65^T

Table 3.5.1.2 Cellular fatty acid composition (%) of Strains JC647^T and "*Crateriforma conspicua*" Mal65^T		
Fatty acid (%)	JC647^T	Mal65^T
anteiso-$C_{12:0}$	0.1	-
$C_{12:0}$	0.1	-
$C_{14:0}$	0.4	0.9
anteiso-$C_{13:0}$	0.1	0.1
$C_{15:0}$2-OH	0.1	0.1
anteiso-$C_{15:0}$	0.1	0.4
$C_{16:1}\omega$9C	0.2	0.1
$C_{15:1}\omega$6C	1.3	0.8
$C_{16:0}$	**20.6**	**23.2**
$C_{18:1}\omega$9c	**44.7**	**40.4**
$C_{18:0\text{-ante}}$ / $C_{18:2}\omega$6,9c	**25.2**	**24.8**
$C_{18:0}$	3.1	4.0
$C_{16:1}\omega$7c/$C_{16:1}\omega$6c	0.9	1.0
$C_{17:0}$	0.4	0.4
$C_{17:0cyclo}$	0.3	0.2
$C_{17:0}$2-OH	0.8	1.0
iso-$C_{19:1}$	1.0	0.9
$C_{20:0}$	-	0.7
iso-$C_{20:0}$	0.2	-
$C_{20:1}\omega$9c	0.3	0.6

3.5.1.6.2 Polar lipid profile

Polar lipids of the strain JC647^T are diphosphatidylglycerol (DPG), phosphatidylcholine (PC), five unidentified phospholipids (PL1,2,3,4,5) and three unidentified lipids (L1,2,3) (Fig. 3.5.1.10a). Polar lipids of the strain "*C. conspicua*" Mal65^T are diphosphatidylglycerol (DPG), phosphatidylcholine (PC), phosphatidyl-monomethylethanolamine (PE1) phosphatidyl-dimethylethanolamine (PE2), four unidentified phospholipids (PL1,2,3,4) and three unidentified lipids (L1,2,3) (Fig. 3.5.1.10b).

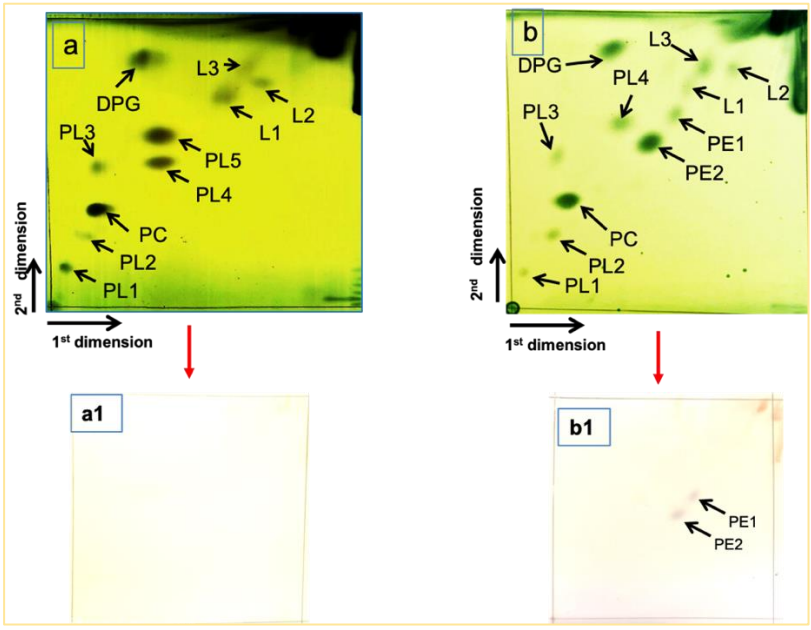

Fig. 3.5.1.10 Two dimensional chromatograms showing polar lipids of the strain (a) JC647^T and (b)"*C.conspicua"* Mal65^T. Ninhydrin stained chromatograms to show the absence (a1) and presence (b1) of amino phospholipids. PC, Phosphatidylcholine; PL1,2,3,4,5, unidentified Phospholipid; PE1, phosphatidyl-monomethylethanolamine; PE2, phosphatidyl-dimethylethanolamine; L1,2,3, unidentified lipid; DPG, Diphosphatidylglycerol.

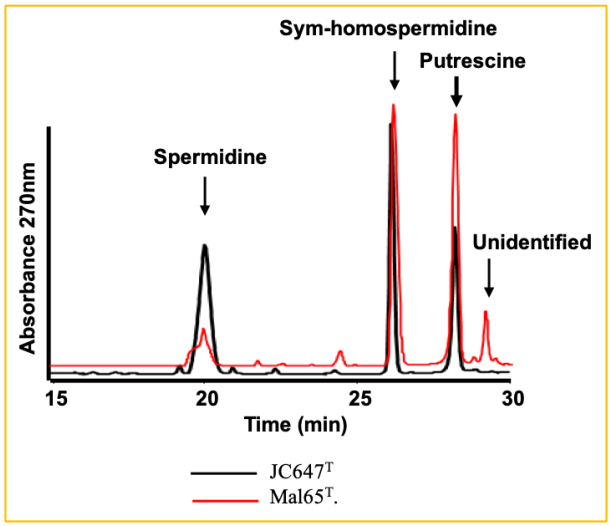

Fig. 3.5.1.11. HPLC chromatogram of polyamines of Strain JC647^T

3.5.1.6.3 Polyamine Profile

The strain JC647^T and "*C. conspicua*" Mal65^T has three polyamines; sym-homospermidine, putrescine and spermidine (Fig. 3.5.1.11). one unidentified polyamine is also present in "*C. conspicua*" Mal65^T

Table 3.5.1.3 Differentiating characters between strain JC647^T and "*Crateriforma conspicua"* Mal65^T

Characters	**Strain JC647^T**	*"C. conspicua"* **Mal65^T**
Cell size (LxW, µm)	1.2-1.6x0.7-1.0	1.8-2.1x0.9-1.3
Cell shape	Pear to ovoid	pear
Pigmentation	Pale pink	pink
Temperature (range, °C)	10-30	10-36
pH (Range)	8.0-9.0	5.0-9.5
Enzyme activities		
Leucine arylamidase	+	-
α-chymotrypsin	+	-
Esterase (C4)	-	+
Esterase Lipase (C 8)	-	+
α-glucosidase	-	+
N-acetyl- β-glucosaminidase	-	+
Carbon sources utilisation		
Fructose	+	-
Starch	+	-
Sorbitol	-	+
Nitrogen sources utilisation		
Glutamic acid	+	-
Glycine	-	+
Alanine	-	+
Vitamin B_{12} requirement	+	-
Polar lipids; PE1, PE2	-	+
Genome information		
Size (nt)	68,65,567	71,82,433
Total genes	6,215	5,298
Protein coding genes	6,095	5,244
RNAs coding genes	72	54
CRISPERs Locus	0	1

Data from this study. Strains JC647^T and *"C. conspicua*" DSM 100706^T; Major polar lipids diphosphatidylglycerol and Phosphatidylcholine are common in both the strains; D-glucose, lactose, mannitol, rhamnose, mannose, sucrose, galactose, maltose are good carbon sources/electron donors supporting growth of both the strains while malic acid, ascorbate, pyruvate, inositol, sodium acetate, propionate, benzoic acid, fumarate, xylose, succinate does not support the growth of both the strains. Ammonium sulphate, lysine, threonine, aspartic acid, peptone, yeast extract, sodium nitrate and glutamine are good nitrogen sources for growth of both the strains while leucine, phenyl alanine, serine, arginine, isoleucine, tryptophan, tyrosine and sorbitol does not support the growth of both

the strain. For the enzyme activity strains JC647^T and "*C. conspicua*" DSM 100706 showed positive for alkaline phosphatase, acid phosphatase, naphthol-AS-BI-phosphohydrolase, and β-galactosidase, while negative for lipase (C 14), valine arylamidase, cysteine arylamidase, trypsin, α-galactosidase, β-glucuronidase, β- glucosidase, α-mannosidase, α-fucosidase.; +, requirement for growth; - not require for growth

3.5.2 Phylo-taxogenomic study of the strain JC658^T

3.5.2.1 *Habitat and nucleotide sequences accession numbers*

The strain JC658^T from a specimen of sponge belonging to the species *Pseudoceratina purpurea*, collected from the sea shore of Rameswaram, India (GPS position: 09°16'52"N 79°10'20"E). The 16S rRNA gene sequence of strain JC658^T was deposited with European Molecular Biology Laboratory (EMBL) with the accession number LR898466. The whole genome sequence of the strain JC658^T (7.4 Mb) was deposited with the NCBI with accession number JAALXT000000000.

3.5.2.2 *Genomic characteristics*

Genome size of the strain JC658^T is 73,61,520 nt present in 24 contigs with a N50 value of 1,105,066. The genome has 5,551 genes of which 5,411 are protein coding genes, 82 genes for RNAs and 58 genes are pseudogenes. The G+C content of the genome of strain JC658^T is 54.6 mol%.

3.5.2.3 BLAST Analysis and Phylogenetic inference

The BLAST analysis of amplicon based 16S rRNA gene sequence of strain JC658^T indicated that it shares highest identity of 87.7% with the species of genus *Rubinisphaera*; Rubinisphaera brasiliensis DSM 5305^T within the family Planctomycetaceae. The 16S rRNA gene sequence based phylogenetic tree with combined bootstrap values obtained from ML, NJ, ME trees (Fig. 3.5.2.1) and 92 core genes based phylogenomic tree (Fig. 3.5.2.2) confirmed the distinct or separate monophyletic clustering of strain JC658^T within the family Planctomycetaceae, suggesting that strain JC658^T forms a novel genus within the family Planctomycetaceae. Comparison of POCP values of strains JC658^T with *Rubinisphaera* spp. and yielded a minimal similarity of 49.1%. These values are below to the POCP value of 50% for delineating taxa of *Planctomycetes* at the level of genus (Peeters et al. 2020a), affirming that the strains JC658^T represent a novel genus within the family

Planctomycetaceae. The AAI values of the strain with *Rubinisphaera* spp. and other members of the family *Planctomycetaceae* yielded a maximal similarity of 56.0%. These values are also below the genus delineating threshold AAI value of 60% (Rodriguez and Konstantinidis 2014) supporting the proposal of a novel genus. Low POCP value and low AAI value between the strains JC658^T and other members of the family *Planctomycetaceae* allow the strains to be classified as the novel genus as per the recommended standards (Qin et al. 2014, Luo et al. 2014).

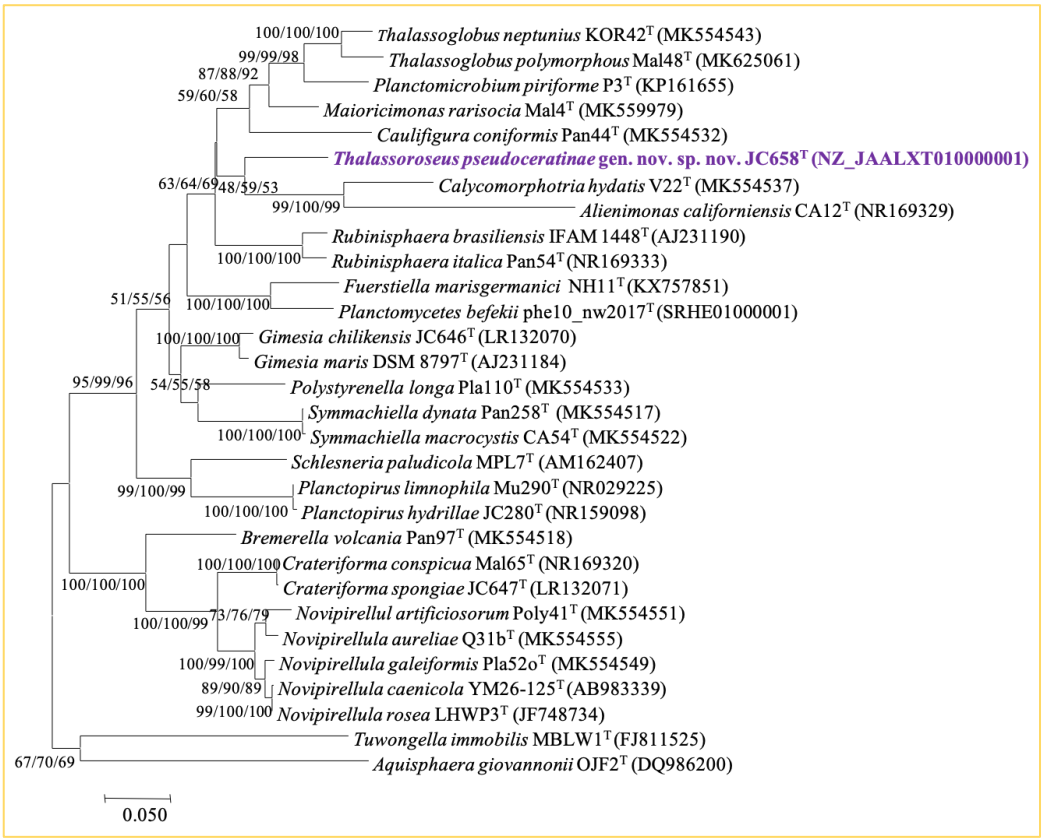

Fig. 3.5.2.1 Phylogenetic tree based on 16S rRNA gene sequences showing the phylogenetic relationship of the strain JC658^{T}within the family *Planctomycetaceae.* The tree was computed with MEGA 7 software and rooted using *Aquisphaera giovannonoi* as the out-group. The GenBank accession numbers for 16S rRNA gene sequences are shown in parentheses. Bootstrap percentages refer to NJ/ML/ME analysis. Bar, 0.050 nucleotide substitution per position.

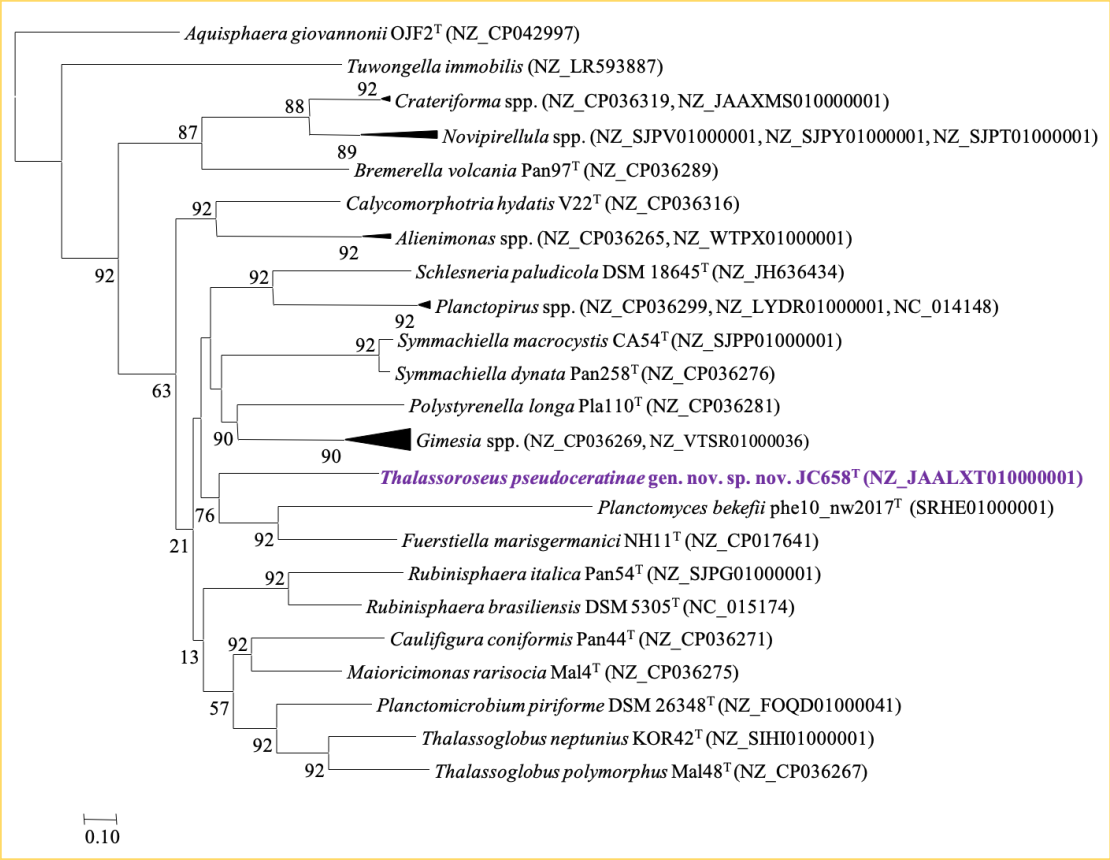

Fig. 3.5.2.2 RAxML based phylogenomics tree of strain JC658^T along with publicly available genome sequence of *Planctomycetaceae*, families. Genome sequence of *Aquisphaera giovannoni* is taken as outgroup. The GenBank accession numbers for genome sequences are shown in parentheses. Bar,0.10 nucleotide substitution per position.

3.5.2.4 *In-silico* metabolic characterization

The genome of the strain JC658^T revealed the presence of genes for cell division related proteins like FtsK, FtsW and FtsH. JC658^T do not have the gene to encode FtsZ protein like other members of the phylum. The analysis of metabolic pathways using genome information revealed that strain JC658^T showed genes encoding for NADH ubiquinone oxidoreductase, succinate dehydrogenase, cytochrome bc1complex, cytochrome c oxidases and an F1F0-type ATP synthase which were the major components of aerobic respiration. The complete Embden-Meyerhof glucolytic pathway, both oxidatative and non-oxidatative stages of pentose phosphate pathway, and the tricarboxylic acid cycle (TCA) were predicted in genome of JC658^T. Genes for De novo purine

biosynthesis are also present in the strain JC658$^{T.}$ Genes encoding for pyruvate dehydrogenase which helps in oxidation of pyruvate generated in the glycolysis and followed by conversion of acetyl-CoA to acetate were predicted. The genome showed the presence of caa3 type cytochrome c oxidases having low affinity to oxygen and is usually used by aerobic microorganisms for respiration. The analysis also revealed the presence cytochrome bd ubiquinol oxidase, an enzyme with high affinity to oxygen often found in anaerobes and microaerophiles (Dedysh et al. 2020). However the capacity of strain JC658^{T} to grow in anerobic conditions is limited. But, the strain JC658^{T} are able to tolerate oxidative stress as its genome has the several genes encoding for *Bacteroides* aerotolerance (Bat) operon proteins (BatA, BatB, BatC, BatD and MoxR) (Nagar et al. 2020). The presence of Bat operon genes in the strain JC658^{T} may be due to the horizontal genes transfer as *Bacteroides* are predominant in the marine sponges. 517 genes are laterally transferred from other domains like Archea, Eukaryota, virus and from eubacterial domain as well. Genes for nitrate/nitrite transporter (NarK) and NAD(P)H-dependent cytoplasmic nitrite reductase that converts nitrate through nitrite to ammonium and NrfAH-type cytochrome c nitrite reductase that helps in dissimilatory reduction of nitrite to ammonium were predicted. The analysis also showed genes encoding for Acetolactate synthase (EC 2.2.1.6), L-lactate dehydrogenase (EC 1.1.1.27), Acetaldehyde dehydrogenase (EC 1.2.1.10), D-lactate dehydrogenase (EC 1.1.1.28) and Acetate kinase (EC 2.7.2.1) which are involved in fermentation. The activity of lactate dehydrogenase could result in the production of lactate among the fermentation products. The strain JC658^{T} are putatively capable of tryptophan synthesis as it genes encode for Phosphoribosyl anthranilate isomerase (EC 5.3.1.24), Anthranilate phosphoribosyl transferase (EC 2.4.2.18), Tryptophan synthase alpha chain (EC 4.2.1.20) Tryptophan synthase beta chain (EC 4.2.1.20), Anthranilate synthase, aminase component (EC 4.1.3.27), ndole-3-glycerol

phosphate synthase (EC 4.1.1.48). The strain JC658^T are putatively capable of degrading lignin derived aromatic compounds to the citric acid intermediates in β- ketoadipate pathway as it contain several genes encoding for the muconate lactonizing enzyme family (Kajander et al. 2003). The strain JC658^T showed complete set of genes encoding for 2-C-methyl-D-erythritol 4-phosphate/1-deoxy-D-xylulose 5-phosphate (MEP) pathway for the biosynthesis of five-carbon isoprene unit (isopentenyl pyrophosphate; IPP) which is eventually the precursor for the synthesis of carotenoids and quinones whereas the complete genes were not observed in *F. marisgermanicae* NH11^T and in case of *R. brasilensis* DSM 5305^T the genes encoding for isopentenyl-diphosphate delta-isomerase [EC:5.3.3.2] were not predicted. The pathways for trehalose biosynthesis, Crassulacean acid metabolism occurring in dark observed in JC658^T and absent in strains *R. brasilensis* DSM 5305^T and *F. marisgermanicae* NH11^T. The pathway for dissimilatory nitrate reduction which involves conversion of nitrate to ammonia is predicted only in *F. marisgermanicae* NH11^T. The genes encoding for enzymes nitrate reductase [EC: 1.9.6.1] involved in dissimilatory nitrate reduction were not observed in JC658 and *R. brasilensis* DSM. The genes encoding for futalosine hydrolase [EC:3.2.2.26] an enzyme involved in conversion of futalosine to dehypoxanthine futalosine a reaction involved in menaquinone biosynthesis was not predicted in both JC658^T and *R. brasilensis* DSM 5305^T. The pathway for Serine biosynthesis was observed in *R. brasilensis* DSM 5305^T and JC658^T

CAZy annotation of genome of the strains JC658^T have number of genes encoding for carbohydrate-active enzymes (CAZymes) and contains more number of glycoside hydrolases (GHs) and followed by carbohydrate binding molecules (CBMs). The strain JC658^T contained GHs, CBM47 and CBM67 as major families and very few are organized in clusters. The genome prediction pattern agrees with the experimentally determined carbohydrate utilization (Fig. 3.5.2.3). Planctomycetes are believed to produce bioactive

secondary metabolites because of their complex life cycle. The number of putative secondary metabolite clusters in strain JC658^T are 11. The strain JC658^T has clusters for terpenes, Type I Polyketide Synthase (TIPKS), TIIIPKS, Non-ribosomal peptide synthetase (NRPS), NRPS-Like and Mixed NRPS-TIPKS.

Table 3.5.2.1 Genome-based analysis of the central carbon metabolism of genus strain JC658^T and closely related strains of Planctomycetaceae.

Enzyme/reaction	**EC number**	**Gene**	**JC658^T**	***Rubinisphaera brasiliensis* DSM 5305^T**	***R. italica***	***Fuerstia marisgermanicae* NH11^T**
Glycolysis						
Glucose-6-phosphate isomerase	5.3.1.9	*pgi*	Yes	Yes	Yes	Yes
ATP-dependent 6-phosphofructokinase isozyme 1	2.7.1.11	*pfkA*	Yes	Yes	Yes	Yes
Fructose-bisphosphate aldolase class 2	4.1.2.13	*fbaA*	Yes	Yes	Yes	Yes
Triosephosphate isomerase	5.3.1.1	*tpiA*	Yes	Yes	Yes	Yes
Glyceraldehyde-3-phosphate dehydrogenase	1.2.1.12	*gapA*	Yes	Yes	Yes	Yes
Phosphoglycerate kinase	2.7.2.3	*pgk*	Yes	Yes	Yes	Yes
2,3-Bisphosphoglycerate-independent phosphoglycerate mutase	5.4.2.12	*gpmI*	Yes	Yes	Yes	Yes
Enolase	4.2.1.11	*eno*	Yes	Yes	Yes	Yes
Pyruvate kinase I	2.7.1.40	*pykF*	Yes	Yes	Yes	Yes
Pyruvate dehydrogenase E1 component	1.2.4.1	*aceE*	Yes	Yes	Yes	Yes
Dihydrolipoyllysine-residue acetyltransferase component of pyruvate dehydrogenase complex	2.3.1.12	*aceF*	Yes	Yes	Yes	Yes
Gluconeogenesis						
Phosphoenolpyruvate carboxylase	4.1.1.31	*ppc*	Yes	No	No	No
Pyruvate, phosphate dikinase	2.7.9.1	*ppdK*	Yes	Yes	Yes	Yes
Phosphoenolpyruvate carboxykinase (ATP)	4.1.1.49	*pckA*	Yes	No	No	No
Phosphoenolpyruvate carboxykinase (GTP)	4.1.1.32	*pckG*	No	No	No	No
Fructose-1,6-bisphosphatase class 2	3.1.3.11	*glpX*	No	No	No	No
Fructose-1,6-bisphosphatase class 1	3.1.3.11	*fbp*	Yes	Yes	Yes	Yes
Pyrophosphate–fructose 6-phosphate 1-phosphotransferase	2.7.1.90	*pfp*	Yes	No	No	Yes

Pentose phosphate pathway						
Glucose-6-phosphate 1-dehydrogenase	1.1.1.49	*zwf*	Yes	Yes	Yes	Yes
6-Phosphogluconolactonase	3.1.1.31	*pgl*	Yes	Yes	Yes	Yes
6-Phosphogluconate dehydrogenase, decarboxylating	1.1.1.44	*gndA*	Yes	Yes	Yes	Yes
Transketolase 2	2.2.1.1	*tktB*	Yes	Yes	Yes	Yes
Transaldolase B	2.2.1.2	*talB*	Yes	Yes	Yes	Yes
Entner–Doudoroff pathway						
KHG/KDPG aldolase	4.1.2.14	*eda*	Yes	Yes	Yes	Yes
Phosphogluconate dehydratase	4.2.1.12	*edd*	No	No	No	No
TCA cycle						
Citrate synthase	2.3.3.16	*gltA*	Yes	Yes	Yes	Yes
Aconitate hydratase A	4.2.1.3	*acnA*	Yes	Yes	Yes	Yes
Isocitrate dehydrogenase (NADP)	1.1.1.42	*icd*	Yes	Yes	Yes	Yes
2-Oxoglutarate dehydrogenase E1 component	1.2.4.2	*sucA*	Yes	Yes	Yes	Yes
Dihydrolipoyllysine-residue succinyltransferase component of 2-oxoglutarate dehydrogenase complex	2.3.1.61	*sucB*	Yes	Yes	Yes	Yes
Succinate–CoA ligase [ADP-forming] subunit alpha	6.2.1.5	*sucD*	Yes	Yes	Yes	Yes
Succinate–CoA ligase [ADP-forming] subunit beta	6.2.1.5	*sucC*	Yes	Yes	Yes	Yes
Succinate dehydrogenase flavoprotein subunit	1.3.5.1	*sdhA*	Yes	Yes	Yes	Yes
Succinate dehydrogenase iron-sulfur subunit	1.3.5.1	*sdhB*	Yes	Yes	Yes	Yes
Succinate dehydrogenase cytochrome b556 subunit	1.3.5.1	*sdhC*	Yes	No	No	No
Succinate dehydrogenase hydrophobic membrane anchor subunit	1.3.5.1	*sdhD*	No	No	No	No
Fumarate hydratase class I, an/aerobic	4.2.1.2	*fumA/B*	No	No	No	No
Fumarate hydratase class II	4.2.1.2	*fumC*	Yes	Yes	Yes	Yes
Malate dehydrogenase	1.1.1.37	*mdh*	Yes	Yes	Yes	Yes
Glyoxylate shunt						
Isocitrate lyase	4.1.3.1	*aceA*	No	No	No	No
Malate synthase G	2.3.3.9	*glcB*	No	No	No	No

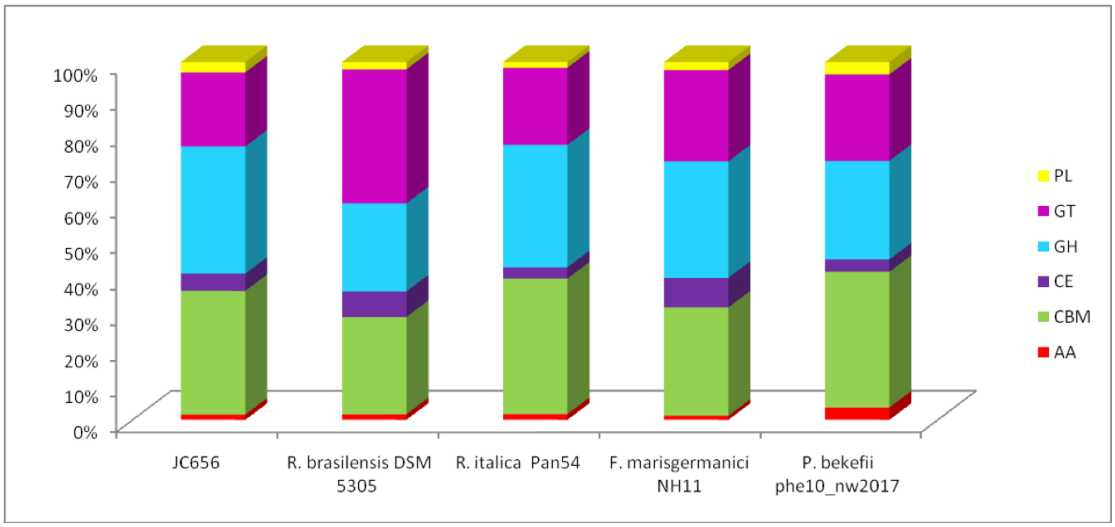

Fig. 3.5.2.3 Comparative analysis of CAZymes of strain JC658^T and and closely related strains of Planctomycetaceae.AA, Auxiliary Activities (AAs); CBM, Carbohydrate-Binding Modules (CBMs); CE, Carbohydrate Esterases (CEs); GH, Glycoside Hydrolases (GHs); GT, Glycosyl Transferases (GTs); PL, Polysaccharide Lyases (PLs).

3.5.2.5 Morphological and physiological analyses

SEM images shows that cells in strain JC658^T are in aggregate or in isolation (Fig. 3.5.2.4a, b). Cells of strain JC658^T are oval to pear shaped (1.7-2.0 x 1.45-1.7 µm; Fig. 4a) having crateriform structures distributed all over the surface isolation (Fig. 3.5.2.4a, b). TEM image of JC658^T cells shows the presence of invagination of cytoplasmic membrane, inclusion body, enlarged periplasm, cytoplasm, nucleoid region and cell reproduction by budding (Fig. 3.5.2.4c). Growth observations with different carbon substrates/nitrogen sources/pH range/NaCl tolerance for the strain JC658^T are given in either species description or in Table 3.5.2.3**.** Enzymatic activity of strain JC658^T was determined using API ZYM kit (BioMérieux), according to the manufacturer's instructions for which results are given in species description or in the Table 3.5.2.3.

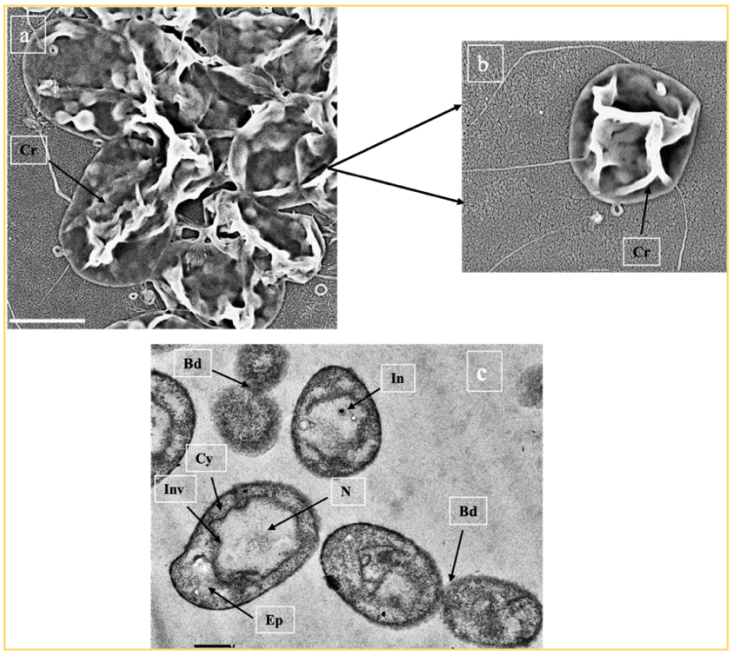

Fig. 3.5.2.4. Electron micrographs of JC658^{T}, SEM image showing oval to pear shaped cells in aggregates Cr, Craterifrom structure

3.5.2.6 Chemotaxonomic characterization

3.5.2.6.1 FAME profile

Table. 3.5.2.2 Distribution of fatty acids in the strain JC658^{T}.

S.No	Fatty acid (%)	JC658^{T}
1.	$C_{12:0}$	1.1
2.	$C_{14:0}$	3.7
3.	Iso-$C_{14:0}$	1.2
4.	$C_{15:0}$ 2-OH	1.2
5.	anteiso-$C_{15:0}$	1.54
6.	$C_{15:1}\omega6c$	2.4
7.	**$C_{16:0}$**	**24.0**
8.	$C_{16:0}$ 3-OH	2.4
9.	**$C_{16:1}\omega7c/C_{16:1}\omega6c$**	**24.9**
10.	$C_{17:0}$	1.6
11.	$C_{12:0}$	1.1
12.	$C_{17:1}\omega8c$	1.4
13.	$C_{17:1}\omega6c$	1.2
14.	anteiso-$C_{17:0}$	1.0
15.	**$C_{18:0}$**	**18.9**
16.	$C_{18:1}\omega9c$	4.5
17.	$C_{18:1}\omega7c$/ $C_{18:1}\omega6c$	2.0
18.	$C_{18:0}$ante/ $C_{18:2}\omega6c,9c$	1.0
19.	$C_{20:1}\omega9c$	1.34
20.	$C_{20:1}\omega7c$	1.0
21.	$C_{20:0}$	1.2
22.	$C_{16:0}$ 10-methyl /iso-$C_{17:1}\omega9c$	1.1

For the strain JC658^T, major proportions of the fatty acids are $C_{16:0}$, $C_{18:0}$, and $C_{16:1}\omega7c/C_{16:1}\omega6c$ (Table. 3.5.2.2).

3.5.2.6.2 Polar lipid profile

Polar lipids of the strain JC658^T are phosphatidylcholine (PC), phosphatidyl-dimethylethanolamine (PE2), phosphatidyl-monomethylethanolamine (PE1), six uncharacterized phospholipids (PL1,2,3,4,5,6) and four uncharacterized lipids (UL1,2,3,4) (Fig. 3.5.2.5).

3.5.2.6.3 Polyamine Profile

Polyamine for the strain JC658^T are sym-homospermidine and putrescine (Fig. 3.5.2.5).

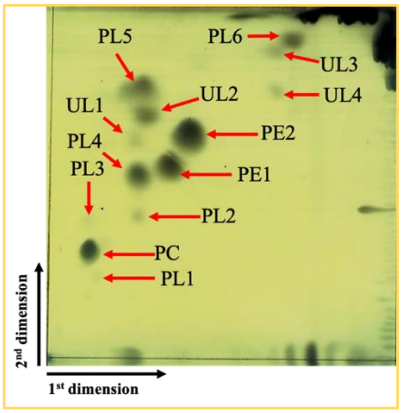

Fig. 3.5.2.5. Two-dimensional thin-layer chromatograms of whole cell polar lipids of strain 1. JC658; PC, phosphatidylcholine; PE2, phosphatidyl-dimethylethanolamine; PE1, phosphatidyl-monomethylethanolamine; PL1,2,3,4,5,6 uncharacterized phospholipids; UL1,2,3,4 uncharacterized lipids.

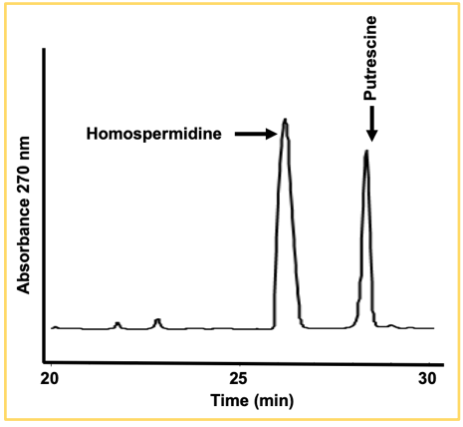

Fig. 3.5.2.6 Polyamine profile of the strain JC658^T

Table 3.5.2.3. Differentiating characters between strains JC658^T and other members of Planctomycetaceae

Characters	**JC658^T**	**2***	**3***	**4***	**5***	**6***	**7***	**8***	**9***	**10***	**11***	**12***	**13***
Cell size (L x W, µm)	1.4 ± 0.2 × 0.7 ± 0.1	1.2–1.6 x 0.7-1.0 or 0.4–1.5	1.4 ± 0.2 × 0.7 ± 0.1	1.6-1.8 x 0.8-1.0	0.8–1.4 x 1.3–2.1	1.0 – 1.4 / 1.2 – 1.5	1.3 ± 0.2	1.6 × 0.8 µm or 0.7 – 1.8 µm	2.0 9 x 1.4	0.9–1.36 x 1.7–2.8	1.6 x 0.9 or 1.7	1.6 ± 0.3 × 0. 7 ± 0.2	2.0 ± 0.2 x 1.5 ± 0.3
Cell shape	Oval to pear shaped	Oval to pear or spherical	Pear shaped	Ovoid to pear shaped	Ellipsoid-like	Spherical to ovoid	Pear-shaped	Pear or spherical to ovoid	Pear-shaped	Ellipsoidal to pear-shaped	Pear shaped or spherical	Round grain rice-shaped	Spherical to ovoid
Cell arrangement	Aggregate	Rosette	Rosette	Rosette	Single, paired or rosette	Rosette	Rosette	Rosette	Rarely aggregates	rosette	Rosette	Rosette	Rosette
Pigmentation	Pale pink	Cream	White	White	Unpigmented	Pink to red	white	White / yellow to orange	Orange	white	Beige or Cream	Pink	Pink
Fimbriae	NR	+	+	+	+		+	+	+	+	+	+	+
NaCl requirement (tolerance; %)	3 (1.0- 6.0)	3(1.0–7.0)	NR	NR	<0.5	0 – 0.5 (0 – 1.5)	NR	0.1 -1.7	NR	< 0.5	NR	NR	NR
Temperature optima (tolerance; °C)	25 (10-40)	30-35 (5-40)	24 (10-27)	24 (15-30)	15-26 (4-32)	20-30 (4 – 50)	26 (15 -30)	26-33 (14-38)	31 (10 – 39)	20 – 28 (10 – 30)	30 – 33 (15 – 36)	30 (15-32)	27 (10-36)
pH optima (tolerance)	8 (7-9)	8 (7-9)	7.5 (6.5-8.5)	7.5 (5.5-9.5)	5.0-6.2 (4.2 – 7.5)	6.5 – 7.5 (6.0 – 9.0)	8.0 (5.0 – 10.0)	9.0 (6.0 – 10 .0)	6.5–9.0 (7.5)	6.0 – 6.5 (4.2 – 7.1)	7.0 – 7.5 (5.5 – 8.5)	8.5 (6.0 – 10.0)	7.5 (6.0 -9.0)
Organic substrate utilization													
NAG	+	+	+	NR	+	+	+	+	NR	+	+	NR	NR
Sucrose	-	+/-	NR	NR	+	+/-	NR	NR	NR	+	+	NR	NR
Maltose	+	+	NR	NR	+	+/-	NR	NR	NR	+	+	NR	NR
Lactose	+	+/-	NR	NR	+/-	-	NR	NR	NR	NR	+	NR	NR
Mannitol	-	-	NR	NR	-	+/-	NR	NR	NR	-	+/-	NR	NR
Nitrogen substrate utilization													
Alanine	+	-	NR	NR	-	+/-	NR	NR	NR	-	-	NR	NR
Asparagine	-	+	NR	NR	-	NR	NR	NR	NR	-	-	NR	NR
Phenylalanine	-	-	NR	NR	-	+/-	NR	NR	NR	-	-	NR	NR
Threonine	-	+	NR	NR	-	NR	NR	NR	NR	-	-	NR	NR
Proline	+	-	NR	NR	-	-	NR	NR	NR	-	-	NR	NR

Nitrate reduction	-	+/-	NR	NR	+	+/-	NR	NR	NR	+	NR	NR	NR
Starch hydrolysis			NR	NR	-	+/-	NR	NR	NR	-	NR	NR	NR
Fatty acids													
$C_{17:1\omega}8c$	+	+	NR	NR	+	++	NR	+	NR	-	+	NR	NR
$C_{16:1}\omega7c/C_{16:1}\omega6c$	++	++	NR	NR	++	++-	NR	++	NR	++	-	NR	NR
$C_{18:1}\omega9c$	+	++	NR	NR	+	++	NR	+	NR	++	++	NR	NR
anteiso-$C_{15:0}$	-	++	NR	NR	-	-	NR	-	NR	-	+	NR	NR
anteiso-$C_{13:0}$	-	++	NR	NR	-	-	NR	-	NR	-	+	NR	NR
Polar lipids													
PG	-	+/-	NR	NR	NR	+	NR		NR	-	NR	NR	NR
DPG	-	+	NR	NR	NR	+	NR		NR	-	NR	NR	NR
PE	++	-	NR	NR	NR	-	NR		NR	-	NR	NR	NR
PC	+	+	NR	NR	NR	+	NR		NR	-	NR	NR	NR
Genome information													
Size (Mbp)	7.4	7.6- 8,9	6.1	7.5 - 7.7		5.4 – 5.7	6.7	6.0 – 6.7	7.7	6.7	6.3 – 6.7	51	5.4
G+C mol%	56.4	50.5-53.2	50.3	55.3	54-57	53.6-53.8	63.2	48.8 – 56.4	63.4	59.0	50.3 – 52.8	53.9	70.7

*, Data taken from the literature

1, Strain JC658^T 2, *Gimesia* (*G. maris*, G.*chilikensis)* 3, *Polystyrenella longa Pla110^T;* 4, *Symmachiella* (S.*dynata Pan258^T*, *S. macrocystis CA54^T*); 5, *Schlesneria paludicola* MPL7^T; 6, *Planctopirus (Planctopirus limnophila Mu290^T* , *Planctopirus hydrillae JC280^T*; 7, *Caulifigura coniformis* Pan44^T ; 8, *Rubinisphaera (R. brasiliensis IFAM 1448^T, R. italica* Pan54^T ; 9, *Maioricimonas rarisocia* Mal4^T ; 10, *Planctomicrobium piriforme* P3^T ; 11, *Thalassoglobus* (*T. neptunius* KOR42^T, *T. polymorphous* Mal48^T); 12, *Calycomorphotria hydatis* V22^T ; 13, *Alienimonas californiensis* CA12^T. (PG), Phosphatidylglycerol; (DPG), Diphosphatidylglycerol; (PE), Phosphatidylethanolamine, (PC), Phosphatidylcholine

3.5.3 Phylo-taxogenomic study of the strains JC639^T and JC637

3.5.3.1 Habitat and nucleotide sequences accession numbers

The strains JC639^T and JC637 were isolated from a specimen of sponges belonging to the genus *Axinella* and *Clathria*, respectively collected from the sea shore of Rameswaram, India (GPS position: 09°16'52"N 79°10'20"E). The 16S rRNA gene sequences of both the strains, JC637 and JC639^T were deposited with European Molecular Biology Laboratory (EMBL) with accession the numbers LR132059 and LR132063, respectively. The whole genome sequences of strains JC637 and JC639^T (7.9Mb and 9.5Mb) were deposited with NCBI with the accession numbers, WRPS00000000 and JACEHH000000000, respectively.

3.5.3.2 Genomic characteristics

Genome size of strain JC637 is 7.9Mb with N_{50} value of 416,970 while the genome size of strain JC639^T is 9.7Mb with N_{50} value of 163,993. Genome of strain JC637 has 5,525 genes of which 5,376 are protein coding genes, 79 genes code for RNAs and 70 genes are pseudogenes. While strain JC639^T has 6,560 genes of which 6,469 are protein coding genes, 67 genes code for RNAs and 69 genes are pseudogenes (Table 3.5.3.1). Genomic DNA G+C content of strains JC637 and JC639^T are 55.1 mol% and 59.5 mol%, respectively. The G+C content between the strain JC639^T and *Roseiconus Lacunae* JC635^T varied by 7.4% which is more than 3% for species delineation (Meier-Kolthoff et al. 2014).

3.5.3.3 BLAST Analysis and Phylogenetic inference

BLAST analysis of amplicon based 16S rRNA gene sequence of strain JC639^T (1446 nt) in EzBiocloud server showed that this strain share highest identity of 96.9% and 96.7% with *Roseiconus nitratereducens* JC645^T and *Roseiconus Lacunae* JC635^T, respectively. While the 16S rRNA gene sequence of strain JC637 (1446 nt) in EzBiocloud server showed that this strain share highest identity of 99.9% with *Roseiconus Lacunae*

JC635^T. The 16S rRNA sequence similarity between strains JC637 and JC639^T is 96.8% (Fig. 3.5.3.1).

Table 3.5.3.1: Comparative genomic features among members of genus *Roseiconus*, JC637, and JC639^T

	Organism	Accession No	Sequencing Technology	Genome size (Mb)	No of contigs	GC %	N50 (bp)	Genes (total)	CDS (Protien)	RNAs
1	JC635^T	NZ_VSZO01000000	Illumina HiSeqX10	7.9	97	55.1	466,683	5,570	5,410	79
2	JC645^T	NZ_VWOX00000000	Illumina HiSeqX10	8.2	108	60.0	403,299	5,806	5,637	83
3	**JC639^T**	JACEHH000000000	Illumina HiSeqX10	9.5	269	59.5	163,993	6,560	6,469	67
4	JC637	WRPS00000000	Illumina HiSeqX10	7.9	113	55.1	416970	5,525	5,376	79

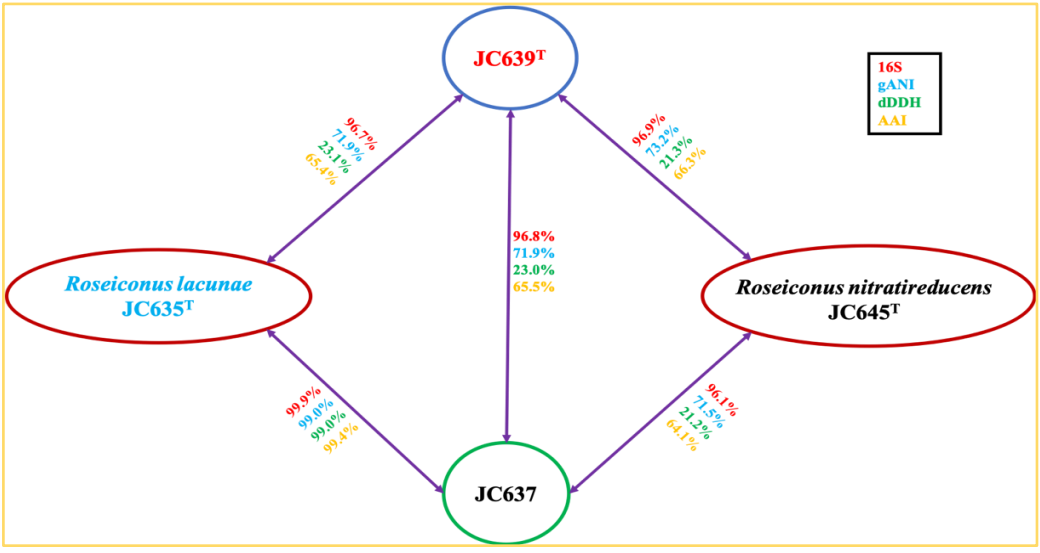

Fig. 3.5.3.1 Analysis of phylogenetic markers for delineation of the novel isolates JC637 and JC639^T. Methods used:16S rRNA gene identity (16S), average amino acid identity (AAI), average nucleotide identity (ANI).

The 16S rRNA gene sequences of strains JC635^T and JC645^T extracted from the genome has sequence length of 1532 nt and 1530 nt respectively and the BLAST search results are also similar. The 16S rRNA gene sequence based phylogenetic tree with combined bootstrap values obtained from NJ, ME, ML trees (Fig. 3.5.3.2) and 92 core genes based phylogenomic tree (Fig. 3.5.3.3) confirmed the clustering of strains JC635^T

and JC645^T within the genus *Roseiconus.* The Strain JC639^T is distinctly separated from both the existing members of *Roseiconus., Roseiconus nitratereducens* JC645^T and *Roseiconus Lacunae* JC635^T. While the strain JC637 is clustered together with *Roseiconus Lacunae* JC635^T. This finding suggest that Strain JC639^T is a novel species within the genus *Roseiconus*.

OrthoANI values of strain JC639^T with *Roseiconus nitratereducens* JC645^T and *Roseiconus Lacunae* JC635^T is 73.2% and 71.9%, respectively. The *d*DDH values strain JC639^T with *Roseiconus nitratereducens* JC645^T and *Roseiconus Lacunae* JC635^T is 21.3% and 23.1, respectively. The OrthoANI and *d*DDH values (Fig. 1) strain JC639^T with *Roseiconus nitratereducens* JC645^T and *Roseiconus Lacunae* JC635^T is far less (95-96% cut off for ANI and 70% cut off for *d*DDH) than the recommended cut-off values for species delineation (Goris et al. 2007; Richter and Rossello-Mora 2009) thus, strain JC639^T represent a novel species within the genus *Roseiconus*. While, the OrthoANI and *d*DDH values strain JC637 have approximately 99% with *Roseiconus Lacunae* JC635^T. These values are far above species delineation threshold, hence the strain JC637 is similar to *Roseiconus Lacunae* JC635^T. The AAI value between the strains JC639^T and *Roseiconus Lacunae* JC635^T is 65.4%. The AAI value between the strains JC639^T and *Roseiconus nitratereducens* JC645^T is 66.3% (Fig. 3.5.3.1). These values are also below the species delineating threshold AAI value of 93.5% supporting the proposal of a novel species within the genus *Roseiconus*. (Qin et al. 2014, Luo et al. 2014).

3.5.3.4 *In-silico* metabolic characterization

Strains JC639^T and JC637 have 2-C-methyl-D-erythritol 4-phosphate/1-deoxy-D-xylulose 5-phosphate (MEP) pathway for the biosynthesis of five-carbon isoprene unit (isopentenyl pyrophosphate; IPP) which is eventually the precursor for the synthesis of carotenoids and quinones (Eisenreich et al. 2004; Zhao et al.2013; Zhang 2018).

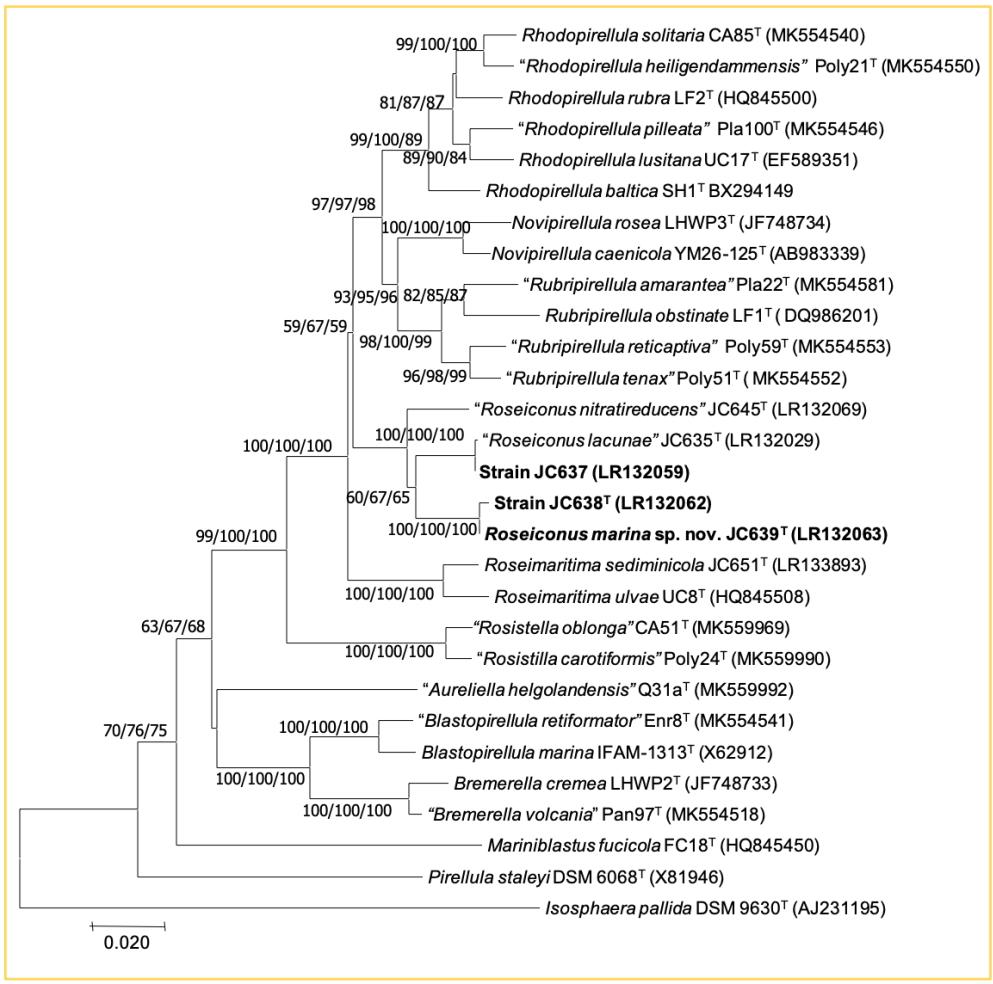

Fig. 3.5.3.2 Phylogenetic tree based on 16S rRNA gene sequences showing the phylogenetic relationship of strains JC637^T, JC639^T within the family *Pirellulaceae*. The tree was computed with MEGA 7 software and rooted using *Isosphaera palida* DSM 9630^T as the out-group. The GenBank accession numbers for 16S rRNA gene sequences are shown in parentheses. Bootstrap percentages refer to NJ/ML/ME analysis. Bar, 0.02 nucleotide substitution per position.

Genes encoding for diapocarotenoid biosynthetic enzymes like diapolycopene oxygenase (1.14.99.44), 4,4'-diapophytoene desaturase (1.3.8.2), 15-cis-phytoene synthase (2.5.1.32) were present in both strains and are capable of forming diaponeurosporenic acid and phytoene. The number of putative gene clusters for the biosynthesis of secondary metabolites in strains *Roseiconus nitratereducens* JC645^T, *Roseiconus Lacunae* JC635^T JC639^T and JC637 are 8, 10, 7 and 9, respectively.

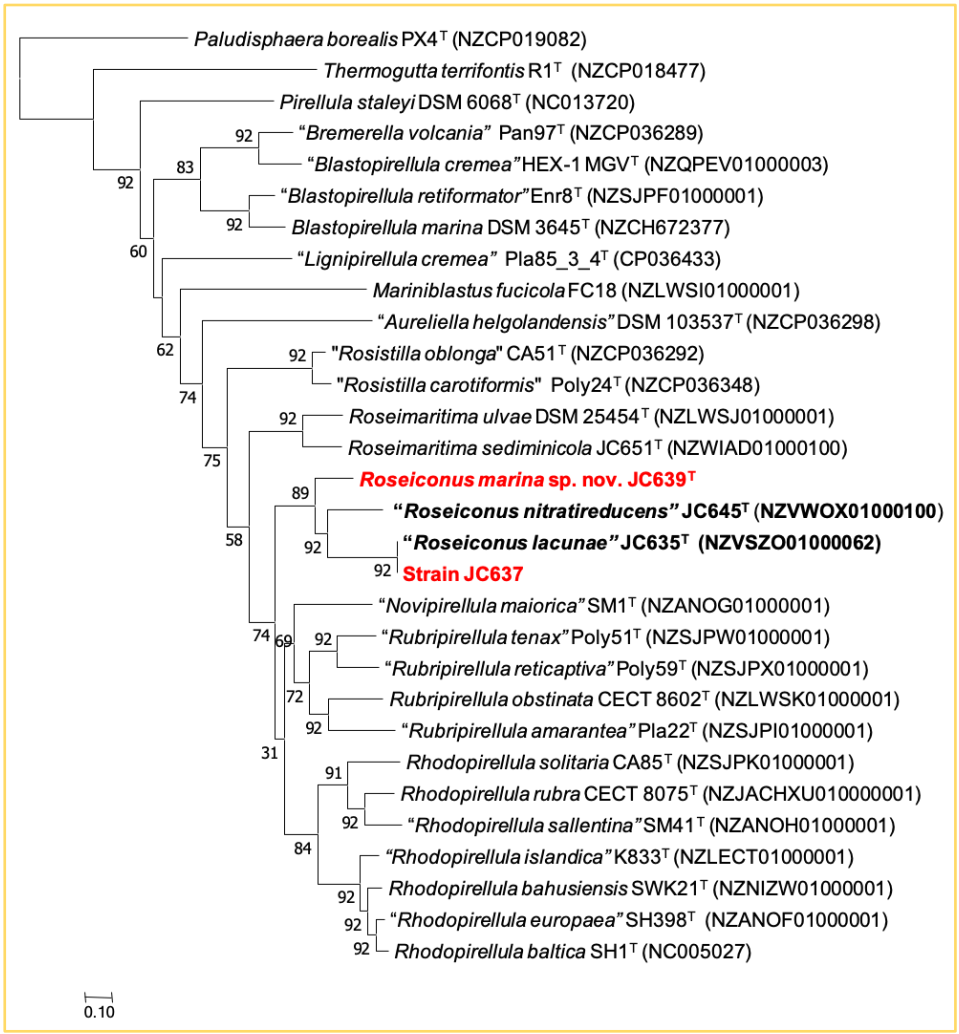

Fig. 3.5.3.3 RAxML based phylogenomic tree of strain JC637 and JC639^T along with publically available genome sequences of *Pirellulaceae* family. The GenBank accession numbers for genome sequences are shown in parentheses. The genome sequence of *Paludisphaera borealis* PX4^T is taken as an outgroup. Bar 0.10 nucleotide substitution per position.

All strains have gene clusters coding for Type III Polyketide Synthase (TIIIPKS), TIPKS, terpenes and acyl amino acid. Non-ribosomal peptide synthetase (NRPS) genes are present in all the strain *Roseiconus Lacunae* JC635^T except *Roseiconus nitratereducens* JC645^T. Interestingly, none of the strains encode for the Bacteriocin and indole as well. Genes coding for pyruvate dehydrogenase (EC 1.2.4.1), lactate dehydrogenase (EC 1.1.1.27), aldehyde dehydrogenase (EC 1.2.1.3) and alcohol dehydrogenase (EC 1.1.1.1) involved in fermentative metabolism are present in all the four strains (Fig. 3.5.3.4).

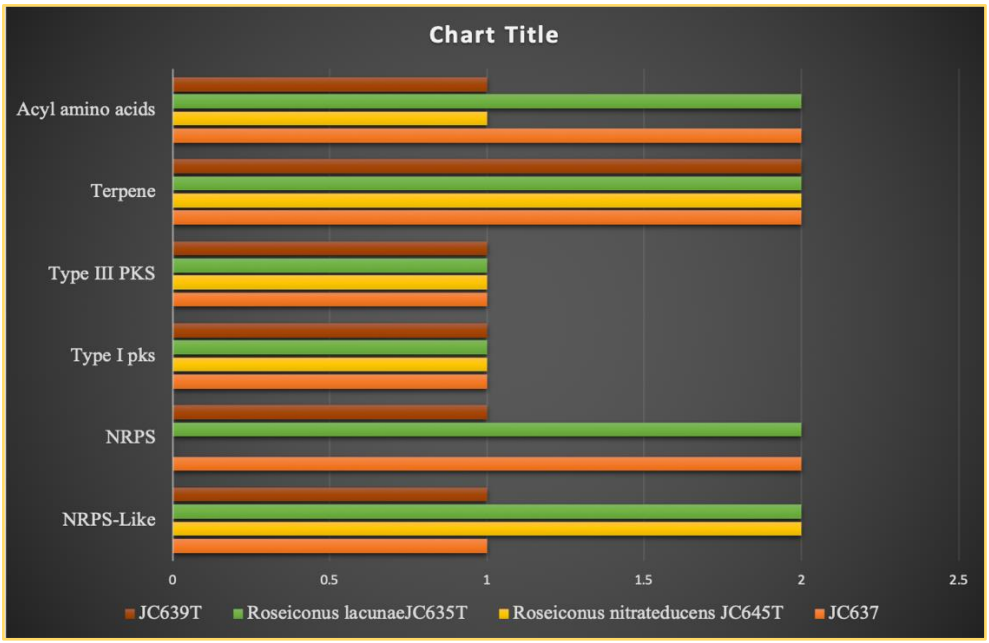

Fig. 3.5.3.4. Number of genetic clusters putatively involved in the production of secondary metabolites. The analysis is based on genome sequences of *R. lacunae* JC635^T, *R. nitrateducens* JC645^T, Strain JC639^T and Strain JC637.

3.5.3.5 Morphological and physiological analyses

Cells of both strains multiply by budding (Fig. 3.5.3.5A,D). Crateriform structures are present throughout the cell surface of both the strains (Fig. 3.5.3.5A,B). TEM image of the strain JC637 show compartment like structure, concentrated nuclear region (Fig. 3.5.3.5C,D) with fimbriae like structures coming out from crateriform structures. Cellular membrane, invagination of cytoplasmic membrane, enlarged periplasm and cytoplasm are distinctly present in the TEM image of strain JC637 (Fig. 3.5.3.5C,D). Growth observations with different carbon substrates/nitrogen sources/pH range/NaCl tolerance for strains JC637 and JC639^T are given in either species description or in Table. 3.5.3.3. Enzymatic activity of strain JC637 and JC639^T was determined using API ZYM kit (BioMérieux), according to the manufacturer's instructions for which results are given in species description or in the Table 3.5.3.3.

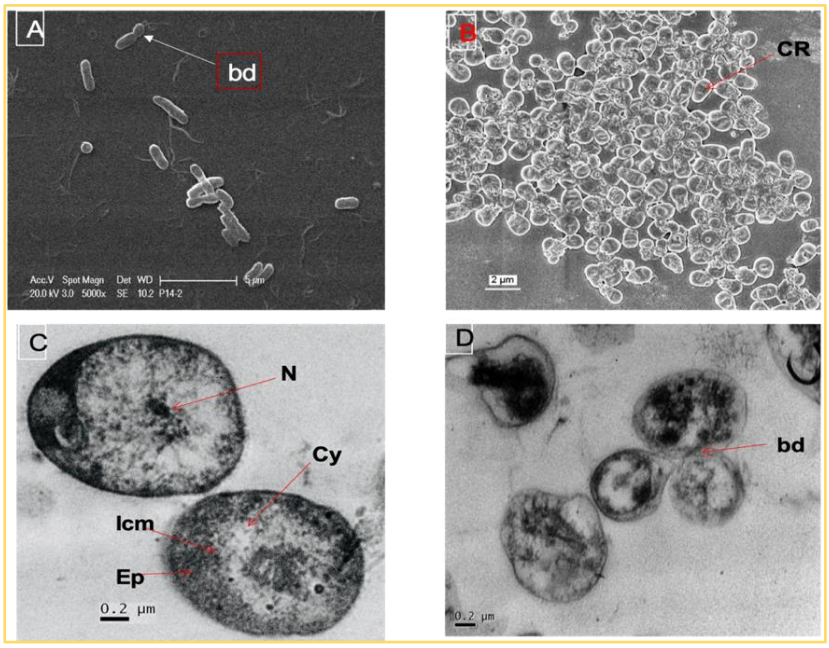

Fig. 3.5.3.5 Electron microscopic image of strain JC639^T and JC637: (A,B) SEM image of the strain JC639^T (A) and the strain JC637 (B) showing Crateriform structure (cr) on the surface; (C,D), TEM image of the cell of the strain JC637 showing reproduction by budding (bd) presence of nucleoid (N), showing intracellular compartmentalization; Cm, Cellular membrane; Icm, Invagination of cytoplasmic membrane; N, Nucleoid; Ep, Enlarged periplasm; Cy, Cytoplasm;

3.5.3.6 Chemotaxonomic characterization

3.5.3.6.1 FAME profile

For the strain JC637, major proportions of the fatty acids are anteiso-$C_{11:0,}$ anteiso-$C_{13:0,}$ anteiso-$C_{15:0,}$ $C_{16:0,}$ and $C_{18:1}\omega9c$. For the strain JC639^T, major proportions of the fatty acids are $C_{15:1}\omega8c$, $C_{16:0,}$ and $C_{18:1}\omega9c$. Interestingly, anteiso-$C_{11:0}$ is exclusive for the strain JC637 (Table. 3.5.3.2).

3.5.3.6.2 Polar lipid profile

Polar lipids of the strain JC637 are diphosphatidylglycerol (DPG), phosphatidylcholine (PC), Phosphotidylglycerol (PG), three unidentified phospholipids (PL1,2,3) and three unidentified lipids (UL1,2,3) and two amino lipid (APL1, 2) (Fig. 3.5.3.6). Polar lipids of the strain JC639^T are phosphatidylcholine (PC),

phosphatidylethanolamine (PE), two unidentified phospholipids (PL1,2) and two unidentified lipids (UL1,2)

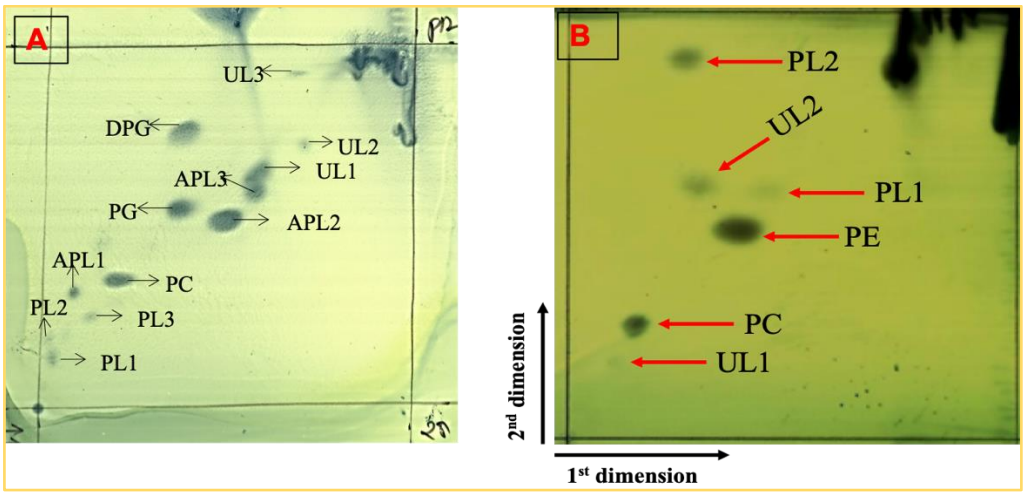

Fig. 3.5.3.6 Two dimensional chromatograms showing polar lipids of (A) strain JC637 and (B) strain JC639^T. PE, phosphatidylethanolamine; PC, Phosphatidylcholine; APL1,2,3 unidentified amino lipid; UL1,2,3 unidentified lipid; PL1,2,3 unidentified phospholipid; DPG, diphosphatidylglycerol

Table 3.5.3.2 Fatty acids distributions among the strains JC639^T, JC637, *R. lacunae* JC635^T, *R. nitrateducens* JC645^T.

S.No	**Fatty acid (%)**	**JC635^T**	**JC645^T**	**JC637**	**JC639^T**
1.	$C_{9:0}$	-	-	-	3.82
2.	$C_{10:0}$	-	-	-	2.32
3.	$C_{10:0}$3-OH	2.1	1.7	-	-
4.	$C_{11:0}$3-OH	1.0	1.0	-	-
5.	anteiso-$C_{11:0}$	-	-	**16.3**	-
6.	$C_{12:0}$	1.0	1.5	-	2.48
8.	anteiso-$C_{12:0}$	3.0	-	3.3	-
9.	anteiso-$C_{13:0}$	10.0	-	**11.8**	-
10.	$C_{14:0}$	1.7	1.5	1.0	3.0
12.	anteiso-$C_{14:0}$	-	-	3.0	-
13.	$C_{15:0}$ 2-OH	-	1.5	-	-
14.	anteiso-$C_{15:0}$	8.0	6.9	**10.0**	1.0
15.	$C_{15:0}$ anteiso A	-	-	-	1.4
16.	iso-$C_{15:0}$	-	-	-	1.3
17.	$C_{15:1}\omega5c$	-	-	1.7	-
18.	$C_{15:1}\omega8c$	-	-	-	10.2
20.	$C_{15:1}$ iso G	-	-	2.0	-
21.	$C_{15:1}$Iso H/$C_{13:0}$ 3-OH	-	-	-	2.7
22.	$C_{16:0}$	16.8	17.4	**8.5**	18.1
23.	$C_{16:0}$ 3-OH	1.0	-	1.6	1.2
24.	iso- $C_{16:0}$	-	-	1.6	-
25.	anteiso-$C_{16:0}$	1.0	-	1.0	-

26.	$C_{16:1}\omega7c/C_{16:1}\omega6c$	5.4	7.0	1.9	6.7
27.	$C_{17:0}$	1.6	2.2	-	1.7
28.	anteiso-$C_{17:1}\omega9c$	-	-	-	4.2
30.	$C_{17:1}\omega8c$	2.2	5.0	1.4	1.7
31.	$C_{17:1}\omega7c$	-	-	-	1.0
33.	anteiso-$C_{17:0}$	5.5	4.6	6.5	-
34.	anteiso-$C_{17:1}$	1.6	-	2.3	-
35.	iso- $C_{17:0}$ 3-OH	-	-	1.9	-
37.	$C_{18:0}$	3.6	1.8	2.3	7.2
38.	$C_{18:0}$3-OH	-	-	2.6	-
40.	$C_{18:1}\omega9c$	21.4	29.5	**9.8**	**22.5**
41.	$C_{18:1}\omega7c/ C_{18:1}\omega6c$	2.3	2.4	2.7	2.3
42.	$C_{18:3}\omega6c,9c,12c$	1.5	1.2	-	-
43.	$C_{18:0}$ante/ $C_{18:2}\omega6c,9c$	-	-	1.0	-
44.	$C_{19:0}$	-	1.4	1.5	-
45.	$C_{19:0}$ iso I	-	-	-	2.3
46.	$C_{20:1}\omega9c$	-	2.5	-	-

3.5.3.6.3 Polyamine Profile

The strain JC637 has three polyamines; 1,2-Diaminopropane, putrescine and sym-homospermidine. The strain JC639^T has two polyamines putrescine and sym-homospermidine (Fig. 3.5.3.7).

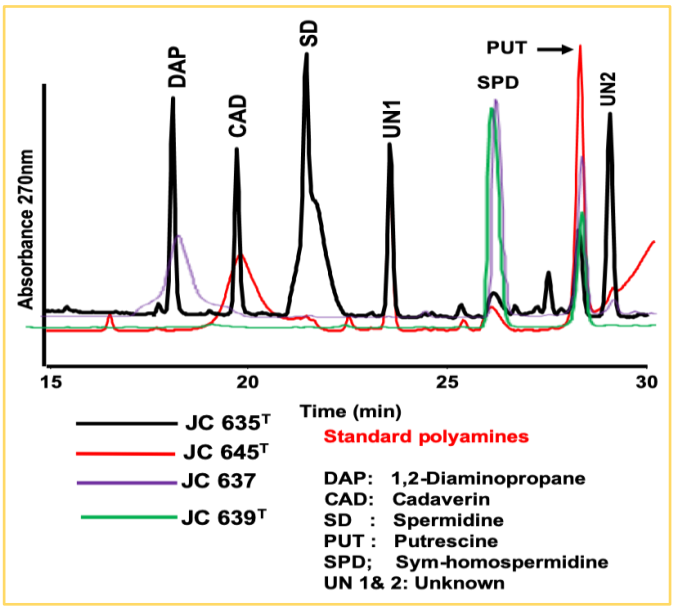

Fig. 3.5.3.7 Polyamine profile of the strains JC639^T, JC637**,** *R. lacunae* JC635^T, *R. nitratereducens* JC645^T

Table 3.5.3.3 Differentiating characters between strain JC639^T, JC637 and other members of the genus *Roseiconus*.

Characteristics	1	2	JC639^T	JC637
Cell shape	Cone to pear	Spherical to ovoid	Cylinderical	oval
Cell size (L x W)	1.2-1.5× 0.5-0.9	1.6-2.3×1.2-1.5	1.9-2.0× 0.5-0.6	1.2-1.5× 0.5-0.9
pH range (optimum)	6.0-9.0 (8.0)	7.0-9.0 (8.0)	7.0- 10.0 (8.0)	7.0- 9.0 (8.0)
NaCl tolerance range (optimum; %)	1-5 (3)	1-7 (4)	1-6 (3)	1-6 (3)
Organic substrates used for growth				
Pyruvate	-	+	-	+
Inulin	-	+	-	-
Lactose	+	-	+	+
D-galactose	+	-	+	+
fructose	+	+	-	-
starch	+	+	+	-
mannitol	-	-	+	-
mannose	+	-	-	+
D-xylose	+	+	-	-
Nitrogen sources used for growth				
Cysteine	-	+	-	+
L-Glutamine	-	+	-	-
L-Proline	-	+	-	+
Urea	-	+	-	-
L-isoleucine	+	-	-	-
L-phenylalanine	+	-	+	-
L-glutamate	+	-	-	+
L-aspartate	+	-	-	-
L-glycine	-	-	+	-
Ammonium sulphate	+	+	+	-
peptone	+	+	+	-
Vit B_{12}requirement	-	+	-	-
API ZYM (Biomeriux)				
Valinearylamidase	-	+	-	+
α-Glucosidase	-	+	-	+
Alkaline phosphatase	+	+	-	+
β-galactosidase	-	-	-	+
Polar lipids				
phosphatidylethanolamine	+	+	+	-
diphosphotidylglycerol	-	-	-	+
Polyamines				
1,2-Diaminopropane	+	-	-	+
Spermidine	+	-	-	-
Sym-homospermidine	-	-	+	+
Unidentified polyamine (UN1,2)	+	-	-	-
Genome Size(Mb)	7.9	8.2	**9.7**	7.9
Genomic DNA G+C content (mol %)	55.5	60.1	59.5	55.5

Data from this study only; 1, *Roseiconus nitratireducens* JC645^T; 2, *Roseiconus lacunae* JC635^T;

3.6 Phylo-taxogenomic studies of the newly isolated axenic culture of Planctomycetes from Loktak lake

Nine strains of Planctomycetes were isolated from the Loktak lake Manipur, India. Total four isolated strains of Planctomycetes remained viable and five strains became silent after 9^{th}-11^{th} sub culturing. Further, phylo-taxogenomic studies of single strain was carried out (Fig. 3.6.1).

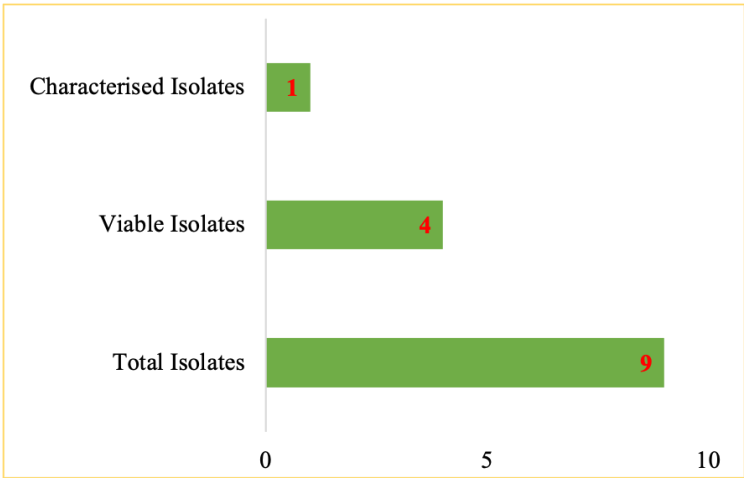

Fig. 3.6.1 Detail about the total Planctomycetal strains isolated, remain viable and strains phylo-taxogenonomic studied (Characterised) from the Loktak lake.

3.6.1 Phylo-taxogenomic study of the strain JC669^T

3.6.1.1 Habitat and nucleotide sequences accession numbers

The strain JC669^T is isolated from rhizospheric soil of *Zizania latifolia* (commonly known as Manchurian wild rice) of the phumdis (floating island) from Loktak lake situated in the northeast state of Manipur (GPS: 24°30'21" N 93°47'43"), India. The 16S rRNA gene sequence of strain JC669^T was deposited with European Molecular Biology Laboratory (EMBL) with the accession number LR782133. The whole genome sequence of strain JC669^T was deposited with the NCBI with accession number JAALJH000000000.

3.6.1.2 Genomic characteristics

Based on the NCBI Prokaryotic Genome Annotation Pipeline (PGAP), the genome size of strain JC669^T is 10.04 Mb with N_{50} value of 90,612 while the genome size of *A. giovannonii* OJF2^T is 10.37 Mb. The genome of strain JC669^T has 7,421 genes of which 7,189 are protein coding genes, 3 rRNA operons, 72 tRNA coding, 154 genes are pseudogenes whereas genome of *Aquisphaera giovannonii* OJF2^T contains a total of 7,692 genes of which 7,415 are protein coding, 73 tRNA genes, 9 rRNA operons and 171 genes are pseudogenes. G+C content of the genome of strain JC669^T is 68.5 mol% which is about 3.2% lower than G+C content (70.8%) of *A. giovannonii* OJF2^T. The difference in G+C between the strains indicate that these two are distinct species since a 3% difference in the G+C content was recommended for species delineation.

Genome sequences of strains JC669^T and *A. giovannonii* OJF2^T were aligned using PATRIC software to identify the multiple maximal matches and local collinear block (LCBs; www. patricbrc.org). The genome sequence of strain JC669^T was used as a reference against *A. giovannonii* OJF2^T. The alignments of the LCBs in both strains differ from each other significantly (Fig. 3.6.1.1). The alignment facilitates detection of homologous regions that are shuffled or inverted due to DNA rearrangement or recombination. The comparison of the genome map based on the protein sequence identity shows that majority of the proteins of strain JC669^T share 60-80% similarity with those of *A. giovannonii* OJF2^T (Fig. 3.6.1.2). Both the strains, JC669^T and *A. giovannonii* OJF2^T share 20-30% similarity with other members of Isosphaeraceae family (Fig. 3.6.1.2). These results suggest a clear-cut dissimilarity between the strains JC669^T and *A. giovannonii* OJF2^T and between the two strains and other taxa of the family Isosphaeraceae.

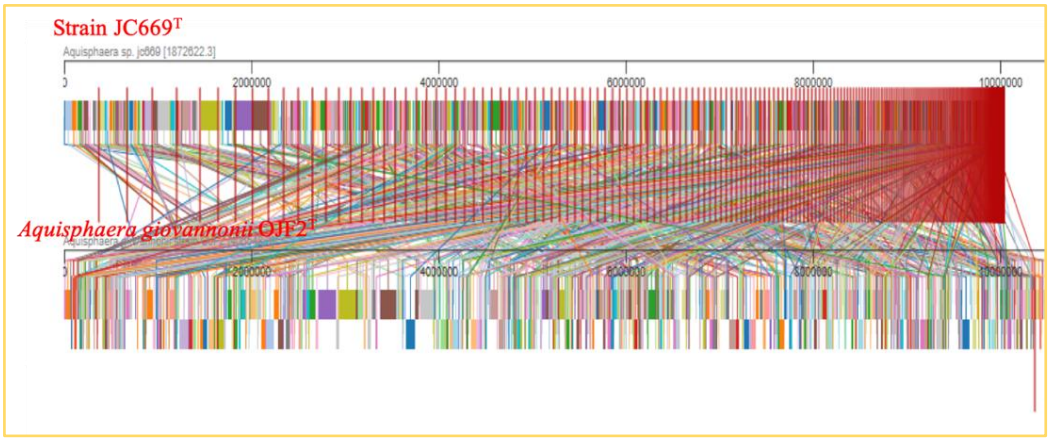

Fig. 3.6.1.1 Genome organization of strain JC669^T and *Aquisphaera giovannonii* OJF2^T. Genome of strain JC669^T was used as reference against which *A. giovannonii* OJF2^T is aligned and compared. LCBs placed under the bars represents reverse complement of the reference DNA sequence. Unmatched regions within LCBs suggests the presence of strain specific sequences.

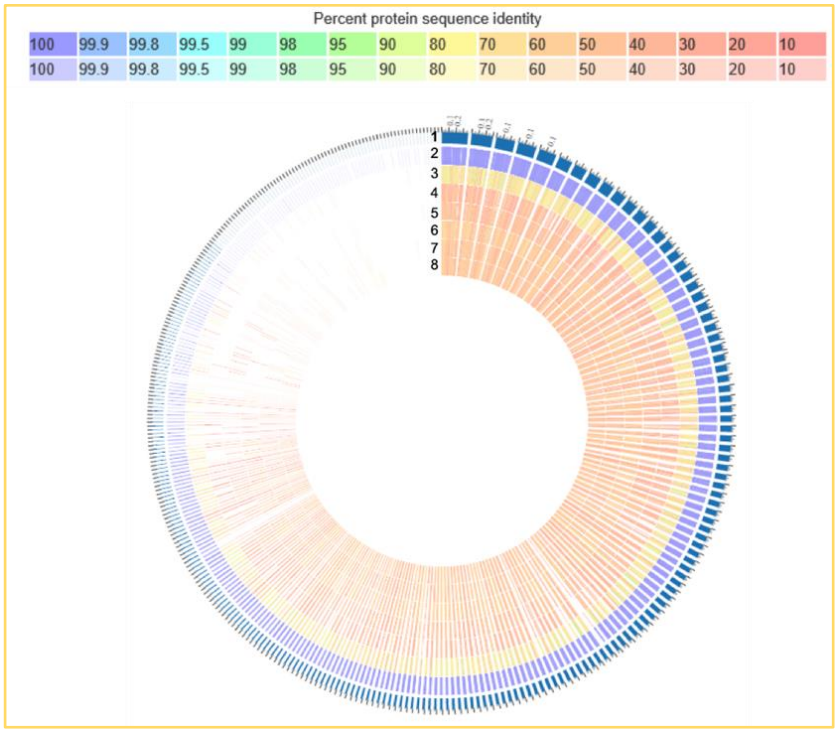

Fig. 3.6.1.2. Genome map based on protein sequence identity between genome of strain JC669^T, *A. giovannonii* OJF2^T, *Isosphaera pallida* ATCC 43644T, *Tautonia sociabilis*GM2012^T, *Paludisphaera borealis* PX4^T , *Singulisphaera acidiphila* DSM 18658^T, *Singulisphaera* sp. GP187. Genome of strain JC669 was used as reference. List of track from outside to inside- 1. Scale showing contigs length, 2. JC669^T 3. *Aquisphaera giovannonii* OJF2 4. *Isosphaera pallida* ATCC 43644^T 5. Tautonia sociabilis GM2012^T 6. *Paludisphaera borealis* PX4^T 7. *Singulisphaera acidiphila* DSM18658^T 8. "*Singulisphaera* sp." GP187.

3.6.1.3 BLAST Analysis and Phylogenetic inference

The 16S rRNA gene sequence of strain JC669^T extracted from the genome has sequence length of 1514nt and the BLAST search results are similar to amplicon 16S rRNA gene sequence having identity of 96.8% (Fig. 2) with sole member of the genus *Aquisphaera*; *Aquisphaera giovannonii*. OrthoANI value between JC669^T and *A. giovannonii* OJF2^T was 81.4%. The *d*DDH value between strains JC669^T and *A. giovannonii* OJF2^T was 24.3 %. The OrthoANI and *d*DDH values of strains JC669^T and *A. giovannonii* OJF2^T were far below than the recommended (Meier et al. 2014; Chun et al. 2018) cut off values (95-96% cut off for ANI and 70% cut off for *d*DDH) for species delineation and thus strain JC669^T represents a new species of the genus *Aquisphaera* (Fig. 2). POCP and AAI values between the strains JC669^T and *A. giovannonii* OJF2^T were 67.3% and 76.6%, respectively. A POCP threshold below 50% was proposed to determine new genera (Qin et al. 2014) and a value of 67.3% between two strains clearly indicates that they belong to the same genus. Further, AAI value of 76.6% between the strains fell close to the recommended cut-off of 80% used for the genus delineation (Rodriguez and Konstantinidis 2016) (Fig. 3.6.1.3). Thus, the strain JC669^T represents a novel species of the genus *Aquisphaera*. The 16S rRNA gene sequence based phylogenetic tree with combined bootstrap values obtained from ML, NJ, ME trees (Fig. 3.6.1.4) and 92 core genes based phylogenomic tree (Fig. 3.6.1.5) confirmed the clustering of strains JC669^T with the type species of the genus *A. giovannonii* OJF2^T.

3.6.1.4 *In-silico* metabolic characterization

CAZy annotation of genomes of the strains JC669^T and *A. giovannonii* OJF2^T shows that they contain more genes for glycosyl transferases, followed by glycoside hydrolases similar to distribution in all the species belonging to genus *Aquisphaera*. The analysis also shows that 80–90% of the enzyme families account to glycoside

hydrolases and glycosyl transferases (Fig. 3.6.1.6). However, the relationship between the presence of higher number of carbohydrate active enzymes and polysaccharide degradation needs further studies.

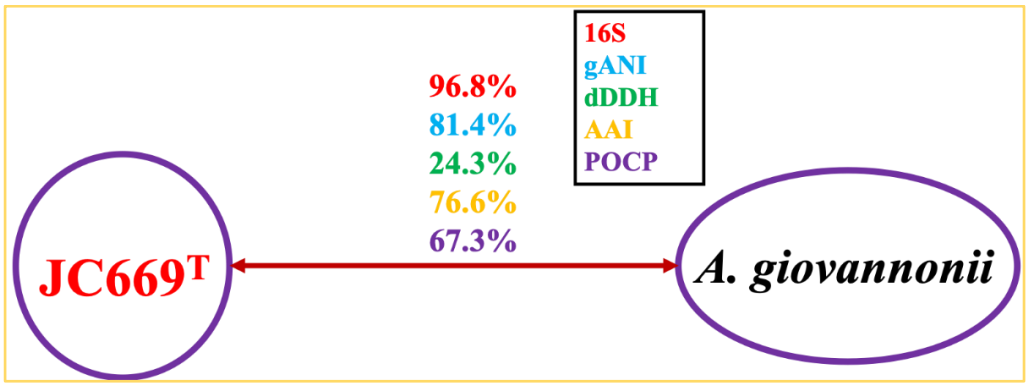

Fig. 3.6.1.3 Analysis of phylogenetic markers for delineation of the novel isolates JC669^T and *Aquisphaera giovannonii* OJF2^T; Methods used: 16S rRNA gene identity (16S), average amino acid identity (AAI), average nucleotide identity (ANI) and digital DNA-DNA Hybridization (*d*DDH).

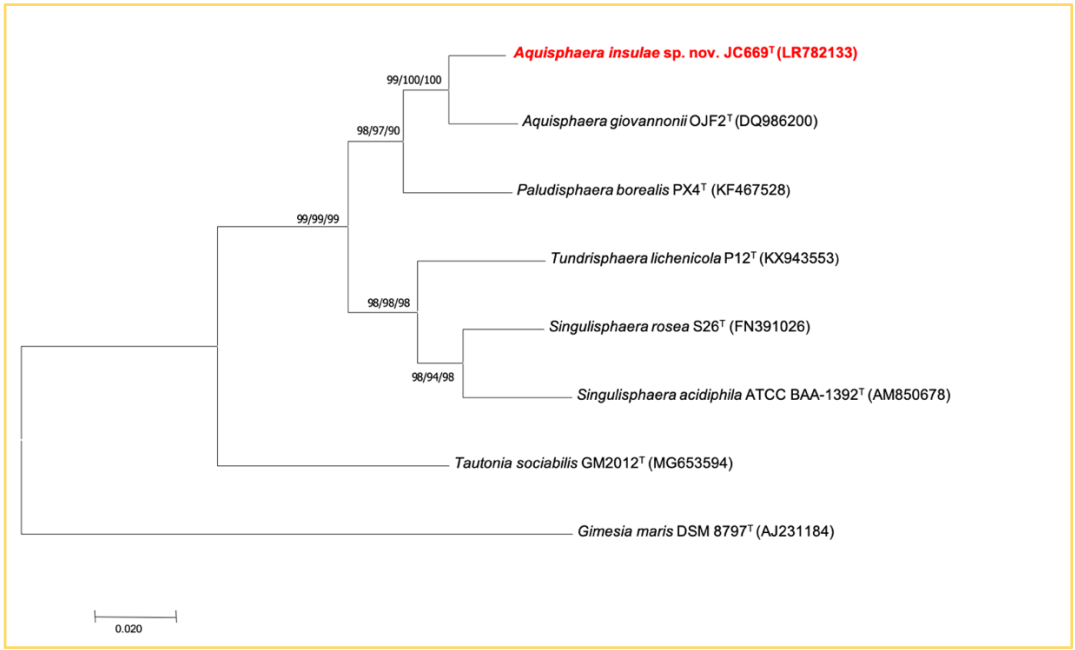

Fig. 3.6.1.4: Phylogenetic tree based on 16S rRNA gene sequences showing the phylogenetic relationship of strain JC669^T with the *A. giovannonii* OJF2^T and other closely related species. The tree was made with MEGA 7 software and *Gimesia maris* DSM 8797^T was used as out-group. The GenBank accession numbers for 16S rRNA gene sequences are shown in parentheses. Numbers at nodes indicate Bootstrap value of 1000 repetition correspond to NJ/ML/ME analysis. Bar,0.02 nucleotide substitution per position.

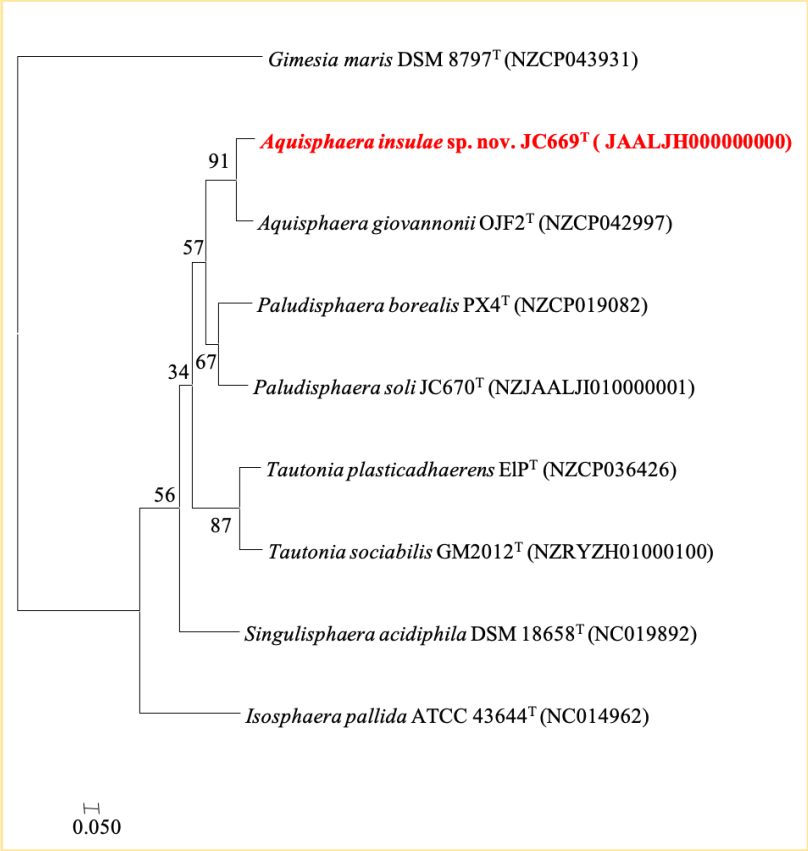

Fig. 3.6.1.5. RAxML based phylogenomics tree of strain JC669^T along with publicly available genome sequence of *Isosphaeraceae* families. The GenBank accession numbers for genome sequences are shown in parentheses. Bar,0.10 nucleotide substitution per position.

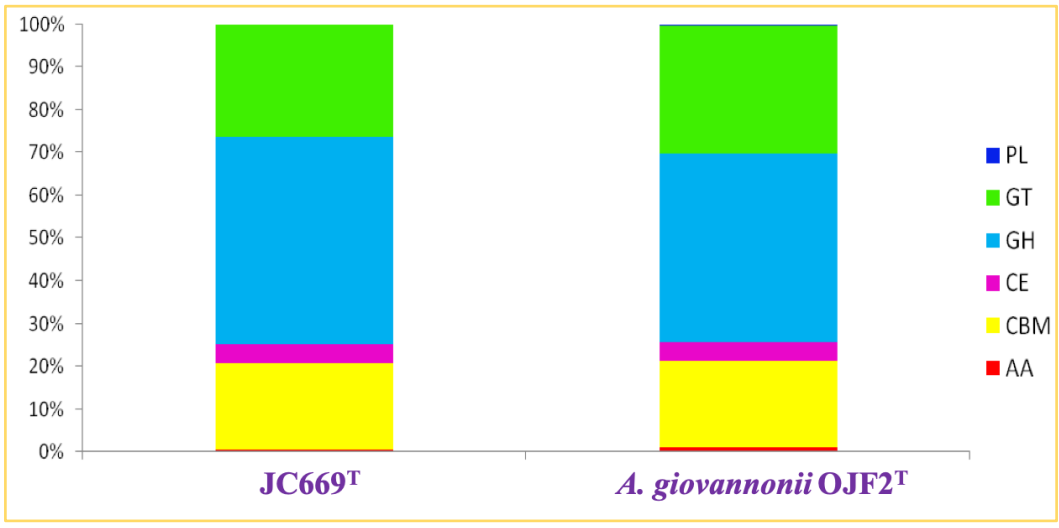

Fig. 3.6.1.6 Comparative analysis of CAZymes of strains JC669^T *and Aquisphaera giovannonii* OJF2^T. Abbreviations: AA, Auxiliary Activities (AAs); CBM, Carbohydrate-Binding Modules (CBMs); CE, Carbohydrate Esterases (CEs); GH,Glycoside Hydrolases (GHs); GT, GlycosylTransferases (GTs); PL, Polysaccharide Lyases (PLs)

In-silico metabolic characterization show that both strain JC669^T and *A. giovannonii* OJF2^T have 2-C-methyl-D-erythritol 4-phosphate/1-deoxy-D-xylulose 5-phosphate (MEP) pathway for the biosynthesis of five carbon isoprene units (isopentenyl pyrophosphate; IPP), which is eventually the precursor for the synthesis of carotenoids and quinones (Eisenreich et al. 2004; Zhao et al. 2013). In both the strains genes encoding for carotenoid biosynthetic enzymes like lycopene β-cyclase (5.5.1.19), β-carotene hydroxylase (1.14.13.129), zeaxanthin epoxidase (1.14.15.21) and neoxanthin synthase (5.3.99.9) are found. Hence, both the strains are putatively capable of forming neoxanthin from lycopene involving important intermediates like γ- carotene, β-carotene, zeaxanthin and violaxanthin (Fig. 3.6.1.7). Both strains JC669^T and *A. giovannonii* have the genes to putatively produce staurosporine (anti-cancerous compound) from L-tryptophan.

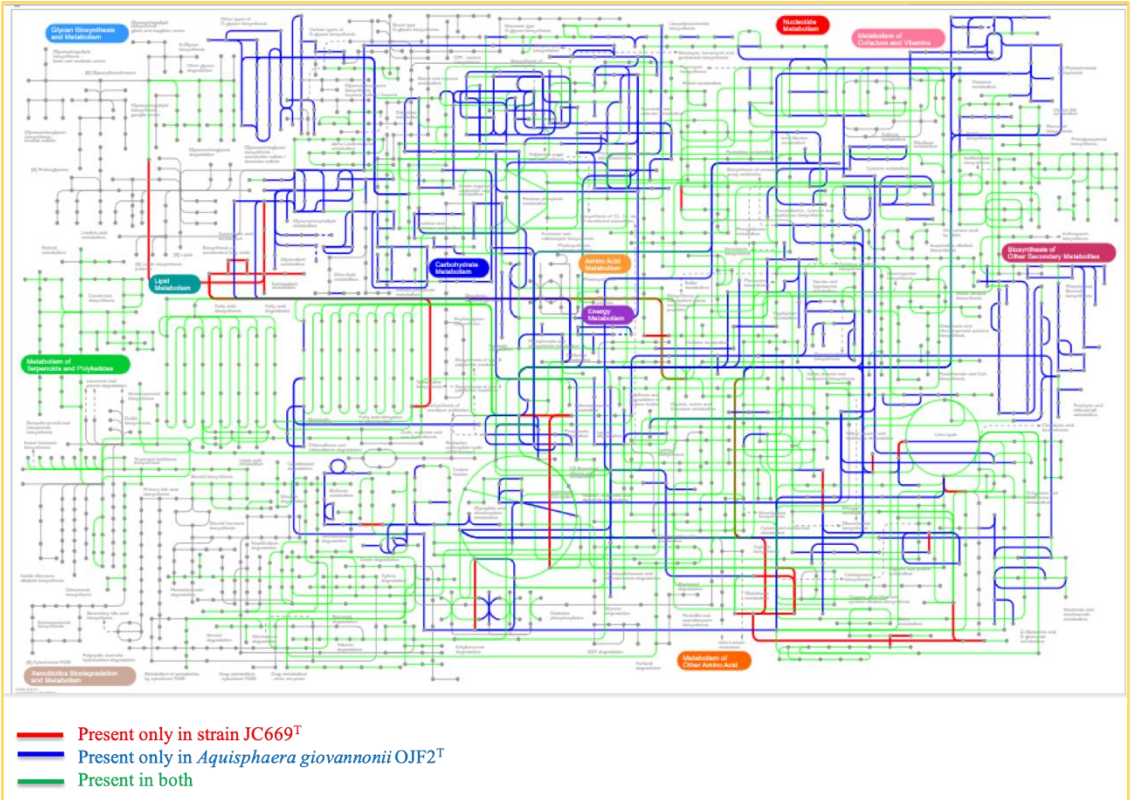

Fig. 3.6.1.7. Common and unique biochemical pathways between strain JC669^T and *A. giovannonii* OJF2 ^{T}

Due to the complex life cycle of planctomycetes, it is believed to produce bioactive secondary metabolites (Wiegand et al. 2020). Both the strains JC669^T and *A. giovannonii* have putative genetic clusters for producing secondary metabolites like bacteriocin, Type I Polyketide Synthase (T1PKS), Non-Ribosomal Peptide Synthetase clusters (NRPS), heterocyst-glycolipid synthase-like PKS (hgIE-KS), terpenes and indole. Putative genetic cluster of lassopeptide and lanthipeptide is exclusive for strain JC669^T and *A. giovannonii* OJF2^T respectively.

3.6.1.5 Morphological and physiological analyses

TEM image of the strain JC669^T show the presence of invagination of enlarge periplasm, cytoplasm, nucleoid region with fimbriae in daughter cell only and cell divide by budding (Fig. 3.6.1.8a). In SEM images, cells of strains JC669^T (Fig. .6.1.8b,c) and *A. giovannonii* DSM 22561^T (Fig. 3.6.1.8d,e) are spherical to oval shaped with crateriform structures distributed throughout their surfaces (Fig. 3.6.1.8b,c,d,e). Both strain JC669^T (Fig. 3.6.1.8b,c) and *A. giovannonii* DSM 22561^T (Fig. 3.6.1.8d,e) produce fruiting bodies which are distinct from each other. Free spore like bodies were also observed (Fig. 3.6.1.8c) which were also stained (Fig. 3.6.1.9a,b) with the spore specific fluorescent stain "sporotan" (Senthilnathan et al., 2020; Ali et al., 2020). To the best of our knowledge this is the first report of a member of the phylum Planctomycetes discovered to produce fruiting bodies and exospores and thus adds one more unique feature to the members of this phylum (Wiegand et al., 2020).

Genome mining of strain JC669^T and *A. giovannonii* was investigated for putative proteins responsible for the formation of fruiting bodies/spores. Amino acids sequences of strain JC669^T and *A. giovannonii* extracted from the NCBI and P-Blast was performed with the amino acids sequences of various important proteins involved in the formation of endospore as in *Firmicutes* represented by *Bacillus subtilis* and exospore as in

Actinobacteria represented by *Stretomyces coelicolor*. Blast analysis in the form of heat maps showed the presence of important proteins of sporulation in strain JC669^T and *A. giovannonii*, although their percentage of identity is low and mainly in the range of 20-40% (Fig. 3.6.1.9a,b). These findings are similar to the peptidoglycan synthesis and cell division proteins discovered among the members of Planctomycetes, where the percentage of identity was also low (Jeske et al., 2015; Wiegand et al., 2020). These finding further support the large evolutionary divergence of Planctomycetes where molecular pathways responsible for forming fruiting bodies is entirely different from those members of the phylum Firmicutes and Actinobacteria.

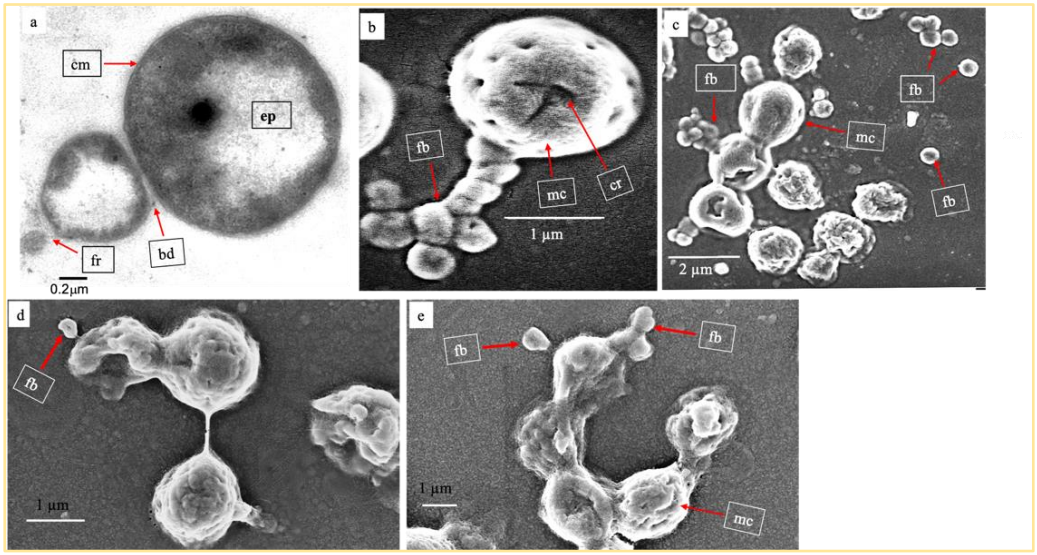

Fig. 3.6.1.8 Transmission (a) and scanning (b,c,d,e) electron micrographs of cell of Strains JC669^T and *A. giovannonii* OJF2^T. (a) Ultrathin section showing cell membrane (cm), cytoplasm (cy), enlarged periplasm (ep), nucleoid (nu), cell multiplication through budding (bd), fimbriae in daughter cell and crateriform like structure (cr) in the sytrain JC669^T. Bars, 0.2µm. (b) Isolated round cells of the strain JC669^T showing crateriform like structure (cr) and fruiting bodies (fb) attached to mother cells (mc). Bars, 1µm. (c) Group of free fruiting bodies (fb) detach from mother cells (mc) of the strain JC669^T. Bars, 2µm. (d,e) round cells of the *A. giovannonii* DSM 22561^T showing crateriform like structure (cr) and fruiting bodies (fb) attached to mother cells (mc). Bars, 1µm.

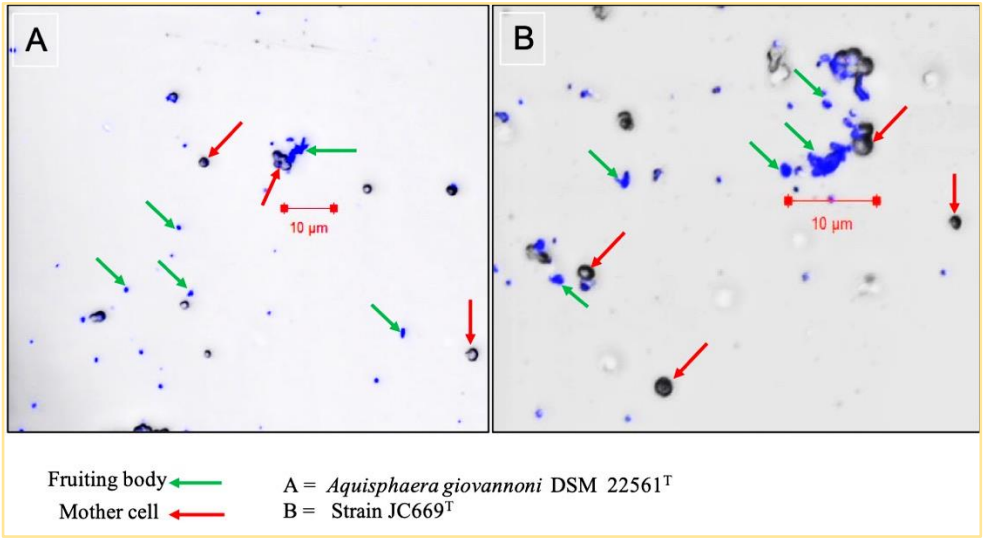

Fig. 3.6.1.9. LSCM images: Sporotan stained fruiting bodies and unstained mother cells of *Aquisphaera giovannoni* DSM 22561^T (A) and the strain JC669^T (B). Green arrows show fruiting bodies; Red arrows show mother cells.

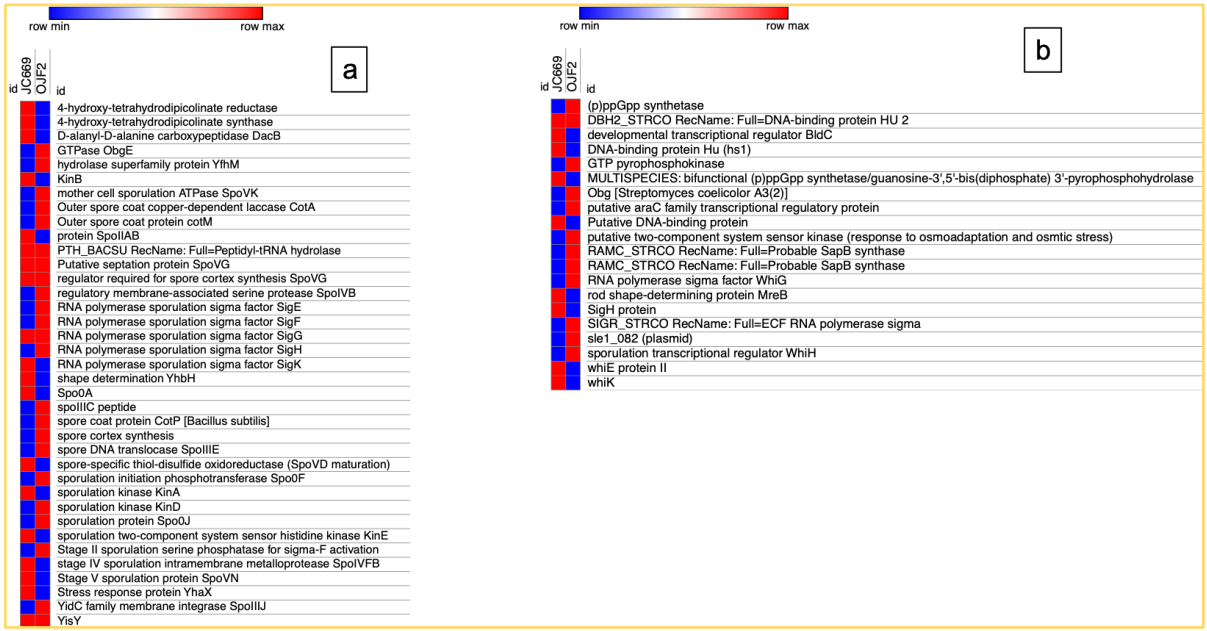

Fig. 3.6.1.10 Heat map representing the Percentage identity of some sporulating proteins in the strains JC669 and OJF2 with the *bacillus subtilis* (a) and *Streptomyces coelicolor* (b).

NaCl tolerance (0-7% w/v; final salt concentration in the media) for both the strain JC669^T and *A. giovannonii* OJF2^T was tested at 25 °C and pH 7. Strains JC669^T and *A. giovannonii* OJF2^T didn't grow in the presence of NaCl even at 0.5%. The optimum temperature (5, 10, 15, 20, 25, 30, 35, 40, 45 °C) required for cell growth was tested at pH

7. The optimum temperature for the cell growth of strain JC669^T was 22-25 °C and no cell growth occurred above 30 °C or below 10°C. The optimum temperature for the cell growth of strain *A. giovannonii* OJF2^T was 28-30 °C and no cell growth occurred above 40 °C or below 15°C pH tolerance (4.0, 5.0, 6.0, 7.0, 8.0, 9.0, 10.0) for cell growth of strain JC669^T was tested at 25 °C in buffered broth, as described earlier (Bondoso et al. 2015). The optimum pH for cell growth of both strain was pH 7.0 and cell growth was observed up to pH 9.0. Both Strain JC669^T and *A. giovannonii* OJF2^T were unable to reduce nitrate and Vitamin B_{12} was not obligate for their cell growth. Cell growth observations with different organic substrates/nitrogen sources of both strain JC669^T and *A. giovannonii* OJF2^T are given in species description and Table 3.6.1.2. Enzymatic activity for strain JC669^T was performed using API ZYM kit, which gave positive results for alkaline phosphatase, esterase (C4), esterase lipase (C8) and napthol-AS-B1-BD-phosphohydrolase and negative for acid phosphatase, lipase (C8), leucine arylamidase, valine arylamidase, cysteine arylamidase, α-chymotrypsin, α-galactosidase, β-galactosidase, β-glucuronidase, α-glucosidase, β-glucosidase, α-mannosidase, trypsin, N-acteyl-β-glucosaminidase and α-fucosidase. While strain *A. giovannonii* DSM 22561^T shows positive for alkaline phosphatase, esterase (C4), esterase lipase (C8), leucine arylamidase, valine arylamidase, cystine arylamidase, trypsin, α chymotrypsin, acid phosphatase, α glucosidase, β-glucosidase and α-fucosidase and negative for napthol-AS-B1-BD-phosphohydrolase, lipase (C14), α-galactosidase, β-galactosidase, β-glucuronidase, α-mannosidase and N-acetyl-β-glucosaminidase.

3.6.1.6 Chemotaxonomic characterization

3.6.1.6.1 FAME profile

The major fatty acid profile of the strain JC669^T was found to be in congruence with the type species of the genus with major proportions of $C_{18:1}\omega9c$, $C_{16:0}$ and $C_{18:0}$.

Anteiso-$C_{15:0}$, $C_{14:0}$, $C_{20:0,}$ $C_{17:1}\omega8c$, $C_{18:1}\omega7c$ summed in feature 3 are present in both strains. While, iso-$C_{19:0}$, iso-$C_{16:0}$, $C_{19:0}$, $C_{20:0,}$ $C_{17:1}$-cyclo, and $C_{20:1}\omega9c$ are exclusively present in the strain JC669^T However, $C_{15:0}$ and $C_{17:0}$ are exclusive for strain *A. giovannonii* DSM 22561^T (Table 3.6.1.1).

Table 3.6.1.1 Major **(>1%)** Cellular fatty acids composition (%) of 1. strain JC669^T and 2. *A. giovannonii* OJF2^T.

Fatty acids (%)	1	2
anteiso-$C_{15:0}$	1.2	4.7
iso-$C_{19:0}$	1.7	-
iso-$C_{16:0}$	1.5	-
$C_{14:0}$	2.2	2.5
$C_{15:0}$	-	3.2
$C_{16:0}$	**23.0**	**22.5**
$C_{17:0}$	-	5.9
$C_{18:0}$	8.8	11.1
$C_{19:0}$	1.3	-
$C_{20:0}$	3.0	-
$C_{17:1}\omega8c$	1.3	3.8
$C_{18:1}\omega9c$	**44.4**	**42.0**
$C_{18:1}\omega7c$	1.2	1.4
$C_{20:1}\omega9c$	1.0	-
$C_{17:1}$-cyclo	1.1	-
Summed in feature 3	2.0	1.4

3.6.1.6.2 Polar lipid profile

The polar lipid profile of strain JC669^T (Fig. 3.6.1.11a) was not in accordance with type species of *Aquisphaera*, *A. giovannonii* DSM 22561^T (both from this study (Fig. 3.6.1.11a, b) and from the literature [3] using *A. giovannonii* OJF2^T). However, the major polar lipids of *A. giovannonii* DSM 22561^T in this study (Fig. 3.6.1.11b) are similar to what was reported earlier except for the absence of unidentified phospholipid, unidentified glycolipids, diphosphatidylglycrol and presence of six unidentified lipids [3]. Polar lipids of strain JC669^T are phosphatidylcholine (PC), an unidentified amino lipid (AL),

unidentified choline lipid (UCL), and six unidentified lipids (UL1-6) (Fig. 3.6.1.11a). For strain *A. giovannonii* DSM 22561^T we identified phosphatidylcholine (PC), a phosphatidylglycerol (PG) and six unidentified lipids (Fig. 3.6.1.11b). Strain JC669^T differ from *A. giovannonii* DSM 22561^T in not having phosphatidylglycerol but additionally having an unidentified aminolipid and an unidentified choline lipid. MK6 is the predominant quinone of both strains.

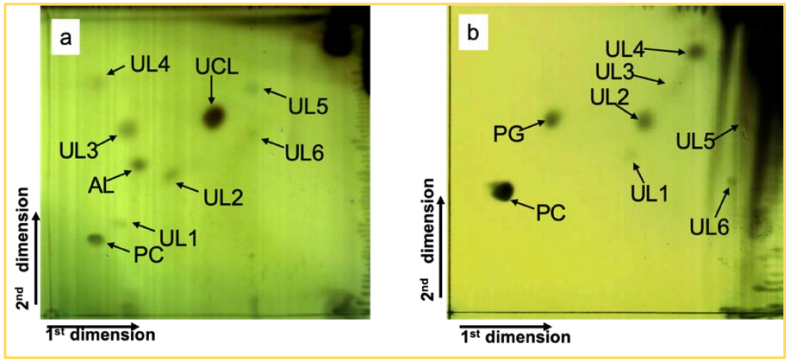

Fig. 3.6.1.11. Two dimensional chromatograms showing polar lipids of (a) strain JC669^T and (b) *A. giovannonii* DSM 22561^T. PC, Phosphatidylcholine; PG, phosphatidylglycerol; AL, unidentified amino lipid; UL1,2, 3,4,5,6 unidentified lipids; UCL, unidentified choline lipid.

3.6.1.6.3 Polyamine Profile

Both strains JC669^T and *A. giovannonii* DSM 22561^T have two polyamines; sym-homospermidine and putrescine, while *A. giovannonii* DSM 22561^T in addition has an unidentified polyamine (Fig. 3.6.1.12).

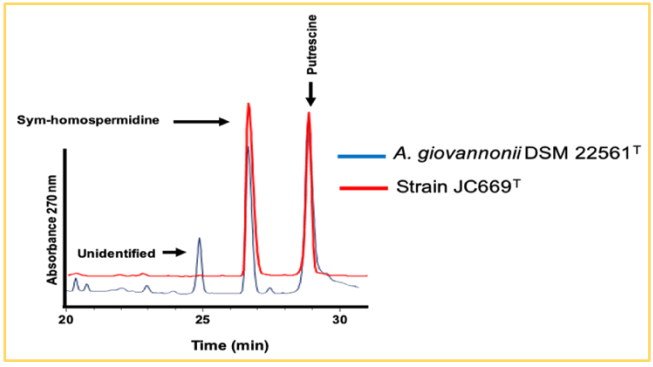

Fig. 3.6.1.12 HPLC chromatograms showing polyamines strain JC669^T and *A. giovannonii* DSM 22561^T

Table 3.6.1.2 Differential characteristics of (1) strain JC669^T and 2. *A. giovannonii* DSM 22561^T.

Characteristics	1	2
Cell shape	Spherical to oval	Spherical
Cell size (diameter µm)	1.8-2.2	1.6-2.0
Organic substrates used for growth		
D-xylose	+	-
Inositol	+	-
Na-succinate	+	-
Sorbitol	+	-
D-fructose	-	+
D-mannitol	-	+
Acetate	-	+
Pyruvate	-	+
Sorbitol	-	+
Nitrogen sources used for growth		
Na- nitrate	+	-
L-phenylalanine	+	-
L-serine	-	+
Aspartate	-	+
Cysteine	-	+
Serine	-	+
Vitamin B_{12} requirement.	-	+
Polar lipids		
PG	-	+
AL	+	-
UCL	+	-
Fatty acids	+	-
iso-$C_{19:0}$	+	-
iso-$C_{16:0}$	-	+
$C_{15:0}$	-	+
$C_{17:0}$	+	-
$C_{20:0}$	+	-
$C_{20:1}\omega 9c$	+	-
$C_{17:1}$-cyclo		
Genomic DNA G+C content (mol %)	68.5	70.8

Data from this study

Species: 1, strain JC669^T; 2, strain *A. giovannonii* OJF2^T.

Both strains have MK6 as the only quinone; both strains grow from pH 7-9 with optima at 7.0. Phosphatidylcholine and six unidentified lipids are common for both strains; major fatty acids are $C_{18:1}\omega 9c$, $C_{16:0}$ and $C_{18:0}$; grow well in the presence of glucose; does not require vitamin B_{12} for growth and can grow without N-acetylglucosamine; PG, phosphatidylglycerol; AL, unidentified amino lipid; UCL, unidentified choline lipids. +, substrate utilized; -, substrate not utilized.

Discussion

4. Discussion

Prior to this thesis studies, there were no reports from India on the diversity of Planctomycetes and their axenic cultures. To understand the diversity of Planctomycetes of India, extensive sampling was done not only in terms of diverse geographical habitats and the nature of samples collected (Annexure 1a,b,c,d,e). Majority of the samples collected were from the coastal regions of Gujarat, Tamil Nadu, and northern coastal areas of Kerala. Samples collected mainly include sponges, sea weeds and sediments, which were used for analysing bacterial communities by culture independent studies with particularly emphasis on the diversity of planctomycetes. While attempts were also made to isolate some of these members using culture dependent studies and describe new taxa, using polyphasic including phylogenomic taxonomic studies.

4.1 Culture independent studies of bacterial communities with special emphasis on taxa belonging to planctomycetes

4.1.1 Bacterial communities of sponges collected from the Little Rann of Kutch, India

Little Rann of Kutch has blooming diversity of sponges and during the survey for Anammox-Planctomycetes of Little Rann of Kutch, several puddles nurturing at least three different species of sponges were observed near Joghad Eco Park. These sponges belongs to the genus *Spongilla* and *Ciocalypta. Spongilla* spp. were collected from three puddles having at a depth of about 20 cm with continuous flow of surface water from different resources. While *Ciocalypta* spp. were collected from the salt marsh puddles on the road side at a distance of about 100 meters between the puddles.

Bacterial communities analysis based on metagenomes and culture-dependent studies revealed that most of the bacteria including Planctomycetes form epibacterial communities on the surfaces of aquatic phototrophic eukaryotes like marine algae and

sponges (Longford et al. 2007; Lage and Bondoso 2011). The bacterial diversity associated with two mini sponge genera, *Ciocalypta* and *Spongilla* (except *Spongilla lacustris*; Gernet et al. 2005) collected from the Little Rann of Kutch, Gujarat showed the association of forty two different bacterial phyla including Planctomycetes. The finding of overall bacterial communities is in the unity with the previous reports (Kaboré et al. 2020) where bacterial phyla like Actinobacteria, Proteobacteria, Bacteroidetes and Firmicutes are primarily dominant. Planctomycetes are well associated with these three sponges and are mainly dominated by taxa of the families Planctomycetaceae, Pirellulaceae, and Isosphaeraceae (Kallscheuer et al. 2020). Among these three sponges, distribution of taxa belonging to the family Phycisphaeraceae is exceptional and are mainly due to the uniqueness of host or environmental parameters (salinity, temperature, and pH) of the Little Rann of Kutch. Comparative bacterial communities analysis of these three sponges also showed that none of the OTUs are shared (Fig. 3.1.1.e). This indicates that environmental parameters like salinity, temperature and pH affect bacterial including Planctomycetal diversity and host specificity.

4.1.2 Bacterial communities of seventeen sponges samples collected from Tamil Nadu

The Gulf of Mannar is one of the important Biosphere Reserves of India (Nammalwar 2008). It consists of 21 islands spread over an area of 623 hectares (10, 500 km^2) and is one of the richest coastal regions in Asia, that contain over 4,000 marine species of flora and fauna (Nammalwar 2008). The Gulf of Mannar is the richest centres of sponge distribution in Indian subcontinent Dendy (1905). The study on the Poriferans (Sponges) of Gulf of Mannar is basically based on extensive collections made during last decade. During the survey for Planctomycetes associated to sponges, approximately seventy dead sponges (Annexure 1c,e) were collected on shore of Tamil Nadu, ranging mainly from Mandapam (Rameswaram) to Tuticorin. Most of these sponges belongs several taxa ranging from species to family. Bacterial communities analysis of sponges from Tamil

Nadu and Gulf of Mannar (east coast of India) showed overall bacterial communities' association. In addition to holistic bacterial communities, these seventeen sponges (Fig. 3.1.2.a) also targeted for the Planctomycetes diversity. Seventeen sponges (Fig. 3.1.2.a) showed the association of forty-two different bacterial phyla dominated by Proteobacteria, Bacteroidetes and firmicutes (Fig. 3.1.2.c) and is in the congruence of bacterial communities of two sponges *Cinachyra cavernosa* and *Haliclona pigmentifera* collected from coral reef ecosystems of the Gulf of Mannar **(**Jasmin et al. 2015**)**. Among these seventeen sponges, the distribution of Planctomycetes are mainly dominated by taxa of the families *Planctomycetaceae, Pirellulaceae, Isosphaeraceae, Gemmataceae* and also by the unclassified taxa of the families of Planctomycetes.

4.1.3 Bacterial communities of fourteen algal samples collected from Tamil Nadu

Macroscopic marine algae, popularly known as seaweeds, constitute one of the important living resources of the ocean. They attach to the bottom of the sea on solid substrate such as rocks, dead corals, pebbles, sponges, shells and plants (Kaboré et al. 2020). The seaweed flora of Tamil Nadu is highly diversified and comprises mostly of tropical species (Sahayaraj et al. 2014). During the survey for Planctomycetes associated to macroalgae, more than hundred macroalgae (Annexure 1c,e) were collected on shore of Tamil Nadu, mostly from Kanyakumari to Ramanathapuram.

Bacterial communities analysis of algal samples showed overall bacteria's distribution, including Planctomycetes on their surfaces as an epibacterial communities (Kaboré et al. 2020). The biofilms on some algal surfaces (*Posidonia oceanica)* are dominated mainly by the members of the phylum Planctomycetes (up to 85%) (Kohn et al. 2020). Bacterial communities analysis of algal samples from Tamil Nadu and Gulf of Mannar (east coast of India) showed the association of overall bacterial communities and is dominated by Proteobacteria, Firmicutes, Bacteroidetes. In addition to holistic bacterial

communities, these fourteen algal samples (Fig. 3.1.3.a) also targeted the Planctomycetes diversity. The fourteen algal samples (Fig. 3.1.3.c) showed the distribution of total forty-three different bacterial phyla and Proteobacteria, Firmicutes, Bacteroidetes and Planctomycetes forms core groups. In addition to this, thirteen to sixteen bacterial phyla are '*Candidatus*'. The Planctomycetes distribution is dominated by taxa of the families Planctomycetaceae, Pirellulaceae, Gemmataceae and unclassified taxa of the families of Planctomycetes. (Fig. 3.1.3.d,e)

4.1.4 Bacterial communities of sediment samples collected from Satapada region of Chilika Lagoon

Chilika lake is the second largest brackish lagoon in the world and largest in Asia. Stapada is part of the outer channel sector and is main mouth of the Chilika Lagoon where several rivers meet the Bay of Bengal. In monsoon season, excess fresh water input from the rivers discharge into the Bay of Bengal. During the summer season, water level in rivers is low and sea water flow back into the Lagoon and make lagoon more saline. Hence, unique temporal salinity gradient that occurs mostly in Satpada region, make Satpada hotspot in term of bacterial diversity as compare to other regions of the Chilika Lagoon.

A recent study on spatial and temporal distribution of bacterial communities inhabiting Chilika lagoon sediment showed that they are heterogeneous and are mostly unexplored, and dominated by several bacterial phyla including planctomycetes (Pramanik et al. 2015; Raina et al. 2019). Bacterial communities analysis of Satapada region of the Chilika lagoon showed a well distribution of sixteen bacterial phyla in which Proteobacteria, Firmicutes, Bacteroidetes and Planctomycetes are dominant (Fig. 3.1.4.a,b). The temporal based bacterial communities analysis revealed rich bacterial diversity, including Planctomycetes during the winter season (December) as compared to summer (May) and monsoon (August) seasons (Fig. 3.1.4.a,b). Bacterial communities analysis provided in-depth insight of the Planctomycetal diversity of the Chilika lagoon (

Satpada region only). Planctomycetes' distribution in Chilika lagoon covers total valid taxa of the families like Planctomycetaceae, Pirellulaceae, Isosphaeraceae, Phycisphaeraceae and Gemmataceae but also the unclassified taxa of the families of Planctomycetes.

4.1.5 Comparative analysis of bacterial communities of samples collected from different habitats of India

Bacterial communities analysis carried out for this study revealed that India harbour rich bacterial diversity including Planctomycetes. Bacterial community studies of all the samples showed a high abundance of up to forty five different bacterial phyla dominated mainly by Proteobacteria, Firmicutes and Bacteroidetes. Bacterial communities analysis of several samples revealed the presence of unclassified taxa. Among all the samples, sediment samples of Satpada region harbour maximum Planctomycetal diversity followed by algae and sponges of Tamil Nadu. The distribution of Planctomycetes covers entire valid taxa of the families like Planctomycetaceae, Pirellulaceae, isosphaeraceae and Gemmataceae and covers several unclassified taxa of the families of Planctomycetes. The maximum unclassified taxa of the families of Planctomycetes are observed in the Chilika lagoon. Distribution of the family Phycisphaeraceae is limited to Little Rann of Kutch's sponges, which could be either because of host or due to the environmental conditions. All sponges (Fig. 3.1.2.a) and algal (Fig. 3.1.3.a) specimen of Tamil Nadu which were residing in similar environmental parameters (Temperature, salinity and pH) harbours rich bacterial diversity and their comparative bacterial analysis showed that they shared maximum OTUs (about 85%) (Fig. 4.1.a). So, overall bacterial communities associated to sponges and algal specimen depends largely on variations in their environmental parameters. Interestingly, only 1% - 3% of the Planctomycetal OTUs were shared among them (Fig. 4.1.b) and hence, distribution of Planctomycetes are host specific. This showed that algae and sponges probably provide a unique niche for the members of Planctomycetes.

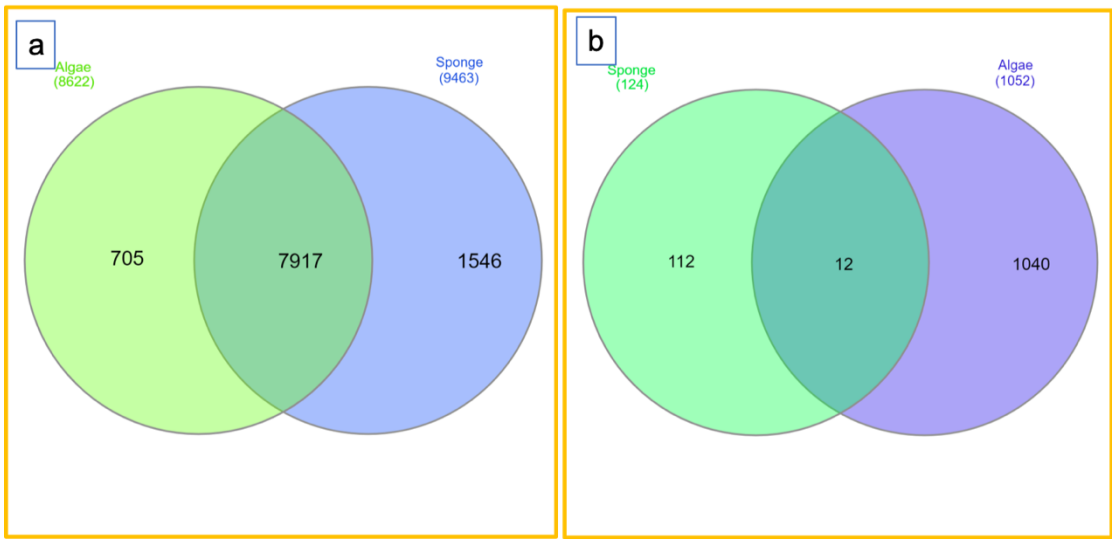

Fig. 4.1 Venn diagram representing diversity of core and shared bacterial (a) and Planctomycetal (b) OTUs among all algal and sponges samples

4.2 The three step enrichment protocol helps in successful cultivation of Planctomycetes

Bacterial communities analysis intimated vast Planctomycetal diversity across India, either associated with hosting or in free form as in Chilika Lagoon. These Planctomycetes' active role in their hosts cannot be grasp unless these members are culture as an axenic strain. In past, various strategies were developed to culture fastidious Planctomycetes by outnumbering other fast-growing bacteria. Few studies revealed the enrichments before cultivation quite useful in the isolation of fastidious members like Planctomycetes. The three steps enrichment strategy applied in this study is a multistep enrichment protocol where fastidious Planctomycetes members are probably outnumbered other fast-growing bacteria at every step. Enrichment of Planctomycetes members are easily monitored through FISH analysis before plating on the solid agar media for their isolation. Hence, FISH analysis narrowed down the enrichment samples size to processed further to isolate the axenic cultures of Planctomycetes.

Onsite inoculation strategy adopted in this protocol prevents the loss of Planctomycetes members and assist in its enrichment during the period of sampling and

transport. Further, the three-step enrichments protocol helps to isolate members of Planctomycetes from the samples of differential geographical locations that include sediments, algae, and sponges (Annexure 1a,b,c,d,e). The three-step enrichment protocol is quite effective in isolating Planctomycetes from the sediment samples as none of the marines and freshwater sediments yielded *Planctomycetes* directly by plating on their respective solid agar media (Table. 2.2,3,4). Few strains of Planctomycetes were isolated from marine algal and sponges specimens, bypassing the three-step enrichment process. Hence, three steps enrichment protocol probably helped us in isolating a large number of Planctomycetes from different habitats of India.

4.3 Proposal and description of new taxa of Planctomycetes

FISH analysis (Fig. 3.2.2,3) showed the enrichment of Planctomycetes in about 35% of the samples **(**Annexure. 1a,b,c,d,e) inoculated for the three steps enrichment. After the enrichment, 53 axenic strains of Planctomycetes were isolated and only 36 strains remained viable after subsequent passaging (Table. 3.3.1). Further, 14 strains of Planctomycetes were processed for the phylo-taxogenomic studies.

4.3.1.1 Proposal of a new genus to accommodate strains JC635^T and JC645^T

The family *Pirellulaceae* presently contains the genera (https://lpsn.dsmz.de/family/pirellulaceae); *Rhodopirellula*, *Pirellula*, *Rubripirellula*, *Roseimaritima*, *Mariniblastus*, *Novopirellula*, "*Stieleria*", *Blastopirellula*, *"Bremerella"*, *"Crateriforma"*, *"Aureliella"*, *"Lignipirellula"* and "*Rosistilla*" (Bondoso et al. 2014b; Yoon et al. 2014; Bondoso et al. 2015; Kallscheuer et al. 2019; Rensink et al. 2019; Dedysh et al. 2020; Wiegand et al. 2020; Kallscheuer et al. 2020; Peeters et al. 2020b; Waqqas et al. 2020). Two pink colored, oxidase-catalase positive, salt and alkali tolerant planctomycetal strains (JC635^T and JC645^T) with pear to spherical shaped, Gram-stain-negative, motile cells were isolated from Chilika lagoon, India. Both the strains share highest 16S rRNA gene sequence identity with members of the genus *Rhodopirellula* (<94%) and *Roseimaritima* (<94%) of the family *Pirellulaceae*. The 16S rRNA sequence identity between the strains JC635^T and JC645^T is 96.1%. Based on phylogenetic, genomic (ANI, AAI, POCP, *d*DDH), chemotaxonomic, physiological and biochemical characteristics, we conclude that both strains belong to a novel genus *Roseiconus* gen. nov. and constitute two novel species for which we propose the names *Roseiconus nitratireducens* sp. nov. JC645^T and *Roseiconus lacunae* sp. nov. JC635^T (Table 3.4.1.5).

4.3.1.2 Description of *Roseiconus* gen. nov.

Roseiconus (Ro.se.i.co'nus. L. adj. *roseus*, pink, rosy; L. masc. n. *conus*, cone; N.L. masc. n. *Roseiconus*, a pink cone)

Cells are spherical or cone to pear shaped and Gram stain-negative. Crateriform structures with fimbriae are common. Daughter cells may be motile with lophotrichous flagella. Cell division is by budding. Mesophilic, heterotrophic and facultatively anaerobic. Major fatty acids are $C_{18:1}\omega9c$ and $C_{16:0}$. Phosphatidylethanolamine and

phosphatidylcholine are the major polar lipids. Cadaverine and putrescine are the major polyamines. In addition, some strains can also have 1,2-diaminopropane and spermidine. MK6 is the only respiratory quinone. The genomic DNA G+C content is 55.1-60.0 mol%. The type species is *Roseiconus nitratireducens*. This genus is a member of the family *Pirellulaceae* (Table 3.4.1.5).

4.3.1.3 Description of *Roseiconus nitratireducens* sp. nov.

Roseiconus nitratireducens (ni.tra.ti.re. du'cens. N.L. n. *nitras, -tis*, nitrate; L. part. adj. *reducens*, reducing; N.L. adj. *nitratireducens*, nitrate-reducing)

Colour of chemotrophically grown culture is pink. Motility could not be demonstrated. NaCl is obligate for growth and can tolerates up to 7% (w/v) NaCl. Optimum pH and temperature for growth are 8.0 (range 7.0-9.0) and 30ºC (range 10-35 °C), respectively. D-glucose, fructose, mannose, maltose, sucrose, starch, D-xylose, rhamnose, pyruvate and inulin are good carbon sources for supporting growth. Ammonium sulphate, peptone, L-serine, DL-threonine, L-leucine, DL-alanine, cysteine, L-glutamine, L-proline and urea can be used as nitrogen sources for growth. Major fatty acids are $C_{18:1}\omega9c$ and $C_{16:0}$. Minor fatty acids include $C_{10:0}$3-OH, $C_{12:0}$, $C_{11:0}$ 3-OH, $C_{14:0}$, anteiso-$C_{15:0}$, $C_{16:1}\omega7c/C_{16:1}\omega6c$, $C_{17:0}$, $C_{17:1}\omega8c$, anteiso-$C_{17:0}$,$C_{18:0}$, $C_{18:1}\omega7c/C_{18:1}\omega6c$, $C_{15:0}$2-OH, $C_{19:0}$ and $C_{20:1}\omega9c$ and $C_{18:3}\omega6,9,12c$. Cadaverine, putrescine and an unidentified polyamine (UN1) are the polyamines. Genomic DNA G+C content is 60 mol% (Table 3.4.1.6)

The type strain JC645^T (=KCTC 72174^T=NBRC 113879^T) is isolated from the sediment of the Chilika lagoon, India. The GenBank accession number for the 16S rRNA gene sequence of *Roseiconus nitratireducens* JC645^{T}is LR132069 and the draft genome has been deposited in GenBank under the accession number VWOX00000000. The version described in this study is version VWOX01000000.1.

4.3.1.4 Description of *Roseiconus lacunae* sp. nov.

Roseiconus lacunae (la.cu'nae. L. gen. n. *lacunae*, of a lagoon)

Colour of chemotrophically grown culture is light pink. Cells are motile with lophotrichous flagella. NaCl is obligate for growth and tolerates up to 5% (w/v) with optimum growth at 3 %. Optimum pH and temperature for growth are 8.0 (range 6.0-9.0) and 30 ºC (range 10-35 °C), respectively. Growth factors are not required for growth. D-glucose, fructose, mannose, maltose, sucrose, starch, D-xylose, lactose, D-galactose and rhamnose are good carbon sources/electron donors for supporting its growth. Ammonium sulphate, peptone, L-serine, DL-threonine, L-leucine and DL-alanine, L-isoleucine, L-phenylalanine, L-glutamic acid and L- aspartic acid are utilized as nitrogen sources for its growth. Major fatty acid are $C_{18:1}\omega9c$, anteiso-$C_{13:0}$ and $C_{16:0}$. Minor fatty acids include; $C_{10:0}$3-OH, $C_{12:0}$, $C_{11:0}$3-OH, $C_{14:0}$, anteiso-$C_{15:0}$, $C_{16:1}\omega7c$/$C_{16:1}\omega6c$, $C_{17:0,}$ $C_{17:1}\omega8c$, anteiso-$C_{17:0}$,$C_{18:0}$, $C_{18:1}\omega7c$/ $C_{18:1}\omega6c$, anteiso-$C_{12:0}$, $C_{16:0}$ 3-OH, anteiso-$C_{17:1}$ A, anteiso-$C_{16:0}$, and $C_{18:3}\omega6,9,12c$. Polyamines are 1,2-Diaminopropane, cadaverine, spermidine, putrescine, and two unidentified polyamines. Polar lipids are phosphatidylethanolamine (PE), phosphatidylcholine (PC), unidentified amino lipids (AL 1), and one unidentified lipid (L1). Genomic DNA G+C content is 55.1 mol% (Table 3.4.1.6).

The type strain JC635^T (=KCTC 72164^T=NBRC 113875^T) was isolated from Chilika lagoon, India. The GenBank accession number for the 16S rRNA gene sequence of *Roseiconus lacunae* JC635^T is LR132029 and the draft genome has been deposited in GenBank under the accession number VSZO00000000. The version described in this study is version VSZO01000000.1.

4.3.2.1 Proposal of a new species to accommodate strain JC646^T

In 1976, Bauld and Staley (Bauld and Staley, 1976) reported a marine, stalked, and budding bacterium as *Planctomyces maris*. Further, in 2014, Scheuner and co-workers (Scheuner et al. 2014), based on more chemotaxonomic and phylogenomic analysis, reclassified the genus *Planctomyces* and emended the description of the family *Planctomycetaceae.* They proposed genus *Gimesia* under which *Gimesia maris* is the only species. The genus *Gimesia* comes under the order *Planctomycetes* and the family *Planctomycetaceae* is having characteristic features of reproduction by budding. The strain JC646^T resembles the type strain of its phylogenetically closest neighbour regarding having white colonies, major polar lipids and fatty acids. However, strain JC646^T has about 5% more in the G+C mol% compared to *G. maris* DSM 8797^T.

Based on phylogenetic, genomic (ANI, AAI, POCP, *d*DDH), chemotaxonomic, physiological and biochemical characteristics, we conclude that strain JC646^T into a new species of the genus *Gimesia* for which we propose the name *Gimesia chilikensis* sp. nov.

4.3.2.2 Description of *Gimesia chilikensis sp. nov*

(chi.li.ken′sis. N.L. fem. adj. *chilikensis* pertaining to Chilika, referring to the isolation of the type strain from Chilika lagoon, Odisha, India).

Colonies are white-colored. Cells are stained Gram-negative, oval to pear-shaped (1.2-1.6x0.7-1.0 μm), non-motile and multiply by polar budding. Stalks and flagellated cells are not observed. NaCl tolerance up to 7% (optimum 3%). Obligate aerobe and mesophilic. Temperature optimum at 25ºC (range 20-30°C).Vitamin B_{12} is not obligate requirement for the growth. Utilizes α-D-glucose, fumarate, lactose, D-galactose, fructose, mannose, sucrose, maltose and D-xylose. Ascorbate, acetate, starch, pyruvate, mannitol, propionate, inositol, malate, inulin, rhamnose, succinate, sorbitol, benzoate and citrate do

not support growth. L-isoleucine, Peptone, L-serine, L-glutamic acid, L-aspartic acid, L-lysine, DL-threonine and L-glycine are good nitrogen sources for growth. While L-tyrosine, cysteine, nitrate, D-valine, L-phenylalanine, DL-ornithine, L-methionine, L-tryptophan, L-glutamine, L-proline, L-arginine, L-histidine, urea L-leucine, L-glycine do not support growth as nitrogen source. API ZYM kit analysis gives positive results for the enzymes esterase, alkaline phosphatase, esterase lipase and acid phosphatase and negative for lipase, leucine arylamidase, cysteine arylamidase, valine arylamidase, α-chymotrypsin, α-galactosidase, β-galactosidase, β-glucuronidase, α-glucosidase, β-glucosidase, trypsin, α-mannosidase and naphthol-AS-BI-phosphohydrolase and α-fucosidase. Nitrate is not reduced. Major fatty acids are $C_{16:0}$ and $C_{16:1}\omega7c/C_{16:1}\omega6c$. MK6 is the major respiratory quinone. Phosphatidylcholine, Phosphatidyl-dimethylethanolamine, an unidentified phospholipid, an unidentified amino lipid and two unidentified lipids make the polar lipids composition. Sym-homospermidine and putrescine are the polyamines. Genomic DNA G+C content of the type strain is 53.20 mol% **(**Table. 3.4.2.5**.)**.

The type strain JC646^T (=KCTC 72175^T =NBRC 113881^T) was isolated from a sediment sample of Chilika lagoon, India. The 16S rRNA gene sequence and the whole genome sequence of *Gimesia chilikensis* JC646^T are deposited to GenBank under the accession number is LR132072 GenBank accession number is VTSR00000000.

4.3.2.3 Proposal for amending the genus description of *Gimesia.*

The genus *Gimesia* is under-studied with only one species (G. maris) described. The original description of this genus is based on the morphological features alone (Bauld and Staley, 1976). It was amended after the analysis of chemotaxonomic data (Scheuner et al. 2014). *G. chilikensis* represents the second species in this genus. We propose to broaden the genus characters of *Gimesia* through emending the genus description.

4.3.2.4 Emended description of the genus *Gimesia.*

Morphological, biochemical, chemotaxonomic characteristics are as previous description (Bauld and Staley 1976; Scheuner et al. 2014), except for presence of stalk in some strains. The genomic G+C content varies from 50.5 to 53.2 mol%. Putrescine and sym-homospermidine are the polyamines. Presence of phosphatidylglycerol and phosphatidyl-monomethylethanolamine is variable. Some strains also contain unidentified aminolipids and unidentified lipids.

4.3.3.1 Proposal of a new species to accommodate strain JC651^T

The genus *Roseimaritima* of phylum Planctomycetes was described by Bondoso and co-workers (Bondoso et al. 2015) to put up a planctomycetes of the family *Pirellulaceae* isolated from the biofilm of marine macroalga *Ulva* sp., collected from the Northern coast of Portugal. The strain JC651^T shows similarity with *R. ulvae* DSM 25454^T concerning cell structure, cell arrangement, major polar lipids, and fatty acids. However, strain JC651^T differs from *R. ulvae* DSM 25454^T in nitrate reduction, absence of vitamin B12 requirement for growth, some of the enzymes' activity, and utilization of some of the nitrogen source for growth (Table 3.4.3.2). Based on phylogenetic, genomic (ANI, AAI, *d*DDH), chemotaxonomic, physiological and biochemical characteristics, we conclude that strain describe the strain JC651^T into a novel species of the genus *Roseimaritima* for which we propose the name *Roseimaritima sediminicola* sp. nov.

4.3.3.2 Description of *Roseimaritima sediminicola* sp. nov

(se.di.mi .ni'co.la. L. neut. n. *sedimen* sediment; L. suff. –*cola* (from L. masc. or fem. n. *incola*) inhabitant, dweller; N.L. fem. n. *sediminicola* dweller of sediments)

Colonies are pale pink. Cells are strictly aerobic, Cells are stain Gram-negative, pear-shaped to spherical, form rosettes of 3-30 cells, and multiply by budding. Motility could not be observed. NaCl is required for growth with optimum at 4% (range 1- 5% (w/v)). Optimum pH and temperature for the growth are 7.5 (range 6.5-9.0) and 25 ºC (range 15-40ºC), respectively. Vitamin B12 is not obligate for growth; however, growth yields are increased in its presence. Utilizes starch, α-D-glucose, lactose, mannitol, sucrose, D-galactose, maltose, D-xylose, rhamnose as the carbon organic sources for the growth. At the same time, ascorbate, acetate, fumarate, pyruvate, propionate, inositol, fructose, mannose, malic acid, sorbitol, succinate, citrate, inulin and benzoic acid do not support

growth. Ammonium sulfate, L-glutamic acid, L-phenylalanine, L-lysine, L-glutamine, proline are utilized as nitrogen sources for the growth. Peptone, L-tyrosin, L-casamino acid, cysteine, nitrate, D-valine, L-isolucine, DL-ornithine, L-methionine, L- aspartic acid, L-tryptophan, DL-threonine, L-arginine, L-histidine, L-leucine, L-glycine, DL-alanine and urea do not assist the growth as nitrogen sources. API ZYM shows positive activities for the enzymes esterase lipase (C8), leucine arylamidase, valine arylamidase, acid phosphatase, alkaline phosphatase, esterase (C4), naphthol-AS-BI-phosphohydrolase. Negative for lipase (C14), cysteine arylamidase, β-glucuronidase, trypsin, α-chymotrypsin, α-galactosidase, β-galactosidase, N-acetyl- β-glucosaminidase, α-glucosidase, β-glucosidase, α-mannosidase and α-fucosidase. The major fatty acids are C18:1ω9c and C16:0. MK6 is the sole respiratory quinone. Diphosphatidylglycerol, an unidentified phospholipid, phosphatidylglycerol and phosphatidylcholine are the constituents of polar lipids. Genomic DNA G+C content of the type strain is 62.4 mol% (Table 3.4.3.2.).

The type strain JC651^{T} (=KCTC 72178^{T} =NBRC 113926^{T}) was isolated from a sediment sample of Chilika lagoon, India. The 16S rRNA gene sequence and the whole genome sequence (6.2 Mb) of *Roseimaritima sediminicola* JC651^{T} are deposited to GenBank under the accession number is LR13389 and WIAD000000000, respectively. The version described in this study is WIAD01000000.

4.3.4.1 Proposal of a new species to accommodate strains JC650^T and JC657^T

Till date the family *Isosphaeraceae* is constituted by 6 genera (*Paludisphaera*, *Tundrisphaera*, *Isosphaera*, *Aquisphaera*, *Singulisphaera* and *Tautonia*) (Bondoso et al. 2011; Giovannoni et al. 1987; Kulichevskaya et al. 2008, 2012, 2016, 2017; Jogler et al. 2020; Kovaleva et al. 2019) which are generally monospecies except for two genera; *Singulisphaera* and *Tautonia* having two species (Jogler et al. 2020; Kovaleva et al. 2019). The family *Isosphaeraceae* is represented by stalk-free planctomycetes with spherical to oval cells divided by polar budding. The members are known to colonize various habitats like peat moss, hot springs and aquatic sediments (Wiegand et al. 2020). The genus *Tautonia* was described under the family *Isosophaeraceae* by Kovaleva and co-workers (Kovaleva et al. 2019) is isolated from microbial mat growing along the thermal water stream emanating from the wall of TauTona gold mine tunnel in South Africa. *Tautonia sociabilis* GM2012^T is a thermotolerant, non-motile, spherical-shaped, capable of budding, aerobic chemoorganoheterotroph and prefer to grow on simple sugars and polysaccharides. The major fatty acids are C18:1ω9c, C16:0, and C18:0 (Kovaleva et al. 2019). Recently, one more species was added to the genus *Tautonia* as *"Tautonia plasticadhaerens"* EIP^T which was isolated from a marine alga gathered from a hydrothermal area. The strains JC650^T and JC657^T have clear phylo-genomic differences with *T. sociabilis* GM2012^T and *"T. plasticadhaerens"* ElP^T and between themselves. The phylo-genomic differences are well supported by some of the phenotypic differences (but not chemotaxonomic; **(**Table 3.4.4.2) which support strains JC650^T and JC657^T as novel species of the genus *Tautonia* for which we propose the names *Tautonia marina* sp. nov. and *Tautonia rosea* sp. nov., for respective strains. Descriptions of *Tautonia marina* sp. nov. and *Tautonia rosea* sp. nov. are given below.

4.3.4.2 Description of *Tautonia marina* sp. nov.

(ma.ri'na. L. fem. adj. *marina* of or belonging to the sea, marine)

Colour of chemotrophically grown culture is pale pink. Cells are spherical to oval shaped, strictly aerobic and are attached to substrate with the help of holdfast. Cell division is through budding. NaCl is obligate for growth and can tolerates up to 6% (w/v). Optimum pH and temperature for growth are 8.0 (range 7.0-10.0) and 25ºC (range 15-37°C) respectively. N-acetylglucosamine (NAG) is obligate for the growth. D-glucose, fructose, mannose, galactose, maltose, sucrose, sorbitol, Na-pyruvate and starch enhances the growth in the presence of NAG. Ammonium sulphate, peptone, DL-aspartic acid, glutamic acid and proline enhance the growth in the presence of NAG. Major fatty acids (>10%) are $C_{18:1}\omega9c$ and $C_{18:0}$. Minor fatty acids include anteiso-$C_{11:0}$, anteiso-$C_{12:0}$, $C_{I4:0}$, anteiso-$C_{13:0}$, $C_{18:0}$3-OH, $C_{19:0}$, anteiso-$C_{15:0}$, $C_{16:0}$ and anteiso-$C_{17:0}$. Putrescine and sym-homospermidine are the polyamines. Polar lipids are one unidentified amino lipid, phosphatidylethanolamine, two unidentified phospholipid and four unidentified lipids. MK6 is a sole quinone. API ZYM shows positive activity for esterase (C4), esterase lipase (C8), lipase (C14), leucine arylamidase, alkaline phosphatase, valine arylamidase, cysteine arylamidase, acid phosphatase, naphthol-AS-BI-phosphohydrolase, and α-fucosidase. Negative for trypsin, α-chymotrypsin, α-galactosidase, β-galactosidase, β-glucuronidase, α-glucosidase, β- glucosidase, N-acetyl- β-glucosaminidase and α-mannosidase. Genomic DNA G+C content of the type strain is 63.9 mol% **(**Table 3.4.4.2**).**

The type strain JC650^T (=KCTC 72177^T =NBRC 113885^T) was isolated from a sediment sample of Chilika lagoon (Balugaon), India. The 16S rRNA gene sequence and the whole genome sequence (7.07 Mb) of *Tautonia marina* JC650^T are deposited to GenBank under the accession number is LR794306 and WEZF00000000, respectively. The version described in this study is WEZF00000000.

4.3.4.3 Description of *Tautonia rosea* sp. nov.

(ro'se.a. L. fem. adj. *rosea* rose-coloured, pink)

Colour of chemotrophically grown culture is dark pink. Cells are spherical to oval shaped, strictly aerobic and are attached to the substrate with the help of holdfast. Cell division is through budding. NaCl is obligate for growth and can tolerates up to 5% (w/v). Optimum pH and temperature for growth are 8.0 (range 7.0-10.0) and 25ºC (range 10-37°C), respectively. N-acetylglucosamine (NAG) is obligate for the growth. D-glucose, fructose, mannose, galactose, maltose, sucrose, sorbitol, sodium pyruvate and starch enhance the growth in the presence of NAG. Ammonium sulphate, peptone, DL-aspartic acid, glutamic acid and proline enhance the growth in the presence of NAG. Major fatty acids (>10%) are $C_{18:1}\omega9c$ and $C_{18:0}$. Minor fatty acids include anteiso-$C_{11:0}$, anteiso-$C_{12:0}$, $C_{I4:0}$, anteiso-$C_{13:0}$, $C_{18:0}$3-OH, anteiso-$C_{15:0}$, $C_{19:0}$, $C_{16:0}$ and anteiso-$C_{17:0}$. Putrescine and sym-homospermidine are the polyamines. Polar lipid consists of phosphatidylethanolamine, one unidentified amino lipid, two unidentified phospholipid and four unidentified lipids. MK6 is a sole quinone. API ZYM shows positive activity for esterase (C4), leucine arylamidase, alkaline phosphatase, cysteine arylamidase, trypsin, naphthol-AS-BI-phosphohydrolase, valine arylamidase and acid phosphatase. Negative for esterase lipase (C8), α-glucosidase, β- glucosidase, lipase (C14), α-chymotrypsin, α-galactosidase, β-galactosidase, β-glucuronidase, N-acetyl- β-glucosaminidase, α-fucosidase and α-mannosidase. Genomic DNA G+C content of the type strain is 62.7 mol% **(**Table 3.4.4.2**)**

The type strain JC657^T (=KCTC 72177^T =NBRC 113885^T) was isolated from a sediment sample of Chilika lagoon (Balugaon), India. The 16S rRNA gene sequence and the whole genome sequence (7.07 Mb) of *Tautonia rosea* JC657^T are deposited to GenBank

under the accession number is LR794311 and JABBYO000000000. respectively. The version described in this study is JABBYO000000000.

4.3.4.4 Proposal to amend the genus description of *Tautonia*

The genus *Tautonia* is under-studied with only two species (*"T. plasticadhaerens"* ElP^T and *T. sociabilis* GM2012^T) described till now. The original description of this genus was mainly based on morphological and genomic features. Chemotaxonomic features were poorly described. With the addition of *T. marina* and *T. rosea* we propose to broaden the genus characters of *Tautonia* through amending the genus description by adding more chemotaxonomic data.

4.3.4.5 Emended description of the genus *Tautonia.*

Morphological, biochemical, some chemotaxonomic characteristics are as previously described (Kovaleva et al. 2019; Jogler et al. 2020) except for presence or absence of holdfast in some strains. Some strains have obligate requirement for NaCl and N-acetylglucosamine (NAG) for their growth. DNA G+C content varies from 62.7 to 71.1mol%. Putrescine and sym-homospermidine are the polyamines. Polar lipid composition of some strains are phosphatidylethanolamine, unidentified aminolipids, unidentified lipids and unidentified phospholipid. Major fatty acids (>10%) are $C_{18:1}\omega9c$, $C_{18:0}$ and $C_{16:0}$. Minor fatty acids include anteiso-$C_{11:0}$, anteiso-$C_{12:0}$, $C_{I4:0}$, anteiso-$C_{13:0}$, $C_{18:0}$3-OH, anteiso-$C_{15:0}$, $C_{19:0}$, $C_{16:0}$, $C_{22:0}$ branched alcohol and anteiso-$C_{17:0}$ are also present in some strains.

4.3.5.1 Proposal of a new genus to accommodate strains JC640 and CH01

Study extends some unique features that were not previously or less studied among the members of the phylum Planctomycetes. The strains JC640 and CH01 are distinctly separated from other members of the genera of the family *Pirellulaceae* (Table 1). Based on the phylogenetic inference supported by differences in genomic (Table S1, S2) and morphology (Fig. 3) we propose a new genus in the family of Pirellulaceae of the phylum Planctomycetes. Since we lost the viability of the cultures on passaging, we propose to describe the new strains giving the status of "*Candidatus*" as "*Candidatus* Laterigemmans baculatus" gen. nov.sp. nov, for which the protologue is given in Table 3.4.5.4.

4.3.5.2 Description of "*Candidatus* Laterigemmans" gen. nov.

Laterigemmans gen. n. (La.te.ri.gem'mans. L. n. *latus*, *-eris*, side; L. v. *gemmo*, to bud; N.L. part. n. *Laterigemmans*, budding on the side, referring to the unusual type of cell fission of this bacterium)

Colonies are pink colored. Cells are rod shaped. Holdfast is present and flagella are absent. Cell divides by lateral budding. Fimbriae and crateriform structures were not observed. Axenic cultures can be obtained, however loose viability on passaging.

4.3.5.3 Description of "*Candidatus* Laterigemmans baculatus" sp. nov.

(ba.cu.la'tus. L. adj. *baculatus*, rod-like)

Description as given for the genus. Cells are 3.0-4.0 µm long and 0.5-0.8 µm wide. Culture grows well till five passages and become non-viable subsequently. *In silico* genome analysis indicate the culture as aerobic and possibly have fermentative growth and both the strains have incomplete menaquinone pathway.

Both the strains JC640 and CH01 were isolated from a sediment sample of Chilika lagoon (Balugaon, Odisha), and Karaikal beach, Tamil Nadu, respectively. The 16S rRNA

gene sequence of both the strains JC640 and CH01 are deposited to GenBank under the accession number are LR536992 and MT975270. The whole genome sequence of the strains JC640 and CH01 (5.77 Mb) are deposited to GenBank under the accession number is WRPR00000000 and JACVRC000000000, respectively.

4.3.6.1 Proposal of a new species to accommodate strain JC647^T

The Strain JC647^T shows clear distinction with "*C. conspicua*" (Peeters et al. 2020a) based on genotypic (ANI, *d*DDH and AAI values) and phenotypic (Table 3.5.1.3) analysis justifying creation of a new species of the genus "*Crateriforma"*.

4.3.6.2 Description of *Crateriforma spongiae* sp. nov.

Crateriforma spongiae (*spon'gi.ae.* L. fem. n. *spongiae*, of a sponge, referring to isolation of the species from the genus *Spongia*).

Colour of chemoheterotrophically grown broth culture is pink. Cells are pear to oval shaped and form rosette. Cell size is 1.2-1.6 x 0.7-1.0 (LxW, µm) and divide by budding. NaCl is required for growth and tolerates up to 5% (w/v). Optimum pH and temperature for growth are 8.0 (range 8.0-9.0) and 25ºC (range 10-30 °C), respectively. D-glucose, fructose, lactose, starch, mannitol, rhamnose, mannose, sucrose, galactose, maltose are good carbon sources/electron donors supporting growth. Carbon sources like malic acid, ascorbate, pyruvate, inositol, sodium acetate, propionate, benzoic acid, fumarate, xylose, succinate and sorbitol does not support the growth. Ammonium sulphate, glutamic acid, lysine, threonine, aspartic acid, peptone, yeast extract, sodium nitrate and glutamine are good nitrogen sources for growth. Nitrogen sources like leucine, glycine, alanine, phenyl alanine, serine, arginine, isoleucine, tryptophan, tyrosine and sorbitol does not support the growth. API ZYM kit analysis gives positive result for alkaline phosphatase, leucine arylamidase, α-chymotrypsin, acid phosphatase, naphthol-AS-BI-phosphohydrolase, and β-galactosidase, while gives negative for Esterase (C 4), Esterase Lipase (C 8), Lipase (C 14), Valine Arylamidase, Cysteine Arylamidase, Trypsin, α-galactosidase, β-glucuronidase, α-glucosidase, β- glucosidase, N-acetyl- β-glucosaminidase, α-mannosidase, and α-fucosidase. Major fatty acids are $C_{18:1}\omega9c$, $C_{16:0}$ and $C_{18:0}$-

$_{ante}$/$C_{18:2}\omega6,9c$. Minor fatty acids include anteiso-$C_{12:0}$, $C_{12:0}$,$C_{14:0}$, anteiso-$C_{13:0}$, $C_{15:0}$2-OH, anteiso-$C_{15:0}$, $C_{16:1}\omega9C$, $C_{15:1}\omega6C$, $C_{18:0}$, $C_{16:1}\omega7c$/$C_{16:1}\omega6c$, $C_{17:0}$, $C_{17:0cyclo}$, $C_{17:0}$2-OH, iso-$C_{19:1}$, iso-$C_{20:0}$ and $C_{20:1}\omega9c$. Polar lipids are diphosphatidylglycerol, phosphatidylcholine, five unidentified phospholipids (PL1,2,3,4,5) and three unidentified lipids (L1,2,3). Spermidine, sym-homospermidine and putrescine are the polyamines. Genomic DNA G+C content of the type strain is 57.8 mol%. The type strain JC647^T(=KCTC 72176^T=NBRC 114068^T) was isolated from marine sponge belonging to the genus *Spongia* from the south eastern coast of India (Table 3.5.1.3).

The GenBank/EMBL/DDBJ accession numbers for the 16S rRNA gene sequences for strain JC647^T is LR132071. This Whole Genome Shotgun project has been deposited at DDBJ/ENA/GenBank under the accession JAAXMS000000000. The version described in this paper is version JAAXMS010000000.

4.3.6.3 Proposal to emend the genus description of "*Crateriforma*"

The genus *"Crateriforma"* is under-studied with only one species ("*C. conspicua*") described. The original description of this genus was based mostly on the morphological and genomic features. Chemotaxonomic features were poorly described (Peeters et al. 2020). *Crateriforma spongiae* represents the second species in this genus. We propose to broaden the genus characters of *"Crateriforma"* through emending the genus description.

4.3.6.4 Emended description of the genus "*Crateriforma*"

In addition to the original description of the genus given by Peeters et al. (2020a), all strains were isolated are from marine algae or sponge. The genomic size varies from 6.9 Mb to 7.2 Mb. DNA G+C content is 57.8 mol%. Putrescine, spermidine and sym-homospermidine are the major polyamines. Major polar lipids are diphosphatidylglycerol and phosphatidylcholine. Some strains in addition can also have phosphatidyl-

monomethylethanolamine and phosphatidyl-dimethylethanolamine. Major fatty acids are $C_{18:1}\omega 9c$, $C_{16:0}$ and $C_{18:0\text{-ante}}/C_{18:2}\omega 6,9c$.

4.3.7.1 Proposal of a new genus to accommodate strain JC658^T

The family Planctomycetaceae presently contains the genera *Gimesia*, *"Polystyrenella"*, *"Symmachiella"*, *Schlesneria*, *Planctopirus*, *"Caulifigura"*, *Rubinisphaera*, *"Maioricimonas"*, *Planctomicrobium*, *"Thalassoglobus"*, *"Calycomorphotria"*, *"Alienimonas"*, *"Novipirellula"* and *Tuwongella* (https://lpsn.dsmz.de/family/pirellulaceae). Pink colored, salt and alkali tolerant planctomycetal strain (JC658^T) with pear to spherical shaped, Gram-stain-negative, motile cells were isolated from sponge, Tamil Nadu, India. The share highest 16S rRNA gene sequence identity with members of the genus *Rubinisphaera* (<88%) of the family Planctomycetaceae. Based on phylogenetic, genomic (ANI, AAI, POCP, *d*DDH), chemotaxonomic, physiological and biochemical characteristics, we conclude that the strain belong to a novel genus *Thalassoroseus* gen. nov. and constitute a species for which we propose the names *Thalassoroseus pseudoceratinae* sp. nov.. JC658^T (Table 3.5.2.3)**.**

4.3.7.2 Description of *Thalassoroseus* gen. nov.

Thalassoroseus [Tha.las.so.ro'se.us. Gr. n. *thalassa*, the sea; L. adj. *roseus*, pink. N.L. masc. n. *Thalassoroseus*, a pink (bug) from the sea].

Cells are oval to pear shaped and Gram stain-negative. Crateriform structures are common. Cell division is by budding. Major fatty acids are $C_{16:0}$, $C_{18:0}$, $C_{16:1}\omega7c$/$C_{16:1}\omega6c$. Phosphatidyl-dimethylethanolamine, Phosphatidyl- monomethylethanolamine and phosphatidylcholine are the major polar lipids. Sym-homospermidine and putrescine are the major polyamines. MK6 is the only respiratory quinone. The genomic DNA G+C content is 56.4 mol%. The type species is *Thalassoroseus pseudoceratinae*. This genus is a member of the family *Planctomycetaceae.*

4.3.7.3 Description of *Thalassoroseus pseudoceratinae* sp. nov.

Thalassoroseus pseudoceratinae (pseu.do.ce.ra.ti'nae. N.L. gen. n. *pseudoceratinae*, of *Pseudoceratina*, a sponge genus from which....)

Colour of chemotrophically grown culture is pink. Motility could not be demonstrated. NaCl is obligate for growth and can tolerates up to 6% (w/v) NaCl. Optimum pH and temperature for growth are 8.0 (range 7.0-9.0) and 25ºC (range 10-40 ˚C), respectively. D-glucose, lactose, ascorbate, pyruvate, galactose, mannose, and maltose and NAG are good carbon sources for supporting growth. Vitamin B_{12} is not obligate for the growth Yeast extract, peptone, sodium nitrate, L-serine, DL-ornithine, DL-alanine, cysteine, L-glutamine, and L-proline can be used as nitrogen sources for growth. Major fatty acids are $C_{16:0,}$ $C_{18:0,}$ and $C_{16:1}\omega7c/C_{16:1}\omega6c$. Minor fatty acids include $C_{15:1}\omega6c$, $C_{16:0}$ 3-OH, $C_{17:0,}$ $C_{17:1}\omega8c$, $C_{17:1}\omega6c$, anteiso-$C_{17:0,}$ $C_{18:1}\omega9c$, $C_{18:1}\omega7c/$ $C_{18:1}\omega6c$, $C_{18:0}$ante/ $C_{18:2}\omega6c,9c$, $C_{20:1}\omega9c$, $C_{20:1}\omega7c$, $C_{20:0}$, $C_{16:0}$ 10-methyl /iso-$C_{17:1}\omega9c$ and $C_{12:0.}$ Sym-homospermidine and putrescine are the polyamines. Phosphatidyl-dimethylethanolamine, Phosphatidyl- monomethyl-ethanolamine and phosphatidylcholine are the major polar lipids. Genomic DNA G+C content is 56.4 mol% (Table 3.5.2.3**)**. The type strain JC658^T (=KCTC 72881^T = NBRC 114371) was isolated from sponge, Tamil Nadu, India. The 16S rRNA gene sequence of the strain JC658^T has been deposited in GenBank under the accession LR898466. The draft genome of the strain JC658^T has been deposited in GenBank under the accession JAALXT000000000. The version described in this study is version JAALXT010000000.

4.3.8.1 Proposal of a new species to accommodate strain JC639^T

The strain JC639^T shows clear distinction with "*Roseiconus nitratereducens*" JC645^T, "*Roseiconus Lacunae*" JC635^T based on genotypic (ANI, *d*DDH and AAI values) and phenotypic and chemotaxonomic **(**Table 3.5.3.3**)** analysis justifying creation of a new species of the genus *Roseiconus*. *Roseiconus nitratereducens* JC645^T and *Roseiconus Lacunae* JC635^T are isolated from the sediment of Chilika lagoon, India (Kumar et al. 2020).

4.3.8.2 Description of *Roseiconus marina* sp. nov.

(ma.ri'na. L. fem. adj. *marina* of or belonging to the sea, marine)

Colour of chemotrophically grown culture is pale pink. Cells are cylinderical shaped and are strictly aerobic. Cell division is through budding. NaCl is obligate for growth and can tolerates up to 6% (w/v). Optimum pH and temperature for growth are 8.0 (range 7.0-10.0) and 25ºC (range 15-37°C) respectively. NAG, lactose, D-glucose, Rhamnose, mannose, galactose, maltose, sucrose, Na-pyruvate, and D-xylose support the growth as the organic carbon sources. Nitrogen sources like cystein, L-methionine, Ammonium sulphate, sodium nitrate, leucine, L-tyrosine, L-arginine, L-glutamic acid, L-serine, DL-alanine, and proline support the growth of the strain. Major fatty acids (>10%) are $C_{15:1}\omega8c$, $C_{16:0}$, and $C_{18:1}\omega9c$. Minor fatty acids include $C_{9:0}$, $C_{10:0}$, $C_{12:0}$, $C_{14:0}$, $C_{15:1}$Iso H/$C_{13:0}$ 3-OH, anteiso-$C_{17:1}\omega9c$, $C_{18:0}$, $C_{18:3}\omega6c,9c,12c$ and $C_{19:0}$ iso I. Putrescine and sym-homospermidine are the polyamines. Polar lipids are phosphatidylcholine (PC), phosphatidylethanolamine (PE), two unidentified phospholipids (PL1,2) and two unidentified lipids (UL1,2). MK6 is the only quinone. API ZYM shows positive activity for alkaline phosphatase, esterase (C 4), esterase Lipase (C8), leucine Arylamidase, valine arylamidase, acid phosphatase, naphthol-AS-BI-phosphohydrolase, β-galactosidase, and α-

glucosidase. Negative for lipase (C 14), cysteine Arylamidase, trypsin, α-chymotrypsin, α-galactosidase, β-glucuronidase, N-acetyl- β-glucosaminidase, α-mannosidase, α-fucosidase. Genomic DNA G+C content of the type strain is 59.5 mol% (Table 3.5.3.3).

The type strain JC639^T (=KCTC 72168^T=NBRC 113878^T) was isolated from marine sponge belonging to the genus *Spongilla* from the eastern coast of India. The GenBank/EMBL/DDBJ accession numbers for the 16S rRNA gene sequences for strain JC639^T is LR132063. This Whole Genome Shotgun project has been deposited at DDBJ/ENA/GenBank under the accession JACEHH000000000. The version described in this paper is version JACEHH010000000.

4.3.9.1 Proposal of a new species to accommodate strain JC669^T

The genus *Aquisphaera* was described by Bondoso et al. (2011) to put up a new planctomycete of the family Isosphaeraceae isolated from the sediments of a fresh water aquarium. So far, the genus *Aquisphaera* has a sole species, namely *Aquisphaera* giovannonii. The species *Aquisphaera* giovannonii OJF2^T is known as an obligate aerobe, slow growing, chemoheterotroph, spherical and pink pigmented bacterium which reproduce through budding (Bondoso et al. 2011). The Loktak lake is the largest freshwater lake of northeast India having spanning area of about 289 km^2. Loktak lake is famous for its floating islands (phumdis), which are heterogeneous biomass of vegetation, soil and organic matter at various stages of decomposition (Reddy et al. 2005). Phumdis constitute dense rhizosphere extending up to the lake sediment and hence, serve as an ecological habitat for several group of bacteria like Actinobacteria, Acidobacteria, Proteobacteria, Verrucomicrobia and Planctomycetes (Puranik et al. 2016). This lake is of ecological hotspot with great diversity of flora and fauna and declared as Ramsar site in 1990. Insight of the previous metagenome study (Puranik et al. 2016) lead us to isolate a strain of planctomycetes from the rhizosphere of the phumdis, which was identified based on 16S rRNA gene sequence as belonging to the genus *Aquisphaera.* The Strain JC669^T isolated from Loktak Lake resembles the type strain of its phylogenetically closest neighbour with respect of having light pink colonies, major polar lipids and major fatty acids. However, strain JC669^T has about 3.2% less in the G+C mol% compared to *A. giovannonii* OJF2^T. Based on phylogenetic, genomic (ANI, AAI, POCP, *d*DDH), chemotaxonomic, physiological and biochemical characteristics, we conclude that strain JC669^T into a new species the genus *Aquisphaera* for which we propose the name *Aquisphaera insulae* sp. nov.

4.3.9.2 Description of *Aquisphaera insulae* sp. nov.

(in'su.lae. L. n. *insula*, island; L. gen. n. *insulae*, from an island, referring to the isolation of type strain from floating island of Loktak lake, Manipur, India).

Colonies are pale to light pink in colour. Cells are Gram-stain-negative, round to oval shaped, non-motile and multiply by budding forming chains and bunches. Stalks and flagellated cells are not observed. Cells are intolerance to NaCl. Obligate aerobe and mesophilic. Temperature optima at 25ºC (range 10-30 °C). Vitamin B_{12} is not obligate for growth. Utilizes lactose, D-galactose, α-D-glucose, sucrose, mannose, maltose, D-xylose, starch, Na-propionate, inositol, rhamnose, Na-succinate and sorbitol. Fumarate, fructose, ascorbate, acetate, pyruvate, mannitol, malate, inulin, benzoate and citrate do not support growth. D-alanine, L-arginine, L-leucine, L-isoleucine, L-glutamine, L-methionine, DL-ornithine, L-glycine, L-histidine, D-valine, L-proline, L-phenylalanine, DL-threonine, Peptone, NAG, yeast extract, and sodium nitrate and casamino acid good nitrogen sources support the growth. L-serine, L-lysine, L-glutamic acid, L-aspartic acid, L-tyrosine, urea cysteine, L-tryptophan, L-glycine do not support growth as nitrogen source. API ZYM kit analysis gives positive for esterase (C4), alkaline phosphatase, and napthol-AS-B1-BD-phosphohydrolase, esterase lipase (C8) and negative for acid phosphatase, lipase, leucine arylamidase, valine arylamidase, esterase lipase (C8), cysteine arylamidase, α-chymotrypsin, β-glucuronidase, α-glucosidase, β-glucosidase, α-mannosidase, α-galactosidase, β-galactosidase, trypsin and α-fucosidase. Nitrate is not reduced. $C_{18:1}\omega 9c$, $C_{16:0}$ and $C_{18:0}$ are the major fatty acids. MK6 is the only respiratory quinone. Phosphatidylcholine, an unidentified amino lipid, unidentified choline lipid and six unidentified lipids make polar lipid composition. Syn-homospermidine and putrescine are the polyamines. Genomic DNA G+C content of the type strain is 68.5 mol% (Table 3.6.1.2).

The type strain JC669^{T} (=KCTC 72672^{T} =NBRC 114306 ^{T}) is isolated from a rhizosphere soil of *Zizania latifolia* of the floating island from Loktak lake, Manipur, India. The 16S rRNA gene sequence and the whole genome sequence of strain JC669^{T} are deposited to GenBank under the accession number is LR794306 and JAALJH000000000 respectively. The version described in this study is JAALJH000000000.

Major findings

5. Major findings

- This study clearly showed the rich diversity of Planctomycetes of India which was otherwise unexplored.
- Guesstimates from the metagenome studies clearly showed that many of the taxa are novel and only about <0.01% of taxa are obtained as pure cultures and many are yet-to-be-cultivated.
- The metagenome and cultured based studies of algal and sponges clearly indicated the vast diversity of Planctomycetes associated with them.
- Diversity of Planctomycetes are host dependent.
- The three steps enrichments strategy helped in efficient culturing of many Planctomycetes.
- Maximum strains were isolated from marine habitats.
- Phylo-taxogenomic studies helped in establishing various new taxa of Planctomycetes with valid taxa.
- The study left with a question to address the sporulation/fruiting bodies among the members of Planctomycetes, which is the novel discovery of this study.

References

Abdelmohsen UR, Bayer K, Hentschel U (2014) Diversity, abundance and natural products of marine sponge-associated actinomycetes. Nat Prod Rep 31:381–99.

Acehan D, Santarella-Mellwig R, Devos DP (2013) A bacterial tubulovesicular network. J Cell Sci 127:277–80.

Akob DM, Mills HJ, Kostka JE (2007) Metabolically active microbial communities in uranium-contaminated subsurface sediments. FEMS Microbiol Ecol 59:95–107.

Arrigo KR (2005) Marine microorganisms and global nutrient cycles. Nature 437: 349–355.

Ali A, Kumar Gaurav, N Senthilnathan, T P Radhakrishnan, Sasikala, Ch, and Ramana, ChV "Sporotan" a new fluorescent stain for identifying *Rhodobacter johrii*. J. Microbiol. Methods. 2020. 177: 106019.

Aziz RK, Bartels D, Best AA, DeJongh M, Disz T et al. (2008) The RAST server: rapid annotations using subsystems technology. BMC Genomics 9:75.

Bacci G, Ceccherini MT, Bani A et al. (2015) Exploring the dynamics of bacterial community composition in soil: the pan- bacteriome approach. Antonie Van Leeuwenhoek 107:785–97.

Bauld J, Staley JT. *Planctomycesmaris* sp. nov. a marine isolate of the *Planctomyces Blastocaulis* group of budding bacteria. Microbiology 97:45-55.

Bayer K, Schmitt S, Hentschel U (2008) Physiology, phylogeny and *in situ* evidence for bacterial and archaeal nitrifiers in the marine sponge *Aplysinaaerophoba*. Environ Microbiol 10:2942–55.

Bergquist PR. Sponges. London: Hutchinson & Co.; 1978.

Blin K, Shaw S, Steinke K, Villebro R, Ziemert N, Lee SY et al. (2019) antiSMASH 5.0: updates to the secondary metabolite genome mining pipeline. Nucleic Acids Res 47(W1):W81-W87.

Blin K, Shaw S, Steinke K, Villebro R, Ziemert N, Lee SY et al. (2019) anti-SMASH 5.0: updates to the secondary metabolite genome mining pipeline. Nucleic Acids Res 47(W1):W81-W87.

Boedeker C, Schu¨ler M, ReintjesG et al. (2017) Determining the bacterial cell biology of Planctomycetes. Nat Commun 8: 14853.

Bondoso J, Albuquerque L, Lobo-da-Cunha A, Da Costa MS, HarderJ,Lage OM (2014b) *Rhodopirellula lusitana* sp. nov. and *Rhodopirellula rubra* sp. nov. isolated from the surface of macroalgae. Syst Appl Microbiol 37:157-164.

Bondoso J, Albuquerque L, Lobo-da-Cunha A, Da Costa, M.S, HarderJ,Lage OM (2014) *Rhodopirellula lusitana* sp. nov. and *Rhodopirellula rubra* sp. nov. isolated from the surface of macroalgae. Syst Appl Microbiol 37:157-164.

Bondoso J, Albuquerque L, Nobre MF, Lobo-da-Cunha A, da Costa MS et al. (2015) *Roseimaritimaulvae* gen. nov. sp. nov. and *Rubripirellula obstinata* gen. nov. sp. nov. two novel planctomycetes isolated from the epiphytic community of macroalgae. Syst Appl Microbiol 38:8-15.

Bondoso J, Albuquerque L, Nobre MF, Lobo-da-Cunha A, da Costa MS, Lage OM (2011) *Aquisphaera giovannonii* gen. nov. sp. nov. a planctomycete isolated from a freshwater aquarium. Int J Syst Evol Microbiol 61:2844-2850.

Boumann HA, Hopmans EC, van de Leemput I, Op den Camp HJM, van de Vossenberg J, Strous M, Jetten MSM, SinninghеDamste JS & Schouten S (2006) Ladderane phospholipids in anammox bacteria comprise phosphocholine and phosphoethanolamine headgroups. FEMS Microbiol Lett 258: 297–304.

Bradley JA, Daille LK, Trivedi CB et al. (2017) Carbonate-rich dendrolitic cones: insights into a modern analog for incipient microbialite formation, Little Hot Creek, Long Valley Caldera, California. npj Biofilms Microbiomes 3:32.

Bray AW, Stewart DI, Courtney R et al. (2017) Sustained bauxite residue rehabilitation with gypsum and organic matter 16 years after initial treatment. Environ Sci Technol 52:152–61.

Buckley DH, Huangyutitham V, Nelson TA et al. (2006) Diversity of *Planctomycetes* in soil in relation to soil history and environmental heterogeneity. Appl Environ Microb 72:4522–31.

Caracciolo AB, Grenni P, Ciccoli R et al. (2005) Simazine biodegradation in soil: analysis of bacterial community structure by in situ hybridization. Pest Manag Sci 61:863–9.

Chen L, Li C, Feng Q et al. (2017a) A Shifts in soil microbial metabolic activities and community structures along a salinity gradient of irrigation water in a typical arid region of China. Sci Total Environ 598:64–70.

Chen YL, Deng Y, Ding JZ et al. (2017b) Distinct microbial communities in the active and permafrost layers on the Tibetan Plateau. MolEcol 26:6608–20.

Croue J, West NJ, Escande ML, Intertaglia L, Lebaron P, Suzuki MT (2013) A single beta-proteobacterium dominates the microbial community of the crambescidine-containing sponge *Crambecrambe*. Sci Rep 3:2583.

Cuskin F, Lowe EC, Temple MJ et al. (2015) Human gut Bacteroidetes can utilize yeast mannan through a selfish mechanism. Nature 517:165–9.

Danilova OV, Belova SE, Gagarinova IV et al. (2016) Microbial community composition and methanotroph diversity of a subarctic wetland in Russia. Microbiology 85:583–91.

Dedysh SN, Kulichevskaya IS, Beletsky AV, Ivanova AA, Rijpstra WIC, Damsté JSS, Ravin NV (2020) *Lacipirellula parvula*gen. nov. sp. nov. representing a lineage of planctomycetes widespread in low-oxygen habitats, description of the family *Lacipirellulaceae* fam. nov. and proposal of the orders *Pirellulales*ord. nov., *Gemmatales*ord. nov. and *Isosphaerales* ord. nov. SystApplMicrobiol 43:126050.

DeLong EF, Franks DG, Alldredge AL (1993) Phylogenetic diversity of aggregate-attached vs. free-living marine bacterial assem- blages. LimnolOceanogr 38:924–34.

Dendy (1905) Report on the sponges collected by Prof.Herdman, at Ceylon, in 1902. Report to the Government of Ceylon on the Pearl Oyster Fisheries of the Gulf of Mannar, Royal Society London suppl 3(18): 57-246.

Devos DP, Dokudovskaya S, Alber F et al. (2004) Components of coated vesicles and nuclear pore complexes share a common molecular architecture. PLoSBio l2:e380.

Dion A, Herbst E (1970) Polyamine changes during development of *Drosophila melanogaster*. Ann NY Acad Sci 171:723–734.

Edgar RC, Haas BJ, Clemente JC, Quince C, Knight R (2011) UCHIME improves sensitivity and speed of chimera detection. Bioinformatics 27:2194-2200.

Egan AJ, Vollmer W (2013) The physiology of bacterial cell division. Ann N Y Acad Sci 1277:8–28.

Egli K, Fanger U, Alvarez PJJ, Siegrist H, van der Meer JR, Zehnder AJB (2001) Enrichment and characterization of ananammox bacterium from a rotating biological contactor treating ammonium-rich leachate. Arch Microbiol 175:198-207.

Eisenreich W, Bacher A, Arigoni D, Rohdich F (2004) Biosynthesis of isoprenoids via thenon-mevalonate pathway. Cell Mol Life Sci 61:1401–1426.

Farghaly A, Enitan AM, Kumari S et al. (2016) Polyhydroxyalkanoates production from fermented paperboard mill wastewater using acetate-enriched bacteria. Clean Techn Environ Policy 19:935–47.

Farias ME, Rasuk MC, Gallagher KL et al. (2017) Prokaryotic diversity and biogeochemical characteristics of benthic microbial ecosystems at La Brava, a hypersaline lake at Salar de Atacama, Chile. PLoS One 12:e0186867.

Felsenstein J (1985) Confidence limits on phylogenies: an approach using thebootstrap. Evolution 39:783-791.

Fernandez AB, Rasuk MC, Visscher PT et al. (2016) Microbial diversity in sediment ecosystems (evaporites domes, microbial mats, and crusts) of hypersaline Laguna Tebenquiche, Salar de Atacama, Chile. Front Microbiol 7:1284.

Fieseler L, Horn M, Wagner M, Hentschel U (2004) Discovery of the novel candidate phylum "Poribacteria" in marine sponges. Appl Environ Microbiol 70:3724–32.

Fonseca JP, Hoffmann L, Cabral BCA et al.(2018) Contrasting the micro- biomes from forest rhizosphere and deeper bulk soil from an Amazon rainforest reserve. Gene 642:389–97.

Frey JC, Rothman JM, Pell AN et al. (2006) Fecal bacterial diversity in a wild gorilla. Appl Environ Microb 72:3788–92.

Fuerst JA, Sagulenko E (2011) Beyond the bacterium: planctomycetes challenge our concepts of microbial structure and function. Nat Rev Microbiol **9**:403–13.

Fuerst JA, Webb RI (1991) Membrane-bounded nucleoid in the eu-bacterium *Gemmataobscuriglobus*. Proc Natl Acad Sci USA 88:8184–8.

Fukunaga Y, Kurahashi M, Sakiyama Y et al. (2009) *Phycisphaerami kurensis* gen. nov. sp. nov, isolated from a marine alga, and proposal of *Phycisphaeraceaefam*. nov., *Phycisphaeralesord*. nov. and *Phycisphaeraeclasses* nov. in the phylum Planctomycetes. J Gen Appl Microbiol 55:267– 75.

Gernert C, Glockner FO, Krohne G, Hentschel U (2005) Microbial diversity of the freshwater sponge *Spongillalacustris*. Microb Ecol 50:206-212.

Gilbert JA, Jansson JK, Knight R. (2014) The Earth Microbiome project: successes and aspirations. BMC Biol 12:69.

Giles EC, Kamke J, Moitinho-Silva L, Taylor MW, Hentschel U, Ravasi T et al. (2013) Bacterial com- munity profiles in low microbial abundance sponges. FEMS Microbiol Ecol 83:232–41.

Gimesi N (1924) *Planctomyces Bekefii Gen.* nov. *gen. sp*. nov Budapest, Hun-gary: Hydrobiologische Studien.

Giovannoni SJ, Schabtach E, Castenholz RW (1987) *Isosphaera pallida* gen. and comb. nov. a gliding, budding eubacterium from hot springs. Arch Microbiol 147, 276-284.

Goris J, Konstantinidis KT, Klappenbach JA, Coenye T, Vandamme P, Tiedje JM (2007). DNA–DNA hybridization values and their relationship to whole-genome sequence similarities. Int J Syst Evol Microbiol 57:81-91.

Gottshall EY, Seebart C, Gatlin JC et al. (2014) Spatially segregated tran- scription and translation in cells of the endomembrane- containing bacterium *Gemmata obscuriglobus*. Proc Natl Acad Sci USA 111:11067–72.

Graca AP, Calisto R, Lage OM (2016) Planctomycetes as novel source of bioactive molecules. Front Microbiol 7:1241.

Halter D, Cordi A, Gribaldo S et al. (2011) Taxonomic and functional prokaryote diversity in mildly arsenic-contaminated sediments. Res Microbiol 162:877–87.

Hammer O, Harper D, Ryan PD (2001) PAST: Paleontological statistics software package for education and data analysis. Palaeontologia Electronica 1:9.

Hentschel U, Fieseler L, Wehrl M, Gernert C, Steinert M, Hacker J, et al. (2003) Microbial diversity of marine sponges. Prog Mol Subcell Biol. 37:59–88.

Hentschel U, Piel J, Degnan SM, Taylor MW (2012) Genomic insights into the marine sponge microbiome. Nat Rev Microbiol 10:641–54.

Hirsch P (1972) Two identical genera of budding and stalked bacteria: *Planctomyces* Gimesi and *Blastocaulis* Henrici and John- son 1935. Int J Syst Evol Microbiol 22:107–11.

Hoffmann F, Radax R, Woebken D, Holtappels M, Lavik G, Rapp HT, et al. (2009) Complex nitrogen cycling in the sponge *Geodiabarretti*. Environ Microbiol 11:2228–43.

Hoffmann F, Rapp HT, Reitner J (2006) Monitoring microbial community composition by fluorescence *in situ* hybridization during cultivation of the marine cold-water sponge *Geodiabarretti*. Mar Biotechnol 8:373–9.

Hou D, Huang Z, Zeng S et al. (2017) Environmental factors shape water microbial community structure and function in shrimp cultural enclosure ecosystems. Front Microbiol 8: 2359.

Hussain S. et al. (2018) MreB filaments align along greatest principal membrane curvature to orient cell wall synthesis. eLife **7**:e32471.

Imhoff JF (1984) Quinones of phototrophic purple bacteria. FEMS Microbiol Lett 25:85-89.

Imhoff JF, Stohr R (2003) Sponge-associated bacteria: general overview and special aspects of bacteria associated with *Halichondriapanicea*. Prog Mol Subcell Biol 37:35–57.

Ivanova AA, Kulichevskaya IS, Merkel AY et al. (2016) High diversity of *Planctomycetes* in soils of two lichen-dominated sub-arctic ecosystems of northwestern Siberia. Front Microbiol 7:2065.

Ivanova AA, Naumoff DG, Miroshnikov KK et al. (2017a) A Comparative genomics of four *Isosphaeraceae* Planctomycetes: a common pool of plasmids and glycoside hydrolase genes shared by *Paludisphaera borealis* PX4T, *Isosphaera pallida* IS1BT, *Singulisphaeraacidiphila* DSM 18658T and strain SH-PL62. Front Microbio l8:412.

Izumi H, Sagulenko E, Webb RI, Fuerst JA (2013) Isolation and diversity of *planctomycetes* from Antonie Van Leeuwenhoek 104:533–46.

Jacquier N, Viollier PH, & Greub G (2015) The role of peptidoglycan in chlamydial cell division: towards resolving the chlamydial anomaly. FEMS Microbiol Rev 39:262–275.

Jarett JK, MacManes MD, Morrow KM et al. (2017) Comparative genomics of color morphs in the coral *Montastraea cavernosa*. Sci Rep**7**:16039.

Jasmin C, Anas A & Nair S (2015) Bacterial diversity associated with *Cinachyra cavernosa* and *Haliclonapigmentifera*, cohabiting sponges in the coral reef ecosystem of Gulf of Mannar, Southeast Coast of India. PLoS One 10(5):e0123222.

Jermy A (2010) Evolution: Bacterial endocytosis uncovered. Nat Rev Microbiol 8:534.

Jeske O, Jogler M, Petersen J et al. (2013) From genome mining to phenotypic microarrays: *Planctomycetes*as source for novel bioactive molecules. Antonie van Leeuwenhoek 104:551–67.

Jeske O, Surup F, Ketteniss M et al. (2016) Developing techniques for the utilization of Planctomycetes as producers of bioactive molecules. Front Microbiol **7**:1242.

Jeske, O, Schüler, M, Schumann, P, Schneider A, Boedeker C, Jogler M, Spring S(2015) Planctomycetes do possess a peptidoglycan cell wall. Nat Commun 6:7116-7123.

Jetten MSM, Niftrik L, Strous M, Kartal B, Keltjens JT & Op den Camp HJM (2009) Biochemistry and molecular biology of anammox bacteria. Crit Rev BiochemMol Biol 44: 65–84.

Jogler C, Glo¨ ckner FO, Kolter R (2011) Characterization of *Planctomyces limnophilus* and development of genetic tools for its manipulation establish it as a model species for the phylum Planctomycetes. Appl Environ Microb 77:5826–9.

Jogler C, Wiegand S, Boedeker C, Heuer A, Peeters SH, Jogler M, JettenMSM, Rohde M, Kalluscheuer N (2020) *Tautoniaplasticadhaerens* sp. nov., a novel species in the family *Isosphaeraceae* isolated from an alga in a hydrothermal area of the Eolian Archipelago. Antonie Van Leeuwenhoek 113:1889-1900.

Jogler C et al. (2012) Identification of proteins likely to be involved in morphogenesis, cell division, and signal transduction in *Planctomycetes* by comparative genomics. J. Bacteriol 194:6419–6430.

Johnson M, Zaretskaya I, Raytselis Y, Merezhuk Y, McGinnis S, Madden T L. (2008) NCBI BLAST: a better web interface. *Nucleic Acids Res* 36:W5-W9.

Jongman M, Chidamba L, Korsten L. (2017) Bacterial biomes and potential human pathogens in irrigation water and leafy greens from different production systems described using pyrosequencing. J Appl Microbiol 123:1043–53.

Kaboré OD, Godreuil S & Drancourt M (2020) Planctomycetes as Host-Associated Bacteria: A Perspective That Holds Promise for Their Future Isolations, by Mimicking Their Native Environmental Niches in Clinical Microbiology Laboratories. Frontiers in Cellular and Infection Microbiology 10:729.

Kallscheuer N, Jeske O, Sandargo B, Boedeker C, Wiegand S, Bartling P, &Surup F (2020a) The planctomycete *Stieleria maiorica* Mal15 T employs *stieleria cines* to alter the species composition in marine biofilms. Commun Biol 3:1-8.

Kallscheuer N, Jogler M, Wiegand S, Peeters S H, Heuer A, Boedeker C, & Jogler C (2019b) Three novel *Rubripirellula* species isolated from plastic particles submerged in the Baltic Sea and the estuary of the river Warnow in northern Germany. Antonie van Leeuwenhoek 113:1767-1778.

Kallscheuer N, Jogler M, Wiegand S, Peeters SH, Heuer A et al. (2019) Three novel *Rubripirellula* species isolated from plastic particles submerged in the Baltic Sea and the estuary of the river Warnow in northern Germany. Antonie van Leeuwenhoek 113:1767-1778.

Kallscheuer N, Wiegand S, Boedeker C, Peeters SH, Jogler M et al. (2020) *Aureliella helgolandensis* gen. nov. sp. nov. a novel Planctomycete isolated from a jellyfish at the shore of the island Helgoland. Antonie Van Leeuwenhoek 113:1839-1849.

Kallscheuer N, Wiegand S, Boedeker C, Peeters SH, Jogler M et al. (2020) *Aureliella helgolandensis* gen. nov. sp. nov. a novel Planctomycete isolated from a jellyfish at the shore of the island Helgoland. Antonie Van Leeuwenhoek 113:1839-1849.

Kallscheuer N, Wiegand S, Boedeker C, Peeters SH, Jogler M, Rast P, Heuer A, Jetten MSM, Rohde M, Jogler C (2020b) *Aureliella helgolandensis* gen. nov. sp. nov. a novel *Planctomycete* isolated from a jellyfish at the shore of the island Helgoland. Antonie Van Leeuwenhoek 113:1839-1849.

Kallscheuer N, Wiegand S, Heuer A, Rensink S, Boersma A S, Jogler M, & Rohde M (2020c) *Blastopirellula retiformator* sp. nov. isolated from the shallow-sea hydrothermal vent system close to Panarea Island. Antonie van Leeuwenhoek 113:1811-1822.

Kallscheuer N, Wiegand S, Jogler M, Boedeker C, Peeters S H, Rast P, & Jogler C (2019a) *Rhodopirellula heiligendammensis* sp. nov. *Rhodopirellula pilleata* sp. nov. and *Rhodopirellula solitaria* sp. nov. isolated from natural or artificial marine surfaces in Northern Germany and California, USA, and emended description of the genus *Rhodopirellula*. Antonie van Leeuwenhoek 113:1737-1750.

Karlsson R, Karlsson A, B€ackman O, Johansson BR & Hulth S (2009) Identification of key proteins involved in the anammox reaction. FEMS Microbiol Lett 297: 87–94.

Kartal B, de Almeida NM, MaalckeWJ et al. *(*2013) How to make a living from anaerobic ammonium oxidation. FEMS Microbiol Rev37:428–61.

Kartal B, Kuenen JG, van Loosdrecht MC (2010) Engineering. Sewage treatment with anammox. Science 328:702–3.

Kaushik R, Sharma M, Gaurav K, Jagadeeshwari U, Shabbir A, Sasikala C, Ramana CV, Pandit MK. (2020) Paludisphaera soli sp. nov., a new member of the family Isosphaeraceae isolated from high altitude soil in the Western Himalaya. Antonie van Leeuwenhoek113:1663-1674.

Kellogg CA, Ross SW, Brooke SD (2016) Bacterial community diversity of the deep-sea octocoral *Paramuriceaplacomus*. Peer J 4:e2529.

Kim HM, Lee MJ, Jung JY et al. (2016) A Vertical distribution of bacterial community is associated with the degree of soil organic matter decomposition in the active layer of moist acidic tundra. J Microbiol 54:713–23.

Kimura M (1980) A simple method for estimating evolutionary rates of base substitutions through comparative studies of nucleotide sequences. J Mol Evol 16:111-120.

Ko¨nig E, Schlesner H, Hirsch P (1984) Cell wall studies on budding bacteria of the *Planctomyces/Pasteuria*group and on a *Prosthecomicrobium*sp. Arch Microbiol 138:200–5.

Kohler T, Stingl U, Meuser K et al. (2008) Novel lineages of *Planctomycetes* densely colonize the alkaline gut of soil-feeding termites (*Cu- bitermes*spp.). Environ Microbiol 10:1260–70.

Kohn T, Heuer A, Jogler M et al. (2016) *Fuerstiamaris germanicae*gen. nov. sp. nov. an unusual member of the phylum Planctomycetes from the German Wadden Sea. Front Microbiol 7:2079.

Kohn T, Rast P, Kallscheuer N, Wiegand S, Boedeker C, Jetten MSM et al. (2020) The Microbiome of Posidoniaoceanica Seagrass Leaves Can Be Dominated by Planctomycetes. Front Microbiol 11:1458.

Kovaleva OL, Elcheninov AG, Toshchakov SV, Novikov AA, Bonch-Osmolovskaya EA, Kublanov IV(2019) *Tautonia sociabilis* gen. nov. sp. nov. a novel thermotolerant planctomycete, isolated from a 4000 m deep subterranean habitat. Int J Syst Evol Microbiol 69:2299-2304.

Kozich JJ, Westcott SL, Baxter NT, Highlander SK, Schloss PD (2013) Development of a dual-index sequencing strategy and curation pipeline for analyzing amplicon sequence data on the MiSeqIllumina sequencing platform. Appl Environ Microbiol 17:5112-5120.

Kulichevskaya IS, Detkova EN, Bodelier PL, Rijpstra WIC, Damste JSS, Dedysh SN (2012) *Singuli sphaerarosea* sp. nov., a planctomycete from acidic aSphagnum peat, and emended description of the genus *Singulisphaera*. Int J Syst Evol Microbiol 62:118-123.

Kulichevskaya IS, Ivanova AA, Detkova EN, Rijpstra WIC, Damsté JSS, Dedysh SN (2017) *Tundrisphaera lichenicola* gen. nov. sp. nov. a psychrotolerant representative of the family *Isosphaeraceae* from lichen-dominated tundra soils. Int J Syst Evol Microbiol 67:3583-3589.

Kulichevskaya IS, Ivanova AA, Suzina NE, Rijpstra WIC, Damste JSS, Dedysh SN (2016) *Paludisphaera borealis* gen. nov. sp. nov. a hydrolytic planctomycete from northern wetlands, and proposal of *Isosphaeraceae* fam. nov. Int J Syst Evol Microbiol 66:837-844.

Kulichevskaya IS, Ivanova AO, Baulina OI, Bodelier PL, Damste JSS, Dedysh SN (2008) *Singulisphaera acidiphila* gen. nov. sp. nov. a non-filamentous, Isosphaera-like planctomycete from acidic northern wetlands. Int J Syst Evol Microbiol 58:1186-1193**.**

Kumar D, Gaurav K, JagadeeshwariU, Deepshikha G, Sasikala Ch, Ramana ChV (2020) *Roseimaritima sediminicola* sp. nov. a new member of Planctomycetaceae isolated from Chilika lagoon. Int J Syst Evol Microbiol 70:2616-2623.

Kumar D, Gaurav K, PK S, Uppada J, ChVR (2020). *Gimesia chilikensis* sp. nov. a haloalkali-tolerant planctomycete isolated from Chilika lagoon and emended description of the genus Gimesia. Int J Syst Evol Microbiol 004211.

Kumar S, Stecher G, Tamura K (2016) MEGA7: molecular evolutionary genetics analysis version 7.0 for bigger datasets. Mol Biol Evol 33:1870-1874.

Kuypers MMM, Sliekers AO, Lavik G, Schmid M, Jørgensen BB, Kuenen JG, SinninghеDamste JS, Strous M &Jetten MSM (2003) Anaerobic ammonium oxidation by anammox bacteria in the Black Sea. Nature 422: 608–611.

Lafi FF, Fuerst JA, Fieseler L, Engels C, Goh WWL, Hentschel U (2009) Widespread distribution of Poribacteria in Demospongiae. Appl Environ Microbiol 75:5695–9.

Lagae, OM, Bondoso J (2014) Planctomycetes and macroalgae, a striking association. Front microbial 5: 267.

Lage O M, Albuquerque L, Lobo-da Cunha A, & da Costa M S (2017) *Mariniblastus fucicola* gen. nov. a novel planctomycete associated with macroalgae. Int J Syst Evol Microbiol 67:1571-1576.

Lage OM and Bondoso J (2011) Planctomycetes diversity associated with macroalgae: Planctomycetes-macroalgae diversity. FEMS Microbiol Ecol 78:366–375.

Lam P, & Kuypers MMM (2011) Microbial nitrogen cycling processes in oxygen minimum zones. Ann Rev Mar Sci 3: 317–345.

Langille M, Zaneveld J, Caporaso JG, McDonald D, Knights D, Reyes J et al. (2013) Predictive functional profiling of microbial communities using 16S rRNA marker gene sequences. Nat. Biotechnol 31:814–821.

Lebaron P, Catala P, Parthuisot N (1998) Effectiveness of SYTOX green stain for bacterial viability assessment. Appl Environ Microbiol 64: 2697-2700.

Lee HW, Roh SW, Shin N R, Lee J, Whon TW, Jung M J, Bae JW (2013) *Blastopirellula cremea* sp. nov. isolated from a dead ark clam. Int J Syst Evol Microbiol 63:2314-2319.

Leser TD, Amenuvor JZ, Jensen TK et al. (2002) Culture-independent analysis of gut bacteria: the pig gastrointestinal tract micro- biota revisited. Appl Environ Microb 68:673–90.

Li XM, Zhu YJ, Yan QY et al. (2014) Do the intestinal microbiotas differ between paddlefish (*Polyodonspathala*) and bighead carp (*Aristichthysnobilis*) reared in the same pond? J Appl Microbiol 117:1245–52.

Liesack W, Ko¨nig H, Schlesner H et al. (1986) Chemical-composition of the peptidoglycan-free cell envelopes of budding bacte- ria of the *Pirella/Planctomyces* group. Arch Microbiol 145: 361–6.

Lindsay MR, Webb RI, Fuerst JA (1997) Pirellulosomes: A new type of membrane-bounded cell compartment in planctomycete bacteria of the genus *Pirellula*. Microbiology-Uk 143:739–48.

Lindsay MR, Webb RI, Strous M et al. (2001) Cell compartmentalisation in planctomycetes: novel types of structural organisation for the bacterial cell. Arch Microbiol 175:413–29.

Longford S, Tujula N, Crocetti G, Holmes A, Holmström C, Kjelleberg S, et al. (2007) Comparisons of diversity of bacterial communities associated with three sessile marine eukaryotes. Aquat Microb Ecol 48:217–229.

Lonhienne TG, Sagulenko E, Webb RI et al. (2010) Endocytosis-like protein uptake in the bacterium *Gemmata obscuriglobus*. Proc Natl Acad Sci USA 107:12883–8.

Lonhienne TG, Sagulenko E, Webb RI et al.(2010) Endocytosis-like protein uptake in the bacterium *Gemmata obscuriglobus*. Proc Natl Acad Sci USA 107:12883–8.

Lovering AL, Safadi SS, Strynadka NC (2012) Structural perspective of peptidoglycan biosynthesis and assembly. Annu Rev Biochem 81:451–78.

Luo C, Rodriguez-r LM, Konstantinidis KT (2014) MyTaxa: an advanced taxonomic classifier for genomic and metagenomic sequences. Nucleic Acids Res 42:e73.

Kajander T, Lehtiö L, Schlömann M, & Goldman A (2003) The structure of Pseudomonas P51 Cl-muconate lactonizing enzyme: Co-evolution of structure and dynamics with the dehalogenation function. Prot sci 12:1855-1864.

Meier-Kolthoff JP, Klenk HP, Göker M (2014) Taxonomic use of DNA G+C content and DNA–DNA hybridization in the genomic age. Int J Syst Evol Microbiol 64:352-356.

Mohamed NM, Saito K, Tal Y, Hill RT (2010) Diversity of aerobic and anaerobic ammonia-oxidizing bacteria in marine sponges. ISME J 4:38–48.

Nagar, Shekhar, Chandni Talwar, Shazia Haider, Akshita Puri, Kalaiarasan Ponnusamy, Madhuri Gupta, Utkarsh Sood, Abhay Bajaj, Rup Lal, and Roshan Kumar. "Phylogenetic Relationships and Potential Functional Attributes of the Genus Parapedobacter: A Member of Family Sphingobacteriaceae. Front in microbiol 11: 1725.

Na SI, Kim YO, Yoon SH, Ha SM, Baek I, Chun J (2018) UBCG: Up-to-date bacterial core gene set and pipeline for phylogenomic tree reconstruction. J Microbiol 56:280-285.

Niu J, Chao J, Xiao Y et al. (2016) Insight into the effects of different cropping systems on soil bacterial community and tobacco bacterial wilt rate. J Basic Microbiol 57:3–11.

N. Senthilnathan, Kumar Gaurav, Ch. Venkata Ramana and T. P. Radhakrishnan. Zwitterionic small molecule based fluorophores for efficient and selective imaging of bacterial endospores. *J Mater Chem B* .2020. 8: 4601-4608.

Parsley LC, Newman MM, Liles MR (2010) Fluorescence in situ hybridization of bacterial cell suspensions. Cold Spring Harb Protoc 9:pdb.prot5493.

Peeters SH, Wiegand S, Kallscheuer N, Jogler M, Heuer A, Jetten MS et al. (2020a) Three marine strains constitute the novel genus and species *Crateriforma* conspicua in the phylum Planctomycetes. Antonie Van Leeuwenhoek 113:1797-1809.

Peeters SH, Wiegand S, Kallscheuer N, Jogler M, Heuer A, Jetten MS, Boedeker C, Rohde M, Jogler C. (2020b) *Lignipirellula cremea* gen. nov. sp. nov. a planctomycete isolated from wood particles in a brackish river estuary. Antonie van Leeuwenhoek 113:1863-1875.

Peeters SH, Wiegand S, Kallscheuer N, Jogler M, Heuer A, Jetten MS, Jogler C (2020) *Lignipirellula cremea* gen. nov. sp. nov. a planctomycete isolated from wood particles in a brackish river estuary. Antonie van Leeuwenhoek 113:1863-1875**.**

Pramanik A, Basak P, Banerjee S, Sengupta S, Chattopadhyay D, Bhattacharyya M (2015) Pyrosequencing based profiling of the bacterial community in the Chilika Lake, the largest lagoon of India. Genom Data 4:112-114.

Prazeres M, Ainsworth T, Roberts TE et al. (2017) Symbiosis and microbiome flexibility in calcifying benthic foraminifera of the Great Barrier Reef. Microbiome 5:38.

Proemse BC, Eberhard RS, Sharples C et al. (2017) Stromatolites on the rise in peat-bound karstic wetlands. Sci Rep 7:15384.

Pruesse E, Quast C, Knittel K, Fuchs BM, Ludwig WG, Peplies J, Glöckner FO (2007) SILVA: a comprehensive online resource for quality checked and aligned ribosomal RNA sequence data compatible with ARB. Nucl Acids Res 35:7188-7196.

Puranik S, Pal RR, More RP, and Purohit HJ (2016) Metagenomic approach to characterize soil microbial diversity of Phumdi at Loktak Lake. Water Sci Technol 74: 2075-2086.

Qin QL, Xie BB, Zhang XY, Chen XL, Zhou BC, Zhou J et al. (2014) A proposed genus boundary for the prokaryotes based on genomic insights. J. Bacteriol 196:2210-2215.

Qiong W, George MG, James MT, James RC (2007) Naive Bayesian Classifier for Rapid Assignment of rRNA Sequences into the New Bacterial Taxonomy. Appl Environ Microbiol 73:5261-5267.

Raina V, Panda AN, Mishra SR, Nayak T, Suar M (2019) Microbial biodiversity study of a brackish water ecosystem in eastern India: the Chilika Lake. In Microbial Diversity in the Genomic Era (pp. 47-63). Academic Press.

Ramesh R, P Nammalwar and VS Gowri (2008). Data base on coastal information of Tamil nadu.

Rattray JE, van de Vossenberg J, Hopmans EC, Kartal B, van Niftrik L, Rijpstra WI, Strous M, Jetten MSM, Schouten S &SinninghеDamste JS (2008) Ladderane lipid distribution in four genera of anammox bacteria. Arch Microbiol 190: 51–66.

Rattray JE, van de Vossenberg J, Jaeschke A et al. (2010) Impact of temperature on ladderane lipid distribution in anammox bacteria. Appl Environ Microbiol 76: 1596–1603.

Reddy HR, Katti RJ, Raveesha KP, Vikas SJ, Babu RN, and Kumar KS (2005) Habitat heterogeneity of the Loktak lake, Manipur. Current Science88:1027.

Reintjes G, Arnosti C, Fuchs BM et al. (2017) An alternative polysaccharide uptake mechanism of marine bacteria. ISMEJ 11:1640–165.

Rensink S, Wiegand S, Kallscheuer N, Rast P, Peeters SH, Heuer A, Boedeker C, Jetten MS, Rohde M, Jogler M, Jogler C. (2020) Description of the novel planctomycetal genus *Bremerella*, containing *Bremerellavolcania* sp. nov. isolated from an active volcanic site, and reclassification of *Blastopirellulacremea* as *Bremerellacremea* comb. nov.Antonie van Leeuwenhoek 113:1823-1837.

Reva O, Tummler B (2008) Think big-giant genes in bacteria. Environ Microbiol 10:768–77.

Richter M, Rossello-Mora R (2009) Shifting the genomic gold standard for the prokaryotic speciesdefinition. Proc Natl Acad Sci (USA) 106:19126-19131.

Ritcher M, Rossello-Mora R (2009) Shifting the genomic gold standard for the prokaryotic species definition. Proc Natl Acad Sci (USA) 106:19126-19131.

Rodriguez RLM, Konstantinidis KT (2014) Bypassing cultivation to identifybacterial species. Microbe 9:111-118.

Roh SW, Lee HW, Yim KJ, Shin NR, Lee J (2013) *Rhodopirellularosea* sp. nov. a novel bacterium isolated from an ark clam *Scapharcabroughtonii*. J Microbiol 51:301-304.

Rzhetsky A, Nei M (1992) A simple method for estimating and testing minimum-evolution trees. Mol Biol Evol 9:945-967.

Sahayaraj K, Rajesh S, Asha A, Rathi JM, & Raja P (2014) Distribution and diversity assessment of the marine macroalgae at four southern districts of Tamil Nadu, India.

Saitou N, Nei M (1987) The neighbor-joining method: a new method for reconstructingphylogenetic trees. Mol Bio Evol 4:406-425.

Sandargo B, Jeske O, Boedeker C, Wiegand S, Wennrich J P, Kallscheuer N, Surup F (2020) Stieleriacines, N-Acyl Dehydrotyrosines From the Marine Planctomycete *Stielerianeptunia* sp. nov. Fron Microbiol 11:1408.

Santarella-Mellwig R, Franke J, Jaedicke A et al. (2010) The compartmentalized bacteria of the Planctomycetes- Verrucomicrobia- Chlamydiae superphylum have membrane coat-like proteins. PLoSBio l8:e1000281.

Santarella-Mellwig R, Pruggnaller S, Roos N et al. (2013) Three- dimensional reconstruction of bacteria with a complex endomembrane system. PLoSBiol 11:e1001565.

Santos-Junior CD, Kishi LT, Toyama D et al. (2017) Metagenome sequencing of prokaryotic microbiota collected from rivers in the upper Amazon basin. Genome Announc 5:e01450–16.

Sasser M. (1990) Identification of bacteria by gas chromatography of cellular fatty acids.

Scheuner C, Tindall BJ, Lu M, Nolan M, Lapidus A, *et al*. Complete genome sequence of *Planctomyces brasiliensis* type strain (DSM 5305^{T}), phylogenomic analysis and reclassification of *Planctomycetes* including the descriptions of *Gimesia* gen. nov. *Planctopirus* gen. nov. and *Rubinisphaera* gen. nov. and emended descriptions of the order Planctomycetales and the family Planctomycetaceae. StandGenomic Sci 9:10-27.

Schleifer K (2004) Microbial diversity: facts, problems and prospects. Syst Appl Microbiol 27:3–9.

Schlesner H, Hirsch P (1984) Assignment of ATCC 27377 to *Pirella*gen. nov. as *Pirellastaleyi* comb. nov. Int J Syst Evol Microbiol 34:492-495.

Schlesner H, Rensmann C, Tindall B J, Gade D, Rabus R, Pfeiffer S, & Hirsch P (2004) Taxonomic heterogeneity within the Planctomycetales as derived by DNA–DNA

hybridization, description of *Rhodopirellula baltica* gen. nov. sp. nov. transfer of *Pirellula marina* to the genus *Blastopirellula* gen. nov. as *Blastopirellula marina* comb. nov. and emended description of the genus *Pirellula*. Int J Syst Evol Microbiol 54:1567-1580.

Schloss PD, Westcott SL, Ryabin T, Hall JR, Hartmann M, Hollister EB, Lesniewski RA, Oakley BB, Parks DH, Robinson CJ, Sahl JW (2009) Introducing mothur: open-source, platform-independent, community-supported software for describing and comparing microbial communities. Appl Environ Microbiol 75:7537-41.

Schmid MC, Maas B, Dapena A, Van de Pas-Schoonen K, Van de Vossenberg J, Kartal B, vanNiftrik L, Schmidt I, Cirpus I et al. (2005) Biomarkersfor *in-situ* detection of anaerobic ammonium-oxidizing (Anammox) bacteria. Appl Environ Microbiol 4:1677-1684.

Schmitt S, Tsai P, Bell J, Fromont J, Ilan M, Lindquist N, Perez T, Rodrigo A, Schupp PJ, et al. (2012) Assessing the complex sponge microbiota: core, variable and species-specific bacterial communities in marine sponges. ISME J 3:564-76.

Selvarajan R, Sibanda T, Tekere M et al. (2017) Diversity analysis and bioresource characterization of halophilic bacteria isolated from a South African saltpan. Molecules 22:E657.

She S, Niu J, Zhang C et al. (2016) Significant relationship between soil bacterial community structure and incidence of bacterial wilt disease under continuous cropping system. Arch Microbiol 2:267–75.

Shi H, Bratton BP, Gitai Z & HuangKC (2018) How to build a bacterial cell: MreB as the foreman of *E. coli* construction. Cell 172: 1294–1305.

Shivani Y, Subhash Y, Sasikala Ch, Ramana ChV (2017) Characterisation of a newly isolated member of a candidatus lineage, *Marispirochaetaaestuarii* gen. nov. sp. nov. Int J Syst Evol Microbiol 67:3829-3936.

Sipkema D, Holmes B, Nichols SA, Blanch HW (2009) Biological characterisation of *Haliclona*(?*gellius*) sp.: sponge and associated microorganisms. Microb Ecol 58:903–20.

Sittig M, Schlesner H (1993) Chemotaxonomic investigation of various prosthecate and/or budding bacteria. Syst Appl Microbiol 16:92-103.

Stackebrandt E, Ludwig W, Schubert W et al. (1984) Molecular genetic evidence for early evolutionary origin of budding peptidoglycan-less eubacteria. Nature 307:735–7.

Stackebrandt E, Wehmeyer U, Liesack W (1986) 16S ribosomal RNA- and cell wall analysis of *Gemmata obscuriglobus*, a new member of the order Planctomycetales. FEMS Microbiol Lett 37:289–92.

Staley JT, Fuerst JA, Giovannoni S, Schlesner, H (1992) The order Planctomycetales and the genera *Planctomyces*, *Pirellula*, *Gemmata*, and *Isosphaera*. In The Prokaryotes. Springer, New York4: 3710–3731.

Steinert G, Wemheuer B, Janussen D, Erpenbeck D, Daniel R, Simon M, Brinkhoff T, Schupp PJ (2019) Prokaryotic diversity and community patterns in Antarctic continental shelf sponges. Front Mar Sci 6:297.

Strous M, Fuerst JA, Kramer EH et al. (1999) Missing lithotroph identified as new planctomycete. Nature 400:446–9.

Taylor MW, Radax R, Steger D, Wagner M (2007) Sponge-associated microorganisms: evolution, ecology, and biotechnological potential. Microbiol Mol Biol Rev 71:295–347.

Taylor MW, Tsai P, Simister RL, Deines P, Botte E, Ericson G, et al. (2013) Sponge-specific bacteria are widespread (but rare) in diverse marine environments. ISME J 7:438–43.

Tla´skalV, Zru˚stova´P, Vrs˘kaTet al. (2017) Bacteria associated with decomposing dead wood in a natural temperate forest. FEMS Microbiol Ecol 93: 432-449.

Tully BJ, Sachdeva R, Graham ED et al. (2017a) 290 metagenome- assembled genomes from the Mediterranean Sea: a resource for marine microbiology. Peer J 5:e3558.

Tully BJ, Wheat CG, Glazer BT et al. (2017b) A dynamic microbial community with high functional redundancy inhabits the cold, oxic sub sea floor aquifer. ISME J 12:1–16.

Van Niftrik L, Geerts WJ, van Donselaar EG, Humbel BM, Webb RI, Fuerst JA, Verkleij AJ, Jetten MSM &Strous M (2008a) A Linking ultrastructure and function in four genera of anaerobic ammonium-oxidizing bacteria: cell plan, glycogen storage, and localization of cytochrome C proteins. J Bacteriol 190: 708–717.

Van Niftrik L, Geerts WJ, van Donselaar EG, Humbel BM, Yakushevska A, Verkleij AJ, Jetten MSM, & Strous M (2008b) Combined structural and chemical analysis of the anammoxosome: a membrane-bounded intracytoplasmic compartment in anammox bacteria. J Struct Biol 161: 401–410.

Van Teeseling MC, Mesman RJ, Kuru E et al. (2015) Anammox Planctomycetes have a peptidoglycan cell wall. Nat Commun 6:6878.

Van Teeseling MCF, Benz R, de Almeida NM et al. (2017) Characterization of the first planctomycetal outer membrane protein identifies a channel in the outer membrane of the anammox bacterium *Kueneniastutt gartiensis*. BiochimBiophys Acta 1860:767–76.

Vergin KL, Urbach E, Stein JL et al. (1998) Screening of a fosmid library of marine environmental genomic DNA fragments reveals four clones related to members of the order Planctomycetales.Appl Environ Microb 64:3075–8.

Vigneron A, Alsop EB, Cruaud P et al. (2017) Comparative metagenomics of hydrocarbon and methane seeps of the Gulf of Mexico. Sci Rep 7:16015.

Vollmer W, Holtje JV (2004) The architecture of the murein (peptidoglycan) in gram-negative bacteria: vertical scaffold or horizontal layer(s)? J Bacteriol 186:5978–87.

Wagner M, Horn M (2006) The Planctomycetes, Verrucomicrobia, Chlamydiae and sister phyla comprise a superphylum with biotechnological and medical relevance. Curr Opin Biotechnol 17, 241-249.

Wagstaff J & Löwe J (2018) Prokaryotic cytoskeletons: protein filaments organizing small cells. Nat. Rev. Microbiol 16:187–201.

Wallner SR, Bauer M, Wu¨rdemann C et al. (2005) Highly enantio selective sec-alkyl sulfatase activity of the marine planctomycete *Rhodopirellula baltica* shows retention of configuration. AngewChemInt Ed 44:6381–4.

Waqqas M, Salbreiter M, Kallscheuer N, Jogler M, Wiegand S, Heuer A, Rast P, Peeters SH, Boedeker C, Jetten MS, Rohde M. (2020) *Rosistilla oblonga* gen. nov. sp. nov. and *Rosistilla carotiformis* sp. nov. isolated from biotic or abiotic surfaces in Northern Germany, Mallorca, Spain and California, USA. Antonie van Leeuwenhoek 113:1939-1952.

Wattam AR, Davis JJ, Assaf R, Boisvert S, Brettin T, Bun C (2017) Improvements to PATRIC, the all-bacterial bioinformatics database and analysis resource centre. Nucleic Acids Res 45:535-542.

Webster NS, Cobb RE, Negri AP (2008) Temperature thresholds for bacterial symbiosis with a sponge. ISME J 2:830–42.

Weisz JB, Hentschel U, Lindquist N, Martens CS (2007) Linking abundance and diversity of sponge-associated microbial communities to metabolic differences in host sponges. Mar Biol 152:475–83.

Wick RR, Judd LM, Gorrie CL, Holt KE (2017) Unicycler: resolving bacterial genome assemblies from short and long sequencing reads. PLoS Comput Biol 13:e1005595.

Wiegand S, Jogler M, Boedeker C, Pinto D, Vollmers J, Rivas-Marín E, Oberbeckmann S et al. (2020) Cultivation and functional characterization of 79 Planctomycetes uncovers their unique biology. Nat Microbio l5:126-140.

Wiegand S, Jogler M, Jogler C (2018) On the maverick Planctomycetes. FEMS Microbiol Rev 42:739-760.

Wilkinson CR (1979) Nutrient translocation from symbiotic cyanobacteria to coral reef sponges. In: Levi C, Boury-Esnault N, editors. Biologie des Spongiaires. Paris: C.N.R.S.; p 373–80.

Woebken D, Teeling H, Wecker P et al. (2007) Fosmids of novel marine *Planctomycetes* from the Namibian and Oregon coast upwelling systems and their cross-comparison with planctomycete genomes. ISMEJ 1:419–435.

Xia W, Jia Z, Bowatte S et al. (2017) Impact of elevated atmospheric CO2 on soil bacteria community in a grazed pasture after 12-year enrichment. Geoderma 285:19–26.

Xu X, Zhang X. (2015) *Lentinula edodes* derived polysaccharide alters the spatial structure of gut microbiota in mice. PLoS One 10:e0115037.

Yang Z (1997) PAML: a program package for phylogenetic analysis by maximum likelihood. Bioinformatics13:555-556.

Yarza P, Yilmaz P, Pruesse E, Glöckner FO, Ludwig W, SchleiferK H,Rosselló-Móra R (2014) Uniting the classification of cultured and uncultured bacteria and archaea using 16S rRNA gene sequences. Nat Rev Microbiol 12:635-645.

Yoon J, Matsuo Y, Kasai H, Lee MK (2014) Phylogenetic and taxonomic analyses of *Rhodopirellulacaenicola* sp. nov. A new marine Planctomycetes species isolatedfrom iron sand. J Phylogenetics Evol Biol 3:143.

Yoon SH, Ha SM, Kwon S, Lim J, Kim Y, et al. (2017) Introducing EzBioCloud: A taxonomically united database of 16S rRNA and whole genome assemblies. Int J Syst Evol Microbiol 67:1613–1617.

Yun J, Deng Y, Zhang H (2017) Anthropogenic protection alters the microbiome in intertidal mangrove wetlands in Hainan Island. Appl Microbiol Biot 101:6241–625.

Zeng S, Huang Z, Hou D et al. (2017) Composition, diversity and function of intestinal microbiota in pacific white shrimp (*Litope- naeusvannamei*) at different culture stages. PeerJ 5: e3986.

Zhang C (2018) "Biosynthesis of carotenoids and apocarotenoids by microorganismsand their industrial potential" *InProgress in Carotenoid Research*, eds L.Q. Zepka,E. Jacob-Lopes, V. Vera de Rosso. Intech Open Ltd.

Zhao L, Chang WC, Xiao Y, Liu HW, Liu P (2013) Methylerythritol phosphate pathway of isoprenoid biosynthesis. Annu Rev Biochem 82:497–530.

Zielin´ska S, Radkowski P, Blendowska A et al. (2017) The choice of the DNA extraction method may influence the outcome of the soil microbial community structure analysis. Microbiology- open 6:e453.

Annexures

Annexure 1a. Gujarat sampling Details (December 2016)

Sample no.	Date of collection	Geographical locations	GPS Coordinate	Type of samples
1	22/12/2016	Near Veraval coast	20° 54' 29" N/ 70° 21' 31" E	Brown sargassam
2	22/12/2016	Near Veraval coast	20° 54' 29" N/ 70° 21' 31" E	Pink sea weed
3	22/12/2016	Near Veraval coast	20° 54' 29" N/ 70° 21' 31" E	Brown gracilaria (gelatinous)
4	22/12/2016	Near Veraval coast	20° 54' 29" N/ 70° 21' 31" E	Green gelatinous alage
5	22/12/2016	Near Veraval coast	20° 54' 29" N/ 70° 21' 31" E	Green algae
6	22/12/2016	Near Veraval coast	20° 54' 29" N/ 70° 21' 31" E	Brown gracilaria
7	22/12/2016	Near Veraval coast	20° 54' 29" N/ 70° 21' 31" E	Rust brown leafy
8	22/12/2016	Near Veraval coast	20° 54' 29" N/ 70° 21' 31" E	Brown broad
9	22/12/2016	Near Veraval coast	20° 54' 29" N/ 70° 21' 31" E	Green-most abundant
10	22/12/2016	Near Veraval coast	20° 54' 29" N/ 70° 21' 31" E	purple
11	22/12/2016	Near Veraval coast	20° 54' 29" N/ 70° 21' 31" E	Brown floating
12	22/12/2016	Near Veraval coast	20° 54' 29" N/ 70° 21' 31" E	Sticking to rock
13	22/12/2016	Near Veraval coast	20° 54' 29" N/ 70° 21' 31" E	sediment
14	22/12/2016	Near Veraval coast	20° 54' 29" N/ 70° 21' 31" E	sediment
15	22/12/2016	Near Veraval coast	20° 54' 29" N/ 70° 21' 31" E	sediment
16	22/12/2016	Near Veraval coast	20° 54' 29" N/ 70° 21' 31" E	Decolourising broad alga
17	22/12/2016	Near Veraval coast	20° 54' 29" N/ 70° 21' 31" E	Pebble with purple layer
18	22/12/2016	Near Veraval coast	20° 54' 29" N/ 70° 21' 31" E	Small water pool with yellow brown biofilm layer at bottom
19	22/12/2016	Near Veraval coast	20° 54' 29" N/ 70° 21' 31" E	Other pebble with brown
20	22/12/2016	Near Veraval coast	20° 54' 29" N/ 70° 21' 31" E	Epilithic green seen at the fringes
21	22/12/2016	Near Veraval coast	20° 54' 29" N/ 70° 21' 31" E	Black color growth on stone
22	22/12/2016	Near Veraval coast	20° 54' 29" N/ 70° 21' 31" E	Green floating
23	22/12/2016	Near Veraval coast	20° 54' 29" N/ 70° 21' 31" E	Green globular gelatinous
24	23/12/2016	Way to Dwarka	21° 32' 35'' N/ 69° 42' 42" E	Algal mat near bridge
25	23/12/2016	Way to Dwarka	21° 32' 35'' N/ 69° 42' 42" E	Sediment
26	23/12/2016	Way to Dwarka	21° 32' 35'' N/ 69° 42' 42" E	Water sea
27	23/12/2016	Way to Dwarka	21° 32' 35'' N/ 69° 42' 42" E	Flower
28	23/12/2016	Way to Dwarka	21° 32' 35'' N/ 69° 42' 42" E	Flower
29	23/12/2016	Way to Dwarka	21° 41' 22'' N/ 69° 33' 61" E	Algal biofilm phytoplanktonic
30	23/12/2016	Way to Dwarka	21° 41' 22'' N/ 69° 33' 61" E	Brown pond without algal phytoplankton
31	23/12/2016	Way to Dwarka	21° 41' 22'' N/ 69° 33' 61" E	Algal sample from brown pond
32	23/12/2016	Way to Dwarka	21° 41' 22'' N/ 69° 33' 61" E	Biofilm on rock

33	23/12/2016	Way to Dwarka	21° 41' 22'' N/ 69° 33' 61" E	Black sediment below brown water and layer
34	23/12/2016	Way to Dwarka	21° 41' 22'' N/ 69° 33' 61" E	Alga in bigger pond like infloresence of onion
35	23/12/2016	Way to Dwarka	21° 41' 22'' N/ 69° 33' 61" E	Alga in smaller pond like grass
36	23/12/2016	Way to Dwarka	21° 41' 22'' N/ 69° 33' 61" E	Border of big pond.brown layer on rock sponge with prawn eggs and small fringes.
37	23/12/2016	Way to Dwarka	21° 41' 22'' N/ 69° 33' 61" E	Hard soil-stone with green layer.
38	23/12/2016	Way to Dwarka	21° 41' 22'' N/ 69° 33' 61" E	Algae
39	23/12/2016	Way to Dwarka	21° 41' 22'' N/ 69° 33' 61" E	Alga big pond
40	23/12/2016	Way to Dwarka	21° 41' 22'' N/ 69° 33' 61" E	Algae floating(like sponge used for absorbing water)
41	23/12/2016	Way to Dwarka	21° 41' 22'' N/ 69° 33' 61" E	Bacterial layer on small pebbles in big pond.
42	23/12/2016	Way to Dwarka	21° 41' 22'' N/ 69° 33' 61" E	Black soil patches
43	23/12/2016	Way to Dwarka	21° 41' 22'' N/ 69° 33' 61" E	Grass
44	23/12/2016	Way to Dwarka	21° 41' 22'' N/ 69° 33' 61" E	Reddish brown path on sediment at the shore.
45	23/12/2016	Way to Dwarka	21° 41' 22'' N/ 69° 33' 61" E	Fecal material of birds
46	24/12/2016	Shivrajpur coast	22° 19' 94'' N/ 68° 57' 08" E	Brown algae(gelatinous)
47	24/12/2016	Shivrajpur coast	22° 19' 94'' N/ 68° 57' 08" E	Globular green
48	24/12/2016	Shivrajpur coast	22° 19' 94'' N/ 68° 57' 08" E	Brown algae
49	24/12/2016	Shivrajpur coast	22° 19' 94'' N/ 68° 57' 08" E	sediments
50	24/12/2016	Shivrajpur coast	22° 19' 94'' N/ 68° 57' 08" E	Epilithic algal biofilm
51	24/12/2016	Shivrajpur coast	22° 19' 94'' N/ 68° 57' 08" E	Algal growth on rock
52	24/12/2016	Shivrajpur coast	22° 19' 94'' N/ 68° 57' 08" E	Epilithic dark green to black
53	24/12/2016	Shivrajpur coast	22° 19' 94'' N/ 68° 57' 08" E	Bone with purple inner and light purple outer layer
54	24/12/2016	Shivrajpur coast	22° 19' 94'' N/ 68° 57' 08" E	Green sponge
55	24/12/2016	Shivrajpur coast	22° 19' 94'' N/ 68° 57' 08" E	Dark brown to black patch pf algae
56	24/12/2016	Shivrajpur coast	22° 19' 94'' N/ 68° 57' 08" E	Brown biofilm on small pebbles
57	24/12/2016	Shivrajpur coast	22° 19' 94'' N/ 68° 57' 08" E	Epilithic biofilm
58	24/12/2016	Shivrajpur coast	22° 19' 94'' N/ 68° 57' 08" E	Pink brown biofilm on pebble
59	24/12/2016	Shivrajpur coast	22° 19' 94'' N/ 68° 57' 08" E	Zoo plankton
60	24/12/2016	Shivrajpur coast	22° 19' 94'' N/ 68° 57' 08" E	Algae
61	24/12/2016	Shivrajpur coast	22° 19' 94'' N/ 68° 57' 08" E	Black coloured sea sediment
62	24/12/2016	Shivrajpur coast	22° 19' 94'' N/ 68° 57' 08" E	Zooplankton different number
63	24/12/2016	Shivrajpur coast	22° 19' 94'' N/ 68° 57' 08" E	Sponges
64	24/12/2016	Shivrajpur coast	22° 19' 94'' N/ 68° 57' 08" E	Green sponge like
65	24/12/2016	Shivrajpur coast	22° 19' 94'' N/ 68° 57' 08" E	Soft tissue sponge

66	24/12/2016	Shivrajpur coast	22° 19' 94'' N/ 68° 57' 08" E	Brown mat
67	24/12/2016	Shivrajpur coast	22° 19' 94'' N/ 68° 57' 08" E	Algae
68	24/12/2016	Shivrajpur coast	22° 19' 94'' N/ 68° 57' 08" E	Sponge like mass
69	24/12/2016	Shivrajpur coast	22° 19' 94'' N/ 68° 57' 08" E	Light green sponge
70	24/12/2016	Shivrajpur coast	22° 19' 94'' N/ 68° 57' 08" E	Green sponge
71	24/12/2016	Shivrajpur coast	22° 19' 94'' N/ 68° 57' 08" E	Young coral-purple and brown
72	24/12/2016	Shivrajpur coast	22° 19' 94'' N/ 68° 57' 08" E	
73	24/12/2016	Shivrajpur coast	22° 19' 94'' N/ 68° 57' 08" E	Reddish sargassam
74	24/12/2016	Shivrajpur coast	22° 19' 94'' N/ 68° 57' 08" E	Brown alga
75	24/12/2016	Shivrajpur coast	22° 19' 94'' N/ 68° 57' 08" E	Green with concentric ring
76	24/12/2016	Shivrajpur coast	22° 19' 94'' N/ 68° 57' 08" E	Green brown Alga
77	24/12/2016	Shivrajpur coast	22° 19' 94'' N/ 68° 57' 08" E	Gelly like
78	24/12/2016	Shivrajpur coast	22° 19' 94'' N/ 68° 57' 08" E	Algae
79	24/12/2016	Shivrajpur coast	22° 19' 94'' N/ 68° 57' 08" E	Brown sargassam
80	24/12/2016	Shivrajpur coast	22° 19' 94'' N/ 68° 57' 08" E	Brown alga with spots
81	24/12/2016	Shivrajpur coast	22° 19' 94'' N/ 68° 57' 08" E	Coral
82	24/12/2016	Shivrajpur coast	22° 19' 94'' N/ 68° 57' 08" E	Algae-new type
83	24/12/2016	Shivrajpur coast	22° 19' 94'' N/ 68° 57' 08" E	Green sponge(grassy)
84	24/12/2016	Shivrajpur coast	22° 19' 94'' N/ 68° 57' 08" E	Molluscan live(moving)
85	24/12/2016	Shivrajpur coast	22° 19' 94'' N/ 68° 57' 08" E	Algae
86	24/12/2016	Shivrajpur coast	22° 19' 94'' N/ 68° 57' 08" E	Light green alga
87	24/12/2016	Shivrajpur coast	22° 19' 94'' N/ 68° 57' 08" E	Other alga
88	24/12/2016	Shivrajpur coast	22° 19' 94'' N/ 68° 57' 08" E	Sponge
89	24/12/2016	Shivrajpur coast	22° 19' 94'' N/ 68° 57' 08" E	Orange soft mass
90	24/12/2016	Shivrajpur coast	22° 19' 94'' N/ 68° 57' 08" E	Bulbous alga
91	24/12/2016	Shivrajpur coast	22° 19' 94'' N/ 68° 57' 08" E	Purple layer on soil sediment
92	24/12/2016	Shivrajpur coast	22° 19' 94'' N/ 68° 57' 08" E	Gracilaria
93	24/12/2016	Shivrajpur coast	22° 19' 94'' N/ 68° 57' 08" E	Gracilaria
94	24/12/2016	Shivrajpur coast	22° 19' 94'' N/ 68° 57' 08" E	Algae
95	24/12/2016	Shivrajpur coast	22° 19' 94'' N/ 68° 57' 08" E	Brown algae
96	24/12/2016	Shivrajpur coast	22° 19' 94'' N/ 68° 57' 08" E	Alga
97	24/12/2016	Shivrajpur coast	22° 19' 94'' N/ 68° 57' 08" E	Green alga like spring
98	24/12/2016	Shivrajpur coast	22° 19' 94'' N/ 68° 57' 08" E	Dark brown alga
99	24/12/2016	Shivrajpur coast	22° 19' 94'' N/ 68° 57' 08" E	Brown alga
100	24/12/2016	Shivrajpur coast	22° 19' 94'' N/ 68° 57' 08" E	Algal sample-compound leaf

101	24/12/2016	Shivrajpur coast	22° 19' 94'' N/ 68° 57' 08" E	Red alga-thin sheet
102	24/12/2016	Shivrajpur coast	22° 19' 94'' N/ 68° 57' 08" E	Light green coral-young and soft
103	24/12/2016	Shivrajpur coast	22° 19' 94'' N/ 68° 57' 08" E	Red alga
104	24/12/2016	Shivrajpur coast	22° 19' 94'' N/ 68° 57' 08" E	Reddish brown and brown biofim
105	24/12/2016	Shivrajpur coast	22° 19' 94'' N/ 68° 57' 08" E	Green alga like grass
106	24/12/2016	Shivrajpur coast	22° 19' 94'' N/ 68° 57' 08" E	sediment
107	24/12/2016	Shivrajpur coast	22° 19' 94'' N/ 68° 57' 08" E	sediment
108	24/12/2016	Shivrajpur coast	22° 19' 94'' N/ 68° 57' 08" E	sediment
109	24/12/2016	Shivrajpur coast	22° 19' 94'' N/ 68° 57' 08" E	sediment
110	24/12/2016	Shivrajpur coast	22° 19' 94'' N/ 68° 57' 08" E	sediment
111	25/12/2016	Bet Dwarka coast	22° 26' 97'' N/ 69° 06' 54" E	Dead sponge
112	25/12/2016	Bet Dwarka coast	22° 26' 97'' N/ 69° 06' 54" E	Hair like dark brown alga
113	25/12/2016	Bet Dwarka coast	22° 26' 97'' N/ 69° 06' 54" E	Soil/sediment near mangrove plant
114	25/12/2016	Bet Dwarka coast	22° 26' 97'' N/ 69° 06' 54" E	Purple sponge
115	25/12/2016	Bet Dwarka coast	22° 26' 97'' N/ 69° 06' 54" E	Sponge like alga but not sponge
116	25/12/2016	Bet Dwarka coast	22° 26' 97'' N/ 69° 06' 54" E	Noodles like sponge-brown in colour
117	25/12/2016	Bet Dwarka coast	22° 26' 97'' N/ 69° 06' 54" E	Brown layer on small rock
118	25/12/2016	Bet Dwarka coast	22° 26' 97'' N/ 69° 06' 54" E	Dry air sac of sargassum washed to the shore
119	25/12/2016	Bet Dwarka coast	22° 26' 97'' N/ 69° 06' 54" E	Brown colour growth on sand
120	25/12/2016	Bet Dwarka coast	22° 26' 97'' N/ 69° 06' 54" E	Sediment composite
121	25/12/2016	Bet Dwarka coast	22° 26' 97'' N/ 69° 06' 54" E	Rocks
122	25/12/2016	Bet Dwarka coast	22° 26' 97'' N/ 69° 06' 54" E	Another green sponge
123	25/12/2016	Bet Dwarka coast	22° 26' 97'' N/ 69° 06' 54" E	sediment
124	25/12/2016	Bet Dwarka coast	22° 26' 97'' N/ 69° 06' 54" E	sediment
125	26/12/2016	Jogadh Eco Park	22° 43' 26'' N/ 70° 28' 40" E	Sediment sample.pond with water.
126	26/12/2016	Jogadh Eco Park	22° 43' 26'' N/ 70° 28' 40" E	Lotus bud
127	26/12/2016	Jogadh Eco Park	22° 43' 26'' N/ 70° 28' 40" E	Fresh water body with yellow brown biofilm
128	26/12/2016	Jogadh Eco Park	22° 43' 26'' N/ 70° 28' 40" E	Sediment water body
129	26/12/2016	Jogadh Eco Park	22° 43' 26'' N/ 70° 28' 40" E	Salt crytalizing with pink
130	26/12/2016	Jogadh Eco Park	22° 43' 26'' N/ 70° 28' 40" E	Sponge like in water body
131	26/12/2016	Jogadh Eco Park	22° 43' 26'' N/ 70° 28' 40" E	Orange salt
132	26/12/2016	Jogadh Eco Park	22° 43' 26'' N/ 70° 28' 40" E	Water in which sponge found+sponge in a falcon tube
133	26/12/2016	Jogadh Eco Park	22° 43' 26'' N/ 70° 28' 40" E	Yellow coloured in a small pond
134	26/12/2016	Jogadh Eco Park	22° 43' 26'' N/ 70° 28' 40" E	Algal mat with APB in the bottom

135	26/12/2016	Jogadh Eco Park	22° 43' 26'' N/ 70° 28' 40" E	Purple bed layer gelatinous below algal mat
136	26/12/2016	Jogadh Eco Park	22° 43' 26'' N/ 70° 28' 40" E	Algal biofilm with brown on top.
137	26/12/2016	Jogadh Eco Park	22° 43' 26'' N/ 70° 28' 40" E	Black sediment with lot of hydrogen sulphide smell
138	26/12/2016	Jogadh Eco Park	22° 43' 26'' N/ 70° 28' 40" E	Brown layer on sediment
139	26/12/2016	Jogadh Eco Park	22° 43' 26'' N/ 70° 28' 40" E	Dark brown growth on grass
140	26/12/2016	Jogadh Eco Park	22° 43' 26'' N/ 70° 28' 40" E	Brown sponge
141	26/12/2016	Jogadh Eco Park	22° 43' 26'' N/ 70° 28' 40" E	Reddish brown sponge
142	26/12/2016	Jogadh Eco Park	22° 43' 26'' N/ 70° 28' 40" E	Brown sponge,salt crystal
143	26/12/2016	Jogadh Eco Park	22° 43' 26'' N/ 70° 28' 40" E	Brown sponge
144	27/12/2016	Wild Ass Sanctuary	23° 08' 45'' N/ 71° 45' 40" E	Sediment brown pond
145	27/12/2016	Wild Ass Sanctuary	23° 08' 45'' N/ 71° 45' 40" E	Brown pond sediment
146	27/12/2016	Wild Ass Sanctuary	23° 08' 45'' N/ 71° 45' 40" E	Sediment brown on top not immersed in water.
147	27/12/2016	Wild Ass Sanctuary	23° 08' 45'' N/ 71° 45' 40" E	Light coloured sediment
148	27/12/2016	Wild Ass Sanctuary	23° 08' 45'' N/ 71° 45' 40" E	Green coloured sponge
149	27/12/2016	Wild Ass Sanctuary	23° 08' 45'' N/ 71° 45' 40" E	sponge
150	27/12/2016	Wild Ass Sanctuary	23° 08' 45'' N/ 71° 45' 40" E	Algal biofilm on the sediment.black at the bottom
151	27/12/2016	Wild Ass Sanctuary	23° 08' 45'' N/ 71° 45' 40" E	Brown layer also on algal mat with grass at the wet soil
152	27/12/2016	Wild Ass Sanctuary	23° 08' 45'' N/ 71° 45' 40" E	Fecal material of wild ass
153	27/12/2016	Wild Ass Sanctuary	23° 08' 45'' N/ 71° 45' 40" E	Floating algal biofilm
154	27/12/2016	Wild Ass Sanctuary	23° 08' 45'' N/ 71° 45' 40" E	Brown layer on the top of a water body
155	27/12/2016	Wild Ass Sanctuary	23° 08' 45'' N/ 71° 45' 40" E	Water body with grass algal mass at the bottom
156	27/12/2016	Wild Ass Sanctuary	23° 08' 45'' N/ 71° 45' 40" E	Brown photosynthetic at the sediment in a shallow water body.
157	27/12/2016	Wild Ass Sanctuary	23° 08' 45'' N/ 71° 45' 40" E	Green florescent,filamentous gelatinous mass.
158	27/12/2016	Wild Ass Sanctuary	23° 08' 45'' N/ 71° 45' 40" E	Floating algal biofilm
159	28/12/2016	Salt pan, way to Bhuj	23° 09' 11'' N/ 70° 44' 16" E	Salt crystallizing as protruding bud
160	28/12/2016	Salt pan, way to Bhuj	23° 09' 11'' N/ 70° 44' 16" E	Normal crystallisation
161	28/12/2016	Salt pan, way to Bhuj	23° 09' 11'' N/ 70° 44' 16" E	Brown layer on black sediment.
162	28/12/2016	Salt pan, way to Bhuj	23° 09' 11'' N/ 70° 44' 16" E	Surface crystals on water.
163	28/12/2016	Salt pan, way to Bhuj	23° 09' 11'' N/ 70° 44' 16" E	Red layer on crystalising salt.
164	28/12/2016	Salt pan, way to Bhuj	23° 09' 11'' N/ 70° 44' 16" E	Brown layer
165	28/12/2016	Salt pan, way to Bhuj	23° 09' 11'' N/ 70° 44' 16" E	Pinkish crystal.
166	29/12/2016	Pingleshwar beach	23° 09' 11'' N/ 70° 44' 16" E	Brown reddish algal mass
167	29/12/2016	Pingleshwar beach	23° 09' 11'' N/ 70° 44' 16" E	Brown reddish alga

168	29/12/2016	Pingleshwar beach	23° 09' 11'' N/ 70° 44' 16" E	Brown red alga
169	29/12/2016	Pingleshwar beach	23° 09' 11'' N/ 70° 44' 16" E	Green alga
170	29/12/2016	Pingleshwar beach	23° 09' 11'' N/ 70° 44' 16" E	Green alga small
171	29/12/2016	Pingleshwar beach	23° 09' 11'' N/ 70° 44' 16" E	Bulbous alga green
172	29/12/2016	Pingleshwar beach	23° 09' 11'' N/ 70° 44' 16" E	Alga on edge with a layer like growth sticking & difficult to remove.
173	29/12/2016	Pingleshwar beach	23° 09' 11'' N/ 70° 44' 16" E	Orange layer on rock
174	29/12/2016	Pingleshwar beach	23° 09' 11'' N/ 70° 44' 16" E	Decolorised alga
175	29/12/2016	Pingleshwar beach	23° 09' 11'' N/ 70° 44' 16" E	Algae with dots
176	29/12/2016	Pingleshwar beach	23° 09' 11'' N/ 70° 44' 16" E	
177	29/12/2016	Pingleshwar beach	23° 09' 11'' N/ 70° 44' 16" E	Fern like alage attached to rock surface
178	29/12/2016	Pingleshwar beach	23° 09' 11'' N/ 70° 44' 16" E	Green sponge like alga
179	29/12/2016	Pingleshwar beach	23° 09' 11'' N/ 70° 44' 16" E	APB growth on alga
180	29/12/2016	Pingleshwar beach	23° 09' 11'' N/ 70° 44' 16" E	Surface sand with black streak
181	29/12/2016	Pingleshwar beach	23° 09' 11'' N/ 70° 44' 16" E	Gelly fish
182	29/12/2016	Pingleshwar beach	23° 09' 11'' N/ 70° 44' 16" E	Green yellow noodle like
183	29/12/2016	Pingleshwar beach	23° 09' 11'' N/ 70° 44' 16" E	Red alga
184	29/12/2016	Pingleshwar beach	23° 09' 11'' N/ 70° 44' 16" E	
185	29/12/2016	Pingleshwar beach	23° 09' 11'' N/ 70° 44' 16" E	Green alga
186	29/12/2016	Pingleshwar beach	23° 09' 11'' N/ 70° 44' 16" E	Green alag-Gelidium like
187	29/12/2016	Pingleshwar beach	23° 09' 11'' N/ 70° 44' 16" E	Green mass like epilithic growth
188	29/12/2016	Pingleshwar beach	23° 09' 11'' N/ 70° 44' 16" E	Thread like green alga
189	29/12/2016	Pingleshwar beach	23° 09' 11'' N/ 70° 44' 16" E	Green alga
190	29/12/2016	Pingleshwar beach	23° 09' 11'' N/ 70° 44' 16" E	Black alga
191	29/12/2016	Pingleshwar beach	23° 09' 11'' N/ 70° 44' 16" E	Green alga unique
192	29/12/2016	Pingleshwar beach	23° 09' 11'' N/ 70° 44' 16" E	Red bottom to green mass on rock
193	29/12/2016	Pingleshwar beach	23° 09' 11'' N/ 70° 44' 16" E	Assorted alagae
194	29/12/2016	Pingleshwar beach	23° 09' 11'' N/ 70° 44' 16" E	Gelidium with pink & attached to rock
195	29/12/2016	Pingleshwar beach	23° 09' 11'' N/ 70° 44' 16" E	Red gelatinous sponge
196	29/12/2016	Pingleshwar beach	23° 09' 11'' N/ 70° 44' 16" E	Red orange sponge
197	29/12/2016	Pingleshwar beach	23° 09' 11'' N/ 70° 44' 16" E	Ash colour
198	29/12/2016	Pingleshwar beach	23° 09' 11'' N/ 70° 44' 16" E	Blue green mass
199	29/12/2016	Pingleshwar beach	23° 09' 11'' N/ 70° 44' 16" E	Green alga
200	29/12/2016	Pingleshwar beach	23° 09' 11'' N/ 70° 44' 16" E	Green alga
201	29/12/2016	Pingleshwar beach	23° 09' 11'' N/ 70° 44' 16" E	B

202	29/12/2016	Pingleshwar beach	23° 09' 11'' N/ 70° 44' 16" E	Brown alga smaller
203	29/12/2016	Pingleshwar beach	23° 09' 11'' N/ 70° 44' 16" E	Transparent in a falcon tube
204	29/12/2016	Pingleshwar beach	23° 09' 11'' N/ 70° 44' 16" E	Plastic cover withAPB biofilm
205	29/12/2016	Pingleshwar beach	23° 09' 11'' N/ 70° 44' 16" E	Black specimen
206	29/12/2016	Pingleshwar beach	23° 09' 11'' N/ 70° 44' 16" E	Reddish brown alga
207	29/12/2016	Pingleshwar beach	23° 09' 11'' N/ 70° 44' 16" E	Dark green floating mat
208	29/12/2016	Pingleshwar beach	23° 09' 11'' N/ 70° 44' 16" E	Algal biomass with APB on.
209	29/12/2016	Pingleshwar beach	23° 09' 11'' N/ 70° 44' 16" E	Algae
210	29/12/2016	Pingleshwar beach	23° 09' 11'' N/ 70° 44' 16" E	Water sample
211	29/12/2016	Pingleshwar beach	23° 09' 11'' N/ 70° 44' 16" E	Water grass
212	29/12/2016	Pingleshwar beach	23° 09' 11'' N/ 70° 44' 16" E	Globular mass ash coloured
213	29/12/2016	Pingleshwar beach	23° 09' 11'' N/ 70° 44' 16" E	Orange sponge polyp
214	29/12/2016	Pingleshwar beach	23° 09' 11'' N/ 70° 44' 16" E	Algal mass with above green,below brown
215	29/12/2016	Pingleshwar beach	23° 09' 11'' N/ 70° 44' 16" E	Transparent gelly
216	30/12/2016	Rann of Kutch	23° 19' 53'' N/ 69° 32' 25" E	Sediment sample
217	30/12/2016	Rann of Kutch	23° 19' 53'' N/ 69° 32' 25" E	Just surface water
218	30/12/2016	Rann of Kutch	23° 19' 53'' N/ 69° 32' 25" E	Orange color salt crystal
219	30/12/2016	Rann of Kutch	23° 19' 53'' N/ 69° 32' 25" E	Brown water along with sediment
220	30/12/2016	Rann of Kutch	23° 19' 53'' N/ 69° 32' 25" E	Salt crystal
221	30/12/2016	Rann of Kutch	23° 19' 53'' N/ 69° 32' 25" E	Alage
222	30/12/2016	Rann of Kutch	23° 19' 53'' N/ 69° 32' 25" E	Alage
223	30/12/2016	Rann of Kutch	23° 19' 53'' N/ 69° 32' 25" E	Sediment brown sample
224	30/12/2016	Rann of Kutch	23° 19' 53'' N/ 69° 32' 25" E	Orange color salt with water
225	30/12/2016	Rann of Kutch	23° 19' 53'' N/ 69° 32' 25" E	Pink colour salt crystals
226	30/12/2016	Rann of Kutch	23° 19' 53'' N/ 69° 32' 25" E	Brown color salt
227	30/12/2016	Rann of Kutch	23° 19' 53'' N/ 69° 32' 25" E	White color salt crystal
228	31/12/2016	Bhuj	23° 16' 47'' N/ 69° 21' 06" E	Termites
229	31/12/2016	Bhuj	23° 16' 47'' N/ 69° 21' 06" E	Gum of accassia
230	31/12/2016	Bhuj	23° 16' 47'' N/ 69° 21' 06" E	Bark with fungal infection
231	31/12/2016	Bhuj	23° 16' 47'' N/ 69° 21' 06" E	Flower and fruits from plant for yeast
232	31/12/2016	Bhuj	23° 16' 47'' N/ 69° 21' 06" E	Cactus plant for yeast
233	31/12/2016	Bhuj	23° 16' 47'' N/ 69° 21' 06" E	Orange brown layer below water with salt crystal
234	31/12/2016	Bhuj	23° 16' 47'' N/ 69° 21' 06" E	Rod like multicolor shining crystal
235	31/12/2016	Bhuj	23° 16' 47'' N/ 69° 21' 06" E	Coral like crystal(above water level)

236	31/12/2016	Bhuj	23° 16' 47'' N/ 69° 21' 06" E	Brown color sediment
237	31/12/2016	Bhuj	23° 16' 47'' N/ 69° 21' 06" E	Falcon with water where shining crystal are seen
238	31/12/2016	Bhuj	23° 16' 47'' N/ 69° 21' 06" E	Crystals on leaf of a grass
239	31/12/2016	Bhuj	23° 16' 47'' N/ 69° 21' 06" E	Water where shiny crystals are formed
240	31/12/2016	Bhuj	23° 16' 47'' N/ 69° 21' 06" E	Algae from pond
241	31/12/2016	Bhuj	23° 16' 47'' N/ 69° 21' 06" E	Red orange mass on dry soil
242	31/12/2016	Bhuj	23° 16' 47'' N/ 69° 21' 06" E	Brown mass on dry soil
243	31/12/2016	Bhuj	23° 16' 47'' N/ 69° 21' 06" E	Salt crystals from where aquatic plant is collected
244	31/12/2016	Bhuj	23° 16' 47'' N/ 69° 21' 06" E	Yellow orange mass
245	31/12/2016	Bhuj	23° 16' 47'' N/ 69° 21' 06" E	Globular salt crystals no water
246	31/12/2016	Bhuj	23° 16' 47'' N/ 69° 21' 06" E	Crystals on algal mat
247	31/12/2016	Bhuj	23° 16' 47'' N/ 69° 21' 06" E	Purple mass-shinning
248	31/12/2016	Bhuj	23° 16' 47'' N/ 69° 21' 06" E	Shinning salt
249	31/12/2016	Bhuj	23° 16' 47'' N/ 69° 21' 06" E	Yellow mass
250	31/12/2016	Bhuj	23° 16' 47'' N/ 69° 21' 06" E	Brown one within shinning layer of salt on soil.
251	31/12/2016	Bhuj	23° 16' 47'' N/ 69° 21' 06" E	Black stones
252	31/12/2016	Bhuj	23° 16' 47'' N/ 69° 21' 06" E	Cow dung on which plant is growing
253	31/12/2016	Bhuj	23° 16' 47'' N/ 69° 21' 06" E	Salt crystal
254	31/12/2016	Koteshwar beach	23° 42' 01'' N/ 68° 50' 33" E	Green algae
255	31/12/2016	Koteshwar beach	23° 42' 01'' N/ 68° 50' 33" E	Infected leaf of peepal plant
256	31/12/2016	Koteshwar beach	23° 42' 01'' N/ 68° 50' 33" E	Grapes
257	31/12/2016	Near Kandla port	23° 10' 03'' N/ 70° 12' 29" E	Water pink pond
258	31/12/2016	Near Kandla port	23° 10' 03'' N/ 70° 12' 29" E	Sediment
259	31/12/2016	Near Kandla port	23° 10' 03'' N/ 70° 12' 29" E	Purple water in 1L bottle
260	31/12/2016	Near Kandla port	23° 10' 03'' N/ 70° 12' 29" E	Sediment
261	31/12/2016	Near Kandla port	23° 10' 03'' N/ 70° 12' 29" E	Yellow brown water small body
262	31/12/2016	Near Kandla port	23° 10' 03'' N/ 70° 12' 29" E	Brownish green body with algal biofilm floating water bodies
263	31/12/2016	Near Kandla port	23° 10' 03'' N/ 70° 12' 29" E	Algal plankton & benthic along with sediment
264	31/12/2016	Near Kandla port	23° 10' 03'' N/ 70° 12' 29" E	Water body with only phytoplankton
265	31/12/2016	Near Kandla port	23° 10' 03'' N/ 70° 12' 29" E	Green sulfur pond water in a 1L pond
266	31/12/2016	Near Kandla port	23° 10' 03'' N/ 70° 12' 29" E	Sediment + algal mat
267	31/12/2016	Near Kandla port	23° 10' 03'' N/ 70° 12' 29" E	Plastic paper
268	31/12/2016	Near Kandla port	23° 10' 03'' N/ 70° 12' 29" E	Brown pond

269	31/12/2016	Near Kandla port	23° 10' 03'' N/ 70° 12' 29" E	Sediment not so black as in green pond.

Annexure 1b. Chhattisgarh, Jharkhand, Bihar, Sikkim, West Bengal, Odisha, Andhra Pradesh sample detail (May-June 2017)

Sample no.	Date	Geographical locations	GPS Coordinate	Type of samples
1	17-05-2017	Chhattisgarh	Hirakud dams	Hydra
2	17-05-2017	Chhattisgarh	Hirakud dams	Water
3	17-05-2017	Jharkhand	22° 49' 10" N/ 84° 9' 18"E	Lichens
4	17-05-2017	Jharkhand	22° 49' 10"N/ 84° 9' 18"E	Green lichen on bark
5	17-05-2017	Jharkhand	22° 49' 10"N/ 84° 9' 18" E	Whitish lichen on bark
6	17-05-2017	Jharkhand	22° 49' 10"N/ 84° 9' 18" E	White lichen on tree bark
7	17-05-2017	Jharkhand	22° 49' 10" N/ 84° 9' 18"E	Rock lichen
8	19-05-2017	Bihar, Gaya	25° 13' 27" (N), 85° 5' 11" (E)	Soil sediment from kako road
9	19-05-2017	Bihar Gaya	25° 13' 27" N/ 85° 5' 11"E	Soil sediment from pond
10	19-05-2017	Bihar, Gaya	25° 13' 12" (N), 85° 15' 4" (E)	Soil sediment from brown pond
11	19-05-2017	Bihar, Gaya	25° 13' 12" (N), 85° 15' 4" (E)	Water sediment from brown pond
12	19-05-2017	Bihar, Rajgirh	25° 0' 54" (N), 85° 25' 10" (E)	Sand from brahmakund hotspring
13	19-05-2017	Bihar Rajgirh	25° 0' 54" (N), 85° 25' 10" (E)	Algal mat
14	19-05-2017	Bihar Rajgirh	25° 0' 54" (N), 85° 25' 10" (E)	Algal mat
15	19-05-2017	Bihar Rajgirh	25° 0' 54" (N), 85° 25' 10" (E)	Biofilm
16	20-05-2017	Bihar	25° 30' 24" (N), 86° 33' 30" (E)	Biofilm and water sediment
17	20-05-2017	Bihar	25° 30' 24" (N), 86° 33' 30" (E)	Sediment
18	20-05-2017	Bihar	25° 24' 21" (N), 86° 52' 8" (E)	Leaf with nodules
19	20-05-2017	Bihar	25° 24' 21" (N), 86° 52' 8" (E)	Leaf with nodules
20	20-05-2017	Gangtok to Nathula Sikkim	27° 20' 12" (N), 86° 37' 18" (E)	Leaf with nodules
21	21-05-2017	Gangtok to Nathula	25° 24' 21" (N), 86° 52' 8" (E)	Lichens
22	21-05-2017	Gangtok to Nathula	25° 33' 08" (N), 86° 56' 32" (E)	Snow with black patches
23	21-05-2017	Gangtok to Nathula	25° 33' 08" (N), 86° 56' 32" (E)	Mud from rock
24	21-05-2017	Gangtok to Nathula	25° 33' 08" (N), 86° 56' 32" (E)	Ferns
25	21-05-2017	Gangtok to Nathula	27° 21' 30" (N), 88° 50' 25" (E)	Soil sediment from stream
26	21-05-2017	Gangtok to Nathula	27° 22' 3" (N), 88° 46' 96" (E)	Sediment
27	21-05-2017	Gangtok to Nathula	27° 22' 9" (N), 88° 49' 20" (E)	Ice with mud
28	22-05-2017	way to Lachung	27° 23' 13" (N), 88° 38' 24" (E)	Fruticose lichen
29	22-05-2017	way to Lachung	27° 23' 13" (N), 88° 38' 24" (E)	Orchids
30	22-05-2017	way to Lachung	27° 23' 13" (N), 88° 38' 24" (E)	Lichen on road
31	22-05-2017	way to Lachung	27° 23' 13" (N), 88° 38' 24" (E)	Sediment froma stream
32	22-05-2017	way to Lachung	27° 23' 13" (N), 88° 38' 24" (E)	Marchantia at waterfall
33	22-05-2017	way to Lachung	27° 23' 13" (N), 88° 38' 24" (E)	Bryophyte
34	22-05-2017	way to Lachung	27° 23' 13" (N), 88° 38' 24" (E)	Moss on rock
35	22-05-2017	way to Lachung	27° 23' 13" (N), 88° 38' 24" (E)	Rhizosphere
36	22-05-2017	way to Lachung	27° 23' 13" (N), 88° 38' 24" (E)	Rhizosphere of wild banana
37	22-05-2017	way to Lachung	27° 23' 13" (N), 88° 38' 24" (E)	Pebbles with algal biofilm
38	22-05-2017	way to Lachung	27° 23' 13" (N), 88° 38' 24" (E)	Decomposing forest litter
39	22-05-2017	way to Lachung	27° 23' 13" (N), 88° 38' 24" (E)	Mosss on a tree trunk
40	22-05-2017	way to Lachung	27° 23' 13" (N), 88° 38' 24" (E)	Bryophyte on a rock

41	22-05-2017	way to Lachung	27° 23' 13" (N), 88° 38' 24" (E)	Gelatinous biofilm
42	22-05-2017	way to Lachung	27° 23' 13" (N), 88° 38' 24" (E)	Organic matter within rhizosphere
43	22-05-2017	way to Lachung	27° 23' 13" (N), 88° 38' 24" (E)	Stem Gall
44	22-05-2017	way to Lachung	27° 23' 13" (N), 88° 38' 24" (E)	Fungus in green leaf and uninfected leaf
45	22-05-2017	way to Lachung	27° 23' 13" (N), 88° 38' 24" (E)	Gelatinous biofilm
46	22-05-2017	way to Lachung	27° 23' 13" (N), 88° 38' 24" (E)	Brown mushroom
47	22-05-2017	way to Lachung	27° 26' 34" (N), 88° 36' 32" (E)	Leaf with patches
48	22-05-2017	way to Lachung	27° 26' 34" (N), 88° 36' 32" (E)	Algal biofilm ,brown
49	22-05-2017	way to Lachung	27° 26' 34" (N), 88° 36' 32" (E)	Filamemtous algae
50	22-05-2017	way to Lachung	27° 26' 34" (N), 88° 36' 32" (E)	Bryophyte on tree trunk
51	22-05-2017	way to Lachung	27° 26' 34" (N), 88° 36' 32" (E)	Orchids
52	22-05-2017	way to Lachung	27° 26' 34" (N), 88° 36' 32" (E)	Orchids
53	22-05-2017	way to Lachung	27° 26' 34" (N), 88° 36' 32" (E)	Decompsing organic matter
54	22-05-2017	way to Lachung	27° 26' 34" (N), 88° 36' 32" (E)	leaf with white anf yellow patches
55	22-05-2017	way to Lachung	26° 27' 20" (N), 88° 36' 25" (E)	Sediment
56	22-05-2017	way to Lachung	26° 27' 20" (N), 88° 36' 25" (E)	Rock green lichen
57	22-05-2017	way to Lachung	26° 27' 20" (N), 88° 36' 25" (E)	Polyporous
58	22-05-2017	way to Lachung	26° 27' 20" (N), 88° 36' 25" (E)	Moss on rock
59	22-05-2017	way to Lachung	26° 27' 20" (N), 88° 36' 25" (E)	White Lichen
60	22-05-2017	way to Lachung	26° 27' 20" (N), 88° 36' 25" (E)	Moss with thin branches
61	22-05-2017	way to Lachung	27° 25' 09" (N), 88° 36' 5" (E)	Orange polyporous
62	22-05-2017	way to Lachung	27° 25' 09" (N), 88° 36' 5" (E)	Water and sediments
63	22-05-2017	way to Lachung	27° 55' 27" (N), 88° 43' 35" (E)	Orange fiungus
64	23-05-2017	Yumthang valley	27° 31' 58" (N), 88° 26' 29" (E)	Green lichen
65	23-05-2017	Yumthang valley	27° 31' 58" (N), 88° 26' 29" (E)	Black lichen
66	23-05-2017	Yumthang valley	27° 31' 58" (N), 88° 26' 29" (E)	Grey lichen
67	23-05-2017	Yumthang valley	27° 31' 58" (N), 88° 26' 29" (E)	Rhizosphere of pink-flowered plant
68	23-05-2017	Yumthang valley	27° 31' 58" (N), 88° 26' 29" (E)	Black fructose lichen
69	23-05-2017	Yumthang valley	27° 31' 58" (N), 88° 26' 29" (E)	Herb
70	23-05-2017	Yumthang valley	27° 31' 58" (N), 88° 26' 29" (E)	Small Azilleas
71	23-05-2017	Yumthang valley	27° 31' 58" (N), 88° 26' 29" (E)	Lichen with spherical spaces
72	23-05-2017	Yumthang valley	27° 31' 58" (N), 88° 26' 29" (E)	Shallow water with algal biofilm
73	23-05-2017	Yumthang valley	27° 31' 58" (N), 88° 26' 29" (E)	Sediment with biofilm
74	23-05-2017	Yumthang valley	27° 31' 58" (N), 88° 26' 29" (E)	White lichen
75	23-05-2017	Yumthang valley	27° 31' 58" (N), 88° 26' 29" (E)	Brown algae
76	23-05-2017	Yumthang valley	27° 31' 58" (N), 88° 26' 29" (E)	Lichen
77	23-05-2017	Yumthang valley	27° 31' 58" (N), 88° 26' 29" (E)	Brown algae
78	23-05-2017	Yumthang valley	27° 31' 58" (N), 88° 26' 29" (E)	Brown mass on water
79	23-05-2017	Yumthang valley	27° 31' 58" (N), 88° 26' 29" (E)	Yellow lichen
80	23-05-2017	Yumthang valley	27° 31' 58" (N), 88° 26' 29" (E)	Small lichen underneath crevices
81	23-05-2017	Yumthang valley	27° 31' 58" (N), 88° 26' 29" (E)	Dark yellow lichen
82	23-05-2017	Yumthang valley	27° 31' 58" (N), 88° 26' 29" (E)	Turmeric colour lichen
83	23-05-2017	Yumthang valley	27° 31' 58" (N), 88° 26' 29" (E)	Light yellow foliose with rhizosphere
84	23-05-2017	Yumthang valley	27° 31' 58" (N), 88° 26' 29" (E)	Floating biofilm

85	23-05-2017	Yumthang valley	27° 31' 58" (N), 88° 26' 29" (E)	Orange coloured mat with green algae
86	23-05-2017	Yumthang valley	27° 31' 58" (N), 88° 26' 29" (E)	Black sediment
87	23-05-2017	Yumthang valley	27° 31' 58" (N), 88° 26' 29" (E)	Black icen in stream
88	23-05-2017	Yumthang valley	27° 31' 58" (N), 88° 26' 29" (E)	Biofilm
89	23-05-2017	Yumthang valley	27° 31' 58" (N), 88° 26' 29" (E)	Orange rock biofilm
90	23-05-2017	Yumthang valley	27° 31' 58" (N), 88° 26' 29" (E)	Brown biofilm on ice
91	23-05-2017	Yumthang valley	27° 31' 58" (N), 88° 26' 29" (E)	Cactus rhizosphere
92	23-05-2017	Yumthang valley	27° 31' 58" (N), 88° 26' 29" (E)	White rhizoids
93	23-05-2017	Yumthang valley	27° 31' 58" (N), 88° 26' 29" (E)	Plant from snow
94	23-05-2017	Yumthang valley	27° 31' 58" (N), 88° 26' 29" (E)	River sediment
95	23-05-2017	Yumthang valley	27° 31' 58" (N), 88° 26' 29" (E)	Pink Rhododendron
96	23-05-2017	Yumthang valley	27° 31' 58" (N), 88° 26' 29" (E)	brown bud Rhododendron
97	23-05-2017	Yumthang valley	27° 48' 24" (N), 88° 42' 15" (E)	Yak excreta
98	23-05-2017	Yumthang valley	27° 48' 24" (N), 88° 42' 15" (E)	Green algal biofilm
99	23-05-2017	Yumthang valley	27° 48' 24" (N), 88° 42' 15" (E)	Brownish riveside sediment
100	23-05-2017	Yumthang valley	27° 48' 24" (N), 88° 42' 15" (E)	Yumthang valley water
101	23-05-2017	Yumthang valley	27° 48' 24" (N), 88° 42' 15" (E)	Soil mat
102	23-05-2017	Yumthang valley	27° 47' 35" (N), 88° 42' 27" (E)	Green lichen
103	23-05-2017	Yumthang valley	27° 47' 35" (N), 88° 42' 27" (E)	Algae from hot water spring
104	23-05-2017	Yumthang valley	27° 47' 35" (N), 88° 42' 27" (E)	Hot water from sulphur spring
105	23-05-2017	Yumthang valley	27° 47' 35" (N), 88° 42' 27" (E)	Algal mat from hot spring
106	23-05-2017	Yumthang valley	27° 47' 35" (N), 88° 42' 27" (E)	Cold water from spring
107	23-05-2017	Yumthang valley	27° 47' 35" (N), 88° 42' 27" (E)	Gelatinous algal biofilm
108	23-05-2017	Yumthang valley	27° 47' 35" (N), 88° 42' 27" (E)	Brown lichen
109	23-05-2017	Yumthang valley	27° 47' 35" (N), 88° 42' 27" (E)	White circular lichen
110	23-05-2017	Yumthang valley	27° 47' 35" (N), 88° 42' 27" (E)	Lichen
111	23-05-2017	Yumthang valley	27° 47' 35" (N), 88° 42' 27" (E)	Large grey lichen
112	23-05-2017	Yumthang valley	27° 47' 35" (N), 88° 42' 27" (E)	Orange lichen on pine tree
113	24-05-2017	Lachung, near homestay	27° 40' 13" (N), 88° 43' 37" (E)	Pink flowers
114	24-05-2017	Lachung, near homestay	27° 40' 13" (N), 88° 43' 37" (E)	brown algal mat
115	24-05-2017	Lachung, near homestay	27° 40' 13" (N), 88° 43' 37" (E)	Green algal mat
116	24-05-2017	Lachung, near homestay	27° 40' 13" (N), 88° 43' 37" (E)	Dried moss
117	24-05-2017	Lachung, near homestay	27° 40' 13" (N), 88° 43' 37" (E)	Brown lichen
118	24-05-2017	Lachung, near homestay	27° 40' 13" (N), 88° 43' 37" (E)	Brown mushroom
119	24-05-2017	Lachung, near homestay	27° 40' 13" (N), 88° 43' 37" (E)	Moss mat with rhizosphere
120	24-05-2017	Lachung, near homestay	27° 40' 13" (N), 88° 43' 37" (E)	Dark brown lichen
121	24-05-2017	Lachung, near homestay	27° 40' 13" (N), 88° 43' 37" (E)	Lichen
122	24-05-2017	Lachung, near homestay	27° 40' 13" (N), 88° 43' 37" (E)	Degrading biomass
123	24-05-2017	Lachung, near homestay	27° 40' 13" (N), 88° 43' 37" (E)	Iron containing rock
124	24-05-2017	Lachung, near homestay	27° 40' 13" (N), 88° 43' 37" (E)	Black sediment
125	24-05-2017	Lachung, near homestay	27° 40' 13" (N), 88° 43' 37" (E)	Decomposing cowdung
126	24-05-2017	Lachung, near homestay	27° 40' 13" (N), 88° 43' 37" (E)	Black fruit
127	24-05-2017	Lachung, near homestay	27° 40' 13" (N), 88° 43' 37" (E)	Decaying organic matter
128	24-05-2017	Lachung, near homestay	27° 40' 13" (N), 88° 43' 37" (E)	Infected leaf with orange colour
129	24-05-2017	Lachung, near homestay	27° 40' 13" (N), 88° 43' 37" (E)	Orange lichen on rock
130	24-05-2017	Lachung, near homestay	27° 40' 13" (N), 88° 43' 37" (E)	Gelatinous brown mat

131	24-05-2017	Lachung, near homestay	27° 40' 13" (N), 88° 43' 37" (E)	Stem
132	24-05-2017	Lachung, near homestay	27° 40' 20" (N), 88° 43' 22" (E)	Orange growth on dead matter
133	24-05-2017	Lachung, near homestay	27° 40' 20" (N), 88° 43' 22" (E)	Powdery layer in leaf
134	24-05-2017	Lachung, near homestay	27° 40' 20" (N), 88° 43' 22" (E)	Rhododendron leaves
135	24-05-2017	Lachung, near homestay	27° 40' 20" (N), 88° 43' 22" (E)	Ecological succession on rock
136	24-05-2017	Lachung, near homestay	27° 40' 20" (N), 88° 43' 22" (E)	Decaying organic matter
137	24-05-2017	Lachung, near homestay	27° 40' 20" (N), 88° 43' 22" (E)	Orange lichen
138	24-05-2017	Lachung, near homestay	27° 40' 20" (N), 88° 43' 22" (E)	Leaves
139	24-05-2017	Lachung, near homestay	27° 40' 20" (N), 88° 43' 22" (E)	Orchids
140	24-05-2017	Lachung, near homestay	27° 40' 20" (N), 88° 43' 22" (E)	Polyporous
141	24-05-2017	Lachung, near homestay	27° 40' 20" (N), 88° 43' 22" (E)	Decomposing leaf litter
142	24-05-2017	Lachung, near homestay	27° 40' 20" (N), 88° 43' 22" (E)	Snake plant
143	24-05-2017	Lachung, near homestay	27° 40' 20" (N), 88° 43' 22" (E)	Yellow mushroom
144	24-05-2017	Lachung, near homestay	27° 40' 20" (N), 88° 43' 22" (E)	Reddish yellow mass
145	24-05-2017	Lachung, near homestay	27° 40' 20" (N), 88° 43' 22" (E)	Stone with biofilm
146	24-05-2017	Lachung, near homestay	27° 40' 20" (N), 88° 43' 22" (E)	Red moss
147	24-05-2017	Lachung, near homestay	27° 40' 20" (N), 88° 43' 22" (E)	Brownish black sediment
148	24-05-2017	Lachung, near homestay	27° 40' 20" (N), 88° 43' 22" (E)	Brown colour sediment
149	24-05-2017	Lachung, near homestay	27° 40' 20" (N), 88° 43' 22" (E)	whitish lichen
150	24-05-2017	Lachung, near homestay	27° 40' 20" (N), 88° 43' 22" (E)	Brown colour mat
151	25-05-2017	Mt. Katao	27° 40' 41" (N), 88° 47' 2" (E)	Coniferous buds
152	25-05-2017	Mt. Katao	27° 40' 41" (N), 88° 47' 2" (E)	Yellow Rhododendron
153	25-05-2017	Mt. Katao	27° 40' 41" (N), 88° 47' 2" (E)	Pink buds
154	25-05-2017	Mt. Katao	27° 40' 41" (N), 88° 47' 2" (E)	Red buds
155	25-05-2017	Mt. Katao	27° 40' 41" (N), 88° 47' 2" (E)	Orange buds
156	25-05-2017	Mt. Katao	27° 40' 41" (N), 88° 47' 2" (E)	Green biofilm
157	25-05-2017	Mt. Katao	27° 40' 41" (N), 88° 47' 2" (E)	Red bud of Rhododendron
158	25-05-2017	Mt. Katao	27° 40' 41" (N), 88° 47' 2" (E)	Orange fungal like growth in roots
159	25-05-2017	Mt. Katao	27° 40' 41" (N), 88° 47' 2" (E)	Light green lichen in root
160	25-05-2017	Mt. Katao	27° 40' 41" (N), 88° 47' 2" (E)	Brown mushroom
161	25-05-2017	Mt. Katao	27° 40' 41" (N), 88° 47' 2" (E)	Green lichen
162	25-05-2017	Mt. Katao	27° 40' 41" (N), 88° 47' 2" (E)	White fungi
163	25-05-2017	Mt. Katao	27° 40' 41" (N), 88° 47' 2" (E)	Orangish mushroom
164	25-05-2017	Mt. Katao	27° 40' 41" (N), 88° 47' 2" (E)	Algal biofilm in stem
165	25-05-2017	Mt. Katao	27° 40' 41" (N), 88° 47' 2" (E)	Tree trunk rotten
166	25-05-2017	Mt. Katao	27° 40' 41" (N), 88° 47' 2" (E)	Degrading wood
167	25-05-2017	Mt. Katao	27° 40' 41" (N), 88° 47' 2" (E)	White lichen
168	25-05-2017	Mt. Katao	27° 40' 41" (N), 88° 47' 2" (E)	Root covered with white layer
169	25-05-2017	Mt. Katao	27° 40' 41" (N), 88° 47' 2" (E)	Rhododendron flower
170	25-05-2017	Mt. Katao	27° 40' 41" (N), 88° 47' 2" (E)	Black mushroom
171	25-05-2017	Mt. Katao	27° 40' 41" (N), 88° 47' 2" (E)	Grey mushroom
172	25-05-2017	Mt. Katao	27° 40' 41" (N), 88° 47' 2" (E)	Dark grey lichen
173	25-05-2017	Mt. Katao	27° 40' 41" (N), 88° 47' 2" (E)	Tiny mushroom with orangish centre
174	25-05-2017	Mt. Katao	27° 40' 41" (N), 88° 47' 2" (E)	Latex from conifer
175	25-05-2017	Mt. Katao	27° 40' 41" (N), 88° 47' 2" (E)	Leaf bud
176	25-05-2017	Mt. Katao	27° 40' 41" (N), 88° 47' 2" (E)	Lichen on rock

177	25-05-2017	Mt. Katao	27° 40' 41" (N), 88° 47' 2" (E)	Creamish mushroom
178	25-05-2017	Mt. Katao	27° 40' 41" (N), 88° 47' 2" (E)	Mushroom creamish small
179	25-05-2017	Mt. Katao	27° 40' 41" (N), 88° 47' 2" (E)	Brown mushroom
180	25-05-2017	Mt. Katao	27° 40' 41" (N), 88° 47' 2" (E)	Black button mushroom
181	25-05-2017	Mt. Katao	27° 40' 41" (N), 88° 47' 2" (E)	Orange lichen
182	25-05-2017	Mt. Katao	27° 40' 41" (N), 88° 47' 2" (E)	Green bryophyte
183	25-05-2017	Mt. Katao	27° 40' 41" (N), 88° 47' 2" (E)	White lichen
184	25-05-2017	Mt. Katao	27° 40' 41" (N), 88° 47' 2" (E)	Yellow lichen
185	25-05-2017	Mt. Katao	27° 40' 41" (N), 88° 47' 2" (E)	Sediment and water
186	25-05-2017	Mt. Katao	27° 40' 41" (N), 88° 47' 2" (E)	Brown biofilm on ice
187	25-05-2017	Mt. Katao	27° 40' 41" (N), 88° 47' 2" (E)	Wild strawberries
188	25-05-2017	Mt. Katao	27° 40' 41" (N), 88° 47' 2" (E)	Fermented radish
189	26-05-2017	Mt. Katao	27° 90' 01" (N), 88° 43' 37" (E)	Garden soil
190	26-05-2017	Lachung to Gangtok	27° 90' 01" (N), 88° 43' 37" (E)	Green fresh lichen
191	26-05-2017	Lachung to Gangtok	27° 90' 01" (N), 88° 43' 37" (E)	Orchids
192	26-05-2017	Lachung to Gangtok	27° 90' 01" (N), 88° 43' 37" (E)	Yellow lichen
193	26-05-2017	Lachung to Gangtok	27° 90' 01" (N), 88° 43' 37" (E)	Sediments
194	26-05-2017	Lachung to Gangtok	27° 30' 56" (N), 88° 34' 08" (E)	Brown bacterial layer on sediment
195	28-05-2017	Darjeeling to Peshok	27° 00' 07" (N), 88° 15' 44" (E)	Orange coloured growth
196	28-05-2017	Darjeeling to Peshok	27° 00' 07" (N), 88° 15' 44" (E)	Marchantia
197	28-05-2017	Darjeeling to Peshok	27° 00' 07" (N), 88° 15' 44" (E)	Decomposing leaves
198	28-05-2017	Darjeeling to Peshok	27° 00' 07" (N), 88° 15' 44" (E)	Bark of conifer
199	28-05-2017	Darjeeling to Peshok	27° 00' 07" (N), 88° 15' 44" (E)	Green patch on bark
200	28-05-2017	Darjeeling to Peshok	27° 00' 07" (N), 88° 15' 44" (E)	Yellow-green lichen on bark
201	28-05-2017	Darjeeling to Peshok	27° 00' 07" (N), 88° 15' 44" (E)	White lichen on bark
202	28-05-2017	Darjeeling to Peshok	27° 00' 07" (N), 88° 15' 44" (E)	Red lichen
203	28-05-2017	Darjeeling to Peshok	27° 00' 07" (N), 88° 15' 44" (E)	Green moss
204	28-05-2017	Darjeeling to Peshok	27° 00' 07" (N), 88° 15' 44" (E)	Orchids
205	28-05-2017	Darjeeling to Peshok	27° 00' 07" (N), 88° 15' 44" (E)	Black lichen
206	28-05-2017	Darjeeling to Peshok	27° 00' 07" (N), 88° 15' 44" (E)	White lichen
207	28-05-2017	Darjeeling to Peshok	27° 00' 07" (N), 88° 15' 44" (E)	Globular black lichen
208	28-05-2017	Darjeeling to Peshok		Nalanda University brick
209	29-05-2017	Darjeeling to Peshok	27° 03' 31" (N), 88° 26' 20" (E)	Red growth
210	29-05-2017	Darjeeling to Peshok	27° 03' 31" (N), 88° 26' 20" (E)	Reddish dried algae
211	29-05-2017	Darjeeling to Peshok	27° 03' 31" (N), 88° 26' 20" (E)	Green lichen
212	29-05-2017	Darjeeling to Peshok	27° 03' 31" (N), 88° 26' 20" (E)	Globular lichen
213	30-05-2017	Darjeeling	Bahrampore	White lichen
214	30-05-2017	Darjeeling	Bahrampore	Green lichen
215	30-05-2017	Darjeeling	Bahrampore	Soil
216	31-05-2017	Darjeeling	24° 05' 08" (N), 87° 43' 58" (E)	Brown pond
217	31-05-2017	Darjeeling	24° 04' 05" (N), 87° 39' 37" (E)	Lichen from teak forest
218	31-05-2017	Darjeeling	23° 52' 55" (N), 87° 27' 23" , Bakreshwar	Decomposing leaf with biofilm
219	31-05-2017	Darjeeling	23° 52' 55" (N), 87° 27' 23" (E)	Orange brown algal biofilm
220	31-05-2017	Darjeeling	23° 52' 55" (N), 87° 27' 23" (E)	water sample from hot spring
221	31-05-2017	Darjeeling	23° 52' 55" (N), 87° 27' 23" (E)	Gelatinous brown growth on branch
222	31-05-2017	Darjeeling	23° 52' 55" (N), 87° 27' 23" (E)	Algal biofilm

223	31-05-2017	Darjeeling	23° 52' 55" (N), 87° 27' 23" (E)	Benthic algal biofilm
224	31-05-2017	Darjeeling	23° 52' 55" (N), 87° 27' 23" (E)	Floating algal biofilm
225	31-05-2017	Darjeeling	23° 52' 55" (N), 87° 27' 23" (E)	Algal biofilm and water
226	31-05-2017	Darjeeling	23° 52' 55" (N), 87° 27' 23" (E)	Algal biofilm
227	31-05-2017	Darjeeling	23° 41' 44" (N), 87° 14' 37" (E)	Soil from coal mine
228	31-05-2017	Darjeeling	23° 41' 44" (N), 87° 14' 37" (E)	Orange coloured fruits
229	31-05-2017	Darjeeling	23° 41' 44" (N), 87° 14' 37" (E)	Black coloured soil from water body
230	31-05-2017	Darjeeling	23° 41' 44" (N), 87° 14' 37" (E)	Peel
231	31-05-2017	Darjeeling	Chandipur beach	Sediment from Chandipur beach
232	31-05-2017	Darjeeling	21° 34' 38" (N), 86° 45' 57" (E)	Water and sediment samplefrom stream
233	31-05-2017	Darjeeling	21° 34' 38" (N), 86° 45' 57" (E)	Lichen on tree
234	31-05-2017	Darjeeling	21° 34' 38" (N), 86° 45' 57" (E)	Aquatic weed
235	31-05-2017	Darjeeling	21° 41' 05" (N), 86° 27' 29" (E) ,Sinlipal Tiger Reserve	Green lichen on the rock
236	31-05-2017	Darjeeling	21° 41' 05" (N), 86° 27' 29" (E)	Green lichen on tree
237	31-05-2017	Darjeeling	21° 41' 05" (N), 86° 27' 29" (E)	Dried twig floating with biofilm
238	31-05-2017	Darjeeling	21° 41' 05" (N), 86° 27' 29" (E)	Fresh water sponge
239	02-06-2017	Odisha	21° 41' 05" (N), 86° 27' 29" (E)	Brown algal mat
240	02-06-2017	Odisha	21° 41' 05" (N), 86° 27' 29" (E)	Red roots in slow folwing warm water
241	02-06-2017	Odisha	21° 41' 05" (N), 86° 27' 29" (E)	Plant root sysytem in floating water
242	02-06-2017	Odisha	21° 41' 05" (N), 86° 27' 29" (E)	Lichen on tree at waterfall
243	02-06-2017	Odisha	21° 41' 05" (N), 86° 27' 29" (E)	Green lichen
244	02-06-2017	Odisha	21° 42' 21" (N), 86° 26' 41" (E)	Epiphytic orchid
245	02-06-2017	Odisha	21° 42' 21" (N), 86° 26' 41" (E)	Small orchid plant on tree
246	02-06-2017	Odisha	21° 42' 21" (N), 86° 26' 41" (E)	Green algal benthic mass in water
247	02-06-2017	Odisha	21° 42' 21" (N), 86° 26' 41" (E)	Inflorescence of wild grape
248	02-06-2017	Odisha	21° 42' 21" (N), 86° 26' 41" (E)	White, big mushroom
249	02-06-2017	Odisha	21° 42' 21" (N), 86° 26' 41" (E)	Poluporous of dead twig
250	02-06-2017	Odisha	21° 42' 21" (N), 86° 26' 41" (E)	White lichen on dry twig
251	02-06-2017	Odisha	21° 38' 09" (N), 86° 34' 25" (E) ,Village Musakhi	Sample from dark brown pond
252	02-06-2017	Odisha	21° 38' 09" (N), 86° 34' 25" (E) ,Village Musakhi	Polyporous sample from tree
253	02-06-2017	Odisha	21° 38' 09" (N), 86° 34' 25" (E) ,Village Musakhi	Algal mat from pond
254	02-06-2017	Odisha	17° 27' 23" (N), 78° 18' 55" (E) ,Way to Konark	Orange growth on standing water
255	02-06-2017	Odisha	17° 27' 23" (N), 78° 18' 55" (E)	Brown water with sediment
256	04-06-2017	Odisha	19° 51' 54" (N), 86° 06' 40" (E) , Konark	Soil from Chandrabagha beach
257	04-06-2017	Odisha	19° 51' 33" (N), 86° 04' 53" (E) , Way to Puri	Brown oily layer on a pond
258	04-06-2017	Odisha	19° 51' 33" (N), 86° 04' 53" (E) , Way to Puri	Surface water from the pond
259	04-06-2017	Odisha	19° 51' 33" (N), 86° 04' 53" (E) , Way to Puri	Black sediment of the pond
260	04-06-2017	Odisha	19° 39' 46" (N), 86° 22' 27" (E) , Otherside of Chilika	Sediment from Chilika

261	04-06-2017	Odisha	19° 39' 46" (N), 86° 22' 27" (E)	Sediment from aquaculture pond
262	04-06-2017	Odisha	19° 37' 52" (N), 85° 17' 20" (E)	Cyanobacterial mat ,brown layer, water and sediment from pond
263	05-06-2017	Odisha	19° 34' 30" (N), 85° 07' 05" (E)	Green lichen
264	05-06-2017	Odisha	19° 34' 30" (N), 85° 07' 05" (E)	Algal sample from Ghantashila hill
265	05-06-2017	Odisha	19° 34' 30" (N), 85° 07' 05" (E)	Thread like algae attached to rock
266	05-06-2017	Odisha	19° 34' 30" (N), 85° 07' 05" (E)	Lichen on rock
267	05-06-2017	Odisha	19° 34' 30" (N), 85° 07' 05" (E)	Surface water of lake
268	05-06-2017	Odisha	19° 34' 30" (N), 85° 07' 05" (E)	Soil sample from died salt pan
269	05-06-2017	Odisha	19° 34' 30" (N), 85° 07' 05" (E)	Algal sample with water nearby salt pan
270	05-06-2017	Odisha	19° 34' 30" (N), 85° 07' 05" (E)	Black sand
271	05-06-2017	Odisha	17° 49' 41" (N), 83° 24' 55" (E)	Sea weed from beach
272	05-06-2017	Odisha	17° 49' 41" (N), 83° 24' 55" (E)	Pebble with biofilm
273	05-06-2017	Odisha	17° 49' 41" (N), 83° 24' 55" (E)	Green lichen
274	05-06-2017	Odisha	17° 49' 41" (N), 83° 24' 55" (E)	Orange brown sidemnt in crevice of rock
275	05-06-2017	Odisha	17° 49' 41" (N), 83° 24' 55" (E)	Black sand
276	05-06-2017	Odisha	17° 49' 41" (N), 83° 24' 55" (E)	Sea weed
277	05-06-2017	Odisha	17° 49' 41" (N), 83° 24' 55" (E)	Yellowish green algae on rock
278	05-06-2017	Odisha	17° 49' 41" (N), 83° 24' 55" (E)	Stone with reddish brown and green biofilm
279	05-06-2017	Odisha	17° 49' 41" (N), 83° 24' 55" (E)	Brown sea weed
280	05-06-2017	Odisha	17° 48' 54" (N), 83° 26' 12" (E)	Redsoil from sand dune
281	05-06-2017		17° 48' 54" (N), 83° 26' 12" (E)	Red sand

Annexure 1c. Tamil Nadu samples detail (June 2018)

Sample No	Date of sampling	Geographical Locations	GPS Coordinate	Type of samples
1	1/6/2018	Parangipettai	11° 44' 06" N/ 79° 46' 43" E	Jelly Fish
2	1/6/2018	Parangipettai	11° 44' 06" N/ 79° 46' 43" E	sediment
3	1/6/2018	Parangipettai	11° 44' 06" N/ 79° 46' 43" E	Molluscs
4	1/6/2018	Parangipettai	11° 44' 06" N/ 79° 46' 43" E	Glass Bottle With Biofilm
5	1/6/2018	Parangipettai coast	11° 44' 17" N/ 79° 43' 45" E	sediment
6	1/6/2018	Parangipettai coast	11° 44' 17" N/ 79° 43' 45" E	Shiny layer on top of water
7	1/6/2018	Parangipettai coast	11° 44' 17" N/ 79° 43' 45" E	Biofilm of paper
8	1/6/2018	Parangipettai coast	11° 44' 17" N/ 79° 43' 45" E	2L bottle plastic cool drink
9	1/6/2018	Parangipettai coast	11° 44' 17" N/ 79° 43' 45" E	Bio film on dead bark
10	1/6/2018	Parangipettai coast	11° 44' 17" N/ 79° 43' 45" E	Sponge (green bark)
11	1/6/2018	Parangipettai coast	11° 44' 17" N/ 79° 43' 45" E	Green sponge
12	1/6/2018	Parangipettai coast	11° 44' 17" N/ 79° 43' 45" E	Green sponge
13	1/6/2018	Parangipettai coast	11° 44' 17" N/ 79° 43' 45" E	Green lump
14	1/6/2018	Parangipettai coast	11° 44' 17" N/ 79° 43' 45" E	Hydrilla
15	1/6/2018	Parangipettai coast	11° 44' 17" N/ 79° 43' 45" E	Other weed
16	1/6/2018	Parangipettai coast	11° 44' 17" N/ 79° 43' 45" E	Jet black sediment
17	1/6/2018	Parangipettai coast	11° 44' 17" N/ 79° 43' 45" E	Algal sample
18	1/6/2018	Parangipettai coast	11° 44' 17" N/ 79° 43' 45" E	Algal sample
19	1/6/2018	Near Parangipettai coast	11° 33' 16" N/ 79° 35' 26" E	Black sediment+water
20	1/6/2018	Near Parangipettai coast	11° 33' 16" N/ 79° 35' 26" E	Algal mat which is fibrous
21	1/6/2018	Near Parangipettai coast	11° 33' 16" N/ 79° 35' 26" E	Purple brown f algal film(filamentous)
22	1/6/2018	Near Parangipettai coast	11° 33' 16" N/ 79° 35' 26" E	Algal sample
23	1/6/2018	Near Parangipettai coast	11° 33' 16" N/ 79° 35' 26" E	Thermocol with brown layer(Bacilli)
24	2/6/2018	Pichavaram mangrove	11° 24' 42" N/ 79° 49' 46" E	Algal biofilm
25	2/6/2018	Pichavaram mangrove	11° 24' 42" N/ 79° 49' 46" E	Sediment
26	2/6/2018	Pichavaram mangrove	11° 24' 42" N/ 79° 49' 46" E	Mangrove root
27	2/6/2018	Pichavaram mangrove	11° 24' 42" N/ 79° 49' 46" E	Dried fruiticose lichen
28	2/6/2018	Pichavaram mangrove	11° 24' 42" N/ 79° 49' 46" E	Dry soil near shallow water body
29	2/6/2018	Pichavaram mangrove	11° 24' 42" N/ 79° 49' 46" E	Salt crystals on shallow water body
30	2/6/2018	Pichavaram mangrove	11° 24' 42" N/ 79° 49' 46" E	Black sediment
31	2/6/2018	Pichavaram mangrove	11° 24' 42" N/ 79° 49' 46" E	Algal sample
32	2/6/2018	Pichavaram mangrove	11° 24' 42" N/ 79° 49' 46" E	Shrimp pond

33	2/6/2018	Pichavaram mangrove	11° 24' 42" N/ 79° 49' 46" E	Black sediment with water
34	2/6/2018	Pichavaram mangrove	11° 24' 42" N/ 79° 49' 46" E	Rhodovulum orange
35	2/6/2018	Pichavaram mangrove	11° 24' 42" N/ 79° 49' 46" E	sediment
36	3/6/2018	Rice field	11° 40' 27" N/ 79° 44' 24" E	sediment
37	3/6/2018	Rice field	11° 40' 27" N/ 79° 44' 24" E	Thread like algae.
38	3/6/2018	Rice field	11° 40' 27" N/ 79° 44' 24" E	Sediment above field
39	3/6/2018	Fishing Harbour, Thirumullaivasal	11° 14' 30" N/ 79° 50' 25" E	Purple marine organism
40	3/6/2018	Fishing Harbour	11° 14' 30" N/ 79° 50' 25" E	Colourless dried sponge
41	3/6/2018	Fishing Harbour	11° 14' 30" N/ 79° 50' 25" E	biofilm
42	3/6/2018	Fishing Harbour	11° 14' 30" N/ 79° 50' 25" E	molluscan
43	3/6/2018	Fishing Harbour	11° 14' 30" N/ 79° 50' 25" E	Yellowish brown water pond
44	3/6/2018	Fishing Harbour	11° 14' 30" N/ 79° 50' 25" E	Black sediment at yellowish brown pond
45	3/6/2018	Fishing Harbour	11° 14' 30" N/ 79° 50' 25" E	Reddish brown pond water
46	3/6/2018	Fishing Harbour	11° 14' 30" N/ 79° 50' 25" E	Black sediment at reddish brown pond
47	3/6/2018	Fishing Harbour	11° 14' 30" N/ 79° 50' 25" E	Decomposing leave at yellowish brown pond
48	3/6/2018	Fishing Harbour, Poompuhar	11° 11' 45" N/ 79° 51' 34" E	Root of water lilly
49	3/6/2018	Fishing Harbour	11° 11' 45" N/ 79° 51' 34" E	Roots of eichorria(water hyacinth)
50	3/6/2018	Fishing Harbour	11° 11' 45" N/ 79° 51' 34" E	Algal sample
51	3/6/2018	Fishing Harbour	11° 11' 45" N/ 79° 51' 34" E	Sediment
52	3/6/2018	Fishing Harbour	11° 11' 45" N/ 79° 51' 34" E	Touch me not like plant
53	3/6/2018	Fishing Harbour	11° 11' 45" N/ 79° 51' 34" E	Gelly fish pieces
54	3/6/2018	Fishing Harbour	11° 11' 45" N/ 79° 51' 34" E	Sea weeds
55	3/6/2018	Fishing Harbour	11° 11' 45" N/ 79° 51' 34" E	sediment
56	3/6/2018	Fishing Harbour	11° 11' 45" N/ 79° 51' 34" E	Sediment
57	3/6/2018	Fishing Harbour	11° 11' 45" N/ 79° 51' 34" E	Sea water
58	3/6/2018	Fishing Harbour	11° 11' 45" N/ 79° 51' 34" E	sediment
59	3/6/2018	Fishing Harbour, Nagapattinam	10°45' 11" N/ 79° 50' 49" E	Water with black sediment
60	3/6/2018	Fishing Harbour	10°45' 11" N/ 79° 50' 49" E	Polluted sea water
61	4/6/2018	Aqua-culture pond	10°45' 11" N/ 79° 50' 49" E	Brown sediment
62	4/6/2018	Aqua-culture pond	10°45' 11" N/ 79° 50' 49" E	Sediment dried
63	4/6/2018	Aqua-culture pond	10°45' 11" N/ 79° 50' 49" E	Brown small pond
64	4/6/2018	Aqua-culture pond	10°45' 11" N/ 79° 50' 49" E	A large marine water channel
65	4/6/2018	Aqua-culture pond	10°45' 11" N/ 79° 50' 49" E	Dry soil on the bund of aquaculture pond

66	4/6/2018	Aqua-culture pond	10°45' 11" N/ 79° 50' 49" E	A large waterbody,not a part of aquaculture pond(algal growth at bottom)
67	4/6/2018	Aqua-culture pond	10°45' 11" N/ 79° 50' 49" E	Rusted iron for clostridia
68	4/6/2018	Aqua-culture pond	10°45' 11" N/ 79° 50' 49" E	Sandy soil
69	4/6/2018	Aqua-culture pond	10°45' 11" N/ 79° 50' 49" E	Sediment of a shallow water standing with algal floating biofilm
70	4/6/2018	Aqua-culture pond	10°45' 11" N/ 79° 50' 49" E	sediment
71	4/6/2018	Aqua-culture pond	10°45' 11" N/ 79° 50' 49" E	Black sediment of brown pond
72	4/6/2018	Aqua-culture pond	10°45' 11" N/ 79° 50' 49" E	Pond with algal biofilm
73	4/6/2018	Aqua-culture pond	10°45' 11" N/ 79° 50' 49" E	Sediment & algal biofilm with orange bottom
74	4/6/2018	Mangrove forest	10°37' 29" N/ 79° 49' 41" E	Hydrilla like wwed
75	4/6/2018	Mangrove forest	10°37' 29" N/ 79° 49' 41" E	Rotting long stalks of aquatic plant
76	4/6/2018	Mangrove forest	10°37' 29" N/ 79° 49' 41" E	Algal biofilm floating.
77	4/6/2018	Mangrove forest	10°37' 29" N/ 79° 49' 41" E	Sediment of the same water body.
78	4/6/2018	Mangrove forest	10°37' 29" N/ 79° 49' 41" E	On the bund,orange layer of growth.
79	4/6/2018	Mangrove forest	10°37' 29" N/ 79° 49' 41" E	Brown growth on plastic in water.
80	4/6/2018	Mangrove forest	10°37' 29" N/ 79° 49' 41" E	Rhizosphere soil.
81	4/6/2018	Mangrove forest	10°37' 29" N/ 79° 49' 41" E	Place where fresh water & salt water meets.
82	4/6/2018	Mangrove forest	10°37' 29" N/ 79° 49' 41" E	Dry soil on the other side(bacilli)
83	4/6/2018	Mangrove forest	10°37' 29" N/ 79° 49' 41" E	Sediment near mangrove.
84	4/6/2018	Mangrove forest	10°37' 29" N/ 79° 49' 41" E	sediment
85	4/6/2018	Mangrove forest	10°37' 29" N/ 79° 49' 41" E	Soil rhizosphere
86	4/6/2018	Vedaranayam, salt pan	10° 21' 11" N/ 79° 50' 41" E	Dark brown layer on crystalised salt.
87	4/6/2018	Vedaranayam, salt pan	10° 21' 11" N/ 79° 50' 41" E	Algal mat at the bottom of water body.no crystallisation of salt.
88	4/6/2018	Vedaranayam, salt pan	10° 21' 11" N/ 79° 50' 41" E	Degrading plastic sheet with algal biofilm
89	4/6/2018	Vedaranayam, salt pan	10° 21' 11" N/ 79° 50' 41" E	Orange brown layer on surface.gelatinous layer.
90	4/6/2018	Vedaranayam, salt pan	10° 21' 11" N/ 79° 50' 41" E	Brown surface layer
91	4/6/2018	Vedaranayam, salt pan	10° 21' 11" N/ 79° 50' 41" E	Salt crystal
92	4/6/2018	Vedaranayam, salt pan	10° 21' 11" N/ 79° 50' 41" E	Dark brown layer at the bottom
93	4/6/2018	Vedaranayam, salt pan	10° 21' 11" N/ 79° 50' 41" E	Salt being harvested
94	4/6/2018	Vedaranayam, salt pan	10° 21' 11" N/ 79° 50' 41" E	Salt floating on the water
95	4/6/2018	Vedaranayam, salt pan	10° 21' 11" N/ 79° 50' 41" E	Floating brown biofilm
96	4/6/2018	Point calimer coast	10° 17' 50" N/ 79° 49' 41" E	fibrous algal
97	4/6/2018	Point calimer coast	10° 17' 50" N/ 79° 49' 41" E	Sea weed

98	4/6/2018	Point calimer coast	10° 17' 50" N/ 79° 49' 41" E	Sea weed
99	4/6/2018	Point calimer coast	10° 17' 50" N/ 79° 49' 41" E	Green algae
100	4/6/2018	Point calimer coast	10° 17' 50" N/ 79° 49' 41" E	Brown algae
101	5/6/2018	Muthupetai lagoon	10° 23' 52" N/ 79° 30' 12" E	Brown algal growth(fibrous)
102	5/6/2018	Muthupetai lagoon	10° 23' 52" N/ 79° 30' 12" E	A plastic cup with brown bacterial growth
103	5/6/2018	Muthupetai lagoon	10° 23' 52" N/ 79° 30' 12" E	Floating thick green algal mat
104	5/6/2018	Muthupetai lagoon	10° 23' 52" N/ 79° 30' 12" E	Black sediment
105	5/6/2018	Muthupetai lagoon	10° 23' 52" N/ 79° 30' 12" E	Rope covered with algal biofilm
106	5/6/2018	Muthupetai lagoon	10° 23' 52" N/ 79° 30' 12" E	Brown gelatinous mass
107	5/6/2018	Muthupetai lagoon	10° 23' 52" N/ 79° 30' 12" E	Sandy soil from bank
108	5/6/2018	Muthupetai lagoon	10° 23' 52" N/ 79° 30' 12" E	sediment
109	5/6/2018	Muthupetai lagoon	10° 23' 52" N/ 79° 30' 12" E	Sediment+water
110	5/6/2018	Muthupetai lagoon	10° 23' 52" N/ 79° 30' 12" E	Alage from lagoon proper
111	5/6/2018	Muthupetai lagoon	10° 23' 52" N/ 79° 30' 12" E	Mass on the wood
112	5/6/2018	Muthupetai lagoon	10° 23' 52" N/ 79° 30' 12" E	Green algae
113	5/6/2018	Muthupetai lagoon	10° 23' 52" N/ 79° 30' 12" E	Black sediment
114	5/6/2018	Muthupetai lagoon	10° 23' 52" N/ 79° 30' 12" E	Degrading sea weed
115	5/6/2018	Muthupetai lagoon	10° 23' 52" N/ 79° 30' 12" E	Dry sponge
116	5/6/2018	Muthupetai lagoon	10° 23' 52" N/ 79° 30' 12" E	Sponge dry
117	5/6/2018	Muthupetai lagoon	10° 23' 52" N/ 79° 30' 12" E	Dry sponge
118	5/6/2018	Muthupetai lagoon	10° 23' 52" N/ 79° 30' 12" E	Sea weed geladium dried
119	5/6/2018	Muthupetai lagoon	10° 23' 52" N/ 79° 30' 12" E	Sponge porous-small
120	5/6/2018	Muthupetai lagoon	10° 23' 52" N/ 79° 30' 12" E	Dry sponge
121	5/6/2018	Muthupetai lagoon	10° 23' 52" N/ 79° 30' 12" E	Sediment with water-brown layer at bottom
122	5/6/2018	Muthupetai lagoon	10° 23' 52" N/ 79° 30' 12" E	Soil of pan dry
123	5/6/2018	Ammapattinam salt pan	09° 59' 02" N/ 79° 12' 09" E	sponge
124	5/6/2018	Ammapattinam salt pan	09° 59' 02" N/ 79° 12' 09" E	Water+sediment
125	5/6/2018	Ammapattinam salt pan	09° 59' 02" N/ 79° 12' 09" E	Yellow brown layer on thermocol
126	5/6/2018	Ammapattinam salt pan	09° 59' 02" N/ 79° 12' 09" E	Sea weed(sargassam)
127	5/6/2018	Ammapattinam salt pan	09° 59' 02" N/ 79° 12' 09" E	sediment
128	5/6/2018	Ammapattinam salt pan	09° 59' 02" N/ 79° 12' 09" E	Water- small water body with orange at the bottom
129	5/6/2018	Ammapattinam salt pan	09° 59' 02" N/ 79° 12' 09" E	Dried sea weed on the shore
130	5/6/2018	Ammapattinam salt pan	09° 59' 02" N/ 79° 12' 09" E	Dark brown sea weed
131	5/6/2018	Ammapattinam salt pan	09° 59' 02" N/ 79° 12' 09" E	Star like sea weed

132	5/6/2018	Ammapattinam salt pan	09° 59' 02" N/ 79° 12' 09" E	Sheet like alga green
133	5/6/2018	Ammapattinam salt pan	09° 59' 02" N/ 79° 12' 09" E	algae
134	5/6/2018	Ammapattinam salt pan	09° 59' 02" N/ 79° 12' 09" E	Purple sponge+same dried
135	5/6/2018	Ammapattinam salt pan	09° 59' 02" N/ 79° 12' 09" E	Purple green gelatinous alga
136	5/6/2018	Ammapattinam salt pan	09° 59' 02" N/ 79° 12' 09" E	Green alga
137	5/6/2018	Ammapattinam salt pan	09° 59' 02" N/ 79° 12' 09" E	Brown alga-live
138	5/6/2018	Ammapattinam salt pan	09° 59' 02" N/ 79° 12' 09" E	Water of decaying sea weed
139	5/6/2018	Ammapattinam salt pan	09° 59' 02" N/ 79° 12' 09" E	Pink biofilm on plastic in a water body
140	6/6/2018	Near pambam bridge	09° 16' 54" N/ 79° 11' 15" E	A red sponge
141	6/6/2018	Near pambam bridge	09° 16' 54" N/ 79° 11' 15" E	Dry sponge
142	6/6/2018	Near pambam bridge	09° 16' 54" N/ 79° 11' 15" E	Dry sponge
143	6/6/2018	Near pambam bridge	09° 16' 54" N/ 79° 11' 15" E	Pink purple layer on soil.bottom jet black
144	6/6/2018	Near pambam bridge	09° 16' 54" N/ 79° 11' 15" E	Sea weed
145	6/6/2018	Near pambam bridge	09° 16' 54" N/ 79° 11' 15" E	Sea weed
146	6/6/2018	Near pambam bridge	09° 16' 54" N/ 79° 11' 15" E	Black sediment
147	6/6/2018	Near pambam bridge	09° 16' 54" N/ 79° 11' 15" E	Alagal bio film with black at the bottom
148	6/6/2018	Near pambam bridge	09° 16' 54" N/ 79° 11' 15" E	Sea weed fibrous
149	6/6/2018	Near pambam bridge	09° 16' 54" N/ 79° 11' 15" E	Sea weed
150	6/6/2018	Near pambam bridge	09° 16' 54" N/ 79° 11' 15" E	Dry sand
151	6/6/2018	Near pambam bridge	09° 16' 54" N/ 79° 11' 15" E	Sediment from sandy beach land-with black
152	6/6/2018	Near pambam bridge	09° 16' 54" N/ 79° 11' 15" E	sediment
153	6/6/2018	Near pambam bridge	09° 16' 54" N/ 79° 11' 15" E	A glass bottle
154	6/6/2018	Near pambam bridge	09° 16' 54" N/ 79° 11' 15" E	thick algal biofilm
155	6/6/2018	Near pambam bridge	09° 16' 54" N/ 79° 11' 15" E	Brown & pink
156	6/6/2018	Near pambam bridge	09° 16' 54" N/ 79° 11' 15" E	Sediment of brown pond
157	6/6/2018	Near pambam bridge	09° 16' 54" N/ 79° 11' 15" E	A drying pond.no water butt moisture.pink surface growth.
158	6/6/2018	Near pambam bridge	09° 16' 54" N/ 79° 11' 15" E	Orange brown layer like the pinkish
159	6/6/2018	Near pambam bridge	09° 16' 54" N/ 79° 11' 15" E	A xerophyte plant
160	6/6/2018	Near pambam bridge	09° 16' 54" N/ 79° 11' 15" E	M.littori sand
161	6/6/2018	Near pambam bridge	09° 16' 54" N/ 79° 11' 15" E	Dry sponge
162	7/6/2018	Sea shore near mandapam	09° 16' 52" N/ 79° 10' 20" E	Sponge
163	7/6/2018	Sea shore near mandapam	09° 16' 52" N/ 79° 10' 20" E	Algae
164	7/6/2018	Sea shore near mandapam	09° 16' 52" N/ 79° 10' 20" E	Sponge
165	7/6/2018	Sea shore near mandapam	09° 16' 52" N/ 79° 10' 20" E	Sponge attached to rock

166	7/6/2018	Sea shore near mandapam	09° 16' 52" N/ 79° 10' 20" E	Sponge small
167	7/6/2018	Sea shore near mandapam	09° 16' 52" N/ 79° 10' 20" E	Sponge attached to rock
168	7/6/2018	Sea shore near mandapam	09° 16' 52" N/ 79° 10' 20" E	Algae
169	7/6/2018	Sea shore near mandapam	09° 16' 52" N/ 79° 10' 20" E	Sponge rock
170	7/6/2018	Sea shore near mandapam	09° 16' 52" N/ 79° 10' 20" E	Brown algae
171	7/6/2018	Sea shore near mandapam	09° 16' 52" N/ 79° 10' 20" E	Red(thick tube like-gelatinous)
172	7/6/2018	Sea shore near mandapam	09° 16' 52" N/ 79° 10' 20" E	Algae
173	7/6/2018	Sea shore near mandapam	09° 16' 52" N/ 79° 10' 20" E	Algal biofilm on shells
174	7/6/2018	Sea shore near mandapam	09° 16' 52" N/ 79° 10' 20" E	Agar yielding agar
175	7/6/2018	Sea shore near mandapam	09° 16' 52" N/ 79° 10' 20" E	Algae
176	7/6/2018	Sea shore near mandapam	09° 16' 52" N/ 79° 10' 20" E	Corals
177	7/6/2018	Sea shore near mandapam	09° 16' 52" N/ 79° 10' 20" E	Noodles like algae
178	7/6/2018	Sea shore near mandapam	09° 16' 52" N/ 79° 10' 20" E	Black sponge In water
179	7/6/2018	Sea shore near mandapam	09° 16' 52" N/ 79° 10' 20" E	Hair like alga
180	7/6/2018	Sea shore near mandapam	09° 16' 52" N/ 79° 10' 20" E	Graclaria like but small being cultivated
181	7/6/2018	Sea shore near mandapam	09° 16' 52" N/ 79° 10' 20" E	Algal biofilm the sticks making the culture vessel
182	7/6/2018	Sea shore near mandapam	09° 16' 52" N/ 79° 10' 20" E	Algae
183	7/6/2018	Sea shore near mandapam	09° 16' 52" N/ 79° 10' 20" E	Orange sponge
184	7/6/2018	Sea shore near mandapam	09° 16' 52" N/ 79° 10' 20" E	Sponge attached to sticks being used for growing algae
185	7/6/2018	Sea shore near mandapam	09° 16' 52" N/ 79° 10' 20" E	Black sponge with star like pores attached to rope
186	7/6/2018	Sea shore near mandapam	09° 16' 52" N/ 79° 10' 20" E	Another sponge
187	7/6/2018	Sea shore near mandapam	09° 16' 52" N/ 79° 10' 20" E	Algae pink with small sponge on it.
188	7/6/2018	Sea shore near mandapam	09° 16' 52" N/ 79° 10' 20" E	Alga with concentric rings
189	7/6/2018	Sea shore near mandapam	09° 16' 52" N/ 79° 10' 20" E	Green gelatinious
190	7/6/2018	Sea shore near mandapam	09° 16' 52" N/ 79° 10' 20" E	Very thin,hairy & gelatinous
191	7/6/2018	Sea shore near mandapam	09° 16' 52" N/ 79° 10' 20" E	Algal biofilm on stone
192	7/6/2018	Sea shore near mandapam	09° 16' 52" N/ 79° 10' 20" E	Small orange,sponge
193	7/6/2018	Sea shore near mandapam	09° 16' 52" N/ 79° 10' 20" E	Brown dry sponge
194	7/6/2018	Sea shore near mandapam	09° 16' 52" N/ 79° 10' 20" E	dry sponge
195	7/6/2018	Sea shore near mandapam	09° 16' 52" N/ 79° 10' 20" E	Algae
196	7/6/2018	Sea shore near mandapam	09° 16' 52" N/ 79° 10' 20" E	dry sponge
197	7/6/2018	Sea shore near mandapam	09° 16' 52" N/ 79° 10' 20" E	dry sponge
198	7/6/2018	Sea shore near mandapam	09° 16' 52" N/ 79° 10' 20" E	Sediment
199	7/6/2018	Sea shore near mandapam	09° 16' 52" N/ 79° 10' 20" E	Algal mat from storage tank

200	7/6/2018	Sea shore near mandapam	09° 16' 52" N/ 79° 10' 20" E	White sponge in falcon
201	6/6/2018	Sea shore near mandapam	09° 16' 52" N/ 79° 10' 20" E	Dry sponge
202	6/6/2018	Sea shore near mandapam	09° 16' 52" N/ 79° 10' 20" E	Green filamentous algae
203	6/6/2018	Sea shore near mandapam	09° 16' 52" N/ 79° 10' 20" E	Sediment along with orange growth
204	6/6/2018	Sea shore near mandapam	09° 16' 52" N/ 79° 10' 20" E	(green color amoeba
205	7/6/2018	Sea shore near mandapam	09° 16' 52" N/ 79° 10' 20" E	Mangrove leaf from mangrove forest
206	7/7/2018	Vallinokkam coast	09° 09' 55" N/ 78° 38' 33" E	sponge
207	7/7/2018	Vallinokkam coast	09° 09' 55" N/ 78° 38' 33" E	Dry sponge
208	7/7/2018	Vallinokkam coast	09° 09' 55" N/ 78° 38' 33" E	Pink coloured on grey sponge
209	7/7/2018	Vallinokkam coast	09° 09' 55" N/ 78° 38' 33" E	Algae
210	7/7/2018	Vallinokkam coast	09° 09' 55" N/ 78° 38' 33" E	Brown alga
211	7/7/2018	Vallinokkam coast	09° 09' 55" N/ 78° 38' 33" E	Orange sponge
212	7/7/2018	Vallinokkam coast	09° 09' 55" N/ 78° 38' 33" E	Dry sponge
213	7/7/2018	Vallinokkam coast	09° 09' 55" N/ 78° 38' 33" E	Sponge(fibrous with pink)
214	7/7/2018	Vallinokkam coast	09° 09' 55" N/ 78° 38' 33" E	Algae fibrous/greenish attached to rope
215	7/7/2018	Vallinokkam coast	09° 09' 55" N/ 78° 38' 33" E	Sponge small-yellow green
216	7/7/2018	Vallinokkam coast	09° 09' 55" N/ 78° 38' 33" E	Veins of a leaf
217	7/7/2018	Vallinokkam coast	09° 09' 55" N/ 78° 38' 33" E	dry sponge
218	7/7/2018	Vallinokkam coast	09° 09' 55" N/ 78° 38' 33" E	Orange layered sponge
219	7/7/2018	Vallinokkam coast	09° 09' 55" N/ 78° 38' 33" E	Dry(semi) muddy color
220	7/7/2018	Vallinokkam coast	09° 09' 55" N/ 78° 38' 33" E	dry sponge
221	7/7/2018	Vallinokkam coast	09° 09' 55" N/ 78° 38' 33" E	Sponge dried
222	7/7/2018	Vallinokkam coast	09° 09' 55" N/ 78° 38' 33" E	Purple live sponge
223	7/7/2018	Vallinokkam coast	09° 09' 55" N/ 78° 38' 33" E	Live sponge on a shell
224	7/7/2018	Vallinokkam coast	09° 09' 55" N/ 78° 38' 33" E	Light green brown live sponge small
225	7/7/2018	Vallinokkam coast	09° 09' 55" N/ 78° 38' 33" E	Dry sponge
226	7/7/2018	Vallinokkam coast	09° 09' 55" N/ 78° 38' 33" E	Coral orange
227	7/7/2018	Vallinokkam coast	09° 09' 55" N/ 78° 38' 33" E	Sponge dried-mud color
228	7/7/2018	Vallinokkam coast	09° 09' 55" N/ 78° 38' 33" E	Live vrick red sponge-attached to shell
229	7/7/2018	Vallinokkam coast	09° 09' 55" N/ 78° 38' 33" E	Dry sponge
230	7/7/2018	Vallinokkam coast	09° 09' 55" N/ 78° 38' 33" E	Dry sponge porous
231	7/7/2018	Vallinokkam coast	09° 09' 55" N/ 78° 38' 33" E	Dry sponge
232	7/7/2018	Vallinokkam coast	09° 09' 55" N/ 78° 38' 33" E	Dry sponge
233	7/7/2018	Vallinokkam coast	09° 09' 55" N/ 78° 38' 33" E	Black live sponge

234	7/7/2018	Vallinokkam coast	09° 09' 55" N/ 78° 38' 33" E	Dry sponge
235	7/7/2018	Vallinokkam coast	09° 09' 55" N/ 78° 38' 33" E	Dry sponge
236	7/7/2018	Vallinokkam coast	09° 09' 55" N/ 78° 38' 33" E	Dry sponge
237	7/7/2018	Vallinokkam coast	09° 09' 55" N/ 78° 38' 33" E	Dry sponge
238	7/7/2018	Vallinokkam coast	09° 09' 55" N/ 78° 38' 33" E	Dry sponge
239	7/7/2018	Vallinokkam coast	09° 09' 55" N/ 78° 38' 33" E	Dry sponge
240	7/7/2018	Vallinokkam coast	09° 09' 55" N/ 78° 38' 33" E	Dry sponge
241	7/7/2018	Vallinokkam coast	09° 09' 55" N/ 78° 38' 33" E	Orange brown sponge
242	7/7/2018	Vallinokkam coast	09° 09' 55" N/ 78° 38' 33" E	Dry sponge
243	7/7/2018	Vallinokkam coast	09° 09' 55" N/ 78° 38' 33" E	Dry sponge
244	7/7/2018	Vallinokkam coast	09° 09' 55" N/ 78° 38' 33" E	Dry sponge
245	7/7/2018	Vallinokkam coast	09° 09' 55" N/ 78° 38' 33" E	Dry sponge
246	7/7/2018	Vallinokkam coast	09° 09' 55" N/ 78° 38' 33" E	Dry sponge(echinodictyum sp.)
247	7/7/2018	Vallinokkam coast	09° 09' 55" N/ 78° 38' 33" E	Dry sponge
248	7/7/2018	Vallinokkam coast	09° 09' 55" N/ 78° 38' 33" E	Dry sponge(Fasciospongia cavernosa)
249	7/7/2018	Vallinokkam coast	09° 09' 55" N/ 78° 38' 33" E	Brick/orange color sponge
250	7/7/2018	Vallinokkam coast	09° 09' 55" N/ 78° 38' 33" E	Orange mushroom sponge
251	7/7/2018	Vallinokkam coast	09° 09' 55" N/ 78° 38' 33" E	Green sponge
252	7/7/2018	Vallinokkam coast	09° 09' 55" N/ 78° 38' 33" E	Blue Green sponge
253	7/7/2018	Vallinokkam coast	09° 09' 55" N/ 78° 38' 33" E	Dark green sponge
254	7/7/2018	Vallinokkam coast	09° 09' 55" N/ 78° 38' 33" E	Light green sponge
255	7/7/2018	Vallinokkam coast	09° 09' 55" N/ 78° 38' 33" E	Dry sponge
256	7/7/2018	Vallinokkam coast	09° 09' 55" N/ 78° 38' 33" E	Dry sponge
257	7/7/2018	Vallinokkam coast	09° 09' 55" N/ 78° 38' 33" E	Dry sponge
258	7/7/2018	Vallinokkam coast	09° 09' 55" N/ 78° 38' 33" E	Dry sponge
259	7/7/2018	Vallinokkam coast	09° 09' 55" N/ 78° 38' 33" E	Dry sponge
260	7/7/2018	Vallinokkam coast	09° 09' 55" N/ 78° 38' 33" E	Dry sponge
261	7/7/2018	Vallinokkam coast	09° 09' 55" N/ 78° 38' 33" E	Dry sponge
262	7/7/2018	Vallinokkam coast	09° 09' 55" N/ 78° 38' 33" E	Dry sponge
263	7/7/2018	Vallinokkam coast	09° 09' 55" N/ 78° 38' 33" E	Dry sponge
264	7/7/2018	Vallinokkam coast	09° 09' 55" N/ 78° 38' 33" E	Dry sponge
265	7/7/2018	Vallinokkam coast	09° 09' 55" N/ 78° 38' 33" E	Dry sponge(echinodictyum sp.)
266	7/7/2018	Vallinokkam coast	09° 09' 55" N/ 78° 38' 33" E	Dry sponge along with rock(echinodictyum sp.)
267	7/7/2018	Vallinokkam coast	09° 09' 55" N/ 78° 38' 33" E	Dry sponge
268	7/7/2018	Vallinokkam coast	09° 09' 55" N/ 78° 38' 33" E	Dry sponge

269	7/7/2018	Vallinokkam coast	09° 09' 55" N/ 78° 38' 33" E	Dry sponge
270	7/7/2018	Vallinokkam coast	09° 09' 55" N/ 78° 38' 33" E	Dry sponge
271	7/7/2018	Vallinokkam coast	09° 09' 55" N/ 78° 38' 33" E	Orange wet sponge(echinodictyu sp.)
272	7/7/2018	Vallinokkam coast	09° 09' 55" N/ 78° 38' 33" E	Orange coral
273	7/7/2018	Vallinokkam coast	09° 09' 55" N/ 78° 38' 33" E	Black coral
274	7/7/2018	Vallinokkam coast	09° 09' 55" N/ 78° 38' 33" E	Wet brown sponge
275	7/7/2018	Vallinokkam coast	09° 09' 55" N/ 78° 38' 33" E	Brown dry sponge
276	7/7/2018	Vallinokkam coast	09° 09' 55" N/ 78° 38' 33" E	Dark brown bulbus algae
277	7/7/2018	Vallinokkam coast	09° 09' 55" N/ 78° 38' 33" E	Black dry sample
278	7/7/2018	Vallinokkam coast	09° 09' 55" N/ 78° 38' 33" E	Merchanta pink(reddish)
279	7/7/2018	Vallinokkam coast	09° 09' 55" N/ 78° 38' 33" E	Big dry sponge
280	7/7/2018	Vallinokkam coast	09° 09' 55" N/ 78° 38' 33" E	Big dry sponge
281	7/7/2018	Vallinokkam coast	09° 09' 55" N/ 78° 38' 33" E	Big dry sponge(spongia sp.)
282	7/7/2018	Vallinokkam coast	09° 09' 55" N/ 78° 38' 33" E	Big dry sponge(echinodictyum sp.)
283	7/7/2018	Vallinokkam coast	09° 09' 55" N/ 78° 38' 33" E	Big dry sponge(echinodictyum sp.)
284	7/7/2018	Vallinokkam coast	09° 09' 55" N/ 78° 38' 33" E	Big dry sponge
285	7/7/2018	Vallinokkam coast	09° 09' 55" N/ 78° 38' 33" E	Big dry sponge
286	7/7/2018	Vallinokkam coast	09° 09' 55" N/ 78° 38' 33" E	Big dry sponge
287	7/7/2018	Vallinokkam coast	09° 09' 55" N/ 78° 38' 33" E	Big dry sponge
288	7/7/2018	Vallinokkam coast	09° 09' 55" N/ 78° 38' 33" E	Orange coral pendula like
289	7/7/2018	Vallinokkam coast	09° 09' 55" N/ 78° 38' 33" E	Black coral pendula like
290	7/7/2018	Kootanguli coast	08° 15' 21" N/ 77° 48' 32" E	Large mushroom like sponge
291	7/7/2018	Kootanguli coast	08° 15' 21" N/ 77° 48' 32" E	Brown colour sponge-mass like appearance
292	7/7/2018	Kootanguli coast	08° 15' 21" N/ 77° 48' 32" E	Sponge having spiny like structure-yellowish brown(dysidea fragilis)
293	7/7/2018	Kootanguli coast	08° 15' 21" N/ 77° 48' 32" E	Black sponge
294	7/7/2018	Kootanguli coast	08° 15' 21" N/ 77° 48' 32" E	Brown color corals
295	7/7/2018	Kootanguli coast	08° 15' 21" N/ 77° 48' 32" E	Flower like blackish brown sponge
296	7/7/2018	Kootanguli coast	08° 15' 21" N/ 77° 48' 32" E	Greenish brown color corals
297	7/7/2018	Kootanguli coast	08° 15' 21" N/ 77° 48' 32" E	Sponge having fringes like appearance
298	7/7/2018	Kootanguli coast	08° 15' 21" N/ 77° 48' 32" E	Brown color porous sponge
299	7/7/2018	Kootanguli coast	08° 15' 21" N/ 77° 48' 32" E	Orange color coral stick
300	7/7/2018	Kootanguli coast	08° 15' 21" N/ 77° 48' 32" E	Lichen(small green flower like)
301	7/7/2018	Kootanguli coast	08° 15' 21" N/ 77° 48' 32" E	
302	7/7/2018	Kootanguli coast	08° 15' 21" N/ 77° 48' 32" E	White color fungi having fringes appearance

303	7/7/2018	Kootanguli coast	08° 15' 21" N/ 77° 48' 32" E	Sponge same growing at bamboo in water
304	7/7/2018	Kootanguli coast	08° 15' 21" N/ 77° 48' 32" E	Polyporous brown color fungi
305	7/7/2018	Kootanguli coast	08° 15' 21" N/ 77° 48' 32" E	Green mass on wood
306	7/7/2018	Kootanguli coast	08° 15' 21" N/ 77° 48' 32" E	Soil sediment

Annexure 1d. Kerala sampling detail (June 2019)

Sample Number	Date of Sampling	Geographical location	GPS Coordinate	Types of samples
1.	4/6/2019	Muthurayana	77° 30' 06"N/13° 04' 92" E	Brick red layer of Lemna
2.	4/6/2019		77° 30' 06"N/13° 04' 92" E	A Brown Pond Spotted Algal
3.	4/6/2019	Coorg gate hotel	77° 30' 06"N/13° 04' 92" E	Brown Pond Spotted Algal
4.	4/6/2019	Coorg gate hotel	77° 30' 06"N/13° 04' 92" E	A brown sponge attached to the algae
5.	4/6/2019	Coorg gate hotel	77° 30' 06"N/13° 04' 92" E	Light ash to white coloured algae attached to sponge
6.	4/6/2019	Coorg gate hotel	77° 30' 06"N/13° 04' 92" E	Sediment rhizosphere soil of grass
7.	4/6/2019	Coorg gate hotel	77° 30' 06"N/13° 04' 92" E	Algal mat on the hill slope with water dripping
8.	4/6/2019	pottandyvame devashanam	77° 35' 06"N/13° 09' 92" E	Green water body vengara
9.	4/6/2019	Ittikulam beach	75° 20' 54"N/12° 00' 67" E	small water body on the beach with black colour
10.	4/6/2019	Ittikulam,	75° 20' 54"N/12° 00' 67" E	brown algae
11.	4/6/2019	Ittikulam,	75° 20' 54"N/12° 00' 67" E	brown fibrous
12.	4/6/2019	Ittikulam,	75° 20' 54"N/12° 00' 67" E	green fibrous
13.	4/6/2019	Pallikkera,	75° 04' 39"N/12° 38' 50" E	mangrove water, orange brown layer with black sediment
14.	4/6/2019	Pallikkera	75° 04' 39"N/12° 38' 50" E	Algal mat adjacent to mangroves
15.	4/6/2019	Pallikkera	75° 04' 39"N/12° 38' 50" E	Green algal mat
16.	5/6/2019	Thalassery	75° 48' 47"N/11° 74' 69" E	algal mat on moist soil
17.	5/6/2019	Thalassery	75° 48' 47"N/11° 74' 69" E	algae attached to rocks, it is fibrous and green
18.	5/6/2019	Thalassery	75° 48' 47"N/11° 74' 69" E	Brown algae, green algae
19.	5/6/2019	thrissur	76° 21' 47"N/10° 52' 43" E	Algal mat
20.	5/6/2019	thrissur	76° 21' 47"N/10° 52' 43" E	a man made water body
21.	6/6/2019	Guruvaayur beach,	76° 03' 93"N/10° 59' 49" E	dry sponge with holes
22.	6/6/2019	Guruvaayur beach	76° 03' 93"N/10° 59' 49" E	White dry sponge with no holes
23.	6/6/2019	Guruvaayur beach	76° 03' 93"N/10° 59' 49" E	Epiozoitic, orange colour on shell, white
24.	6/6/2019	Guruvaayur beach	76° 03' 93"N/10° 59' 49" E	White sponge, like mushroom
25.	6/6/2019	Guruvaayur beach	76° 03' 93"N/10° 59' 49" E	Sargassam
26.	6/6/2019	Guruvaayur beach	76° 03' 93"N/10° 59' 49" E	Tar/oil/ for PAH, crude
27.	6/6/2019	Guruvaayur beach	76° 03' 93"N/10° 59' 49" E	Sand composite,
28.	6/6/2019	Guruvaayur beach	76° 03' 93"N/10° 59' 49" E	Green algal mat
29.	6/6/2019	Guruvaayur beach	76° 03' 93"N/10° 59' 49" E	Colorless biofilm
30.	6/6/2019	Guruvaayur beach	76° 03' 93"N/10° 59' 49" E	Wetland biofilm
31.	7/6/2019	Athirapally fall	76° 56' 91"N/10° 28' 47" E	Algal mat
32.	7/6/2019	Athirapally fall	76° 56' 91"N/10° 28' 47" E	Black algae, benthic, fresh water,
33.	7/6/2019	Athirapally fall	76° 56' 91"N/10° 28' 47" E	Decaying wood
34.	7/6/2019	Athirapally fall	76° 56' 91"N/10° 28' 47" E	Root of a plant growing on rock
35.	7/6/2019	Athirapally fall	76° 56' 91"N/10° 28' 47" E	Algae floating in the rock
36.	7/6/2019	Athirapally fall	76° 56' 91"N/10° 28' 47" E	Small pebble
37.	7/6/2019	Athirapally fall	76° 56' 91"N/10° 28' 47" E	Green algae
38.	7/6/2019	Athirapally fall	76° 56' 91"N/10° 28' 47" E	Algal biofilms in the small holes
39.	7/6/2019	Athirapally fall	76° 56' 91"N/10° 28' 47" E	dark green colour algal mat
40.	7/6/2019	Athirapally fall	76° 56' 91"N/10° 28' 47" E	Light green fibrous algae
41.	7/6/2019	Athirapally fall	76° 56' 91"N/10° 28' 47" E	White polyparous
42.	7/6/2019	Athirapally fall	76° 56' 91"N/10° 28' 47" E	Root of plants in water
43.	7/6/2019	Athirapally fall	76° 56' 91"N/10° 28' 47" E	Mat on palm blue
44.	7/6/2019	Athirapally fall	76° 56' 91"N/10° 28' 47" E	Red coloured lichen
45.	7/6/2019	Athirapally fall	76° 56' 91"N/10° 28' 47" E	Green coloured lichen

46.	7/6/2019	Athirapally fall	76° 56' 91"N/10° 28' 47" E	Lichen
47.	7/6/2019	Athirapally fall	76° 56' 91"N/10° 28' 47" E	Lichen
48.	7/6/2019	Athirapally fall	76° 56' 91"N/10° 28' 47" E	Lichen
49.	7/6/2019	Athirapally fall	76° 56' 91"N/10° 28' 47" E	Decaying leaf
50.	7/6/2019	Athirapally fall	76° 56' 91"N/10° 28' 47" E	Decaying leaf

Annexure 1e. Tamil Nadu samples detail (December 2019)

Sample no.	**Date of sampling**	**Geographical location**	**GPS Coordinate**	**Type of samples**
1	26/12/2019	Sea shore near mandapam	09° 16' 52" N/ 79° 10' 20" E	sediment
2	26/12/2019	Sea shore near mandapam	09° 16' 52" N/ 79° 10' 20" E	sediment
3	26/12/2019	Sea shore near mandapam	09° 16' 52" N/ 79° 10' 20" E	sediment
4	26/12/2019	Sea shore near mandapam	09° 16' 52" N/ 79° 10' 20" E	algal sample (fibrous alga)
5	26/12/2019	Sea shore near mandapam	09° 16' 52" N/ 79° 10' 20" E	Sand
6	26/12/2019	Sea shore near mandapam	09° 16' 52" N/ 79° 10' 20" E	Yellowish Green,long sea weed
7	26/12/2019	Sea shore near mandapam	09° 16' 52" N/ 79° 10' 20" E	Green,long sea weed
8	26/12/2019	Sea shore near mandapam	09° 16' 52" N/ 79° 10' 20" E	Grey dead sponge
9	26/12/2019	Sea shore near mandapam	09° 16' 52" N/ 79° 10' 20" E	Green leaf-sea weed-
10	26/12/2019	Sea shore near mandapam	09° 16' 52" N/ 79° 10' 20" E	Shell on which white shells are
11	26/12/2019	Sea shore near mandapam	09° 16' 52" N/ 79° 10' 20" E	Orange color sea weed-fibrous
12	26/12/2019	Sea shore near mandapam	09° 16' 52" N/ 79° 10' 20" E	Orange fibrous algae
13	26/12/2019	Sea shore near mandapam	09° 16' 52" N/ 79° 10' 20" E	Leafy-macro algae-brownish
14	26/12/2019	Sea shore near mandapam	09° 16' 52" N/ 79° 10' 20" E	Sea weed-umbrella like
15	26/12/2019	Sea shore near mandapam	09° 16' 52" N/ 79° 10' 20" E	Light green colour-branching-sea weed thin branches.
16	26/12/2019	Sea shore near mandapam	09° 16' 52" N/ 79° 10' 20" E	Bluish green-mass
17	26/12/2019	Sea shore near mandapam	09° 16' 52" N/ 79° 10' 20" E	Sea weed-branching
18	26/12/2019	Sea shore near mandapam	09° 16' 52" N/ 79° 10' 20" E	Pinkish brown coloured sand
19	26/12/2019	Sea shore near mandapam	09° 16' 52" N/ 79° 10' 20" E	Greenish yellow dead sponge

20	26/12/2019	Sea shore near mandapam	09° 16' 52" N/ 79° 10' 20" E	Sea weed-green
21	26/12/2019	Sea shore near mandapam	09° 16' 52" N/ 79° 10' 20" E	Stone
22	26/12/2019	Sea shore near mandapam	09° 16' 52" N/ 79° 10' 20" E	Stone
23	26/12/2019	Sea shore near mandapam	09° 16' 52" N/ 79° 10' 20" E	Shell
24	26/12/2019	Sea shore near mandapam	09° 16' 52" N/ 79° 10' 20" E	Dead sponge
25	26/12/2019	Sea shore near mandapam	09° 16' 52" N/ 79° 10' 20" E	Shell
26	26/12/2019	Sea shore near mandapam	09° 16' 52" N/ 79° 10' 20" E	Red coloured,shiny macroalgae
27	26/12/2019	Sea shore near mandapam	09° 16' 52" N/ 79° 10' 20" E	Phytoplankton
28	26/12/2019	Sea shore near mandapam	09° 16' 52" N/ 79° 10' 20" E	Green algae ball like structure
29	26/12/2019	Sea shore near mandapam	09° 16' 52" N/ 79° 10' 20" E	Shell
30	26/12/2019	Sea shore near mandapam	09° 16' 52" N/ 79° 10' 20" E	Sargassam
31	26/12/2019	Sea shore near mandapam	09° 16' 52" N/ 79° 10' 20" E	Green slimy mass of alga
32	26/12/2019	Sea shore near mandapam	09° 16' 52" N/ 79° 10' 20" E	Sargassam leaves pink patch
33	26/12/2019	Sea shore near mandapam	09° 16' 52" N/ 79° 10' 20" E	Solidified sand with rock
34	26/12/2019	Opposite CFMR coast	09° 16' 57" N/ 78° 55' 07" E	pinkish spot-seaweed leaf
35	26/12/2019	Opposite CFMR coast	09° 16' 57" N/ 78° 55' 07" E	Live spinge-yellowish green
36	26/12/2019	Opposite CFMR coast	09° 16' 57" N/ 78° 55' 07" E	Green fibrous algae
37	26/12/2019	Opposite CFMR coast	09° 16' 57" N/ 78° 55' 07" E	Yellow sponge-appear black associated with algae
38	26/12/2019	Opposite CFMR coast	09° 16' 57" N/ 78° 55' 07" E	Sponge associated with algae
39	26/12/2019	Opposite CFMR coast	09° 16' 57" N/ 78° 55' 07" E	Round sponge-green color
40	26/12/2019	Opposite CFMR coast	09° 16' 57" N/ 78° 55' 07" E	Coral
41	26/12/2019	Opposite CFMR coast	09° 16' 57" N/ 78° 55' 07" E	Algae attached to coral
42	26/12/2019	Opposite CFMR coast	09° 16' 57" N/ 78° 55' 07" E	Green alage
43	26/12/2019	Opposite CFMR coast	09° 16' 57" N/ 78° 55' 07" E	Green alga with dry pink branch
44	26/12/2019	Opposite CFMR coast	09° 16' 57" N/ 78° 55' 07" E	Chara
45	27/12/2019	Pudumadam coast	09° 16' 33" N/ 78° 48' 37" E	Fibrous sea weed
46	27/12/2019	Pudumadam coast	09° 16' 33" N/ 78° 48' 37" E	Green algae

47	27/12/2019	Pudumadam coast	09° 16' 33" N/ 78° 48' 37" E	Fibrous,slimy,green algae,small leaf like structure
48	27/12/2019	Pudumadam coast	09° 16' 33" N/ 78° 48' 37" E	Cream color sponge(white spike)
49	27/12/2019	Pudumadam coast	09° 16' 33" N/ 78° 48' 37" E	Green macro algae
50	27/12/2019	Pudumadam coast	09° 16' 33" N/ 78° 48' 37" E	Macroalgae(sargassam)
51	27/12/2019	Pudumadam coast	09° 16' 33" N/ 78° 48' 37" E	Orange sponge
	27/12/2019	Pudumadam coast	09° 16' 33" N/ 78° 48' 37" E	Blue sponge
53	27/12/2019	Pudumadam coast	09° 16' 33" N/ 78° 48' 37" E	Grey sponge
54	27/12/2019	Pudumadam coast	09° 16' 33" N/ 78° 48' 37" E	Reddhish white sponge-tightly attached to rock
55	27/12/2019	Pudumadam coast	09° 16' 33" N/ 78° 48' 37" E	Yellow sponge
56	27/12/2019	Pudumadam coast	09° 16' 33" N/ 78° 48' 37" E	Orangish greenish sponge
57	27/12/2019	Vallinokkam coast	09° 09' 22" N/ 78° 38' 48" E	Ball like sponge associated with other sponge
58	27/12/2019	Vallinokkam coast	09° 09' 22" N/ 78° 38' 48" E	Pink color sponges
59	27/12/2019	Vallinokkam coast	09° 09' 22" N/ 78° 38' 48" E	Brown coloured sponge-grren algae attached on
60	27/12/2019	Vallinokkam coast	09° 09' 22" N/ 78° 38' 48" E	Small ball like yellow sponge
61	27/12/2019	Vallinokkam coast	09° 09' 22" N/ 78° 38' 48" E	Sponge red
62	27/12/2019	Vallinokkam coast	09° 09' 22" N/ 78° 38' 48" E	Green sea weed covered with green macroalga
63	27/12/2019	Vallinokkam coast	09° 09' 22" N/ 78° 38' 48" E	Unnamed
64	27/12/2019	Pudumadam coast	09° 16' 33" N/ 78° 48' 37" E	Macroalagae(mucilaginous)(green)
65	27/12/2019	Pudumadam coast	09° 16' 33" N/ 78° 48' 37" E	Reddish fibre kind algae
66	27/12/2019	Pudumadam coast	09° 16' 33" N/ 78° 48' 37" E	Reddish fibre kind algae
67	27/12/2019	Pudumadam coast	09° 16' 33" N/ 78° 48' 37" E	Leaf like alage(green)
68	27/12/2019	Pudumadam coast	09° 16' 33" N/ 78° 48' 37" E	Rock
69	27/12/2019	Pudumadam coast	09° 16' 33" N/ 78° 48' 37" E	Small fibrous green algae
70	27/12/2019	Pudumadam coast	09° 16' 33" N/ 78° 48' 37" E	Green dead sponge
71	27/12/2019	Pudumadam coast	09° 16' 33" N/ 78° 48' 37" E	Green ball like algae(sea weed)
72	27/12/2019	Pudumadam coast	09° 16' 33" N/ 78° 48' 37" E	Salt pan
73	27/12/2019	Pudumadam coast	09° 16' 33" N/ 78° 48' 37" E	Brown algae(fibrous)
74	27/12/2019	Pudumadam coast	09° 16' 33" N/ 78° 48' 37" E	Sand on shell
75	27/12/2019	Pudumadam coast	09° 16' 33" N/ 78° 48' 37" E	
76	27/12/2019	Pudumadam coast	09° 16' 33" N/ 78° 48' 37" E	Phytoplankton
77	27/12/2019	Pudumadam coast	09° 16' 33" N/ 78° 48' 37" E	Algal mat over salt pan
78	27/12/2019	Pudumadam coast	09° 16' 33" N/ 78° 48' 37" E	White patches on brown algae
79	27/12/2019	Pudumadam coast	09° 16' 33" N/ 78° 48' 37" E	Green wrinked macroalgae
80	27/12/2019	Pudumadam coast	09° 16' 33" N/ 78° 48' 37" E	Greenish macroalgae

81	27/12/2019	Pudumadam coast	09° 16' 33" N/ 78° 48' 37" E	Sargassum
82	27/12/2019	Pudumadam coast	09° 16' 33" N/ 78° 48' 37" E	Green algae
83	27/12/2019	Pudumadam coast	09° 16' 33" N/ 78° 48' 37" E	Kelp-sea weed

Publications

Publications

From this thesis

Gaurav Kumar., Dhanesh K., Jagadeeshwari U., Sreya PK., Shabbir A., Sasikala, Ch. and Ramana, Ch.V. (2021) *Crateriforma spongiae* sp. nov., isolated from a marine sponge. Antonie van Leeuwenhoek. (doi.org/10.1007/s10482-020-01515-1)

[$]Dhanesh K., [$]**Gaurav Kumar.,** [$]Jagadeeshwari U., Sasikala, Ch. and Ramana Ch.V. (2021) "*Candidatus* Laterigemmans baculatus" gen. nov. sp. nov., the first representative of rod shaped planctomycetes with lateral budding in the family *Pirellulaceae.* Syst Appl Microbiol. (doi.org/10.1016/j.syapm.2021.126188)

[$]**Gaurav Kumar.,** [$]Radha Vaddavalli., [$]Jagadeeshwari, U., Sasikala, Ch. and Ramana, Ch.V. (2020) Bacterial communities of sponges from the wetland ecosystem of Little Rann of Kutch, India with particular reference to Planctomycetes. 3 Biotech. 10:1-10

[$]Dhanesh Kumar., [$]**Kumar Gaurav.,** Jagadeeshwari U., Deepshikha G., Sasikala, Ch. and Ramana, Ch.V. (2020) *Roseimaritima sediminicola* sp. nov., a new member in Planctomycetaceae isolated from Chilika lagoon. Int J Syst Evol Microbiol.70:2613-2623.

[$]Dhanesh Kumar., [$]**Gaurav Kumar.,** Shabbir A., Jagadeeshwari, U., Sasikala, Ch. and Ramana, Ch.V. (2020) Descriptions of *Roseiconus nitratireducens* gen. nov. sp. nov. and *Roseiconus lacunae* sp. nov. Arch Microbiol. 12:1-14

[$]Dhanesh Kumar., [$]**Kumar Gaurav.,** Sreya PK, Shabbir A, Jagadeeshwari, U., Deepshikha G., Sasikala, Ch. and Ramana, Ch.V. (2020) *Gimesia chilikensis* sp. nov., a haloalkali tolerant planctomycete isolated from Chilika lagoon and emended description of the genus *Gimesia.* Int J Syst Evol Microbiol.70:3647-3655.

[$]**Gaurav Kumar.,** [$] Dhanesh K., Jagadeeshwari U., Shabbir A., Sasikala, Ch. and Ramana, Ch.V (2021) Phylo-taxogenomics of the genus *Tautonia* with descriptions of *Tautonia marina* sp. nov., *Tautonia rosea* sp. nov., and emended description of the genus. Syst Appl Microbiol. (Under Revision)

[$]**Gaurav Kumar.,** [$]Lhingjakim Khongsai L., Shabbir A., Jagadeeshwari, U., ., Sasikala Ch. and Ramana Ch.V. (2021) *Aquisphaera insulae* sp. nov., a new member in Isosphaeraceae isolated from the floating island of Loktak lake and emended description of the genus *Aquisphaera*. Antonie van Leeuwenhoek. (Communicated)

Note:- $, First and Equal authorship

Others Publications

N. Senthilnathan, **Kumar Gaurav,** Ch. Venkata Ramana and T. P. Radhakrishnan. Zwitterionic small molecule based fluorophores for efficient and selective imaging of bacterial endospores. J Mater Chem B .2020. 8: 4601-4608.

Ashif A., **Gaurav Kumar.,** N. Senthilnathan, T. P. Radhakrishnan, Sasikala, Ch., and Ramana, Ch.V. (2020) "Sporotan" a new fluorescent stain for identifying *Rhodobacter johrii*. J. Microbiol. Methods. 177: 106019

[$]Kaushik Rishabh., [$]Meesha Sharma., **Kumar Gaurav.,** U. Jagadeeshwari., A. Shabbir., Ch Sasikala., Ch V. Ramana., and Maharaj K. Pandit. (2020) "Paludisphaera soli sp. nov., a new member of the family Isosphaeraceae isolated from high altitude soil in the Western Himalaya." Antonie van Leeuwenhoek. 113: 1663-1674.

Indu B., **Kumar Gaurav.,** Smita N., Shabbir A., Sasikala Ch. and Ramana Ch.V. (2020) Chryseobacterium candidae sp. nov., isolated from a yeast (Candida tropicalis). Int J Syst Evol Microbiol. 70: 93-99.

Kumar, D, Nandardhane Smita, **Kumar Gaurav,** Gandham Suresh, Uppada Jagadeeshwari, Chintalapati Sasikala, and Chintalapati Venkata Ramana. "Arenibacter lacus sp. nov., Isolated from Chilika Lagoon, India." Current Microbiol. 2020.77:4152-4159.

Anusha R, Indu, N. Smita, G. Deepshikha, **Kumar Gaurav,** K. Dhanesh, G. Suresh, Ch. Sasikala, and Ch. V. Ramana Emerging Concepts in Bacterial Taxonomy. Microbial Diversity in Ecosystem Sustainability and Biotechnological Applications. Springer, Singapore.

Pre-Patent Application

N. Senthilnathan., **Kumar Gaurav.,** Ch. Venkata Ramana and T. P. Radhakrishnan, Sporotan: A Spore Selective Fluorescent Dye for Identification of Cryptic Bacterial Spores, Indian patent 201941052617 dated 18.12.2019.

Presented in the following conference

Kumar Gaurav., Radha Vaddavalli., Jagadeeshwari Uppadda., Ramana, Ch.V. and Sasikala, Ch. (2018). "Anaerobic ammonium oxidation bacteria (anammox) bacteria associated with sponges collected from little Rann of Kutch, Gujarat, India". Poster presentation in 59th Annual conference of AMI during 9th-12th December, 2018 in Hyderabad, India.

Antonie van Leeuwenhoek
https://doi.org/10.1007/s10482-020-01515-1

ORIGINAL PAPER

Crateriforma spongiae sp. nov., isolated from a marine sponge and emended description of the genus "*Crateriforma*"

Gaurav Kumar · Dhanesh Kumar · U. Jagadeeshwari · P. K. Sreya · A. Shabbir · Ch. Sasikala · Ch. V. Ramana

Received: 17 August 2020 / Accepted: 22 December 2020
© The Author(s), under exclusive licence to Springer Nature Switzerland AG part of Springer Nature 2021

Abstract A Gram-stain-negative, aerobic, pear to oval shaped, rosette forming bacterium with crateriform structures well distributed on the cell surface designated as strain JC647^T was isolated from a sponge specimen belonging to the genus *Spongia*. Strain JC647^T reproduces through budding. Strain JC647^T shared highest 16S rRNA gene sequence identity of 99.9% with "*Crateriforma conspicua*" Mal65^T (not a valid species name). The genome size of strain JC647^T is 6.9 Mb with a G + C content of 57.8 mol %. For the resolution of the phylogenetic congruence of the novel strain, the phylogeny was also constructed with the sequences of ninety-two housekeeping genes. Based on the phylogenetic analyses, low *d*DDH value (51.0%), low gANI (93.2%), low AAI (94.9%) results, chemotaxonomic characteristics and differential physiological properties, strain JC647^T is recognized as a new species of the genus "*Crateriforma*", for which we propose the name *Crateriforma spongiae* sp. nov. The type species is JC647^T (= KCTC 72176^T = NBRC 114068^T).

Keywords Planctomycetes · Crateriforma · Sponge · New species

A1 The GenBank/EMBL/DDBJ accession numbers for the 16S
A2 rRNA gene sequences of the strains JC647^T is LR132071. This
A3 Whole Genome Shotgun project has been deposited at DDBJ/
A4 ENA/GenBankunder the accession JAAXMS000000000. The
A5 version described in this paper is version JAAXMS010000000.

A6 **Supplementary Information** The online version of this
A7 article (https://doi.org/10.1007/s10482-020-01515-1) contains
A8 supplementary material, which is available to authorized users.

A9 G. Kumar · D. Kumar · P. K. Sreya ·
A10 A. Shabbir · Ch. V. Ramana (✉)
A11 Department of Plant Sciences, School of Life Sciences,
A12 University of Hyderabad, P.O. Central University,
A13 Hyderabad 500046, India
A14 e-mail: cvr449@gmail.com

A15 U. Jagadeeshwari · Ch. Sasikala (✉)
A16 Bacterial Discovery Laboratory,Centre for Environment,
A17 Institute of Science and Technology, JNT University
A18 Hyderabad, Kukatpally, Hyderabad 500085, India
A19 e-mail: sasi449@yahoo.ie; sasikala.ch@gmail.com

Abbreviations

NCBI	National Centre for Biotechnology Information
*g*ANI	Genome Average Nucleotide Identity
AAI	Average Amino Acid Identity
*d*DDH	Digital DNA–DNA Hybridization
POCP	Percentage Of Conserved Proteins
HPLC	High-Pressure Liquid Chromatography
KCTC	Korean Collection for Type Cultures
NBRC	Biological Resource Centre, NITE

Introduction

The phylum Planctomycetes along with Verrucomicrobia, Lentisphaerae, Kiritimatiellaeota, Candidatus

REVISED PROOF

Journal : Medium 10482 | Dispatch : 15-1-2021 | Pages : 13
Article No. : 1515 | ☐ LE | ☐ TYPESET
MS Code : ANTO-D-20-00318R1 | ☑ CP | ☑ DISK

Systematic and Applied Microbiology 44 (2021) 126188

Contents lists available at ScienceDirect

Systematic and Applied Microbiology

journal homepage: http://www.elsevier.com/locate/syapm

"*Candidatus* Laterigemmans baculatus" gen. nov. sp. nov., the first representative of rod shaped planctomycetes with lateral budding in the family *Pirellulaceae*

Dhanesh Kumar[a,1], Gaurav Kumar[a,1], Uppada Jagadeeshwari[b,1], Chintalapati Sasikala[b,*], Chintalapati Venkata Ramana[a,*]

[a] *Department of Plant Sciences, School of Life Sciences, University of Hyderabad, P.O. Central University, Hyderabad 500046, India*
[b] *Bacterial Discovery Laboratory, Centre for Environment, Institute of Science and Technology, J. N. T. University Hyderabad, Kukatpally, Hyderabad 500085, India*

ARTICLE INFO

Article history:
Received 24 September 2020
Received in revised form 5 February 2021
Accepted 8 February 2021

Keywords:
Planctomycetes
Pirellulaceae
Candidatus taxa
gen. nov
sp. nov.

ABSTRACT

Two axenic cultures of *Planctomycetes* were isolated from distinct geographical regions of the east coast of India. The two closely related strains (JC640 and CH01) showed <93.3% 16S rRNA gene sequence identity with members of the genus *Roseimaritima* followed by *Rhodopirellula* (<91%). Both strains displayed non-canonical cell morphology of *Planctomycetes*, such as rod shaped cells with division by lateral budding. Both strains showed crateriform structures on their surfaces and cells lack fimbriae. The genomes have a size of about 5.76 Mb and DNA G+C content of 63.6 mol%. Phylogenetic analysis based on 16S rRNA gene sequence and 92 core genes based RAxML phylogenetic tree place both the strains in the family *Pirellulaceae* and indicated *Roseimaritima sediminicola* as their closest relative. The AAI and POCP values differentiate both strains from rest of the members of the family *Pirellulaceae*. The axenic cultures of both strains were able to grow up to 8–10 passages and subsequently the cells became non-viable with pleomorphic shapes. Supported by genomic, phylogenetic and morphological differences, we conclude that both strains belong to a novel genus. However, since the new isolates lost their viability on passaging, we propose the novel genus as "*Candidatus* Laterigemmans" gen. nov. and the novel species as "*Candidatus* Laterigemmans baculatus" sp. nov.

© 2021 Elsevier GmbH. All rights reserved.

The GenBank/EMBL/DDBJ accession numbers for the 16S rRNA gene sequences of the strains JC640 and CH01 are LR536992 and MT975270 respectively. The GenBank/EMBL/DDBJ accession for the whole genome shotgun sequences are WRPR01000000 and JACVRC010000000 for strains JC640and CH01, respectively.

Introduction

The phylum *Planctomycetes* along with *Verrucomicrobia*, *Lentisphaerae*, *Kiritimatiellaeota*, "*Candidatus* Omnitrophica" and *Chlamydiae* forms PVC superphylum [6,8,12,13,39–41,44]. Members of the phylum *Planctomycetes* are ubiquitously distributed [35,39] and mostly isolated from brackish and marine sources [4,5,22,25,26,28,32,48,49,51]. Taxonomically, the phylum *Planctomycetes* is subdivided into three classes: *Phycisphaerae*, *Planctomycetia*, and "*Candidatus* Brocadiae". At present, the class *Planctomycetia* consists of a majority of the validly described names of the taxa classified within four orders (*Pirellulales, Gemmatales, Isosphaerales*, and *Planctomycetales*) and each order (except for *Pirellulales)* is represented by a single family (*Gemmataceae*, *Isosphaeraceae* and *Planctomycetaceae*). The Order *Pirellulales* has three families; *Pirellulaceae, Lacipirellulaceae* and *Thermoguttaceae*. The family *Pirellulaceae* is represented by thirteen genera, among which several genera names still need validation (https://lpsn.dsmz.de/family/pirellulaceae); *Rhodopirellula*, *Pirellula*, *Rubripirellula*, *Roseimaritima*, *Mariniblastus*, *Novopirellula, Blastopirellula, "Bremerella", "Crateriforma", "Aureliella" "Lignipirellula"*, "*Stieleria*" and "*Rosistilla*" [4,5,7,17–21,32,35,38,45,49,51].

Members of the class "*Candidatus* Brocadiae" are capable of performing anaerobic ammonium oxidation (anammox) [48,49] and

Abbreviations: NCBI, National Centre for Biotechnology Information; AAI, Average Nucleotide Index; POCP, Percentage of Conserved Protein.

* Corresponding authors.
E-mail address: sasikala.ch@gmail.com (C. Sasikala).
[1] Equal contribution as first authors.

https://doi.org/10.1016/j.syapm.2021.126188
0723-2020/© 2021 Elsevier GmbH. All rights reserved.

3 Biotech (2020) 10:478
https://doi.org/10.1007/s13205-020-02449-1

ORIGINAL ARTICLE

Bacterial communities of sponges from the wetland ecosystem of Little Rann of Kutch, India with particular reference to Planctomycetes

Gaurav Kumar[1] · Vaddavalli Radha[1] · Uppadda Jagadeeshwari[2] · Chintalapati Sasikala[2] · Chintalapati Venkata Ramana[1]

Received: 1 June 2020 / Accepted: 21 September 2020
© King Abdulaziz City for Science and Technology 2020

Abstract

Five sponge specimens belonging to the genera *Spongilla* and *Ciocalypta* were collected from Little Rann of Kutch (in Gujarat, India) and analysed for associated microbiomes. Critical analysis was done with respect to members of the phylum Planctomycetes, using two different strategies; 1. Culture-independent metagenomic approach and 2. culture-dependent anaerobic enrichment for anammox-planctomycetes. The 16S rRNA gene (V1-V3 region) amplicon metagenome analysis revealed significant divergence in bacterial diversity, including Planctomycetes among the sponges analysed. Community metagenomics revealed a total of 376 Operational Taxonomic Units (OTUs) belonging to 41 different phyla. OTUs belonging to Proteobacteria was the most abundant (38%) among the sponge analysed. The KEGG annotation predicted a total of 6909 KEGG orthologs (KOs); most of the KOs are associated with membrane transport, xenobiotic degradation, production of secondary metabolites, amino acid metabolism and carbohydrate metabolism. In the culture-dependent study, FISH analysis confirmed the association of anammox-planctomycetes with sponges. Partial 16S rRNA gene sequences of two planctomycetes (JC545, JC543) were cladding with those of uncultured *Phycisphaerae* class. The other three putative anammox bacteria (JC541, JC542, JC544) formed a different clade with "*Candidatus* Brocadia anammoxidans". These three putative bacteria believably represent new species/genus related to "*Candidatus* Brocadia".

Keywords Sponges · Culture independent · Metagenome · Culture dependent · Planctomycetes · Anammox bacteria

Introduction

An unprecedented amount of information through high-throughput sequencing methods revealed the structural and functional diversity of microbial communities, particularly those associated with sponges (Thomas et al. 2016). Sponges have highly diverse and specific symbiont communities. Due to the filter-feeding activities of sponges, they maintain a constant influx of seawater microorganisms. Approximately 40% of sponge volume comprises of sponge-associated microorganisms having densities over 10^9 CFU of sponge tissue, several orders higher than those typical for seawater (Abdelmohsen et al. 2014). Sponge microbiome consists of all the three domains of life which play an essential role in shaping sponge evolution (Hentschel et al. 2003, 2012; Imhoff and Stohr 2003; Taylor et al. 2007). Sponge symbionts are capable of producing secondary metabolites and provide a chemical defence to the sponge. On the other hand,

Gaurav Kumar, Vaddavalli Radha and Uppadda Jagadeeshwari contributed equally and considered as first authors.

Electronic supplementary material The online version of this article (https://doi.org/10.1007/s13205-020-02449-1) contains supplementary material, which is available to authorized users.

✉ Chintalapati Venkata Ramana
cvr449@gmail.com

Chintalapati Sasikala
sasi449@yahoo.ie

[1] Department of Plant Sciences, School of Life Sciences, University of Hyderabad, P.O. Central University, Hyderabad 500046, India

[2] Bacterial Discovery Laboratory, Centre for Environment, Institute of Science and Technology, J. N. T. University Hyderabad, Kukatpally, Hyderabad 500085, India

Published online: 17 October 2020

INTERNATIONAL JOURNAL OF SYSTEMATIC AND EVOLUTIONARY MICROBIOLOGY

TAXONOMIC DESCRIPTION
Kumar *et al.*, *Int. J. Syst. Evol. Microbiol.* 2020;70:2616–2623
DOI 10.1099/ijsem.0.004076

MICROBIOLOGY SOCIETY

Roseimaritima sediminicola sp. nov., a new member of *Planctomycetaceae* isolated from Chilika lagoon

Dhanesh Kumar[1]†, Kumar Gaurav[1]†, Jagadeeshwari U[2], Deepshikha G[1], Sasikala Ch.[2,*] and Ramana Ch.V.[1,*]

Abstract

Strain JC651^T was isolated from a sediment sample collected from Chilika lagoon, which is one of the world's most important brackish water lakes with estuarine characteristics. Colonies of this strain are light pink and cells are Gram-stain negative, spherical to pear shaped and form rosettes. Strain JC651^T grows well up to pH 9.0 and tolerates up to 5% NaCl (w/v). The respiratory quinone is MK6. The detected major fatty acids are $C_{18:1}$ $\omega 9c$ and $C_{16:0}$. Its polar lipids are diphosphatidylglycerol, an unidentified phospholipid, phosphatidylglycerol and phosphatidylcholine. Strain JC651^T shows highest 16S rRNA gene sequence similarity (97.8%) to the type species of the genus *Roseimaritima*, *Roseimaritima ulvae* UC8^T. The genome size of strain JC651^T is 6.2 Mb with a G+C content of 62.4 mol%. For the resolution of the phylogenetic congruence of the novel strain, the phylogeny was also reconstructed with the sequences of 92 core genes. Based on the phylogenetic analyses, low digital DNA–DNA hybridization values (19.5%), low (74.9%) genome average nucleotide identity results, chemotaxonomic characteristics and differential physiological properties, strain JC651^T is recognized as a new species of the genus *Roseimaritima* for which we propose the name *Roseimaritima sediminicola* sp. nov. The type strain is JC651^T (=KCTC 72178^T=NBRC 113926^T).

The genus *Roseimaritima* of the phylum *Planctomycetes* was described by Bondoso and co-workers [1] to accommodate a planctomycetes of the family *Planctomycetaceae* isolated from the biofilm of marine macroalga *Ulva* sp., collected from the Northern coast of Portugal. *Roseimaritima ulvae* is the only species of this genus. It is a chemoheterotrophic, strictly aerobic and mesophilic marine bacterium with spherical to oval-shaped cells forming rosettes. $C_{18:1}$ ω9*c* and $C_{16:0}$ are the major fatty acids with MK6 as the respiratory quinone. The predominant polar lipids are phosphatidylcholine, phosphatidylglycerol and diphosphatidylglycerol.

Chilika lagoon is the largest brackish water lagoon of India and is situated in the Eastern part of the country. With an area of about 1100 km^2, it is connected to sea on one side and fed by rivers on other, making a salinity gradient of about 0–3%. The lagoon is an ecological hotspot with great diversity of flora and fauna and declared as Ramsar site in 1981. During our survey for planctomycetes of this lagoon, we have isolated a few members of this phylum; however, most of these became non-cultivable on passaging. Here we describe strain JC651^T isolated from a sediment sample of Chilika lagoon and propose it as a representative of a new species of the genus *Roseimaritima* using the polyphasic approach together with genomic information. This is apparently the first report of planctomycetes from India.

HOME, HABITAT AND ISOLATION

Strain JC651^T was isolated from a sediment sample collected from the Satapada region (19° 40′ 12.0″ N 85° 25′ 48.0″ E) of the Chilika lagoon from a depth of 1.5 meters. The pH and temperature of the sample site were 7.5 and 24 °C, respectively. The Satapada region is near to the sea mouth of the lagoon with about 3% (w/v) salinity. Modified M30 medium [2] containing 1.0 g l^{-1} $MgCl_2 \cdot 6H_2O$, 2.0 g l^{-1} *N*-acetylglucosamine, 0.1 g l^{-1} $Na_2HPO_4 \cdot 2H_2O$, 10 ml l^{-1} vitamin solution, 50 ml l^{-1} 0.1 M Tris–HCl (pH 8) and 20 ml l^{-1} Hutner's basal salts

Author affiliations: [1]Department of Plant Sciences, School of Life Sciences, University of Hyderabad, P.O. Central University, Hyderabad 500046, India; [2]Bacterial Discovery Laboratory, Centre for Environment, Institute of Science and Technology, J. N. T. University Hyderabad, Kukatpally, Hyderabad-500085, India.
***Correspondence:** Ramana Ch.V., cvr449@gmail.com; Sasikala Ch., sasi449@yahoo.ie
Keywords: Planctomycetaceae, Roseimaritima, sp. nov., Chilika lagoon.
Abbreviations: AAI, average amino acid identity; ANI, average nucleotide indentity; ASW, artificial sea water; dDDH, digital DNA–DNA hybridization; LCB, local collinear block; ME, minimum-evolution; ML, maximum-likelihood; NJ, neighbour-joining.
The GenBank/EMBL/DDBJ accession number for the 16S rRNA gene sequence of strains JC651^T is LR133893. The GenBank/EMBL/DDBJ accession for the whole genome shotgun sequence is WIAD01000000.
†These authors contributed equally to this work
Four supplementary figures and one supplementary table are avaliable with the online version of this article.

004076 © 2020 The Authors

Archives of Microbiology
https://doi.org/10.1007/s00203-020-02078-5

ORIGINAL PAPER

Descriptions of *Roseiconus nitratireducens* gen. nov. sp. nov. and *Roseiconus lacunae* sp. nov.

Dhanesh Kumar[1] · Gaurav Kumar[1] · Jagadeeshwari Uppada[2] · Shabbir Ahmed[1] · Chintalapati Sasikala[2] · Chintalapati Venkata Ramana[1]

Received: 19 June 2020 / Revised: 25 August 2020 / Accepted: 1 October 2020
© Springer-Verlag GmbH Germany, part of Springer Nature 2020

Abstract

Two pink-coloured, oxidase–catalase-positive, salt and alkali-tolerant planctomycetal strains (JC635^T and JC645^T) with pear to spherical-shaped, Gram-stain-negative, motile cells were isolated from Chilika lagoon, India. Both strains share highest 16S rRNA gene sequence identity with members of the genus *Rhodopirellula* (< 94%) and *Roseimaritima* (< 94%) of the family *Pirellulaceae*. The 16S rRNA sequence identity between the strains JC635^T and JC645^T is 96.1%. Respiratory quinone for both strains is MK6. Major fatty acids are $C_{18:1}\omega9c$ and $C_{16:0}$. Major polar lipids are phosphatidylethanolamine, phosphatidylcholine, unidentified amino lipids and an unidentified lipid. The genomic size of strain JC635^T and JC645^T are 7.95 Mb and 8.2 Mb with DNA G + C content of 55.1 and 60.0 mol%, respectively. Based on phylogenetic, genomic (ANI, AAI, POCP, *d*DDH), chemotaxonomic, physiological and biochemical characteristics, we conclude that both strains belong to a novel genus *Roseiconus* gen. nov. and constitute two novel species for which we propose the names *Roseiconus nitratireducens* sp. nov. and *Roseiconus lacunae* sp. nov. The two novel species are represented by the type strains JC645^T (= KCTC 72174^T = NBRC 113879^T) and JC635^T (= KCTC 72164^T = NBRC 113875^T), respectively.

Keywords Chilika lagoon · *Planctomycetes* · *Pirellulaceae* · Gen. nov. · Sp. nov.

Introduction

Members of the phylum *Planctomycetes* are widely distributed and are most commonly isolated from aquatic habitats (Wiegand et al. 2018). Species of this phylum have unique physiology and cell morphology compared to other bacteria (Lage et al. 2013; Wiegand et al. 2020). Phylogenetically, the phylum *Planctomycetes*, along with *Chlamydiae*, *Verrucomicrobia* and others sister phyla forms the PVC superphylum (van Niftrik and Devos 2017). The phylum *Planctomycetes* is subdivided into three classes: *Planctomycetia*, *Phycisphaerae* and "*Candidatus* Brocadiae". Members of "*Candidatus* Brocadiae" are capable of performing anaerobic ammonium oxidation (anammox) (Strous et al. 1999) and thereby convert toxic ammonium to dinitrogen gas. The class *Planctomycetia* has the highest number of species and in the past decade, a large number of strains representing new taxa were isolated from aquatic habitats (Storesund and Øvreås 2013; Bondoso et al. 2014, 2017; Vollmers et al. 2017; Kallscheuer et al. 2019a, b, 2020; Boersma et al. 2019; Peeters et al. 2020a, b; Schubert et al. 2020; Dedysh et al. 2020; Kumar et al. 2020a, b; Waqqas et al. 2020). The

Communicated by Erko stackebrandt.

Dhanesh Kumar and Kumar Gaurav share equal authorship and are considered as first authors.

Electronic supplementary material The online version of this article (https://doi.org/10.1007/s00203-020-02078-5) contains supplementary material, which is available to authorized users.

✉ Chintalapati Sasikala
sasi449@yahoo.ie; sasikala.ch@gmail.com

✉ Chintalapati Venkata Ramana
cvr449@gmail.com

[1] Department of Plant Sciences, School of Life Sciences, University of Hyderabad, P.O. Central University, Hyderabad 500046, India

[2] Bacterial Discovery Laboratory, Centre for Environment, Institute of Science and Technology, J. N. T. University Hyderabad, Kukatpally, Hyderabad 500085, India

Published online: 12 October 2020

INTERNATIONAL JOURNAL OF SYSTEMATIC AND EVOLUTIONARY MICROBIOLOGY

TAXONOMIC DESCRIPTION
Kumar *et al.*, *Int. J. Syst. Evol. Microbiol.*
DOI 10.1099/ijsem.0.004211

MICROBIOLOGY SOCIETY

Gimesia chilikensis sp. nov., a haloalkali-tolerant planctomycete isolated from Chilika lagoon and emended description of the genus *Gimesia*

Dhanesh Kumar[1]†, Kumar Gaurav[1]†, Sreya PK[1], Shabbir A.[1], Jagadeeshwari Uppada[2], Sasikala Ch.[2,*] and Ramana Ch.V.[1,*]

Abstract

A Gram-stain-negative, aerobic, non-motile, salt- and alkali-tolerant, pear to oval shaped, rosette-forming, white coloured, bacterium, designated as strain JC646^T, was isolated from a sediment sample collected from Chilika lagoon, India. Strain JC646^T reproduced through budding, grew well at up to pH 9.0 and tolerated up to 7% NaCl. Strain JC 646^T utilized α-D-glucose, fumarate, lactose, sucrose, fructose, D-galactose, mannose, maltose and D-xylose as carbon sources. Peptone, L-isoleucine, L-serine, L-lysine, L-glutamic acid, L-aspartic acid, DL-threonine and L-glycine were used by the strain as nitrogen sources for growth. The respiratory quinone was MK6. Major fatty acids were $C_{16:1}\,\omega7c/C_{16:1}\,\omega6c$ and $C_{16:0}$. The polar lipids of strain JC646^T comprised phosphatidyl-dimethylethanolamine, phosphatidylcholine, diphosphatidylglycerol, an unidentified amino lipid and two unidentified lipids. Strain JC646^T had highest (97.3%) 16S rRNA gene sequence identity to the only species of the genus *Gimesia*, *Gimesia maris* DSM 8797^T. The genome of strain JC646^T was 7.64 Mbp with a DNA G+C content of 53.2 mol%. For the resolution of the phylogenetic congruence of the novel strain, the phylogeny was also reconstructed with the sequences of 92 housekeeping genes. Based on phylogenetic analyses, digital DNA–DNA hybridization (19.0%), genome average nucleotide identity (74.5%) and average amino acid identity/percentageof conserved proteins (77%) results, chemotaxonomic characteristics, and differential physiological properties, strain JC646^T is recognized as representing a new species of the genus *Gimesia*, for which we propose the name *Gimesia chilikensis* sp. nov. The type strain is JC646^T (=KCTC 72175^T=NBRC 113881^T).

In 1976, Bauld and Staley [1] reported a marine, stalked and budding bacterium as *Planctomyces maris*. Later, in 2014, Scheuner and co-workers [2] on the basis of the results of further chemotaxonomic and phylogenomic analyses reclassified the genus *Planctomyces* and emended the description of the family *Planctomycetaceae*. They proposed the genus *Gimesia* under which *Gimesia maris* is the only species. The genus *Gimesia* comes under order *Planctomycetes* and family *Planctomycetaceae* having characteristic features of reproduction by budding. The genus *Gimesia* is characterized by the presence of sym-homospermidine as the polyamine, diphosphatidylglycerol, phosphatidyl-monomethyl-ethanolamine and phosphatidyl-dimethylethanolamine as major polar lipids, and $C_{16:0}$ and $C_{16:1}\,\omega7c/C_{16:1}\,\omega6c$ as major fatty acids. *G. maris* is a slow-growing, obligately aerobic, mesophilic, heterotrophic marine bacterium with spherical to ovoid, rosette-forming cells. It reproduces by budding at the opposite pole of the cell, exhibiting longitudinal symmetry and has a single fibrillar appendage located at one pole of mature cells [1]. During our survey of planctomycetes from Chilika lagoon, strain JC646^T was isolated and its 16S rRNA gene sequence identity value was highest (97.3%) with *G. maris* DSM 8797^T. Strain JC646^T was characterized by using a polyphasic approach together with genomic information.

Author affiliations: [1]Department of Plant Sciences, School of Life Sciences, University of Hyderabad, P.O. Central University, Hyderabad 500046, India; [2]Bacterial Discovery Laboratory, Centre for Environment, Institute of Science and Technology, JNT University Hyderabad, Kukatpally, Hyderabad-500085, India.
***Correspondence:** Sasikala Ch., sasikala.ch@gmail.com; Ramana Ch.V., cvr449@gmail.com
Keywords: planctomycetes; *Gimesia chilikensis* sp. nov.; Chilika lagoon.
Abbreviations: AAI, average amino acid identity; ASW, artificial seawater; dDDH, digital DNA–DNA hybridization; gANI, genome average nucleotide identity; LCB, local collinear block; ME, minimum-evolution; ML, maximum-likelihood; NJ, neighbour-joining; POCP, percentage of conserved proteins.
The GenBank/EMBL/DDBJ accession number for the 16S rRNA gene sequence of the strains JC646^T is LR132072. The GenBank/EMBL/DDBJ accession for the whole genome shotgun sequence is VTSR00000000.
†These authors contributed equally to this work
Four supplementary tables and six supplementary figures are available with the online version of this article.

004211 © 2020 The Authors

Journal of Materials Chemistry B

ROYAL SOCIETY OF CHEMISTRY

PAPER

View Article Online
View Journal

Published on 11 May 2020. Downloaded by University of Hyderabad on 5/11/2020 3:16:25 PM.

Check for updates

Cite this: DOI: 10.1039/d0tb00470g

Zwitterionic small molecule based fluorophores for efficient and selective imaging of bacterial endospores†

N. Senthilnathan,[a] Kumar Gaurav,[b] Ch. Venkata Ramana *[b] and T. P. Radhakrishnan *[a]

Received 20th February 2020,
Accepted 23rd April 2020

DOI: 10.1039/d0tb00470g

rsc.li/materials-b

In the emerging scenario of increasing antibiotic resistance and pathogen transmission channels, the grave danger posed by bacterial endospores in critical fields like food industry, health and medicine highlights the urgent need to develop efficient probes for their detection; their sturdy and impermeable multilayer coat makes desirable methods like fluorescence imaging extremely difficult. Selective imaging of the endospores in the presence of the bacteria is even more challenging. Furthermore, it is preferable to maintain the dormant state of endospores through the imaging process, if extended monitoring is required; many of the available techniques involve lethal germination or destruction of the endospores. We show that simple zwitterionic diaminodicyanoquinodimethane (DADQ) molecules with selected functionalities are efficient dyes for fluorescence imaging due to their dipolar structure that facilitates the penetration into the endospore system, and the enhanced fluorescence in their rigid/aggregated state. The facile structural tailorability allows DADQs with various appendage moieties to be synthesized; a derivative with ionic substituents (BT_2), and another with optimally long alkyl chains and the resultant hydrophobic character (BHADQ) are shown to be excellent fluorescent probes for endospores. Nanomolar amounts of dyes provide effective staining; while BT_2 stains bacteria and endospores, most significantly, BHADQ stains endospores selectively. To the best of our knowledge, this is the first example of selective fluorescence imaging of endospores in their dormant state. A range of spectroscopy, microscopy and calorimetry studies provide insight into the molecular level interactions that enable efficient staining and bright images. DADQ fluorophores are photostable and non-cytotoxic, hence useful in practical applications. The versatile structural tailorability of these dye molecules holds great promise for targeted imaging.

Introduction

Endospore formation is an ingenious mechanism that allows bacteria to survive adverse environmental conditions and transfer their genetic information to ensuing generations. These dormant states are highly resistant to debilitating effects such as heat, dehydration, radiation and chemicals; causative factors include the exosporium that provides adherence and biocide resistance, keratin based spore coat, cortex and spore wall made of peptidoglycan, and dipicolinate and the low water content in the core.[1] The increasing susceptibility of humans and animals to infections arising from the bourgeoning antibiotic resistance of several bacterial strains has reached alarming levels. Since antibiotics and sterilization techniques are often ineffective against endospores, food and medical industries are at great risk;[2–4] endospores can also act as ominous biological weapons.[5,6] Development of efficient, cost-effective and facile methods for the detection of endospores and assessment of their viability is an urgent and critical imperative.[7–10]

Even though optical absorption and fluorescence emission based imaging are desirable and facile techniques, the chemical resistance and permeability barriers due to the protective coats of endospores pose inherent challenges. The exosporium allows the penetration of molecules with sizes typically <150 kDa, whereas the coat/outer membrane allows only sizes <8 kDa. For even smaller molecules such as water, the permeability of the coat including the inner membrane is very low, with the structure of the coat being critical.[11] Non-fluorescence based imaging

[a] School of Chemistry, University of Hyderabad, Hyderabad – 500 046, India. E-mail: tpr@uohyd.ac.in; Web: http://chemistry.uohyd.ac.in/Btpr/; Tel: 91-40-2313-4827

[b] Department of Plant Science, School of Life Sciences, University of Hyderabad, Hyderabad – 500 046, India. E-mail: cvr449@gmail.com

† Electronic supplementary information (ESI) available: Characterization of the dye molecules, control experiments (imaging, microscopy and spectroscopy details), cytotoxicity assay and additional references. CCDC 1950536. For ESI and crystallographic data in CIF or other electronic format see DOI: 10.1039/d0tb00470g

Journal of Microbiological Methods 177 (2020) 106019

Contents lists available at ScienceDirect

Journal of Microbiological Methods

journal homepage: www.elsevier.com/locate/jmicmeth

"Sporotan" a new fluorescent stain for identifying cryptic spores of *Rhodobacter johrii*

Ashif Ali[a], Kumar Gaurav[a], Senthilnathan N.[b], Radhakrishnan T.P.[b], Sasikala Ch[c], Ramana Ch.V.[a,*]

[a] Department of Plant Sciences, School of Life Sciences, University of Hyderabad, Hyderabad 500046, Telangana, India
[b] School of Chemistry, University of Hyderabad, Hyderabad 500046, Telangana, India
[c] Centre for Environment, Institute of Science & Technology, JNT University Hyderabad, Hyderabad 500085, Telangana, India

ARTICLE INFO

Keywords:
Endospores
Fluorescent stain
Proteobacterium
Rhodobacter johrii

ABSTRACT

We propose a new fluorescent stain "sporotan" and staining protocol which aid in the identification of cryptic endospores which are otherwise mistaken as poly-β-hydroxyalkanoate granules.

1. Introduction

A spore is the tough, dormant, non-reproductive structure usually formed when bacteria go through extreme adverse environmental conditions. This is a survival strategy that evolves among many bacteria which are human pathogens such as *Bacillus anthracis, Bacillus cereus, Bacillus thuringiensis, Clostridium botulinum, Clostridium tetani* (Bottone, 2010). However, spores are major contaminants in food processing industry (Heyndrickx, 2011). Spores are also advantageous for humans as potential probiotics (Elshaghabee et al., 2017) because they are heat, acid, bile salt and gastric juice resistant, which are generally used for their antimicrobial, anti-oxidant, immune-modulatory and pathogen exclusion properties (Shobharani et al., 2015; Ripert et al., 2016; Lefevre et al., 2015).

Bacteria produce spores either endogenously (endospores) or exogenously (exospores). It is widely believed that endospore producers are confined to the members of the phylum *Firmicutes*. Other endospore producers discovered include *Rhodobacter johrii* (Girija et al., 2010), *Serratia marcescens* subsp. *sakuensis* (Ajithkumar et al., 2003), *Rhodopseudomonas palustris* (Venkidusamy and Megharaj, 2016), *Coxiella burnetii* (McCaul and Williams, 1981) and *Myxococcus xanthus* (Kroos, 2007; Kaiser, 2006) belonging to the phylum Proteobacteria. *Mycobacterium* species like *Mycobacterium marinum*, *Mycobacterium bovis BCG* (Ghosh et al., 2009) and *Mycobacterium avium* subsp. *paratuberculosis* (MAP) (Lamont et al., 2012) belong to the phylum *Actinobacteria,* indicating clearly that the phenomenon of endospores is wide spread in bacteria and not confined to the members of the phylum Firmicutes, as believed previously (Abecasis et al., 2013). On the other hand, exospore producing bacteria are wide spread among the members of the phylum Actinobacteria (Reed and Dugan, 1979; Reed et al., 1980) and a few members of Proteobacteria (Kimble-Long and Madigan, 2001; Wu et al., 2005). Detection of bacterial spores is an important part of medical science, as well as food, bio-fertilizers and pharma industry. Therefore, an easy, rapid method for their visualization and identification is required, as the existing spore staining methods have various drawbacks.

The classical methods for endospore staining are Gram stain and Schaeffer–Fulton method (Schaeffer and Fulton, 1933) which was modified from Dorner's method (Dorner, 1922) which is lengthy, tedious and hazardous. The recent method of "Flood to microliter" developed by Siguenza and coworkers (Siguenza et al., 2019) for bacterial endospore staining utilizes microliters of the dye, still flooding of dyes is practiced. There are a large number of fluorescence dyes also used for endospore staining, however, they all still have several drawbacks (Table.1). Some of these like 4–6-diamino-2- phenylindole [DAPI] and propidium monoazide [PMA] cause impairment of living cells and are only permeable in membrane–compromised dead cells; thus, they bind to both vegetative cells as well as dead spores. Acridine orange [AO], DAPI, PMA and flow cytometery fluorescent probes like, SYBR1, SYBR2 (Invitrogen™) are not specific for binding spore DNA (Schichnes et al., 2006; Tarnowski et al., 1991; Probst et al., 2012; Karava et al., 2019). Auromine 0, Thioflavin T [ThT] and Hoechst 34580 exhibit binding for both vegetative cells and spores (Bartholomew et al., 1965; Xia et al., 2011; D'Incecco et al., 2018). We propose a new fluorescent bacterial spore stain "Sporotan" which is chemically: 7,7-(*n*-hexylamino)-8,8-

* Corresponding author.
E-mail address: chvrsl@uohyd.ernet.in (C.V. Ramana).

https://doi.org/10.1016/j.mimet.2020.106019
Received 9 May 2020; Received in revised form 21 July 2020; Accepted 23 July 2020
Available online 14 August 2020
0167-7012/ © 2020 Elsevier B.V. All rights reserved.

Author's personal copy

Antonie van Leeuwenhoek
https://doi.org/10.1007/s10482-020-01471-w

ORIGINAL PAPER

Paludisphaera soli sp. nov., a new member of the family *Isosphaeraceae* isolated from high altitude soil in the Western Himalaya

Rishabh Kaushik · Meesha Sharma · Kumar Gaurav · U. Jagadeeshwari · A. Shabbir · Ch. Sasikala · Ch. V. Ramana · Maharaj K. Pandit

Received: 8 June 2020 / Accepted: 1 September 2020
© Springer Nature Switzerland AG 2020

Abstract A novel strain of Planctomycetes, designated JC670^T, was isolated from a high altitude (~ 2900 m above sea level) soil sample collected from Garhwal region in the Western Himalaya. Colonies of this strain were observed to be light pink coloured with spherical to oval shaped cells having crateriform structures distributed all over the cell surface. The cells divide by budding. Strain JC670^T was found to grow well at pH 7.0 and pH 8.0 and to tolerate up to 2% NaCl (w/v). MK6 was the only respiratory quinone identified. The major fatty acids of strain JC670^T were identified as $C_{18:1}\omega9c$, $C_{18:0}$ and $C_{16:0}$, and phosphatidylcholine, two unidentified phospholipids and six unidentified lipids are present as the polar lipids. The polyamines putrescine and sym-homospermidine were detected. Strain JC670^T shows high 16S rRNA gene sequence identity (95.4%) with *Paludisphaera borealis* PX4^T. The draft genome size of strain JC670^T is 7.97 Mb, with G + C content of 70.4 mol%. Based on phylogenetic analyses with the sequences of ninety-two core genes, low *d*DDH value (20.6%), low gANI (76.8%) and low AAI (69.1%) results, differential chemotaxonomic and physiological properties, strain JC670^T (= KCTC 72850^T = NBRC 114339^T) is recognised as the type strain of a new species of the genus *Paludisphaera,* for which we propose the name *Paludisphaera soli* sp. nov.

Keywords Soil bacteria · Western himalaya · Planctomycetes · Isosphaeraceae · *Paludisphaera* · High altitude

Abbreviations

NCBI	National Center for Biotechnology Information
ANI	Average Nucleotide Index
AAI	Average Nucleotide Index
*d*DDH	Digital DNA-DNA Hybridization
HPLC	High-Pressure Liquid Chromatography
KCTC	Korean Collection for Type Cultures

Rishabh Kaushik and Meesha Sharma having equal authorship and consider as first authors.

Electronic supplementary material The online version of this article (https://doi.org/10.1007/s10482-020-01471-w) contains supplementary material, which is available to authorized users.

R. Kaushik · M. Sharma · M. K. Pandit (✉)
Department of Environmental Studies, University of Delhi, Delhi 110007, India
e-mail: rajkpandit@gmail.com

K. Gaurav · A. Shabbir · Ch. V. Ramana (✉)
Department of Plant Sciences, School of Life Sciences, University of Hyderabad, P.O. Central University, Hyderabad 500046, India
e-mail: cvr449@gmail.com

U. Jagadeeshwari · Ch. Sasikala
Bacterial Discovery Laboratory, Centre for Environment, Institute of Science and Technology, J. N. T. University Hyderabad, Kukatpally, Hyderabad 500085, India

Published online: 16 September 2020

INTERNATIONAL JOURNAL OF SYSTEMATIC AND EVOLUTIONARY MICROBIOLOGY

TAXONOMIC DESCRIPTION

B. *et al.*, *Int J Syst Evol Microbiol* 2020;70:93–99

DOI 10.1099/ijsem.0.003716

MICROBIOLOGY SOCIETY

Chryseobacterium candidae sp. nov., isolated from a yeast (*Candida tropicalis*)

Indu B.,[1] Kumar G.,[1] Smita N.,[1] Shabbir A.,[2] Sasikala Ch.[1,*] and Ramana Ch. V.[1]

Abstract

A Gram-stain-negative, rod shaped, non-motile, aerobic bacterium (strain JC507^T) was isolated from a yeast (*Candida tropicalis* JY101). Strain JC507^T was oxidase- and catalase-positive. Complete 16S rRNA gene sequence comparison data indicated that strain JC507^T was a member of the genus *Chryseobacterium* and was closely related to *Chryseobacterium indologenes* NBRC 14944^T (98.7 %), followed by *Chryseobacterium arthrosphaerae* CC-VM-7^T (98.6 %), *Chryseobacterium gleum* ATCC 35910^T (98.5 %) and less than 98.5 % to other species of the genus *Chryseobacterium*.The genomic DNA G+C content of strain JC507^T was 36.0 mol%. Strain JC507^T had phosphatidylethanolamine, four unidentified amino lipids and four unidentified lipids. MK-6 was the only respiratory quinone. The major fatty acids (>10 %) were anteiso-$C_{11:0}$, iso-$C_{15:0}$ and iso-$C_{17:0}$3OH. The average nucleotide identity and *in silico* DNA–DNA hybridization values between strain JC507^T and *C. indologenes* NBRC 14944^T, *C. arthrosphaerae* CC-VM-7^T and *C. gleum* ATCC 35910^T were 80.2, 83.0 and 87.0 % and 24, 26.7 and 32.7 %, respectively. The results of phenotypic, phylogenetic and chemotaxonomic analyses support the inclusion of strain JC507^T as a representative of a new species of the genus *Chryseobacterium,* for which the name *Chryseobacterium candidae* sp. nov. is proposed. The type strain is JC507^T (=KCTC 52928^T=MCC 4072^T=NBRC 113872^T).

The family *Flavobacteriaceae* comprises the genus *Chryseobacterium* which was first established by Vandamme *et al.* [1]. At the time of writing, more than 100 species of bacteria (www.bacterio.net/chryseobacterium.html) have been placed in the genus *Chryseobacterium* and were isolated either from clinical samples [2], fish [3], fresh water [4], sewage and plants [5], soils [6, 7], meat [8] or waste water [9]. New species with valid names added during 2018–2019 included *Chryseobacterium salipaludis* [10] *Chryseobacterium aurantiacum* [11], *Chryseobacterium phosphatilyticum* [12], *Chryseobacterium glaciei* [13] and *Chryseobacterium populi* [14]. The typical characteristics of the genus *Chryseobacterium* include the presence of an aerobic type of metabolism, branched-chain fatty acids, iso-$C_{15:0}$ and iso-$C_{17:0}$3-OH as the major fatty acids, phosphatidylethanolamine as a major polar lipid, menaquinone-6 (MK-6) as the characteristic respiratory quinone, and production of flexirubin-type pigments [15–17]. Some of the members of this genus are associated as endophytes [12, 17] and during our study on yeast diversity, we have isolated an endobacterium (strain JC507^T) of a yeast (*Candida tropicalis*) which was characterized by a genomic and polyphasic taxonomic approach.

A yeast (strain JY101) was isolated from a soil sample collected from Hyderabad, India (22° 98′ N 71° 47′ E). The soil sample was serially diluted and plated onto a nutrient agar plate containing chloramphenicol (100 µg ml^{-1}). Several white-coloured colonies were observed which were further purified and sequenced using yeast-specific primers used for amplification of the ITS regions and the D1/D2 domain of the 26S rRNA gene. The Internal transcribed spacer (ITS) region was amplified with ITS1 (5′-GTCGTAACAAGGTTTCCGTAGGTG-3′) and ITS4 (5′-TCCTCCGCTTATTGATATGC-3′) primers (31). The D1/D2 domain of the 26S rRNA gene was amplified using NL1 (5′-GCATATCAATAAGCGGAGGAAAAG-3′) and NL4 (5′-GGTCCGTGTTTCAAGACGG-3′) primers. NCBI/CBS BLAST analysis of strain JY101 for D1/D2 (599 bp; NCBI accession numberLT999794) and ITS (340 bp; NCBI accession number LT795043) showed 100 % sequence similarity

Author affiliations: [1]Department of Plant Sciences, School of Life Sciences, University of Hyderabad, P.O. Central University, Hyderabad 500046, India; [2]Bacterial Discovery Laboratory, Centre for Environment, Institute of Science and Technology, J. N. T. University Hyderabad, Kukatpally, Hyderabad 500085, India.

***Correspondence:** Sasikala Ch., cvr449@gmail.com *or* sasi449@yahoo.ie

Keyword: *Chryseobacterium* .

Abbreviations: EDTA, Ethylenediaminetetraaceticacid; EMSA, ElectrophoreticMobility Shift Assay; SPI-1, *Salmonella*PathogenicityIsland 1; MR/P, Mannose-Resistant/*Proteus*; PAGE, PolyacrylamideGel Electrophoresis; PBS, PhosphateBuffered Saline; PCR, PolymeraseChain Reaction; UAS, UpstreamActivating Sequence.

The GenBank/EMBL/DDBJ accession number for the 16S rRNA gene sequence of strainJC507^T is LT838865. The GenBank/EMBL/DDBJ accession for the whole genome shotgun sequence is SDLV00000000.

One supplementary table and three supplementary figures are available with the online version of this article.

003716 © 2020 The Authors

Current Microbiology
https://doi.org/10.1007/s00284-020-02205-x

Arenibacter lacus sp. nov., Isolated from Chilika Lagoon, India

Dhanesh Kumar[1] · Nandardhane Smita[1] · Gaurav Kumar[1] · Gandham Suresh[1] · Uppada Jagadeeshwari[2] · Chintalapati Sasikala[2] · Chintalapati Venkata Ramana[1]

Received: 16 May 2020 / Accepted: 5 September 2020
© Springer Science+Business Media, LLC, part of Springer Nature 2020

Abstract
A shiny dark yellow pigmented, Gram-stain-negative, rod-shaped, non-motile bacterium, designated as strain JC631^T, was isolated from the sediment ecosystem of Chilika lagoon, India. Strain JC631^T tolerates up to pH 10 and NaCl up to 3% (w/v). MK6 is the only respiratory quinone. Predominant (> 10%) cellular fatty acids are anteiso-$C_{11:0}$, anteiso-$C_{13:0}$, and anteiso-$C_{15:0}$. Major polar lipids are phosphatidylethanolamine, phosphatidylcholine, a few unidentified phospholipids, and a few unidentified aminolipids. 16S rRNA gene sequencing showed that strain JC631^T shared the highest sequence identity (98.7%) with *Arenibacter latericius* KMM 426^T followed by *Arenibacter certesii* CCUG 48006^T (98.6%) and other members of the genus *Arenibacter* (< 97%). The genome size of strain JC631^T is 4.16 Mb with a GC content of 40.8 mol%. Strain JC631^T has ANI scores of 78.3% and 78.1%; *d*DDH values of 22.2% and 21.8%, respectively, with the type strains of *A. latericius* and *A. certesii*. The genomic distinction is well supported by chemotaxonomic characteristics and differential physiological properties. This supports strain JC631^T to be described as a new species of the genus *Arenibacter,* named as *Arenibacter lacus* sp. nov. The type strain is JC631^T (= KCTC 72002^T = NBRC 114071^T).

Introduction

The genus *Arenibacter* was first described by Ivanova et al. [1] to accommodate a rod-shaped bacterium, *Arenibacter latericius* within the family *Flavobacteriaceae*, which was further amended by Nedashkovskaya et al. [2]. Currently, the genus *Arenibacter* has 10 species with validly published names (https://lpsn.dsmz.de/genus/arenibacter). All species of the genus *Arenibacter* except *A. antarcticus*, *A. catalasegens*, and *A. aquaticus* were reported to have the capacity of degrading polycyclic aromatic hydrocarbons (PAHs) such as phenanthrene and naphthalene, indicating the industrial importance of the genus *Arenibacter* [3]. Members of the genus *Arenibacter* are exclusively marine and are isolated from different habitats such as sediment, sea weed, sea urchin, and tidal flat. During our study on the cultivable bacterial diversity of Chilika lagoon, we have isolated an obligately aerobic bacterium which has highest (94–99%) 16S rRNA gene sequence identity with the members of the genus *Arenibacter*. Polyphasic characterization including phylogenomic analysis was carried out to classify the new isolate.

Materials and Methods

Home, Habitat and Isolation

Strain JC631^T was isolated from a sediment sample collected from Chilika lagoon at Satapada, Odisa, India (GPS of the sampling site was 19° 40′ 12.0″ N 85° 25′ 48.0″ E), depth of 10 feet from the water surface; sample pH was 8.0 and

The GenBank/EMBL/DDBJ accession number for the 16S rRNA gene sequences of the strains JC631^T is LR215975. The GenBank/EMBL/DDBJ accession number for the whole-genome shotgun sequence is VVIN00000000.

Electronic supplementary material The online version of this article (https://doi.org/10.1007/s00284-020-02205-x) contains supplementary material, which is available to authorized users.

✉ Chintalapati Sasikala
sasikala.ch@gmail.com

✉ Chintalapati Venkata Ramana
cvr449@gmail.com; chvrsl@uohyd.ernet.in

[1] Department of Plant Sciences, School of Life Sciences, University of Hyderabad, P.O. Central University, Hyderabad 500046, India

[2] Bacterial Discovery Laboratory, Centre for Environment, Institute of Science and Technology, J. N. T. University Hyderabad, Kukatpally, Hyderabad 500085, India

Published online: 21 September 2020

Emerging Concepts in Bacterial Taxonomy

1

Anusha Rai, Indu, N. Smita, G. Deepshikha, K. Gaurav, K. Dhanesh, G. Suresh, Ch. Sasikala, and Ch. V. Ramana

Abstract

Bacterial taxonomy has progressed over the years by virtue of the brisk and competent scientific developments. Ground-breaking molecular techniques have added an edge in the phylogenetic studies, resulting in the quality description of the taxa under studies. New avenues are rapidly developing whose validation has always been embraced and included, which will assist in resolution. It began with the simple application of objective procedures for classification, and now we have arrived at the genome-based taxonomy. This pedantic step has led to the meticulous examination and served to reconcile certain conflicts of the status of the taxa. This field is dynamic and is exploring more options like proteomics and metabolomics in gaining more insights into the lineal heritage. Even though there has been a significant change and addition, there is an ever-growing need for a comprehensive study, which would thread all the attributes together into one functional unit of classification. In this review, we examine the paradigm shift from traditional taxonomy to integrated taxonomy useful in the characterisation of bacteria which in addition aids in the identity of biotechnological targets.

Keywords

Bacterial taxonomy · Polyphasic · Phylogenomics · Integrated taxonomy · Average nucleotide sequence index (ANI)

A. Rai · Indu · N. Smita · G. Deepshikha · K. Gaurav · K. Dhanesh · G. Suresh · C. V. Ramana (✉)
Department of Plant Sciences, School of Life Sciences, University of Hyderabad, Hyderabad, Telangana, India

C. Sasikala (✉)
Centre for Environment, Institute of Science & Technology, JNT University Hyderabad, Hyderabad, Telangana, India

© Springer Nature Singapore Pte Ltd. 2019

T. Satyanarayana et al. (eds.), *Microbial Diversity in Ecosystem Sustainability and Biotechnological Applications*, https://doi.org/10.1007/978-981-13-8315-1_1

Genetic and culture diversity of Planctomycetes from different habitats of India

ORIGINALITY REPORT

41%	13%	38%	6%
SIMILARITY INDEX	INTERNET SOURCES	PUBLICATIONS	STUDENT PAPERS

PRIMARY SOURCES

1	Gaurav Kumar, Vaddavalli Radha, Uppadda Jagadeeshwari, Chintalapati Sasikala, Chintalapati Venkata Ramana. "Bacterial communities of sponges from the wetland ecosystem of Little Rann of Kutch, India with particular reference to Planctomycetes", 3 Biotech, 2020 Publication	11%
2	Dhanesh Kumar, Gaurav Kumar, Jagadeeshwari Uppada, Shabbir Ahmed, Chintalapati Sasikala, Chintalapati Venkata Ramana. "Descriptions of Roseiconus nitratireducens gen. nov. sp. nov. and Roseiconus lacunae sp. nov.", Archives of Microbiology, 2020 Publication	9%
3	Gaurav Kumar, Dhanesh Kumar, U. Jagadeeshwari, P. K. Sreya, A. Shabbir, Ch. Sasikala, Ch. V. Ramana. "Crateriforma spongiae sp. nov., isolated from a marine	7%

This paper is published by student itself

Prof. Ch. Venkata Ramana Ph.D
Department of Plant Sciences School of Life Sciences
University of Hyderabad, P.O. Central University,
Hyderabad - 500 046, India

18/3/2021

Scanned with CamScanner

sponge and emended description of the genus "Crateriforma"", Antonie van Leeuwenhoek, 2021
Publication

4 Dhanesh Kumar, Gaurav Kumar, Uppada Jagadeeshwari, Chintalapati Sasikala, Chintalapati Venkata Ramana. ""Candidatus Laterigemmans baculatus" gen. nov. sp. nov., the first representative of rod shaped planctomycetes with lateral budding in the family Pirellulaceae", Systematic and Applied Microbiology, 2021 — 4%
Publication

This paper is published by student itself
Prof. Ch. Venkata Ramana Ph.D
Department of Plant Sciences, School of Life Sciences
University of Hyderabad - 500 046, India
19/8/2024

5 Submitted to University of Hyderabad, Hyderabad — 1%
Student Paper

6 link.springer.com — 1%
Internet Source

7 Rishabh Kaushik, Meesha Sharma, Kumar Gaurav, U. Jagadeeshwari, A. Shabbir, Ch. Sasikala, Ch. V. Ramana, Maharaj K. Pandit. "Paludisphaera soli sp. nov., a new member of the family Isosphaeraceae isolated from high altitude soil in the Western Himalaya", Antonie van Leeuwenhoek, 2020 — 1%
Publication

This paper is published by student itself
Prof. Ch. Venkata Ramana Ph.D
Department of Plant Sciences, School of Life Sciences
University of Hyderabad, PO Central University
Hyderabad - 500 046, India
18/8/2021

8 Sandra Wiegand, Mareike Jogler, Christian

Scanned with CamScanner

	Jogler. "On the maverick Planctomycetes", FEMS Microbiology Reviews, 2018 Publication	1%
9	www.microbiologyresearch.org Internet Source	1%
10	res.mdpi.com Internet Source	<1%
11	"The Prokaryotes", Springer Science and Business Media LLC, 2014 Publication	<1%
12	repository.tudelft.nl Internet Source	<1%
13	Dhanesh Kumar, Nandardhane Smita, Gaurav Kumar, Gandham Suresh et al. "Arenibacter lacus sp. nov., Isolated from Chilika Lagoon, India", Current Microbiology, 2020 Publication	<1%
14	Submitted to Jawaharlal Nehru Technological University Student Paper	<1%
15	baadalsg.inflibnet.ac.in Internet Source	<1%
16	Goodfellow, Michael. "Phylum XXVI. Actinobacteria phyl. nov.", Bergey's Manual® of Systematic Bacteriology, 2012. Publication	<1%

17	Anusha Rai, N. Smita, A. Shabbir, U. Jagadeeshwari, T. Keertana, Ch. Sasikala, Ch. V. Ramana. "Mesobacillus aurantius sp. nov., isolated from an orange-colored pond near a solar saltern", Archives of Microbiology, 2021 Publication	<1%
18	onlinelibrary.wiley.com Internet Source	<1%
19	crdd.osdd.net Internet Source	<1%
20	hdl.handle.net Internet Source	<1%
21	ijs.sgmjournals.org Internet Source	<1%
22	edepot.wur.nl Internet Source	<1%
23	Karl-Heinz Schleifer. "Phylum XIII. Firmicutes Gibbons and Murray 1978, 5 (Firmacutes [sic] Gibbons and Murray 1978, 5)", Systematic Bacteriology, 2009 Publication	<1%
24	www.frontiersin.org Internet Source	<1%
25	Submitted to National Chung Hsing University Student Paper	<1%

26	d-nb.info Internet Source	<1%
27	lrd.yahooapis.com Internet Source	<1%
28	repository.dl.itc.u-tokyo.ac.jp Internet Source	<1%
29	en.wikipedia.org Internet Source	<1%
30	Rikuan Zheng, Ruining Cai, rui liu, Yeqi Shan, Ge Liu, Chaomin Sun. "Cultivation and characterization of a novel clade of deep-sea Chloroflexi: providing a glimpse of the phylum Chloroflexi involved in sulfur cycling", Cold Spring Harbor Laboratory, 2021 Publication	<1%
31	www.i-scholar.in Internet Source	<1%
32	Xu Qiu, Xiaorong Cao, Guangxin Xu, Huangming Wu, Xixiang Tang. "Halomonas Maris Sp. Nov., a Moderately Halophilic Bacterium Isolated From Marine Sediment in the Southwest Indian Ocean", Research Square, 2021 Publication	<1%
33	sheethub.com Internet Source	<1%

34	www.semanticscholar.org Internet Source	<1%
35	bioruby.org Internet Source	<1%
36	dx.doi.org Internet Source	<1%
37	manualzz.com Internet Source	<1%
38	studyres.com Internet Source	<1%
39	Bergey's Manual of Systematic Bacteriology, 2010. Publication	<1%
40	ijs.microbiologyresearch.org Internet Source	<1%
41	Submitted to University of Hong Kong Student Paper	<1%
42	Submitted to Incheon National University Student Paper	<1%
43	The Prokaryotes, 2014. Publication	<1%
44	www.science.gov Internet Source	<1%